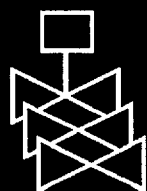
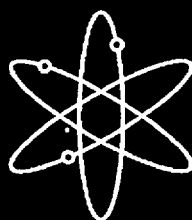
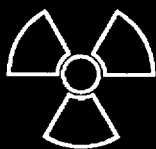
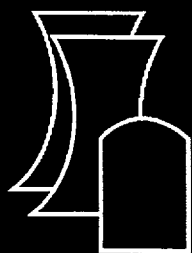


Technical Basis for Revision of Regulatory Guidance on Design Ground Motions: Development of Hazard- and Risk-consistent Seismic Spectra for Two Sites

Risk Engineering, Inc.

**U.S. Nuclear Regulatory Commission
Office of Nuclear Regulatory Research
Washington, DC 20555-0001**



AVAILABILITY OF REFERENCE MATERIALS IN NRC PUBLICATIONS

NRC Reference Material

As of November 1999, you may electronically access NUREG-series publications and other NRC records at NRC's Public Electronic Reading Room at www.nrc.gov/NRC/ADAMS/index.html.

Publicly released records include, to name a few, NUREG-series publications; *Federal Register* notices; applicant, licensee, and vendor documents and correspondence; NRC correspondence and internal memoranda; bulletins and information notices; inspection and investigative reports; licensee event reports; and Commission papers and their attachments.

NRC publications in the NUREG series, NRC regulations, and *Title 10, Energy*, in the Code of *Federal Regulations* may also be purchased from one of these two sources.

1. The Superintendent of Documents
U.S. Government Printing Office
Mail Stop SSOP
Washington, DC 20402-0001
Internet: bookstore.gpo.gov
Telephone: 202-512-1800
Fax: 202-512-2250
2. The National Technical Information Service
Springfield, VA 22161-0002
www.ntis.gov
1-800-553-6847 or, locally, 703-605-6000

A single copy of each NRC draft report for comment is available free, to the extent of supply, upon written request as follows:

Address: Office of the Chief Information Officer,
Reproduction and Distribution
Services Section
U.S. Nuclear Regulatory Commission
Washington, DC 20555-0001

E-mail: DISTRIBUTION@nrc.gov
Facsimile: 301-415-2289

Some publications in the NUREG series that are posted at NRC's Web site address www.nrc.gov/NRC/NUREGS/indexnum.html are updated periodically and may differ from the last printed version. Although references to material found on a Web site bear the date the material was accessed, the material available on the date cited may subsequently be removed from the site.

Non-NRC Reference Material

Documents available from public and special technical libraries include all open literature items, such as books, journal articles, and transactions, *Federal Register* notices, Federal and State legislation, and congressional reports. Such documents as theses, dissertations, foreign reports and translations, and non-NRC conference proceedings may be purchased from their sponsoring organization.

Copies of industry codes and standards used in a substantive manner in the NRC regulatory process are maintained at—

The NRC Technical Library
Two White Flint North
11545 Rockville Pike
Rockville, MD 20852-2738

These standards are available in the library for reference use by the public. Codes and standards are usually copyrighted and may be purchased from the originating organization or, if they are American National Standards, from—

American National Standards Institute
11 West 42nd Street
New York, NY 10036-8002
www.ansi.org
212-642-4900

Legally binding regulatory requirements are stated only in laws; NRC regulations; licenses, including technical specifications; or orders, not in NUREG-series publications. The views expressed in contractor-prepared publications in this series are not necessarily those of the NRC.

The NUREG series comprises (1) technical and administrative reports and books prepared by the staff (NUREG-XXXX) or agency contractors (NUREG/CR-XXXX), (2) proceedings of conferences (NUREG/CP-XXXX), (3) reports resulting from international agreements (NUREG/IA-XXXX), (4) brochures (NUREG/BR-XXXX), and (5) compilations of legal decisions and orders of the Commission and Atomic and Safety Licensing Boards and of Directors' decisions under Section 2.206 of NRC's regulations (NUREG-0750).

DISCLAIMER: This report was prepared as an account of work sponsored by an agency of the U.S. Government. Neither the U.S. Government nor any agency thereof, nor any employee, makes any warranty, expressed or implied, or assumes any legal liability or responsibility for any third party's use, or the results of such use, of any information, apparatus, product, or process disclosed in this publication, or represents that its use by such third party would not infringe privately owned rights.

Technical Basis for Revision of Regulatory Guidance on Design Ground Motions: Development of Hazard- and Risk-consistent Seismic Spectra for Two Sites

Manuscript Completed: March 2002

Date Published: April 2002

Prepared by

R. K. McGuire¹

W. J. Silva²

C. J. Costantino³

¹Risk Engineering, Inc., Principal Contractor

4155 Darley Avenue, Suite A

Boulder, CO 80305

Subcontractor:

²Pacific Engineering & Analysis

311 Pomona Avenue

El Cerrito, CA 94530

³Carl J. Costantino, Consultant

4 Rockingham Road

Spring Valley, NY 10977

R. M. Kenneally, NRC Project Manager

Prepared for

Division of Engineering Technology

Office of Nuclear Regulatory Research

U.S. Nuclear Regulatory Commission

Washington, DC 20555-0001

NRC Job Code W6248



**NUREG/CR-6769 has been reproduced
from the best available copy.**

Abstract

We develop recommendations for design spectra at two sites, one in the Mojave desert, California, and the second at Columbia, South Carolina. These sites were chosen because local, small earthquakes dominate the high frequencies ($f \geq 10$ Hz), but large distant events dominate the low frequencies ($f \leq 1$ Hz). Both rock and soil conditions are examined at each site.

For rock conditions, the uniform hazard spectrum (UHS) is determined at each site with a probabilistic seismic hazard analysis (PSHA). The hazard at 10 Hz and 1 Hz is deaggregated to determine the dominant magnitude M and distance R , and these values are used to generate two sets of spectral shapes. The first set comes from the recommended functions documented in McGuire et al. (2001); the second set comes from the attenuation equations used in the PSHA. In the CEUS there are separate shapes for the 1- and 2-corner seismic source model, and these are weighted using weights justified in the PSHA. The two sets of spectral shapes are scaled to the UHS amplitudes at 10 Hz and 1 Hz, as a consistency check on the shape of the UHS.

We calculate a scale factor to derive a rock uniform reliability spectrum (URS) based on the slopes of the hazard curves across the frequency range of interest at each site. The URS achieves an approximately consistent annual frequency of plant component seismic failures for all sites and across all structural frequencies. For these examples the 10^{-4} URS is illustrated by scaling the 10^{-4} UHS. The attenuation equation spectral shapes derived from the UHS are scaled to the 10 Hz and 1 Hz URS amplitudes. If the scaled spectra match the URS within a designated criterion, the scaled spectra may be used as separate design motions. This will be more accurate and realistic for sites where a broad-banded earthquake motion is not likely.

The database of strong motion records provides a source of rock motions with the correct magnitudes and distances. To develop design motions, these records are used as the starting point to develop artificial records fit to the individual scaled spectra. Matching criteria are applied to ensure compatibility between the target spectra and the artificial motions.

For soil sites, we illustrate the development of design spectra using a profile of the Meloland station in California assumed to lie at the Mojave site, and a generalized profile of the Savannah River site in South Carolina assumed to lie at the Columbia site. Soil amplification is calculated for these two sites using an equivalent-linear formulation of dynamic soil response, and using as input the rock motions calculated from the PSHA. For the Mojave site it is necessary to remove the effects of the shallow soft-rock velocity gradient to a depth corresponding to a shear-wave velocity of 4000 ft/sec, in order to provide an accurate input to the base of the soil column. We calculate soil amplification factors for rock motions corresponding to the 10^{-4} and 10^{-5} hazard, accounting for uncertainties in soil properties and documenting the uncertainty in soil response. From these calculations we can determine with sufficient accuracy the 10^{-4} and 10^{-5} UHS on soil. This accuracy is illustrated with a separate calculation of the soil hazard, using soil-specific attenuation equations developed specifically for the two profiles studied here. From the UHS on soil we derive the 10^{-4} URS on soil.

We scale soil spectra to the 10 Hz and 1 Hz UHS and URS, using the soil-specific amplification studies, because generic shapes for soil sites are not appropriate. The soil-specific shapes are scaled to the UHS to check consistency, and are scaled to the URS as optional design spectra. If these scaled shapes are to be used for design, they must match the URS within a stated criterion.

Artificial motions for soil sites are created in a manner similar to that for rock sites. The database of records includes soil motions for the WUS and the CEUS, and records with the appropriate magnitudes and distances are adjusted to match the target spectra (either a broad-banded spectrum or individual scaled spectra).

Overall, the procedures recommended in McGuire et al. (2001) work well in developing design spectra for the rock and soil sites examined here. Care must be taken in calculating the URS from the UHS, and in determining soil response given a rock PSHA, but sufficient consistency checks are illustrated so that one can make a determination of the validity of the final recommended spectra.

Reference

McGuire, R.K., W.J. Silva, and C. Costantino (2001). *Tech. Basis for Rev. of Reg. Guidance on Dsgn. Grnd. Motions: Hazard and Risk-consistent Grnd. Motion Spectra Guidelines*, US Nuc. Reg. Comm., Rept. NUREG/CR-6728, Oct.

Contents

Abstract	iii
List of Figures	vii
List of Tables	xv
List of Terms	xvii
1. Introduction	1-1
1.1 Background	1-1
1.2 Summary of procedures for rock and soil sites	1-1
1.3 Purpose of current report	1-2
1.4 Organization of report	1-2
2. Two Sites Chosen for Implementation Study	2-1
2.1 Mojave site seismic environment	2-1
2.2 Columbia site seismic environment	2-1
2.3 Development of WUS and CEUS attenuation relations for generic rock and site specific soil sites	2-2
2.3.1 Point source model parameters	2-2
2.3.2 Soil profiles and nonlinear properties	2-5
2.3.3 Form of attenuation relations	2-7
2.3.4 Attenuation relations for WUS and CEUS rock site conditions	2-7
2.3.5 Attenuation relations for WUS and CEUS soil site conditions	2-9
3. Seismic Hazard	3-1
3.1 Mojave site	3-1
3.1.1 Rock site conditions	3-1
3.1.2 Soil site conditions	3-2
3.2 Columbia site	3-3
3.2.1 Rock site conditions	3-3
3.2.2 Soil site conditions	3-4
4. Uniform Hazard and Reliability Spectra, Rock	4-1
4.1 Mojave site	4-1
4.1.1 Derivation of uniform reliability spectrum (URS)	4-1
4.1.2 Derivation of scaled spectra	4-2
4.1.3 Vertical motions	4-2
4.2 Columbia site	4-3
4.2.1 Derivation of URS	4-3
4.2.2 Derivation of scaled spectra	4-3
4.2.3 Vertical motions	4-4
5. Generating Artificial Time Histories for WUS Rock Sites	5-1
5.1 Spectral Matching Methodology	5-1
5.2 Mojave Site	5-2

6.	Estimation of Uniform Hazard Spectra on Soil	6-1
6.1	Background on estimation of uniform hazard spectra for horizontal motions .	6-1
6.1.1	Overview of approaches to developing hazard-consistent site-specific soil motions incorporating profile uncertainties	6-1
6.1.2	Theoretical basis of methods for soil analyses	6-3
6.2	Steps for estimating uniform hazard spectra for horizontal motions	6-5
6.3	Approaches for vertical motions	6-7
6.4	Horizontal motions for Mojave site	6-9
6.4.1	Results for Approaches 1, 2A, and 2B	6-9
6.4.2	Results for Approach 2A/3	6-12
6.5	Horizontal motions for Columbia site	6-14
6.5.1	Results for Approaches 1, 2A, and 2B	6-14
6.5.2	Results for Approach 2A/3	6-15
6.6	Vertical motions	6-16
6.6.1	Mojave site	6-16
6.6.2	Columbia site	6-16
7.	Uniform Reliability Spectrum on Soil	7-1
7.1	Mojave site	7-1
7.1.1	Derivation of uniform reliability spectrum (URS)	7-1
7.1.2	Scaled spectra on soil	7-1
7.2	Columbia site	7-2
7.2.1	Derivation of URS	7-2
7.2.2	Scaled spectra on soil	7-2
8.	Generating Artificial Motions for Soil Sites	8-1
9.	Summary of Recommendations	9-1
9.1	Rock Sites	9-1
9.2	Soil Sites	9-6
Appendix A	Approximate Method to Calculate Soil Hazard	A-1
Appendix B	Comparison of Horizontal Soil Response Using Equivalent Linear and Nonlinear Methods	B-1
B.1	Methods of analysis	B-1
B.2	Site model	B-2
B.3	Initial computations	B-3
B.4	Revised input motions for western sites	B-3
B.5	Conclusions	B-5

List of Figures

Figure	Description	Page No.
Figure 1-1	Flowchart of design ground motion procedure and application to rock sites.	1-4
Figure 1-2	Flowchart of design ground motion procedure and application to soil sites.	1-5
Figure 2-1	Seismic sources used for WUS example site (Mojave Desert)	2-21
Figure 2-2	Seismic sources used for CEUS example site (Charleston, South Carolina).	2-22
Figure 2-3	Comparison of generic shear-wave velocity profiles for WUS (Los Angeles) and CEUS crustal conditions.	2-23
Figure 2-4	Variations in base case shallow crustal velocities.	2-24
Figure 2-5	Generic G/G_{max} and hysteretic damping curves for soft rock.	2-25
Figure 2-6a	Base case WUS soil shear-wave velocity profile.	2-26
Figure 2-6b	Base case CEUS soil shear-wave velocity profile.	2-27
Figure 2-7a	Variation in base case shear-wave velocity for the Meloland profile based on thirty realizations.	2-28
Figure 2-7b	Variation in base case shear-wave velocity for the Savannah River generic profile based on thirty realizations.	2-29
Figure 2-8a	Generic G/G_{max} and hysteretic damping curves for Imperial Valley soils. Used for soil site Meloland.	2-30
Figure 2-8b	Generic G/G_{max} and hysteretic damping curves for Peninsular Range cohesionless soil site conditions (Silva et al., 1997), assumed for Savannah River generic profile.	2-31
Figure 2-9	Generic G/G_{max} and hysteretic damping curves from SHAKE 1991.	2-32
Figure 2-10	Generic G/G_{max} and hysteretic damping curves for cohesive soils.	2-33
Figure 2-11	Peak acceleration estimates and regression fit at M 7.5 for WUS rock site conditions.	2-34
Figure 2-12	Peak acceleration estimates and regression fit at M 7.5 for CEUS (1-corner source model) rock site conditions.	2-35
Figure 2-13	Attenuation of median peak horizontal acceleration at M 5.5, 6.5, and 7.5 for WUS rock site conditions.	2-36
Figure 2-14a	Attenuation of median peak horizontal acceleration at M 5.5, 6.5, and 7.5 for CEUS rock site conditions (single-corner source model).	2-37
Figure 2-14b	Attenuation of median peak horizontal acceleration at M 5.5, 6.5, and 7.5 for CEUS rock site conditions (double-corner source model).	2-38
Figure 2-15	Median response spectra (5% damping) at a distance of 10 km for magnitudes M 5.5, 6.5, and 7.5: WUS rock site.	2-39
Figure 2-16	Response spectra (5% damping) at a distance of 10 km for M 6.5 showing median and $\pm 1 \sigma$ estimates (parametric and regression uncertainty): WUS rock site.	2-40

Figure 2-17a	Median response spectra (5% damping) at a distance of 10 km for M 5.5, 6.5, and 7.5: CEUS rock site (single-corner source model).	2-41
Figure 2-17b	Median response spectra (5% damping) at a distance of 10 km for M 5.5, 6.5, and 7.5: CEUS rock site (double-corner source model).	2-42
Figure 2-18a	Response spectra (5% damping) at a distance of 10 km for M 6.5 showing median and $\pm 1 \sigma$ estimates (parametric and regression uncertainty): CEUS rock site (single corner source model).	2-43
Figure 2-18b	Response spectra (5% damping) at a distance of 10 km for M 6.5 showing median and $\pm 1 \sigma$ estimates (parametric and regression uncertainty): CEUS rock site (double corner source model) variability in stress drop not included.	2-44
Figure 2-19	Variability in response spectral ordinates at WUS and CEUS rock sites resulting from parametric variability and regression fit over all magnitudes and distances (Tables 2-5 and 2-6).	2-45
Figure 2-20	Attenuation of median peak horizontal acceleration at M 5.5, 6.5, and 7.5 for Meloland profile and WUS conditions.	2-46
Figure 2-21	Median response spectra (5% damping) at a distance of 10 km for M 5.5, 6.5, and 7.5 for Meloland profile and WUS conditions.	2-47
Figure 2-22a	Attenuation of median peak horizontal acceleration at M 4.5, 5.5, 6.5, and 7.5 for Savannah River generic profile and CEUS conditions (single-corner source model).	2-48
Figure 2-22b	Attenuation of median peak horizontal acceleration at M 4.5, 5.5, 6.5, and 7.5 for Savannah River generic profile and CEUS conditions (double-corner source model).	2-49
Figure 2-23a	Median response spectra (5% damping) at a distance of 10 km for M 4.5, 5.5, 6.5, and 7.5 for Savannah River generic profile and CEUS conditions (single-corner source model).	2-50
Figure 2-23b	Median response spectra (5% damping) at a distance of 10 km for M 4.5, 5.5, 6.5, and 7.5 for Savannah River generic profile and CEUS conditions (double-corner source model).	2-51
Figure 2-24	Variability in response spectral ordinates for Meloland profile (WUS) and Savannah River generic profile (CEUS) resulting from parametric variability and regression fit over all magnitudes and distances (Tables 2-7 and 2-8).	2-52
Figure 3-1	PGA seismic hazard curve for Mojave site, rock conditions.	3-14
Figure 3-2	UHS for Mojave site, rock conditions.	3-15
Figure 3-3	Contribution to 10 Hz spectral acceleration hazard by source for Mojave site, rock conditions.	3-16
Figure 3-4	Contribution to 1 Hz spectral acceleration hazard for Mojave site, rock conditions.	3-17
Figure 3-5	Magnitude and distance deaggregation of 10^{-4} hazard at 10 Hz for Mojave site, rock conditions.	3-18

Figure 3-6	Epsilon deaggregation of 10^{-4} hazard at 10 Hz for Mojave site, rock conditions.	3-19
Figure 3-7	Magnitude and distance deaggregation of 10^{-4} hazard at 1 Hz for Mojave site, rock conditions.	3-20
Figure 3-8	Epsilon deaggregation of 10^{-4} hazard at 1 Hz for Mojave site, rock conditions.	3-21
Figure 3-9	PGA seismic hazard curve for Mojave site, soil conditions.	3-22
Figure 3-10	UHS for Mojave site, soil conditions.	3-23
Figure 3-11	Contribution to 10 Hz spectral acceleration hazard by source for Mojave site, soil conditions.	3-24
Figure 3-12	Contribution to 1 Hz spectral acceleration hazard for Mojave site, soil conditions.	3-25
Figure 3-13	Magnitude and distance deaggregation of 10^{-4} hazard at 10 Hz for Mojave site, soil conditions.	3-26
Figure 3-14	Epsilon deaggregation of 10^{-4} hazard at 10 Hz for Mojave site, soil conditions.	3-27
Figure 3-15	Magnitude and distance deaggregation of 10^{-4} hazard at 1 Hz for Mojave site, soil conditions.	3-28
Figure 3-16	Epsilon deaggregation of 10^{-4} hazard at 1 Hz for Mojave site, soil conditions.	3-29
Figure 3-17	PGA seismic hazard, Columbia site, rock conditions.	3-30
Figure 3-18	UHS for Columbia site, rock: 10^{-5} (top three curves), 10^{-4} (middle three curves), 10^{-3} (bottom three curves).	3-31
Figure 3-19	Contribution to 10 Hz hazard by source for Columbia site, rock, 1-corner model.	3-32
Figure 3-20	Contribution to 1 Hz hazard by source for Columbia site, rock, 1-corner model.	3-33
Figure 3-21	$1E-4$ 10 Hz M-R deaggregation for Columbia site, rock, 1-corner and 2-corner models.	3-34
Figure 3-22	$1E-4$, 10 Hz, ϵ deaggregation for Columbia site, rock, 1-corner and 2-corner models.	3-35
Figure 3-23	$1E-4$, 1 Hz, M-R deaggregation for Columbia site, rock, 1-corner and 2-corner models.	3-36
Figure 3-24	$1E-4$, 1 Hz, ϵ deaggregation, Columbia site, rock, 1-corner and 2-corner models.	3-37
Figure 3-25	PGA seismic hazard, Columbia site, Savannah profile.	3-38
Figure 3-26	UHS for Columbia site, Savannah profile: 10^{-5} (top three curves), 10^{-4} (middle three curves), and 10^{-3} (bottom three curves).	3-39
Figure 3-27	Contribution to 10 Hz hazard by source for Columbia site, Savannah profile, rock, 1-corner model.	3-40

Figure 3-28	Contribution to 1Hz hazard by source for Columbia site, Savannah profile, rock, 1-corner model.	3-41
Figure 3-29	1E-4 10 Hz M-R deaggregation for Columbia site, Savannah profile, 1-corner and 2-corner models.	3-42
Figure 3-30	1E-4, 10 Hz ϵ deaggregation for Columbia site, Savannah profile, 1-corner and 2-corner models.	3-43
Figure 3-31	1E-4 M-R deaggregation for Columbia site, Savannah profile, 1-corner and 2-corner models.	3-44
Figure 3-32	1E-4, 1Hz ϵ deaggregation for Columbia site, Savannah profile, 1-corner and 2-corner models.	3-45
Figure 4-1	10 ⁻⁴ UHS and URS for Mojave site, rock conditions.	4-11
Figure 4-2	10 ⁻⁴ UHS and scaled spectra at Mojave site, rock conditions, from attenuation equations and from recommended spectral shapes (labeled "Equation 4-8").	4-12
Figure 4-3	10 ⁻⁴ URS and scaled design spectra for 10 Hz and 1 Hz, Mojave site, rock conditions.	4-13
Figure 4-4a	Recommended V/H ratios (for 5% damping) for WUS soft rock site conditions for ranges in expected horizontal component peak accelerations (McGuire et al., 2001)	4-14
Figure 4-4b	Recommended V/H ratios (for 5% damping) for CEUS hard rock site conditions for ranges in horizontal component peak accelerations.	4-15
Figure 4-5	WUS rock horizontal 10 ⁻⁴ URS and corresponding vertical URS.	4-16
Figure 4-6	10 ⁻⁴ UHS and URS for Columbia site, rock conditions.	4-17
Figure 4-7	10 ⁻⁴ UHS and scaled spectra at Columbia site, rock conditions, from attenuation equations and from recommended spectral shapes (labeled "Equation 4-8").	4-18
Figure 4-8	10 ⁻⁴ URS and scaled spectra for 10 Hz and 1 Hz, Columbia site, rock conditions.	4-19
Figure 4-9	CEUS rock horizontal 10 ⁻⁴ URS and corresponding vertical URS.	4-20
Figure 5-1	Spectral match to corrected (base of soil) rock horizontal 1E-4 UHS, Mojave site.	5-11
Figure 5-2	Acceleration, velocity, and displacement time histories corresponding to the rock horizontal UHS spectral match.	5-12
Figure 5-3	Spectral match to rock vertical component 1E-4 spectrum, at base of soil for Mojave site.	5-13
Figure 5-4	Acceleration, velocity, and displacement time histories corresponding to the rock vertical component spectral match at base of soil for Mojave site.	5-14
Figure 5-5	Spectral match to corrected (base of soil) 1 Hz rock 1E-4 spectrum: ML.	5-15
Figure 5-6	Acceleration, velocity, and displacement time histories corresponding to the corrected (base of soil) 1 Hz rock spectral match: ML.	5-16

Figure 5-7	Spectral match to corrected (base of soil) 1 Hz rock 1E-4 spectrum: MM.	5-17
Figure 5-8	Acceleration, velocity, and displacement time histories corresponding to the corrected (base of soil) 1 Hz rock spectral match: MM.	5-18
Figure 5-9	Spectral match to corrected (base of soil) 1 Hz rock 1E-4 spectrum: MH.	5-19
Figure 5-10	Acceleration, velocity, and displacement time histories corresponding to the corrected (base of soil) 1 Hz rock spectral match: MH.	5-20
Figure 5-11	Spectral match to corrected (base of soil) 10 Hz rock 1E-4 spectrum: ML.	5-21
Figure 5-12	Acceleration, velocity, and displacement time histories corresponding to the corrected (base of soil) 10 Hz rock spectral match: ML.	5-22
Figure 5-13	Spectral match to corrected (base of soil) 10 Hz rock 1E-4 spectrum: MM.	5-23
Figure 5-14	Acceleration, velocity, and displacement time histories corresponding to the corrected (base of soil) 10 Hz rock spectral match: MM.	5-24
Figure 5-15	Spectral match to corrected (base of soil) 10 Hz rock 1E-4 spectrum: MH.	5-25
Figure 5-16	Acceleration, velocity, and displacement time histories corresponding to the corrected (base of soil) 10 Hz rock spectral match: MH.	5-26
Figure 6-1	Comparison of 5% damped rock outcrop 10^{-4} UHS spectra for CEUS and WUS conditions.	6-23
Figure 6-2	Comparison of WUS rock 10^{-4} UHS (solid line) with UHS corrected for base-of-soil conditions (dashed line).	6-24
Figure 6-3	Mojave site, rock, 1 Hz, 10 Hz and UHS corrected to base of soil.	6-25
Figure 6-4	Columbia site, rock outcrop 1 Hz, 10 Hz and UHS.	6-26
Figure 6-5	Comparison of spectral match (dotted line) to corrected WUS rock UHS.	6-27
Figure 6-6	Median and $\pm \sigma$ spectra computed for $M = 7.5$ at a distance of 1 km using the Meloland profile with site variations only (profile, G/G_{max} , and hysteretic damping): WUS conditions.	6-28
Figure 6-7	Median and $\pm \sigma$ spectra computed for $M = 7.5$ at a distance of 1 km for the Meloland profile, WUS conditions, source, path, and site variations.	6-29
Figure 6-8	Comparison of median spectral estimates computed for $M=7.5$ at a distance of 1 km using the Meloland profile, WUS conditions, varying site properties only and varying source, path, and site properties.	6-30
Figure 6-9	Comparison of soil spectra computed using Approaches 1, 2A, 2B, and 4 (Table 6-1) for Meloland profile, WUS conditions.	6-31
Figure 6-10	Median and $\pm 1\sigma$ effective strains for Meloland profile using Approach 1, WUS conditions.	6-32
Figure 6-11	Comparison of transfer functions computed for the scaled 1 Hz design earthquake for the Meloland profile, WUS conditions.	6-33
Figure 6-12	Comparison of transfer functions computed for the scaled 10 Hz design earthquake for the Meloland profile, WUS conditions.	6-34
Figure 6-13	Comparison of weighted mean transfer functions computed for the 1 Hz and 10 Hz scaled spectra for the Meloland profile, WUS conditions.	6-35

Figure 6-14	Mojave site rock spectra for 10^{-3} , 10^{-4} , and 10^{-5} annual frequencies.	6-36
Figure 6-15	Mojave site, M-R deaggregation of rock seismic hazard for 10^{-3} .	6-37
Figure 6-16	Mojave site, M-R deaggregation of rock seismic hazard for 10^{-4} .	6-38
Figure 6-17	Mojave site, M-R deaggregation of rock seismic hazard for 10^{-5} .	6-39
Figure 6-18	Mean amplification factor, soil/rock, from Approach 2A for 10^{-3} , 10^{-4} , and 10^{-5} rock input motions, Mojave site, Meloland profile.	6-40
Figure 6-19	Mojave site 10^{-4} UHS for Meloland profile from Approach 4 and Approaches 2A and 2A/3.	6-41
Figure 6-20	Mojave site $1E-5$ UHS for Meloland profile from Approach 4 (direct method) and Approaches 2A and 2A/3.	6-42
Figure 6-21	Comparison of soil spectra computed using Approaches 1, 2A, 2B, and 4 (Table 6-1) for Savannah profile, CEUS conditions.	6-43
Figure 6-22	Median and $\pm 1\sigma$ effective strains for Savannah profile using Approach 1: CEUS conditions.	6-44
Figure 6-23	Comparison of transfer functions computed for the scaled 1 Hz motion for Savannah profile, CEUS conditions.	6-45
Figure 6-24	Comparison of transfer functions computed for the scaled 10 Hz motion for Savannah profile, CEUS conditions.	6-46
Figure 6-25	Comparison of weighted mean transfer functions computed for the scaled 1 Hz and 10 Hz motions for Savannah profile, CEUS conditions.	6-47
Figure 6-26	Columbia site UHS for 1- and 2-corner models and mean, for 10^{-3} (lower 3 curves), 10^{-4} (middle 3 curves), and 10^{-5} (top 3 curves).	6-48
Figure 6-27a	Columbia site M-R deaggregation for 10^{-3} , 1-corner model, 10 Hz (top) and 1 Hz (bottom).	6-49
Figure 6-27b	Columbia site M-R deaggregation for 10^{-3} , 2-corner model, 10 Hz (top) and 1 Hz (bottom).	6-50
Figure 6-28a	Columbia site M-R deaggregation for 10^{-4} , 1-corner model, 10 Hz (top) and 1 Hz (bottom).	6-51
Figure 6-28b	Columbia site M-R deaggregation for 10^{-4} , 2-corner model, 10 Hz (top) and 1 Hz (bottom).	6-52
Figure 6-29a	Columbia site M-R deaggregation for 10^{-5} , 1-corner model, 10 Hz (top) and 1 Hz (bottom).	6-53
Figure 6-29b	Columbia site M-R deaggregation for 10^{-5} , 2-corner model, 10 Hz (top) and 1 Hz (bottom).	6-54
Figure 6-30	Mean amplification factor, soil/rock, from Approach 2A for 10^{-3} , 10^{-4} , and 10^{-5} rock input motions, Columbia site, Savannah profile.	6-55
Figure 6-31	Columbia site 10^{-4} UHS for Savannah profile from Approach 4 and Approaches 2A and 2A/3.	6-56
Figure 6-32	Columbia site 10^{-5} UHS for Savannah profile from Approach 4 and Approaches 2A and 2A/3.	6-57

Figure 6-33	Empirical WUS deep soil V/H ratios for 5% damped response spectra. Mean ratio is used to scale the horizontal soil design spectrum.	6-58
Figure 6-34	Elements used to develop CEUS deep soil V/H ratio. The solid line is used to scale the horizontal soil spectrum to produce the vertical soil spectrum.	6-59
Figure 7-1	Mojave site, 10^{-4} soil URS from Approach 4 and Approximate Approach 2A/3, and 10^{-4} UHS from Approach 4.	7-8
Figure 7-2	Hazard consistent soil spectrum along with 1 Hz and 10 Hz soil spectra, horizontal motion, Mojave site.	7-9
Figure 7-3	Mojave site 10^{-4} soil URS (Approximate Approach 2A/3) and 10 Hz and 1 Hz scaled spectra.	7-10
Figure 7-4	Horizontal and vertical URS for Mojave site, Meloland profile.	7-11
Figure 7-5	Columbia site, 10^{-4} soil URS from Approaches 4 and Approximate Approach 2A/3, and 10^{-4} UHS from Approach 4.	7-12
Figure 7-6	Hazard consistent soil spectrum along with 1 Hz and 10 Hz soil spectra, horizontal motions, Columbia site.	7-13
Figure 7-7	Columbia site 10^{-4} soil URS (Approximate Approach 2A/3) and 10 Hz and 1 Hz scaled spectra.	7-14
Figure 7-8	Horizontal and vertical URS for Columbia site, Savannah profile	7-15
Figure 8-1	Target spectrum, spectral match and spectral ratio, component H1, Mojave site, soil.	8-5
Figure 8-2	Target spectrum and spectral match on linear scale, component H1, Mojave site, soil.	8-6
Figure 8-3	Power spectral density for component H1, Mojave site, soil.	8-7
Figure 8-4	Time histories for component H1, Mojave site, soil.	8-8
Figure 8-5	Target spectrum, spectral match and spectral ratio, component H2, Mojave site, soil.	8-9
Figure 8-6	Target spectrum and spectral match on linear scale, component H2, Mojave site, soil.	8-10
Figure 8-7	Power spectral density for component H2, Mojave site, soil.	8-11
Figure 8-8	Time histories for component H2, Mojave site, soil.	8-12
Figure 8-9	Target spectrum, spectral match and spectral ratio, component V, Mojave site, soil.	8-13
Figure 8-10	Target spectrum and spectral match on linear scale, component V, Mojave site, soil.	8-14
Figure 8-11	Power spectral density for component V, Mojave site, soil.	8-15
Figure 8-12	Time histories for component V, Mojave site, soil.	8-16
Figure 8-13	Target spectrum, spectral match and spectral ratio, component H1, Columbia site, soil.	8-17

Figure 8-14	Target spectrum and spectral match on linear scale, component H1, Columbia site, soil.	8-18
Figure 8-15	Power spectral density for component H1, Columbia site, soil	8-19
Figure 8-16	Time histories for component H1, Columbia site, soil	8-20
Figure 8-17	Target spectrum, spectral match, and spectral ratio, component H2, Columbia site, soil	8-21
Figure 8-18	Target spectrum and spectral match on linear scale, component H2, Columbia site, soil	8-22
Figure 8-19	Power spectral density for component H2, Columbia site, soil	8-23
Figure 8-20	Time histories for component H2, Columbia site, soil	8-24
Figure 8-21	Target spectrum, spectral match, and spectral ratio, component V, Columbia site, soil	8-25
Figure 8-22	Target spectrum and spectral match on linear scale, component V, Columbia site, soil	8-26
Figure 8-23	Power spectral density for component V, Columbia site, soil	8-27
Figure 8-24	Time histories for component V, Columbia site, soil	8-28

List of Tables

Table	Title	Page No.
Table 2-1	Parameters for WUS Rock Outcrop Simulations	2-12
Table 2-2	Parameters for CEUS Rock Outcrop Simulations	2-13
Table 2-3	Southern California Crustal Model	2-14
Table 2-4	CEUS Crustal Model (EPRI, 1993 Midcontinent)	2-14
Table 2-5	WNA Rock Attenuation Coefficients	2-15
Table 2-6a	ENA Rock Attenuation Coefficients Single-corner Model	2-16
Table 2-6b	ENA Rock Attenuation Coefficients Double-corner Model	2-17
Table 2-7	WNA Soil Attenuation Coefficients Meloland Profile	2-18
Table 2-8a	ENA Soil Attenuation Coefficients Single-corner Model	2-19
Table 2-8b	ENA Soil Attenuation Coefficients Double-corner Model	2-20
Table 3-1	Seismic hazard curves, Mojave site, rock conditions	3-6
Table 3-2	Uniform hazard spectra, Mojave site, rock conditions	3-7
Table 3-3	Seismic hazard curves, Mojave site, Meloland profile	3-8
Table 3-4	Uniform hazard spectra, Mojave site, Meloland profile	3-9
Table 3-5	Seismic hazard curves, Columbia site, rock	3-10
Table 3-6	Uniform hazard spectra, Columbia site, rock	3-11
Table 3-7	Seismic hazard curves, Columbia site, Savannah River generic profile	3-12
Table 3-8	Uniform hazard spectra, Columbia site, Savannah River generic profile	3-13
Table 4-1	Slope parameters for rock hazard curves, Mojave site	4-5
Table 4-2	Spectra scaled to 10^{-4} UHS, Mojave site, rock conditions	4-6
Table 4-3	Spectra scaled to 10^{-4} URS, Mojave site, rock conditions	4-7
Table 4-4	Slope parameters for rock hazard curves, Columbia site	4-8
Table 4-5	Spectra scaled to 10^{-4} UHS, Columbia site, rock conditions	4-9
Table 4-6	Spectra scaled to 10^{-4} URS, Columbia site, rock conditions	4-10
Table 5-1a	WUS Time History Bins	5-4
Table 5-1b	CEUS Time History Bins	5-5
Table 5-2	WUS Statistical Shape Bins	5-6
Table 5-3	Magnitude and Distance Bins and Duration Criteria	5-9
Table 5-4	Rock Motion Durations (Annual Probability of Exceedence 10^{-4})	5-10
Table 6-1	Overview of Approaches for Developing Soil UHS	6-19
Table 6-2	Details of Approaches for Developing Soil UHS	6-19

Table 6-3	Magnitudes and Distances Used for Soil Amplification Calculations at Mojave Site	6-20
Table 6-4	Magnitudes and Distances Used for Soil Amplification Calculations at Columbia Site	6-21
Table 7-1	Scale factor for soil URS, Mojave site, Approximate Approach 2A/3	7-4
Table 7-2	Scale factor for soil URS, Mojave site, Approach 4	7-5
Table 7-3	Scale factors for soil URS, Columbia site, Approximate Approach 2A/3	7-6
Table 7-4	Scale factors for soil URS, Columbia site, Approach 4	7-7
Table 8-1	WUS Soil Motion Durations	8-3
Table 8-2	CEUS Soil Motion Durations	8-4

List of Terms

a,b	parameters of geometric attenuation
a_{rp}	rock amplitude for return period rp
$\frac{AF}{AF_{rp}}$	amplification factor, soil amplitude/rock amplitude
A_R	mean amplification factor for rock motion with return period rp
A^S	ratio of 10^{-5} spectral amplitude to 10^{-4} spectral amplitude
	ground motion amplitude on soil
b	Richter b-value, a parameter of the exponential magnitude distribution
$c_1, c_2, c_4, c_6, c_7, c_{10}$	coefficients used to define ground motion attenuation for the WUS and the CEUS (eq. 2-1)
CDMG	California Division of Mines and Geology
CEUS	central and eastern United States
d_1, d_2, d_3	parameters of soil amplification
D	source depth
f	frequency in Hz
f_c	intersection frequency
F_{SM}	minimum seismic margin factor
G/G_{max}	shear modulus behavior of non-linear soils
H	horizontal component of motion
H_D	annual hazard exceedence frequency
$H(a)$	hazard associated with amplitude a
H1	one horizontal component of motion
H2	second horizontal component of motion
HCLPF	high confidence of low probability of failure point on fragility curve
k, K_H	slope parameter of hazard curve
m'	mean magnitude from deaggregation
M, m	earthquake magnitude (moment magnitude scale)
m_L, m_M, m_H	low, medium, and high magnitudes used to discretize a magnitude distribution
M_{min}	minimum magnitude
M_x	maximum magnitude
P[]	probability of event []
P_F	annual frequency of component failure
PGA	peak ground acceleration
PGD	peak ground displacement

List of Terms (continued)

PGV	peak ground velocity
PSD	power spectral density
PSHA	probabilistic seismic hazard analysis
Q_0	frequency-independent component of Q model
$Q(f)$	deep crustal damping quality factor
R, r	source-to-site distance
rp	return period
R_p	probability ratio of hazard frequency to failure frequency
RS	response spectrum of artificial record
RVT	random vibration theory
SA	spectral acceleration
SF	scale factor for converting UHS to URS
TH	time history of motion
UHS	uniform hazard spectrum
URS	uniform reliability spectrum
USGS	United States Geological Survey
V	vertical component of motion
V_s	shear-wave velocity
WUS	western United States
z	soil amplitude
z_{rp}	soil amplitude for return period rp
Δt	time step for strong motion records
$\Delta\sigma$	earthquake stress drop
δ	logarithmic variation of soil amplification
ε	logarithmic deviation of rock motion for predicted value
η	frequency exponent of Q model
σ	standard deviation
ν_0	frequency (rate) of earthquake occurrence on a fault or in a source

1.0 INTRODUCTION

1.1 Background

This report documents the application of recommended procedures to derive seismic design ground motions at two sites. A companion report (McGuire et al., 2001) describes the recommended procedures in detail and documents the earthquake ground motion database that is recommended for development of ground motion time histories. These procedures are implemented in this report as a demonstration of how they work at two sites, one in the western US (WUS) and the other in the central and eastern US (CEUS).

The overall objectives of the project (McGuire et al., 2001) are to (1) update the standardized design spectra used in the evaluation of nuclear facilities to accommodate the effects of magnitude, site condition, distance, and tectonic environment, (2) assemble a database of strong motion records appropriate for use in design analyses, (3) recommend procedures and requirements for the scaling of ground motion records to be consistent with design spectra, (4) develop recommendations for conducting site response analyses to produce soil motions consistent with rock outcrop hazard results (hazard consistency), and (5) develop recommendations on how to derive seismic design spectra that provide risk consistency (uniform conservatism) across structural frequency. These objectives support the goal of developing uniform hazard spectra and design spectra that take into account the seismic threat at a site and the response of surficial rock and soil to that threat.

1.2 Summary of procedures for rock and soil sites

Figures 1-1 and 1-2 present flowcharts of the recommended procedures for developing design ground motions on rock and soil, respectively.

The procedure for rock sites (Figure 1-1) starts with a probabilistic seismic hazard analysis (PSHA) at a site using rock conditions. The hazard results at 10 and 1 Hz are then deaggregated at 10 Hz and 1 Hz, to define two deaggregation events (defined by M and R). We define two sets of spectra from these M and R values: one from PSHA, and a second from the spectra defined in this project. These spectra are used for a consistency check on the shape of the UHS.

We then derive a Uniform Reliability Spectrum (URS) from the UHS, and scale the spectra from attenuation equations to the URS at 10 and 1 Hz. For these scaled spectra, time histories are selected from the appropriate M - R bin. The time history spectra are compared to the scaled spectra, and are adjusted to match the target. For rock sites these adjusted time histories are used to conduct building dynamic analysis.

For soil sites (Figure 1-2) the first five steps are the same as for rock sites, except that the UHS is not scaled to a URS but is used as calculated to define the target spectra. The reason is that the scaling of UHS to URS depends on the slope of the hazard curve, and for soil sites, the slope must be determined by several soil analyses at different amplitudes. Following the adjustment of time histories to match the target spectra, dynamic soil analysis is performed with parameter uncertainty, using the scaled rock time histories as input. The relevant soil response is calculated as the average

spectrum (or spectra) over earthquake and soil uncertainties. The soil response calculations lead to a soil URS that accounts for the slope of the soil hazard curves. Next, time histories from soil sites are chosen based on the dominant M and R values (in a similar manner to rock time histories). The soil time histories are then adjusted to target soil spectra and are used as input to building dynamic analysis.

1.3 Purpose of current report

It is often observed in developing new procedures that “the devil is in the details,” and that is certainly true with the recommended methods for design ground motions. With that in mind, the current report’s purpose is to apply the recommended procedures at two sites and to confront and resolve any problems in application of the procedures. In this way, recommendations on how to handle the details can be made in a manner consistent with how the procedures were developed.

1.4 Organization of report

Section 2 of this report describes the two sites chosen for this implementation study, one in the WUS and one in the CEUS. For each site, design ground motions for both rock and soil conditions are developed. Soil properties for the WUS site are assumed to be those from Meloland, a deep soil site in the Imperial Valley of California. Soil properties for the CEUS site represent a generic Savannah River profile, a deep soil site typical of the CEUS. Section 2 also documents the attenuation equations developed for rock and soil conditions and used in the calculation of seismic hazard. Section 3 describes the seismic hazard at the two sites, including the UHS, and Section 4 documents the Uniform Reliability Spectra for rock conditions at each site, including the estimation of vertical motions. Artificial time histories for rock conditions are derived and explained in Section 5, which completes the derivation of design ground motions for rock conditions.

Results for soil conditions are addressed beginning in Section 6. This section illustrates the estimation of the Uniform Hazard Spectra (UHS) on soil for the two test sites, including the estimation of vertical motions. The UHS is modified into a URS for soil conditions in Section 7 for the two sites. Finally, Section 8 illustrates the generation of artificial time histories of motion for the soil sites, given the URS documented in Section 7. In addition, Section 9 summarizes all recommendations for deriving design spectra for both rock and soil sites.

Overall, the report illustrates the derivation of seismic ground motions for two sites, starting with a description of the seismic threat and proceeding to the estimation of UHS, URS, and artificial motions. For comparison purposes at soil sites, the direct approach is used, in which we derive an attenuation equation for site-specific soil conditions and calculate the seismic hazard directly using this attenuation equation. This allows demonstration of the accuracy of approximate procedures based on rock UHS. The methods based on rock UHS are less cumbersome and are more applicable to a site with multiple soil depths and profiles.

The implementation at soil sites illustrates that simplistic methods of estimating soil UHS are not accurate. Specifically, one cannot use a broad-banded rock UHS as input to a soil analysis that disregards uncertainties in soil properties, to estimate a soil UHS. Additionally, the slope of the soil

hazard curve must be determined, to estimate a soil URS from which design motions can be obtained.

REFERENCE

McGuire, R.K., W.J. Silva, C.J. Costantino (2001). "Technical Basis for Revision of Regulatory Guidance on Design Ground Motions: Hazard and Risk-consistent Ground Motion Spectra Guidelines," U.S. Nuclear Reg. Comm., Rept NUREG/CR-6728, October.

Overview of Design Ground Motion Procedure and Application to Rock Sites

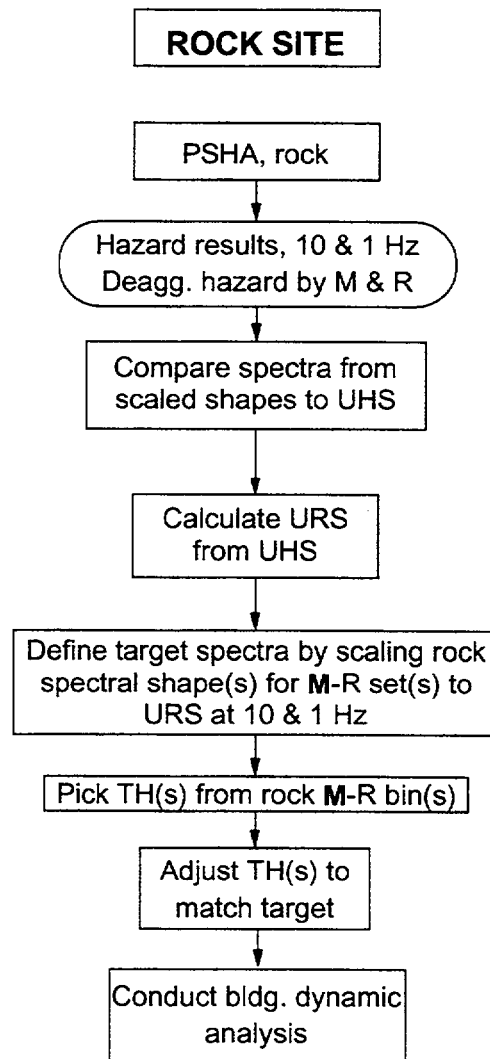


Figure 1-1. Flowchart of design ground motion procedure and application to rock sites.
TH = time history

Overview of Design Ground Motion Procedure and Application to Soil Sites

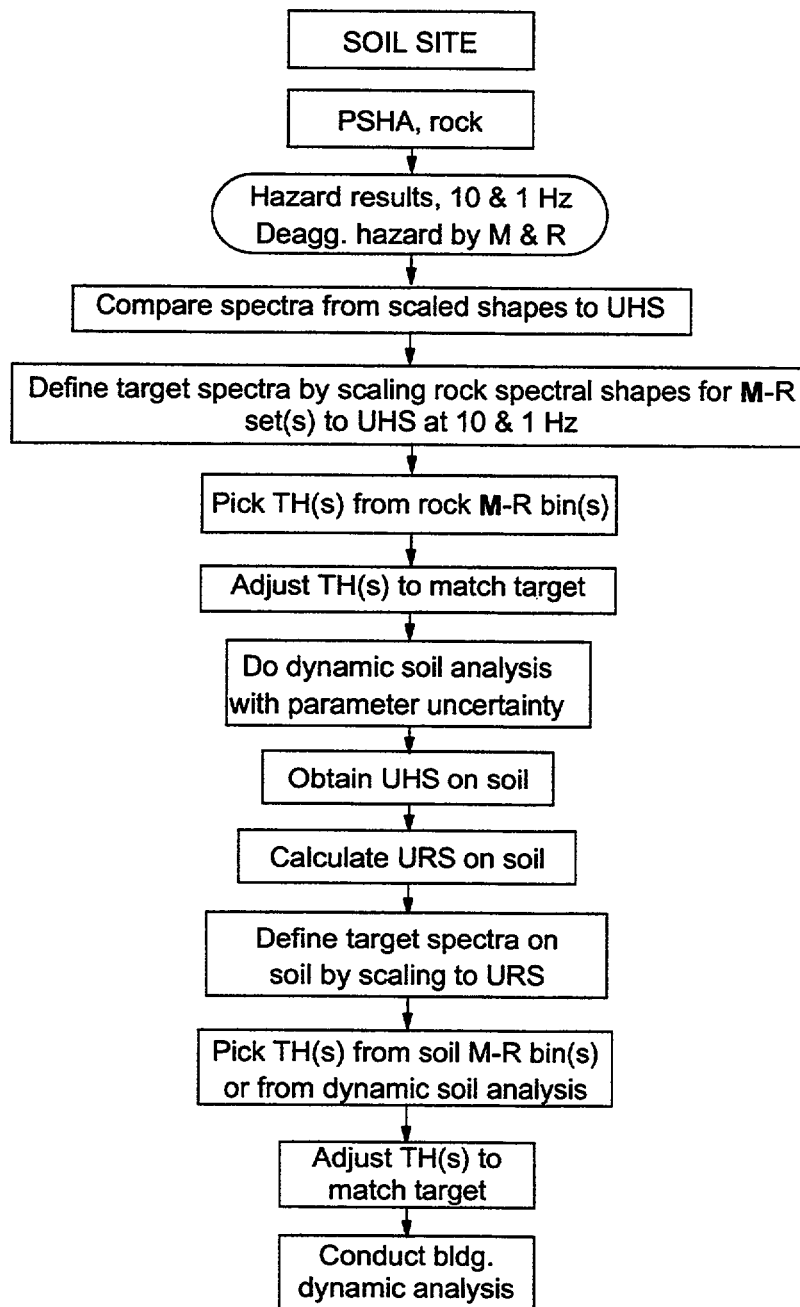


Figure 1-2. Flowchart of design ground motion procedure and application to soil sites.
TH = time history

2.0 TWO SITES CHOSEN FOR IMPLEMENTATION STUDY

2.1 Mojave site seismic environment

A site in the Mojave Desert in California was chosen as the example site for the WUS. This site, the nearby faults, and background seismicity points are illustrated in Figure 2-1. The site is located at 117.5° W, 34.6° N.

Seismicity parameters for the faults and background points were selected following the USGS/CDMG interpretation for California. In this interpretation, major earthquakes ($M > 6.5$) are ascribed to faults, and lower-level seismicity is ascribed to background points. The rate of activity of these background points, spaced at 0.1° longitude and latitude, is calculated based on a smoothed interpretation of historical seismicity. An exponential magnitude distribution with a $b=0.9$ is assigned to these points.

The seismicity model for the faults was taken to be that used by the USGS/CDMG in deriving seismic hazard maps for California. That is, each fault is assumed to produce a single characteristic magnitude with a specified annual frequency of occurrence. The characteristic magnitudes and associated frequencies were taken from the USGS/CDMG work.

Important sources that contribute to the hazard at the Mojave site are the San Andreas Fault and the background seismicity. All faults with a closest approach within 50 km of the site were modeled, for completeness.

2.2 Columbia site seismic environment

Columbia, South Carolina was the site chosen as the example site in the CEUS. Its seismic hazard is affected by a local source and by the Charleston earthquake zone, represented here by a fictitious fault (see Figure 2-2).

Seismicity parameters of the two earthquake sources affecting Columbia were as follows. The local source consisted of a box surrounding Columbia, 220 km on a side, with a minimum magnitude M_{\min} of 4.5 (corresponding to $m_{Lg} = 5$, which is standard for CEUS seismic hazard assessments) and a maximum magnitude M_x of 6.5. The seismicity in the local source was taken to be exponentially distributed and spatially homogeneous, with an annual rate of occurrence (v_o) of 1.13E-2 and a Richter b-value of 0.9. Both values came from the US Geological Survey assessment of seismicity for the national hazard maps, the rate being calculated as an average over the spatially-varying rate for the southeastern US derived by the USGS.

For the fictitious Charleston fault, earthquakes between $M=6.5$ and 7.8 were considered equally likely, that is a characteristic magnitude model was used between these two magnitudes with a rate of occurrence $v_o=1.54E-3$, meaning a mean recurrence period of 650 years. This is the rate used by the USGS for the Charleston fault, although they used a single characteristic magnitude of 7.3. We assumed a range of magnitudes for this test example to make the task of choosing a single (or a few) analysis earthquakes more challenging.

Both sources contribute to the hazard at Columbia as demonstrated in the next section. The background seismicity dominates the high-frequency motion, and the Charleston fault dominates the low-frequency motion.

2.3 Development of WUS and CEUS attenuation relations for generic rock and site specific soil sites

Regional- and site-(soil column) specific attenuation relations are required to evaluate the suitability of various approaches in developing soil spectra with hazard levels that are consistent with the control motions (rock outcrop UHS spectra). Soil-column-specific attenuation relations (median spectra and uncertainties) are used to generate uniform hazard spectra at the soil surface while regional-specific rock profiles are used to develop attenuation relations for outcropping rock. The soil uniform hazard spectra are then compared to soil motions generated by applying traditional equivalent-linear site response analyses using the rock UHS or scaled spectra as control motions. This process is applied to the California strong motion recording site Meloland assumed to be located in the WUS, and to a generic Savannah River profile assumed to be located in the CEUS (Sections 2.1 and 2.2). We developed appropriate attenuation relations for ground motions on these profiles, including parameter uncertainties and reflecting the appropriate crustal environments.

The process of developing site- and region-specific attenuation relations involves exercising the stochastic point source model (McGuire et al., 2001) for a suite of magnitudes and distances, and then regressing on the predicted ground motions. Site- and region-specific elements are introduced through the selection of appropriate model parameters and their uncertainties. Parametric uncertainty about the median ground motion regression (which includes regression uncertainty) is estimated through multiple ground motion estimates at each magnitude and distance based on random model parameters. This process results in a regression equation for median ground motions (5% damped response spectra) as a function of magnitude and distance, and in estimates of the uncertainty, both of which are required by probabilistic seismic hazard analyses. This process has been applied to a number of Department of Energy sites and to many other commercial projects and forms the basis for a number of CEUS attenuation relations. As a result, the process is both mature and stable, having undergone the scrutiny of widespread applications to engineered structures.

2.3.1 Point source model parameters

Dependent parameters for the point-source model include source depth (D), stress drop ($\Delta\sigma$), $Q(f)$ model (deep crustal damping), kappa (shallow crustal damping), a crustal model, and a shallow profile along with nonlinear dynamic material properties parameterized through G/G_{max} and hysteretic damping curves. Independent parameters are magnitude and distance, which were selected to cover the appropriate range in M and R in the hazard analyses. Three magnitudes were run for the WUS (M 5.5, 6.5, and 7.5) and four magnitudes were run for the CEUS (M 4.5, 5.5, 6.5 and 7.5) over the distance range of 1 to 400 km (Tables 2-1 and 2-2).

For the dependent parameters, base case (mean or median) values and their uncertainties are listed in Table 2-1 for the WUS and Table 2-2 for the CEUS. Source depth distributions are based on region specific seismicity while $Q(f)$ [$Q(f) = Q_0 f^n$] models are based on inversions using the point-

source model (Silva et al., 1997). WUS stress drops are based on inversions of the Abrahamson and Silva (1997) empirical attenuation relation and show a magnitude dependency (EPRI, 1993; Atkinson and Silva, 1997). CEUS stress drops (Table 2-2) are assumed to follow the same magnitude scaling as WUS. The M 5.5 stress drop was set to 160 bars to correspond to Atkinson's (1993) value, which is based on high frequency spectral levels from CEUS earthquakes. In her database of CEUS earthquakes the mean magnitude is about 5.5. Interestingly, these stress drop values result in an average (over magnitude) difference of about a factor of two between CEUS (122 bars, Table 2-2) and WUS (65 bars, Table 2-1), in agreement with Hanks and Johnston's (1992) analyses of intensity data.

Kappa values are based on ground motion observations at hard rock sites in the CEUS (EPRI, 1993; Silva and Darragh, 1995) and soft rock sites in the WUS. The WUS kappa value of 0.025 sec (Table 2-1) applied to the shallow portions of the Wald and Heaton (1994) crust (Table 2-3) and this value was adjusted to give a total kappa value of about 0.04 sec for WUS rock (EPRI, 1993; Silva and Darragh, 1995; Silva et al., 1997; Boore and Joyner, 1997). The remaining kappa, 0.015 sec, is contributed by the shallow geotechnical portion of the profile, which has a shear-wave velocity of about 250 m/sec at the surface and increases roughly linearly to 1 km/sec at a depth of 30m, where it merges with the Wald and Heaton (1994) crustal model (Figure 2-3). The shallow geotechnical profile was based on shear-wave velocity measurements at strong motion sites classified as rock (Silva et al., 1997). The profile is considered nonlinear to a depth of 30m (shear-wave velocity of 1 km/sec, Table 2-3) and the damping for the shallow kappa contribution is taken from the rock damping curve (Figure 2-5). The crustal model is shown in Figure 2-3 along with the generic CEUS hard rock crustal model (Table 2-4).

The kappa value for the CEUS rock site is 0.006 sec (Table 2-2), which is significantly lower than the 0.04 sec value for the WUS rock site and is based on analyses of recordings at hard rock CEUS sites (EPRI, 1993). The variability in kappa, $\sigma_{\ln k} = 0.30$, is assumed to be the same in WUS and CEUS and is the observed variability in kappa values at rock sites in northern California that recorded the M 6.9 1989 Loma Prieta earthquake (EPRI, 1993). While this uncertainty of 0.3 for kappa may seem low to characterize both epistemic (uncertainty in the median value) and aleatory (uncertainty about the median value) variability in a site specific kappa value, the point-source modeling uncertainty (Silva et al., 1997) already accommodates the effects of kappa variability. This is the case because a fixed kappa value of 0.03 sec was used to characterize the linear rock damping at all rock sites in the validation exercises. As a result, site specific departures of kappa from the assumed constant value of 0.03 sec increases model deviations from recorded motions, and this results in larger estimates of model uncertainty. This also applies to shallow rock profiles and soil profiles (to a depth of 300m [1,000 ft]), both of which were randomized in developing the attenuation relations. While it is possible that the total variability in the attenuation relations is overestimated due to this probable double counting, validations are sparse for the CEUS (and are nonexistent for deep soil sites), and are sparse for M larger than about 7.0 in the WUS. Thus the assessment and partitioning of appropriate variability is not an unambiguous issue, particularly in the CEUS, and the approach taken here is to follow prudent design practice and not underestimate uncertainty.

To illustrate the profile variability (which was assessed over the top 300m, to be consistent with the deepest soil profile also described in the next section), Figure 2-4 shows median and $\pm 1\sigma$ shear-wave velocity profiles for the WUS and CEUS rock sites (Figure 2-3). The profile randomization scheme was developed by Toro (1997) based on an analysis of variance of over 500 measured profiles. The analysis is appropriate for WUS rock (both hard and soft) and soil conditions (EPRI, 1993; Silva et al., 1997). For WUS rock the soft rock model was used. For the CEUS profile, the WUS hard rock model was used, since there are few, if any, shallow CEUS rock geotechnical profiles with which to develop statistics on variability.

The profile variability models for rock are based on an analysis of variance of all rock profiles in the database and therefore are appropriate for generic applications. Site-specific applications would likely result in a lower variability that reflects random (aleatory) variations over the dimensions of a foundation (or to a foundation dimension extending outside the footprint) as well as uncertainty in the mean or base case profile (epistemic). To develop these non-generic or small area models, multiple closely spaced holes are necessary. Such an analysis was undertaken at a deep soil site in the CEUS, and a footprint correlation model was developed by Silva et al., 1997. However, similar data are not currently available for rock sites. The use of a generic statistical model for both WUS and CEUS rock sites therefore may also contribute to an overestimate of the variability in the rock outcrop attenuation relations.

To accommodate potential nonlinear response in the shallow portion (top 30m) of the soft rock profile (Table 2-3, Figures 2-3 and 2-4), the modulus reduction and hysteretic damping curves shown in Figure 2-5 were used. These curves were developed by modeling the rock site motions produced by a recently developed empirical attenuation relation (Abrahamson and Silva, 1997). The generic WUS rock profile (Figure 2-3) was used in developing the G/G_{\max} and hysteretic damping curves and were validated by modeling the motions recorded from 17 earthquakes at about 150 soft rock sites (Silva et al., 1997).

As with the soil material strain dependencies (Section 2.3.2), the rock G/G_{\max} and hysteretic damping curves were randomized based on an analysis of variance of recent laboratory dynamic test results. To develop probabilistic models, multiple test results were analyzed and yielded standard errors (natural log) of 0.1 and 0.3 for G/G_{\max} and hysteretic damping respectively, these values calculated at cyclic shear strains of 0.03%. These variabilities are appropriate for within-class (cohesionless or cohesive soil) uncertainties and were used to generate suites of random curves that follow the shapes of the base case G/G_{\max} and hysteretic damping curves (EPRI, 1993). In the randomization process, upper and lower bounds of about $\pm 2\sigma$ were used to prohibit physically implausible excursions (EPRI, 1993).

To model nonlinear response at the WUS rock site and at the soil sites, RVT equivalent-linear analyses were performed (EPRI, 1993). This process, the use of the simple point-source model coupled to RVT equivalent-linear site response, has been validated at about 500 sites for 17 earthquakes (Silva et al., 1997). This validation showed that the process results in an acceptably accurate characterization of strong ground motions for engineering design.

2.3.2 Soil profiles and nonlinear properties

The Meloland measured shear-wave velocity profile was analyzed at the WUS site and the generic Savannah profile was analyzed at the CEUS site, for the application of soil-site procedures. The soil profile was either merged (WUS) or placed on top (CEUS) of the rock crustal models (the Wald and Heaton, 1994 model for the WUS site, see Table 2-3; the hard rock profile developed here for the CEUS, see Table 2-4). The Meloland profile in the Imperial Valley is actually located at a strong motion site that recorded the 1979 M 6.5 Imperial Valley earthquake. The site recorded a maximum horizontal peak acceleration of about 0.4g with about 0.6g reflecting the highest peak acceleration at similar sites in the region.

The base case shear-wave velocity profile for the Meloland site is shown in Figure 2-6a. Meloland is a “bottomless” soft profile (i.e. it has no sharp shear-wave contrast at the soil-bedrock interface) consisting mainly of silty clays and silty sands with clay zones having a plasticity index (PI) less than about 20 but with some medium hard (MH) clays (PI \approx 40). The soil profile was truncated at a depth of 300m. For the CEUS site, the generic Savannah River profile is shown in Figure 2-6b. The profile reaches a shear-wave velocity of 1 km/sec at a depth of about 220m, which was extended to 300m. It is placed on top of the CEUS crustal model (Table 2-4).

As with the shallow rock profile, the soil profiles (top 300m) were randomized using the same approach but with a soil statistical model appropriate for a footprint areal extent. The resulting median and $\pm 1 \sigma$ profiles are shown in Figures 2-7a and 2-7b for the Meloland and generic Savannah River profiles, respectively. Compared to the rock site generic variability shown in Figure 2-4, the footprint soil site variability is significantly smaller. Part of the difference is caused by deep soil sites showing significantly smaller absolute variability than rock sites (EPRI, 1993; Silva et al., 1997). The remaining difference is attributed to variability over a limited area or similar depositional environment vs. generic conditions.

In addition to velocity and layer thickness variability, depth to underlying bedrock material (1 km/sec for the WUS, Table 2-3; 2.83 km/sec for the CEUS, Table 2-4) was also varied $\pm 10\%$ (uniform distribution) to accommodate changes that may occur over a site.

For the Meloland soil site, a regional set of G/G_{max} and hysteretic damping curves were used. Validation exercises using the stochastic point-source model at Meloland for the Imperial Valley earthquake showed that the Vucetic and Dobry (1991) (depth-independent) curves for cohesive soils resulted in too much nonlinearity (overdamping). Additional validation exercises for the Los Angeles area (Peninsular Range) soils showed too much nonlinearity using the recently developed EPRI curves for cohesionless soils. As a result, revised sets of curves were developed for Imperial Valley and Peninsular Range soils by modeling exercises at a number of soil sites (Silva et al.,

1997). The Peninsular Range curves were assumed for the relatively stiff cohesionless soils of the Savannah River generic profile (Figure 2-8b). The revised sets of region-specific curves are shown in Figure 2-8a for Imperial Valley soils. For reference, G/G_{max} and hysteretic damping curve recommendations from SHAKE (1991) and Vucetic and Dobry (1991) are shown in Figures 2-9 and 2-10. The revised curves generally reflect more linear response, particularly at depth. This may result from the maximum depth over which the profiles are considered nonlinear, which was taken to be 150m based on extensive validation exercises. The SHAKE (1991) and Vucetic and Dobry (1991) curves are independent of depth and may not have been intended to be implemented over such large depth ranges.

For the soil profiles, material damping was fixed at the low-strain value from the corresponding damping curves and linear analyses assumed for depths exceeding 150m (500 ft). The kappa value for the rock material was kept at 0.006 sec for CEUS sites and 0.03 sec for the WUS sites. For the WUS soil sites, the total kappa values were about 0.04 sec, similar to WUS rock and consistent with observations at low strains (Silva et al., 1997). For the CEUS soil sites, this process resulted in total kappa values for the soil sites between about 0.01 and 0.02 sec, as the low strain kappa values for the soil columns was about 0.01 sec. This suggests the possibility of different spectral shapes for the same soil profile located in the WUS and CEUS, particularly at low loading levels and with similar limited depth to base rock material.

In general the evaluation of appropriate nonlinear properties (e.g. G/G_{max} and hysteretic damping curves) for a particular site requires considerable judgment.

The curves used in this study (and in McGuire et al., 2001) are generic. They are based on both high quality laboratory testing as well as validation and refinement through analyses of recorded motions at moderate-to-high loading conditions. Recently these soil models have become increasingly linear; that is, less modulus degradation and lower hysteretic damping occurs with induced cyclic shear strain. These characteristics have been required to better reproduce recorded motions through convolution studies.

In addition, detailed review of some proposed soil models developed from laboratory studies have indicated potential problems. These problems have tended to arise from disturbance effects induced in the sample from both sampling and sample preparation processes. Such disturbance effects can lead to soil models which are too nonlinear which can tend to seriously erode the proper characterization of soil site response and will tend to lead to underestimates of ground response at the soil surface.

As a result, site specific or alternate generic nonlinear dynamic material properties could depart significantly from the curves presented here (and in McGuire et al., 2001). It is therefore critical for these cases to ensure that where nonlinear dynamic material properties are deduced from laboratory studies, the sampling and testing programs are critically peer reviewed to ensure that the generated soil models are appropriate to properly characterize site response. If possible, the selected nonlinear properties should be validated at sites with appropriate soil conditions and with recordings reflecting moderate-to-high levels of loading conditions.

2.3.3 Form of attenuation relations

The functional form used in the regression analyses accommodates magnitude saturation, from a magnitude-dependent stress drop and potential nonlinear response, and accommodates a magnitude-dependent, far-field attenuation (Tables 2-1 and 2-2):

$$\ln(y) = c_1 + c_2 M + (c_6 + c_7 M) \cdot \ln(R + e^{c_4}) + c_{10} (M - 6)^2 \quad (2-1)$$

where R is taken as the closest distance to the surface projection of the rupture (Boore et al., 1997). In arriving at this functional form, about 15 variations were used in regression analyses. This particular form resulted in the best combination of low sigma, accommodation of significant trends with M and R , stability over oscillator frequency (smoothness in spectral shape), and simplicity. The fictitious depth term c_4 in equation (2-1) appears to be related to nonlinear site response, being nearly constant for CEUS rock (with a value near 3) and increasing strongly with frequency for WUS rock and for soil profiles (Tables 2-5 to 2-8). For the CEUS both single- and double-corner source models (McGuire et al., 2001) were run to replicate epistemic uncertainties in CEUS ground motion models and to show how this uncertainty should be treated.

To illustrate the nature of the fits to the simulations and the distribution about the regression lines, Figures 2-11 and 2-12 show peak accelerations for M 7.5, for WUS and CEUS (single- corner source model) rock conditions, respectively. The model captures the trends in the simulations for both rock site conditions. Variability about the regression for the CEUS (Figure 2-12) is larger than for the WUS (Figure 2-11) reflecting the larger variability in stress drop and source depth (Tables 2-1 and 2-2) and in the shallow profile (Figure 2-4). The increase in variability at large distance for both WUS and CEUS results from the effects of variability in $Q(f)$. The large variability at close distance for the CEUS results from the large range in source depth. The difference in the variability between WUS and CEUS rock site conditions for peak acceleration is significant, being about 0.65 for CEUS and 0.57 for WUS (this is presented below in connection with Figure 2-19).

2.3.4 Attenuation relations for WUS and CEUS rock site conditions

Attenuation curves of peak acceleration for M 5.5, 6.5, and 7.5 for WUS and CEUS rock site conditions predicted by the regression equations are shown in Figures 2-13 and 2-14 respectively. Figure 2-14a plots results for the single-corner source model, and Figure 2-14b plots results for the double-corner source model (Atkinson, 1993). Magnitude saturation at close distances is apparent in the decreasing jumps in peak acceleration as M increases. This results primarily from the magnitude dependent stress drops (Tables 2-1 and 2-2). CEUS peak accelerations for the single-corner source model exceed WUS by about 30% to 50% at large distance and are comparable at close distances, because of the greater CEUS source depths (Tables 2-1 and 2-2). For the double-corner CEUS relation, the implied stress drop associated with high frequency ($f \geq 1$ Hz) ground motion is independent of magnitude with a value of about 150 bars (for the CEUS crustal model, see Figure 2-3 and Table 2-4). This results in significantly higher large magnitude high frequency motions (McGuire et al., 2001) and no magnitude saturation (Figure 2-14b). The WUS relation is generally consistent with empirical relations for comparable site conditions. The CEUS single-corner relation shows lower peak accelerations than the Toro et al., 1997 and EPRI, 1993 relations,

particularly at large magnitude. This difference results from the assumption of decreasing stress drop with increasing magnitude in the CEUS (Table 2-2). Toro et al. (1997) used a constant stress drop of 120 bars, resulting in motions that may be too high at large magnitudes and somewhat low at small magnitudes. Tables 2-5 and 2-6 list the regression coefficients for rock sites, and includes the uncertainty due to parametric variability and regression fit. For the CEUS double-corner source model, variabilities were not available for the low and high frequency stress drops (corner frequencies), so the single-corner parametric variability was assumed to be appropriate for the double-corner model (for both the rock and soil attenuation relations).

To illustrate the resulting spectra for typical conditions, Figure 2-15 shows spectral accelerations (5% of critical damping) at a distance of 10 km for magnitudes 5.5, 6.5, and 7.5 for WUS rock site conditions. Since the regression coefficients (equation (2-1)) were not smoothed, some of the crustal resonances are present in the spectra. Shallow profile resonances (top 30m) were smoothed in the profile randomization, and the bump in the spectra near 0.5 Hz results from a deeper crustal velocity discontinuity (Figure 2-3). For M 6.5, Figure 2-16 shows median and $\pm 1\sigma$ estimates of the WUS rock site spectra. Interestingly, the logarithmic standard deviation displayed in Figure 2-16 decreases at low frequency, which is opposite the trend in most empirical regressions (Abrahamson and Shedlock, 1997). The modeling uncertainty, however, increases with decreasing frequency (Silva et al., 1997) and, when combined with the parametric uncertainty, reverses the trend exhibited in Figure 2-16. Apparently neither the model nor regressions on recorded motions capture deterministic elements in the WUS strong ground motions at low frequency. Interesting, the empirical relation of Campbell (1997), which includes depth to basement material ($V_s \approx 3$ km/sec), results in a largely frequency-independent sigma. Since sigma is computed over all site conditions, the depth dependency suggests that the effects of deep sedimentary basins may not be fully captured in other empirical relations that neglect the depth-to-basement term.

For the CEUS rock site conditions, Figures 2-17 and 2-18 show corresponding plots prepared using equation (2-1) and the coefficients of Table 2-6. The CEUS spectra show the expected shift in peak to higher frequencies (near 30 Hz) and the larger uncertainty in CEUS predictions (Figure 2-18). Figures 2-17a and 2-18a plot the single-corner source model and Figures 2-17b and 2-18b plot the double-corner source model. The difference in motions between the two source models depends on magnitude and frequency. The single-corner source model generally shows larger low-frequency motions and smaller high-frequency motions than the double-corner source model (McGuire et al., 2001), with the difference being greatest at large magnitude ($M \geq 6.5$). The large difference in ground motion variabilities between the single- and double-corner source models (Figures 2-18a and 2-18b) reflects the large contribution of stress drop variability. This variability is not included in the double-corner estimates of variability shown in Figure 2-18b, as explained previously.

Logarithmic uncertainties for WUS and CEUS rock site conditions are plotted in Figure 2-19. This sigma reflects variation about the median regression over the magnitude and distances listed in Tables 2-1 and 2-2. It includes only the variability in motions due to parametric variability and goodness-of-fit using the functional form shown in equation (2-1). The difference between CEUS and WUS sigmas ranges up to about 30% at high frequency (above 10 Hz), but the two uncertainties are comparable moderate and low frequency (less than 10 Hz). As previously mentioned, the uncertainty for CEUS rock site conditions exceeds that for WUS because of the larger variability in

stress drop and source depth (see Tables 2-1 and 2-2) and in the shallow (300m) part of the crustal models.

These rock outcrop attenuation relations are not intended for use exclusively of others. They are used in this study to provide consistency between the rock and site specific soil attenuation relations. For applications to WUS crustal conditions, if appropriate empirical relations are available their use is preferred. For the CEUS and regions of the WUS where ground motion data are sparse, provided the relations presented here reflect appropriate parameter values and produce motions consistent with available recordings, they may be used in hazard evaluations.

2.3.5 Attenuation relations for WUS and CEUS soil site conditions

This section illustrates the attenuation of peak acceleration and the magnitude dependence of response spectra at a distance of 10 km for the soil profiles Meloland (WUS) and Savannah River generic (CEUS). Results are presented for WUS and CEUS source and path conditions, as appropriate.

Figures 2-20 through 2-23 show the attenuation of peak acceleration and the magnitude dependence of spectra at 10 km for the two profiles and, in the case of the CEUS, for the single- and double-corner source models. Tables 2-7 and 2-8 list the coefficients.

For both the Meloland and Savannah River generic profiles, the magnitude saturation effect is very strong near 10 Hz (Figures 2-21 and 2-23). This trend indicates that the soils saturate in the levels of motion they can transmit as strains increase to high levels. This observation is not new, since soils are known to fail (lose shear strength) at very high loading levels and simply will not propagate waves with wave lengths shorter than about four times the width of the failed zone. However, early predictions on saturation of peak acceleration have routinely been exceeded, suggesting an incorrect assumption in the dynamic nonlinear properties of soils, particularly soft soils. The revised sets of G/G_{\max} and hysteretic damping curves, based on modeling high levels of motions (Figure 2-8), are believed to capture nonlinear properties reasonably well, meaning that the saturation displayed in spectral plots for the Meloland and Savannah River generic profiles are appropriate for these sites. These results should be confirmed with nonlinear (effective stress) analyses with properties adjusted so that the nonlinear soil models produce the same G/G_{\max} and hysteretic damping curves used in the equivalent-linear analyses. This is an important issue and may have significant impacts on probabilistic seismic hazard analyses since the uncertainties typically used in attenuation relations assume a lognormal distribution, symmetric about the median in log spectral ordinates. Saturation, on the other hand, suggests a negatively skewed distribution (in log space) with a lower probability of motions above the median $+1\sigma$ level than below the median -1σ level, with the difference increasing with increasing cyclic shear-strains. To partially accommodate this effect, a magnitude- and distant-dependent uncertainty was used in the hazard analyses (Section 4).

The uncertainties about the regression equations over all magnitudes and distances (Tables 2-7 and 2-8) are shown in Figure 2-24 for WUS and CEUS (single-corner source model) conditions. These uncertainties result from the regression analyses and reflect parametric variability as well as goodness-of-fit provided by the regression functional form (equation (2-1)). They average about 0.5

to 0.6 (natural log units), lower than the corresponding sigmas for rock site conditions (Figure 2-19). This reduction is likely due to the reduced profile variability, (compare Figures 2-4 and 2-7), and the effect of nonlinear response, which dampens variability in the input motions (EPRI, 1993). Modeling (or model) uncertainty has not been added to the parametric plus regression uncertainty for the hazard study because it would mask the differences in approaches to soil hazard being examined here (see Section 6). Total uncertainty, which includes the addition of modeling uncertainty, would be the appropriate uncertainty to use in applications to assess probabilistic hazard at a site for actual design purposes (EPRI, 1993).

REFERENCES

- Abrahamson, N.A and K.M. Shedlock (1997). "Overview." *Seis. Res. Let.*, 68(1), 9-23.
- Abrahamson, N.A. and W.J. Silva (1997). "Empirical response spectral attenuation relations for shallow crustal earthquakes." *Bull. Seism. Soc. Am.*, 68(1), 94-127.
- Atkinson, G.M and W.J. Silva (1997). "An empirical study of earthquake source spectra for California earthquakes." *Bull. Seism. Soc. Am.* 87(1), 97-113.
- Atkinson, G.M. (1993). "Source spectra for earthquakes in eastern North America." *Bull. Seism. Soc. Am.*, 83(6), 1778-1798.
- Boore, D.M, and W.B. Joyner (1997). "Site amplifications for generic rock sites." *Bull. Seism. Soc. Am.*, 87(2), 327-341.
- Boore, D.M., W.B. Joyner and T.E. Fumal (1997). "Equations for estimating horizontal response spectra and peak acceleration from Western North American earthquakes: A summary of recent work." *Seism. Res. Let.*, 68(1), 128-153.
- Campbell, K W. (1997). "Empirical near-source attenuation relationships for horizontal and vertical components of peak ground acceleration, peak ground velocity, and pseudo-absolute acceleration response spectra." *Bull. Seism. Soc. Am.*, 68(1), 154-176.
- Electric Power Research Institute (1993). "Guidelines for determining design basis ground motions." Electric Power Research Institute, Palo Alto, CA, EPRI TR-102293, vol. 1-5:
vol. 1: Methodology & guidelines for estimating earthquake ground motion in eastern NA
vol. 2: Appendices for ground motion estimation.
vol. 3: Appendices for field investigations.
vol. 4: Appendices for laboratory investigations.
vol. 5: Quantification of seismic source effects.
- Hanks, T.C. and A.C. Johnston (1992). "Common features of the excitation and propagation of strong ground motion for north American earthquakes." *Bull. Seism. Soc. Am.*, 82(1), 1-23.

- McGuire, R.K., W.J. Silva, C.J. Costantino (2001). "Technical Basis for Revision of Regulatory Guidance on Design Ground Motions: Hazard and Risk-consistent Ground Motion Spectra Guidelines," U.S. Nuclear Reg. Comm., Rept NUREG/CR-6728, October.
- SHAKE (1991). "*A computer program for conducting equivalent linear seismic response analyses of horizontally layered soil deposits.*" Sponsored by Structures Building and Fire Research Lab., Nat'l Institute of Standards and Technology, Gaithersburg, Maryland. Modifications by I. Idriss and J. Sun.
- Silva, W.J. and R. Darragh (1995). "Engineering characterization of earthquake strong ground motion recorded at rock sites." Electric Power Res. Inst., Palo Alto, CA, Rept TR-102261.
- Silva, W.J., N. Abrahamson, G. Toro, C. Costantino (1997). "Description and validation of the stochastic ground motion model." Report to Brookhaven National Laboratory, Associated Universities, Inc. Upton, New York, Contract 770573.
- Toro, G.R. (1997). "Probabilistic Models of Site Velocity Profiles for Generic and Site-Specific Ground Motion Amplification Studies." Published as an appendix in Silva et al (1997).
- Toro, G.R., N.A. Abrahamson, and J.F. Schneider (1997). "Model of strong ground motions from earthquakes in Central and Eastern North America: Best estimates and uncertainties." *Seism. Res. Let.*, 68(1), 41-57.
- Vucetic, M. and R. Dobry (1991). "Effects of Soil Plasticity on Cyclic Response," *Journal of Geotechnical Engineering, ASCE*, 117(1), 89-107.
- Wald, D.J. and T.H. Heaton (1994). "A dislocation model of the 1994 Northridge, California, earthquake determined from strong ground motions." *USGS, Open-File Rpt.* 94-278.

Table 2-1
Parameters for WUS Rock Outcrop Simulations

M 5.5, 6.5, 7.5
R(km) 1, 5, 10, 20, 50, 75, 100, 200, 400

30 simulations for each **M**, **R** pair = 810 runs

Randomly vary source depth, $\Delta\sigma$, kappa, Q_o , profile

Depth, $\sigma_{\ln D} = 0.6$, \bar{R} ($M > 5$) = 8 km; Source, California Seismicity

<u>M</u>	<u>Lower Bound (km)</u>	<u>\bar{R} (km)</u>	<u>Upper Bound (km)</u>
5.5	2	6	25
6.5	4	8	20
7.5	5	8	15

$\Delta\sigma$, $\sigma_{\ln \Delta\sigma} = 0.5$, Based on California earthquake inversions (Silva et al., 1997)

<u>M</u>	<u>$\Delta\sigma$ (bars)</u>	AVG. $\Delta\sigma$ (bars) = 65
5.5	85	Based on inversions of the Abrahamson and Silva (1997) relation.
6.5	64	
7.5	50	

$Q(f)$, $\bar{Q}_o = 275$, *Southern California inversions*; $\sigma_{\ln Q_o} = 0.4$, (Silva et al., 1997)

$\eta = 0.60$, *Southern California inversions*; $\sigma_\eta = 0$, (Silva et al., 1997)

Varying Q_o only is sufficient, since $\pm 1 \sigma$ covers range of Southern California inversions from 1 to 20 Hz

Kappa, $\bar{\kappa} = 0.025$ sec, $\sigma_{\ln \kappa} = 0.3$ (EPRI, 1997): linear zone ($V_s \geq 1$ km/sec)

Profile, California soft rock: GEOMATRIX A + B over Wald and Heaton (1994) Los Angeles Crust, randomize to 30m.

Geometrical attenuation $R^{-(a+bM)}$, $a = 1.0296$, $b = -0.0422$
 $R^{-(a+bM)/2}$, $R > 65$ km

Based on inversions of the Abrahamson and Silva (1997) relation

Table 2-2
Parameters for CEUS Rock Outcrop Simulations

M 5.5, 6.5, 7.5
D(km) 1, 5, 10, 20, 50, 75, 100, 200, 400

30 simulations for each **M, R** pair = 810 runs

Randomly vary source depth, $\Delta\sigma$, kappa, Q_o , η , profile

Depth, $\sigma_{\ln D} = 0.6$, \bar{R} (**M** > 5) = 10 km; Intraplate Seismicity (EPRI, 1993)

M	<u>Lower Bound (km)</u>	<u>\bar{R} (km)</u>	<u>Upper Bound (km)</u>
5.5	3	8	30
6.5	4	10	30
7.5	5	12	30

$\Delta\sigma$, $\sigma_{\ln \Delta\sigma} = 0.7$ (EPRI, 1993)

M	<u>$\Delta\sigma$ (bars)</u>	AVG. $\Delta\sigma$ (bars) = 122; Assumes M 5.5 = 160 bars (Atkinson, 1993) with magnitude scaling taken from WUS (Table 2-1)
5.5	160	
6.5	120	
7.5	95	

$Q(f)$, $\bar{Q}_o = 351$, *Saguenay earthquake inversions*; $\sigma_{\ln Q_o} = 0.4$, (Silva et al., 1997)

$\eta = 0.84$, *Saguenay earthquake inversions*; $\sigma_\eta = 0$, (Silva et al., 1997)

Varying Q_o only is sufficient, since $\pm 1 \sigma$ covers range of CEUS inversions from 1 to 20 Hz

Kappa, $\bar{\kappa} = 0.006 \text{ sec}$ $\sigma_{\ln \kappa} = 0.3$, (EPRI, 1993)

Profile, Midcontinent Crust (EPRI, 1993), randomize to 300m

Geometrical attenuation $R^{-(a+bM)}$, $a = 1.0296$, $b = -0.0422$
 $R^{-(a+bM)/2}$, $R > 100 \text{ km}$

Based on inversions of the Abrahamson and Silva (1997) relation

Table 2-3
Southern California Crustal Model*

<u>Thickness (km)</u>	<u>V_s (km/sec)</u>	<u>Density (cgs)</u>
0.0015239	0.24383	2.0
0.0024383	0.30478	2.0
0.0030479	0.42670	2.0
0.0042670	0.53337	2.0
0.0033526	0.63091	2.0
0.0042670	0.71624	2.0
0.0057909	0.83016	2.0
0.0067503	0.96617	2.0
0.5	1.0	2.1
1.5	2.0	2.3
2.5	3.2	2.5
23.0	3.6	2.6
5.0	3.9	2.9
	4.5	3.0

Table 2-4
CEUS Crustal Model (EPRI, 1993 Midcontinent)

<u>Thickness (km)</u>	<u>V_s (km/sec)</u>	<u>Density (cgs)</u>
1.0	2.830	2.52
11.0	3.520	2.71
28.0	3.750	2.78
	4.620	3.35

*Wald and Heaton (1994) begins at V_s = 1 km/sec

Table 2-5
WNA Rock Attenuation Coefficients

Freq. (Hz)	ξ_1	ξ_2	ξ_4	ξ_6	ξ_7	ξ_{10}	$\xi_{10,y}$
0.2	-15.07355	2.28803	2.0	-1.42561	.05553	-.49468	.4089
0.4	-8.68981	1.56496	2.3	-1.76499	.08297	-.39232	.4721
0.5	-6.47823	1.30499	2.4	-1.91086	.09548	-.33494	.4886
0.6	-5.24277	1.14930	2.4	-1.98227	.10227	-.29832	.4712
1.	-1.33267	.70799	2.6	-2.30588	.12753	-.18914	.5187
1.3	.67113	.48815	2.7	-2.53819	.14943	-.14236	.5515
2.	3.95381	.15441	2.9	-2.98310	.19125	-.08925	.5724
2.5	5.55431	.00724	3.0	-3.20781	.21165	-.07728	.6010
3.	6.94024	-.12170	3.1	-3.42954	.23215	-.07278	.6221
4.	8.66812	-.28522	3.2	-3.71372	.25897	-.06717	.6291
5.	10.06003	-.40764	3.3	-3.95717	.27975	-.06039	.6370
6.	11.31119	-.51492	3.4	-4.18633	.29881	-.05821	.6367
7.	11.71011	-.56219	3.4	-4.27015	.30773	-.05541	.6388
8.	12.92842	-.66660	3.5	-4.49380	.32645	-.05512	.6390
10.	13.35592	-.72377	3.5	-4.59214	.33758	.05646	.6397
12.	13.54154	-.75771	3.5	-4.64435	.34432	-.05630	.6392
14.	13.65565	-.78728	3.5	-4.68724	.35100	-.05612	.6385
16.	12.75687	-.73975	3.4	-4.55259	.34412	-.05604	.6356
18.	12.65100	-.74165	3.4	-4.54515	.34469	-.05561	.6304
20.	12.47129	-.73133	3.4	-4.52315	.34314	-.05542	.6258
25.	11.24288	-.64422	3.3	-4.33387	.32974	-.05790	.6144
31.	10.09850	-.55919	3.2	-4.14941	.31588	-.05892	.5997
40.	9.69120	-.52302	3.2	-4.08971	.31031	-.06071	.5830
50.	8.72729	-.44775	3.1	-3.92599	.29736	-.06070	.5720
100.	8.49206	-.42582	3.1	-3.88996	.29388	-.06198	.5647
PGA	8.51069	-.42805	3.1	-3.88703	.29324	-.06028	.5655
PGV	5.27143	.39517	2.5	-3.04853	.24741	-.17693	.4586

Table 2-6a
 ENA Rock Attenuation Coefficients
 Single-corner Model

<u>Freq. (Hz)*</u>	ϵ_1	ϵ_2	ϵ_4	ϵ_6	ϵ_7	ϵ_{10}	$\epsilon_{10,y}$
0.2	-16.20991	2.49652	2.7	-1.58692	.05635	-.59273	.4167
0.4	-10.16041	1.83310	2.8	-1.87976	.08425	-.57716	.5078
0.5	-7.71149	1.54904	2.9	-2.03483	.09820	-.51778	.5194
0.6	-6.08736	1.33854	2.9	-2.11588	.10738	-.46899	.5220
1.	-1.84398	.81332	3.0	-2.44002	.14132	-.35788	.5276
1.3	.00430	.57674	3.0	-2.57387	.15757	-.29458	.5581
2.	2.43166	.27522	3.0	-2.75419	.17904	-.19872	.5634
2.5	3.39155	.16089	3.0	-2.83133	.18792	-.18914	.5783
3.	4.07443	.07375	3.0	-2.89207	.19480	-.13571	.5751
4.	5.29015	-.02768	3.1	-3.05076	.20786	-.13790	.5827
5.	5.81926	-.07821	3.1	-3.09271	.21166	-.13063	.5888
6.	6.14411	-.10668	3.1	-3.12637	.21465	-.11957	.5922
7.	6.45032	-.13433	3.1	-3.15042	.21655	-.11286	.5961
8.	6.64633	-.14804	3.1	-3.17080	.21812	-.10990	.6050
10.	7.63608	-.22487	3.2	-3.30190	.22694	-.09675	.6225
12.	7.85878	-.23912	3.2	-3.32890	.22891	-.09573	.6381
14.	8.02846	-.25176	3.2	-3.35244	.23069	-.09286	.6482
16.	8.18918	-.26865	3.2	-3.37280	.23226	-.08486	.6519
18.	8.34875	-.28887	3.2	-3.39042	.23362	-.07596	.6540
20.	8.49056	-.30814	3.2	-3.40586	.23484	-.06867	.6573
25.	8.79761	-.35210	3.2	-3.43792	.23746	-.05063	.6725
31.	9.67978	-.42541	3.3	-3.58327	.24787	-.04007	.6929
40.	10.04410	-.46691	3.3	-3.62090	.25119	-.05504	.7326
50.	10.15048	-.49206	3.3	-3.63049	.25133	-.01202	.7451
100.	8.32910	-.39607	3.2	-3.49089	.24863	-.05120	.6534
PGA	8.01521	-.36903	3.2	-3.47207	.24770	-.06451	.6387
PGV	5.60957	.38668	2.9	-3.12813	.24391	-.23165	.5251

*SA and PGA in g, PGV in cm/sec

Table 2-6b
 ENA Rock Attenuation Coefficients
 Double-corner Model

Freq. (Hz)	ϵ_1	ϵ_2	ϵ_4	ϵ_6	ϵ_7	ϵ_{10}	$\epsilon_{in,y}$
0.2	-13.34719	1.91021	2.7	-1.54032	.04731	-.38333	.4167
0.4	-8.16519	1.39932	2.9	-1.90878	.08018	-.23634	.5078
0.5	-6.80414	1.26025	2.9	-2.02956	.09463	-.19126	.5194
0.6	-5.79540	1.15773	2.9	-2.13792	.10789	-.16775	.5220
1.	-3.11160	.92878	3.0	-2.52258	.15109	-.18150	.5276
1.3	-1.84321	.81242	3.0	-2.64729	.16641	-.18533	.5581
2.	.27394	.60149	3.0	-2.80138	.18464	-.16462	.5634
2.5	1.30196	.49268	3.0	-2.86111	.19122	-.17390	.5783
3.	2.09397	.39888	3.0	-2.90936	.19644	-.12758	.5751
4.	3.53297	.27523	3.1	-3.05421	.20762	-.13367	.5827
5.	4.22534	.20596	3.1	-3.08968	.21056	-.12575	.5888
6.	4.66605	.16347	3.1	-3.12045	.21318	-.11309	.5922
7.	5.05561	.12547	3.1	-3.14287	.21486	-.10489	.5961
8.	5.31133	.10435	3.1	-3.16283	.21639	-.10100	.6050
10.	6.37944	.01780	3.2	-3.29300	.22504	-.08614	.6225
12.	6.65330	-.00290	3.2	-3.32066	.22708	-.08411	.6381
14.	6.85694	-.01977	3.2	-3.34480	.22891	-.08055	.6482
16.	7.04234	-.03969	3.2	-3.36590	.23053	-.07201	.6519
18.	7.21940	-.06199	3.2	-3.38405	.23190	-.06274	.6540
20.	7.37512	-.08287	3.2	-3.40016	.23315	-.05512	.6573
25.	8.34631	-.17182	3.3	-3.54380	.24297	-.03648	.6725
31.	8.60903	-.20481	3.3	-3.57998	.24612	-.02542	.6929
40.	8.99110	-.24821	3.3	-3.61832	.24933	-.03957	.7326
50.	9.12345	-.27688	3.3	-3.63110	.24966	.00639	.7451
100.	7.30879	-.18410	3.2	-3.49724	.24682	-.02587	.6534
PGA	6.98479	-.15610	3.2	-3.47944	.24601	-.03936	.6387
PGV	6.51003	.23997	3.0	-3.18672	.23808	-.12459	.5251

Table 2-7
WNA Soil Attenuation Coefficients
Meloland Profile

<u>Freq. (Hz)</u>	ϵ_1	ϵ_2	ϵ_4	ϵ_6	ϵ_7	ϵ_{10}	σ_{ny}
0.2	-14.79366	2.34611	2.0	-1.30310	.03351	-.44903	.4236
0.4	-7.57877	1.53337	2.2	-1.77620	.08364	-.34626	.4590
0.5	-4.57983	1.14690	2.4	-2.09712	.12540	-.29611	.4363
0.6	-2.32052	.85779	2.6	-2.33181	.15398	-.25486	.4444
1.	2.97459	.22254	2.9	-2.91186	.22047	-.16493	.4599
1.3	4.26798	.08493	3.0	-3.06475	.22888	-.13884	.4820
2.	9.49210	-.53398	3.3	-3.87960	.32441	-.10106	.5015
2.5	12.71682	-.90851	3.5	-4.39494	.38377	-.08527	.5036
3.	14.75347	-1.15533	3.6	-4.71940	.42266	-.07488	.5118
4.	17.48099	-1.50130	3.7	-5.21022	.48190	-.06209	.5294
5.	21.00123	-1.89390	3.9	-5.79498	.54618	-.05371	.5312
6.	21.29599	-1.94596	3.9	-5.86151	.55512	-.05182	.5290
7.	21.28144	-1.95033	3.9	-5.86701	.55507	-.04711	.5283
8.	21.20482	-1.94677	3.9	-5.86410	.55400	-.04046	.5264
10.	20.91175	-1.91782	3.9	-5.82368	.54829	-.03502	.5262
12.	18.99363	-1.71934	3.8	-5.51762	.51534	-.03331	.5188
14.	18.37632	-1.63593	3.8	-5.42634	.50172	-.03389	.5134
16.	16.62846	-1.45166	3.7	-5.14314	.47122	-.03515	.5074
18.	15.09565	-1.29202	3.6	-4.89674	.44538	-.03854	.5016
20.	14.74662	-1.24279	3.6	-4.84672	.43782	-.04137	.4971
25.	13.20808	-1.07739	3.5	-4.60376	.41156	-.04580	.4887
31.	11.97449	-.95102	3.4	-4.40563	.39138	-.04922	.4837
40.	11.76486	-.92102	3.4	-4.37960	.38739	-.05189	.4800
50.	11.67101	-.90757	3.4	-4.36871	.38572	-.05332	.4782
100.	11.58735	-.89572	3.4	-4.35865	.38419	-.05448	.4769
PGA	10.79847	-.82842	3.3	-4.21658	.37161	-.05187	.4774
PGV	5.52514	.47014	2.6	-2.84291	.21580	-.15289	.4340

Table 2-8a
 ENA Soil Attenuation Coefficients
 Single-corner Model

<u>Freq. (Hz)</u>	\underline{c}_1	\underline{c}_2	\underline{c}_4	\underline{c}_6	\underline{c}_7	\underline{c}_{10}	$\underline{\sigma}_{ln,y}$
0.20	-13.46820	2.17130	2.7	-1.67419	.05839	-.33475	.4575
0.40	-9.89286	1.95352	2.7	-1.68767	.04480	-.45054	.5365
0.50	-8.04432	1.77492	2.7	-1.80349	.05968	-.46856	.5399
0.60	-5.32191	1.43172	2.8	-2.11656	.10825	-.47163	.5168
1.00	-2.80428	1.11337	2.9	-2.29798	.12009	-.40219	.5625
1.30	00.19768	.74467	3.0	-2.60912	.16359	-.35786	.5643
2.00	2.142000	.46727	3.0	-2.78470	.18589	-.28980	.5789
2.50	5.108680	.06749	3.2	-3.17610	.24345	-.25946	.5536
3.00	5.730590	.00237	3.2	-3.27162	.24991	-.23697	.5941
4.00	7.202390	-.23007	3.2	-3.45317	.28163	-.20367	.5918
5.00	9.068490	-.49378	3.3	-3.73124	.32256	-.18881	.5735
6.00	10.51087	-.68183	3.4	-3.96146	.35227	-.17356	.5743
7.00	11.02282	-.77051	3.4	-4.02002	.36418	-.16911	.5702
8.00	12.30466	-.92417	3.5	-4.22802	.38865	-.16348	.5801
10.00	13.04199	-1.06225	3.5	-4.33863	.41066	-.15138	.5809
12.00	14.36650	-1.22462	3.6	-4.55542	.43635	-.14297	.5730
14.00	14.60592	-1.27242	3.6	-4.59270	.44329	-.13784	.5720
16.00	15.81457	-1.40855	3.7	-4.79204	.46486	-.13234	.5723
18.00	15.83779	-1.41944	3.7	-4.79439	.46539	-.12877	.5766
20.00	15.79335	-1.41821	3.7	-4.79295	.46497	-.12554	.5776
25.00	15.60403	-1.39813	3.7	-4.76756	.46027	-.11831	.5866
31.00	15.20687	-1.33830	3.7	-4.72216	.45059	-.11664	.5904
40.00	13.62076	-1.15201	3.6	-4.48030	.41966	-.11532	.5877
50.00	13.03486	-1.05485	3.6	-4.41445	.40545	-.11948	.5836
100.0	10.12073	-.69989	3.4	-4.00714	.35364	-.13737	.5696
PGA	10.00517	-.67940	3.4	-3.99504	.35058	-.13799	.5706
PGV	5.970300	.48921	2.9	-2.99431	.22119	-.24318	.5551

Table 2-8b
 ENA Soil Attenuation Coefficients
 Double-corner Model

<u>Freq. (Hz)</u>	\underline{c}_1	\underline{c}_2	\underline{c}_4	\underline{c}_6	\underline{c}_7	\underline{c}_{10}	\underline{c}_{iny}
0.2	-11.68753	1.75687	2.7	-1.67563	.05803	-.31947	.4575
0.4	-8.53757	1.61478	2.8	-1.76645	.05208	-.28536	.5365
0.5	-7.44955	1.56539	2.8	-1.81054	.05412	-.25663	.5399
0.6	-5.32462	1.33981	2.9	-2.07425	.09220	-.24186	.5168
1.	-3.44962	1.12158	2.9	-2.27562	.11334	-.18710	.5625
1.3	-1.00704	.88393	3.0	-2.53903	.14750	-.18048	.5643
2.	0.888050	.65634	3.0	-2.72212	.17064	-.17311	.5789
2.5	3.370070	.31278	3.1	-3.02331	.22163	-.18018	.5536
3.	3.837880	.29120	3.1	-3.06863	.21864	-.17275	.5941
4.	6.102460	-.00163	3.2	-3.36031	.25959	-.16476	.5918
5.	8.148440	-.28331	3.3	-3.64975	.30241	-.16424	.5735
6.	9.054380	-.43569	3.3	-3.77384	.32498	-.15811	.5743
7.	10.38986	-.59729	3.4	-3.96016	.34793	-.15892	.5702
8.	11.01992	-.70282	3.4	-4.05205	.36406	-.15818	.5801
10.	12.82658	-.95201	3.5	-4.33487	.40417	-.15305	.5809
12.	14.43801	-1.16336	3.6	-4.59703	.43820	-.14936	.5730
14.	14.90221	-1.25136	3.6	-4.67086	.45208	-.14746	.5720
16.	16.30052	-1.42129	3.7	-4.90004	.47925	-.14443	.5723
18.	16.43841	-1.45524	3.7	-4.92024	.48350	-.14092	.5766
20.	16.47880	-1.47228	3.7	-4.93247	.48607	-.13676	.5776
25.	17.54555	-1.58996	3.8	-5.11309	.50360	-.12705	.5866
31.	17.17517	-1.54047	3.8	-5.06993	.49480	-.12083	.5904
40.	16.49071	-1.43517	3.8	-4.97584	.47601	-.11247	.5877
50.	14.67235	-1.21557	3.7	-4.70503	.44066	-.11021	.5836
100.	11.31446	-.79933	3.5	-4.23331	.37818	-.11554	.5696
PGA	10.34848	-.70192	3.4	-4.07802	.36229	-.11577	.5706
PGV	7.184400	.25885	3.0	-3.17174	.24092	-.12760	.5551

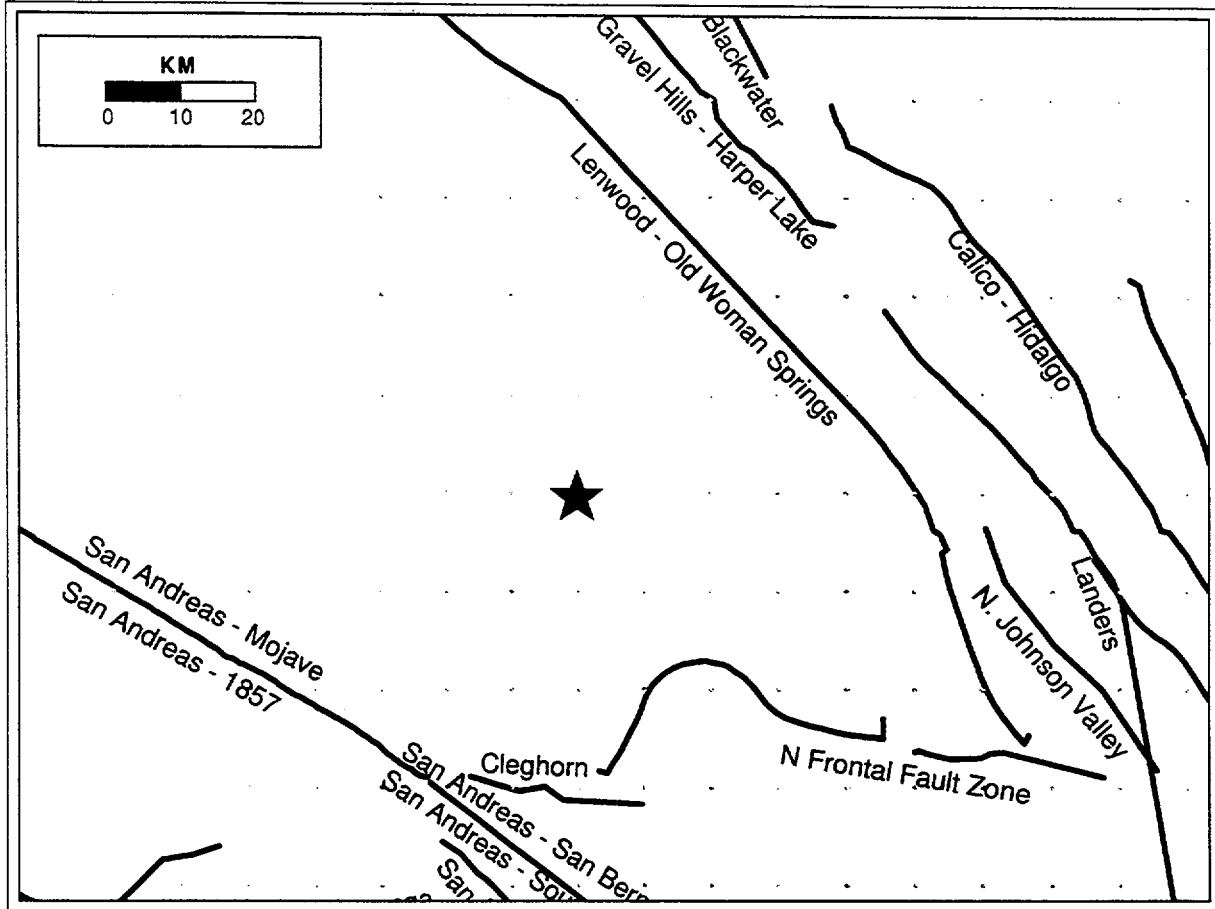


Figure 2-1. Seismic sources used for WUS example site (Mojave Desert), including nearby faults and background seismicity points.

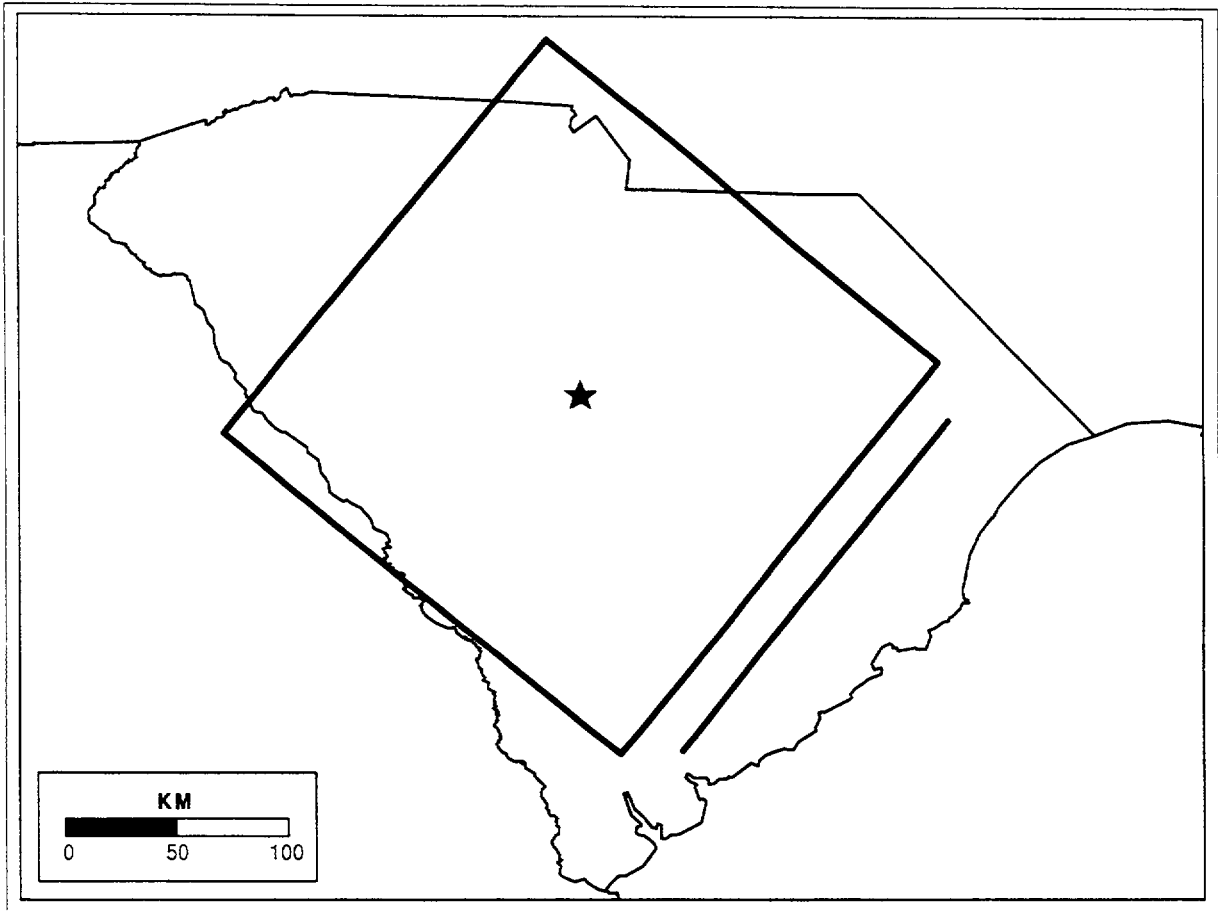
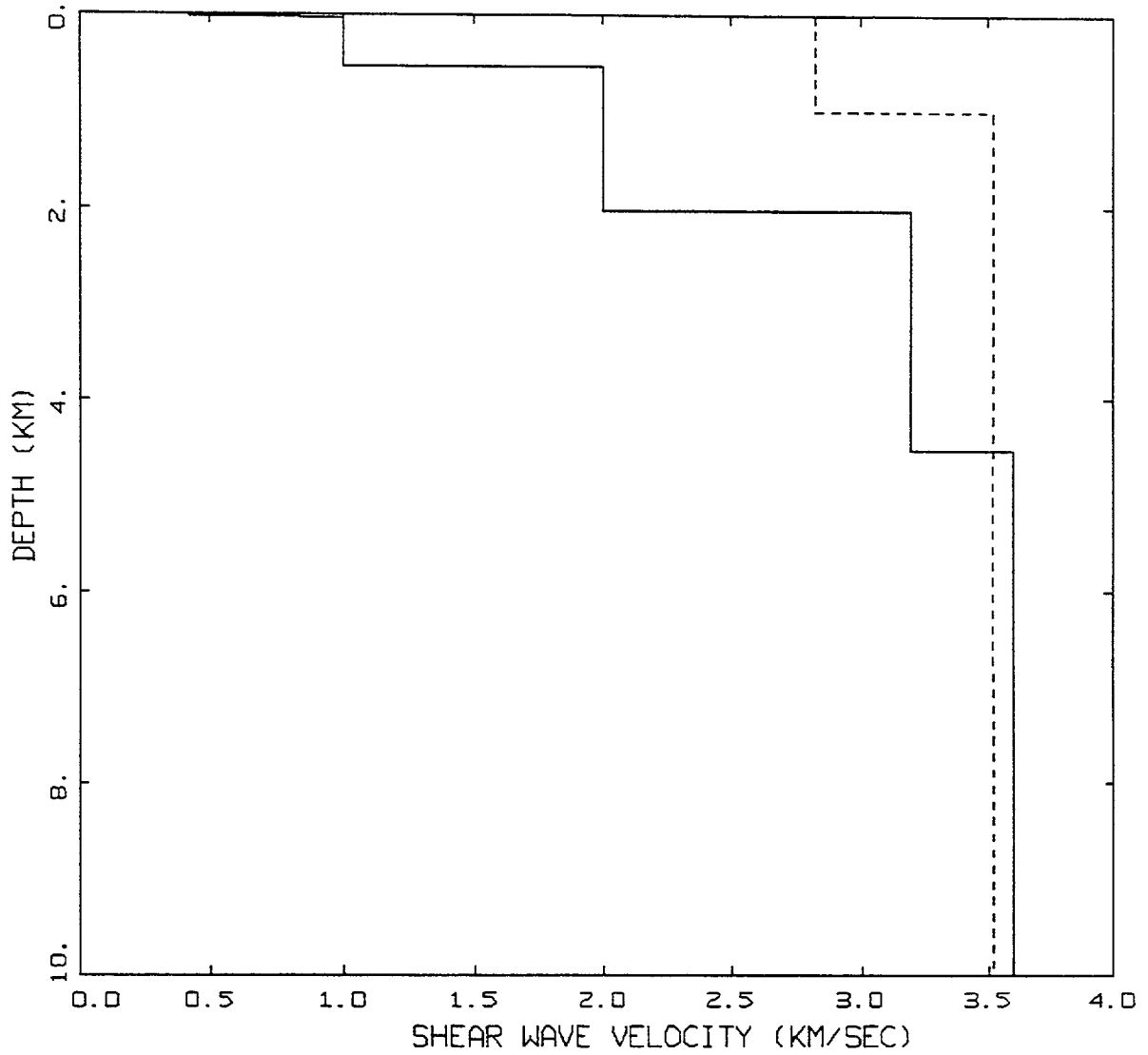


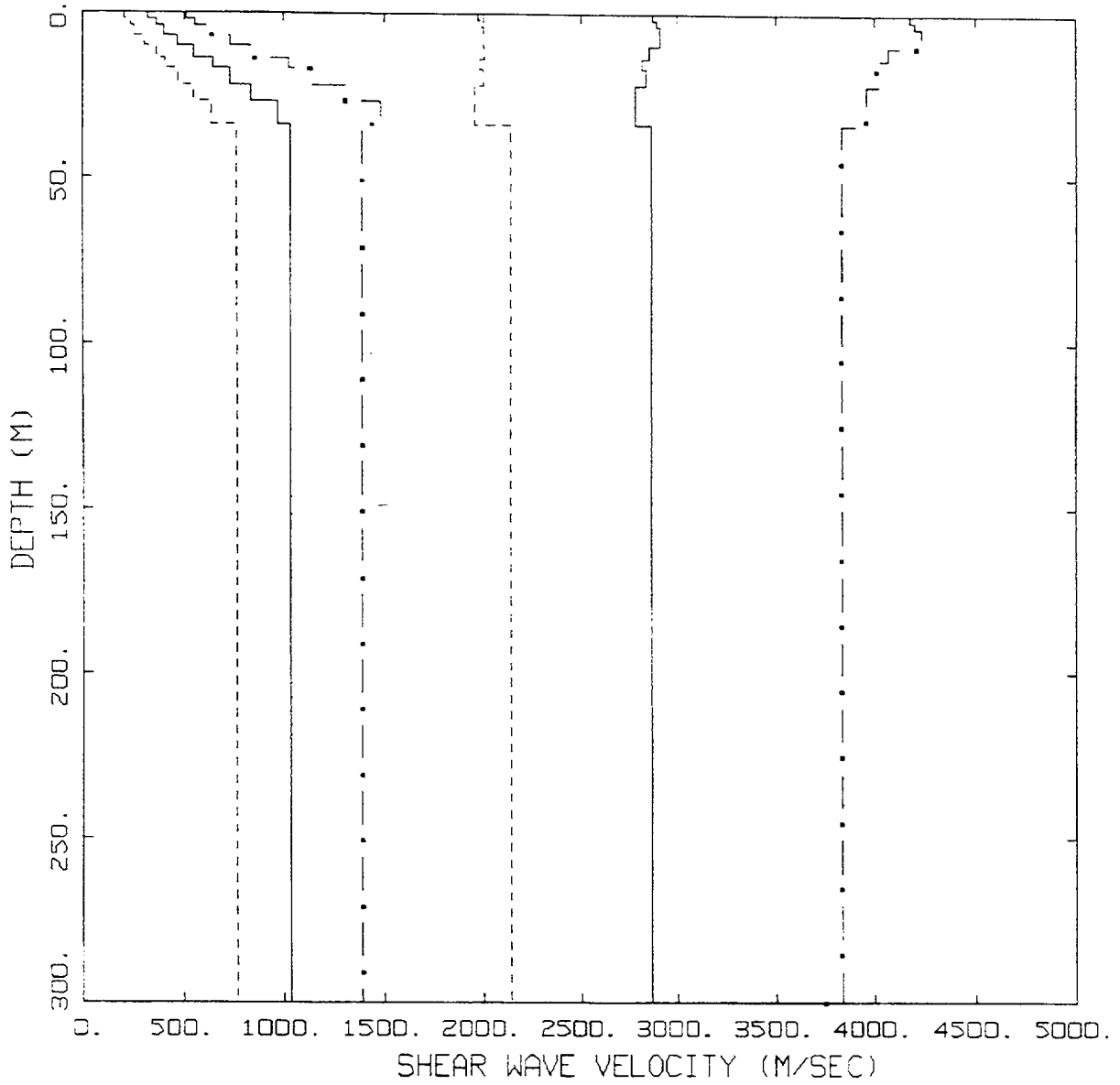
Figure 2-2. Seismic sources used for CEUS example site (Charleston, South Carolina).



GENERIC WUS AND CEUS
CRUSTAL MODELS

LEGEND
 _____ WUS
 - - - - - CEUS

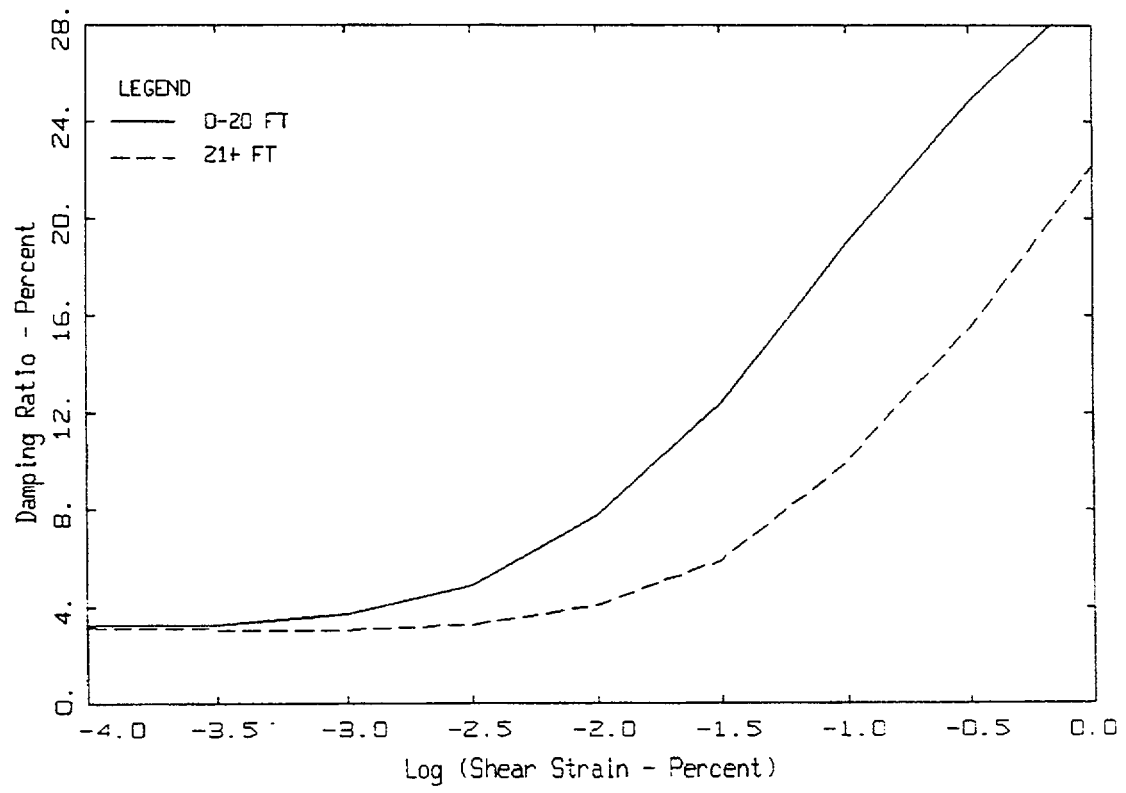
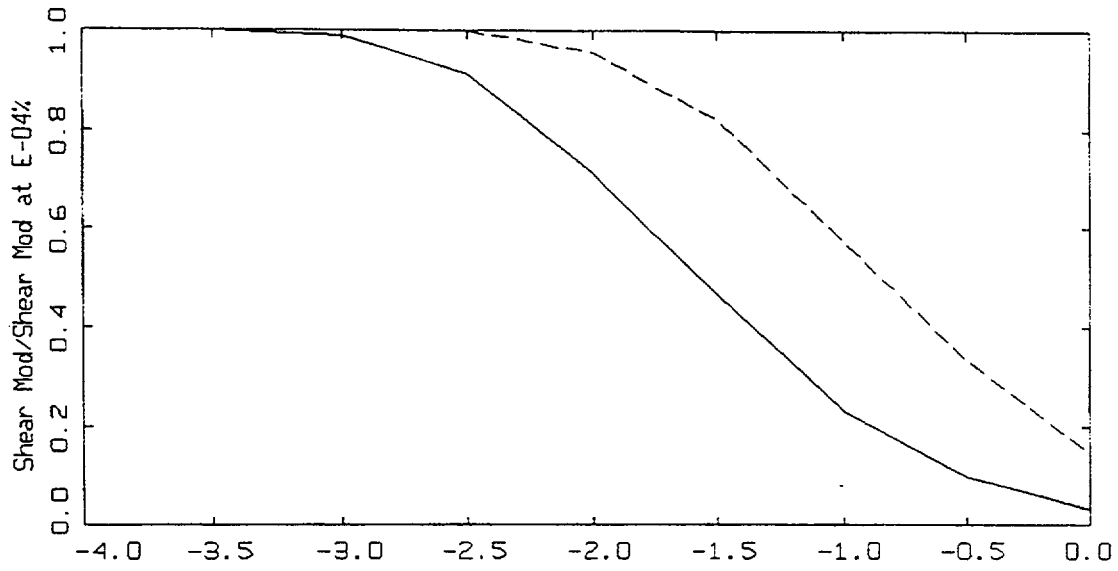
Figure 2-3. Comparison of generic shear-wave velocity profiles for WUS (Los Angeles) and CEUS crustal conditions.



SHALLOW CRUSTAL MODEL
 WUS AND CEUS ROCK

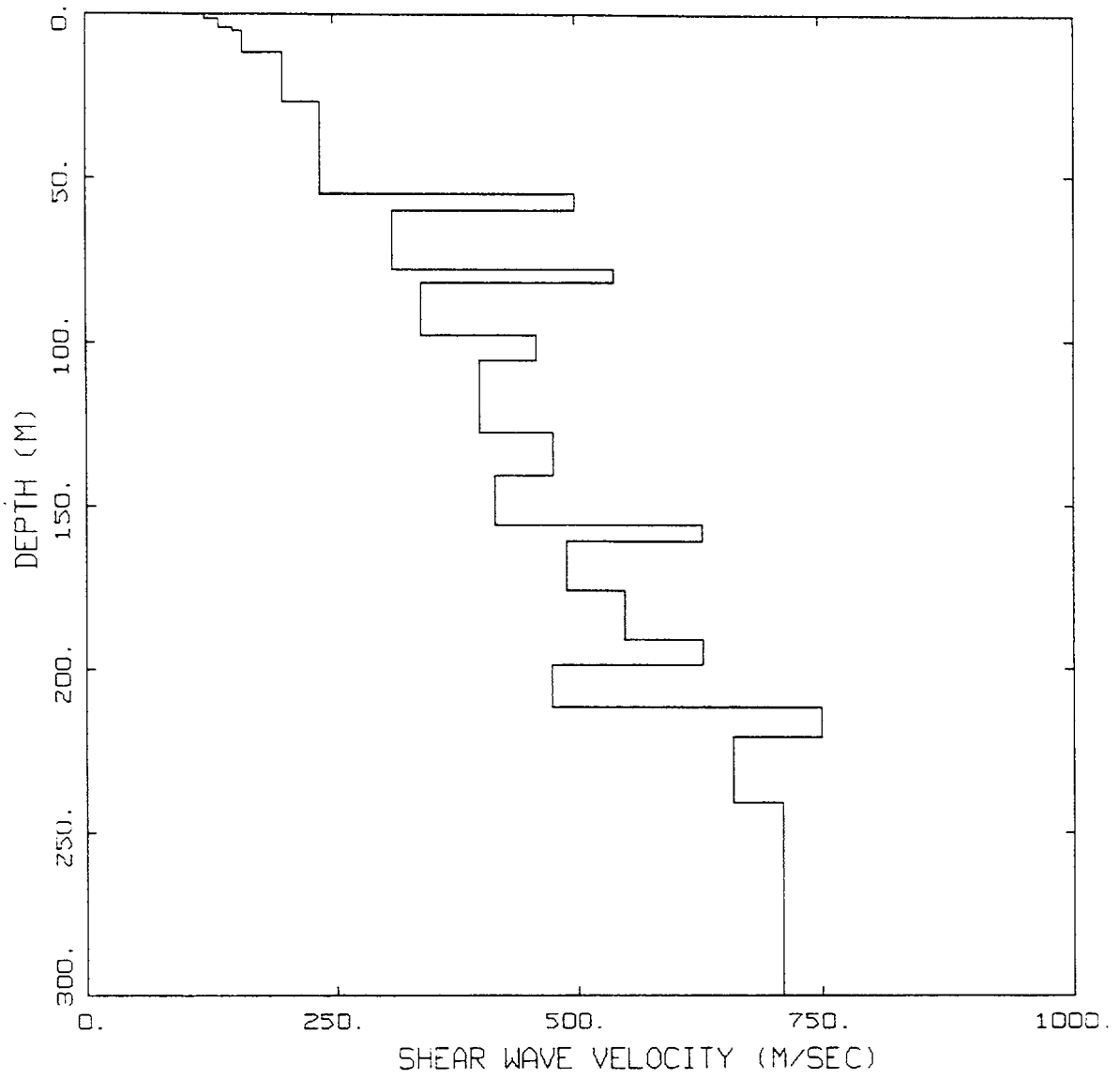
- LEGEND
- WUS ROCK, MEDIAN
 - . - . WUS ROCK, +1 SIGMA
 - - - - WUS ROCK, -1 SIGMA
 - CEUS ROCK, MEDIAN
 - . - . CEUS ROCK, +1 SIGMA
 - - - - CEUS ROCK, -1 SIGMA

Figure 2-4. Variations in base case shallow crustal velocities. Solid lines are median estimates from a suite of randomly generated profiles (30) using base-case profiles (Figure 2-3) as input. Ranges reflect $\pm 1 \sigma$ estimates.



MODULUS REDUCTION AND DAMPING CURVES FOR ROCK

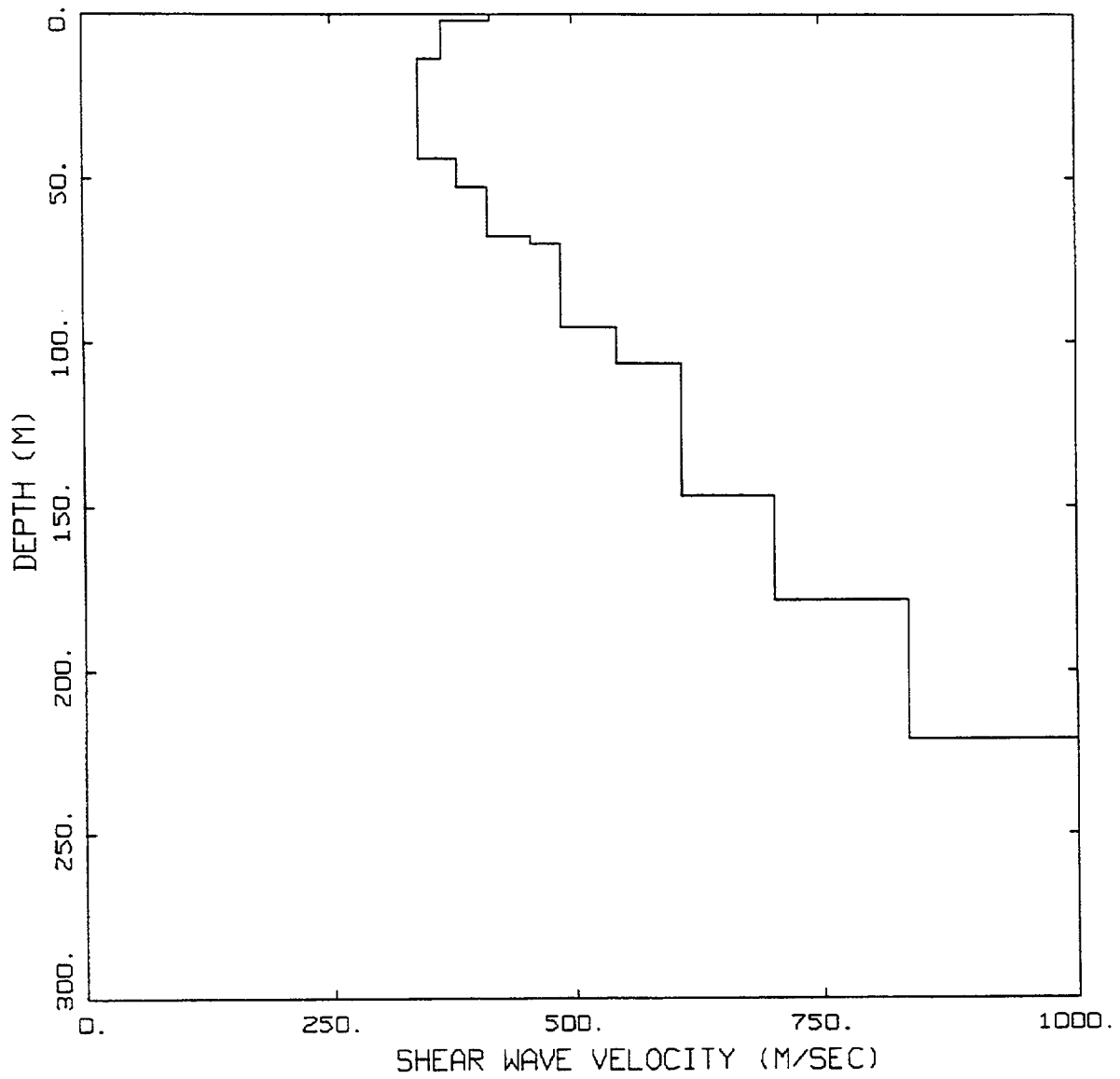
Figure 2-5. Generic G/G_{max} and hysteretic damping curves for soft rock.



MELOLAND PROFILE

— LEGEND
 — MELOLAND

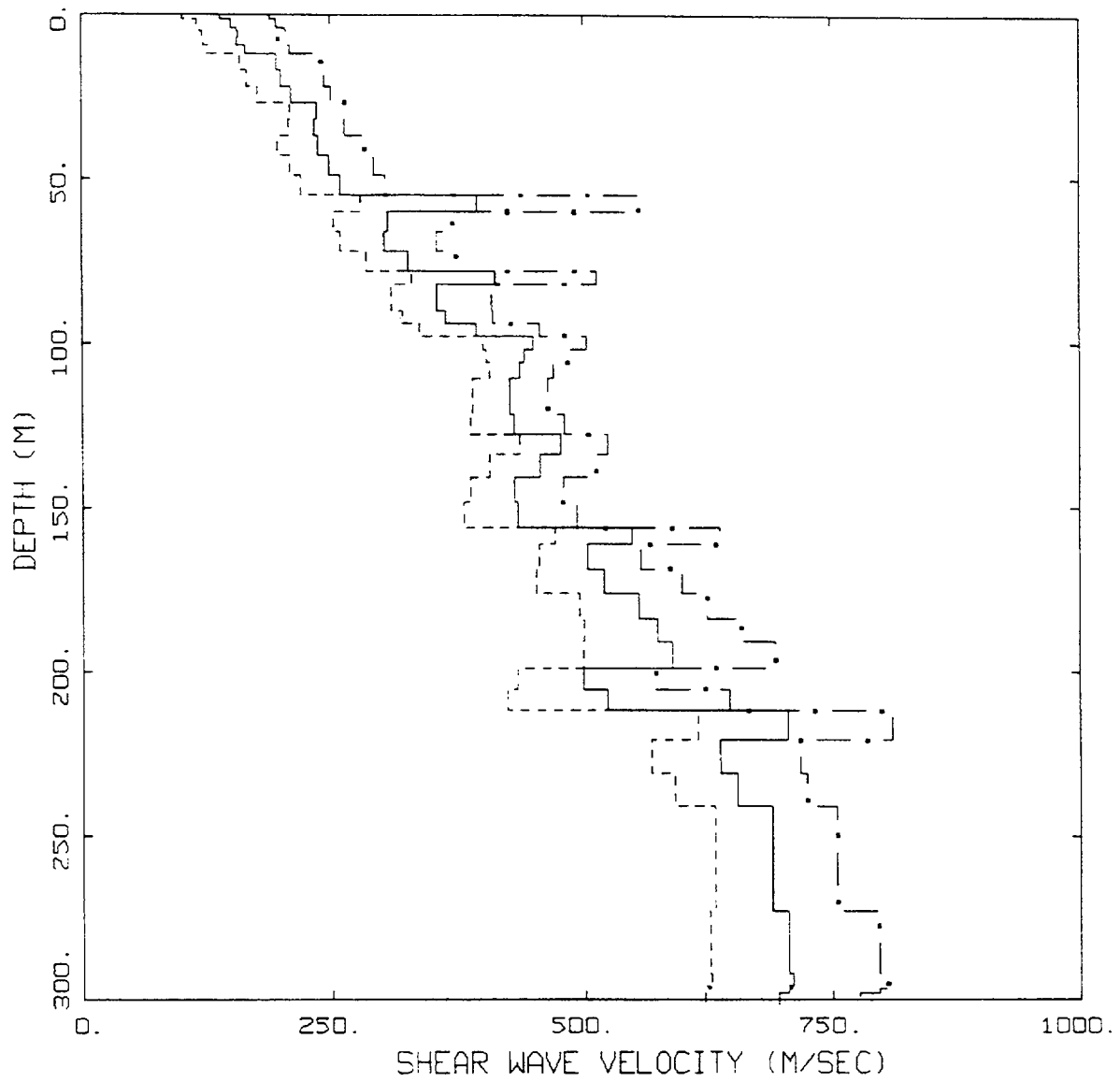
Figure 2-6a. Base case WUS soil shear-wave velocity profile based on suspension logging measurements. Placed on top of Wald and Heaton (1994) crustal model (Table 2-3).



SAVANNAH RIVER GENERIC PROFILE

_____ LEGEND
 SAVANNAH RIVER

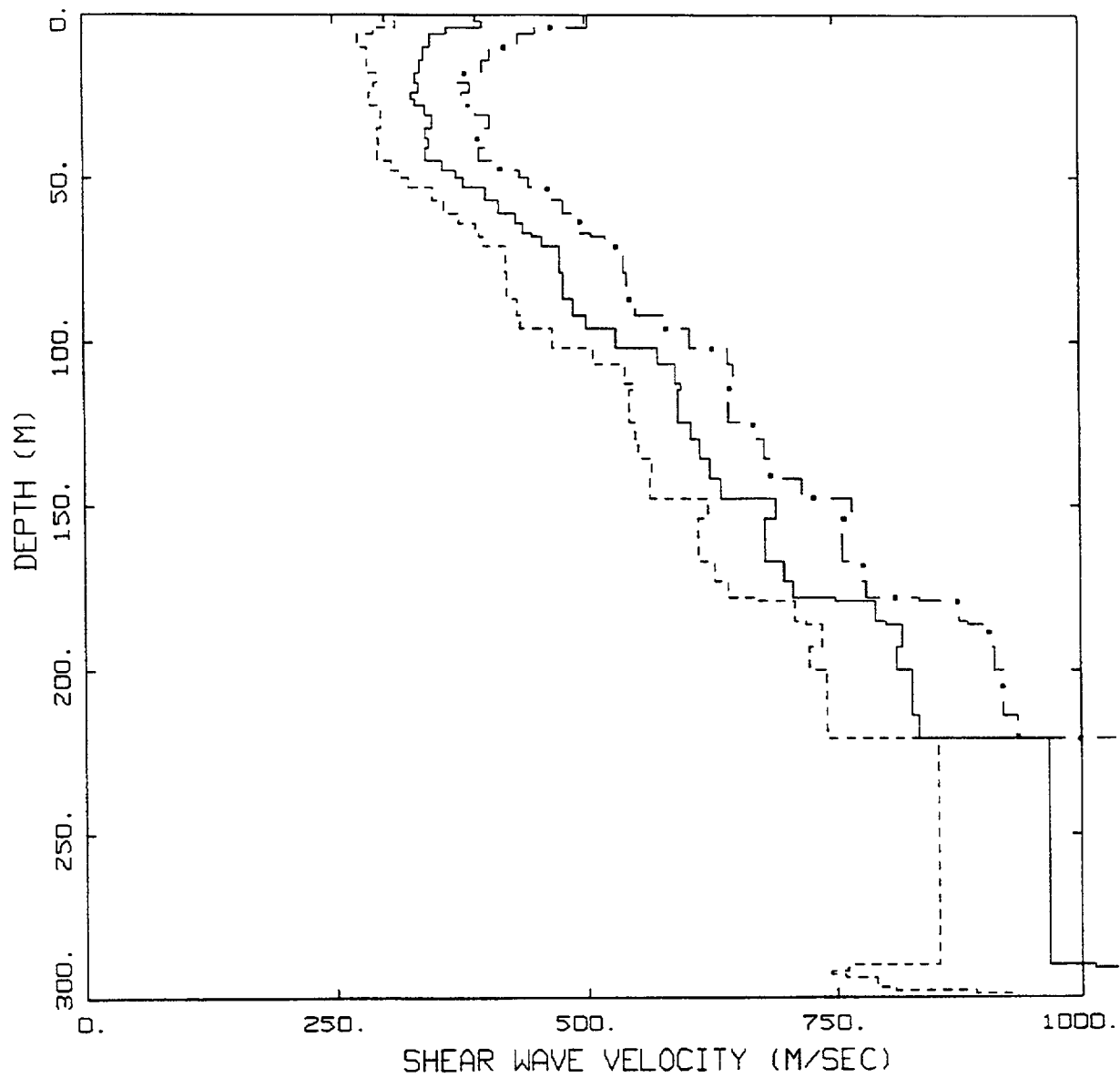
Figure 2-6b. Base case CEUS soil shear-wave velocity profile based on suspension logging measurements. Placed on top of CEUS crustal model (Table 2-3).



MELOLAND PROFILE

- LEGEND
- 16TH PERCENTILE
 - 50TH PERCENTILE
 - · - · 84TH PERCENTILE

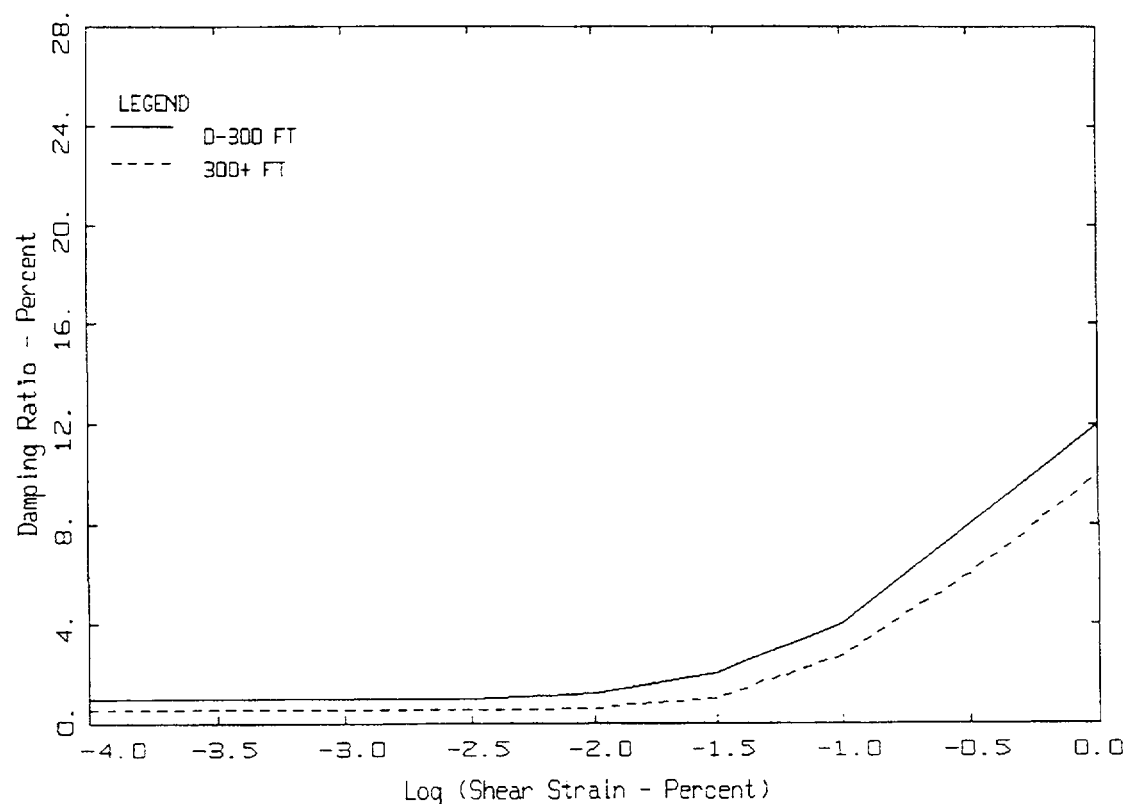
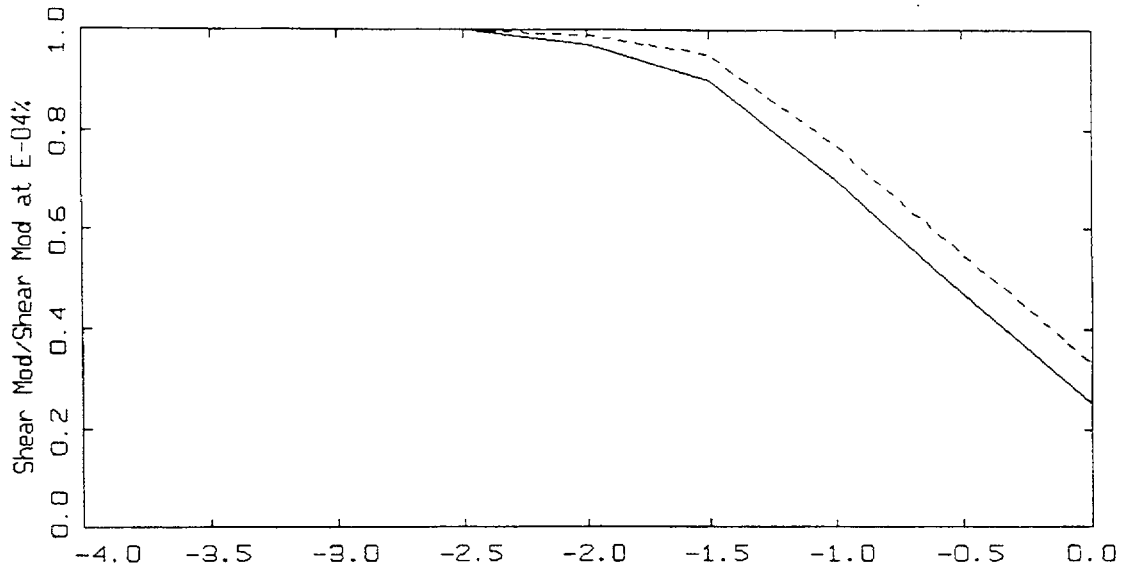
Figure 2-7a. Variation in base case shear-wave velocity for the Meloland profile (Figure 2-6a) based on thirty realizations. Median estimate along with $\pm \sigma$ values.



SAVANNAH RIVER GENERIC PROFILE

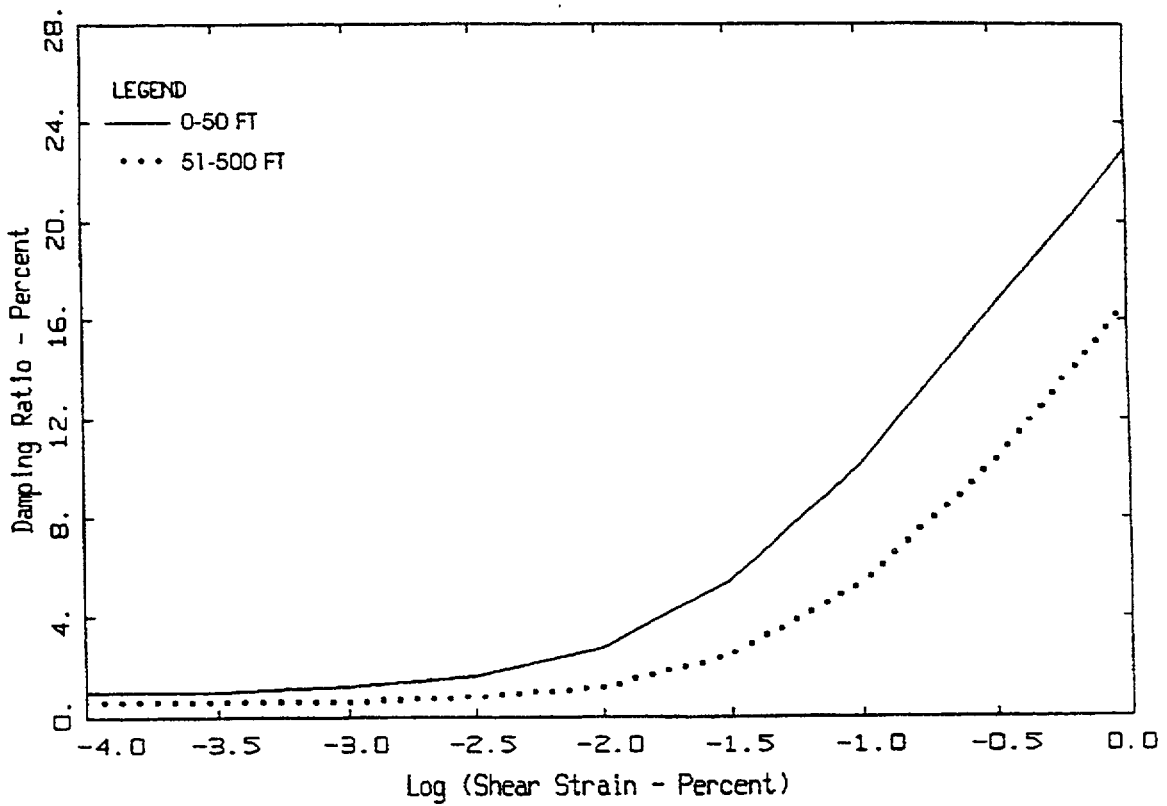
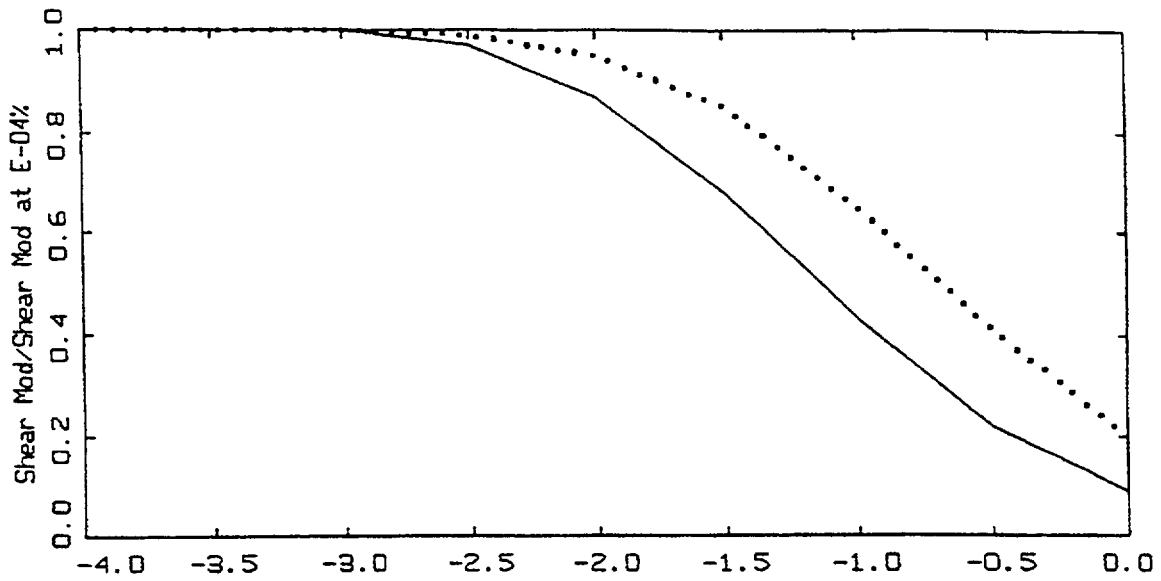
- LEGEND
- 16TH PERCENTILE
 - 50TH PERCENTILE
 - · - · 84TH PERCENTILE

Figure 2-7b. Variation in base case shear-wave velocity for the Savannah River generic profile (Figure 2-6b) based on thirty realizations. Median estimate along with $\pm \sigma$ values.



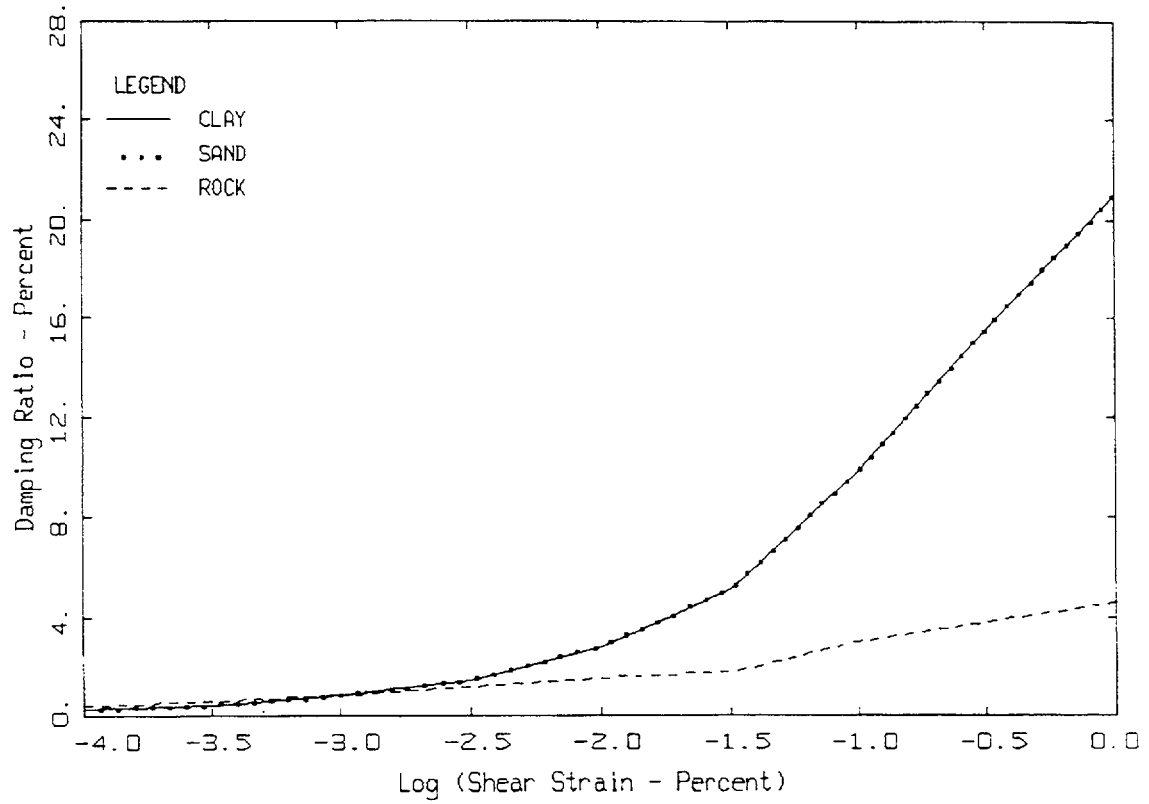
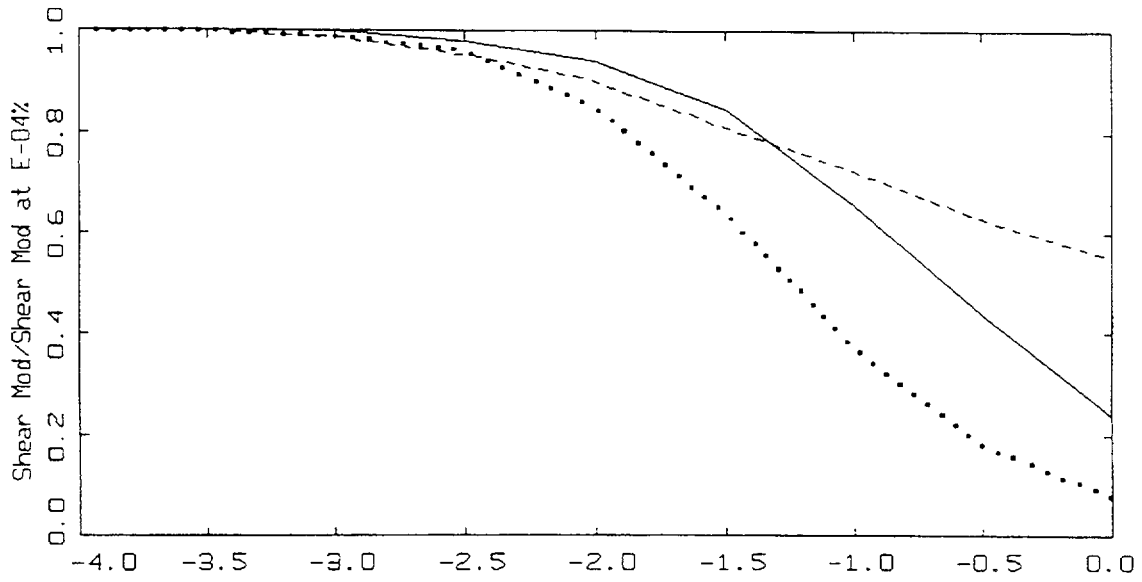
MODULUS REDUCTION AND DAMPING CURVES FOR MELOLAND

Figure 2-8a. Generic G/G_{max} and hysteretic damping curves for Imperial Valley soils. Used for soil site Meloland.



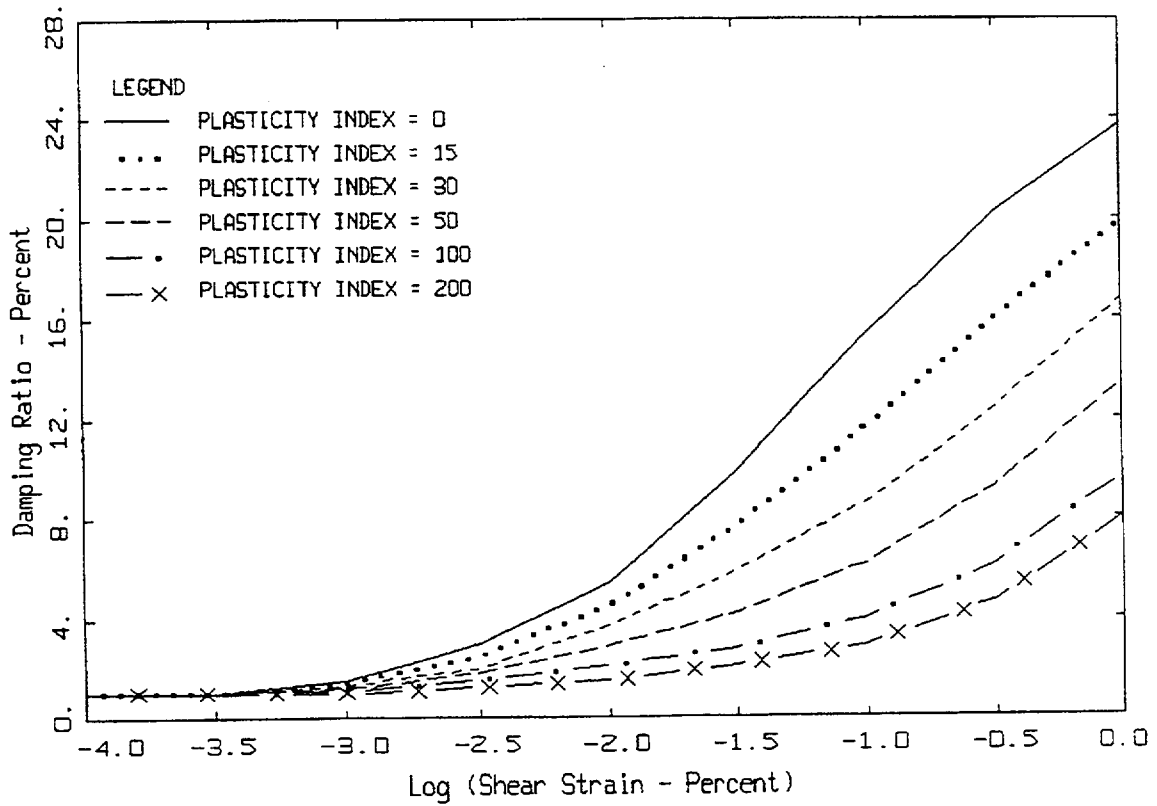
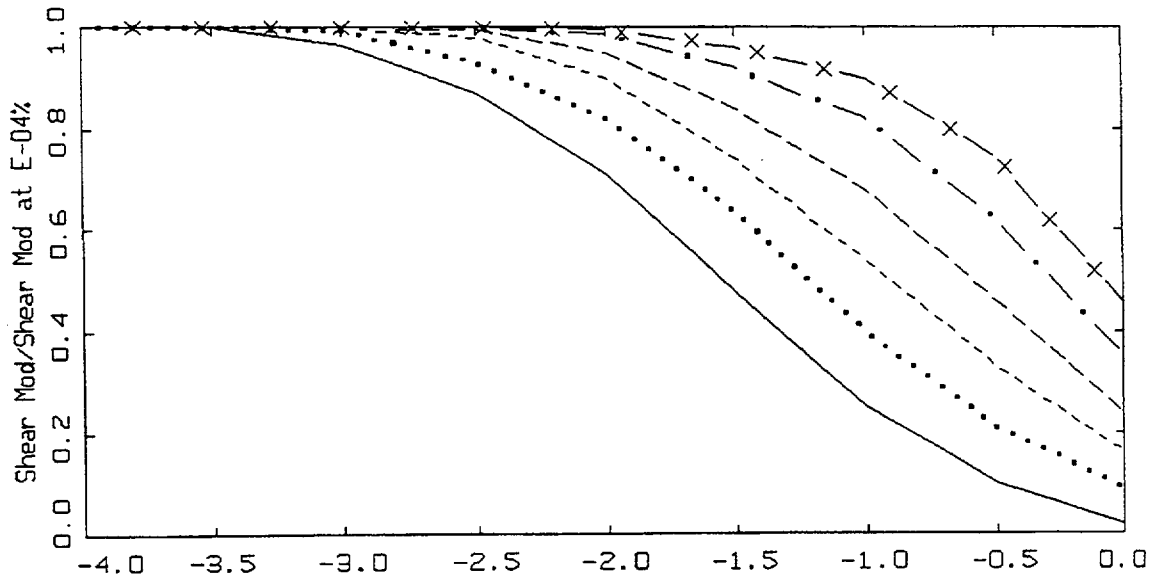
MODULUS REDUCTION AND DAMPING CURVES FOR COHESIONLESS SOILS

Figure 2-8b. Generic G/G_{max} and hysteretic damping curves for Peninsular Range cohesionless soil site conditions (Silva et al., 1997), assumed for Savannah River generic profile.



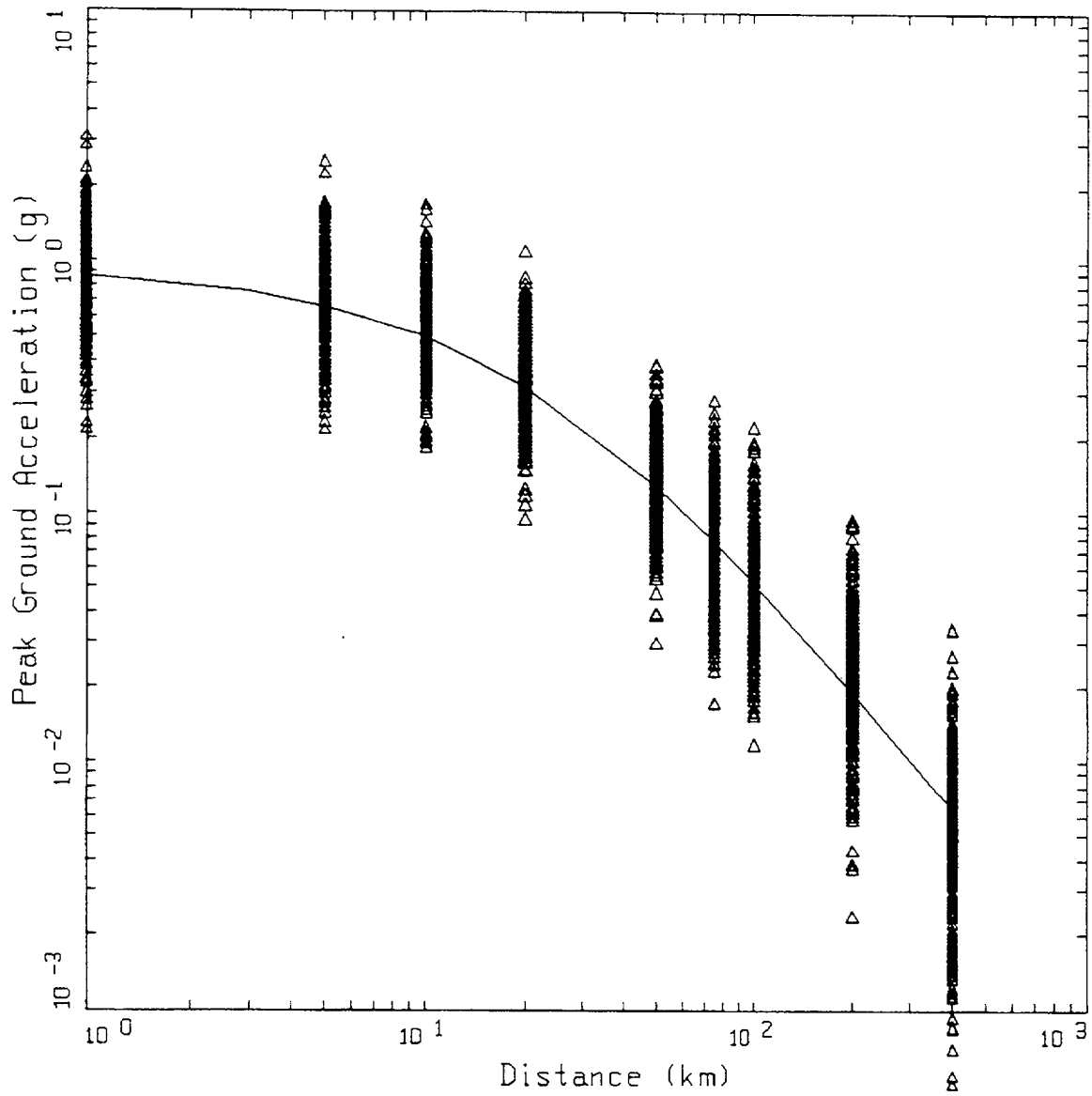
MODULUS REDUCTION AND DAMPING CURVES FROM SHAKE MANUAL

Figure 2-9. Generic G/G_{max} and hysteretic damping curves from SHAKE, 1991.



VUCETIC/DOBRY MODULUS REDUCTION AND DAMPING CURVES

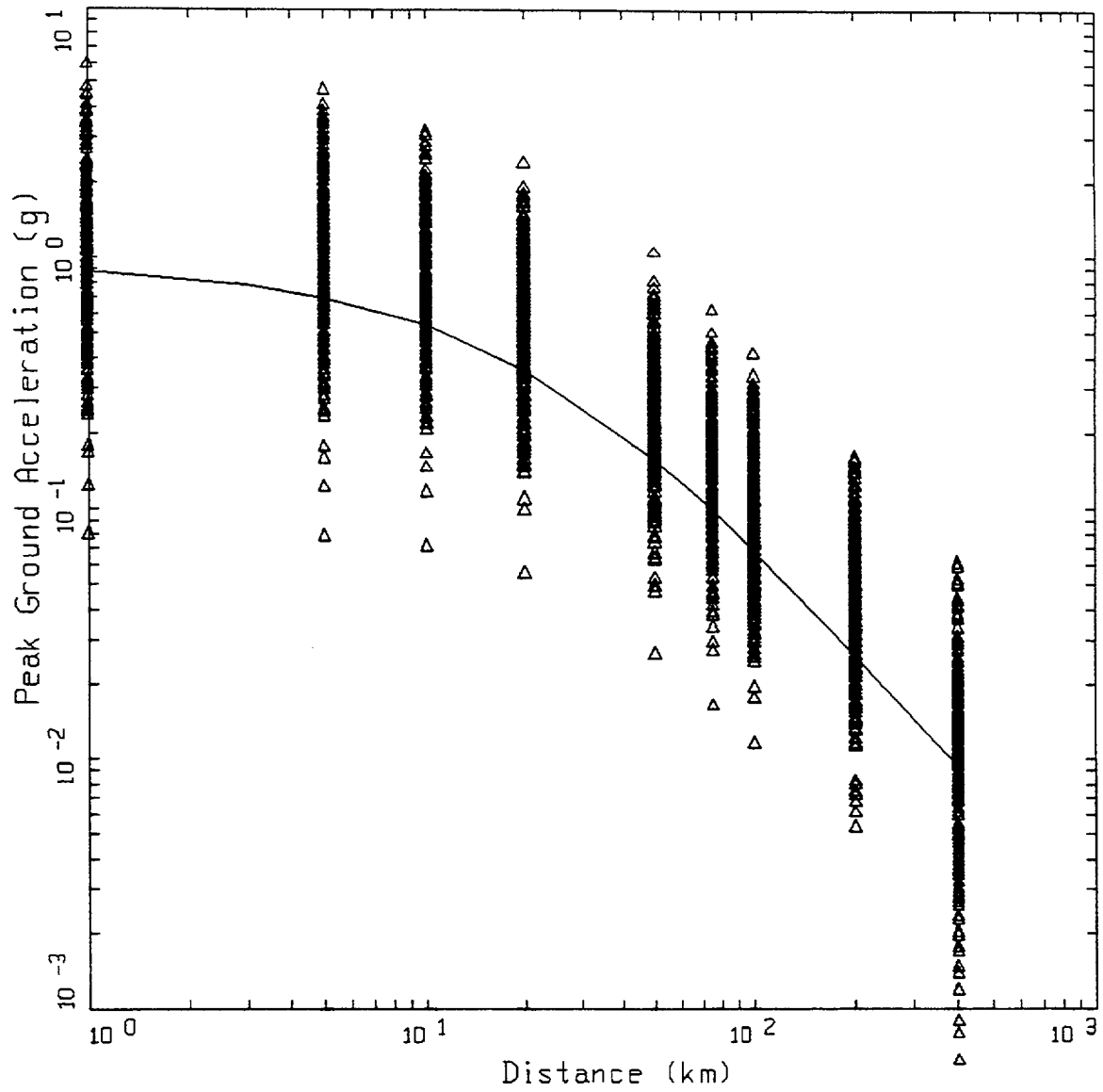
Figure 2-10. Generic G/G_{max} and hysteretic damping curves for cohesive soils (Vucetic and Dobry, 1991).



WUS ROCK
M=7.5

Δ Δ LEGEND
 — DATA: PGA
 M=7.5, SIGMA=0.5655

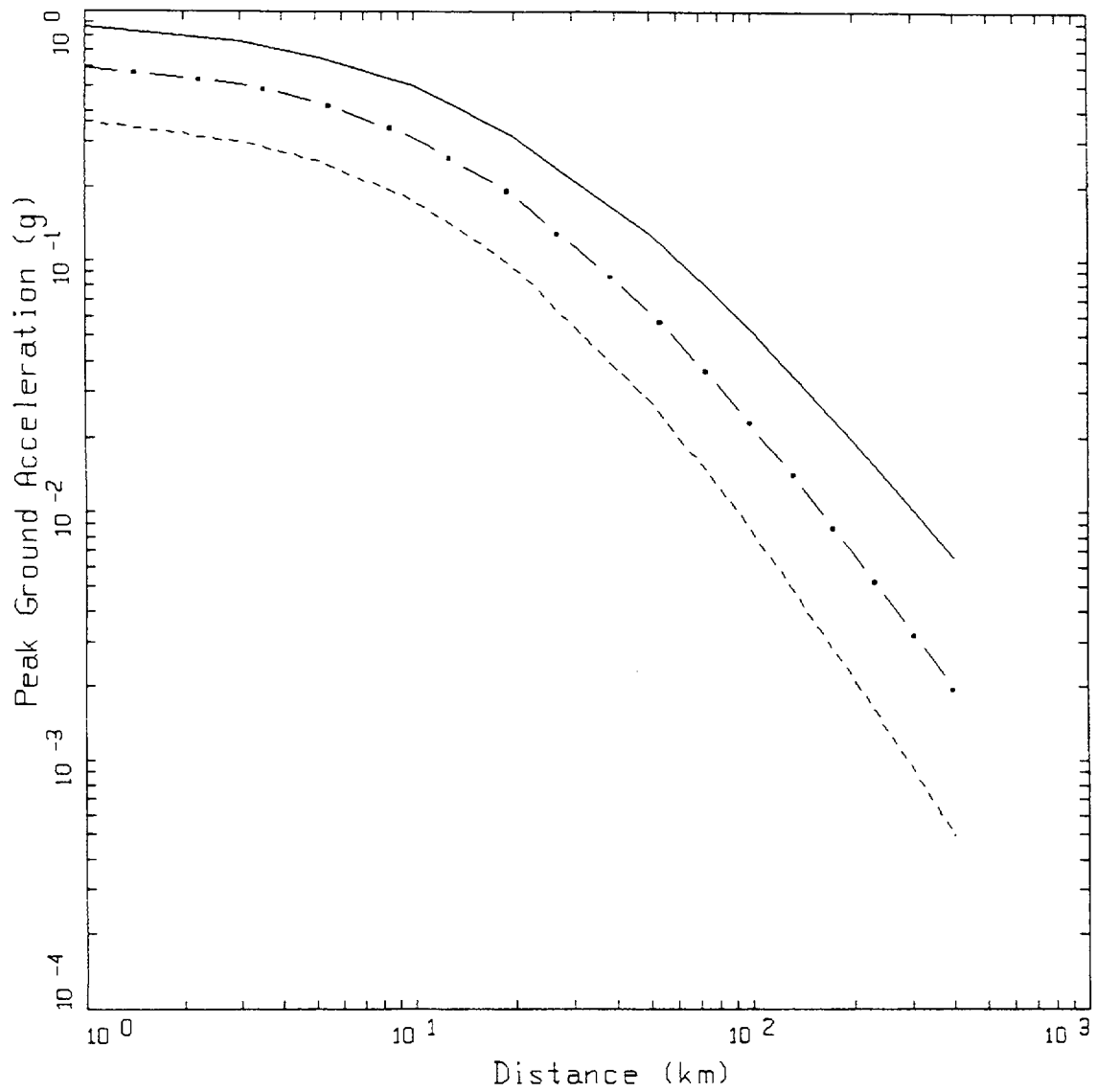
Figure 2-11. Peak acceleration estimates and regression fit at M 7.5 for WUS rock site conditions.



CEUS ROCK
M=7.5

LEGEND
Δ DATA: PGA
— M=7.5, SIGMA=0.6387

Figure 2-12. Peak acceleration estimates and regression fit at M 7.5 for CEUS (1-corner source model) rock site conditions.

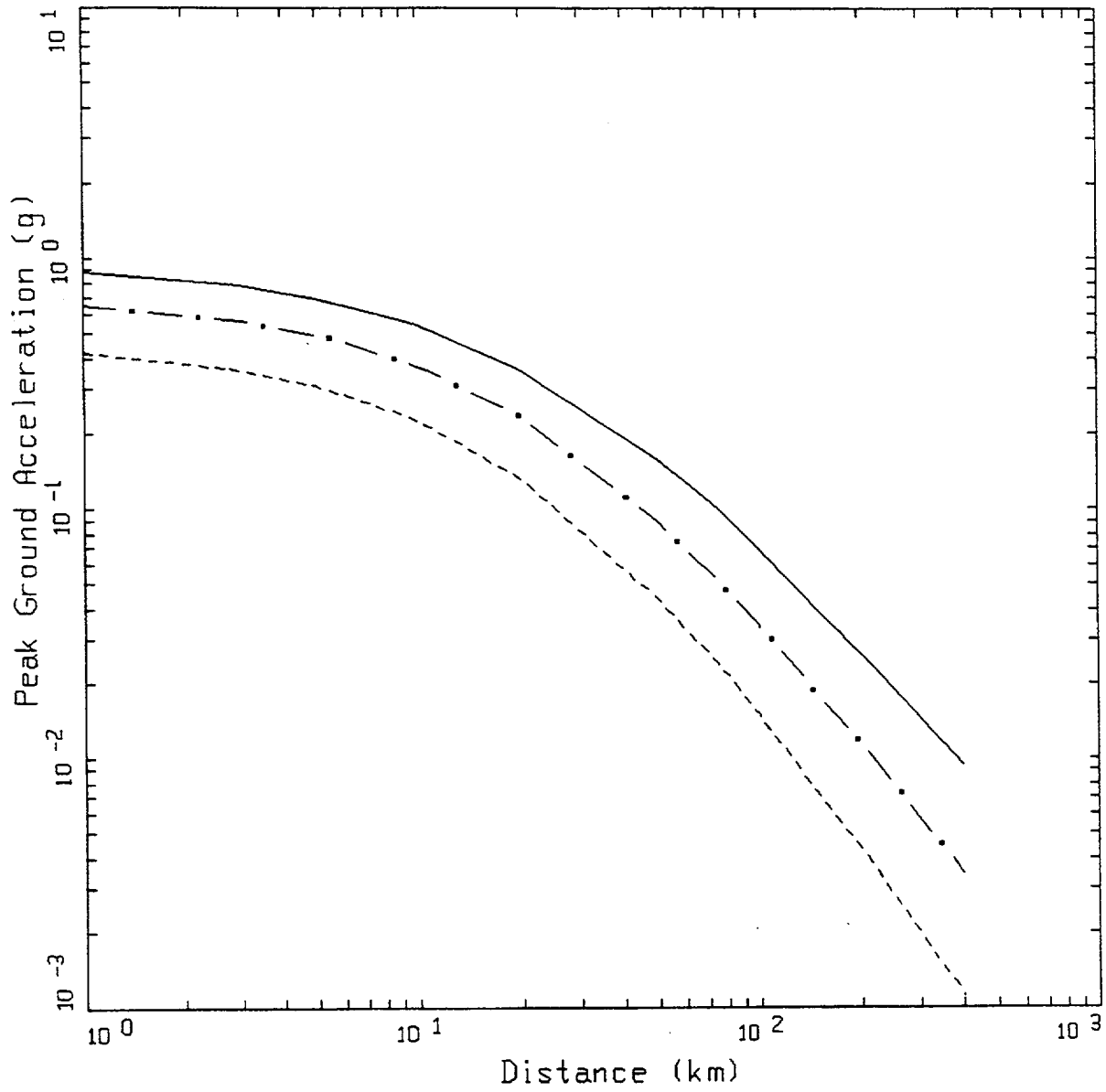


WUS ROCK

LEGEND

- M=5.5, SIGMA=0.5655
- . - M=6.5, SIGMA=0.5655
- M=7.5, SIGMA=0.5655

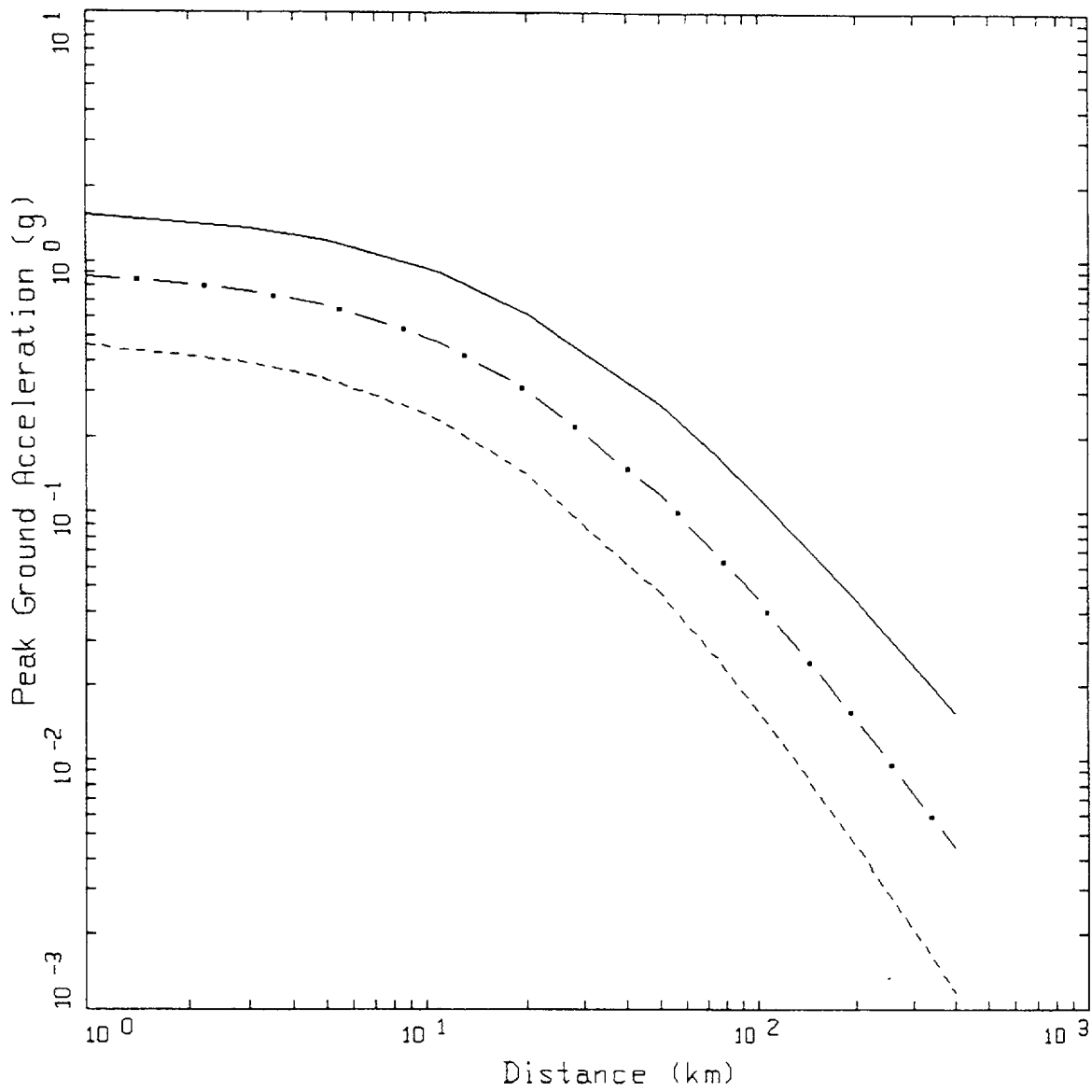
Figure 2-13. Attenuation of median peak horizontal acceleration at **M** 5.5, 6.5, and 7.5 for WUS rock site conditions.



CEUS ROCK

- LEGEND
- M=5.5, SIGMA=0.6387
 - . - M=6.5, SIGMA=0.6387
 - M=7.5, SIGMA=0.6387

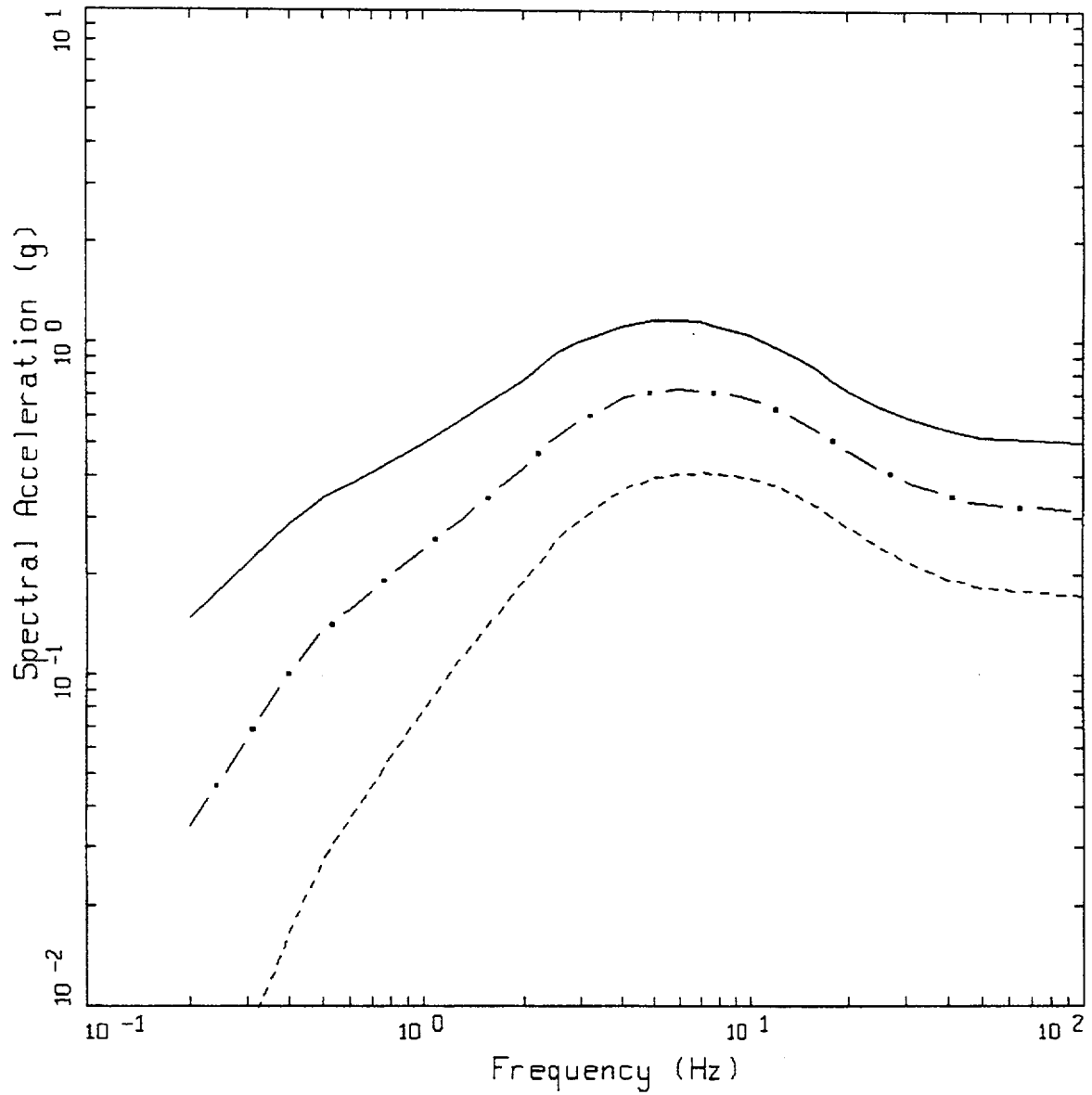
Figure 2-14a. Attenuation of median peak horizontal acceleration at M 5.5, 6.5, and 7.5 for CEUS rock site conditions (single-corner source model).



CEUS ROCK

- LEGEND
- M=5.5, SIGMA=0.4854
 - . - M=6.5, SIGMA=0.4854
 - M=7.5, SIGMA=0.4854

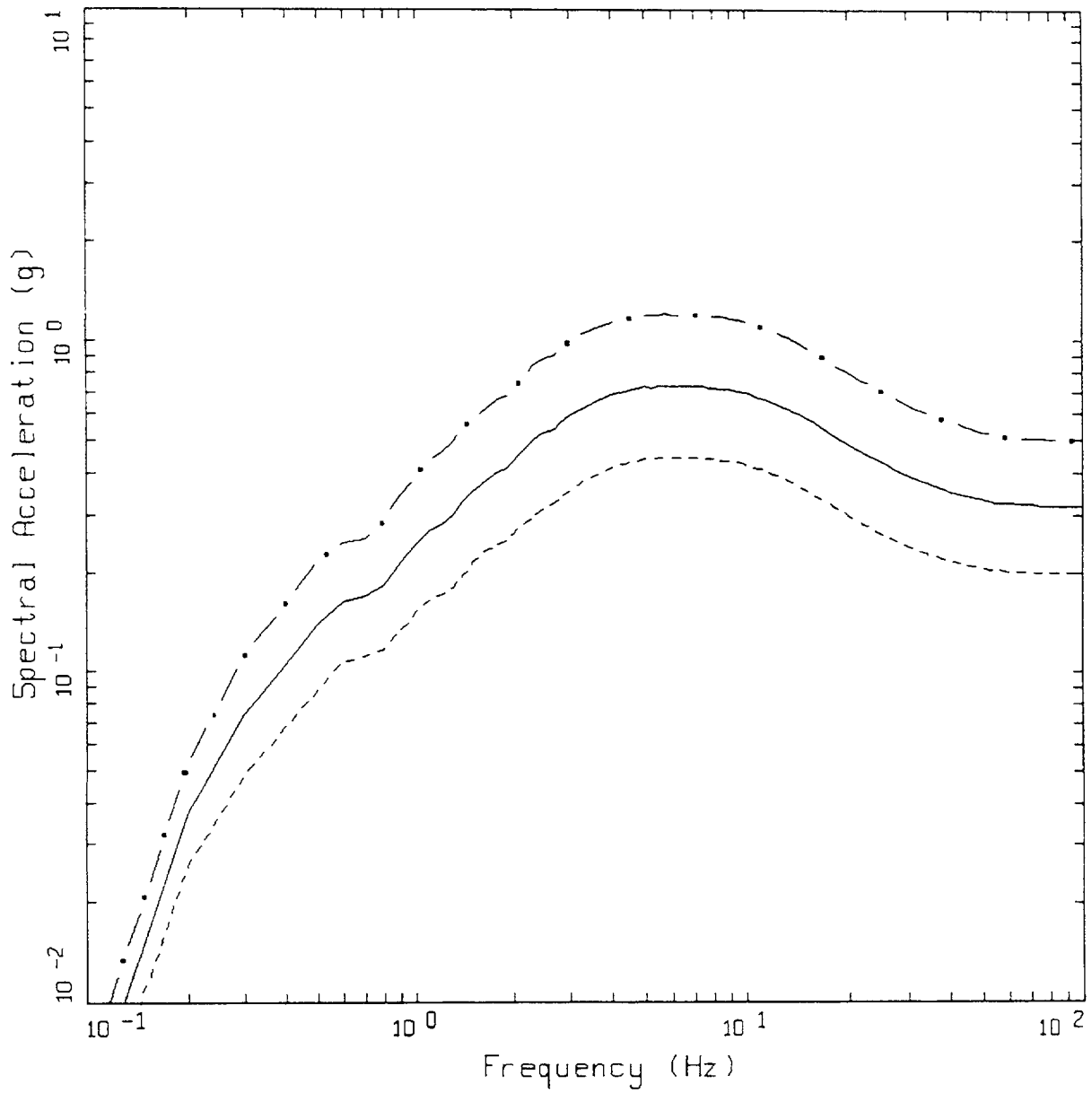
Figure 2-14b. Attenuation of median peak horizontal acceleration at M 5.5, 6.5, and 7.5 for CEUS rock site conditions (double corner source model).



WUS ROCK
 DISTANCE = 10 KM

LEGEND
 - - - - - M=5.5
 - . - - - M=6.5
 ——— M=7.5

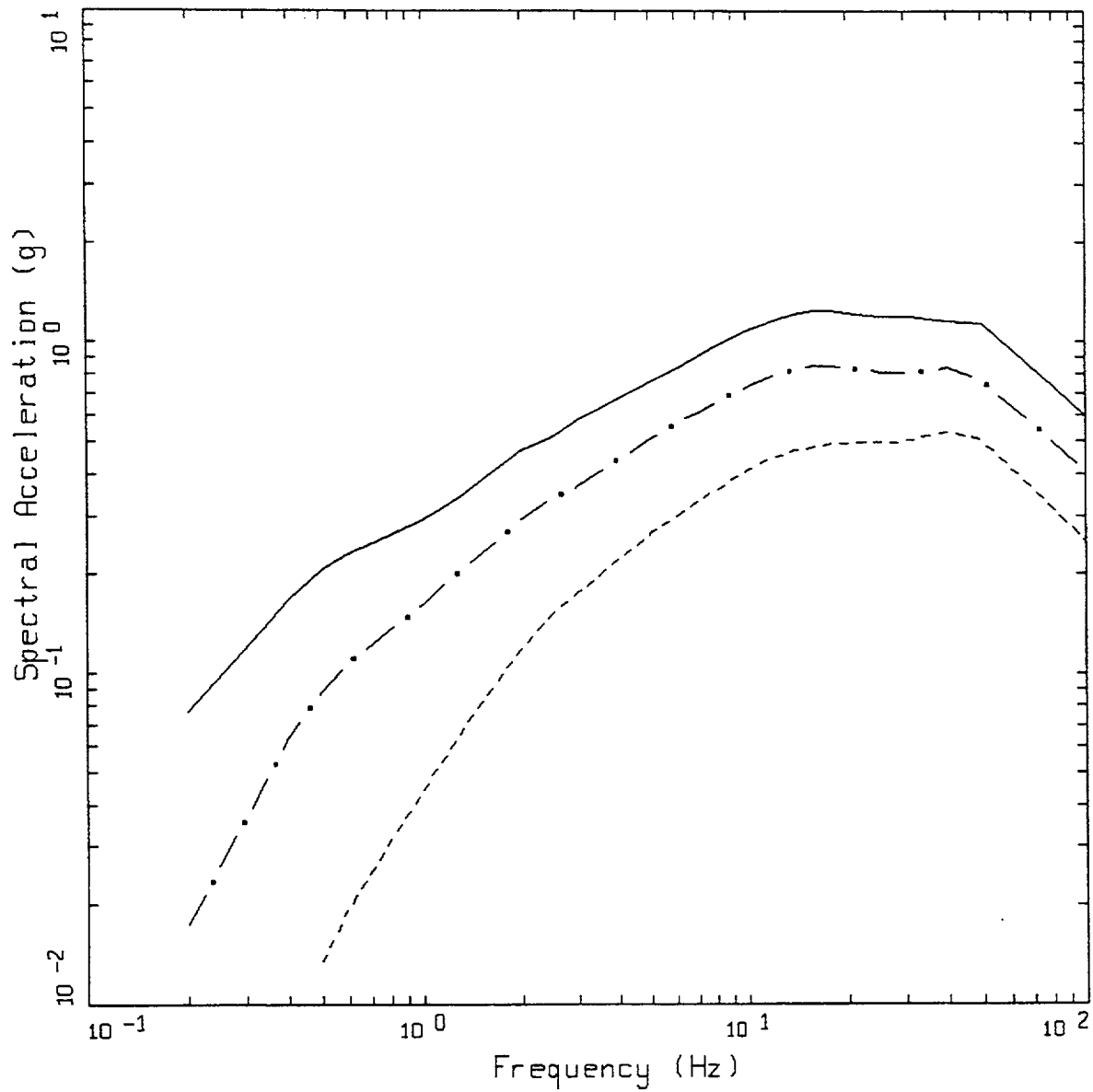
Figure 2-15. Median response spectra (5% damping) at a distance of 10 km for magnitudes **M** 5.5, 6.5, and 7.5: WUS rock site.



WUS ROCK
M=6.5, DISTANCE=10 KM

LEGEND
- · - 84TH PERCENTILE, PGA = 0.500 G
— 50TH PERCENTILE, PGA = 0.315 G
- - - 16TH PERCENTILE, PGA = 0.199 G

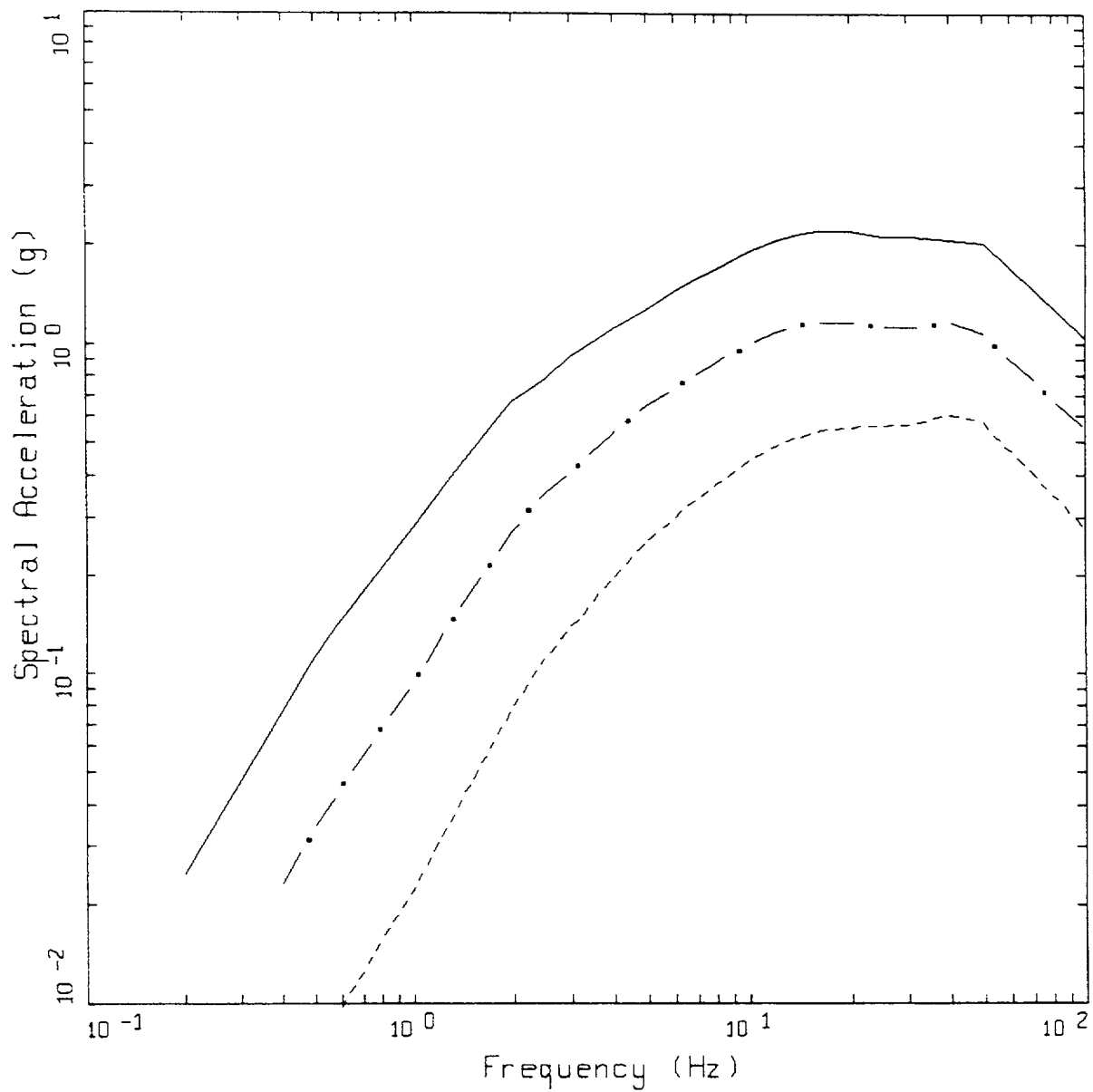
Figure 2-16. Response spectra (5% damping) at a distance of 10 km for M 6.5 showing median and $\pm 1 \sigma$ estimates (parametric and regression uncertainty): WUS rock site.



CEUS ROCK
 DISTANCE = 10 KM

LEGEND
 - - - - - M=5.5
 - . - - - M=6.5
 ——— M=7.5

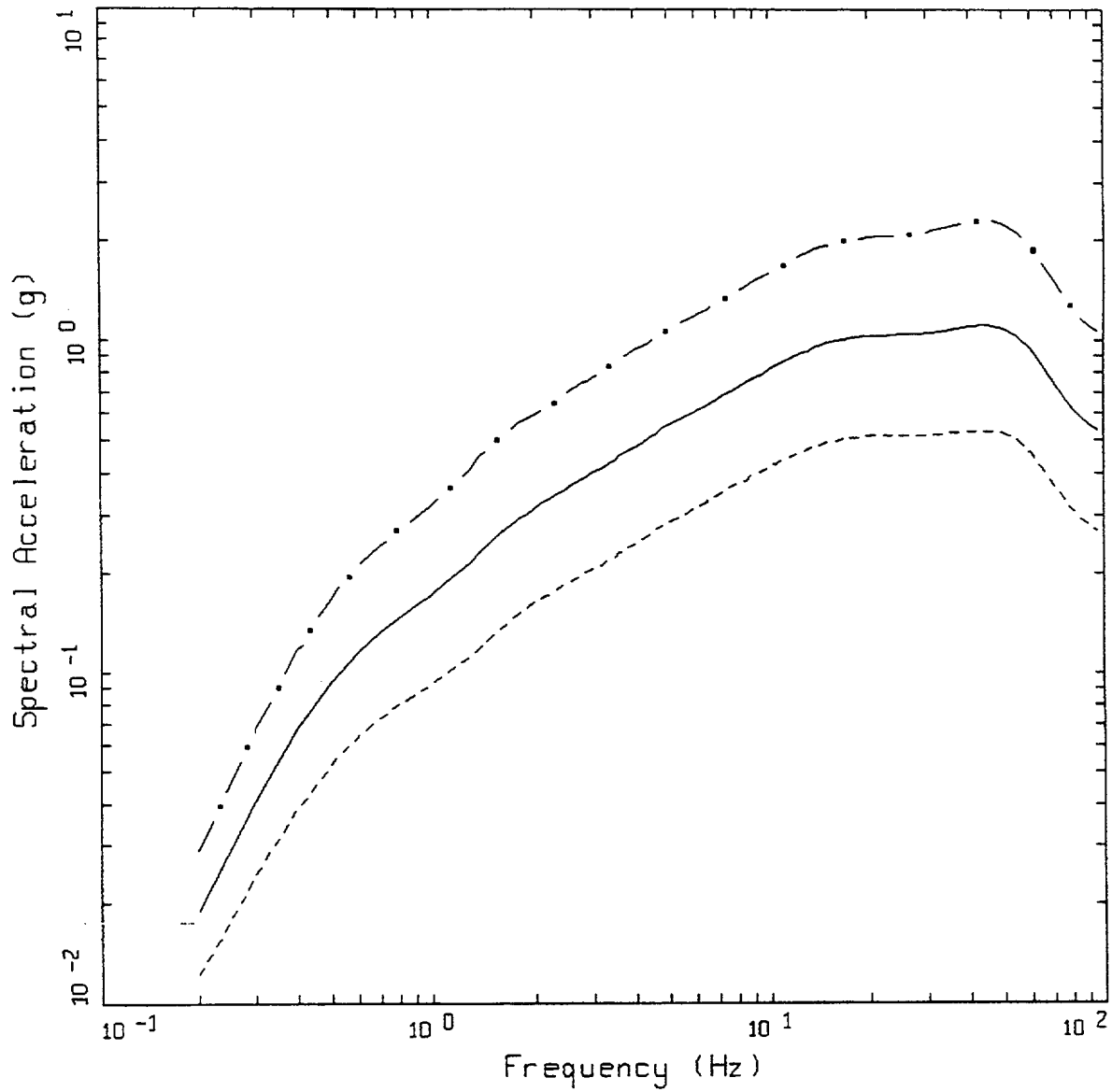
Figure 2-17a. Median response spectra (5% damping) at a distance of 10 km for M 5.5, 6.5, and 7.5: CEUS rock site (single-corner source model).



CEUS ROCK
 DISTANCE = 10 KM

- LEGEND
- M=5.5
 - . - . M=6.5
 - M=7.5

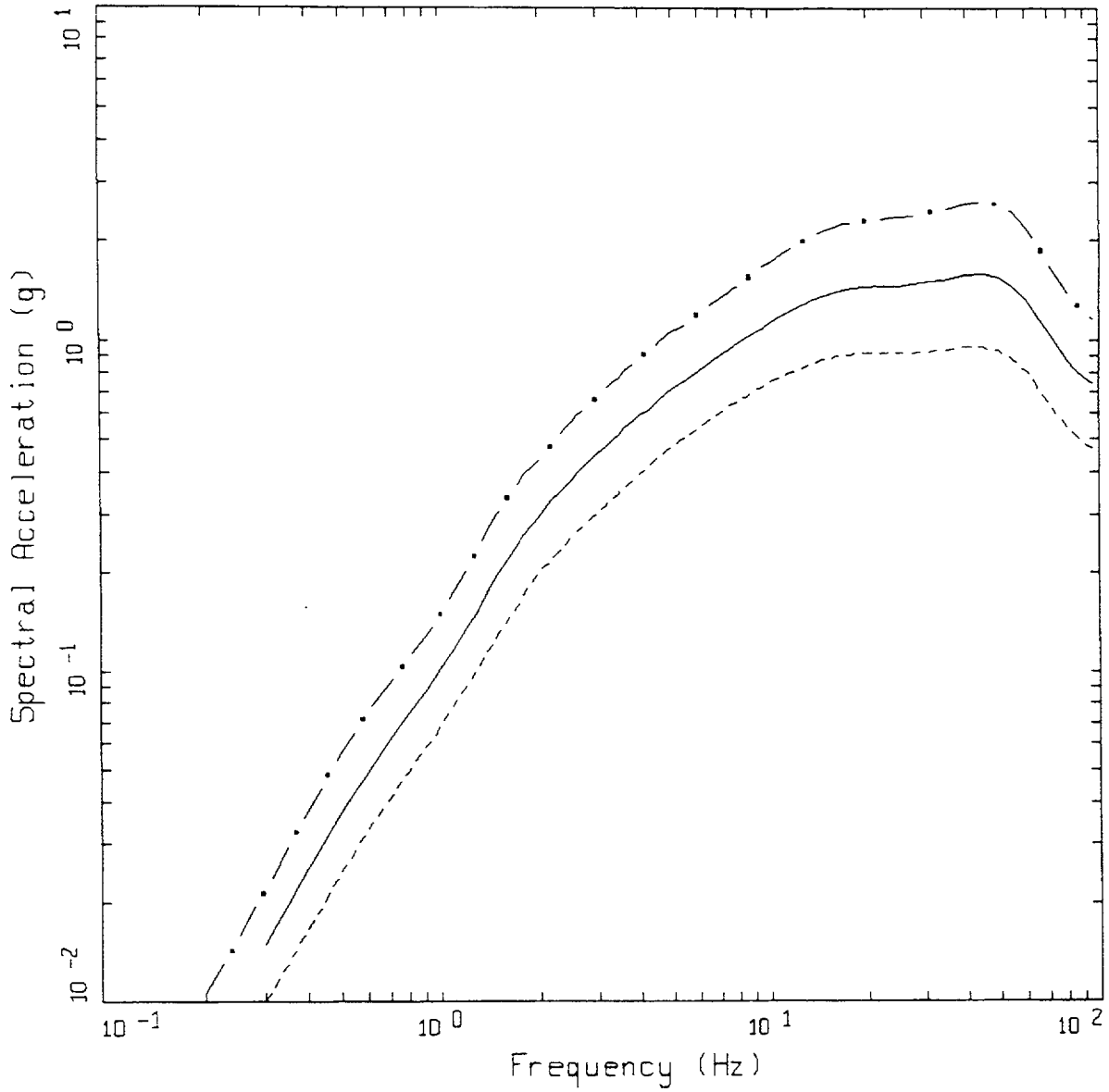
Figure 2-17b. Median response spectra (5% damping) at a distance of 10 km for M 5.5, 6.5, and 7.5: CEUS rock site (double-corner source model).



CEUS ROCK
 M=6.5, DISTANCE=10 KM

LEGEND
 - · - 84TH PERCENTILE, PGA = 1.033 G
 ——— 50TH PERCENTILE, PGA = 0.520 G
 - - - 16TH PERCENTILE, PGA = 0.262 G

Figure 2-18a. Response spectra (5% damping) at a distance of 10 km for M 6.5 showing median and $\pm 1 \sigma$ estimates (parametric and regression uncertainty): CEUS rock site (single corner source model).

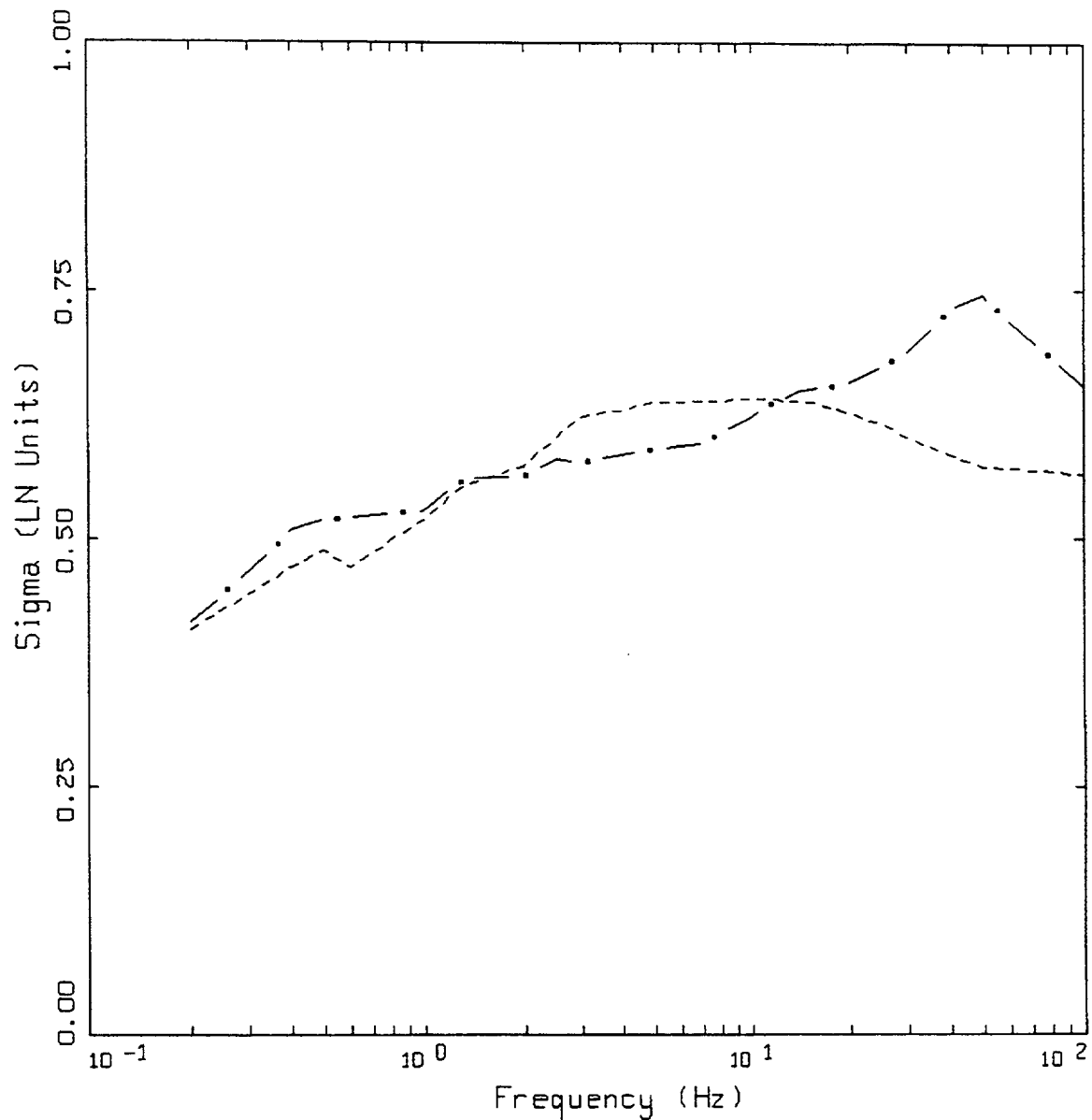


CEUS ROCK
 M=6.5, DISTANCE=10 KM

LEGEND

- • — 84TH PERCENTILE, PGA = 1.130 G
- 50TH PERCENTILE, PGA = 0.723 G
- 16TH PERCENTILE, PGA = 0.462 G

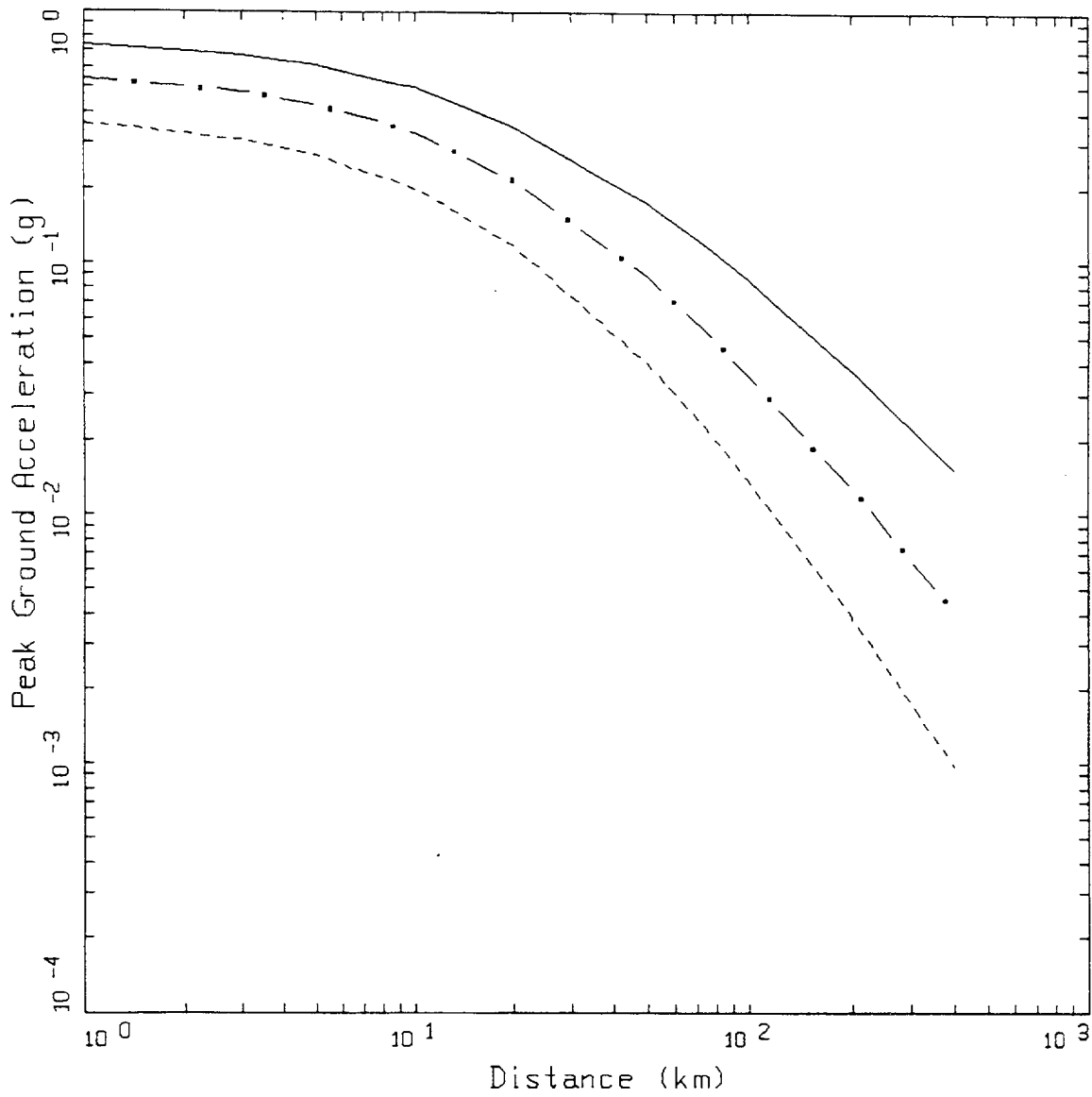
Figure 2-18b. Response spectra (5% damping) at a distance of 10 km for **M** 6.5 showing median and $\pm 1 \sigma$ estimates (parametric and regression uncertainty): CEUS rock site (double corner source model) variability in stress drop not included.



ROCK SITE VARIABILITY

- LEGEND
- WUS SIGMA
 - • — CEUS SINGLE CORNER SOURCE MODEL SIGMA

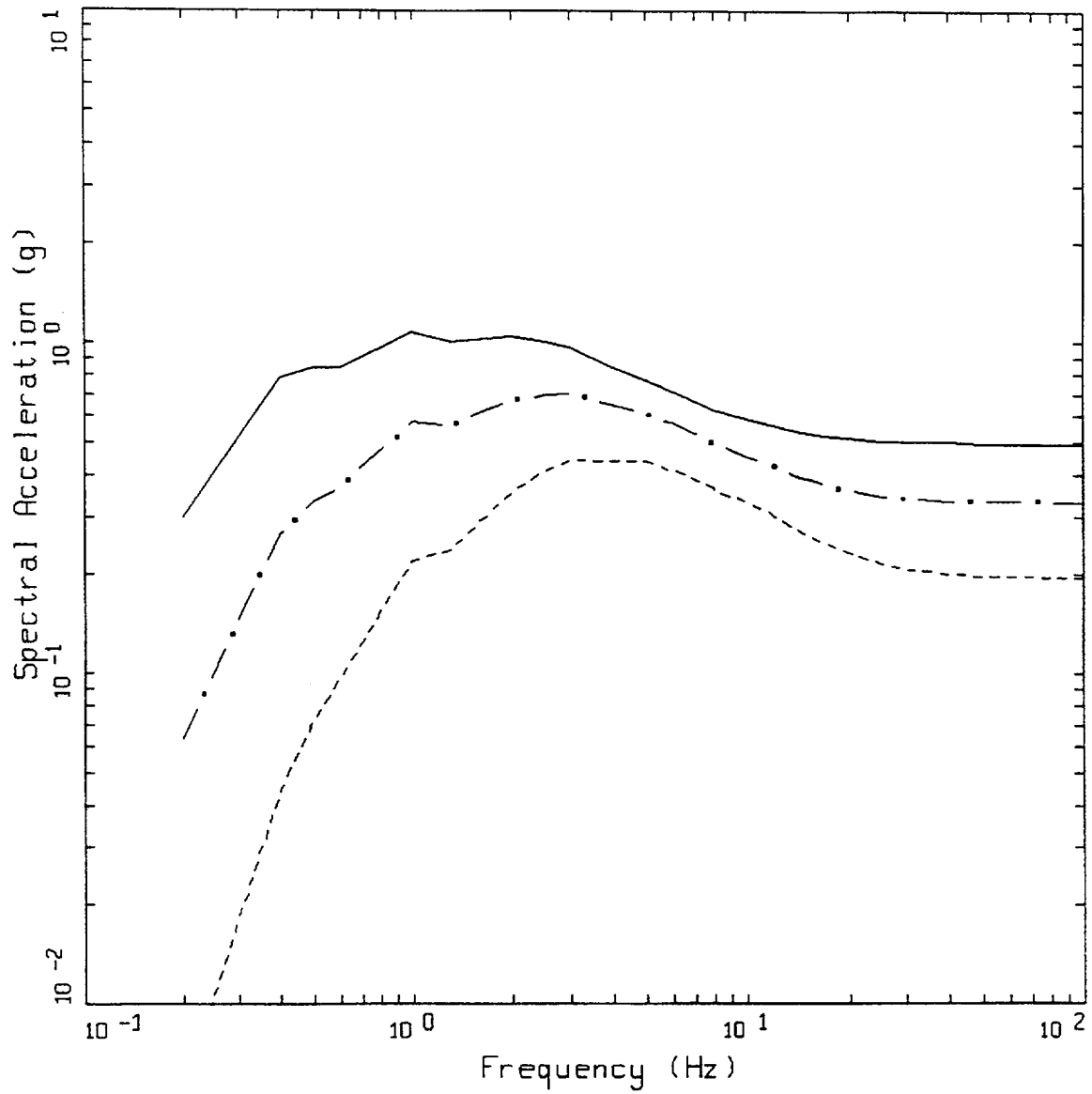
Figure 2-19. Variability in response spectral ordinates at WUS and CEUS rock sites resulting from parametric variability and regression fit over all magnitudes and distances (Tables 2-5 and 2-6).



WUS SOIL, MELOLAND

LEGEND
 - - - - M=5.5, SIGMA=0.4774
 - . - M=6.5, SIGMA=0.4774
 ——— M=7.5, SIGMA=0.4774

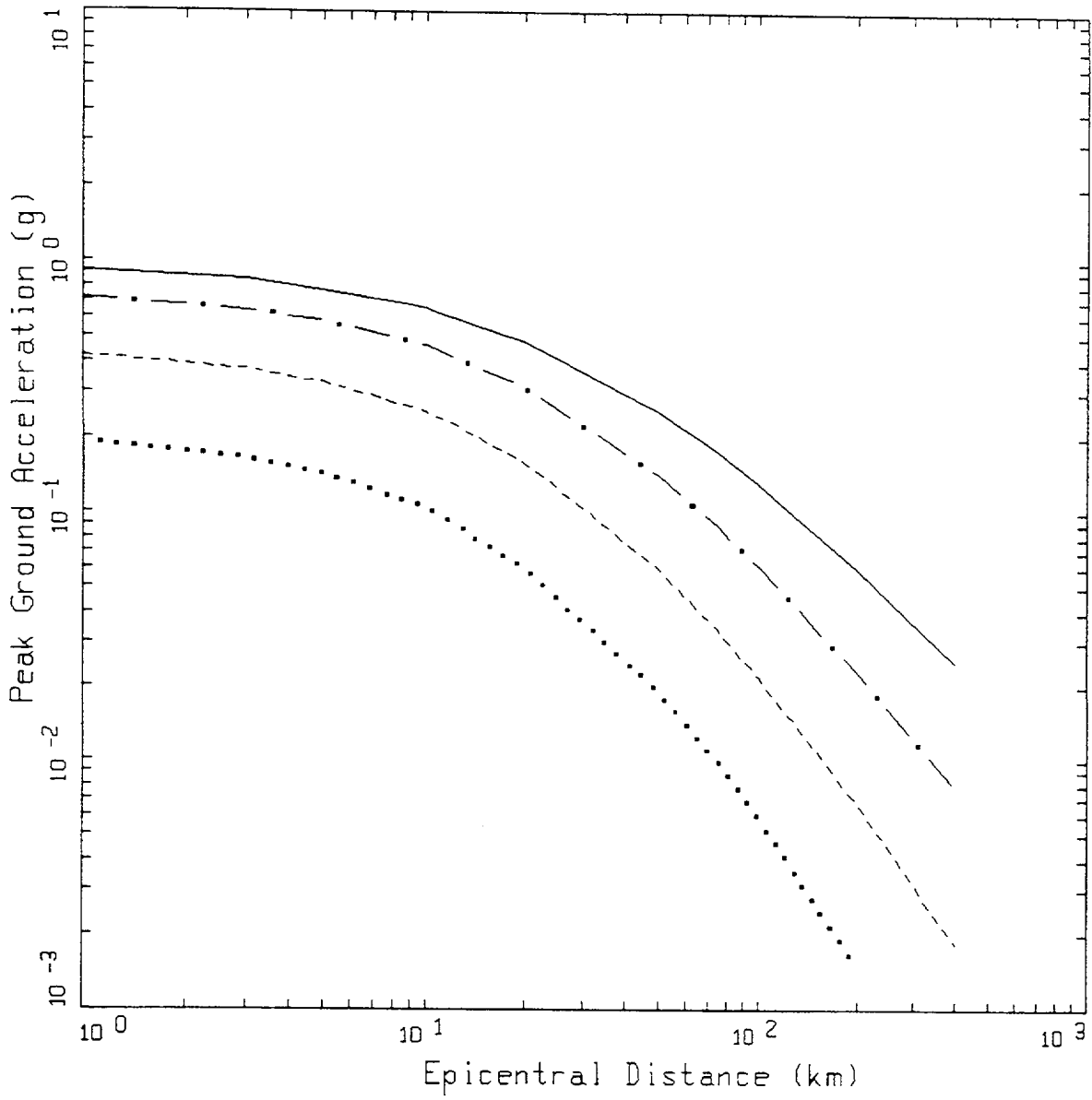
Figure 2-20. Attenuation of median peak horizontal acceleration at **M** 5.5, 6.5, and 7.5 for Meloland profile and WUS conditions.



WUS SOIL, MELOLAND
 DISTANCE = 10 KM

LEGEND
 - - - - M=5.5
 - . - - M=6.5
 ——— M=7.5

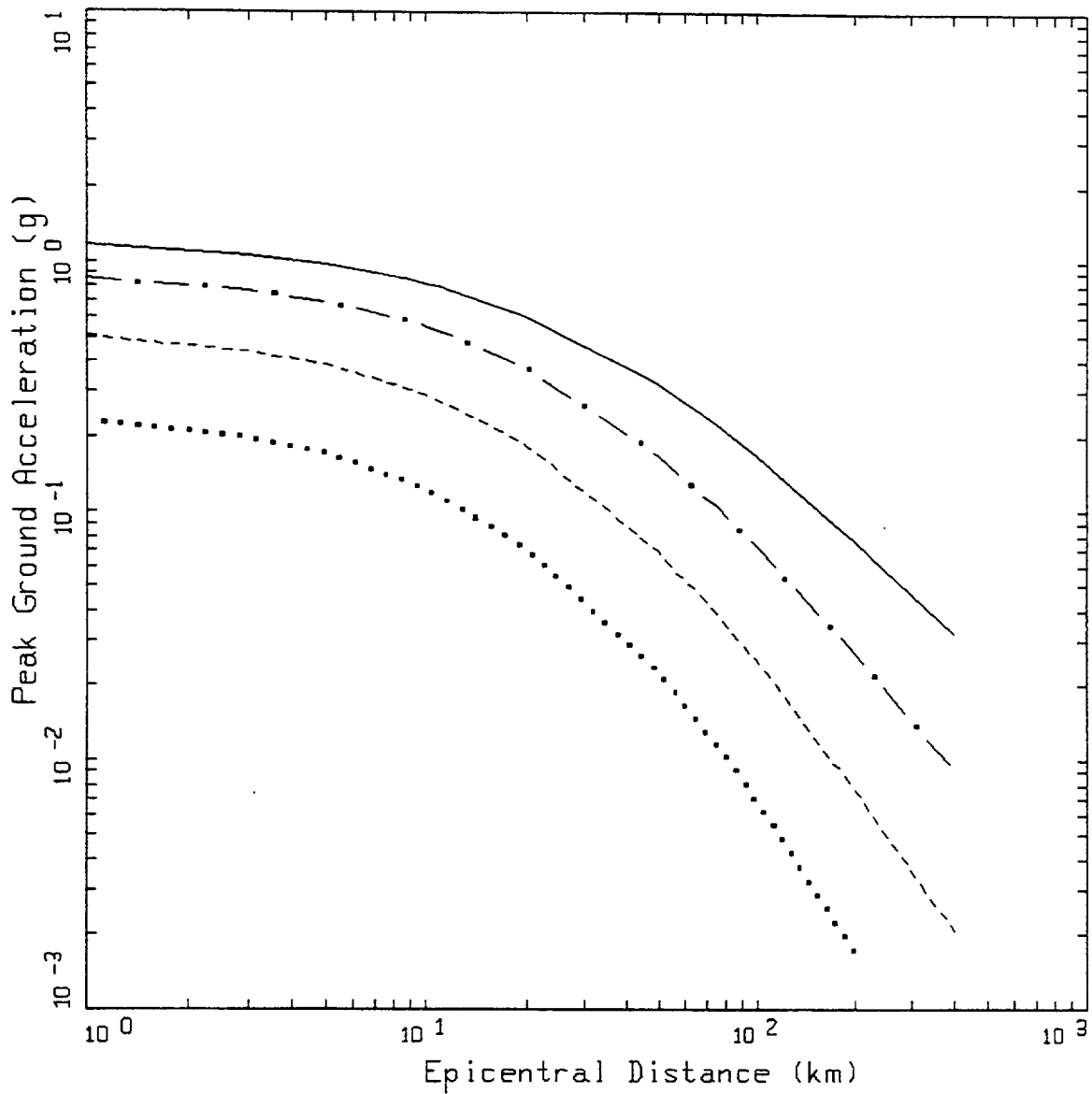
Figure 2-21. Median response spectra (5% damping) at a distance of 10 km for M 5.5, 6.5, and 7.5 for Meloland profile and WUS conditions.



CEUS SOIL
 SAVANNAH RIVER GENERIC

- LEGEND
- M=4.5, SIGMA=0.5706
 - M=5.5, SIGMA=0.5706
 - . - M=6.5, SIGMA=0.5706
 - M=7.5, SIGMA=0.5706

Figure 2-22a. Attenuation of median peak horizontal acceleration at **M** 4.5, 5.5, 6.5, and 7.5 for Savannah River generic profile and CEUS conditions (single-corner source model).

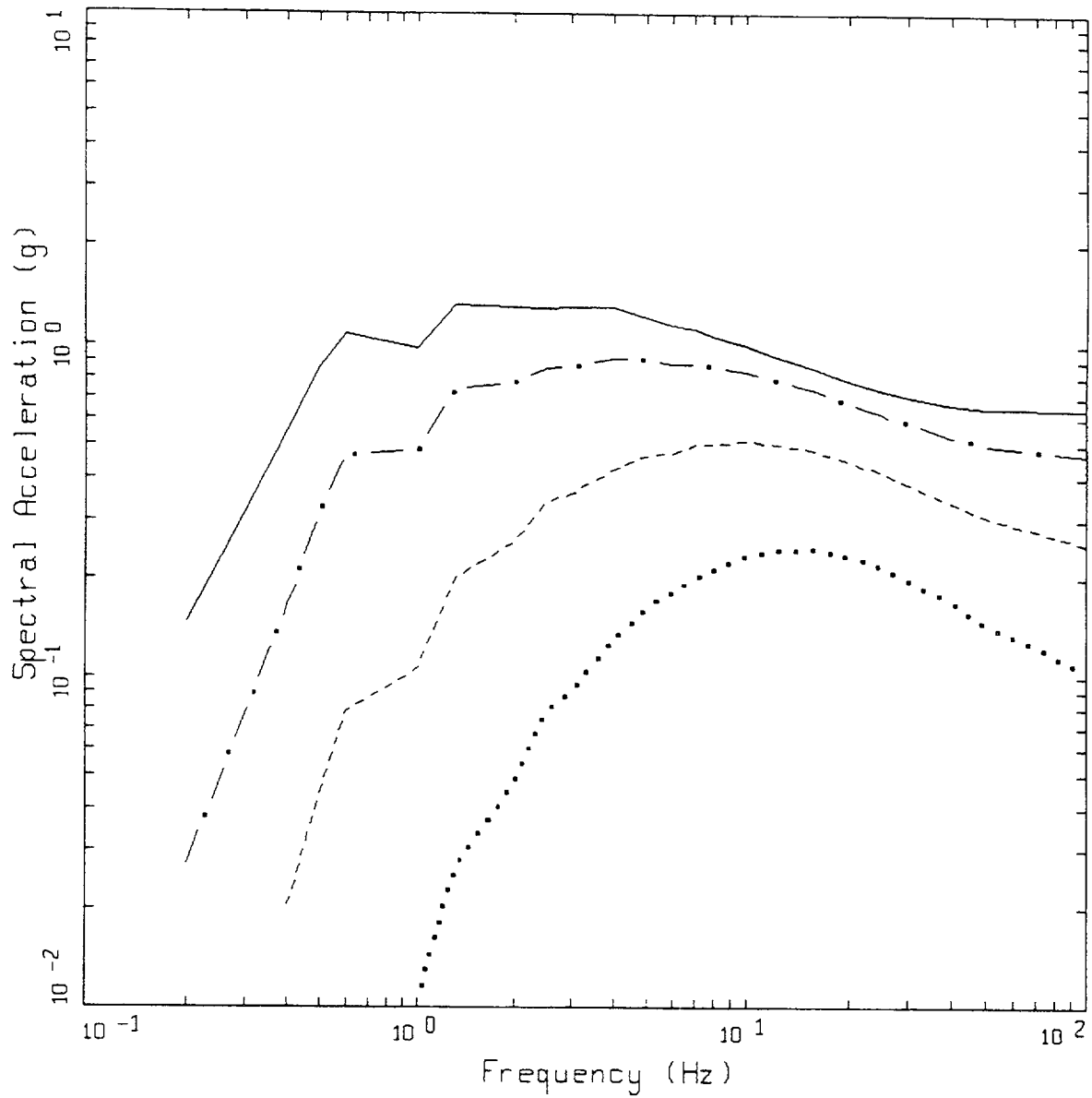


CEUS SOIL
SAVANNAH RIVER GENERIC

LEGEND

- M=4.5, SIGMA=0.4219
- M=5.5, SIGMA=0.4219
- . - . M=6.5, SIGMA=0.4219
- M=7.5, SIGMA=0.4219

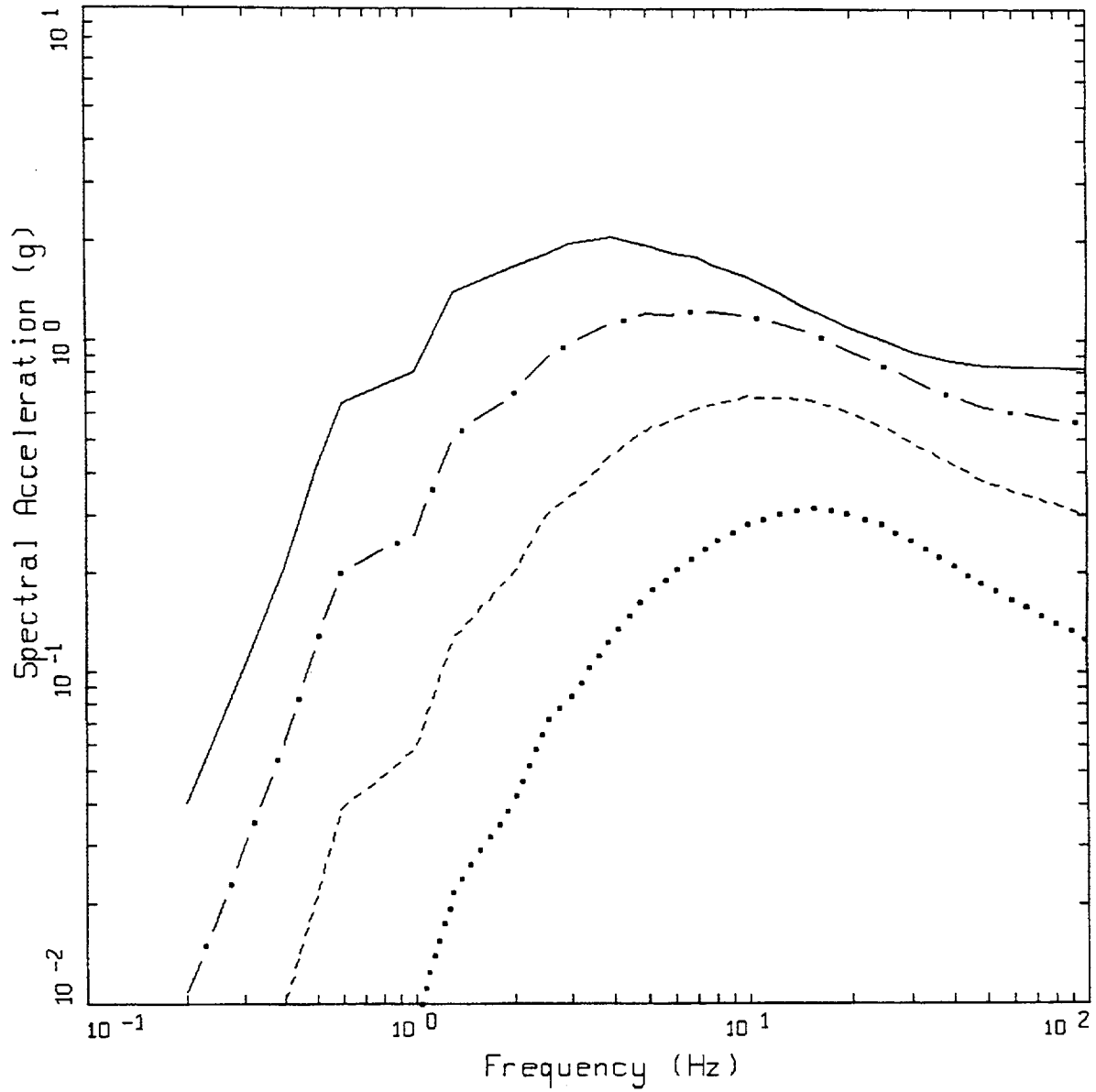
Figure 2-22b. Attenuation of median peak horizontal acceleration at M 4.5, 5.5, 6.5, and 7.5 for Savannah River generic profile and CEUS conditions (double-corner source model).



CEUS SOIL, DISTANCE=10 KM
 SAVANNAH RIVER GENERIC

LEGEND
 M=4.5
 - - - - M=5.5
 - . - . M=6.5
 _____ M=7.5

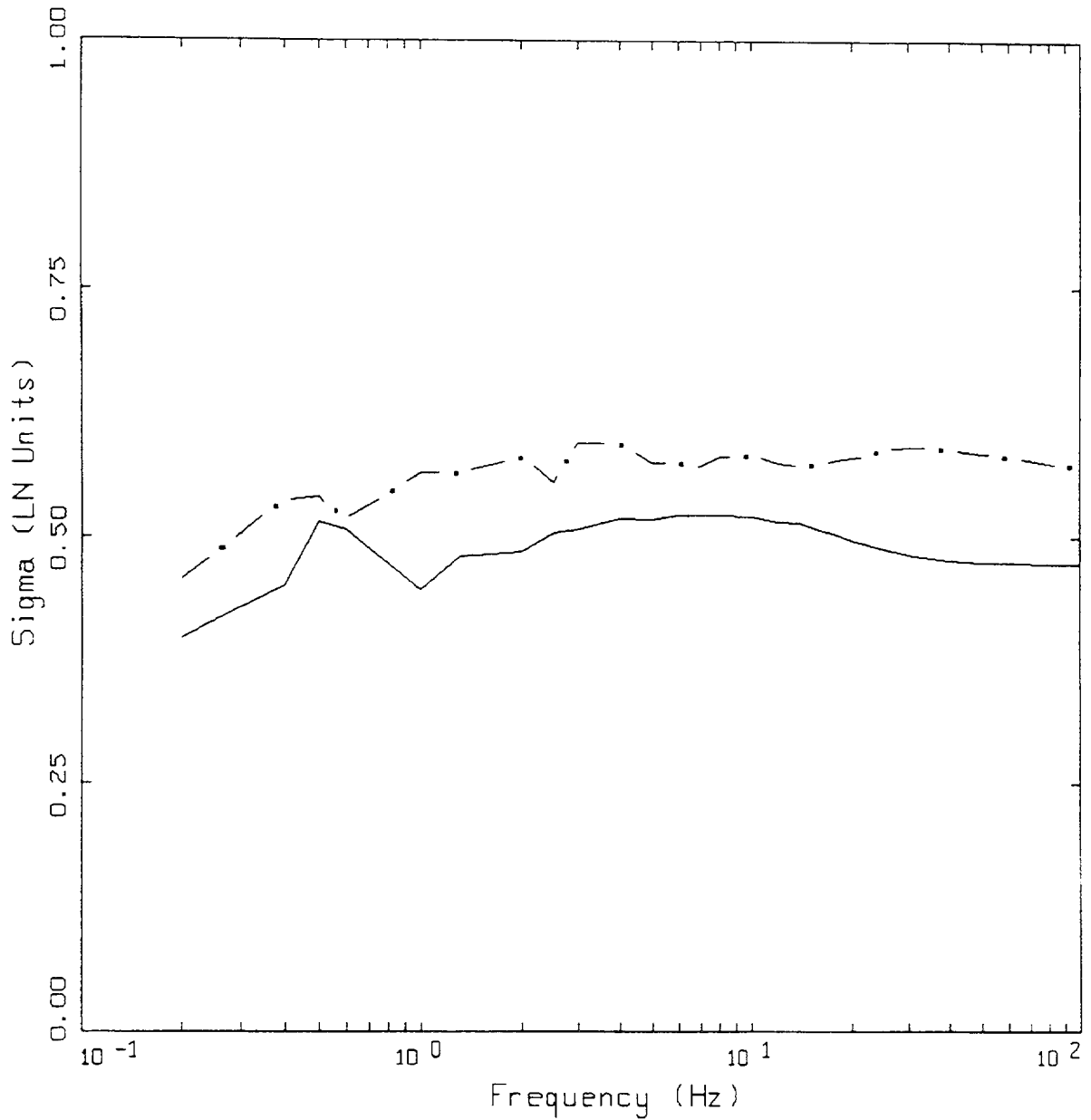
Figure 2-23a. Median response spectra (5% damping) at a distance of 10 km for **M** 4.5, 5.5, 6.5, and 7.5 for Savannah River generic profile and CEUS conditions (single-corner source model).



CEUS SOIL, DISTANCE=10 KM
 SAVANNAH RIVER GENERIC

- LEGEND
- M=4.5
 - M=5.5
 - . - . M=6.5
 - M=7.5

Figure 2-23b. Median response spectra (5% damping) at a distance of 10 km for M 4.5, 5.5, 6.5, and 7.5 for Savannah River generic profile and CEUS conditions (double-corner source model).



SOIL SITE VARIABILITY

- LEGEND
- WUS SOIL (MELOLAND) SIGMA
 - · - CEUS SOIL (SAVANNAH RIVER GENERIC) SIGMA

Figure 2-24. Variability in response spectral ordinates for Meloland profile (WUS) and Savannah River generic profile (CEUS) resulting from parametric variability and regression fit over all magnitudes and distances (Tables 2-7 and 2-8).

3.0 SEISMIC HAZARD

3.1 Mojave site

3.1.1 Rock site conditions

A probabilistic seismic hazard analysis (PSHA) was conducted at the Mojave site using the seismic sources and parameters described in Section 2.1 and using the attenuation equation for rock site conditions described in Section 2.3. In all respects the PSHA was typical of the analysis that would be conducted for a critical facility except that epistemic uncertainties in seismicity parameters and attenuation equations were not considered, for simplicity. The application of procedures to develop design spectra and ground motions will be the same whether applied to a single seismic hazard curve or to the mean of a family of seismic hazard curves.

Figure 3-1 shows the seismic hazard in terms of peak ground acceleration (PGA) vs. annual frequency of exceedence. This illustrates that the site is in a location of relative high seismic hazard, with $PGA \approx 0.32g$ for a 500-year return period, and $PGA \approx 0.9g$ for 10,000-year return period. (Note that PGA results are shown in Figure 3-1 only because they provide a common benchmark for experience.) Seismic hazard curves are documented in Table 3-1 for PGA, 10 Hz, 5 Hz, 2.5 Hz, and 1 Hz. The uniform hazard spectra (UHS) are shown in Figure 3-2 for annual frequencies of exceedence of $1E-3$, $1E-4$, and $1E-5$, and these spectra are documented in Table 3-2.

The Mojave site was chosen because small, close earthquakes dominate the hazard at high frequencies ($f > 10$ Hz), but large distant events on the San Andreas fault contribute significantly at lower frequencies (1 Hz and less). This is illustrated in Figures 3-3 and 3-4, which show hazard contributions at 10 and 1 Hz, respectively, for the individual sources affecting the site. Particularly in the range of annual frequencies of $1E-3$ to $1E-4$, the San Andreas Fault has an important effect on 1 Hz hazard. This influence also occurs at lower structural frequencies.

The contribution of sources can be seen by deaggregating the hazard by magnitude, distance, and the attenuation equation ϵ term. These deaggregations are shown in Figures 3-5 through 3-8 for ground motions at 10 and 1 Hz corresponding to $1E-4$ annual frequency of exceedence. The strong contribution of the San Andreas ($M=7.8$ at 30 km) for 1 Hz is apparent. The ϵ distributions are similar for 10 and 1 Hz; both indicate that ground motion above the median ($\epsilon > 0$) dominate the hazard at the $1E-4$ level of motion. Mean ϵ values are 1.36 and 1.23 for 10 and 1 Hz, respectively.

Magnitudes and distances chosen from deaggregation to represent the range of values contributing to hazard are as follows:

<u>Annual Frequency</u>	<u>Structural Frequency</u>	<u>description</u>	<u>M</u>	<u>R</u>	<u>weight</u>
1E-4	10 Hz	lower magnitude	5.1	10 km	0.2
„	„	mean magnitude	6.1	14 km	0.6
„	„	upper magnitude	7.8	30 km	0.2
„	1 Hz	lower magnitude	5.4	10 km	0.2
„	„	mean magnitude	6.6	18 km	0.6
„	„	upper magnitude	7.8	30 km	0.2

For each frequency all three magnitudes are used to develop “deaggregation spectra” for Approach 2B (see Section 6.1.2). Only the mean magnitude is used to develop spectra for Approach 2A (Section 6.1.2). The lower and upper magnitude values were selected from the deaggregation results, identifying the magnitude associated with 5% and 95% cumulative probability from the magnitude deaggregation and then selecting the most likely distance associated with this magnitude (from Figures 3-5 and 3-7). The mean magnitude and associated distance (selected as the mean distance) were chosen from deaggregation.

For application of Approach 3 (Section 6.2), we also deaggregated the seismic hazard at 1E-3 and 1E-5 annual frequencies, to select appropriate magnitudes and distances. These are as follows:

<u>Annual Frequency</u>	<u>Structural Frequency</u>	<u>description</u>	<u>M</u>	<u>R</u>
1E-3	10 Hz	mean magnitude	6.1	23 km
„	1 Hz	mean magnitude	7.1	28 km
1E-5	10 Hz	mean magnitude	5.9	12 km
„	1 Hz	mean magnitude	6.4	14 km

3.1.2 Soil site conditions

A PSHA was conducted for the Mojave site assuming soil conditions as described in Section 2.1.2. For this analysis the soil attenuation equation was used to compute directly the hazard at the soil surface.

Figure 3-9 illustrates the PGA hazard at the site. By comparison to rock conditions, the soil hazard indicates slightly higher ground motions (0.34g) for the 500-year motion, and somewhat lower ground motions (0.7g) for the 10,000-year motion. This is evidence that the soil is undergoing non-linear response at high levels of input shaking, which is consistent with the deep soil profile and soil parameters chosen for this example (see Section 2.1.2). Table 3-3 documents the seismic hazard curves for soil, for PGA, 10 Hz, 5 Hz, 2.5 Hz, and 1 Hz. Figure 3-10 shows the 1E-3, 1E-4, and 1E-5 UHS for soil conditions, and Table 3-4 indicates the values of UHS for the three annual frequencies. Comparison with the UHS on rock illustrates the larger low-frequency content on soil and the decreased high frequencies.

Figures 3-11 and 3-12 show the contribution to 10 and 1 Hz seismic hazard, respectively, by seismic source. As is the case for the rock site conditions, the San Andreas Fault plays an important role in the seismic hazard at low frequencies, particularly in the range of amplitudes corresponding to 1,000- to 10,000-year return periods.

The deaggregation of seismic hazard by M , R , and ϵ is illustrated in Figures 3-13 through 3-16 for the two natural frequencies and for ground motion amplitudes corresponding to $1E-4$ annual exceedence frequency. The contribution of the San Andreas Fault at 1 Hz is clear (Figure 3-15). As for rock conditions, the ϵ distribution for soil indicates that ground motions above the median ($\epsilon > 0$) dominate the hazard for $1E-4$. The mean values are 1.73 and 1.40 for 10 and 1 Hz, respectively.

3.2 Columbia site

3.2.1 Rock site conditions

We conducted a PSHA for the Columbia site using the seismic sources described in Section 2.2 and the rock attenuation equation described in Section 2.3. These consist of a 1-corner and a 2-corner ground motion model, which were weighted equally in order to produce a composite seismic hazard. Note that the use of equal weights here is only for example and is not meant as a recommendation. The weights actually used in seismic hazard calculations must be justified with sound technical arguments and comparisons to data, where relevant. For the same reasons given for the Mojave site, no epistemic uncertainties were included in the Columbia site analysis other than those just mentioned for the attenuation equation.

Figure 3-17 shows the PGA seismic hazard curve for Columbia. The seismic hazard is, of course, much lower than in California, with a 500-year PGA of about 0.05g and a 10^{-4} PGA of 0.27g. Table 3-5 documents seismic hazard levels for PGA and for 10, 5, 2.5, and 1 Hz SA. Figure 3-18 shows the UHS for Columbia for 10^{-3} , 10^{-4} , and 10^{-5} annual frequencies of exceedence, and the mean UHS are documented in Table 3-6.

The Columbia site was chosen because small earthquakes in the local background dominate the high-frequency hazard, and large distant earthquakes from the Charleston fault dominate the low-frequency hazard. These dominances are illustrated in Figures 3-19 and 3-20, which show the contribution by seismic source for 10 Hz and 1 Hz SA, respectively, for the 1-corner model (results for the 2-corner model are similar). In the annual frequency range of 10^{-3} to 10^{-4} , the Charleston fault controls the seismic hazard at 1 Hz and lower frequencies.

Deaggregation of the seismic hazard shows the contribution by M , R , and ϵ . This deaggregation is illustrated for 10^{-4} annual frequency in Figures 3-21 through 3-24. The first of these figures indicates the contribution by M and R for 10 Hz, for the 1-corner and 2-corner models where the dominance of small, local earthquakes is evident. Figure 3-22 shows the ϵ distributions, where generally positive ϵ values contribute most to the hazard. Figure 3-23 indicates the contribution by M and R for 1 Hz, where the large contribution of Charleston-size events ($M \approx 7.8$, $R \approx 130$ km) is clear for

both ground motion models. The ϵ distribution from these events also indicates positive values (Figure 3-24).

Values of **M** and **R** chosen from deaggregation of the hazard at 10^{-4} to represent the range of magnitudes and distances contributing to hazard are as follows:

<u>Annual Frequency</u>	<u>Structural Frequency</u>	<u>description</u>	<u>M</u>	<u>R</u>	<u>weight</u>
1E-4	10 Hz:	lower magnitude	4.6	10 km	0.22
„	„	mean magnitude	6.0	46 km	0.58
„	„	upper magnitude	7.7	130 km	0.20
„	1 Hz:	lower magnitude	6.0	10 km	0.07
„	„	mean magnitude	7.2	110 km	0.73
„	„	upper magnitude	7.7	130 km	0.20

For each frequency all three magnitudes were used to develop “deaggregation spectra” for Approach 2B (see Section 6.1.2). Only the mean magnitude at each frequency is used to develop spectra according to Approach 2A (Section 6.1.2). The lower and upper magnitudes were selected from the **M** and **R** deaggregation to represent the contributions of local and Charleston earthquakes, respectively. The weights on the upper magnitudes were calculated to reflect the contribution to the 10^{-4} hazard from the Charleston source, and the weights on the lower magnitudes were calculated to give the correct mean magnitude.

To apply Approach 3 we also deaggregated the seismic hazard at amplitudes corresponding to 10^{-3} and 10^{-5} annual frequencies, to select appropriate magnitudes and distances. These are as follows:

<u>Annual Frequency</u>	<u>Structural Frequency, Hz</u>	<u>description</u>	<u>M</u>	<u>R</u>
1E-3	10 Hz	mean magnitude	6.2	73 km
„	1 Hz	mean magnitude	7.1	115 km
1E-5	10 Hz	mean magnitude	5.8	20 km
„	1 Hz	mean magnitude	7.1	90 km

3.2.2 Soil site conditions

We conducted a PSHA for the Columbia site, using the soil conditions described in Section 2.3. For this analysis we used the soil attenuations for the CEUS (Section 2.3.5), consisting of 1- and 2-corner models weighted equally.

Figure 3-25 shows the PGA hazard at the Columbia site for soil conditions. By comparison to the rock hazard curves (Figure 3-17), the soil shows slightly higher amplitudes at 10^{-3} annual frequency

(0.11g vs. 0.08g on rock), about the same amplitudes at 10^{-4} annual frequency (~ 0.28 g on both soil and rock), and lower amplitudes at 10^{-5} annual frequency (0.59g vs. 0.68g on rock). This indicates that the soil is behaving more nonlinearly for the extreme motions (low annual frequencies). Table 3-7 documents the seismic hazard curves for soil for PGA and for 10 Hz, 2.5 Hz, and 1 Hz SA. Figure 3-26 plots the 10^{-3} , 10^{-4} , and 10^{-5} UHS for soil, and Table 3-8 indicates the numerical values of UHS for these annual frequencies. Comparison of these spectra with UHS for rock (Figure 3-18) indicates the larger long period content of the soil motion and the spectral peak around 10 Hz.

Figures 3-27 and 3-28 show the contribution to 10 Hz and 1 Hz hazard, respectively, by source. As for the rock hazard analysis, the local background source dominates at 10 Hz and the Charleston source dominates at 1 Hz for annual frequencies between 10^{-3} and 10^{-5} .

The deaggregation of seismic hazard by M , R , and ϵ at 10 and 1 Hz is illustrated in Figures 3-29 through 3-32, for ground motions corresponding to 10^{-4} annual frequency. The contribution of the Charleston source is clear in both the M - R deaggregations and in the ϵ deaggregations (the Charleston source causes the highest spike in both ϵ plots). As is the case for rock conditions, ϵ values for soil are generally greater than zero. Mean values for ϵ are 1.10 and 1.18 for 10 and 1 Hz, respectively.

Table 3-1
Seismic hazard curves
Mojave site, rock conditions

<u>Amplitude, g</u>	<u>PGA</u>	<u>Annual frequency of exceedence</u>			
		<u>10 Hz</u>	<u>5 Hz</u>	<u>2.5 Hz</u>	<u>1 Hz</u>
0.05	6.246E-2	1.281E-1	1.359E-1	9.855E-2	4.614E-2
0.1	2.871E-2	7.086E-2	7.388E-2	5.292E-2	1.983E-2
0.2	7.001E-3	3.432E-2	3.661E-2	2.245E-2	4.234E-3
0.3	2.282E-3	1.788E-2	1.983E-2	1.036E-2	1.311E-3
0.4	9.724E-4	9.716E-3	1.115E-2	5.236E-3	5.235E-4
0.5	5.069E-4	5.567E-3	6.567E-3	2.893E-3	2.520E-4
0.6	3.036E-4	3.370E-3	4.058E-3	1.726E-3	1.398E-4
0.7	1.989E-4	2.149E-3	2.625E-3	1.098E-3	8.610E-5
0.8	1.380E-4	1.436E-3	1.770E-3	7.362E-4	5.703E-5
0.9	9.937E-5	1.001E-3	1.239E-3	5.163E-4	3.972E-5
1	7.343E-5	7.242E-4	8.968E-4	3.759E-4	2.866E-5
1.25	3.712E-5	3.674E-4	4.518E-4	1.926E-4	1.401E-5
1.5	2.015E-5	2.135E-4	2.600E-4	1.119E-4	7.488E-6
1.75	1.152E-5	1.355E-4	1.641E-4	7.049E-5	4.246E-6
1.91	8.230E-6	1.045E-4	1.265E-4	5.400E-5	3.025E-6
2	6.857E-6	9.111E-5	1.102E-4	4.685E-5	2.517E-6
2.5	2.679E-6	4.586E-5	5.597E-5	2.295E-5	9.790E-7
3	1.160E-6	2.523E-5	3.127E-5	1.229E-5	4.223E-7
4	2.728E-7	8.946E-6	1.149E-5	4.175E-6	9.812E-8
5	7.986E-8	3.651E-6	4.847E-6	1.650E-6	2.818E-8

Table 3-2
Uniform hazard spectra
Mojave site, rock conditions

Structural frequency, Hz	Spectral amplitudes, g		
	<u>10⁻³ UHS</u>	<u>10⁻⁴ UHS</u>	<u>10⁻⁵ UHS</u>
100	3.962E-1	8.980E-1	1.816
50	4.178E-1	9.522E-1	1.929
40	4.494E-1	9.974E-1	2.001
31	4.993E-1	1.120	2.259
25	5.621E-1	1.240	2.481
20	6.432E-1	1.396	2.778
18	6.889E-1	1.503	2.999
16	7.412E-1	1.625	3.240
14	7.968E-1	1.715	3.398
12	8.464E-1	1.831	3.658
10	9.003E-1	1.939	3.878
8	9.427E-1	2.002	4.004
7	9.527E-1	2.054	4.138
6	9.646E-1	2.043	4.083
5	9.651E-1	2.065	4.146
4	9.175E-1	1.969	3.951
3	8.228E-1	1.759	3.523
2.5	7.221E-1	1.557	3.170
2	5.710E-1	1.228	2.500
1.3	4.097E-1	8.644E-1	1.806
1	3.266E-1	6.675E-1	1.379
0.6	2.340E-1	4.529E-1	8.561E-1
0.5	2.191E-1	4.170E-1	7.669E-1
0.4	1.755E-1	3.298E-1	5.879E-1
0.2	8.502E-2	1.499E-1	2.412E-1

Table 3-3
 Seismic hazard curves
 Mojave site, Meloland profile

<u>Amplitude, g</u>	<u>PGA</u>	<u>Annual frequency of exceedence</u>			
		<u>10 Hz</u>	<u>5 Hz</u>	<u>2.5 Hz</u>	<u>1 Hz</u>
0.01	3.913E-1	5.622E-1	6.552E-1	6.597E-1	5.163E-1
0.05	8.873E-2	1.589E-1	2.084E-1	1.894E-1	1.192E-1
0.07	6.484E-2	1.151E-1	1.518E-1	1.367E-1	8.675E-2
0.1	4.426E-2	8.086E-2	1.078E-1	9.710E-2	6.372E-2
0.2	1.214E-2	3.283E-2	5.125E-2	4.851E-2	3.282E-2
0.3	3.450E-3	1.344E-2	2.654E-2	2.704E-2	1.665E-2
0.4	1.152E-3	5.538E-3	1.345E-2	1.482E-2	8.445E-3
0.5	4.594E-4	2.396E-3	6.831E-3	8.115E-3	4.485E-3
0.6	2.140E-4	1.111E-3	3.555E-3	4.526E-3	2.503E-3
0.7	1.118E-4	5.542E-4	1.921E-3	2.599E-3	1.459E-3
0.8	6.291E-5	2.959E-4	1.085E-3	1.546E-3	8.838E-4
0.9	3.712E-5	1.672E-4	6.418E-4	9.553E-4	5.547E-4
1	2.260E-5	9.876E-5	3.961E-4	6.137E-4	3.601E-4
1.25	7.136E-6	3.036E-5	1.382E-4	2.369E-4	1.401E-4
1.5	2.465E-6	1.059E-5	5.625E-5	1.083E-4	6.436E-5
1.75	9.140E-7	4.014E-6	2.520E-5	5.508E-5	3.333E-5
2	3.601E-7	1.623E-6	1.205E-5	2.988E-5	1.870E-5
3	1.402E-8	6.954E-8	9.486E-7	3.600E-6	2.738E-6
4	9.571E-10	5.083E-9	1.150E-7	5.949E-7	5.427E-7
5	9.619E-11	5.341E-10	1.855E-8	1.229E-7	1.292E-7

Table 3-4
 Uniform hazard spectra
 Mojave site, Meloland profile

Structural frequency, Hz	Spectral amplitudes, g		
	10^{-3} UHS	10^{-4} UHS	10^{-5} UHS
100	4.140E-1	7.183E-1	1.171
50	4.165E-1	7.233E-1	1.179
40	4.192E-1	7.285E-1	1.187
31	4.252E-1	7.402E-1	1.205
25	4.377E-1	7.470E-1	1.198
20	4.599E-1	7.716E-1	1.218
18	4.741E-1	7.965E-1	1.255
16	4.960E-1	8.189E-1	1.272
14	5.247E-1	8.546E-1	1.310
12	5.627E-1	9.231E-1	1.412
10	6.141E-1	9.975E-1	1.514
8	6.607E-1	1.083	1.665
7	7.048E-1	1.157	1.776
6	7.499E-1	1.234	1.901
5	8.148E-1	1.336	2.060
4	8.535E-1	1.450	2.298
3	9.049E-1	1.550	2.492
2.5	8.900E-1	1.528	2.467
2	8.576E-1	1.490	2.434
1.3	7.511E-1	1.348	2.316
1	7.741E-1	1.353	2.282
0.6	5.545E-1	9.735E-1	1.650
0.5	5.248E-1	9.488E-1	1.648
0.4	4.691E-1	8.799E-1	1.592
0.2	1.704E-1	3.232E-1	5.142E-1

Table 3-5
 Seismic hazard curves*
 Columbia site, rock

<u>Acceleration, g</u>	<u>PGA</u>	<u>Annual frequency of exceedence for:</u>			
		<u>10 Hz</u>	<u>5 Hz</u>	<u>2.5 Hz</u>	<u>1 Hz</u>
.001	1.284E-2	1.284E-2	1.284E-2	1.258E-2	7.906E-3
.005	1.137E-2	1.234E-2	1.109E-2	7.905E-3	3.033E-3
.01	8.574E-3	1.056E-2	8.220E-3	5.097E-3	1.946E-3
.02	5.304E-3	7.487E-3	5.189E-3	3.008E-3	1.033E-3
.05	2.094E-3	3.674E-3	2.261E-3	1.112E-3	1.933E-4
.1	7.655E-4	1.690E-3	8.752E-4	3.207E-4	2.134E-5
.2	2.035E-4	5.596E-4	2.199E-4	5.298E-5	1.426E-6
.3	8.145E-5	2.439E-4	7.908E-5	1.485E-5	3.196E-7
.4	4.040E-5	1.248E-4	3.540E-5	5.736E-6	1.148E-7
.5	2.288E-5	7.124E-5	1.840E-5	2.728E-6	5.117E-8
.6	1.416E-5	4.407E-5	1.064E-5	1.487E-6	2.582E-8
.7	9.336E-6	2.898E-5	6.656E-6	8.899E-7	1.419E-8
.8	6.456E-6	2.000E-5	4.418E-6	5.688E-7	8.294E-9
.9	4.630E-6	1.433E-5	3.068E-6	3.818E-7	5.092E-9
1	3.418E-6	1.060E-5	2.208E-6	2.661E-7	3.252E-9
1.25	1.762E-6	5.523E-6	1.087E-6	1.215E-7	1.210E-9
1.5	1.002E-6	3.200E-6	5.995E-7	6.251E-8	5.175E-10
2	3.921E-7	1.312E-6	2.256E-7	2.079E-8	1.252E-10

* mean results from 1- and 2-corner models

Table 3-6
Uniform hazard spectra*
Columbia site, rock

<u>Structural</u> <u>Frequency, Hz</u>	<u>Spectral Acceleration, g</u>		
	<u>1E-3 UHS</u>	<u>1E-4 UHS</u>	<u>1E-5 UHS</u>
100	8.410E-2	2.740E-1	6.824E-1
50	1.777E-1	6.241E-1	1.611
40	1.815E-1	6.282E-1	1.600
31	1.725E-1	5.853E-1	1.467
25	1.687E-1	5.679E-1	1.407
20	1.664E-1	5.516E-1	1.354
18	1.661E-1	5.461E-1	1.330
16	1.643E-1	5.361E-1	1.296
14	1.599E-1	5.173E-1	1.238
12	1.517E-1	4.847E-1	1.146
10	1.390E-1	4.369E-1	1.020
8	1.199E-1	3.728E-1	8.604E-1
7	1.117E-1	3.422E-1	7.829E-1
6	1.024E-1	3.086E-1	6.964E-1
5	9.140E-2	2.733E-1	6.123E-1
4	7.711E-2	2.309E-1	5.079E-1
3	6.180E-2	1.838E-1	3.959E-1
2.5	5.349E-2	1.566E-1	3.381E-1
2	4.309E-2	1.301E-1	2.729E-1
1.3	2.573E-2	8.420E-2	1.676E-1
1	2.036E-2	6.307E-2	1.214E-1
0.6	1.203E-2	4.230E-2	8.431E-2
0.5	1.020E-2	3.566E-2	7.352E-2
0.4	7.111E-3	2.771E-2	2.388E-2
0.2	2.384E-3	1.240E-2	2.388E-2

* mean results from 1- and 2-corner models

Table 3-7
 Seismic hazard curves*
 Columbia site, Savannah River generic profile

<u>Acceleration, g</u>	Annual frequency of exceedence for:				
	<u>PGA</u>	<u>10 Hz</u>	<u>5 Hz</u>	<u>2.5 Hz</u>	<u>1 Hz</u>
.002	1.276E-2	1.284E-2	1.283E-2	1.279E-2	8.157E-3
.005	1.171E-2	1.271E-2	1.255E-2	1.155E-2	4.855E-3
.01	9.324E-3	1.196E-2	1.115E-2	8.750E-3	3.250E-3
.02	6.259E-3	9.855E-3	8.333E-3	5.785E-3	2.207E-3
.05	2.946E-3	5.881E-3	4.570E-3	3.063E-3	1.110E-3
.07	1.843E-3	4.294E-3	3.293E-3	2.206E-3	6.677E-4
.1	1.208E-3	3.301E-3	2.514E-3	1.664E-3	4.091E-4
.2	2.896E-4	1.400E-3	1.043E-3	6.155E-4	7.165E-5
.3	9.458E-5	6.833E-4	4.985E-4	2.566E-4	1.767E-5
.4	3.849E-5	3.652E-4	2.617E-4	1.183E-4	5.801E-6
.5	1.823E-5	2.098E-4	1.478E-4	5.955E-5	2.402E-6
.6	9.593E-6	1.279E-4	8.862E-5	3.235E-5	1.188E-6
.7	5.444E-6	8.193E-5	5.589E-5	1.878E-5	6.696E-7
.8	3.266E-6	5.459E-5	3.676E-5	1.153E-5	4.138E-7
1	1.325E-6	2.668E-5	1.760E-5	4.990E-6	1.891E-7
1.5	2.146E-7	6.390E-6	4.155E-6	1.049E-6	4.515E-8
2	5.015E-8	2.064E-6	1.367E-6	3.341E-7	1.537E-8

* mean results from 1- and 2-corner models

Table 3-8
Uniform hazard spectra*
Columbia site, Savannah River generic profile

Structural Frequency, Hz	Spectral Acceleration, g		
	<u>1E-3 UHS</u>	<u>1E-4 UHS</u>	<u>1E-5 UHS</u>
100	1.101E-1	2.940E-1	5.930E-1
50	1.415E-1	3.700E-1	7.299E-1
40	1.634E-1	4.217E-1	8.256E-1
31	1.885E-1	4.830E-1	9.475E-1
25	2.087E-1	5.390E-1	1.0567
20	2.221E-1	5.811E-1	1.147
18	2.308E-1	6.065E-1	1.201
16	2.382E-1	6.258E-1	1.240
14	2.389E-1	6.360E-1	1.274
12	2.428E-1	6.469E-1	1.292
10	2.419E-1	6.540E-1	1.321
8	2.306E-1	6.280E-1	1.282
7	2.250E-1	6.170E-1	1.255
6	2.129E-1	5.891E-1	1.196
5	2.046E-1	5.747E-1	1.172
4	1.825E-1	5.328E-1	1.104
3	1.483E-1	4.516E-1	9.365E-1
2.5	1.456E-1	4.224E-1	8.309E-1
2	1.089E-1	3.345E-1	6.802E-1
1.3	9.595E-2	3.063E-1	6.036E-1
1	5.435E-2	1.790E-1	3.475E-1
0.6	5.226E-2	1.848E-1	3.511E-1
0.5	2.875E-2	1.190E-1	2.379E-1
0.4	1.648E-2	7.465E-2	1.485E-1
0.2	3.390E-3	2.179E-2	4.559E-2

* mean results from 1- and 2-corner models

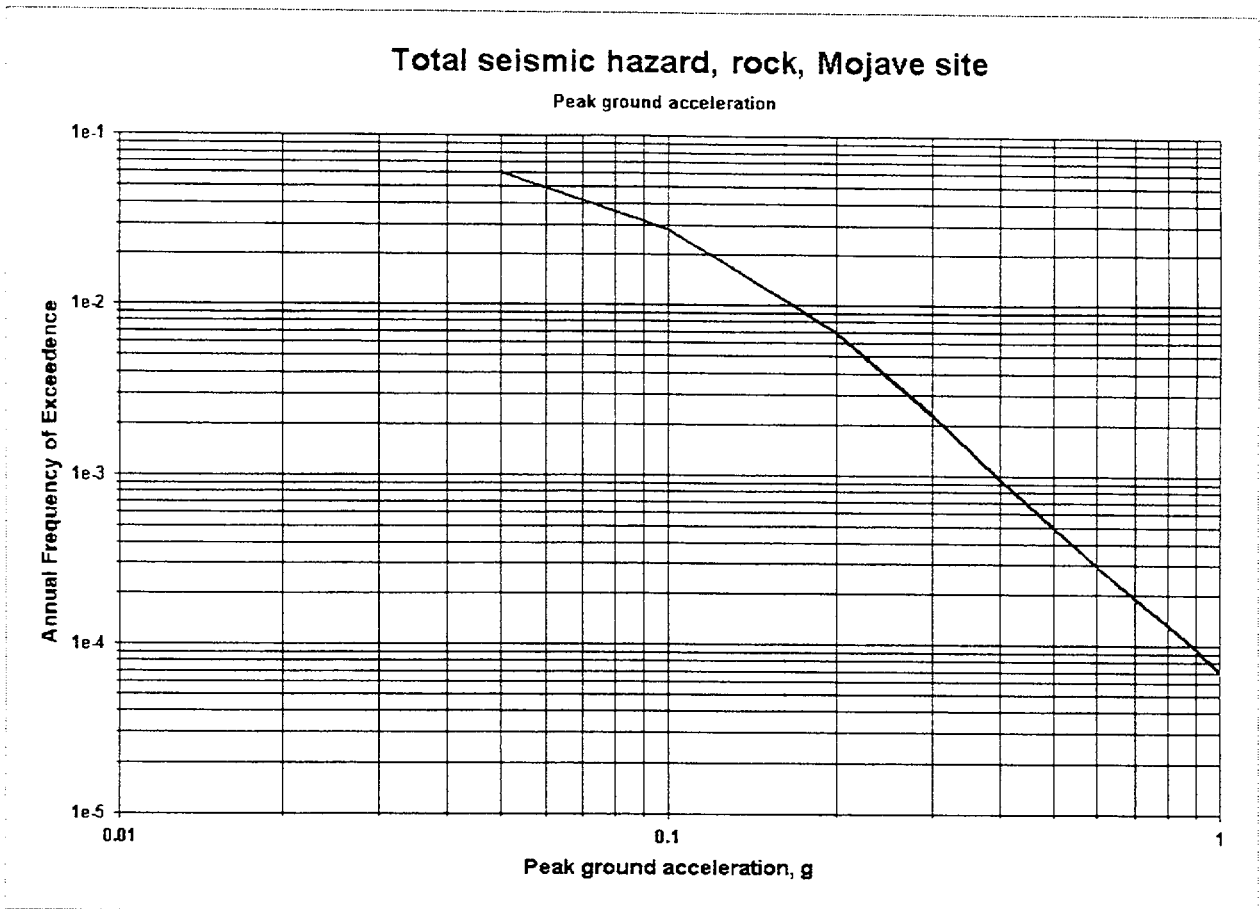


Figure 3-1. PGA seismic hazard curve for Mojave site, rock conditions.

Uniform hazard spectra, rock, Mojave site

Annual frequencies 1E-3, 1E-4, 1E-5

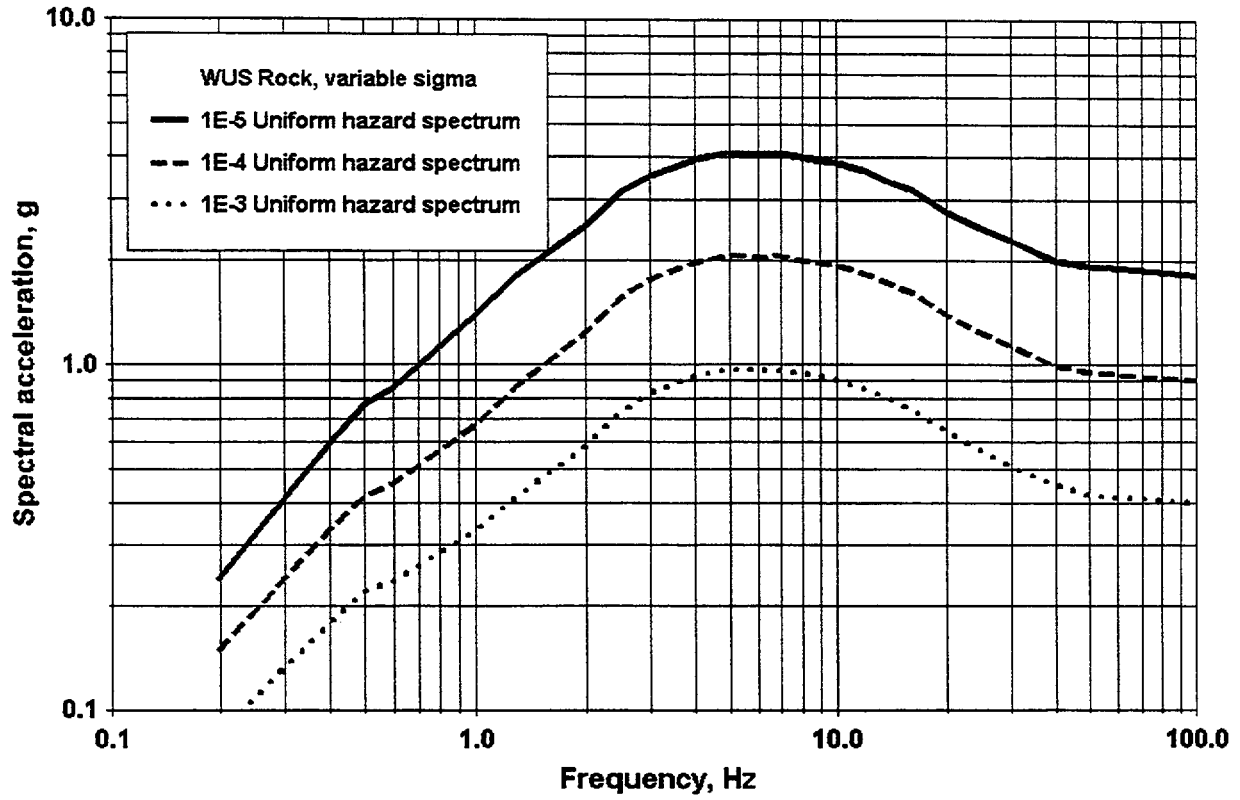


Figure 3-2. UHS for Mojave site, rock conditions.

Hazard contribution by source, 10 Hz, rock, Mojave site

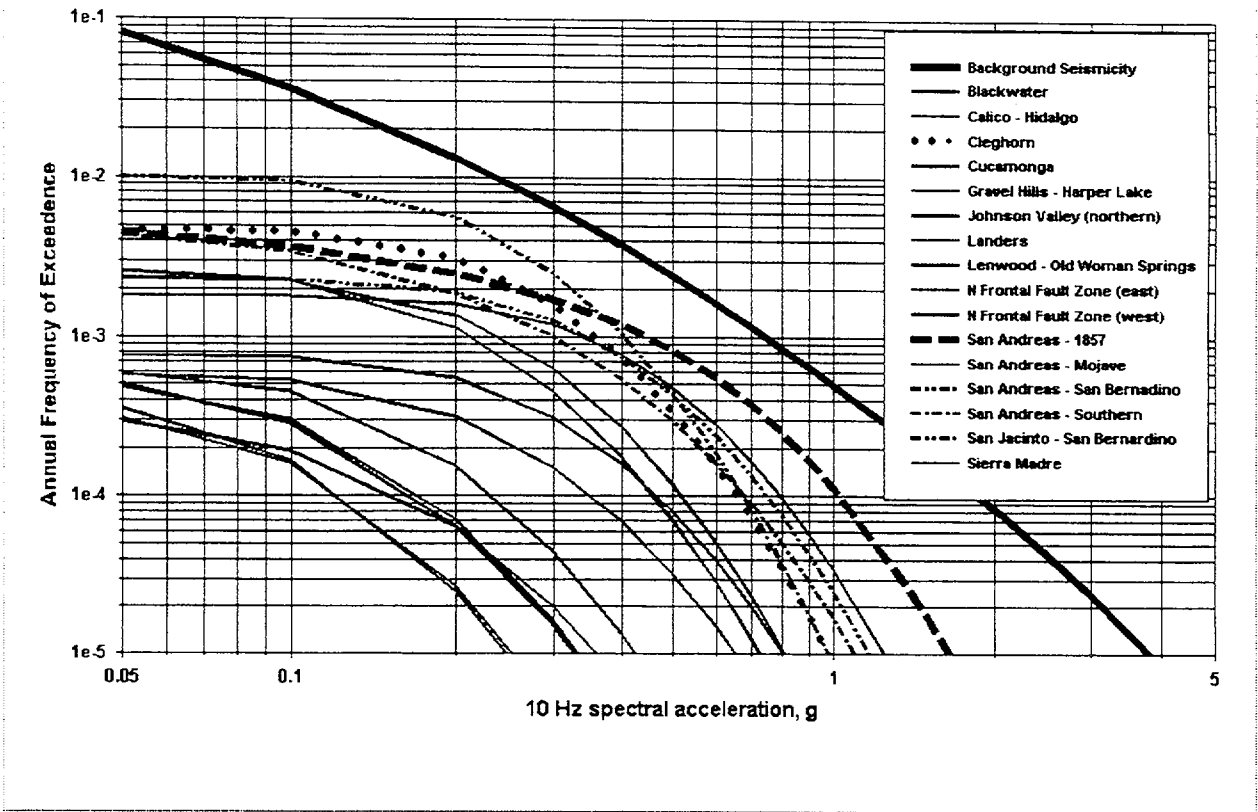


Figure 3-3. Contribution to 10 Hz spectral acceleration hazard by source for Mojave site, rock conditions.

Hazard contribution by source, 1 Hz, rock, Mojave site

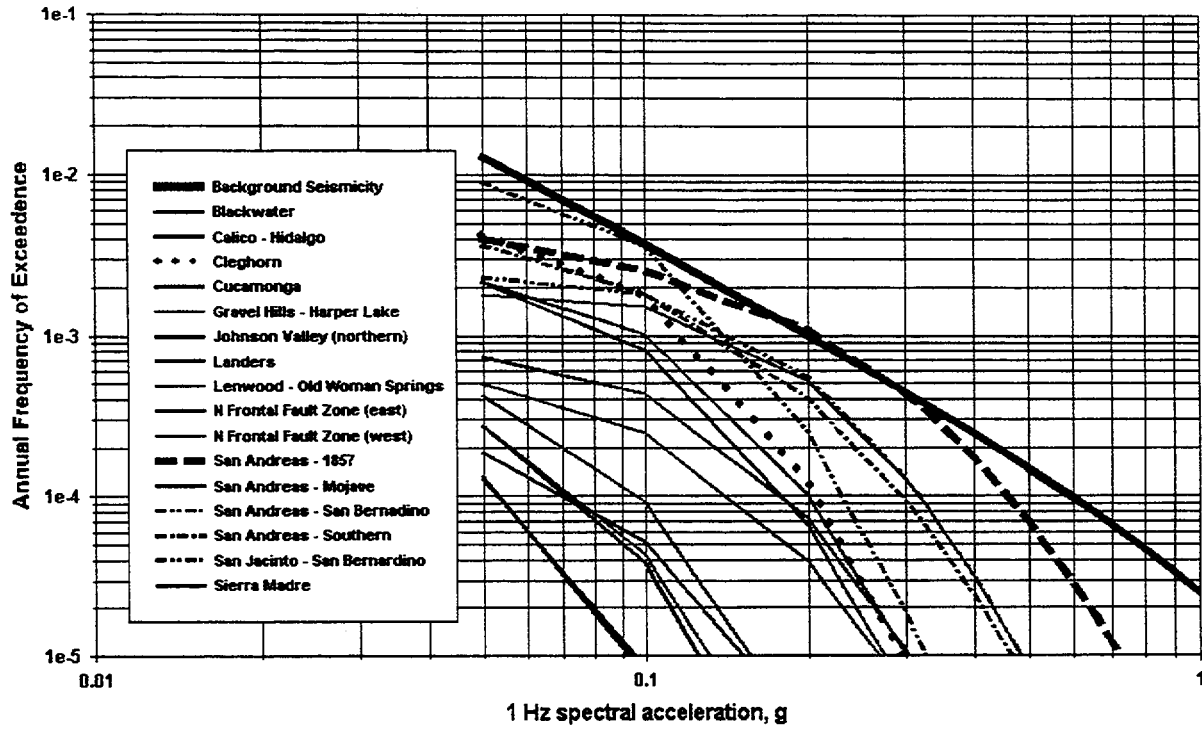


Figure 3-4. Contribution to 1 Hz spectral acceleration hazard for Mojave site, rock conditions.

Magnitude-Distance Deaggregation

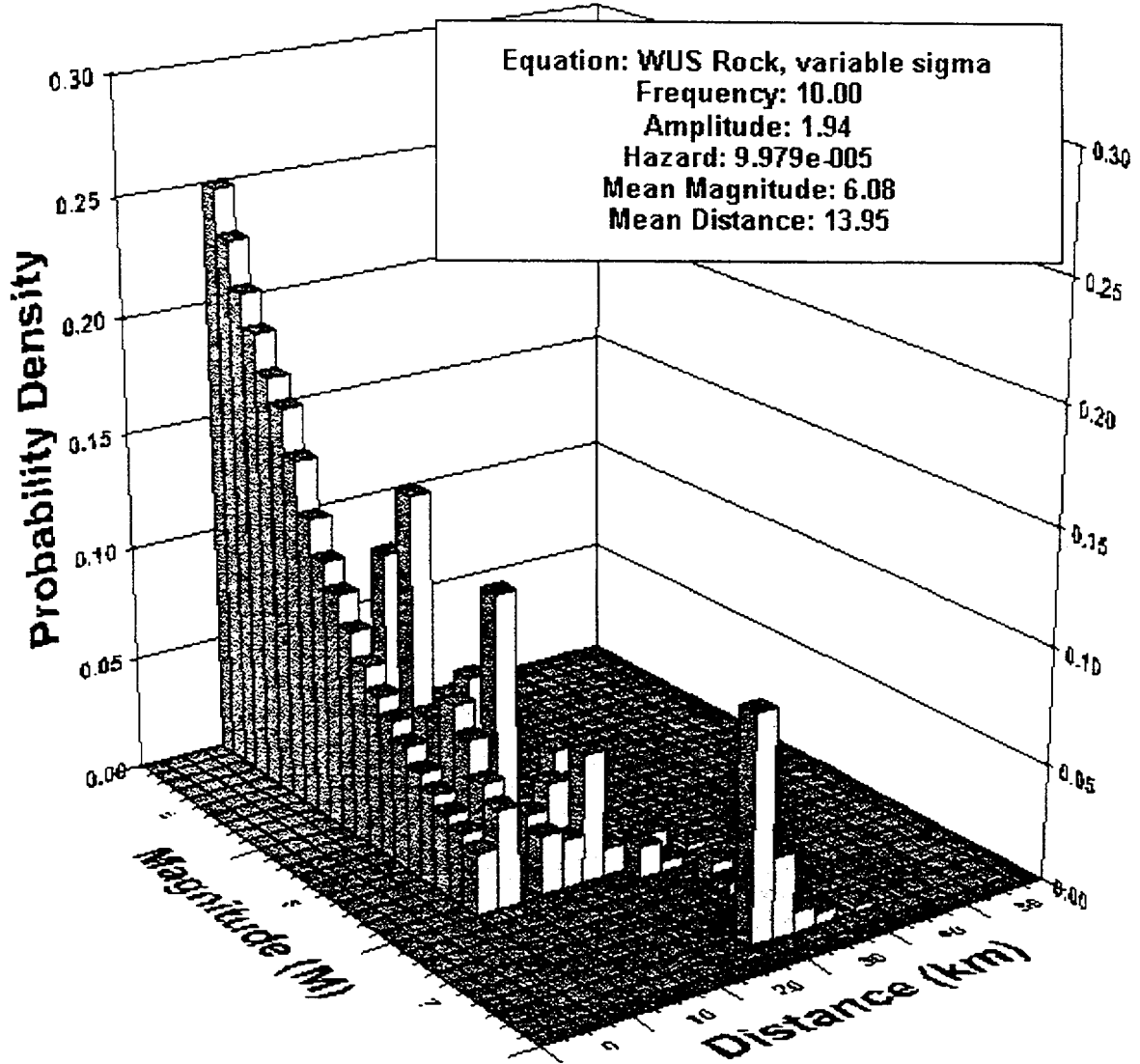


Figure 3-5. Magnitude and distance deaggregation of 10^{-4} hazard at 10 Hz for Mojave site, rock conditions.

Epsilon deaggregation, 10 Hz, rock, Mojave site

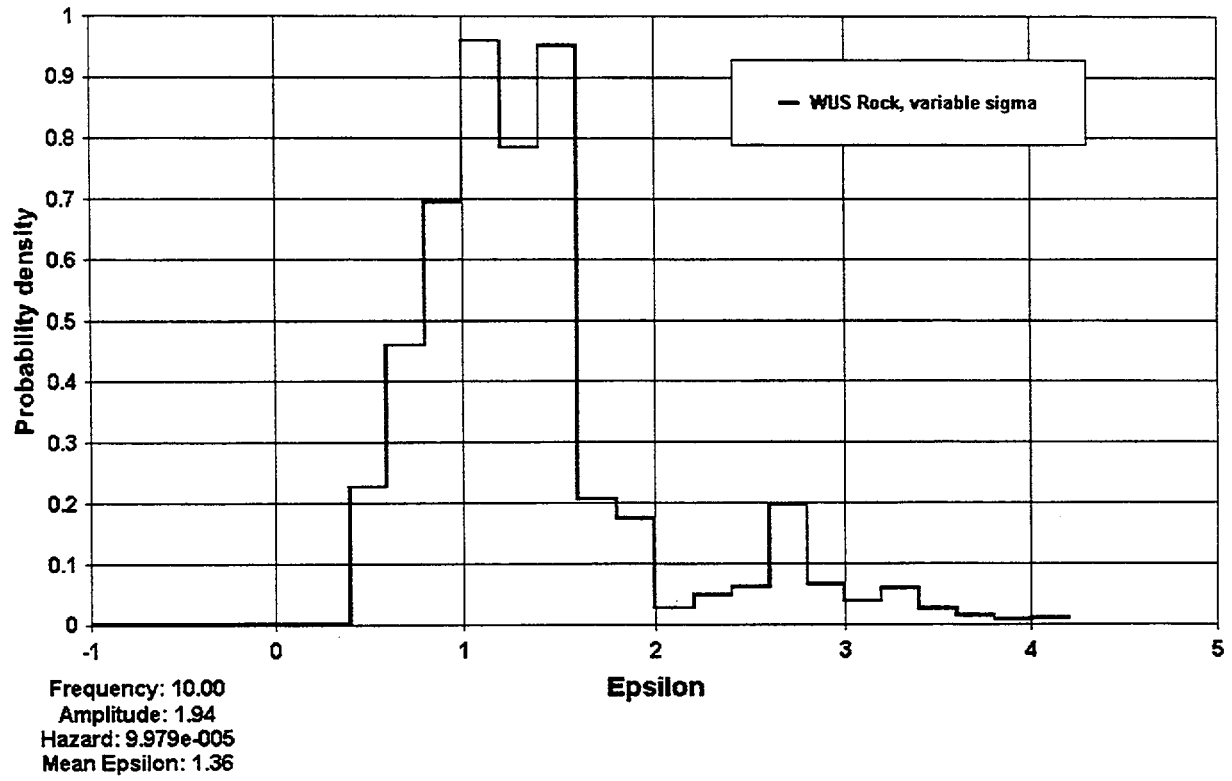


Figure 3-6. Epsilon deaggregation of 10^{-4} hazard at 10 Hz for Mojave site, rock conditions.

Magnitude-Distance Deaggregation

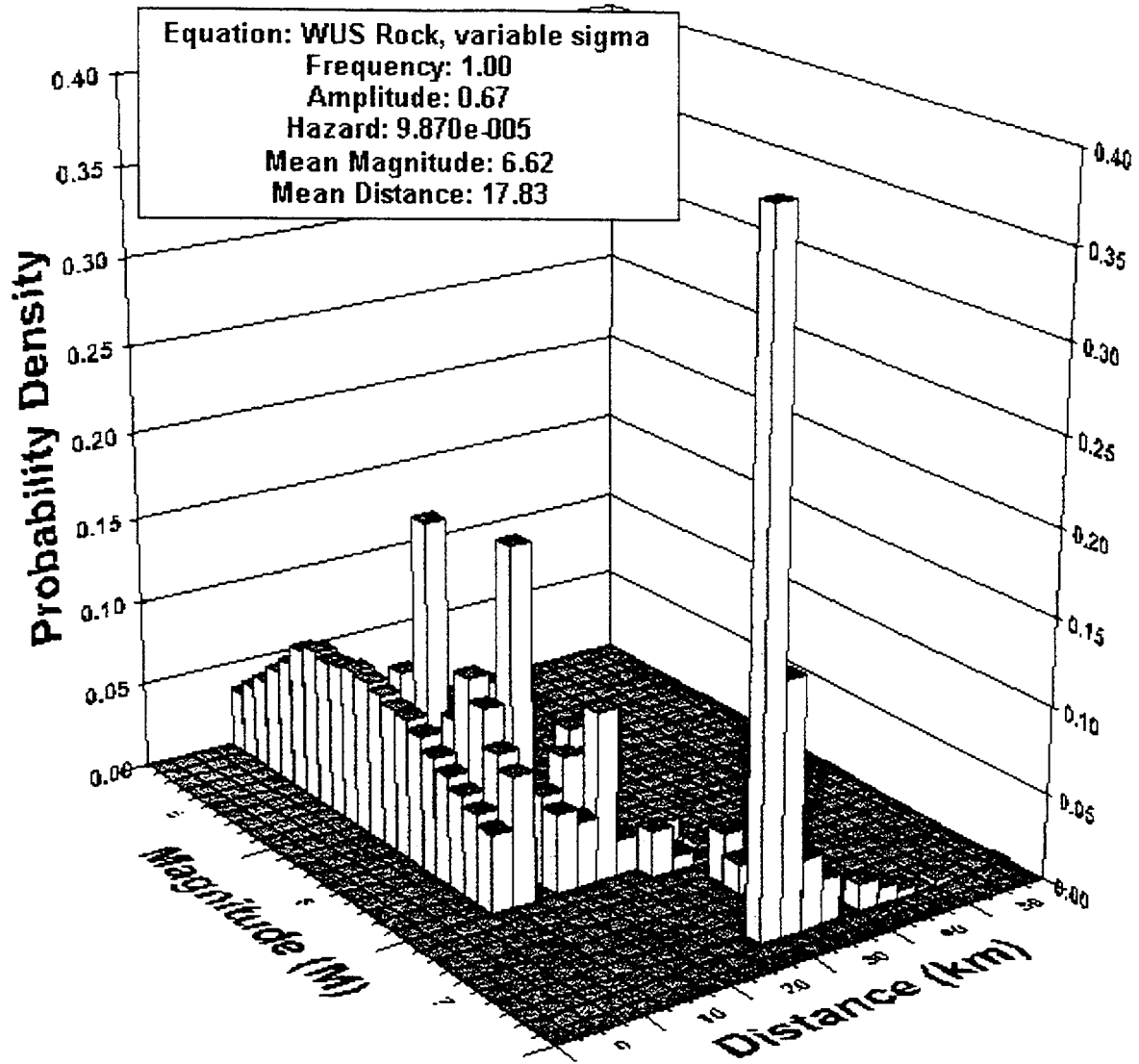


Figure 3-7. Magnitude and distance deaggregation of 10^{-4} hazard at 1 Hz for Mojave site, rock conditions.

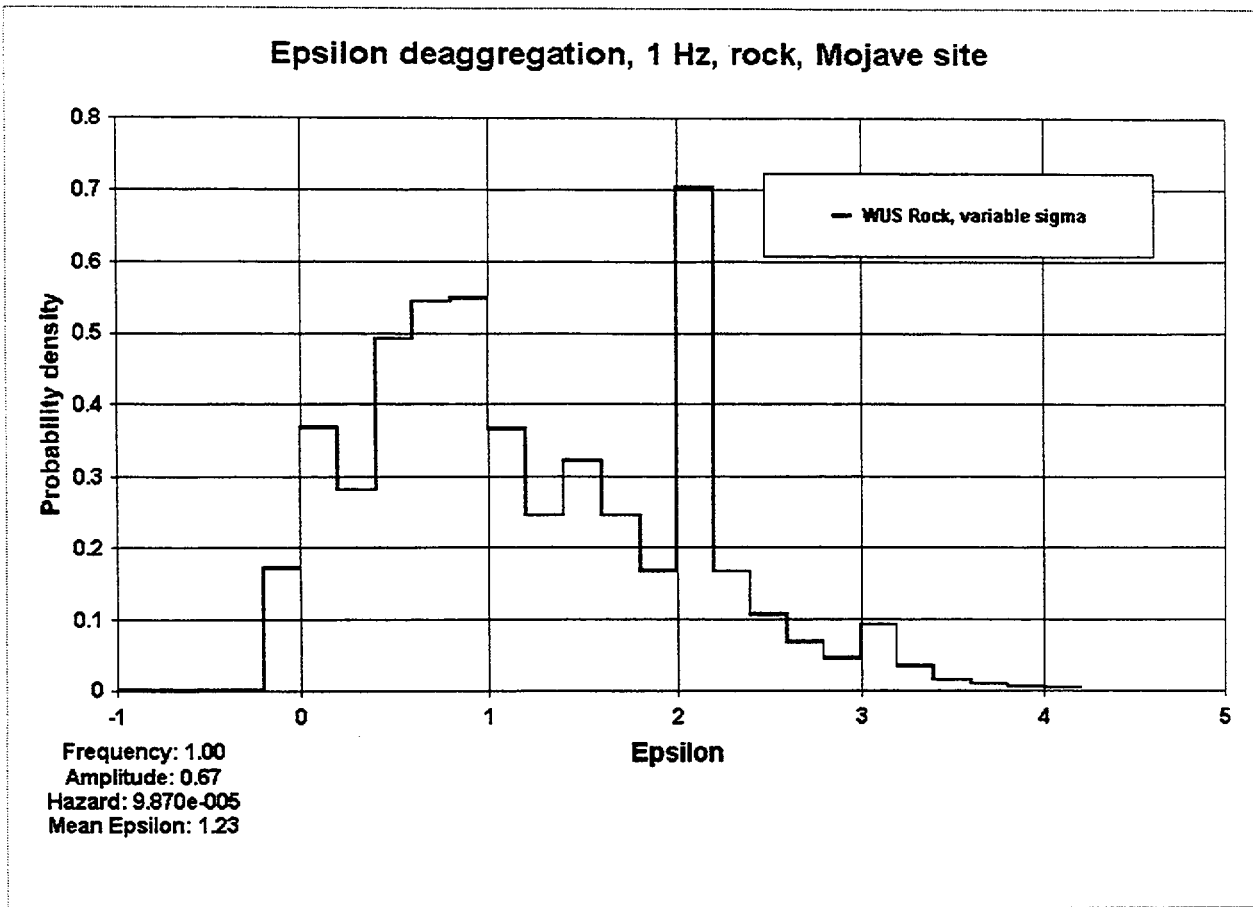


Figure 3-8. Epsilon deaggregation of 10^{-4} hazard at 1 Hz for Mojave site, rock conditions.

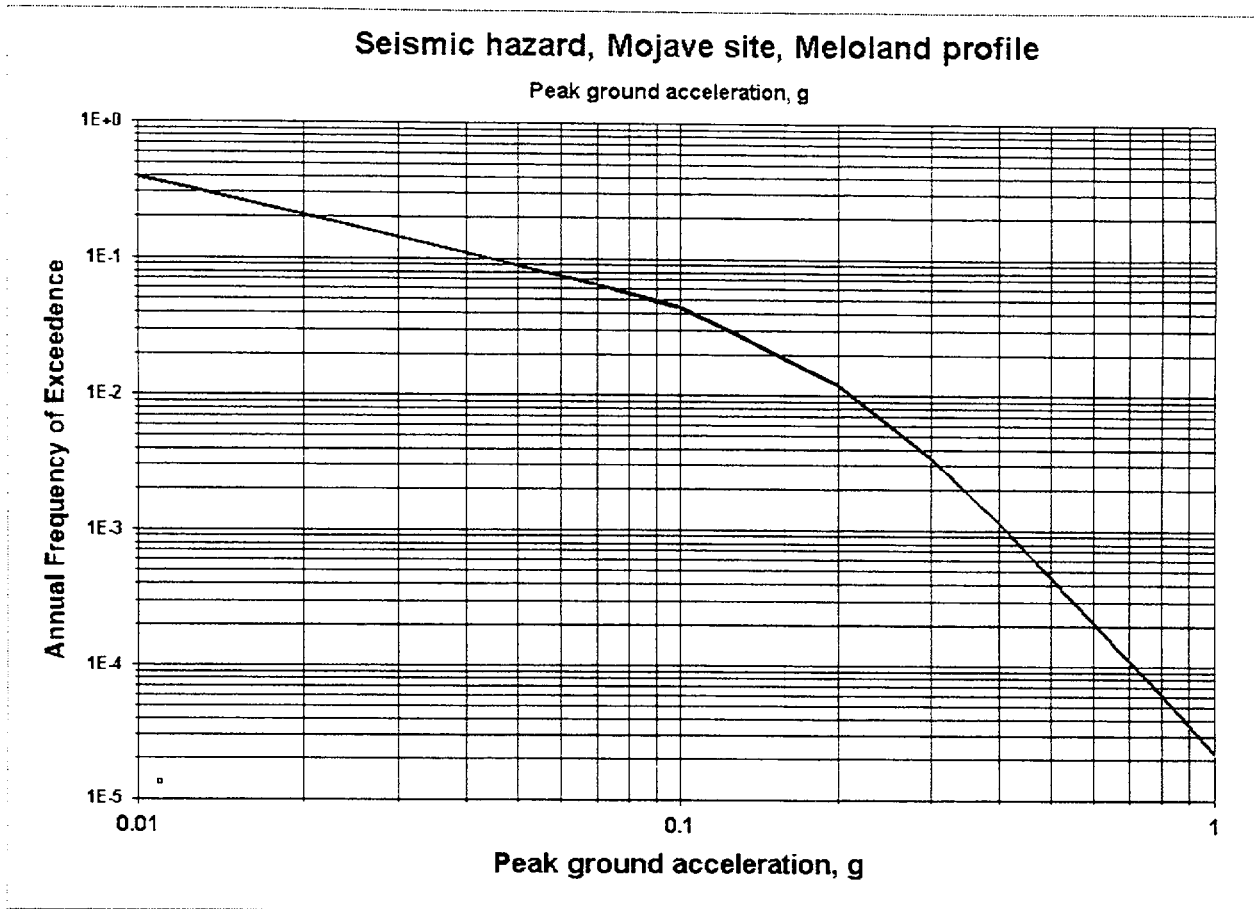


Figure 3-9. PGA seismic hazard curve for Mojave site, soil conditions.

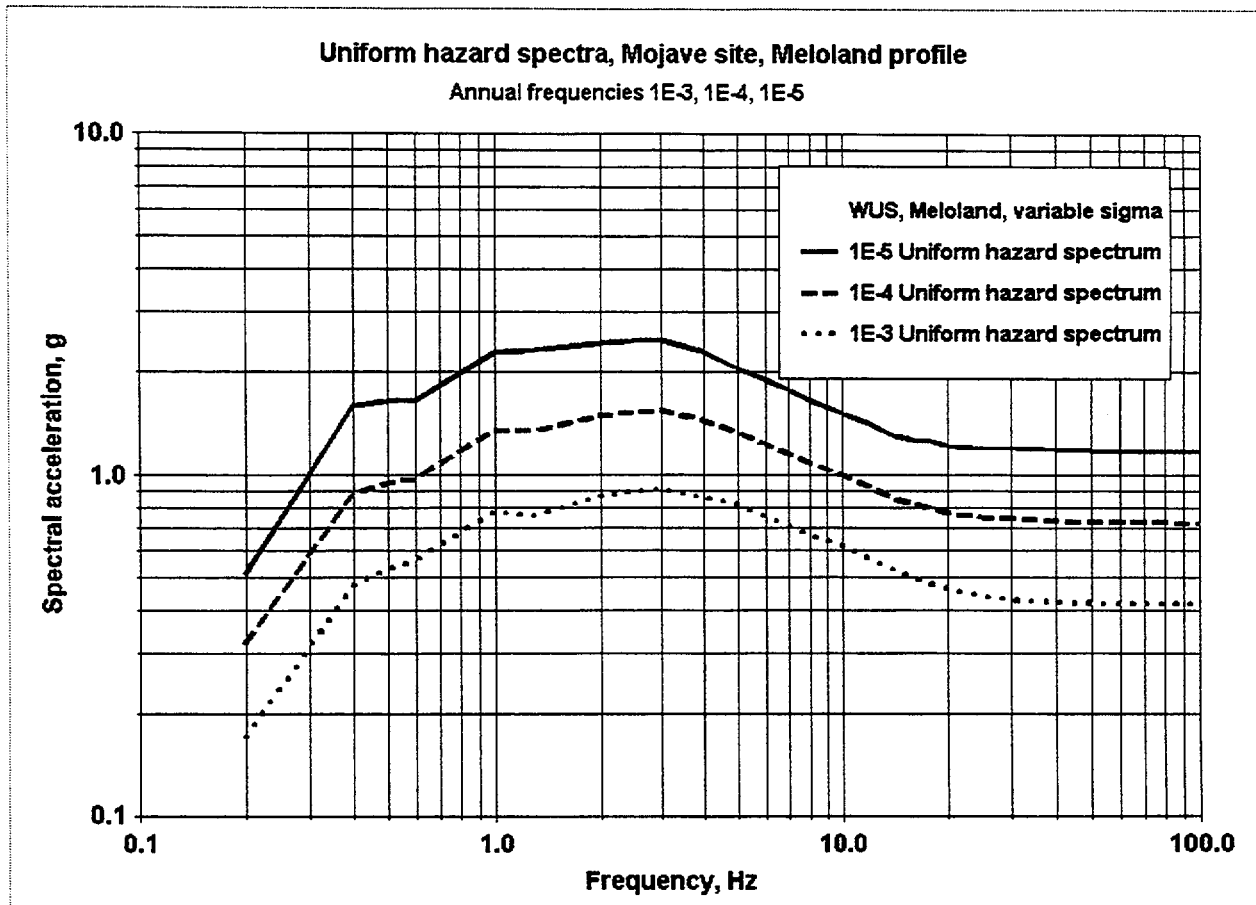


Figure 3-10. UHS for Mojave site, soil conditions.

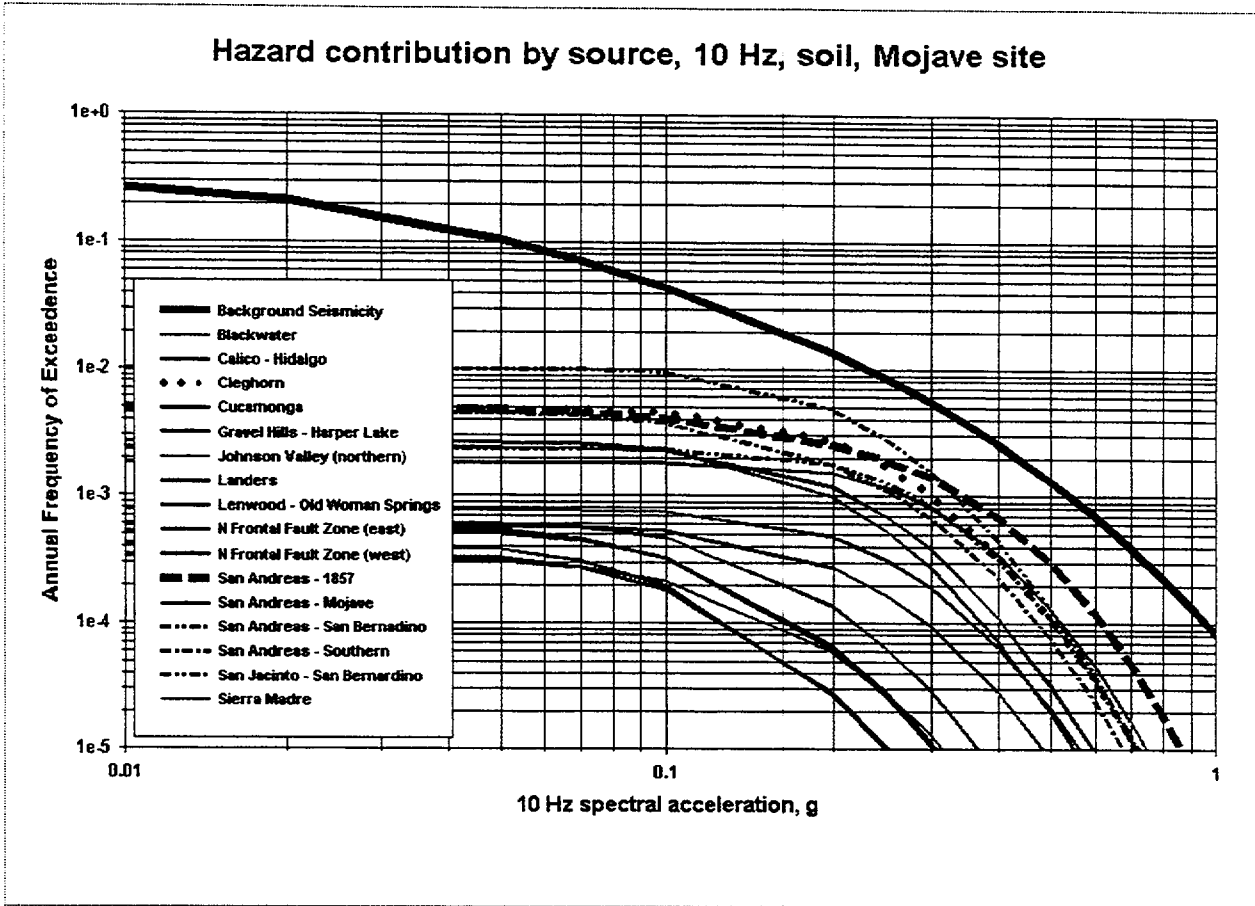


Figure 3-11. Contribution to 10 Hz spectral acceleration hazard by source for Mojave site, soil conditions.

Hazard contribution by source, 1 Hz, soil, Mojave site

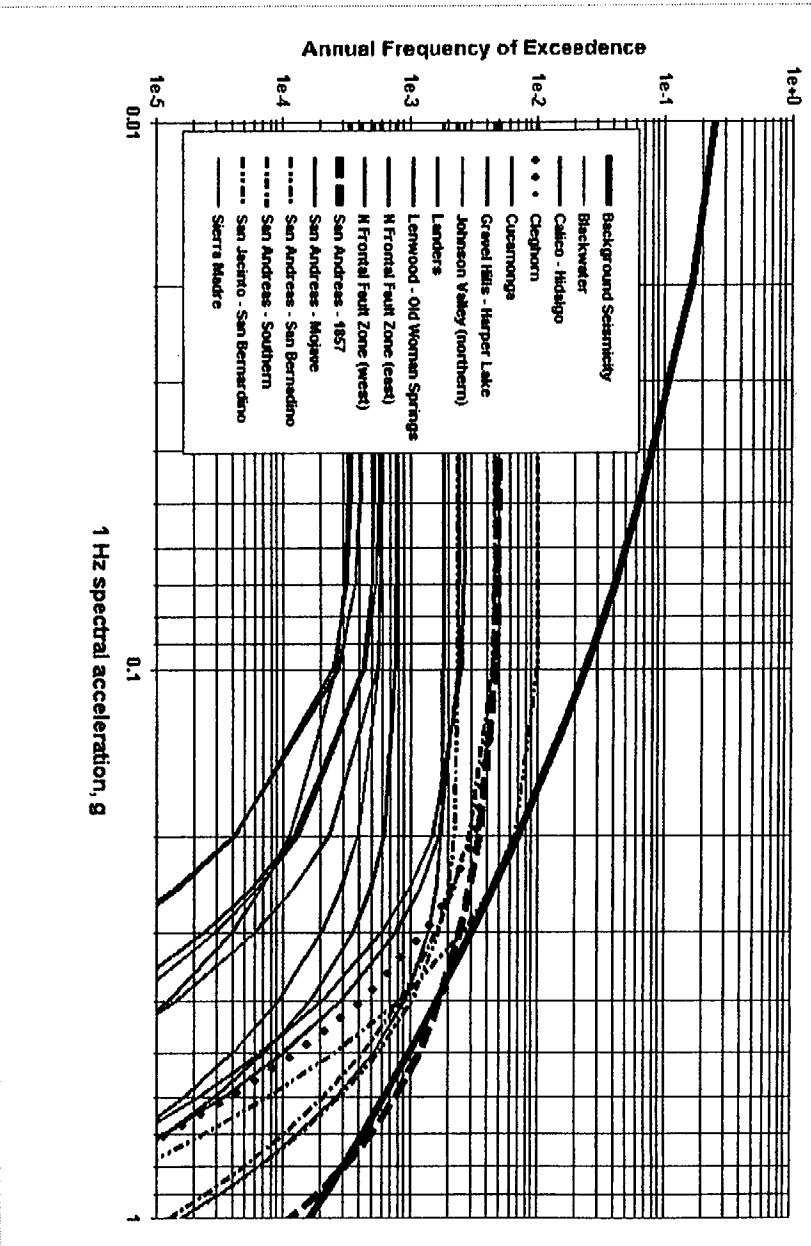


Figure 3-12. Contribution to 1 Hz spectral acceleration hazard for Mojave site, soil conditions.

Magnitude-distance deaggregation, 10 Hz Mojave site, Meloland profile

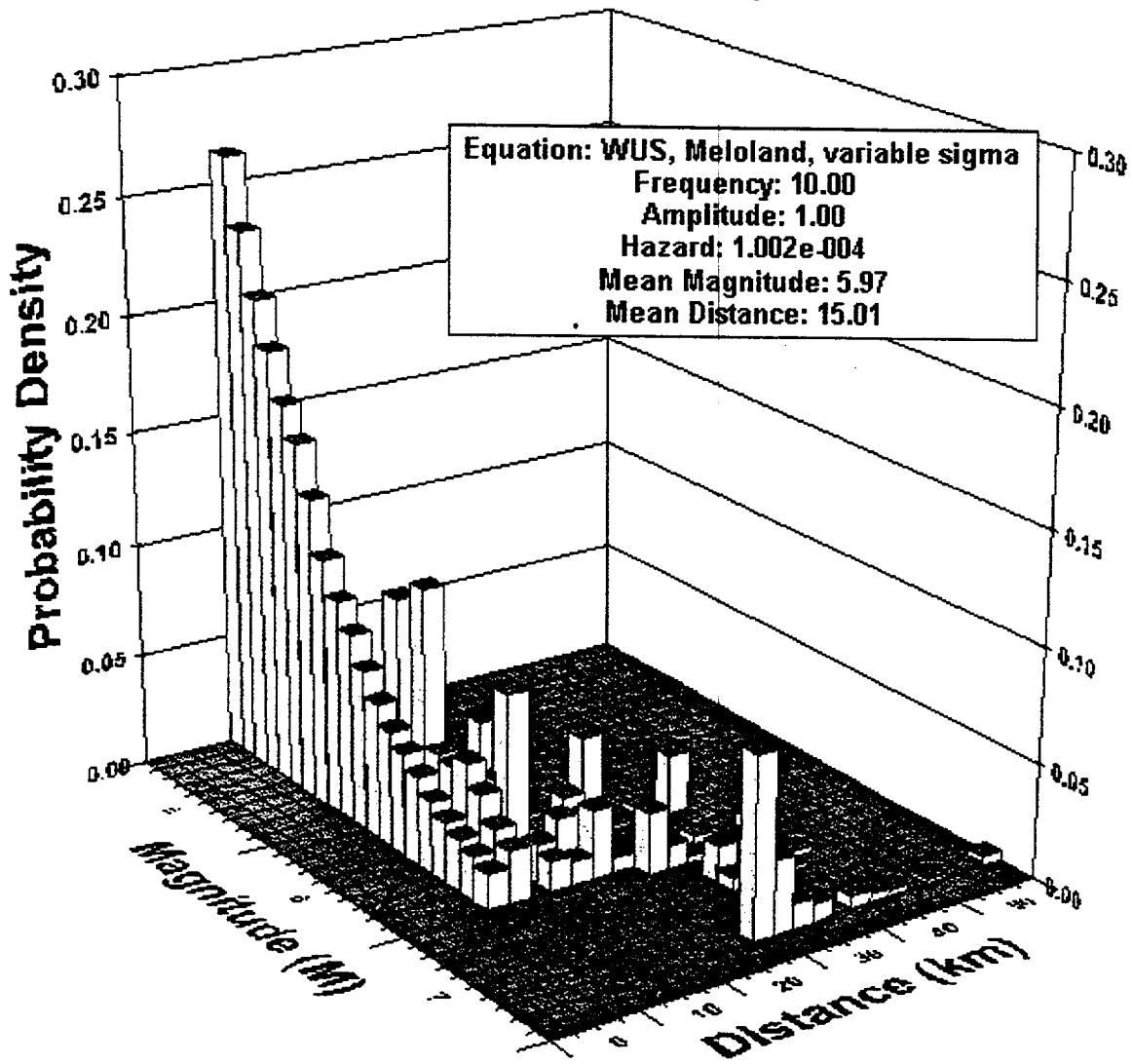


Figure 3-13. Magnitude and distance deaggregation of 10^{-4} hazard at 10 Hz for Mojave site, soil conditions.

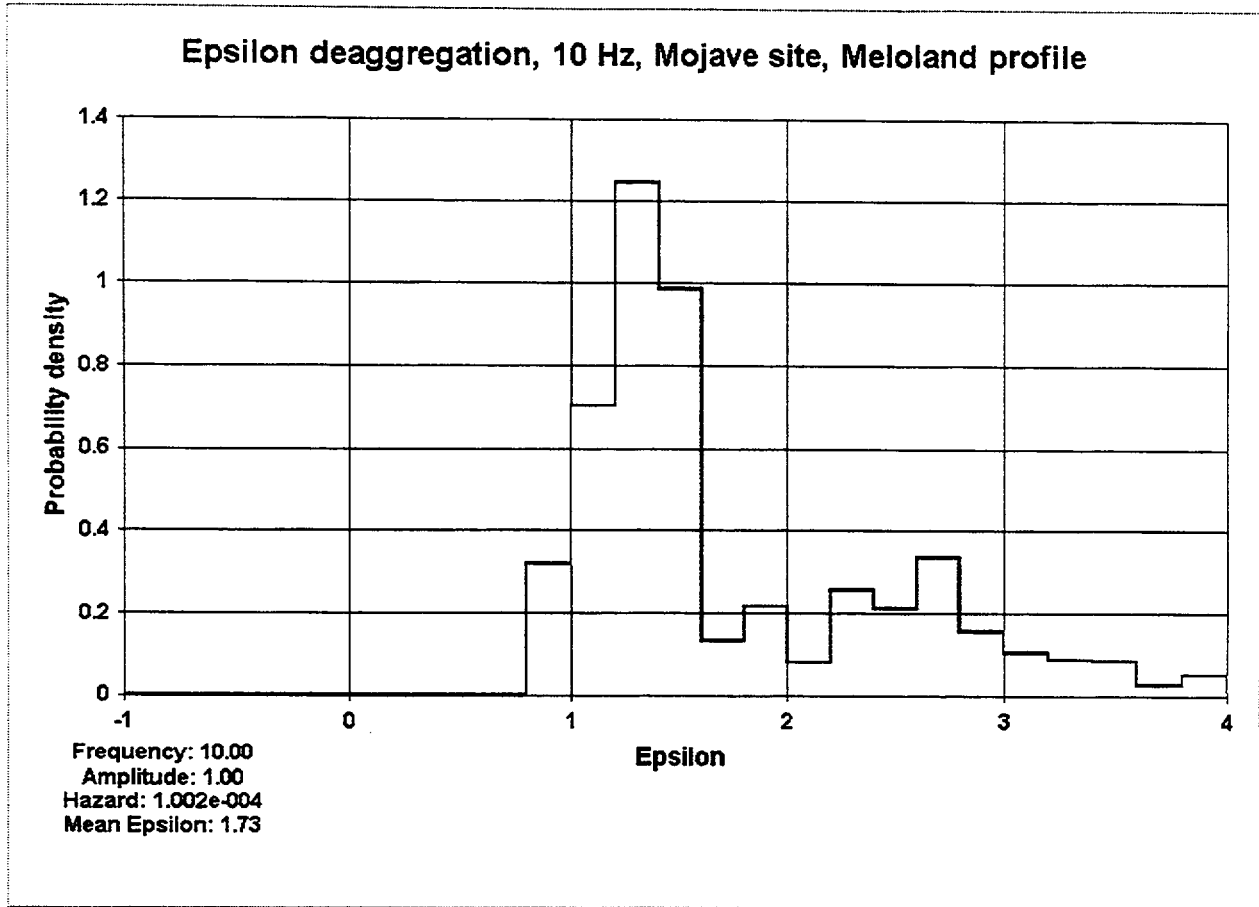


Figure 3-14. Epsilon deaggregation of 10^{-4} hazard at 10 Hz for Mojave site, soil conditions.

Magnitude-distance deaggregation, 1 Hz Mojave site, Meloland profile

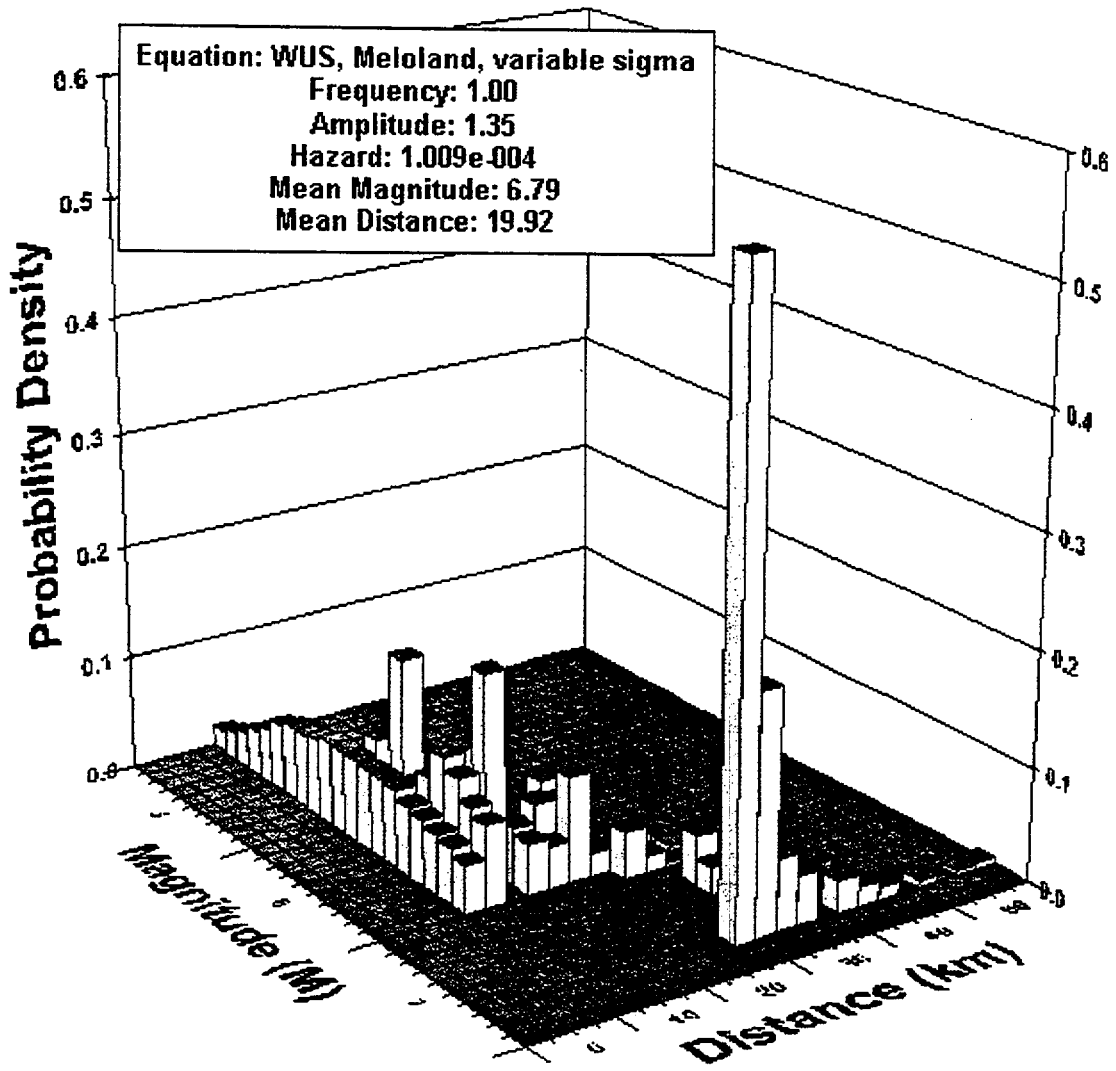


Figure 3-15. Magnitude and distance deaggregation of 10^{-4} hazard at 1 Hz for Mojave site, soil conditions.

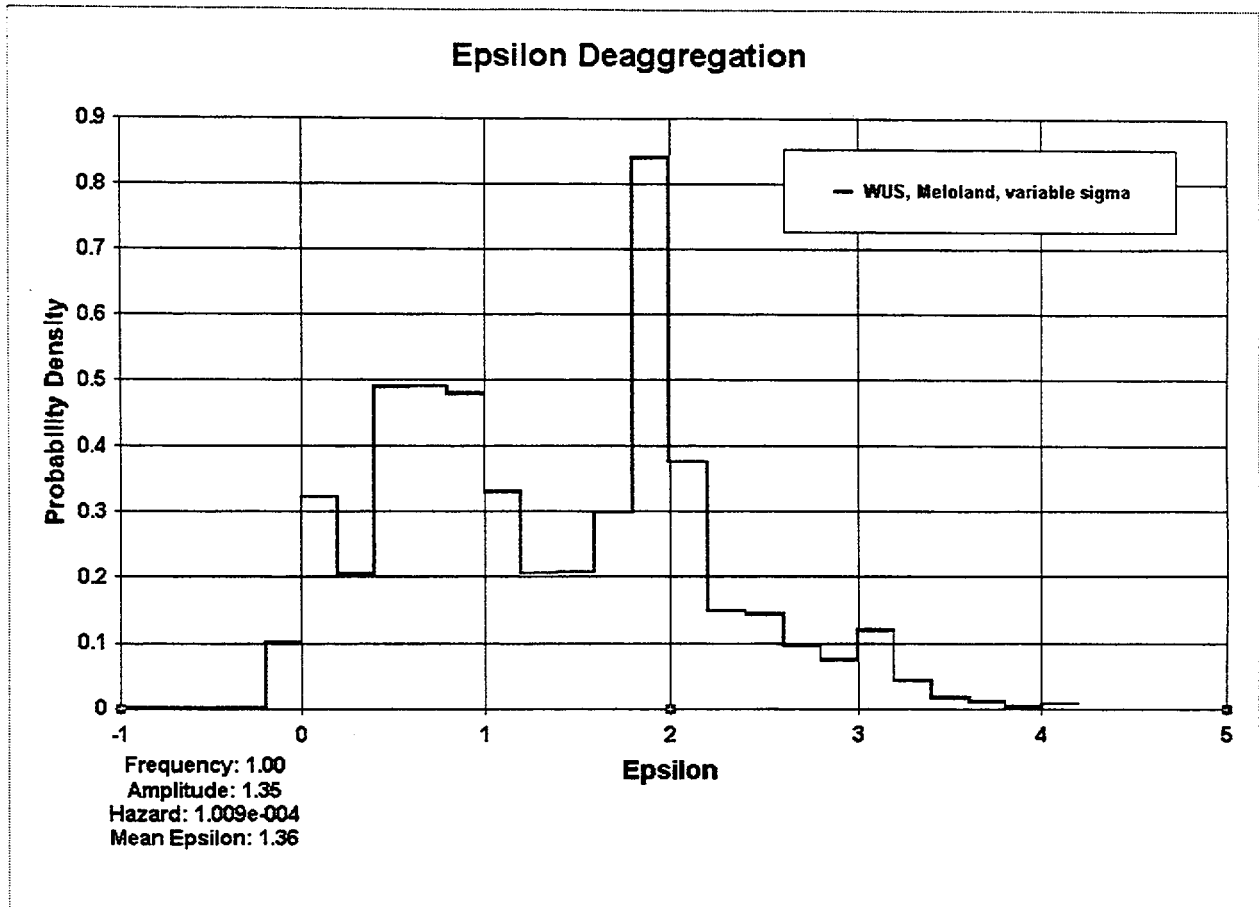


Figure 3-16. Epsilon deaggregation of 10^{-4} hazard at 1 Hz for Mojave site, soil conditions.

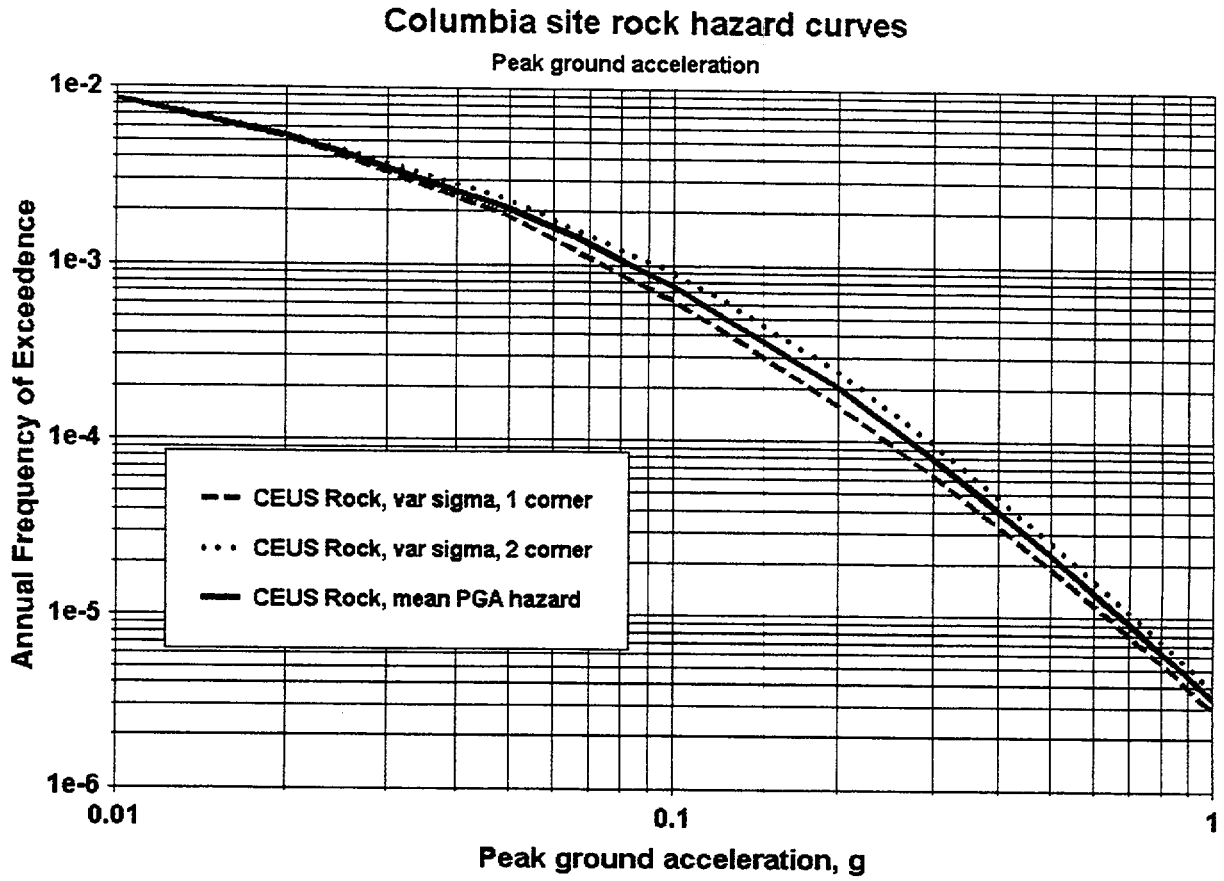


Figure 3-17. PGA seismic hazard, Columbia site, rock.

Uniform hazard spectra, Columbia site
Annual frequencies 1E-3, 1E-4, and 1E-5

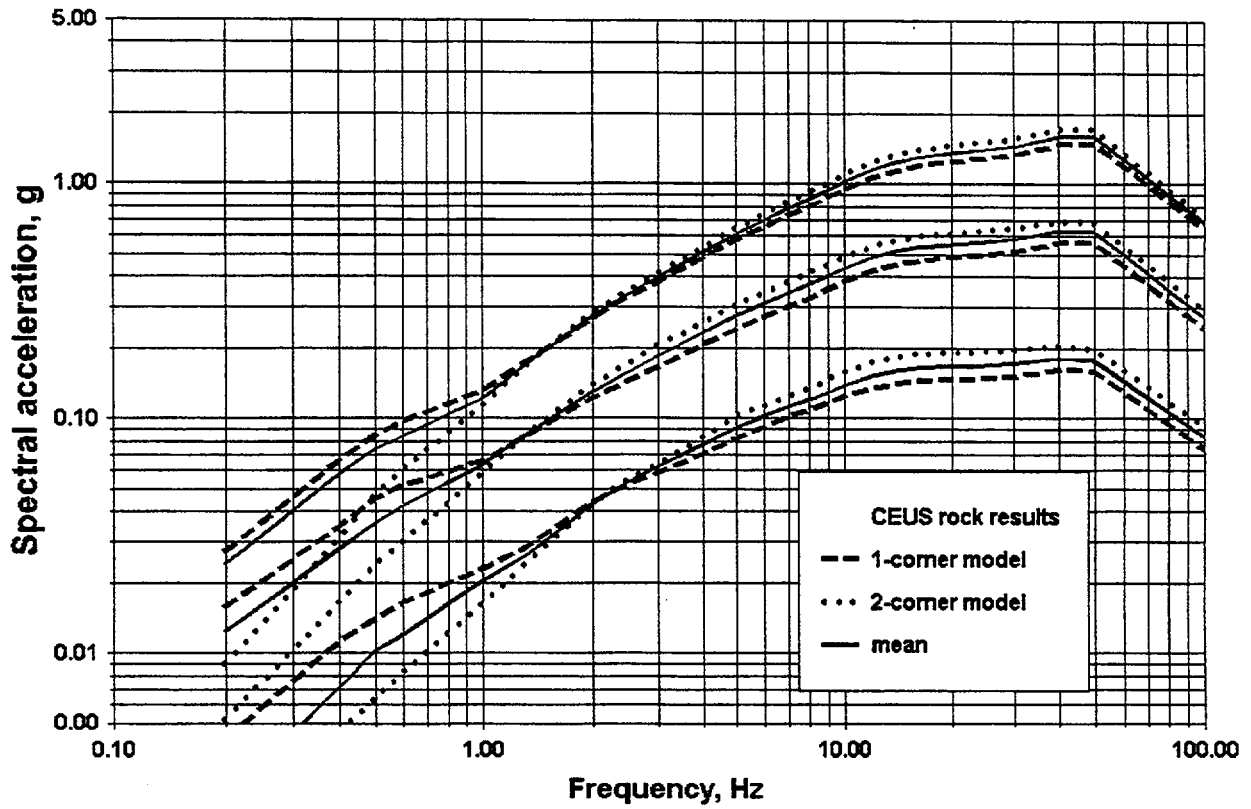


Figure 3-18. UHS for Columbia site, rock: 10^{-5} (top three curves), 10^{-4} (middle three curves), 10^{-3} (bottom three curves).

10 Hz SA hazard contribution by source

CEUS rock, variable sigma, 1-corner model
Frequency = 10 Hz

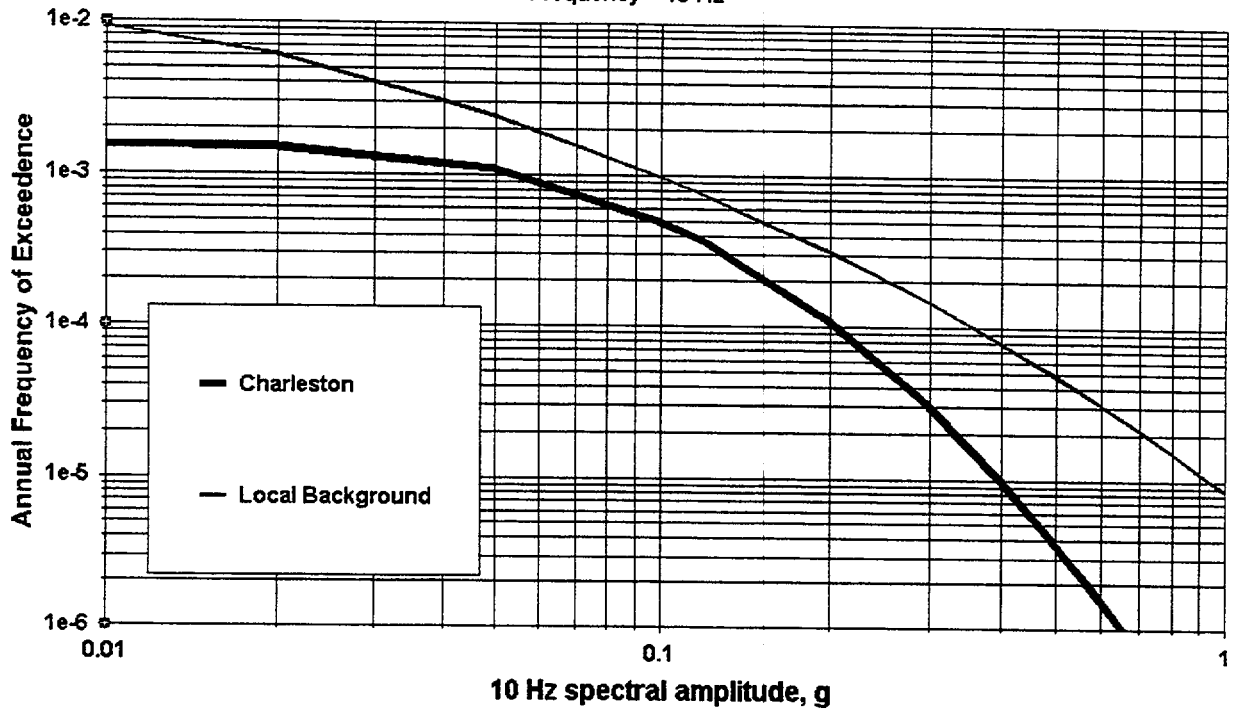


Figure 3-19. Contribution to 10 Hz hazard by source for Columbia site, rock, 1-corner model.

1 Hz SA hazard contribution by source

CEUS rock, variable sigma, 1-corner model
Frequency = 1 Hz

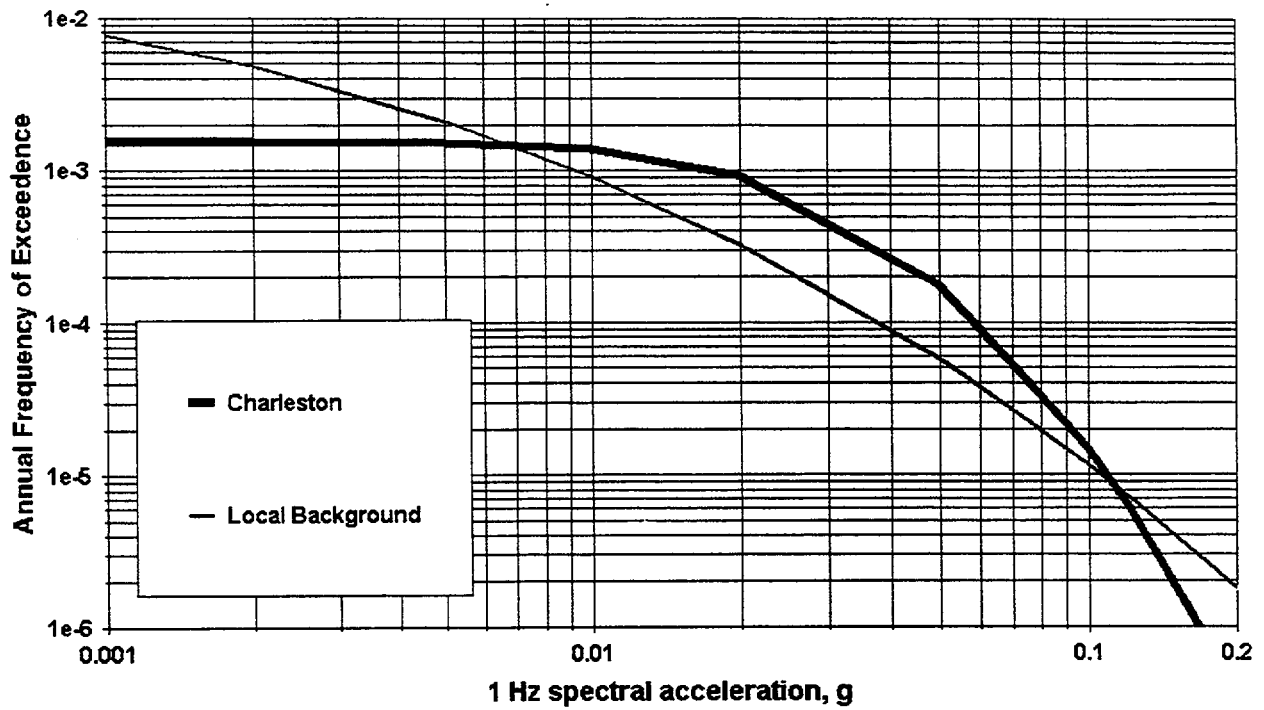
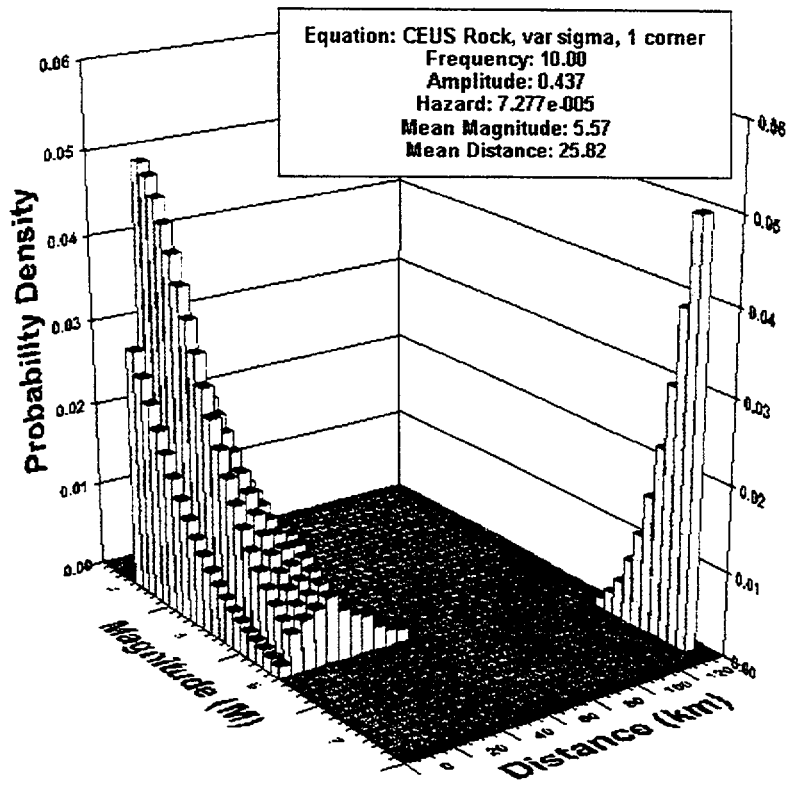


Figure 3-20. Contribution to 1 Hz hazard by source for Columbia site, rock, 1-corner model.

Magnitude-Distance Deaggregation



Magnitude-Distance Deaggregation

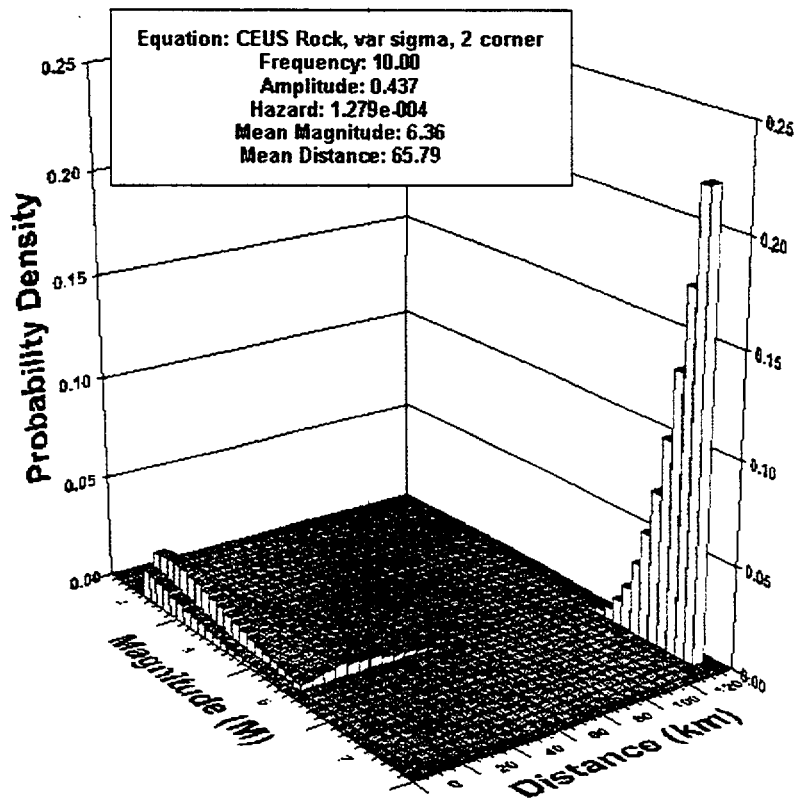


Figure 3-21. $1E-4$ 10 Hz M-R deaggregation for Columbia site, rock, 1-corner model (top) and 2-corner model (bottom).

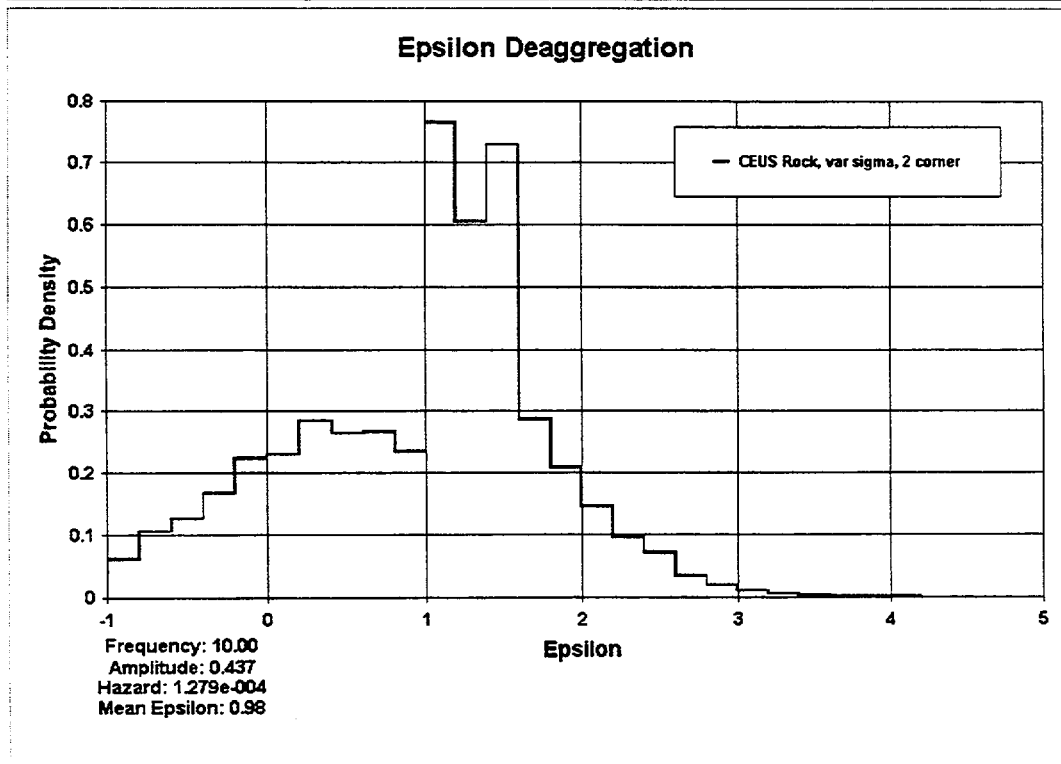
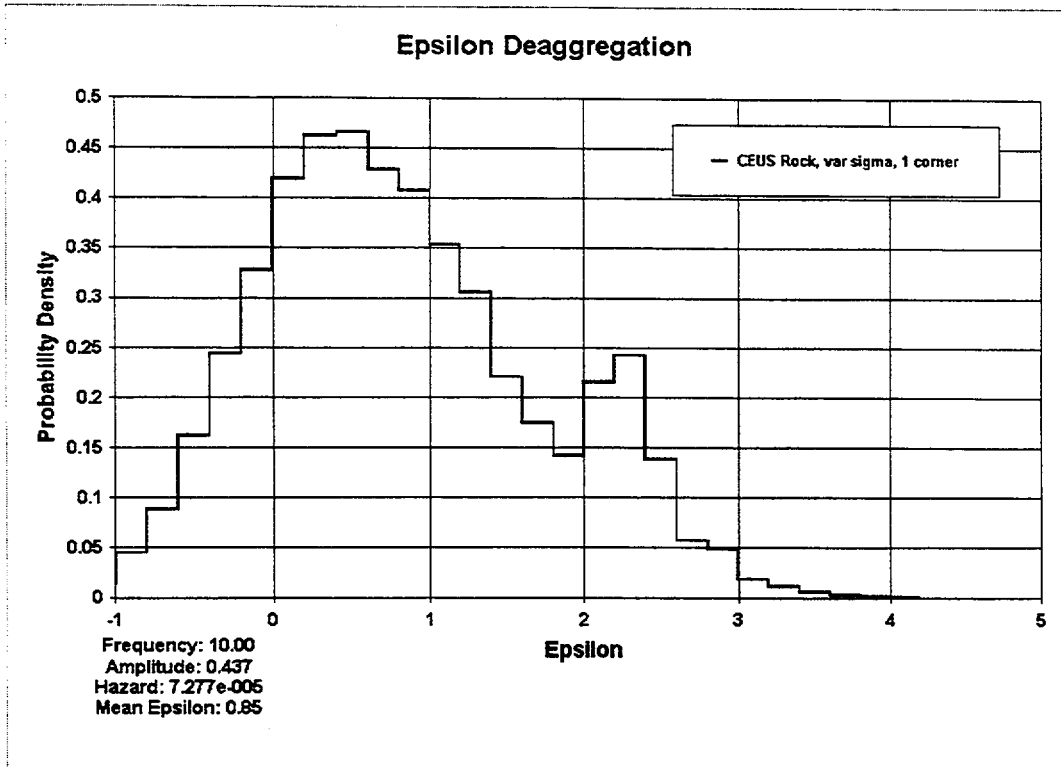
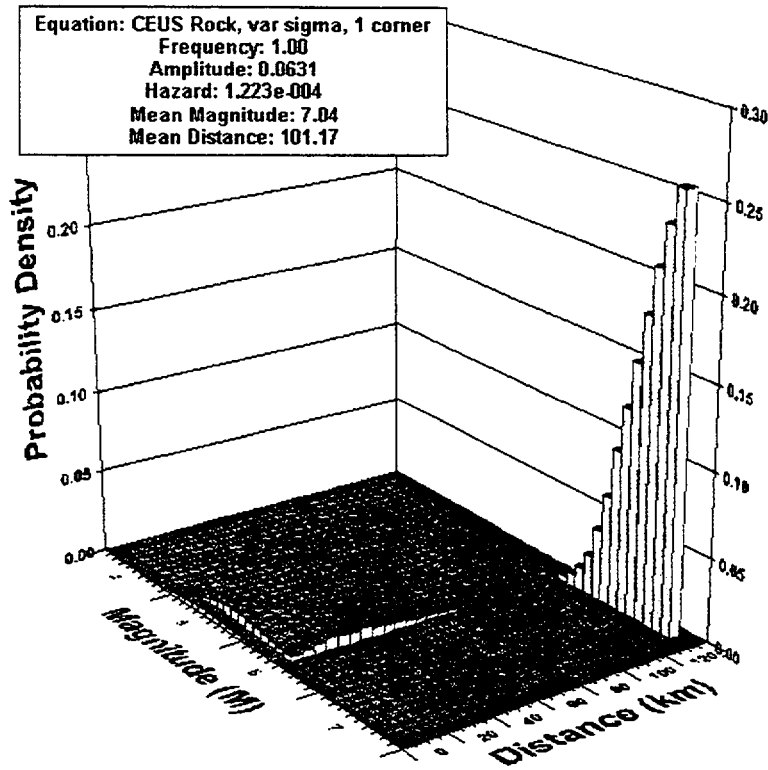


Figure 3-22. 1E-4, 10 Hz, ϵ deaggregation for Columbia site, rock, 1-corner model (top) and 2-corner model (bottom).

Magnitude-Distance Deaggregation



Magnitude-Distance Deaggregation

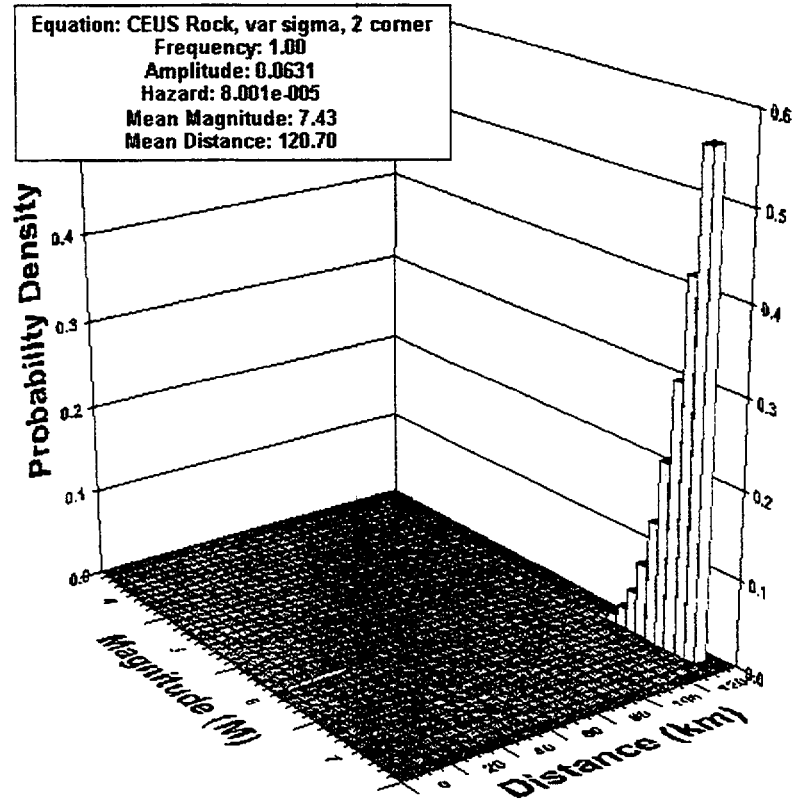


Figure 3-23. 1E-4, 1 Hz, M-R deaggregation for Columbia site, rock, 1-corner model (top) and 2-corner model (bottom).

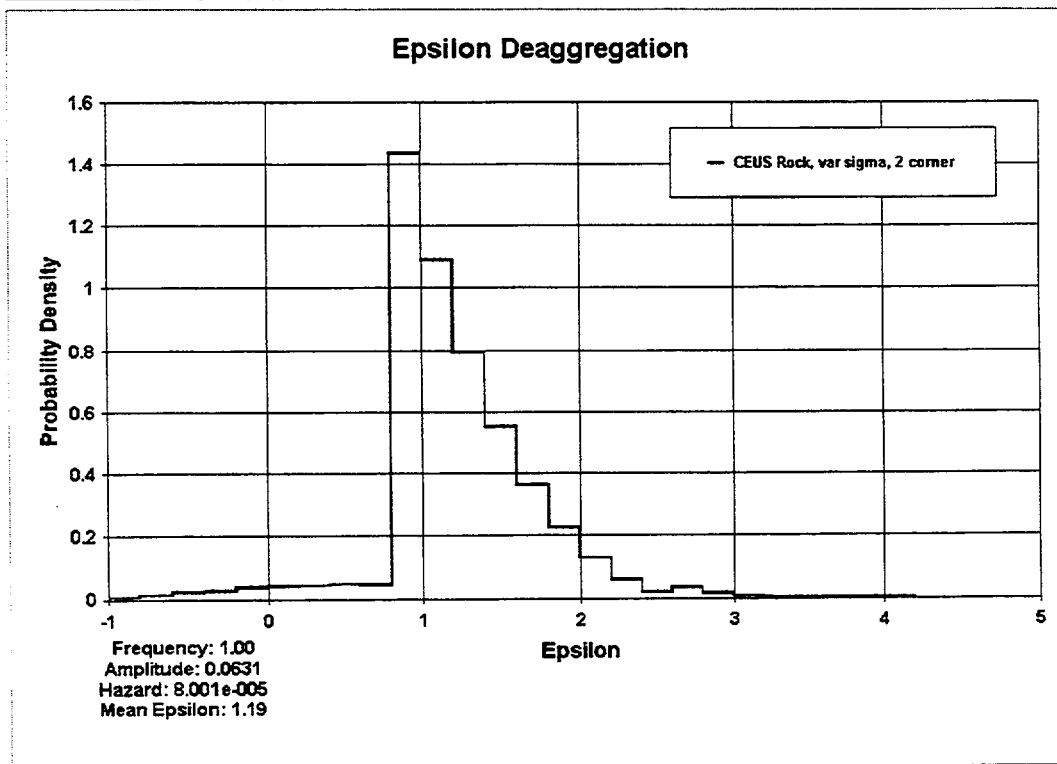
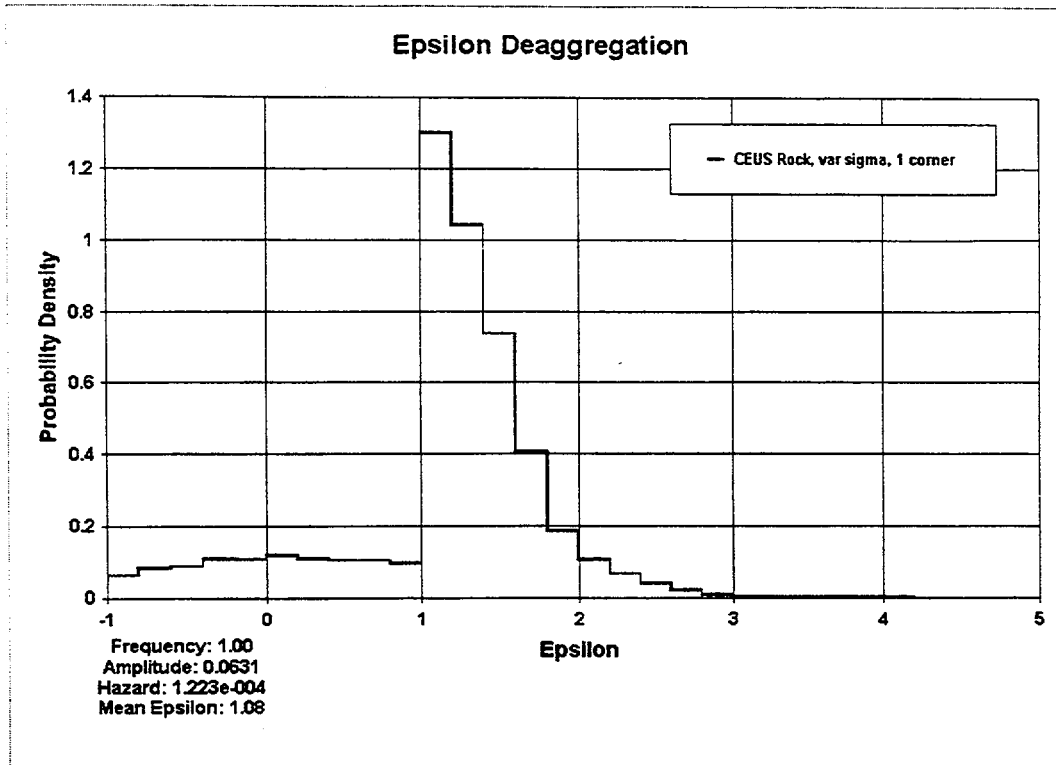


Figure 3-24. $1E-4$, 1 Hz, ϵ deaggregation, Columbia site, rock, 1-corner model (top) and 2-corner model (bottom).

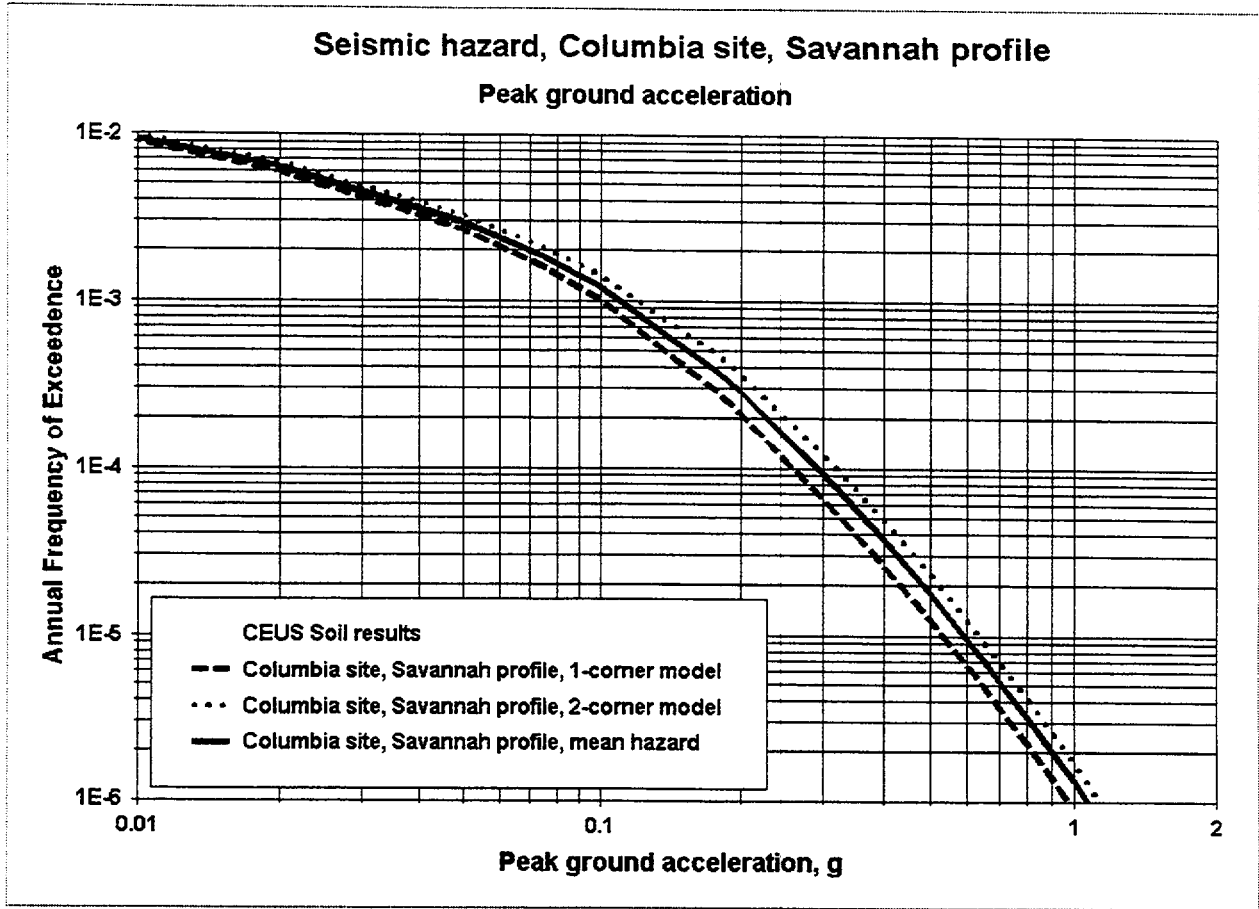


Figure 3-25. PGA seismic hazard, Columbia site, Savannah profile.

Uniform hazard spectra, Columbia site, Savannah profile
Annual frequencies 1E-3, 1E-4, and 1E-5

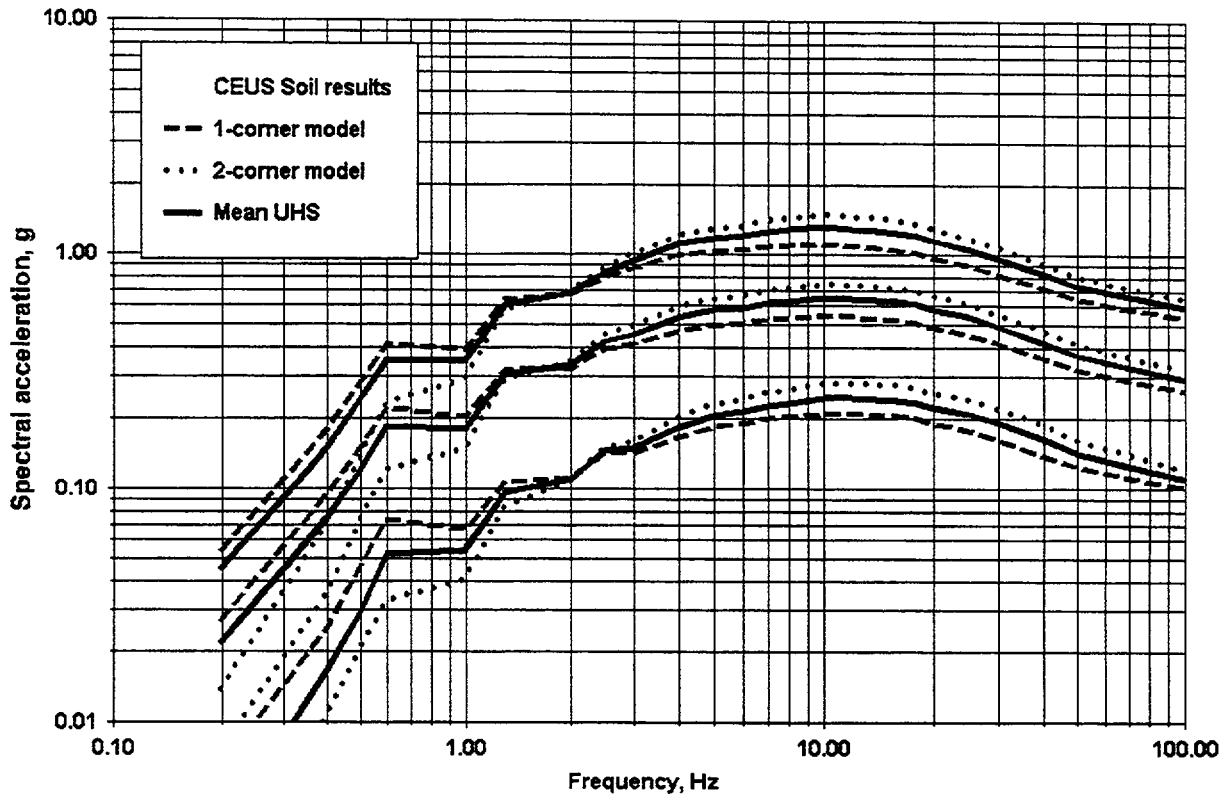


Figure 3-26. UHS for Columbia site, Savannah profile: 10^{-5} (top three curves), 10^{-4} (middle three curves), and 10^{-3} (bottom three curves).

10 Hz SA hazard contribution by source
Columbia site, Savannah profile, 1-corner model

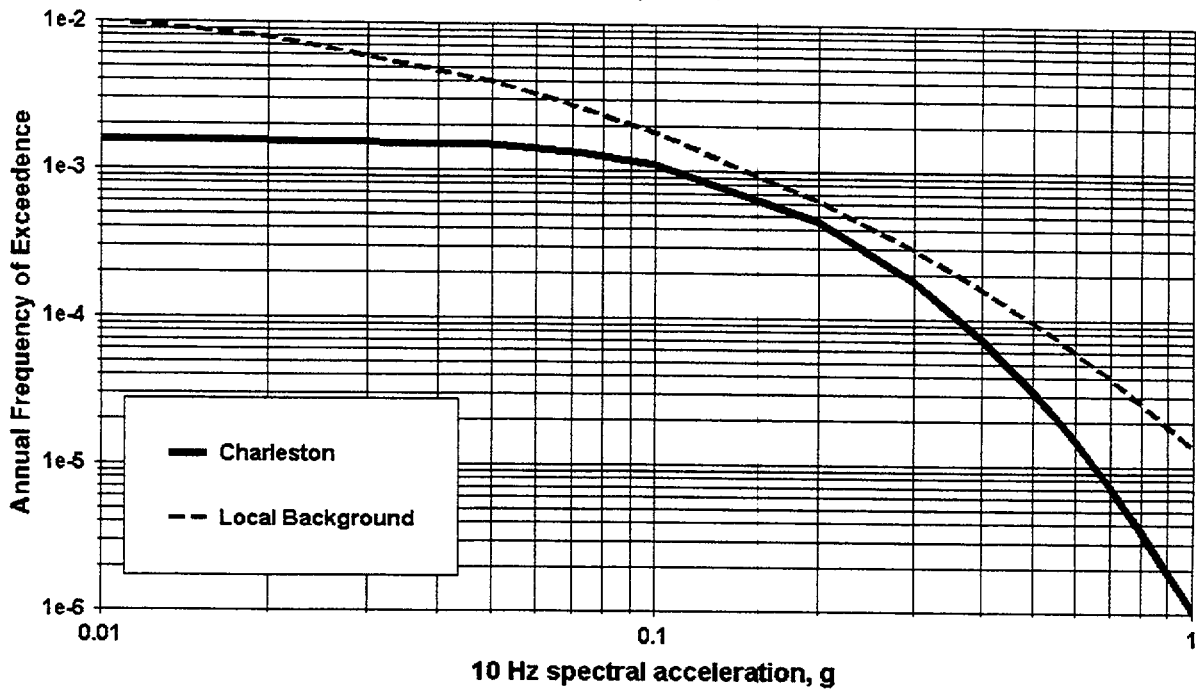


Figure 3-27. Contribution to 10 Hz hazard by source for Columbia site, Savannah profile, rock, 1-corner model.

1 Hz SA hazard contribution by source
Columbia site, Savannah profile, 1-corner model

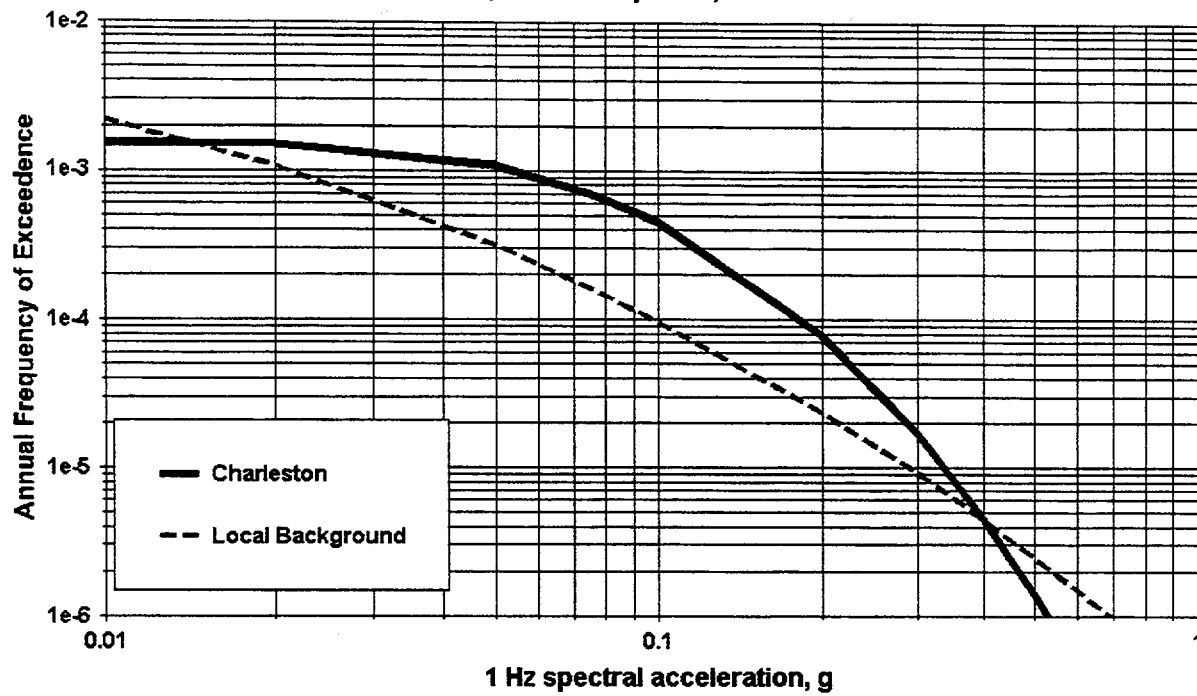
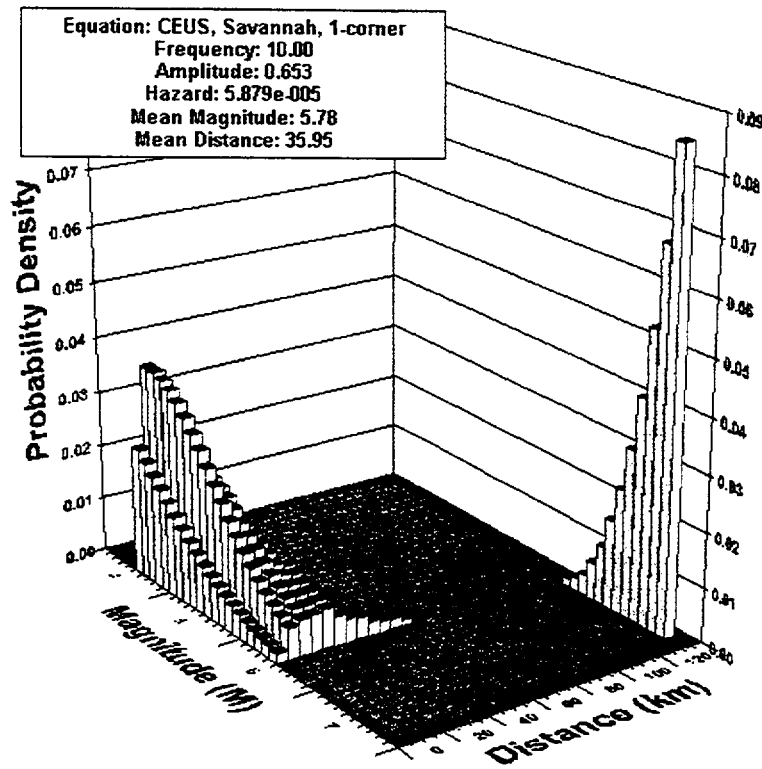


Figure 3-28. Contribution to 1Hz hazard by source for Columbia site, Savannah profile, rock, 1-corner model.

Magnitude-Distance Deaggregation



Magnitude-Distance Deaggregation

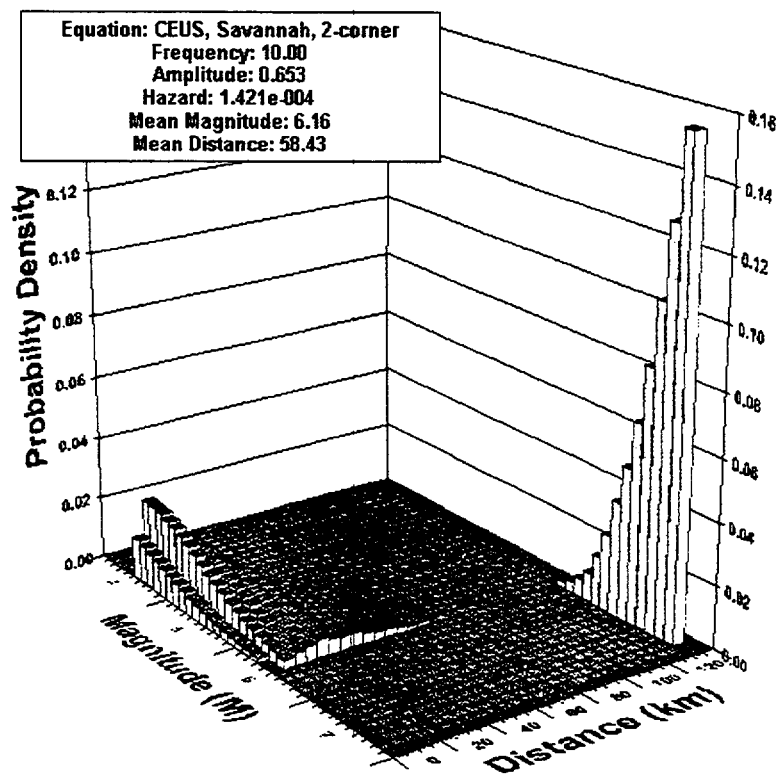


Figure 3-29. $1E-4$ 10 Hz M-R deaggregation for Columbia site, Savannah profile, 1-corner model (top) and 2-corner model (bottom).

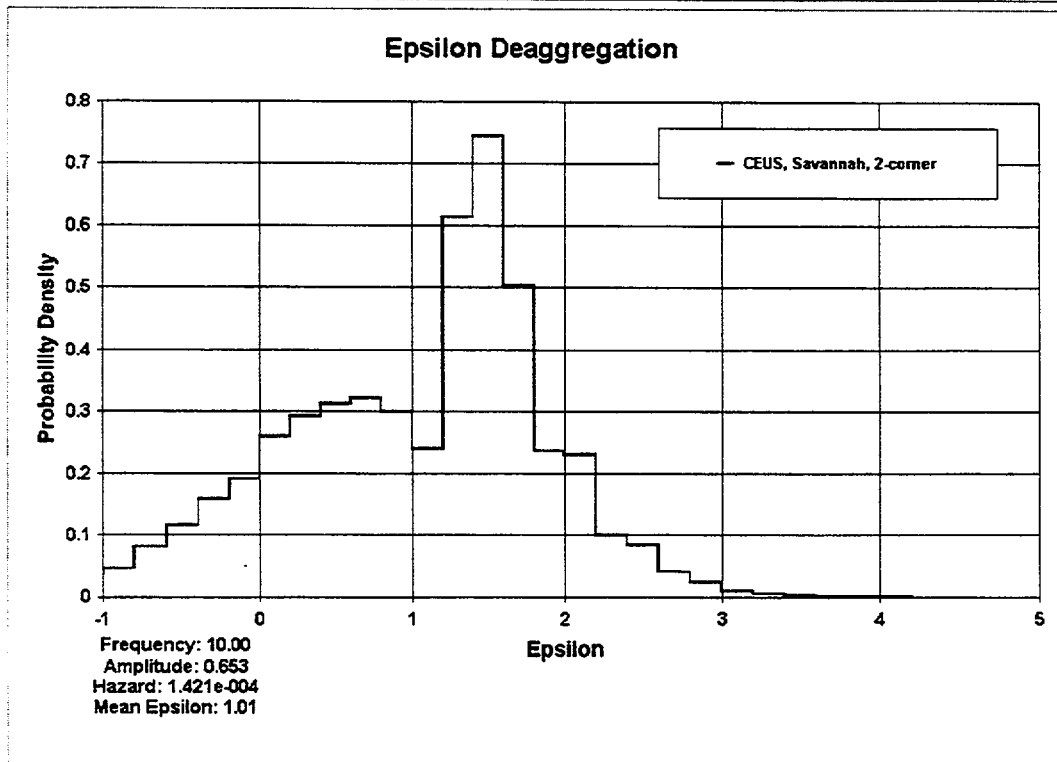
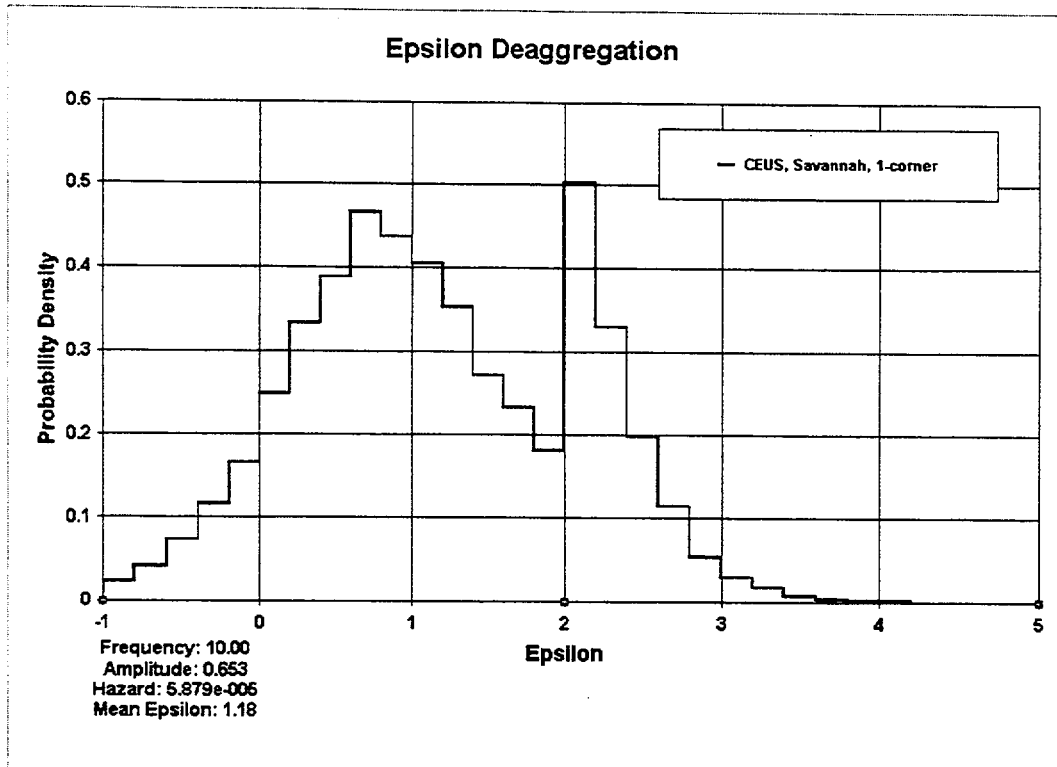
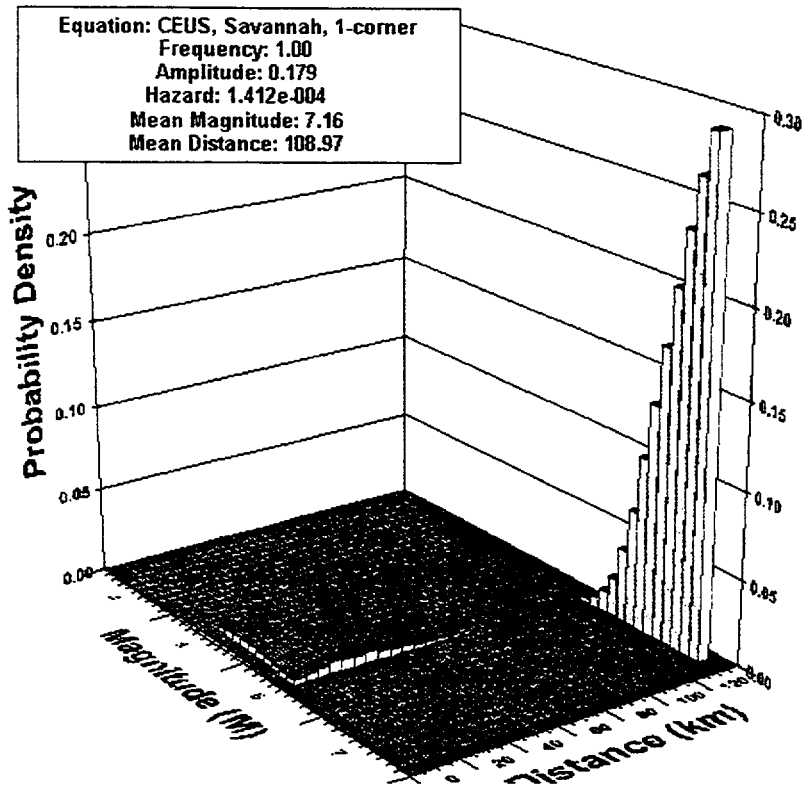


Figure 3-30. $1E-4$, 10 Hz ϵ deaggregation for Columbia site, Savannah profile, 1-corner model (top) and 2-corner model (bottom).

Magnitude-Distance Deaggregation



Magnitude-Distance Deaggregation

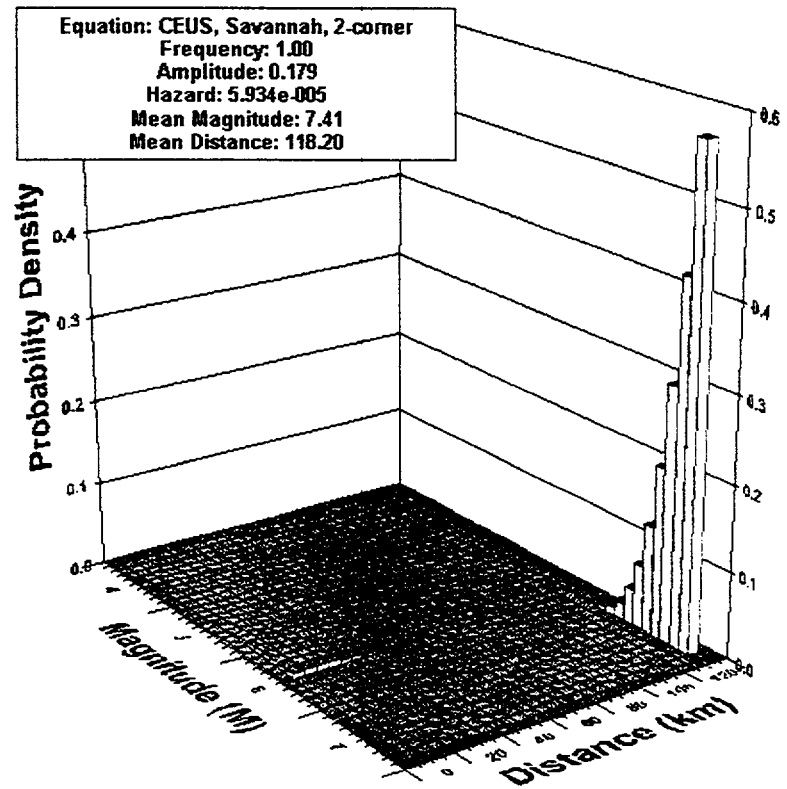


Figure 3-31. 1E-4 M-R deaggregation for Columbia site, Savannah profile, 1-corner model (top) and 2-corner model (bottom).

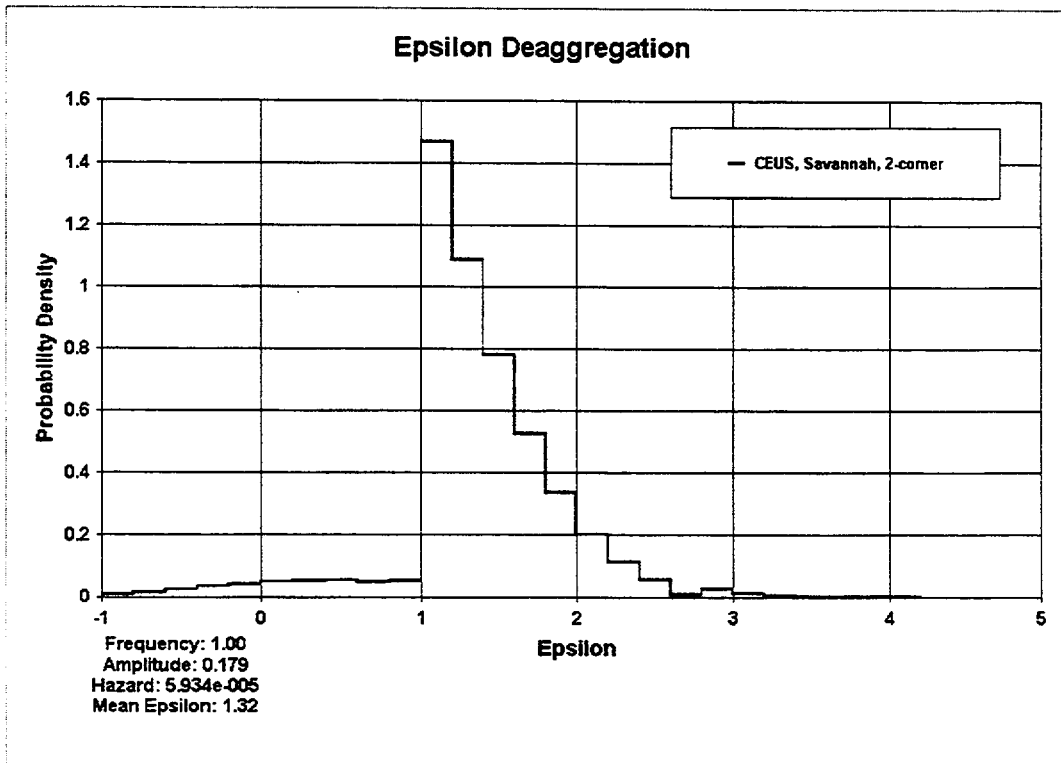
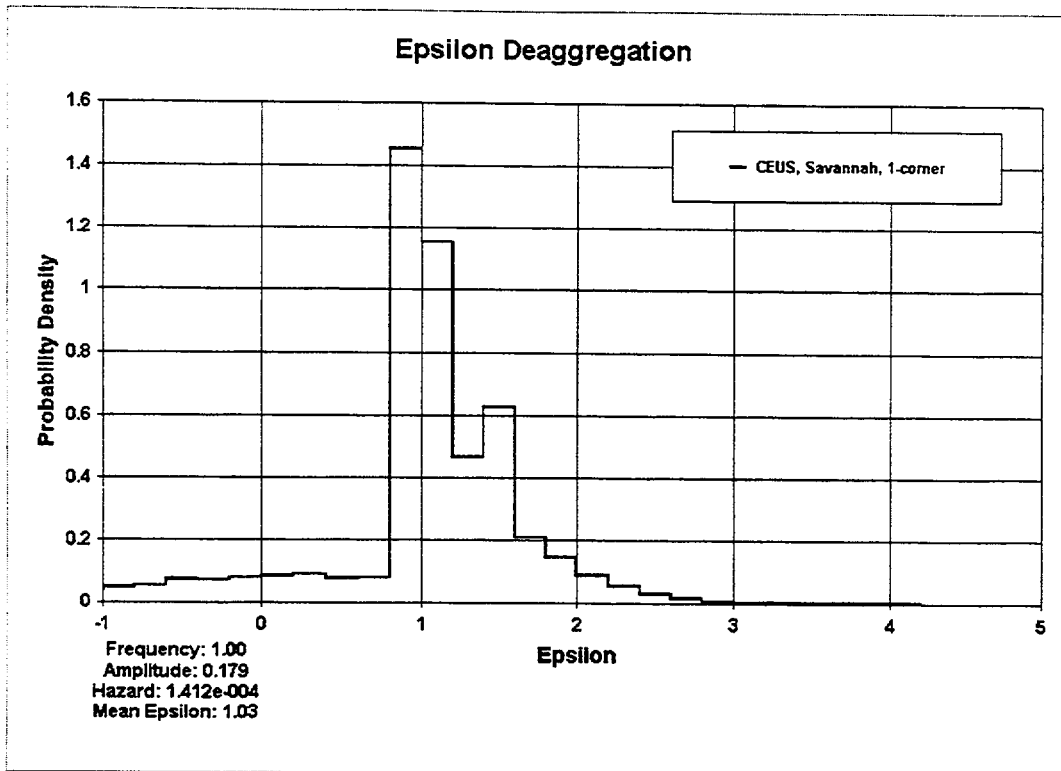


Figure 3-32. $1E-4$, 1Hz ϵ deaggregation for Columbia site, Savannah profile, 1-corner model (top) and 2-corner (bottom).

4.0 UNIFORM RELIABILITY SPECTRA, ROCK

4.1 Mojave site

4.1.1 Derivation of uniform reliability spectrum (URS)

As discussed in McGuire et al., (2001), the uniform reliability spectrum (URS) is a spectrum derived from the UHS that accounts for differences in hazard levels, slopes of hazard curves for different structural periods, and the seismic ruggedness of components (and the uncertainty in that ruggedness) from site to site. By its nature, of course, the URS is a general spectrum that “corrects” the UHS for seismic hazard levels, slopes of hazard curves, and generic component response, but it corrects different sites in appropriate ways to achieve an approximate uniform reliability of seismic components across sites and structural periods.

The URS is derived from the UHS by multiplying the amplitude at each structural frequency by a scale factor SF:

$$\text{URS} = \text{UHS} \times \text{SF} \quad (4-1)$$

where, for this example,

$$\text{SF} = \max\{0.7, 0.35 A_R^{1.2}\} \quad (4-2)$$

The basis for this scale factor is described in Section 7.3 of McGuire et al., (2001). The procedure to obtain other scale factors is described in Section 9.1.

Table 4-1 documents the 10^{-4} and 10^{-5} UHS from the rock hazard analysis at the Mojave site. These are the same UHS described in Section 3. In addition, Table 4-1 shows the values of A_R and K_H calculated from these UHS. Recall that A_R is the ratio of 10^{-5} to 10^{-4} ground motion at each frequency, and K_H is the negative logarithmic slope between 10^{-4} and 10^{-5} . The 10^{-4} URS value for each frequency is shown in the last column of Table 4-1, calculated using equation (4-1).

The Mojave site lies in an area of high seismic hazard, and as a result the hazard curves are dropping steeply at 10^{-4} annual frequency. As described in Section 7.3 of McGuire et al., (2001), if the A_R value at any frequency is less than 2.4, the URS will be less than the UHS. This is the case for the Mojave site. Because the seismic hazard curves are falling off steeply above the 10^{-4} UHS amplitudes, there is relatively low probability of ground motions say twice the 10^{-4} UHS, so the design spectrum can be reduced from the UHS somewhat. Note that from equation (4-2), the URS is never decreased by more than 30%.

We assume for this example that the URS will be based on the UHS at 10^{-4} annual frequency of exceedence. Figure 4-1 compares the UHS and URS spectra for the Mojave site. The URS is typically 18% - 20% below the UHS. This URS is the spectrum to which seismic structures, equipment, and components would be designed.

4.1.2 Derivation of scaled spectra

Deaggregation of the rock seismic hazard was described in Section 3.1. At the 10^{-4} hazard level, the mean magnitude and associated distances are:

10 Hz: $M = 6.1$, $R = 14$ km,

1 Hz: $M = 6.6$, $R = 18$ km.

Using these magnitudes and distances, spectral amplitudes were calculated from the rock attenuation equations described in Section 2.3, and were scaled to the UHS at 10 and 1 Hz, as appropriate. That is, the $M=6.1$ spectrum was scaled to the 10 Hz UHS amplitude, and the $M=6.6$ spectrum was scaled to the 1 Hz UHS amplitude.

The above magnitudes and distances were also used to develop scaled spectra using equation (4-8) of McGuire et al., (2001). These are the recommended spectral shapes developed from the strong motion database of this project. The same magnitudes and distances were used, and the spectra also were scaled to the 10 Hz and 1 Hz UHS.

Figure 4-2 shows the UHS and these four scaled design spectra. Because the two mean magnitudes differ by only 0.5 units, the spectral shapes are similar. Also, the spectra derived from the attenuation equations are similar to those derived from the recommended spectral shapes. The purpose of this comparison is a consistency check, to ensure that the shape of the UHS is consistent with spectra from individual events representing both the high- and low-frequency motion. The values of the scaled design spectra are shown in Table 4-2.

Figure 4-3 shows the 10^{-4} URS and spectra scaled from the attenuation equations to the 10 Hz and 1 Hz URS amplitudes. These individual spectra represent an alternative design criterion to the broad-banded URS. For the spectra in Figure 4-3, there is not much advantage in designing to the individual spectra, so the designer would likely opt to use the broad-banded URS. As discussed above, this results from the 10 Hz and 1 Hz dominant magnitudes differing by only 0.5 magnitude units. The values for the spectra scaled to the URS are given in Table 4-3.

4.1.3 Vertical motions

WUS rock site vertical motions corresponding to the horizontal rock URS were estimated by applying the recommended WUS empirical V/H ratios (McGuire et al., 2001) to the URS. For the WUS, these ratios were developed from empirical WUS rock attenuation relations. For the CEUS they were based on model predictions using inclined P-SV waves (Silva, 1997; McGuire et al., 2001). Both WUS and CEUS V/H ratios were based on expected horizontal component peak acceleration values, equal to the UHS value at 100 Hz. The dependency of V/H ratios on expected horizontal component peak acceleration captures the general trends in V/H ratios with magnitude and distance in a manner that is unambiguous in the context of probabilistic seismic hazard analyses. The ratios are shown in Figure 4-4a for WUS rock site conditions and Figure 4-4b for CEUS rock site conditions. These V/H ratios were developed and presented in Section 4 of McGuire et al. (2001). For the WUS, the ratios are applied to the horizontal rock URS because the ratios are based

on horizontal and vertical motions recorded at soft rock sites (McGuire et al., 2001). Figure 4-5 shows the horizontal and vertical rock URS for the Mojave site.

4.2 Columbia Site

4.2.1 Derivation of URS

The URS for the Columbia site was derived in a parallel manner to the URS for the Mojave site. For the Columbia site, the average hazard from the two ground motion models was used to establish the ratio A_R of amplitudes at annual frequencies of 10^{-4} and 10^{-5} . These values of A_R for each structural frequency were then used with equations (4-1) and (4-2) to calculate the URS. Table 4-4 documents the values of A_R and the URS at each frequency.

Figure 4-6 shows the UHS and URS for the Columbia site for rock conditions. For frequencies below 15 Hz, the hazard curves are steep ($K_H > 2.63$), so the UHS is decreased to obtain the URS. At higher frequencies the hazard curves are shallow ($K_H < 2.63$), so the UHS is increased to obtain the URS.

This characteristic, that the high frequency hazard curves are shallower than the low frequency hazard curves, results from the specific sources and their characteristics that we have assumed to affect the Columbia site. Often all frequencies will have a shallow slope in the CEUS, and the calculated URS will exceed the UHS at all frequencies. For an example, see Section 7.3.2 and Figure 7.12 of McGuire et al., 2001.

4.2.2 Derivation of scaled spectra

Deaggregation of rock hazard for the Columbia site was described in Section 3.2. At the 10^{-4} hazard level the mean magnitudes and associated distances are:

10 Hz:	$M = 6.0, R = 46 \text{ km}$
1 Hz:	$M = 7.2, R = 110 \text{ km}$

These magnitudes and distances, and the CEUS rock attenuation equations, were used to estimate one spectrum scaled to the 10 Hz UHS, and a second spectrum scaled to the 1 Hz UHS. These spectra were the average of spectra calculated from the two ground motion models. In addition, two spectra were derived from the recommended spectral shapes from this project, using equation (4-9) of McGuire et al., (2001). The procedure was the same as described above for the Mojave site. Figure 4-7 shows the UHS and the two scaled spectra. For the Columbia site the two magnitudes differ by 1.2 units, so the spectral shapes differ markedly.

In general, however, the UHS at high frequencies is consistent with the 10 Hz scaled spectra, and the UHS at low frequencies is consistent with the 1 Hz scaled spectra. This illustrates the purpose of the comparison, to determine the consistency of the UHS shape with several scaled spectra. The spectral values are documented in Table 4-5.

Figure 4-8 shows a comparison of the 10^{-4} URS with spectra calculated from the CEUS rock attenuation equations (weighting the 1- and 2-corner models equally, as was done in the PSHA). Here the 1.2 magnitude unit difference in dominant magnitudes between 10 and 1 Hz leads to a significant difference across the entire frequency band. If the designer were concerned about a structure with both high-frequency and long-period response, he might elect to use one spectrum for low frequencies and the other at high frequencies. Values of the spectra scaled to the URS are documented in Table 4-6.

Figure 4-8 shows that there is a mismatch between the URS at high frequencies ($f > 20$ Hz) and the spectrum scaled to 10 Hz. This results from the scale factor at high frequencies being > 1.0 (see Table 4-4). To avoid scaling the 10 Hz spectrum up to achieve a match at these high frequencies, the designer could add a third spectrum scaled to 30 or 50 Hz that would replicate the URS for design purposes and not impact frequencies below 10 Hz.

4.2.3 Vertical motions

For the CEUS, V/H ratios were developed based on model predictions using inclined P-SV waves (Silva, 1997; McGuire et al., 2001). The resulting ratios are summarized in Figure 4-4b, and are a function of horizontal component peak acceleration (equal to the URS at 100 Hz). Figure 4-9 illustrates the resulting CEUS rock vertical URS, compared to the corresponding horizontal URS. This vertical URS was produced with the 0.2 to 0.5g hard rock V/H ratio (Figure 4-4b). The V/H ratios were developed and presented in Section 4 of McGuire et al., (2001).

REFERENCE

McGuire, R.K., W.J. Silva, and C. Costantino (2001). "Technical Basis for Revision of Regulatory Guidance on Design Ground Motions: Hazard and Risk-consistent Ground Motion Spectra Guidelines," US Nuclear Reg. Comm., Rept NUREG/CR-6728, October.

Table 4-1
Slope parameters for rock hazard curves
Mojave site

<u>Structural</u> <u>Frequency, Hz</u>	<u>10⁻⁴ UHS, g</u>	<u>10⁻⁵ UHS, g</u>	<u>A_R</u>	<u>K_H</u>	<u>SF</u>	<u>10⁻⁴ URS, g</u>
100	8.98E-1	1.82	2.02	3.27	8.14E-1	7.31E-1
50	9.52E-1	1.93	2.03	3.26	8.17E-1	7.78E-1
40	9.97E-1	2.00	2.01	3.31	8.07E-1	8.05E-1
31	1.12	2.26	2.02	3.28	8.12E-1	9.10E-1
25	1.24	2.48	2.00	3.32	8.04E-1	9.98E-1
20	1.40	2.78	1.99	3.35	7.99E-1	1.12
18	1.50	3.00	2.00	3.33	8.02E-1	1.21
16	1.63	3.24	1.99	3.34	8.01E-1	1.30
14	1.72	3.40	1.98	3.37	7.95E-1	1.36
12	1.83	3.66	2.00	3.33	8.03E-1	1.47
10	1.94	3.88	2.00	3.32	8.04E-1	1.56
8	2.00	4.00	2.00	3.32	8.04E-1	1.61
7	2.05	4.16	2.02	3.27	8.15E-1	1.67
6	2.04	4.09	2.00	3.31	8.06E-1	1.65
5	2.07	4.16	2.02	3.28	8.12E-1	1.68
4	1.97	3.95	2.01	3.31	8.07E-1	1.59
3	1.76	3.52	2.00	3.32	8.05E-1	1.42
2.5	1.56	3.17	2.04	3.24	8.21E-1	1.28
2	1.23	2.50	2.04	3.24	8.21E-1	1.01
1.3	8.64E-1	1.81	2.09	3.12	8.47E-1	7.32E-1
1	6.67E-1	1.38	2.07	3.17	8.36E-1	5.58E-1
.6	4.53E-1	8.56E-1	1.89	3.62	7.51E-1	3.40E-1
.5	4.17E-1	7.67E-1	1.84	3.78	7.27E-1	3.03E-1
.4	3.30E-1	5.88E-1	1.78	3.98	7.00E-1	2.31E-1
.2	1.50E-1	2.41E-1	1.61	4.84	7.00E-1	1.05E-1

Table 4-2
Spectra scaled to 10^{-4} UHS
Mojave site, rock conditions

Structural frequency, Hz	10 Hz scaled spectrum from attenuation eq.	1 Hz scaled spectrum from attenuation eq.	10 Hz scaled spectrum from spectral shapes	1 Hz scaled spectrum from spectral shapes
100	8.578E-1	8.127E-1	1.002	9.513E-1
50	9.022E-1	8.470E-1	1.035	9.722E-1
40	9.592E-1	9.019E-1	1.070	9.973E-1
31	1.053	9.784E-1	1.138	1.050
25	1.176	1.087	1.226	1.121
20	1.345	1.241	1.355	1.230
18	1.441	1.324	1.430	1.294
16	1.556	1.427	1.522	1.376
14	1.688	1.560	1.638	1.481
12	1.820	1.684	1.778	1.613
10	1.940	1.805	1.940	1.774
8	2.016	1.898	2.101	1.955
7	2.029	1.913	2.161	2.038
6	2.030	1.932	2.186	2.100
5	1.993	1.907	2.146	2.113
4	1.851	1.793	2.000	2.037
3	1.573	1.564	1.696	1.811
2.5	1.370	1.394	1.471	1.620
2	1.074	1.127	1.193	1.366
1.3	7.124E-1	8.068E-1	7.285E-1	9.003E-1
1	5.522E-1	6.670E-1	5.148E-1	6.670E-1
.6	3.258E-1	4.610E-1	2.398E-1	3.418E-1
.5	2.701E-1	4.075E-1	1.776E-1	2.623E-1
.4	1.911E-1	3.200E-1	1.205E-1	1.861E-1
.2	5.253E-2	1.223E-1	3.057E-2	5.489E-2

Table 4-3
Spectra scaled to 10^4 URS
Mojave site, rock conditions

<u>Structural Frequency, Hz</u>	<u>URS, g</u>	<u>10 Hz spectrum scaled from atten. eq.</u>	<u>1 Hz spectrum scaled from atten. eq.</u>
100	7.31E-1	6.898E-1	7.041E-1
50	7.78E-1	7.254E-1	7.339E-1
40	8.05E-1	7.713E-1	7.827E-1
31	9.10E-1	8.467E-1	8.501E-1
25	9.98E-1	9.460E-1	9.466E-1
20	1.12	1.082	1.082
18	1.21	1.159	1.155
16	1.30	1.251	1.243
14	1.36	1.358	1.359
12	1.47	1.464	1.467
10	1.56	1.560	1.571
8	1.61	1.621	1.650
7	1.67	1.632	1.661
6	1.65	1.633	1.676
5	1.68	1.602	1.652
4	1.59	1.488	1.550
3	1.42	1.265	1.346
2.5	1.28	1.102	1.196
2	1.01	8.640E-1	9.610E-1
1.3	7.32E-1	5.729E-1	6.809E-1
1	5.58E-1	4.440E-1	5.580E-1
.6	3.40E-1	2.620E-1	3.787E-1
.5	3.03E-1	2.172E-1	3.314E-1
.4	2.31E-1	1.537E-1	2.563E-1
.2	1.05E-1	4.224E-2	9.260E-2

Table 4-4
Slope parameters for rock hazard curves
Columbia site

<u>Structural</u> <u>Frequency, Hz</u>	<u>10⁻⁴ UHS, g</u>	<u>10⁻⁵ UHS, g</u>	<u>A_R</u>	<u>K_H</u>	<u>SF</u>	<u>10⁻⁴ URS, g</u>
100	2.74E-1	6.82E-1	2.49	2.52	1.05	2.87E-1
50	6.24E-1	1.61	2.58	2.43	1.09	6.81E-1
40	6.28E-1	1.60	2.55	2.46	1.07	6.75E-1
31	5.85E-1	1.47	2.51	2.51	1.05	6.17E-1
25	5.68E-1	1.41	2.48	2.54	1.04	5.90E-1
20	5.52E-1	1.35	2.45	2.56	1.03	5.67E-1
18	5.46E-1	1.33	2.44	2.59	1.02	5.56E-1
16	5.36E-1	1.30	2.42	2.61	1.01	5.41E-1
14	5.17E-1	1.24	2.39	2.64	9.97E-1	5.16E-1
12	4.85E-1	1.15	2.36	2.68	9.82E-1	4.76E-1
10	4.38E-1	1.02	2.33	2.72	9.66E-1	4.23E-1
8	3.72E-1	8.60E-1	2.31	2.75	9.57E-1	3.56E-1
7	3.42E-1	7.83E-1	2.29	2.78	9.46E-1	3.23E-1
6	3.09E-1	6.96E-1	2.26	2.83	9.30E-1	2.87E-1
5	2.73E-1	6.12E-1	2.24	2.85	9.21E-1	2.52E-1
4	2.31E-1	5.08E-1	2.20	2.92	9.01E-1	2.08E-1
3	1.84E-1	3.96E-1	2.15	3.00	8.79E-1	1.62E-1
2.5	1.57E-1	3.38E-1	2.16	2.99	8.81E-1	1.38E-1
2	1.30E-1	2.73E-1	2.10	3.11	8.52E-1	1.11E-1
1.3	8.39E-2	1.68E-1	2.00	3.33	8.03E-1	6.74E-2
1	6.32E-2	1.21E-1	1.92	3.53	7.66E-1	4.84E-2
.6	4.23E-2	8.41E-2	1.99	3.35	7.98E-1	3.38E-2
.5	3.57E-2	7.32E-2	2.05	3.20	8.29E-1	2.96E-2
.4	2.77E-2	5.77E-2	2.08	3.14	8.44E-1	2.34E-2
.2	1.24E-2	2.39E-2	1.93	3.51	7.69E-1	9.53E-3

Table 4-5
Spectra scaled to 10^{-4} UHS
Columbia site, rock conditions

<u>Structural frequency, Hz</u>	<u>10 Hz scaled spectrum from atten. eq.</u>	<u>1 Hz scaled spectrum from atten. eq.</u>	<u>10 Hz. scaled spectrum from spectral shapes</u>	<u>1 Hz scaled spectrum from spectral shapes</u>
100	2.548E-1	1.500E-1	2.790E-1	1.660E-1
50	4.987E-1	2.672E-1	5.647E-1	3.379E-1
40	5.392E-1	2.831E-1	6.136E-1	3.687E-1
31	5.119E-1	2.911E-1	6.274E-1	3.793E-1
25	5.120E-1	2.977E-1	6.177E-1	3.770E-1
20	5.188E-1	3.112E-1	5.919E-1	3.674E-1
18	5.196E-1	3.182E-1	5.747E-1	3.609E-1
16	5.164E-1	3.214E-1	5.520E-1	3.520E-1
14	5.044E-1	3.192E-1	5.226E-1	3.404E-1
12	4.786E-1	3.100E-1	4.851E-1	3.250E-1
10	4.380E-1	2.911E-1	4.380E-1	3.050E-1
8	3.840E-1	2.646E-1	3.804E-1	2.789E-1
7	3.532E-1	2.488E-1	3.473E-1	2.630E-1
6	3.172E-1	2.318E-1	3.114E-1	2.447E-1
5	2.827E-1	2.125E-1	2.725E-1	2.237E-1
4	2.351E-1	1.878E-1	2.299E-1	1.989E-1
3	1.818E-1	1.577E-1	1.814E-1	1.687E-1
2.5	1.601E-1	1.413E-1	1.534E-1	1.504E-1
2	1.260E-1	1.232E-1	1.214E-1	1.283E-1
1.3	7.374E-2	8.172E-2	7.064E-2	8.614E-2
1	5.178E-2	6.320E-2	4.866E-2	6.320E-2
.6	2.730E-2	4.259E-2	2.240E-2	3.177E-2
.5	2.060E-2	3.642E-2	1.673E-2	2.464E-2
.4	1.358E-2	2.842E-2	1.157E-2	1.801E-2
.2	2.944E-3	1.169E-2	3.251E-3	6.545E-3

Table 4-6
 Spectra scaled to 10^{-4} URS
 Columbia site, rock conditions

<u>Structural frequency, Hz</u>	<u>10 Hz scaled spectrum from attenuation equation</u>	<u>1 Hz scaled spectrum from attenuation equation</u>
100	2.346E-1	1.187E-1
50	4.554E-1	2.140E-1
40	4.951E-1	2.263E-1
31	4.762E-1	2.325E-1
25	4.753E-1	2.370E-1
20	4.819E-1	2.466E-1
18	4.849E-1	2.515E-1
16	4.847E-1	2.538E-1
14	4.782E-1	2.522E-1
12	4.570E-1	2.442E-1
10	4.230E-1	2.290E-1
8	3.680E-1	2.068E-1
7	3.417E-1	1.941E-1
6	3.086E-1	1.808E-1
5	2.783E-1	1.656E-1
4	2.344E-1	1.460E-1
3	1.810E-1	1.218E-1
2.5	1.617E-1	1.090E-1
2	1.298E-1	9.481E-2
1.3	7.901E-2	6.276E-2
1	5.703E-2	4.840E-2
0.6	3.137E-2	3.233E-2
0.5	2.426E-2	2.761E-2
0.4	1.619E-2	2.145E-2
0.2	3.724E-3	8.716E-3

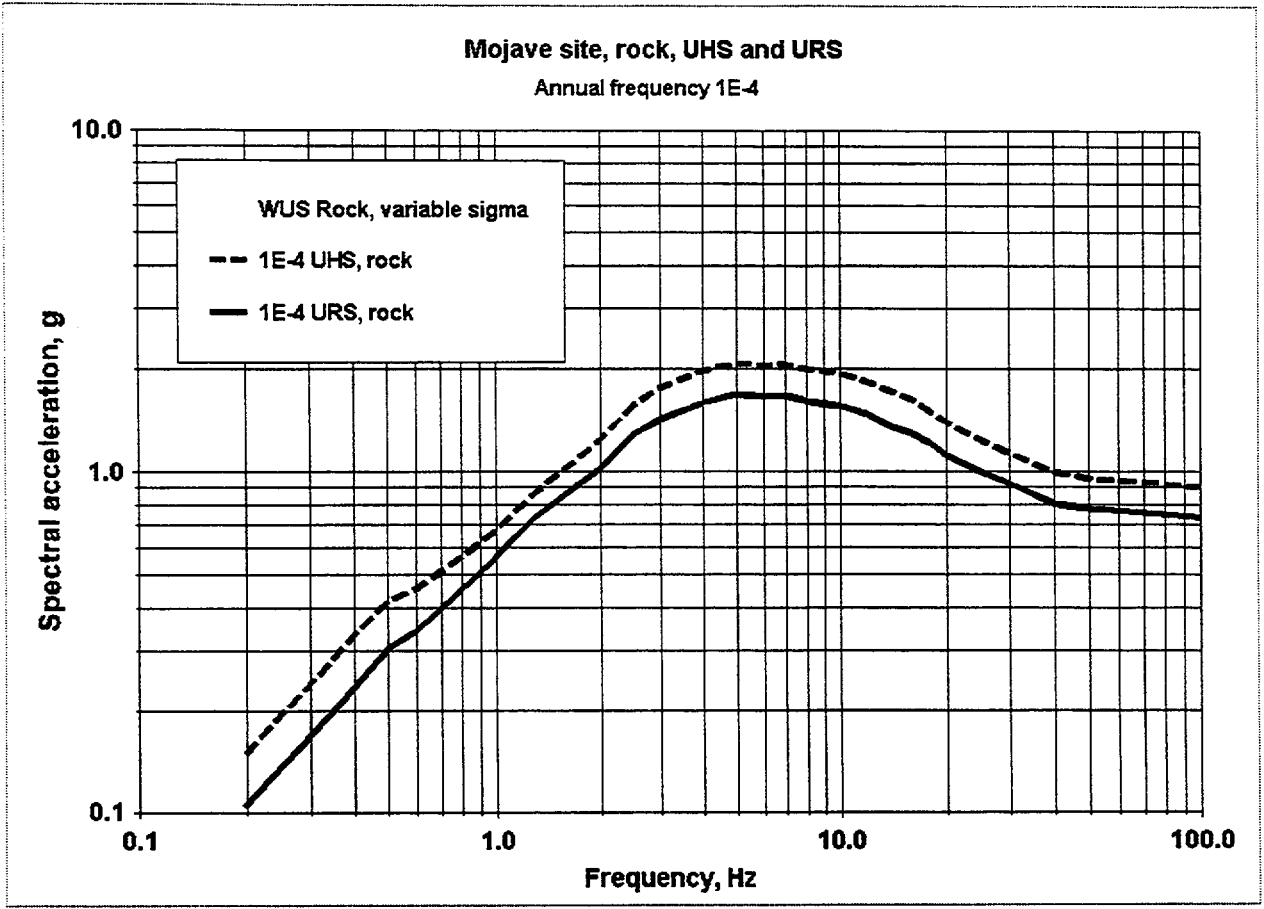


Figure 4-1. 10^{-4} UHS and URS for Mojave site, rock conditions.

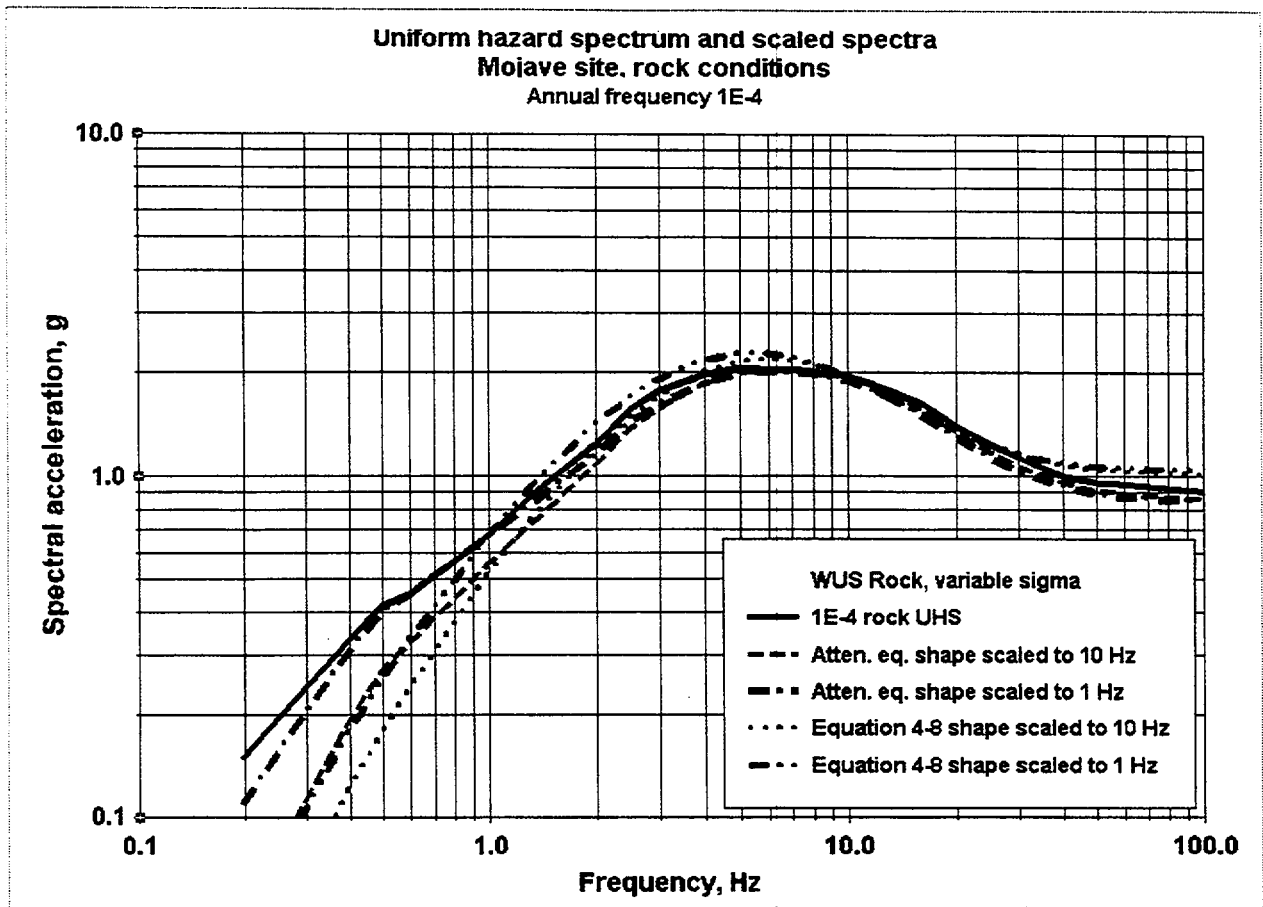


Figure 4-2. 10^{-4} UHS and scaled spectra at Mojave site, rock conditions, from attenuation equations and from recommended spectral shapes (labeled "Equation 4-8").

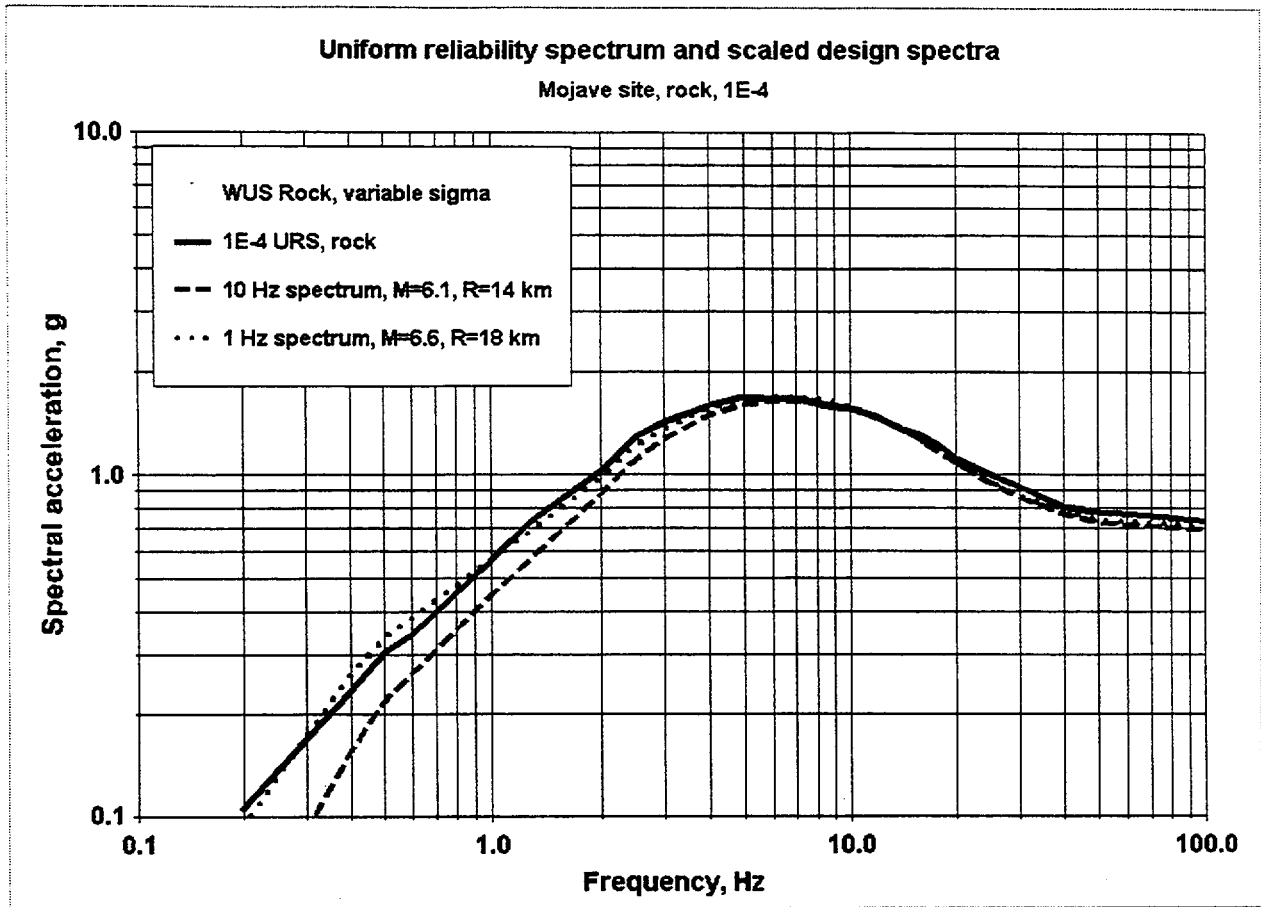


Figure 4-3. 10^{-4} URS and scaled spectra at Mojave site, rock conditions.

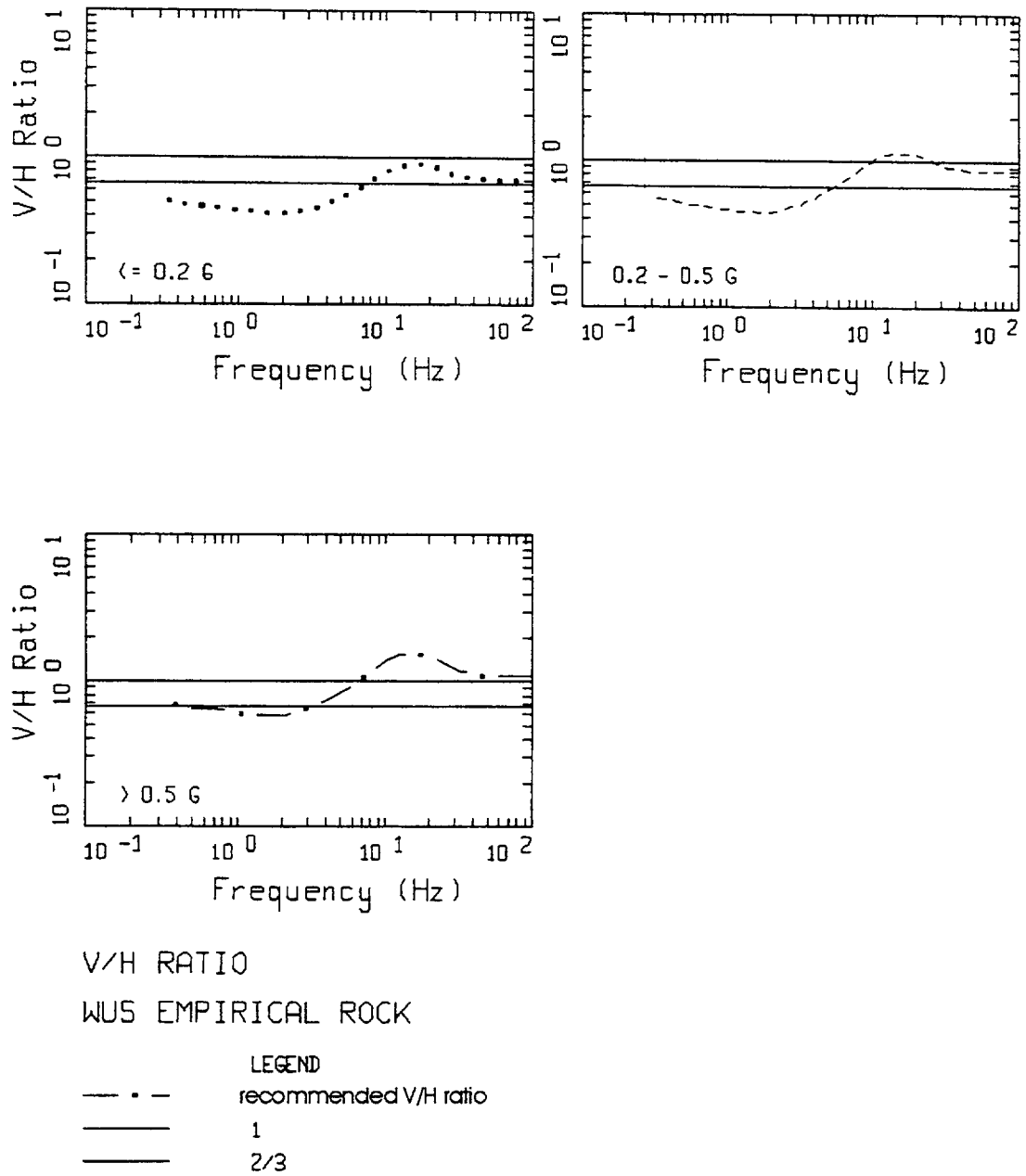
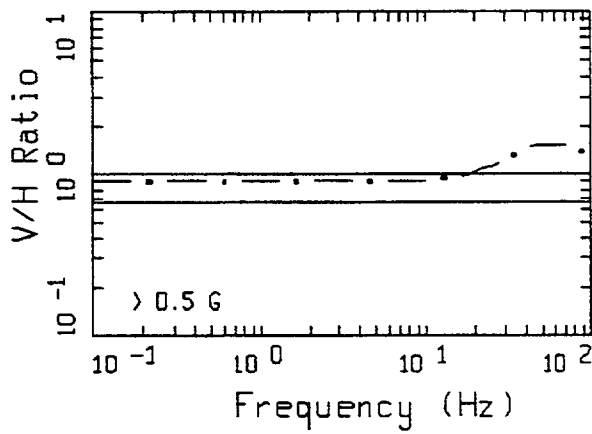
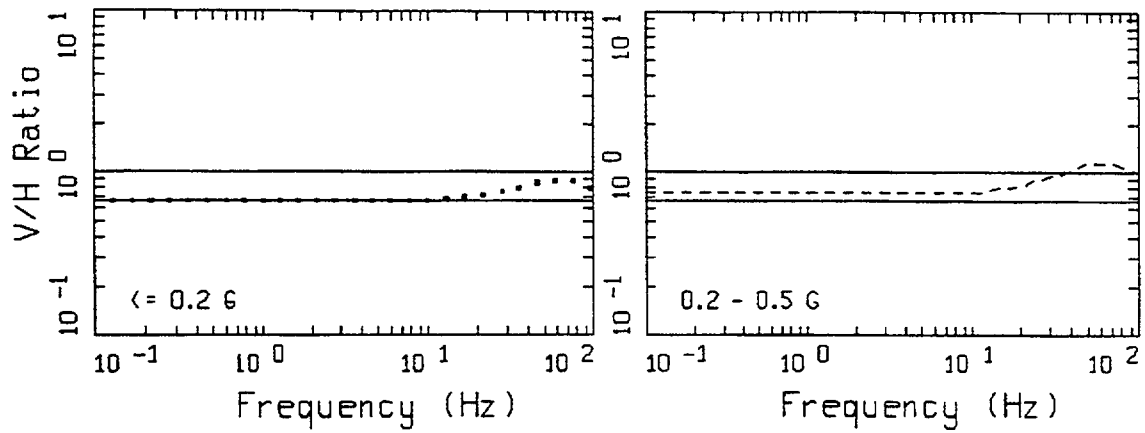


Figure 4-4a. Recommended V/H ratios (for 5% damping) for WUS soft rock site conditions for ranges in expected horizontal component peak accelerations (McGuire et al., 2001)



V/H RATIO

CEUS RECOMMENDATIONS

LEGEND
 - • - recommended V/H ratio
 — 1
 — 2/3

Figure 4-4b. Recommended V/H ratios (for 5% damping) for CEUS hard rock site conditions for ranges in horizontal component peak accelerations.

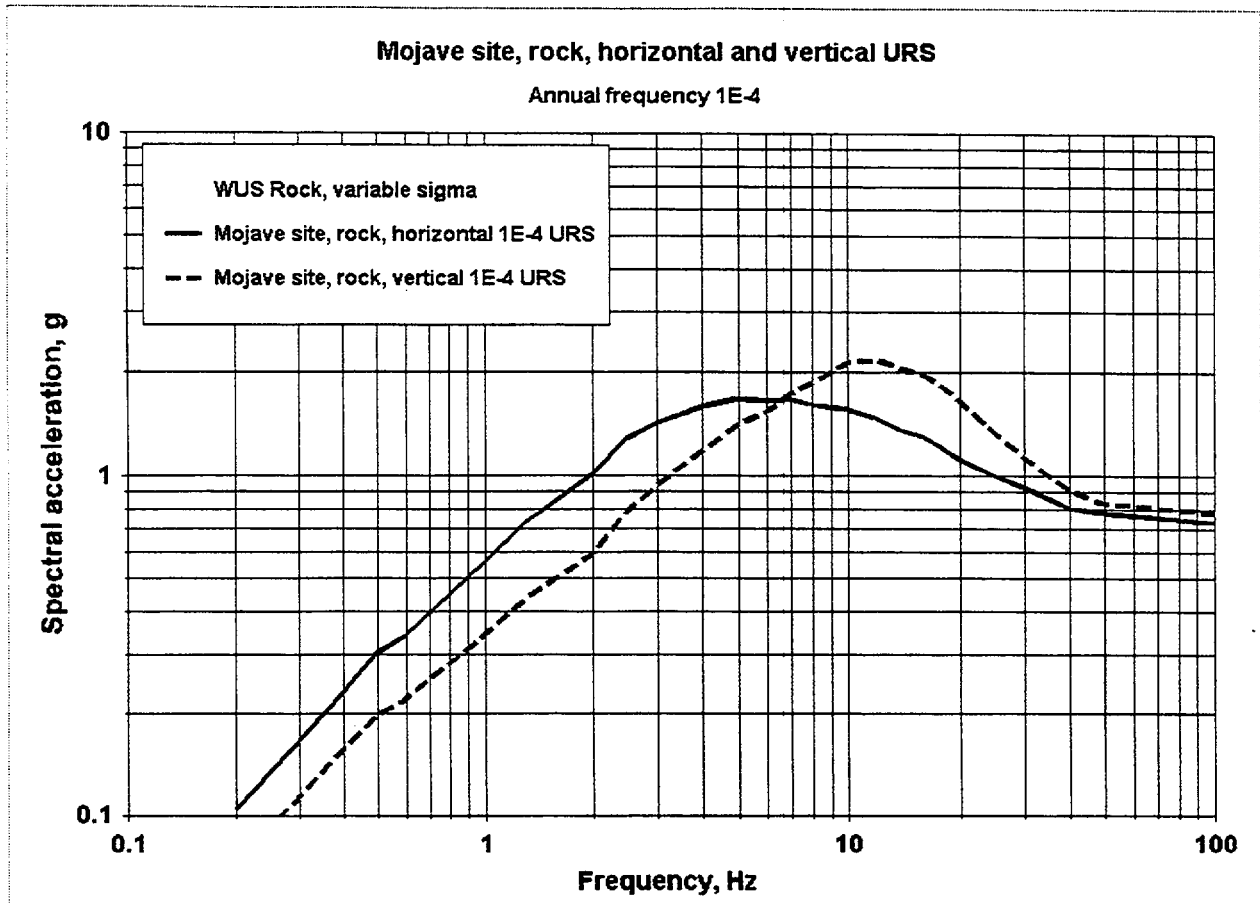


Figure 4-5. WUS rock horizontal 10^{-4} URS and corresponding vertical URS.

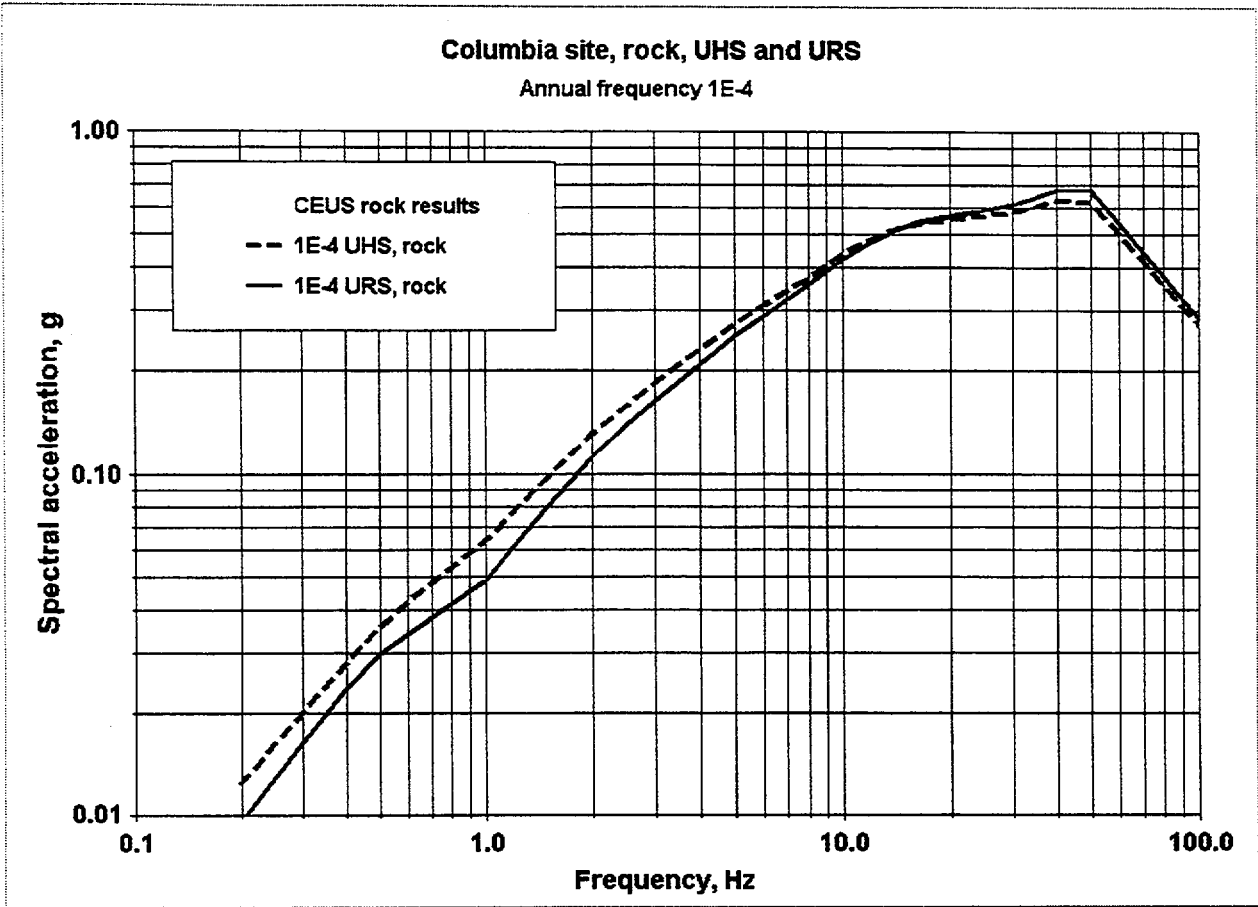


Figure 4-6. 10^{-4} UHS and URS for Columbia site, rock conditions.

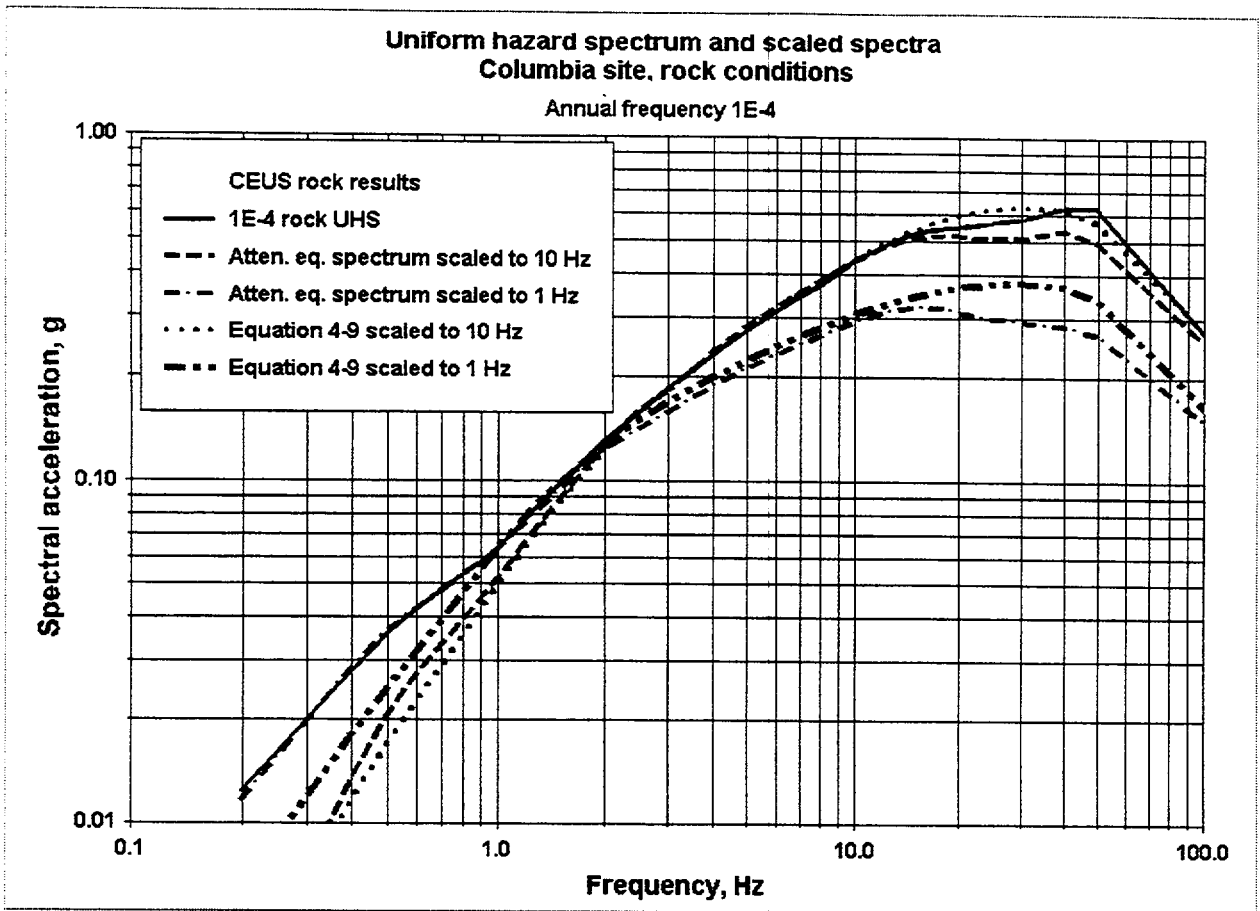


Figure 4-7. 10^{-4} UHS and scaled spectra at Columbia site, rock conditions, from attenuation equations and from recommended spectral shapes (labeled "Equation 4-8").

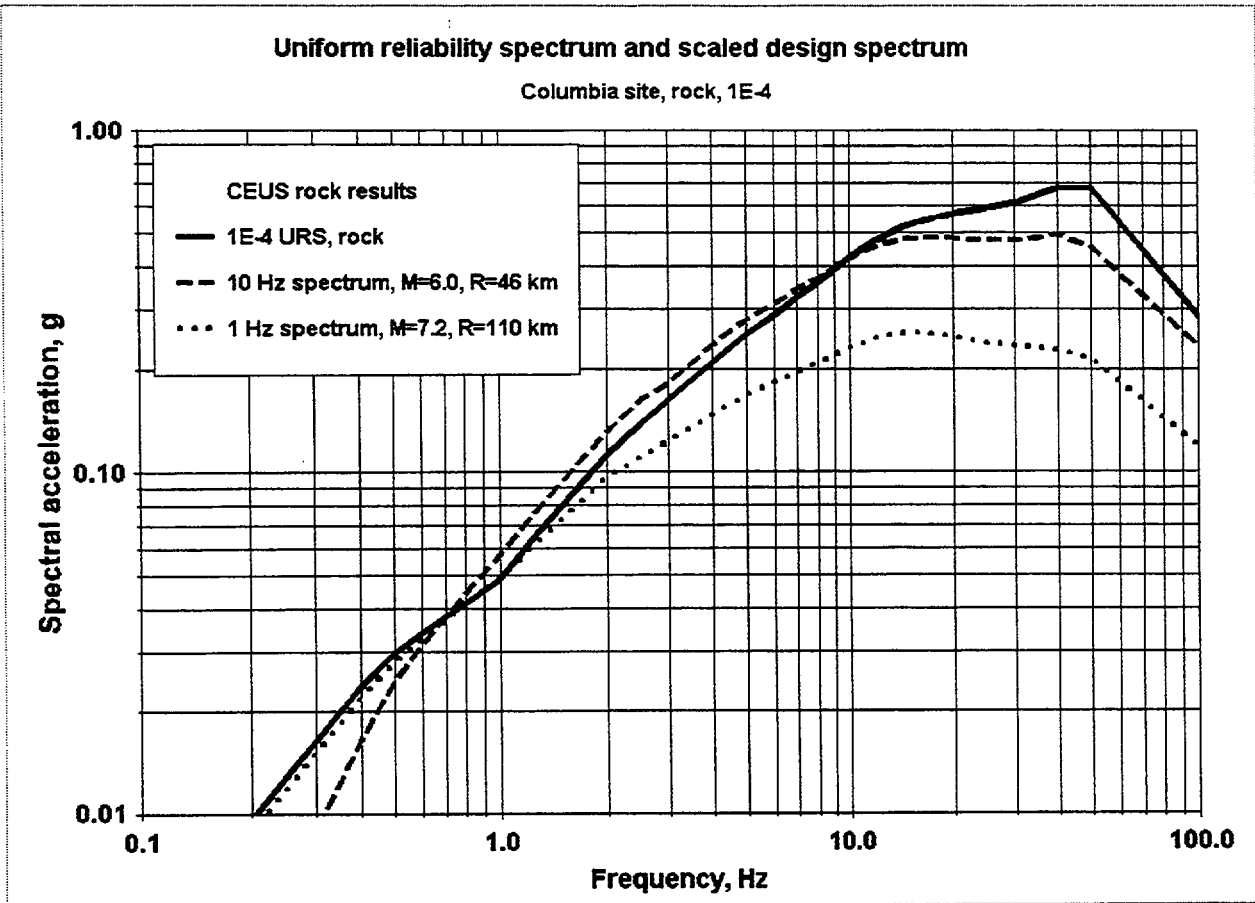


Figure 4-8. 10^{-4} URS and scaled spectra for 10 Hz and 1 Hz, Columbia site, rock conditions.

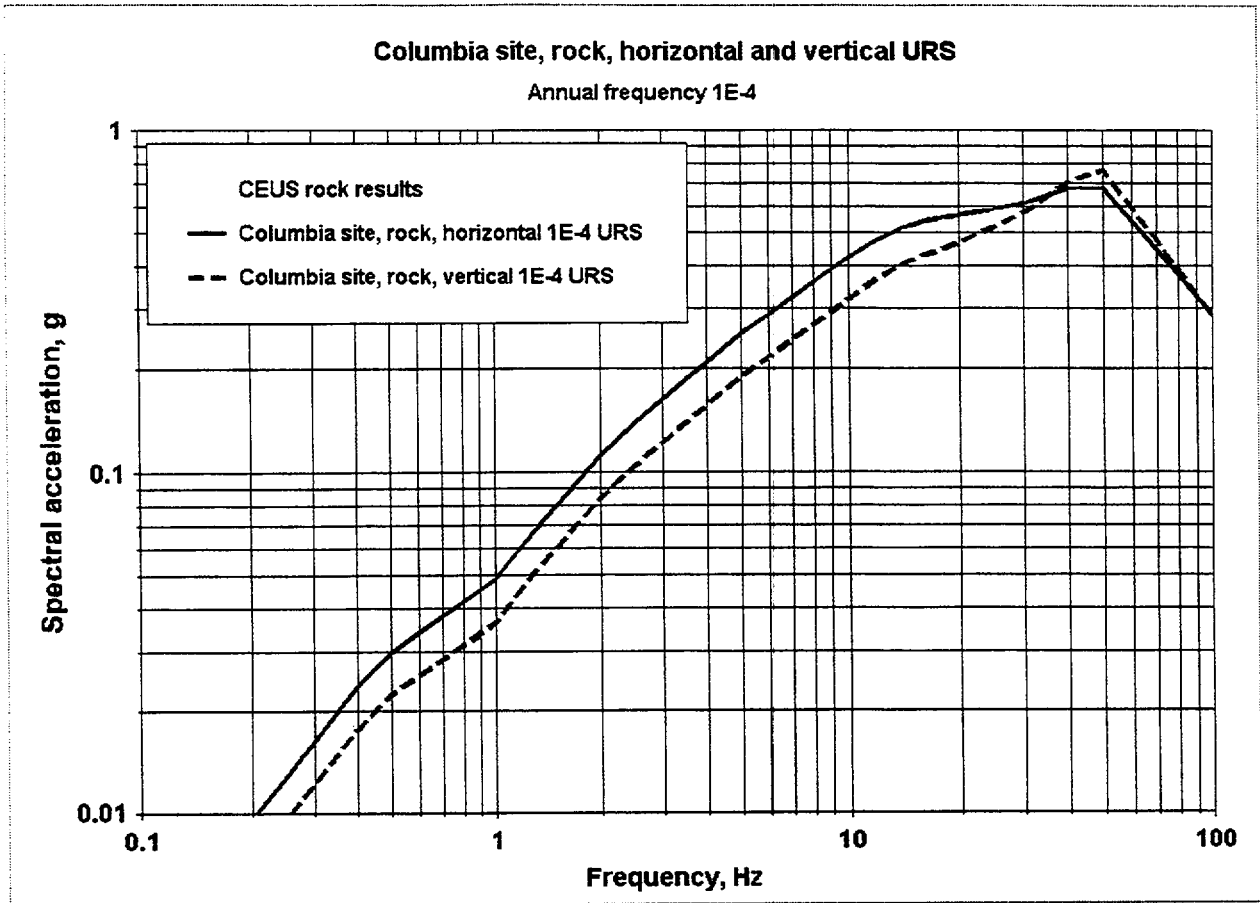


Figure 4-9. CEUS rock horizontal 10^{-4} URS and corresponding vertical URS.

5.0 GENERATING ARTIFICIAL TIME HISTORIES FOR WUS ROCK SITES

Control motions for the site response analyses using Approaches 1, 2A, and 2B (Section 6.1) are represented with Fourier amplitude spectra, because the equivalent-linear random vibration technique (RVT) is used (Schneider et al., 1993; Silva et al., 1997; McGuire et al., 2001). In general, development of a Fourier amplitude spectrum and associated response spectrum that are consistent with a specified target response spectrum results in a close match. Examples are shown in Section 6.4 for the WUS rock UHS and in McGuire et al. (2001). Time histories are generated for comparisons of equivalent-linear results with fully nonlinear site response analyses. Since control motion time histories are generally used in conventional equivalent-linear (SHAKE-type) analyses, the time history spectral matching is presented here in detail.

5.1 Spectral matching methodology

Spectral matching to the target spectra was conducted using the procedure described in Silva and Lee (1987). In this procedure, acceleration time histories are produced by combining a Fourier amplitude spectrum (which is generated by matching the target spectrum) with a phase spectrum from an observed strong ground motion recording. This approach has been used extensively for NRC, DOE, and other federal agencies in developing appropriate time histories for seismic design.

To avoid any tendency of the spectral matching process to develop gaps or low points in the time history power spectrum, this matching process begins with a smooth Fourier amplitude spectrum based on the Brune source model. Initial RVT-based matches are used to produce a smooth response spectrum that is close to the target. Subsequent matching is done by combining the Fourier phase spectrum from the recording with the smooth Fourier amplitude spectrum resulting from the RVT matching and computing the response spectrum from the resulting time history. The time history response spectrum is then used for final matching, resulting in a time history (acceleration, velocity, and displacement) that resembles the original recording in time domain characteristics, and that possesses realistic frequency-to-frequency variability in response and power spectra. Additionally, a baseline correction is included by high-pass filtering the acceleration record at 0.1 Hz. The result is a synthetic time history that closely matches the target spectrum and that possess realistic integrations to velocity and displacement.

The two most important criteria in selecting the phase spectrum from a recorded earthquake for the matching are that the seismic moment (or M) and the source-to-site distance should be comparable. These criteria produce synthetic records with appropriate durations and timing of the major phase arrivals so that the distribution of energy with time in the synthetic record is realistic. The time histories are intended to approximate expected durations and therefore to be appropriate for nonlinear analyses.

This project has recommended a duration criterion based on target spectra deaggregation magnitude, distance, and site condition (rock or soil), and has documented recorded motions in a time history database (McGuire et al., 2001). The time history database is segmented into M , R , and site condition bins (Table 5-1) so that appropriate input records for generating artificial motions can be appropriately selected. Statistics on PGA, PGV, PGD, PGV/PGA, and $PGA \cdot PGD/PGV^2$ are shown

in Table 5-2. Table 5-3 shows the duration guidelines for the corresponding record bins. The durations represent the 5 to 75% cumulative Arias Intensity, a duration measure considered significant in nonlinear analyses of nuclear facility structures (Kennedy et al., 1985; McGuire et al., 2001). The listed duration ranges are meant to reflect guidelines rather than strict criteria (McGuire et al., 2001).

5.2 Mojave Site

For the Mojave site, the deaggregation magnitudes (target spectra) and distances are listed in Table 5-4 along with the applicable duration guidelines from Table 5-3. The time histories selected from the WUS rock motion bins for inputs to the spectral matching are listed in Table 5-4 with their associated durations, both prior and subsequent to the matching process. The resulting spectra, their targets, spectral matches, and time histories are plotted in Figures 5-1 through 5-16 for the UHS horizontal and vertical components, for the 1 Hz low, moderate, and high magnitudes (designated ML, MM, and MH, respectively), and for the 10 Hz low, moderate, and high magnitudes. Note that all of these spectra are for rock motions at the base of the soil column, rather than at the rock surface, so the spectra are different from the rock surface spectra shown in Section 3.

The spectra were computed and matched at 298 points from 0.1 Hz to 100 Hz (peak acceleration) following the guidelines in McGuire et al., (2001). The associated matching criteria, no points exceeding 30% above the target nor more than 20 points below the target (with none more than 10% below) have not been applied here. In this case, the motions are used as control motions for site response analyses so mean based time histories, with respect to the target spectra, are desired. Applying the matching criteria (McGuire et al., 2001) necessarily results in spectra that are biased high with respect to target spectra, an undesirable feature in site response analyses. An examination of the spectral matches shows the fits to be quite good overall, mean-based, and with no spectral ordinates falling significantly below the targets over the important frequency range 0.3 Hz to 25 Hz. For example, in the mean based fit to the rock UHS (Figure 5-1) from 0.2 Hz to 100 Hz, 130 out of 268 points are below the target with about 100 less than 5% below and only 3 points are more than 10% under the target. The lowest point is only about 15% below the target and the maximum exceedence is about 15% (about 3 points). The remaining mean based fits show similar distributions around the targets.

REFERENCES

- Kennedy, R.P., Kincaid, R.H., and Short, S.A. (1985). "Engineering characterization of ground motion, Task II: Effects of ground motion characteristics on structural response considering localized structural nonlinearities and soil-structure interaction effects." Prepared for U.S. Nuclear Regulatory Commission. NUREG/CR-3805, vol. 2.
- McGuire, R.K., W.J. Silva, and C. Costantino (2001). "Technical Basis for Revision of Regulatory Guidance on Design Ground Motions: Hazard- and Risk-consistent Ground Motion Spectra Guidelines," U.S. Nuclear Reg. Comm., Rept NUREG/CR-6728, October.

- Schneider, J.F., W.J. Silva, and C.L. Stark (1993). "Ground motion model for the 1989 M 6.9 Loma Prieta earthquake including effects of source, path and site." *Earthquake Spectra*, 9(2), 251-287.
- Silva, W.J. and Lee, K. (1987). "*WES RASCAL code for synthesizing earthquake ground motions.*" State-of-the-Art for Assessing Earthquake Hazards in the United States, Report 24, U.S. Army Engineers Waterways Experiment Station, Miscellaneous Paper S-73-1.
- Silva, W.J., N. Abrahamson, G. Toro, C. Costantino (1997). "Description and validation of the stochastic ground motion model." Report to Brookhaven National Laboratory, Associated Universities, Inc. Upton, New York, Contract 770573.

Table 5-1a
WUS Time History Bins

M, site conditions	\bar{M}	R (km)	\bar{R} (km)	Number of Sets
5 - 6, rock	5.50	0 - 50	17.29	15
	6.00	50 - 100	64.88	15
5 - 6, soil	5.77	0 - 50	16.97	15
	5.77	50 - 100	63.81	15
6 - 7, rock	6.53	0 - 10	6.00	15
	6.39	10 - 50	31.29	30
	6.38	50 - 100	66.12	15
	6.66	100 - 200	89.03*	15
6 - 7, soil	6.51	0 - 10	6.65	15
	6.41	10 - 50	27.83	15
	6.57	50 - 100	67.10	15
	6.64	100 - 200	131.53	15
7+, rock	7.34	0 - 10	4.95	15
	7.38	10 - 50	31.48	15
	7.49	50 - 100	80.56	15
	7.49	100 - 200	134.85	15
7+, soil	7.47	0 - 10	4.62	15
	7.47	10 - 50	29.81	15
	7.53	50 - 100	67.84	15
	7.44	100 - 200	133.50	15

*Supplemented with records from 50 to 100 km bin which had durations within 30% of the 100 to 200 km bin minimum.

Table 5-1b
CEUS Time History Bins*

M, site conditions	\bar{M}	R (km)	\bar{R} (km)	Number of Sets
5 - 6, rock	5.50	0 - 50	17.29	15
	5.85	50 - 100	78.34	15
5 - 6, soil	5.69	0 - 50	18.81	15
	5.38	50 - 100	72.30	15
6 - 7, rock	6.51	0 - 10	6.55	15
	6.32	10 - 50	28.58	15
	6.35	50 - 100	66.47	15
	6.66	100 - 200	89.03	15
6 - 7, soil	6.51	0 - 10	6.65	15
	6.34	10 - 50	29.04	15
	6.50	50 - 100	66.49	15
	6.64	100 - 200	131.53	15
7+, rock	7.34	0 - 10	4.95	15
	7.38	10 - 50	31.43	15
	7.49	50 - 100	80.56	15
	7.49	100 - 200	134.85	15
7+, soil	7.47	0 - 10	5.72	15
	7.47	10 - 50	29.81	15
	7.53	50 - 100	67.84	15
	7.44	100 - 200	133.50	15

*Supplemented with WUS to CEUS scaled records (McGuire et al., 2001; Section 3)

Table 5-2
WUS Statistical Shape Bins

Distance Bin (km)	<u>Range</u>			<u>Magnitude Bins (M)</u>					
	\bar{M}	\bar{R} (km)	Number of Spectra	Bin Center	PGA** (g), σ_{ln}	PGV** (cm/sec), σ_{ln}	PGD** (cm), σ_{ln}	$\frac{PGV^*}{PGA} (\frac{cm/sec}{g}), \sigma_{ln}$	$\frac{PGA \cdot PGD'}{PGV^2}, \sigma_{ln}$
				5 - 6					
				6 - 7					
				7+					
0 - 10, rock	5.54	7.91	30	5.5	0.18, 0.91	8.14, 1.14	0.80, 1.60	44.50, 0.58	2.17, 0.28
	6.53	5.75	32	6.5	0.44, 0.76	32.65, 0.93	6.22, 1.26	73.51, 0.40	2.54, 0.42
	7.51	4.99	27	7.5	0.45, 0.62	60.41, 0.49	38.47, 0.86	135.42, 0.50	4.61, 0.55
0 - 10, soil	5.76	7.80	24	5.5	0.26, 0.65	18.57, 0.56	3.11, 0.46	70.72, 0.33	2.32, 0.35
	6.46	6.00	77	6.5	0.38, 0.43	46.88, 0.59	14.79, 0.89	122.00, 0.44	2.54, 0.41
	7.50	5.77	42	7.5	0.27, 0.52	51.81, 0.31	43.08, 0.36	194.11, 0.44	4.20, 0.42
10 - 50, rock	5.57	21.80	180	5.5	0.11, 0.87	5.08, 0.85	0.54, 1.04	46.96, 0.37	2.24, 0.38
	6.43	30.28	238	6.5	0.13, 0.73	8.81, 0.76	1.96, 1.01	70.41, 0.49	3.09, 0.54
	7.52	34.57	64	7.5	0.12, 0.87	15.31, 0.84	9.11, 1.15	126.39, 0.59	4.62, 0.59
10-50, soil	5.69	21.82	378	5.5	0.11, 0.73	6.63, 0.77	0.87, 0.94	59.88, 0.34	2.16, 0.33
	6.35	28.27	542	6.5	0.14, 0.63	10.77, 0.74	2.25, 1.04	78.78, 0.41	2.57, 0.41

**Median values

Table 5-2 (cont.)
WUS Statistical Shape Bins

Distance Bin (km)	<u>Magnitude Bins (M)</u>			<u>Bin Center</u>				
	<u>Range</u> 5 - 6 6 - 7 7+				5.5 6.5 7.5			
	\bar{M}	\bar{R} (km)	Number of Spectra	PGA** (g), σ_{ln}	PGV** (cm/sec), σ_{ln}	PGD** (cm), σ_{ln}	$\frac{PGV^*}{PGA}$ ($\frac{cm/sec}{g}$), σ_{ln}	$\frac{PGA \cdot PGD^*}{PGV^2}$, σ_{ln}
10 - 50, soil	7.53	32.27	169	0.12, 0.59	24.04, 0.70	16.39, 0.86	207.08, 0.51	3.23, 0.50
50 - 100, rock	5.91	64.27	34	0.05, 0.40	2.22, 0.53	0.21, 0.83	41.16, 0.43	2.24, 0.57
	6.51	76.29	132	0.06, 0.48	8.62, 0.63	7.55, 0.88	152.29, 0.45	5.64, 0.48
	7.58	81.46	10	0.06, 0.52	5.16, 0.87	2.64, 1.17	80.63, 0.45	6.23, 0.50
50 - 100, soil	5.80	67.22	42	0.06, 0.80	3.12, 0.78	0.38, 0.92	53.20, 0.23	2.28, 0.49
	6.49	67.34	158	0.07, 0.67	6.23, 0.78	1.26, 0.99	88.00, 0.42	2.26, 0.44
	7.59	73.86	196	0.07, 0.49	13.42, 0.43	10.75, 0.56	203.68, 0.37	3.86, 0.45
100 - 200, rock	5.40	107.80	2	0.02, ----	1.16, ----	0.10, ----	49.72, ----	1.74, ---
	6.64	114.57	14	0.02, 0.86	2.03, 0.38	1.09, 0.68	132.54, 0.59	3.98, 0.27
	7.53	134.32	52	0.03, 0.60	5.97, 0.64	4.61, 0.96	214.91, 0.37	3.52, 0.37
100-200, soil	6.00	105.00	2	0.03, ----	1.50, ----	0.11, ----	42.92, ----	1.74, ----
	6.64	132.97	28	0.03, 0.78	3.05, 0.58	0.89, 0.97	98.24, 0.53	2.90, 0.42
	7.50	128.34	206	0.04, 0.55	9.95, 0.55	6.78, 0.70	224.81, 0.31	2.97, 0.41

Table 5-2 (cont.)
WUS Statistical Shape Bins

Distance Bin (km)	<u>Magnitude Bins (M)</u>							
	<u>Range</u> 5 - 6 6 - 7 7+			<u>Bin Center</u> 5.5 6.5 7.5				
	\bar{M}	\bar{R} (km)	Number of Spectra	PGA** (g), σ_{ln}	PGV** (cm/sec), σ_{ln}	PGD** (cm), σ_{ln}	$\frac{PGV^*}{PGA} \left(\frac{cm/sec}{g} \right)$, σ_{ln}	$\frac{PGA \cdot PGD^*}{PGV^2}$, σ_{ln}
0 - 50, rock	5.57	19.91	208	0.12, 0.89	5.39, 0.91	0.57, 1.14	46.73, 0.40	2.22, 0.37
	6.44	27.39	270	0.15, 0.84	10.27, 0.89	2.24, 1.10	70.77, 0.48	3.02, 0.53
	7.52	25.92	89	0.18, 1.00	22.81, 0.98	14.16, 1.27	129.78, 0.56	4.69, 0.57
0 - 50, soil	5.69	21.10	398	0.12, 0.75	7.02, 0.79	0.93, 0.97	60.48, 0.34	2.16, 0.33
	6.37	25.50	619	0.16, 0.70	12.93, 0.87	2.85, 1.20	83.17, 0.44	2.57, 0.41
	7.52	27.02	211	0.14, 0.66	27.99, 0.71	19.85, 0.87	204.45, 0.50	3.40, 0.49

Table 5-3
Magnitude and Distance Bins and Duration Criteria

M	R (km)	Duration (sec)**	
		Rock	Soil
5.5 (5 - 6)	0 - 50*	1.1 - 3.6*	1.6 - 4.8*
	50 - 100	3.6 - 8.2	2.9 - 6.4
6.5 (6 - 7)	0 - 10	2.6 - 5.8	3.1 - 7.0
	10 - 50	3.1 - 7.0	3.6 - 8.2
	50 - 100	5.1 - 11.6	5.7 - 12.8
	100 - 200	8.1 - 18.3	8.7 - 19.5
	200 - 400***		
7.5 (7+)	0 - 10	6.1 - 13.8	6.6 - 15.0
	10 - 50	6.6 - 14.9	7.2 - 16.1
	50 - 100	8.7 - 19.5	12.2 - 27.5
	100 - 200	11.7 - 26.3	16.2 - 36.5
	200 - 400***		

*For the M 5.5 bin, there were too few records in the 0-10 km, so distance bins 0-10 and 10-50 were combined into one 0-50 km bin

**5% - 75% total cumulative Arias Intensity

***CEUS only

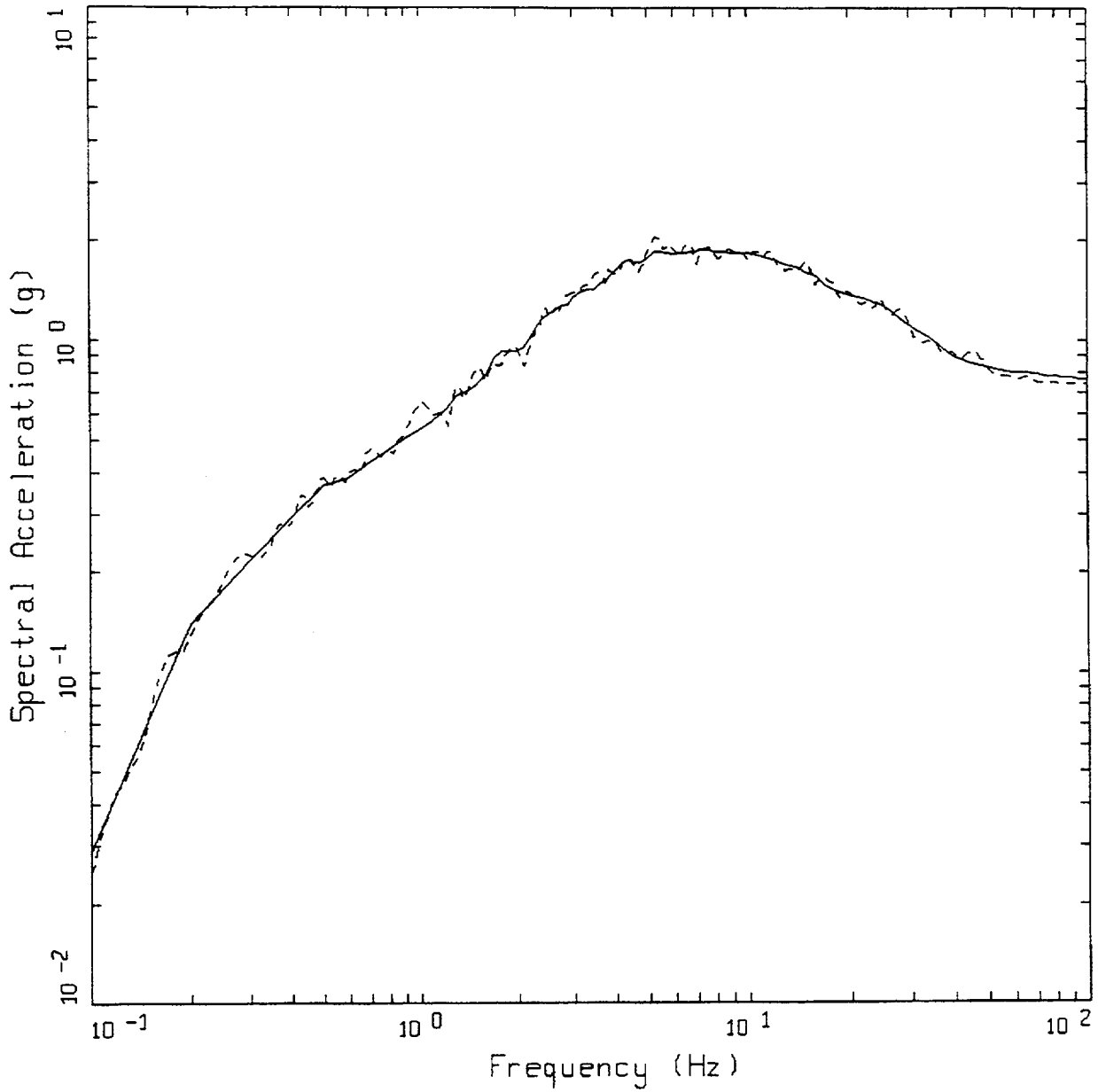
Table 5-4
 Rock Motion Durations (Annual Probability of Exceedence 10^{-4})

UHS	Magnitude	Distance (km)	Durations (5 to 75%) (sec)		
			Input	Match	Target
1 Hz	ML: 5.4	10	2.843	4.944	1.1 - 3.6
	MM: 6.6	18	5.643	8.400	3.1 - 7.0
	MH: 7.8	30	15.85	18.98	6.6 - 14.9
10 Hz	ML: 5.1	10	2.843	4.749	1.1 - 3.6
	MM: 6.1	14	5.678	7.715	3.1 - 7.0
	MH: 7.8	30	15.85	19.05	6.6 - 14.9

RECORDS SELECTED

Target M	Earthquake	M	Site	Distance (km)	Site Condition
5.1, 5.4	Coalinga*	5.2	C-OLP, 270	11.9	rock
6.1	Morgan Hill	6.2	Gilroy 1, 320	16.2	rock
6.6	Loma Prieta	6.9	UCSC, 000	18.1	rock
7.8	Chi Chi	7.5	TCUO78; EW, Z	7.5	rock

* Coalinga aftershock on July 9, 1983.



WUS, 10⁻⁴, UHS, HORIZONTAL
 UHS, M=6.6

LEGEND
 - - - - 5 %, SPECTRAL MATCH; PGA = 0.736 G
 ——— 5 %, CORRECTED TARGET; PGA = 0.767 G

Figure 5-1. Spectral match to corrected (base of soil) rock horizontal 1E-4 UHS, Mojave site.

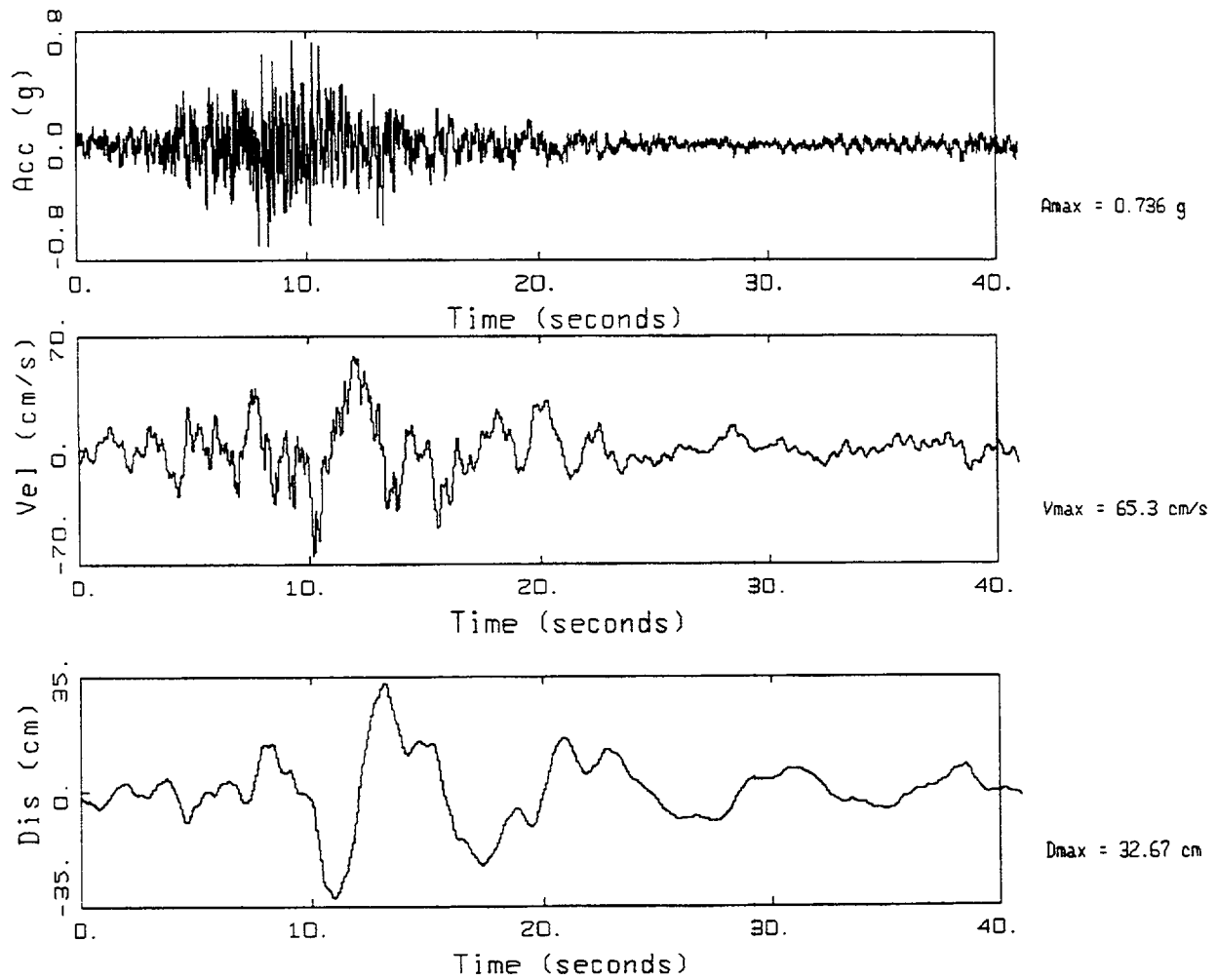
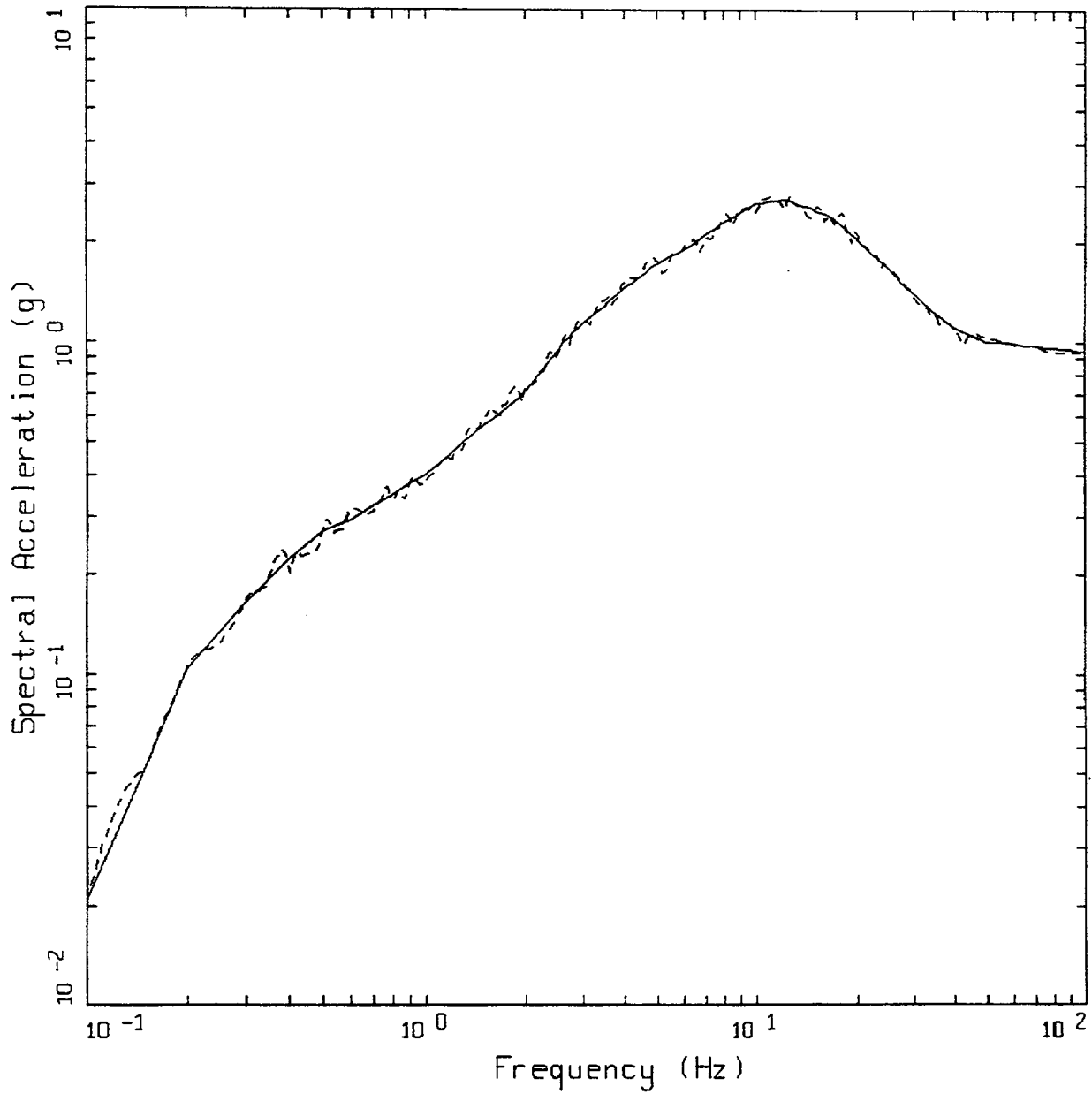


Figure 5-2. Acceleration, velocity, and displacement time histories corresponding to the corrected (base of soil) rock horizontal UHS spectral match, Mojave site.



WUS, 10^{-4} , VERTICAL
 M=6.6

LEGEND
 ——— 5 %, TARGET; PGA = 0.945 g
 - - - - 5 %, SPECTRAL MATCH; PGA = 0.928 g

Figure 5-3. Spectral match to rock vertical component $1E-4$ spectrum, at base of soil for Mojave site.

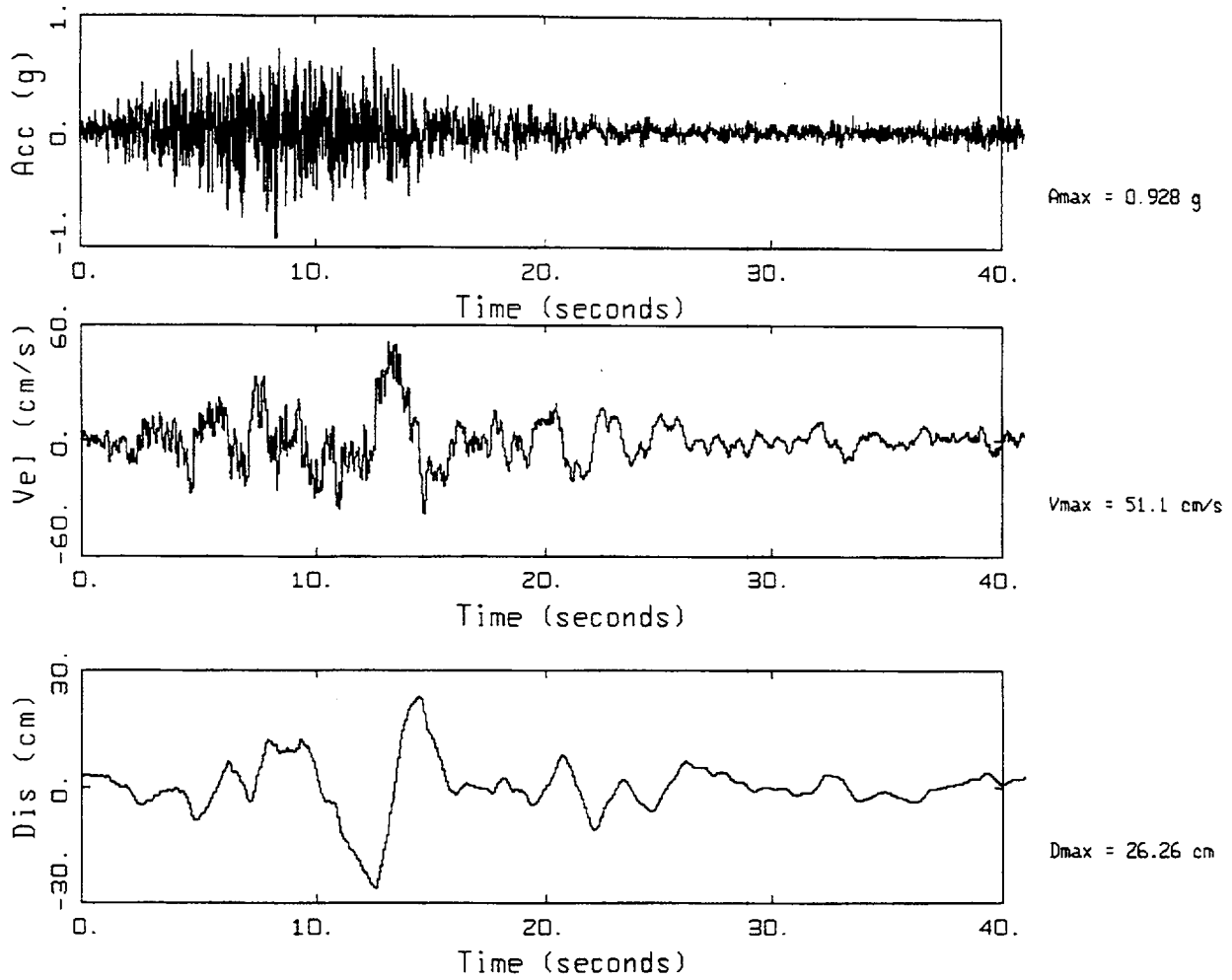
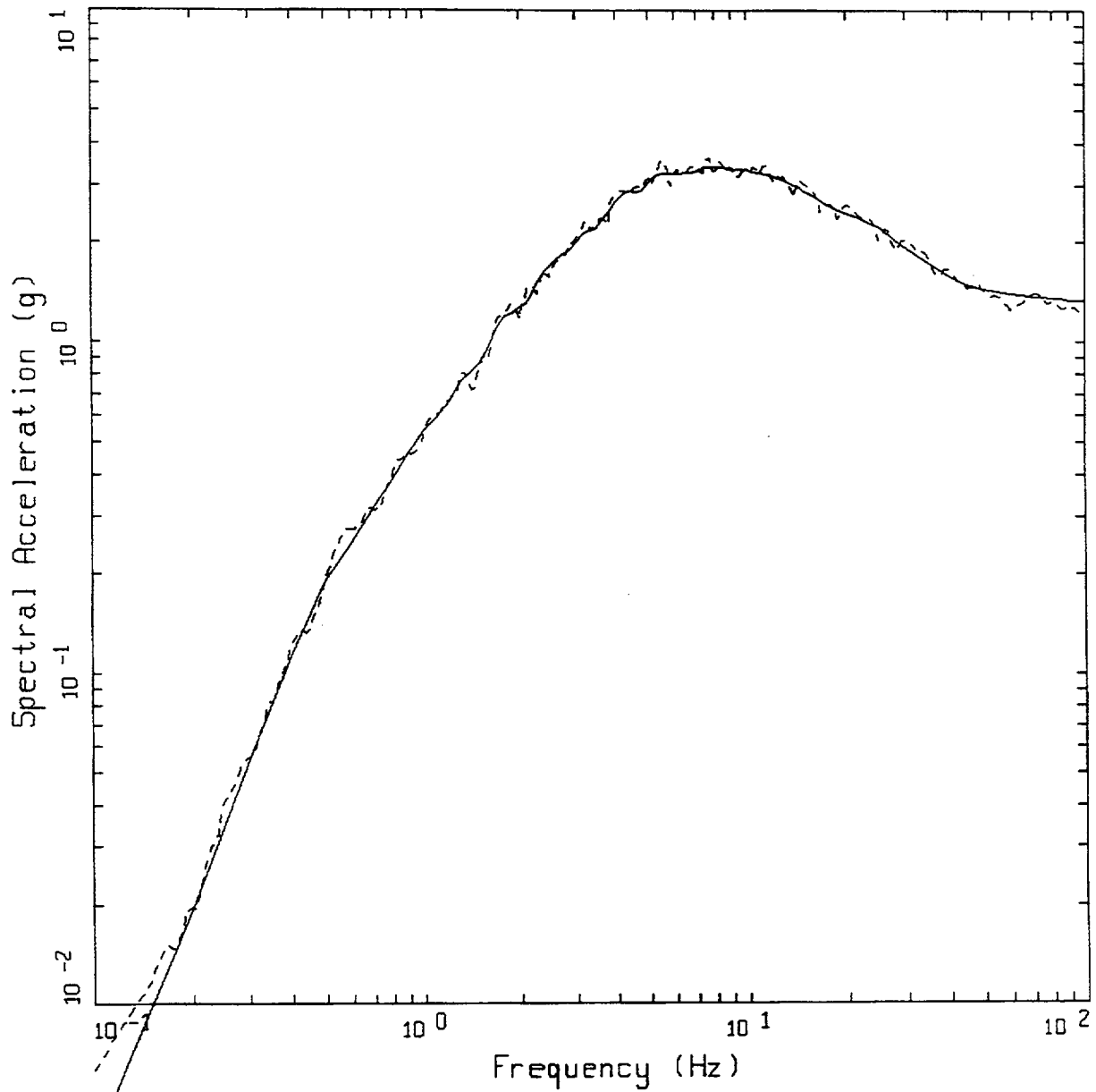


Figure 5-4. Acceleration, velocity, and displacement time histories corresponding to the rock vertical component spectral match at base of soil for Mojave site.



WUS, 10⁻⁴, 1 HZ, HORIZONTAL
 ML, M=5.4

LEGEND
 - - - - 5 %, SPECTRAL MATCH; PGA = 1.221 G
 ——— 5 %, CORRECTED TARGET; PGA = 1.327 G

Figure 5-5. Spectral match to corrected (base of soil) 1 Hz rock 1E-4 spectrum: ML.

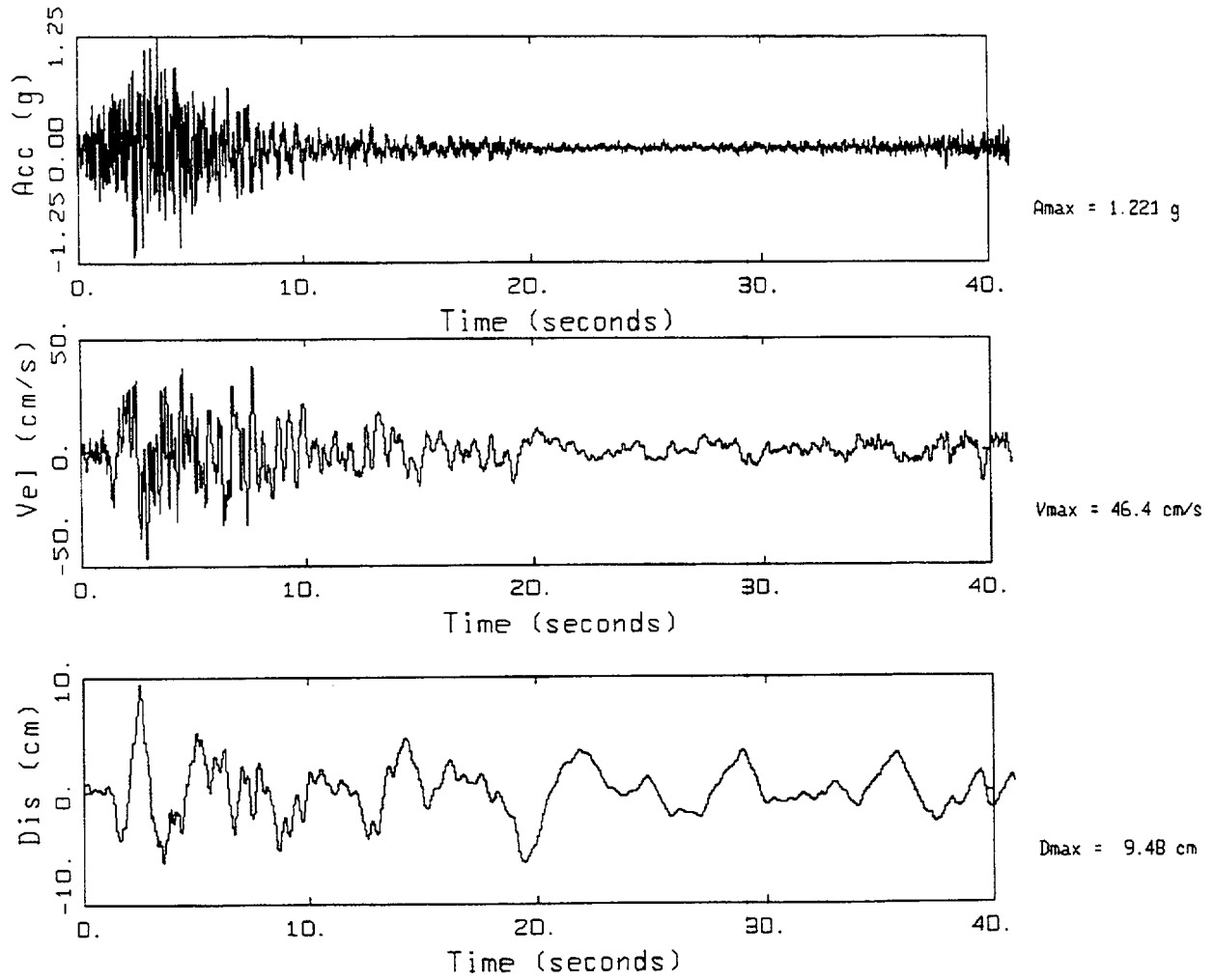
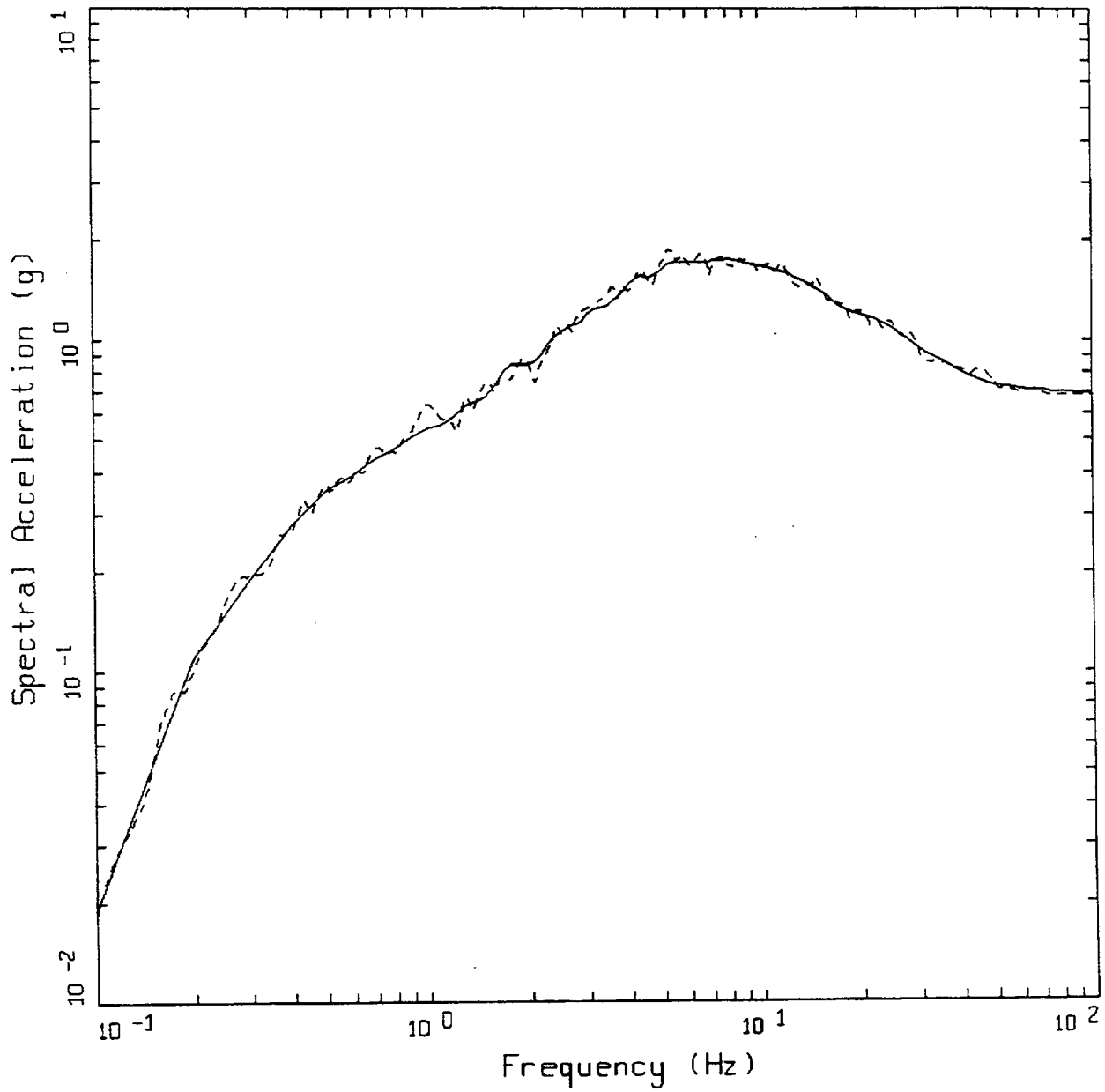


Figure 5-6. Acceleration, velocity, and displacement time histories corresponding to the corrected (base of soil) 1 Hz rock spectral match: ML.



WUS, 10-4, 1 HZ, HORIZONTAL
 MM, M=6.6

- LEGEND
- 5 %, SPECTRAL MATCH; PGA = 0.680 G
 - 5 %, CORRECTED TARGET; PGA = 0.689 G

Figure 5-7. Spectral match to corrected (base of soil) 1 Hz rock 1E-4 spectrum: MM.

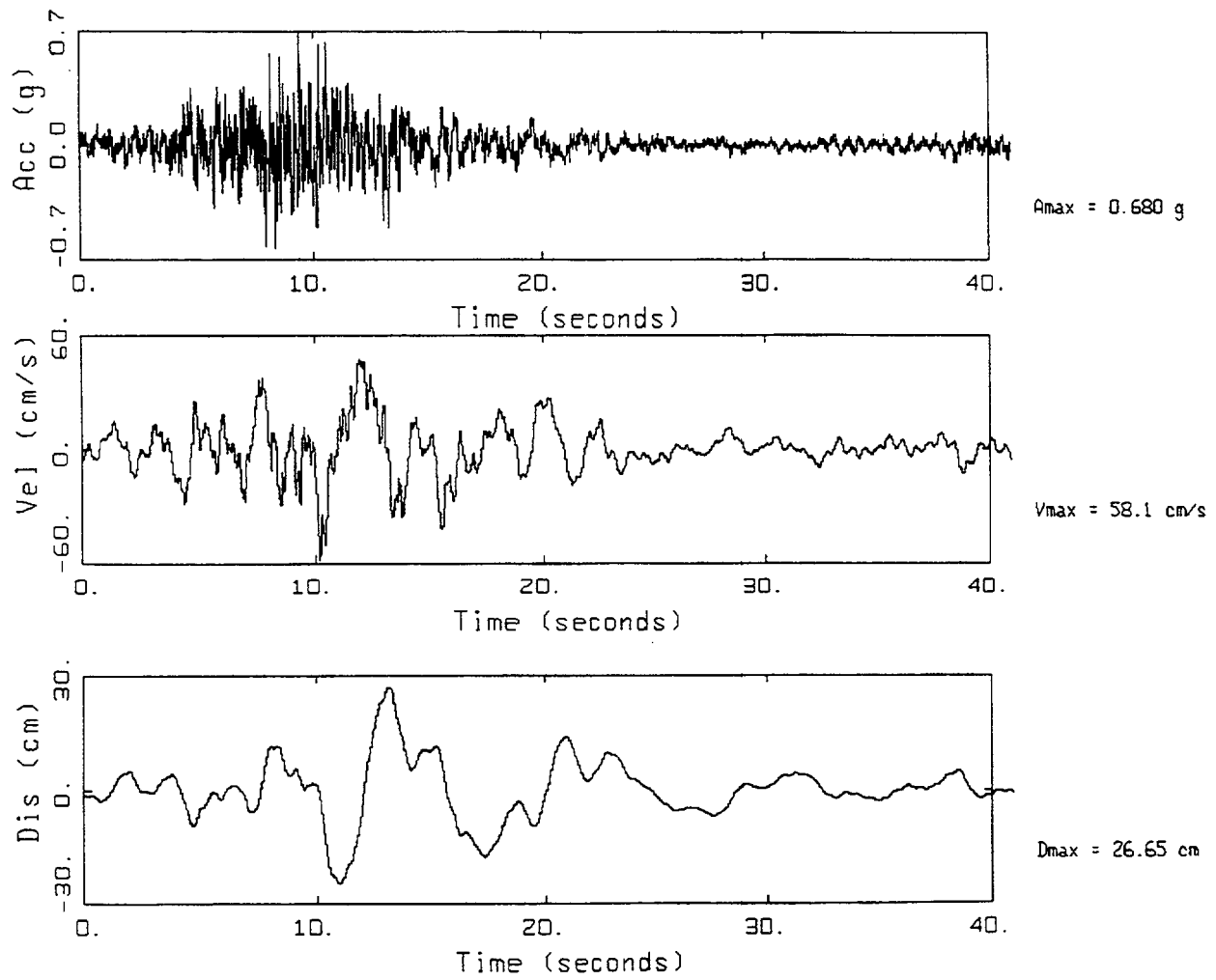
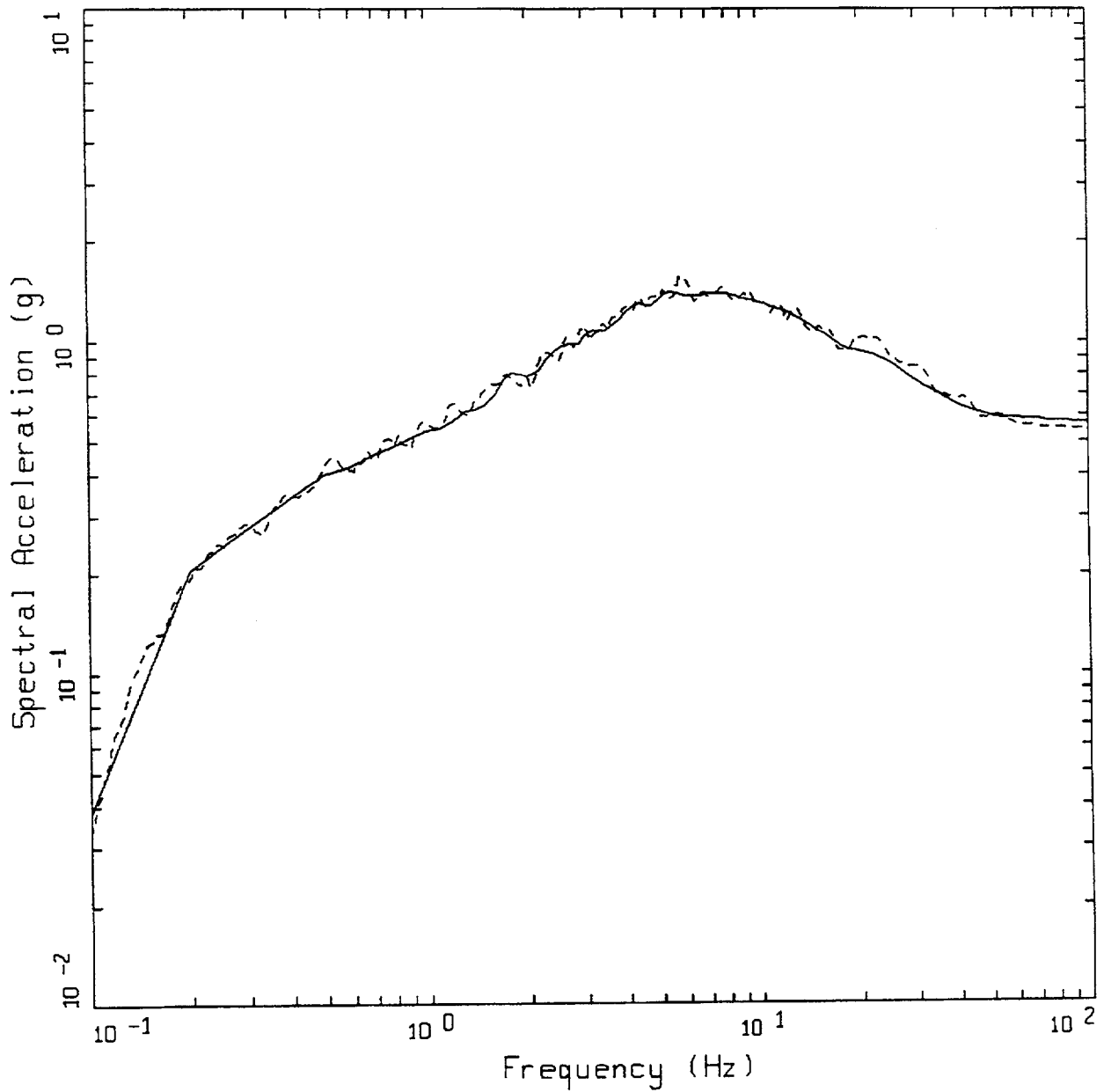


Figure 5-8. Acceleration, velocity, and displacement time histories corresponding to the corrected (base of soil) 1 Hz rock spectral match: MM.



WUS, 10⁻⁴, 1 HZ, HORIZONTAL
 MH, M=7.8

- LEGEND
- 5 %, SPECTRAL MATCH; PGA = 0.539 G
 - 5 %, CORRECTED TARGET; PGA = 0.567 G

Figure 5-9. Spectral match to corrected (base of soil) 1 Hz rock 1E-4 spectrum: MH.

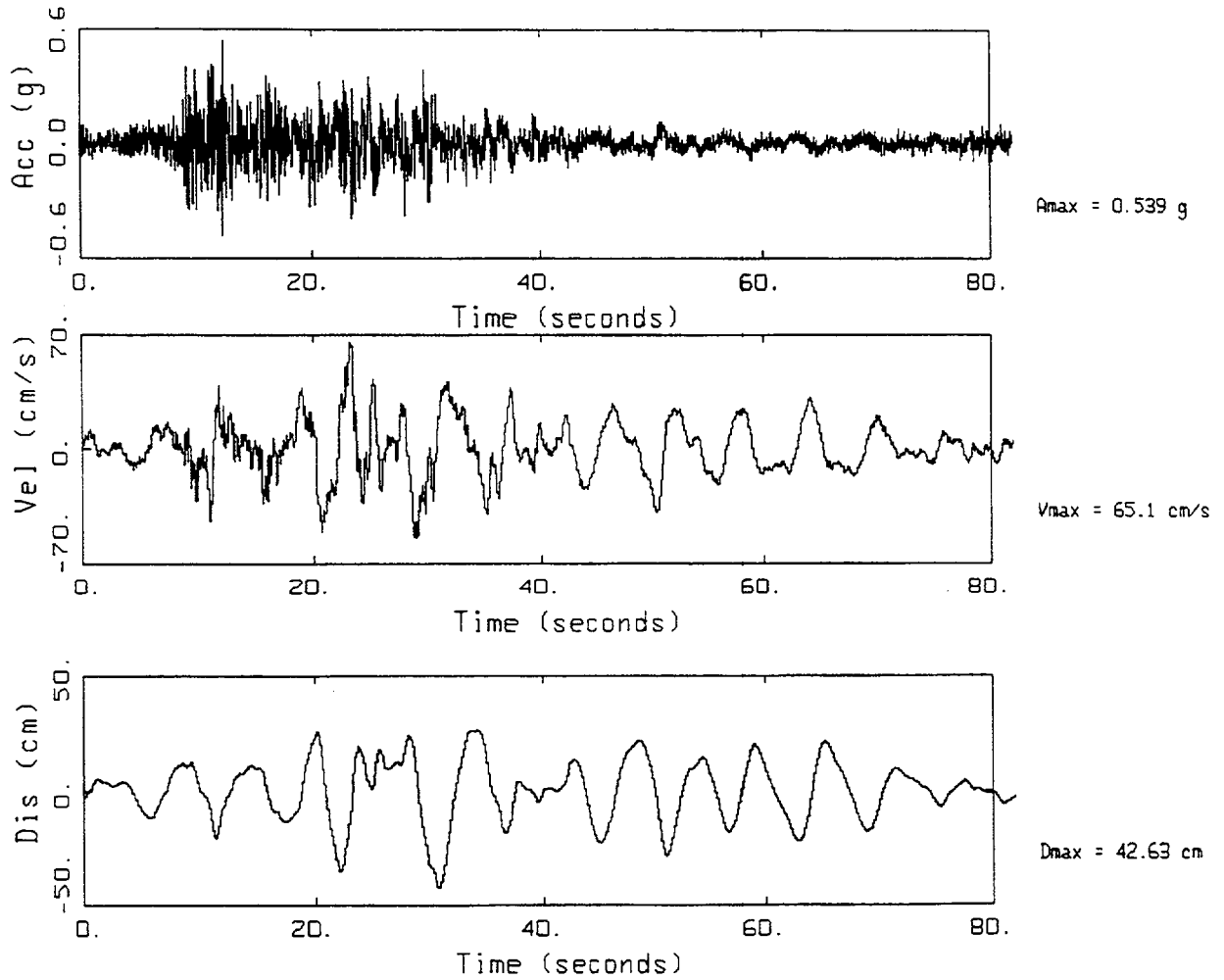
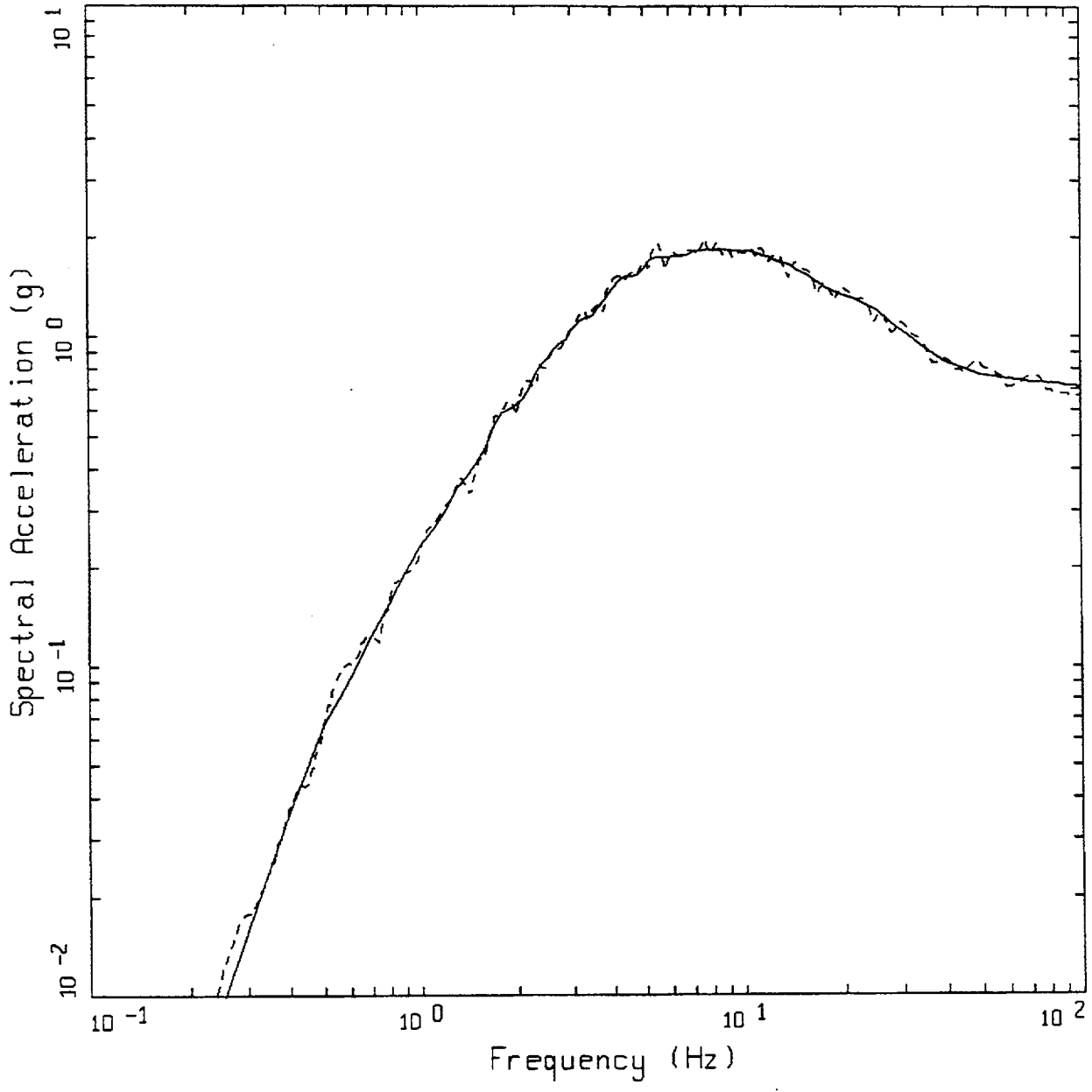


Figure 5-10. Acceleration, velocity, and displacement time histories corresponding to the corrected (base of soil) 1 Hz rock spectral match: MH.



WUS, 10-4, 10HZ, HORIZONTAL
 ML, M=5.1

LEGEND
 - - - - 5 %, SPECTRAL MATCH; PGA = 0.662 G
 ——— 5 %, CORRECTED TARGET; PGA = 0.710 G

Figure 5-11. Spectral match to corrected (base of soil) 10 Hz rock 1E-4 spectrum: ML.

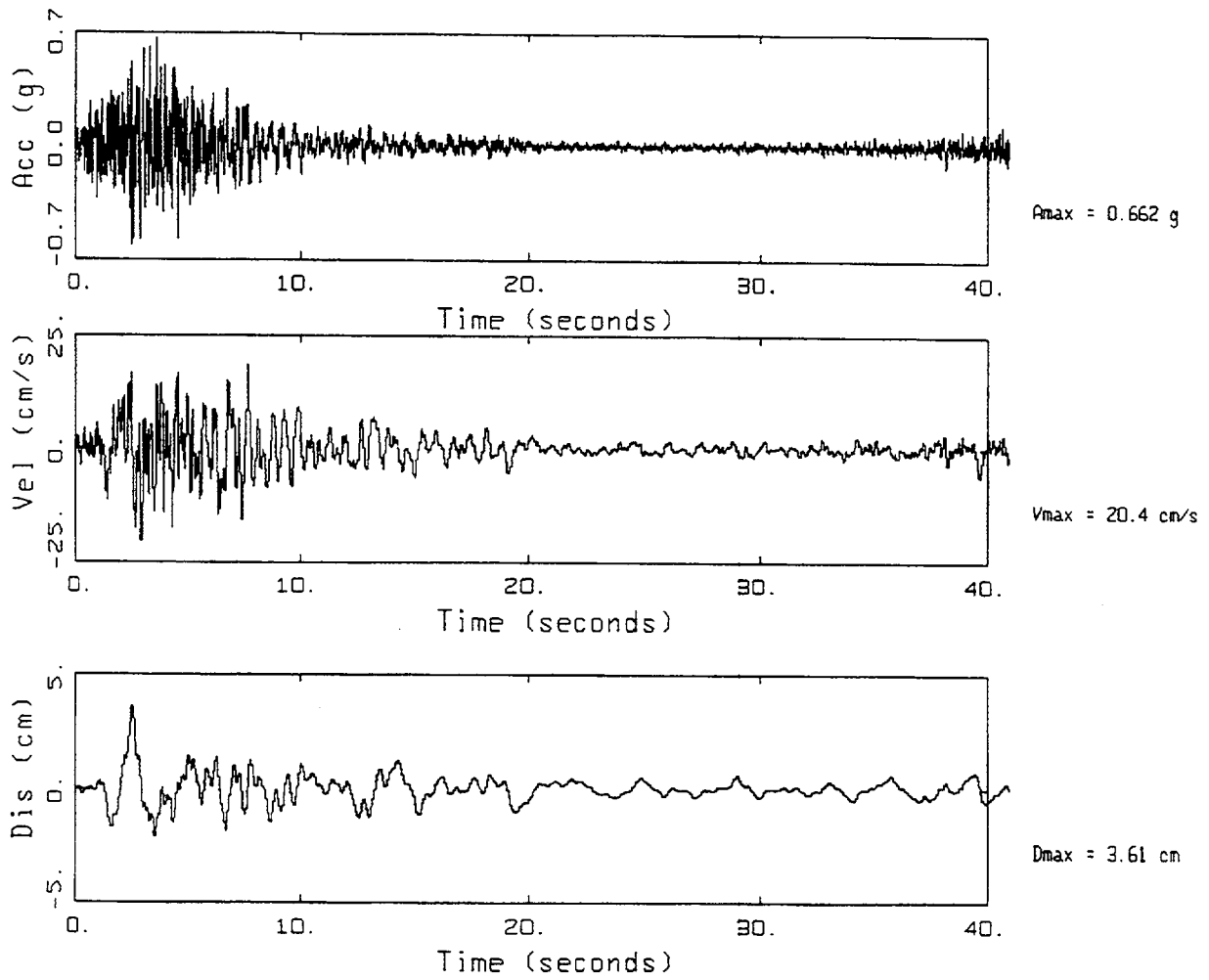
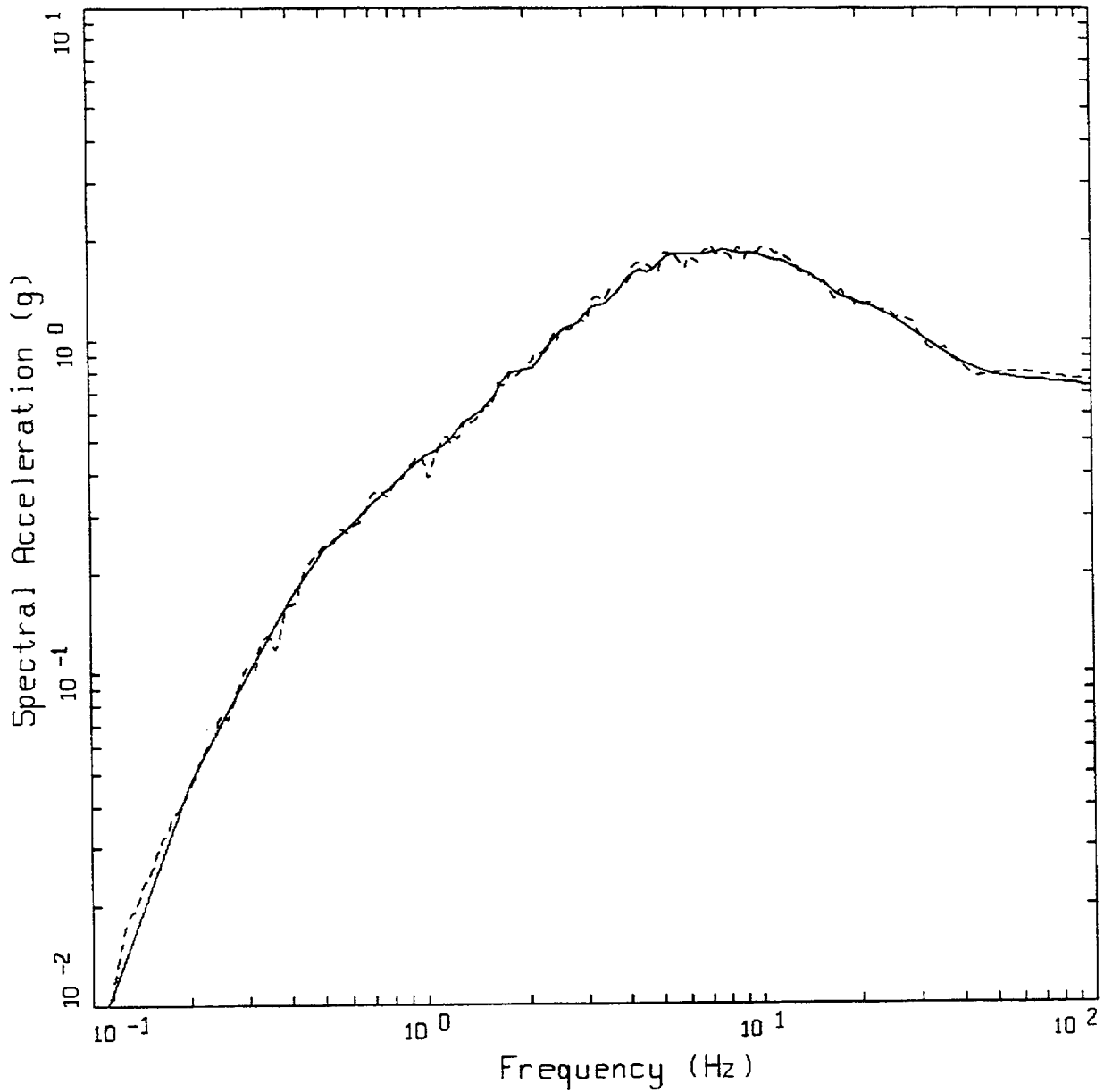


Figure 5-12. Acceleration, velocity, and displacement time histories corresponding to the corrected (base of soil) 10 Hz rock spectral match: ML.



WUS, 10⁻⁴, 10HZ, HORIZONTAL
MM, M=6.1

LEGEND
 - - - - - 5 %, SPECTRAL MATCH; PGA = 0.759 G
 ————— 5 %, CORRECTED TARGET; PGA = 0.733 G

Figure 5-13. Spectral match to corrected (base of soil) 10 Hz rock 1E-4 spectrum: MM.

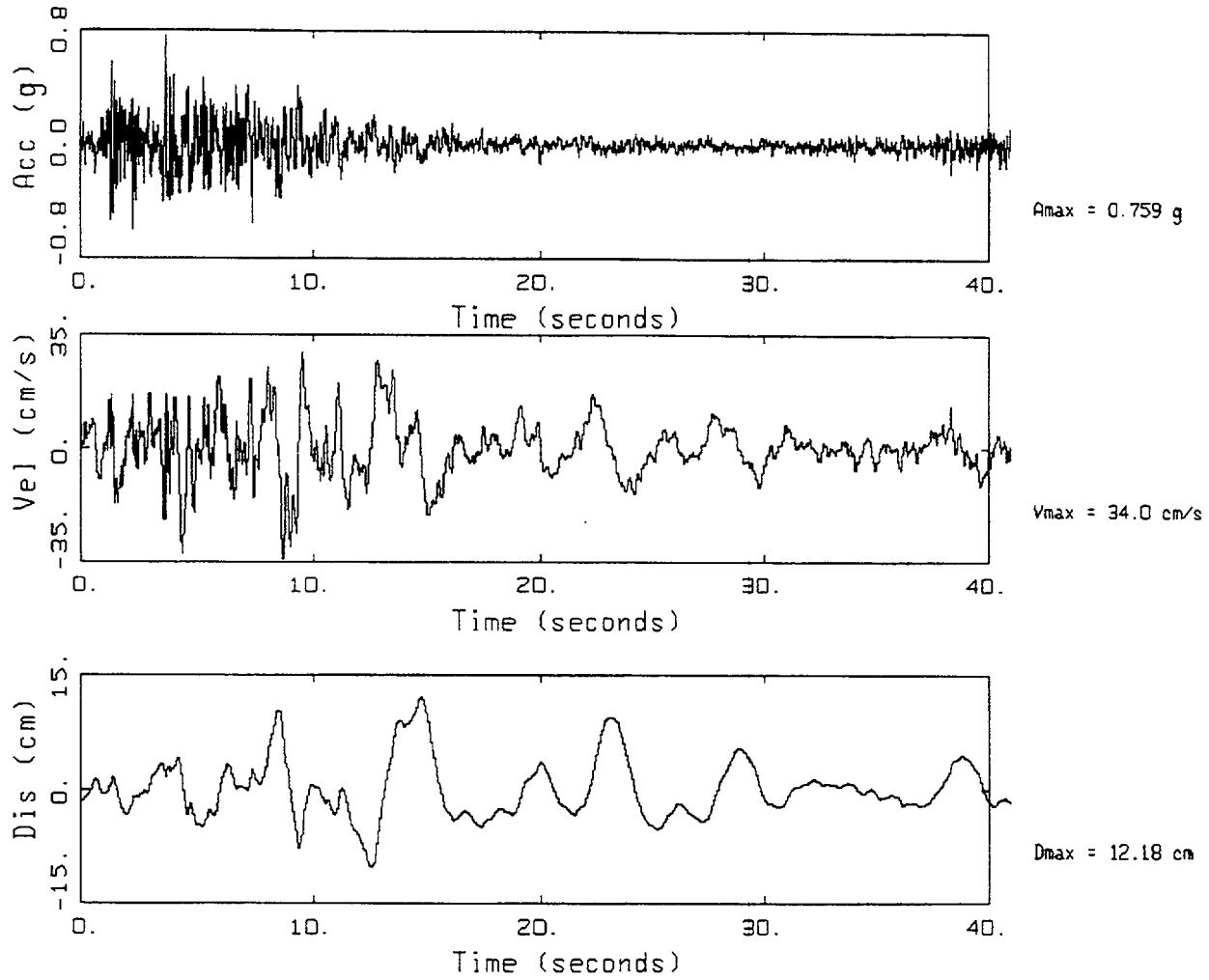
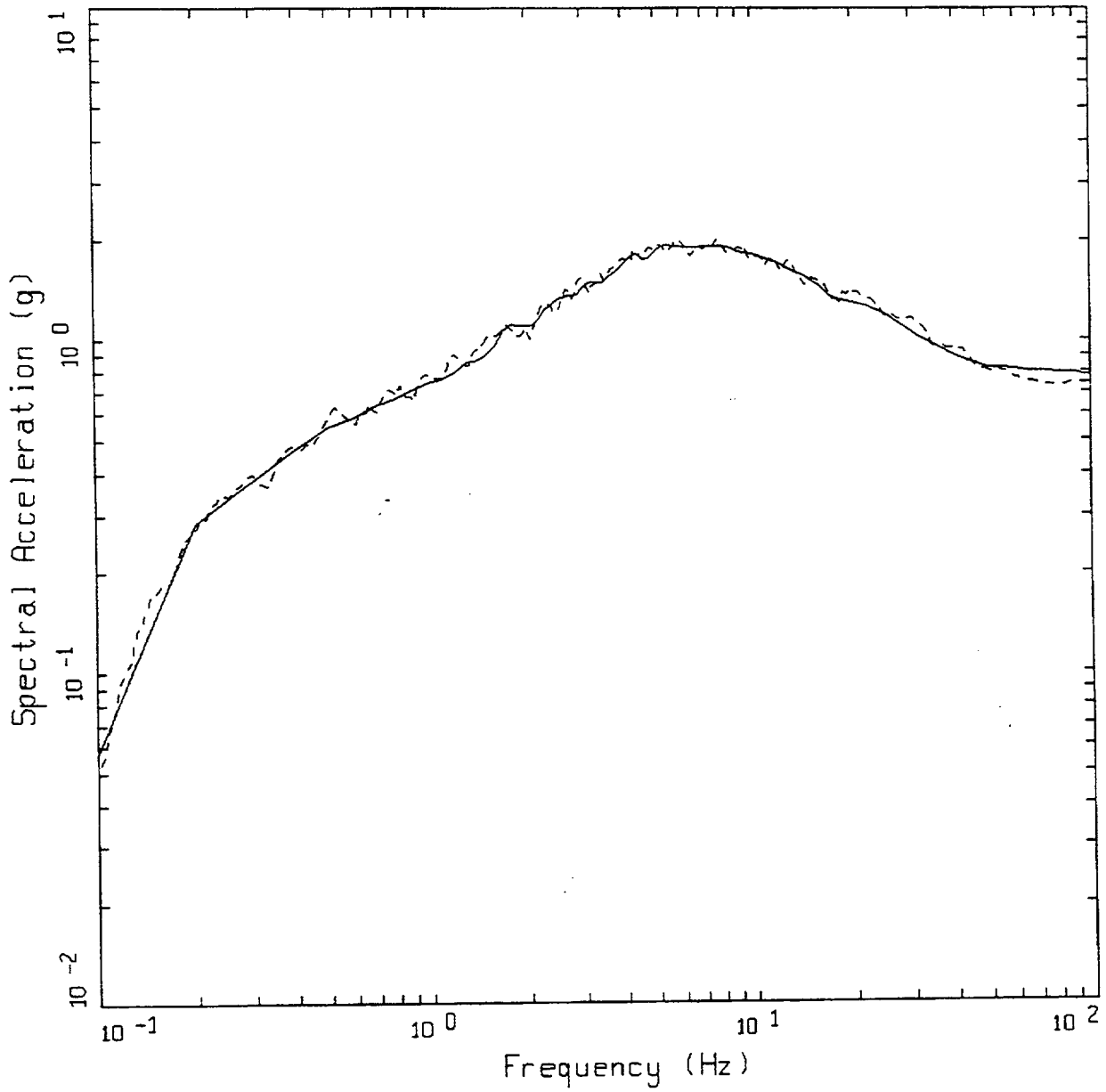


Figure 5-14. Acceleration, velocity, and displacement time histories corresponding to the corrected (base of soil) 10 Hz rock spectral match: MM.



WUS, 10⁻⁴, 10HZ, HORIZONTAL
 MH, M=7.8

LEGEND
 - - - - - 5 %, SPECTRAL MATCH; PGA = 0.730 G
 ————— 5 %, CORRECTED TARGET; PGA = 0.785 G

Figure 5-15. Spectral match to corrected (base of soil) 10 Hz rock 1E-4 spectrum: MH.

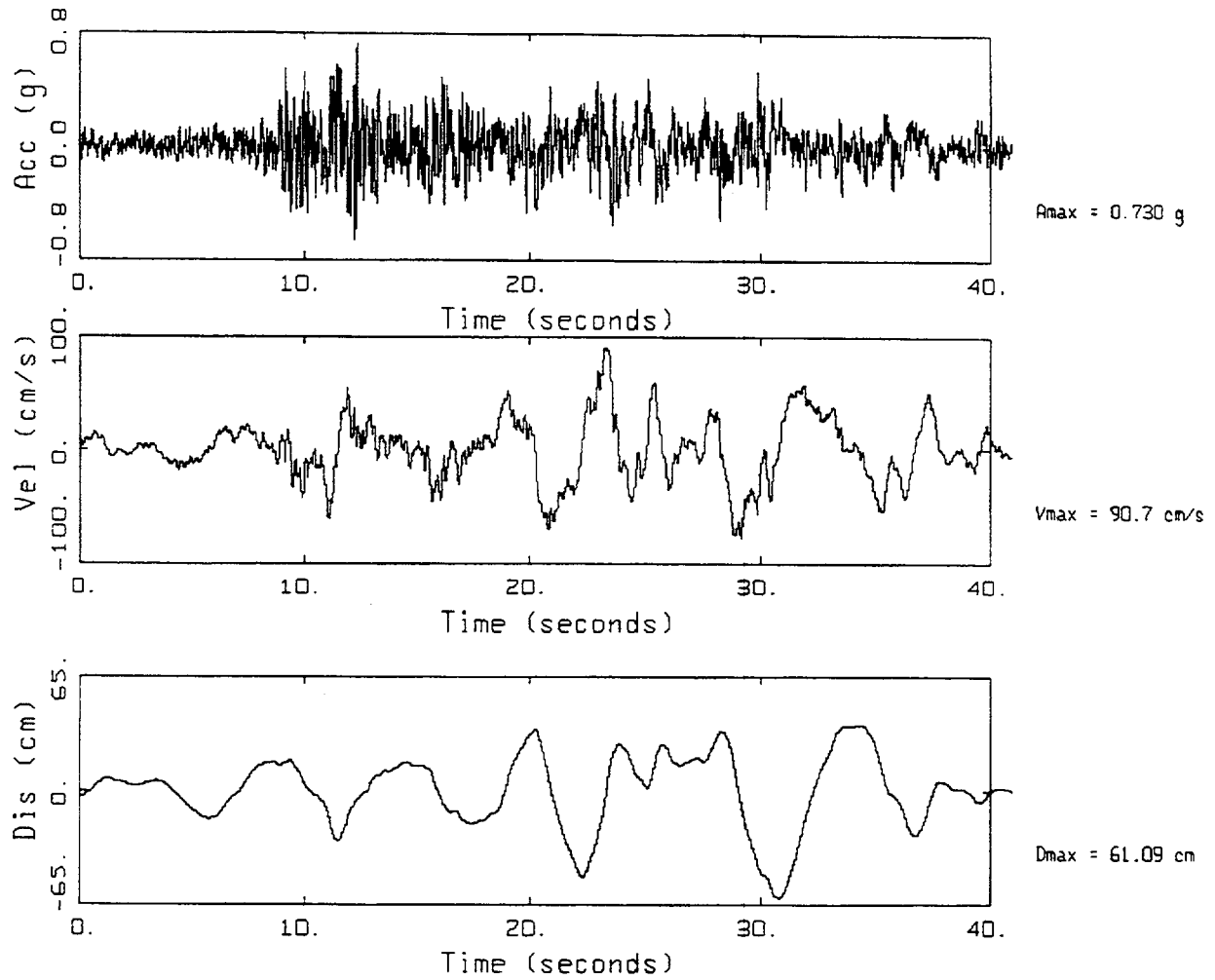


Figure 5-16. Acceleration, velocity, and displacement time histories corresponding to the corrected (base of soil) 10 Hz rock spectral match: MH.

6.0 ESTIMATION OF UNIFORM HAZARD SPECTRA ON SOIL

6.1 Background on estimation of uniform hazard spectra for horizontal motions

The objective in developing site specific soil motions for engineering design is to produce seismic demands that reflect a desired hazard level or degree of conservatism that is uniform across structural frequency. An essential aspect of this process is the accommodation of appropriate degrees of uncertainty and variability in source, path, and site processes.

The usual approach to developing site specific soil motions involves defining regionally generic rock (or very firm conditions) outcrop motions and then performing site response analyses to accommodate the effects of local soils. In this approach the hazard level is usually set at the base of the soil column (in defining the control motions) and the actual hazard level corresponding to the resulting soil motion is not well known. To provide conservatism, that is, to ensure that the resulting soil motions do not reflect a higher hazard level than the control motions at some frequencies, parametric site response analyses are performed to incorporate both uncertainty and variability in dynamic material properties and to account for site response model deficiencies. The resulting suite of soil motions is then either smoothly enveloped or the mean value is computed. Since the effects of site variability have been counted twice, once in developing the control (rock outcrop) motions and again in the parametric site response analyses, the resulting soil motions can reflect significantly different hazard levels than desired, as well as hazard levels that vary with frequency. This is particularly true for frequencies near soil column resonances. Design motions then generally reflect both unknown as well as highly variable hazard levels, making the achievement of risk consistency or uniformity in structural analyses a difficult task.

To evaluate approaches to achieving hazard consistent soil spectra (consistent with rock motions) in the context of probabilistic seismic hazard analyses, a suite of site response analyses using rock outcrop UHS are compared to site-specific soil UHS.

6.1.1 Overview of approaches to developing hazard-consistent site-specific soil motions incorporating profile uncertainties

The conventional approach to developing site-specific soil motions involves convolutional analysis, either equivalent-linear or fully nonlinear, using rock outcrop control motions at the soil/rock transition zone. For “bottomless” profiles the “rock” control motions may be input at a sufficiently deep location such that soil amplification extends to the lowest frequency of interest, about 0.5 Hz (generally about 500 ft, McGuire et al., 2001). In the convolutional analyses, uncertainty in dynamic material properties is generally accommodated through parametric variations, either deterministically with upper-, mid-, and lower-range moduli or through a Monte Carlo approach using randomly generated properties with statistically based distributions. Uncertainties in soil properties and in model deficiencies (in the convolutional formulation) are accommodated by either smoothly enveloping the deterministic variations, or by selecting the mean (or a fractile level) for the Monte Carlo approach. Both of these procedures often result in conservative spectral estimates since site variability is already accommodated in the variability associated with the attenuation relations used in developing the control (rock) motions. The approach that uses randomized material properties

is preferred since the conservatism is quantified, provided the parameter distributions reflect a realistic assessment of uncertainty in the base case profile and nonlinear properties (epistemic uncertainty) and variability over the site or footprint (aleatory uncertainty). One motivation for using the more conservative mean rather than median spectral estimates, which acknowledges double counting site variability, is to accommodate a degree of model uncertainty (vertically propagating shear-waves and equivalent-linear approximation) in the convolutional formulation. Since this component of model uncertainty is currently unquantified, it is not possible to add it explicitly. It is, however, thought to be relatively small, based on validation exercises of a complete model (including source, path, and site, see Silva et al., 1997). As a result, the possible double counting of site variability may be largely offset by neglecting the deficiencies in the convolutional formulation. For attenuation relations based solely on validated stochastic point- or finite-source models (Silva et al., 1997) the inclusion of model uncertainty accommodates the site model deficiencies for the vertically propagating shear-wave model using the equivalent-linear approximation.

The various approaches to developing hazard-consistent site-specific soil spectra in increasing order of accuracy are listed in Table 6-1. Approaches 1, 2A, 2B, 3, and 4 are compared in the following sections. Approach 1 involves driving the soil column with the broad rock UHS spectrum (control motions) and may result in unconservative high frequency motions, particularly in the context of equivalent-linear site response analyses. Additionally, the appropriate magnitude and time history duration are ambiguous using Approach 1 for hazard environments that do not result in strongly unimodal *M* and *R* deaggregation. Approach 2A recognizes that different earthquakes may dominate the high and low frequencies, and uses separate transfer functions for these events. This is the approach recommended by Regulatory Guide 1.165 (USNRC, 1997). Approach 2B requires some elucidation. In this approach, mean, high and low percentile magnitudes from deaggregations for each design earthquake (e.g., 1 Hz and 10 Hz) are used to scale spectral shapes to the 1 Hz and 10 Hz rock UHS, and the resulting control motions are used to develop weighted mean transfer functions for each design earthquake. The transfer functions are then used to scale each design earthquake or are combined to scale the rock UHS (illustrated in the following sections). The use of a three-point magnitude distribution for each design earthquake accounts for non-linear effects caused by a wide range of earthquake magnitudes contributing to the hazard.

To provide some insulation from the effects of inappropriate nonlinear dynamic material properties, principally in the context of equivalent-linear analyses, Approach 2 uses the envelope of the two (or more) transfer functions to scale the rock outcrop UHS (McGuire et al., 2001). In this approach, for frequencies above the fundamental column resonance, the soil amplification resulting from the lowest input (control) motion is used to scale the rock UHS. If there is high confidence that the nonlinear properties reflect in-situ conditions, the analyst may use either the mean (of the two or more) transfer function or a composite that, at any frequency, simply uses the transfer function appropriate for the controlling scaled earthquake.

Approach 3 involves approximations to the hazard integration using suites of transfer functions. Its development is recent (Bazzurro, 1998; Bazzurro et al., 1999) and it has been implemented at the Department of Energy site Savannah River (Richard Lee, personal communication, 1998). In this approach, complete hazard curves may be generated, as this approach is a direct approximation to

Approach 4, essentially substituting suites of transfer functions in place of the site specific soil attenuation relation. The approach is attractive, although requiring significant computations in site response and hazard deaggregation. The approximations implemented in the hazard integrations have been evaluated for a limited number of profiles and loading conditions (Bazzurro et al., 1999). An approximate form of Approach 3 is described in the next section and is used in Section 8 to estimate spectra on soil.

In Approach 4, as Table 6-1 states, a site specific soil attenuation relation is used in the hazard analysis. This approach assumes that appropriate parametric variations are incorporated in the development of the attenuation relation and that they are also reflected in the uncertainty about the median ground motions.

6.1.2 Theoretical basis of methods for soil analyses

The previous section gave a general overview of four approaches to estimating seismic hazard for soil sites; this section presents the theoretical basis for those approaches. In developing this theoretical basis we have benefitted from discussions with C.A. Cornell and P. Bazzurro, who have pursued similar work, most recently documented in Bazzurro (1998) and Bazzurro et al (1999).

Available approaches to estimating soil UHS can be divided into two broad categories. First are those that integrate over multiple rock amplitudes to calculate soil hazard (probability of exceedence vs. amplitude), from which UHS on soil can be derived. Second are approaches that use the rock UHS at a given annual probability to derive a soil UHS at that same probability. Both approaches and their variants are described here, and in subsequent sections we present examples of applications using soil data from actual sites. Table 6-2 lists these approaches, with a short description and an indication of whether the approach integrates over multiple earthquakes and multiple amplitudes. A more detailed description of each approach is given in McGuire et al., (2001). It is most convenient to start with the most accurate method, Approach 4.

Approach 4 (Based on Integration). If we define the amplitude on soil at a certain natural frequency to be A_s , then the straightforward approach to calculate soil hazard is directly through a PSHA:

$$P[A_s > z] = \iint P[A_s > z | m, r] f_{m,r}(m, r) dm dr \quad (6-1)$$

which is the standard PSHA equation in which z is soil amplitude, m is magnitude and r is distance. (Equation (6-1) ignores, for simplicity, rates of occurrence on different faults and is therefore the probability of exceedence for one random earthquake. Rates of occurrence from multiple sources could be incorporated into this and subsequent equations, at the expense of more cumbersome equations.) We call this "Approach 4." It can lead to a defensible representation of soil hazard. Approach 4 is used as the baseline for evaluating other approaches in subsequent sections.

Approach 3 (Based on Integration). Approach 4 can be simplified by recognizing that soil response can be determined from the level of input motion and the magnitude and distance of the causative earthquake. Thus we can modify equation (6-1) to the following:

$$P[A_s > z] = \iiint P[A_s > z | m, r, a] f_{M,R|A}(m, r; a) f_A(a) dm dr da \quad (6-2)$$

or

$$P[A_s > z] = \iiint P[AF > \frac{z}{a} | m, r, a] f_{M,R|A}(m, r; a) f_A(a) dm dr da \quad (6-3)$$

where a is the amplitude of shaking on rock, for example the spectral acceleration at the same frequency as A_s , and $f_A(a)$ is derived from the hazard curve for this frequency. We call this "Approach 3." The first equation above calculates $P[A_s > z]$ from the deaggregated rock hazard, i.e. from $[a, m, r]$ sets. The second equation is equivalent except that it defines soil response by an amplification factor:

$$AF = A_s / a \quad (6-4)$$

where AF is a random variable with a distribution that can potentially be a function of m and r as well as a .

Approach 3 can be approximated by recognizing that soil response is governed primarily by the level of rock motion and the magnitude of the event; given these two variables, distance does not have a significant effect. Thus:

$$P[A_s > z] = \iint P[A_s > z | m, a] f_{M|A}(m; a) f_A(a) dm da \quad (6-5)$$

$$P[A_s > z] = \iint P[AF > \frac{z}{a} | m, a] f_{M|A}(m; a) f_A(a) dm da \quad (6-6)$$

For this variant of Approach 3, we would need only the conditional magnitude distribution for relevant amplitudes of a .

There are several ways to implement equations (6-5) and (6-6) in practice. We can represent the magnitude distribution $f_{M|A}(m; a)$ with a continuous function, with three discrete points, or with a single point located for example at the mean magnitude given a . Also, the probabilities of $A_s > z$ or of $AF > z/a$ can be calculated from a broad-banded motion or from motions scaled to specific frequencies (see Approaches 1 and 2 below). We present a comparison of several implementations in Section 6.2 below.

Approach 1 (based on UHS Scaling). Approach 3 above prompts the idea of further simplification by eliminating the integrals on magnitude and spectral amplitude, and scaling the rock UHS to calculate a soil UHS. If soil uncertainties are small, or if we can account for them explicitly, we can estimate the soil UHS accurately, for a given rock UHS. This would certainly be the most straightforward, intuitive approach. We label the simplest scaling "Approach 1."

This scaling works as follows. For a chosen annual probability p' , the corresponding rock UHS is calculated. This UHS becomes a target spectrum, and one (or preferably multiple) rock motions are matched to the target. These rock motions are then used to drive a model of the soil column that includes uncertainties in soil properties. From all of the rock motions and soil properties, the mean soil spectrum is calculated, and this is the Approach 1 estimate of the soil UHS corresponding to

annual probability p' . Of course a less accurate estimate could be obtained by ignoring uncertainty in soil properties.

Approach 2 (Based on UHS Scaling). Approach 1 implies that a single, broadband motion representing the rock UHS will be used to drive the soil calculations. It has been recognized that a broadbanded motion may be inaccurate in many applications (e.g. USNRC, 1997) and may in fact be unconservative. The reason is that one earthquake (e.g., a small, local event) may dominate the high-frequency hazard, but a different event (e.g. a large, distant shock) may dominate the low frequencies. In this case a single earthquake that drives all frequencies to the UHS level is unlikely. As an alternative, two earthquakes can be used: one that dominates at high frequencies (10 Hz) and another that dominates at low frequencies (1 Hz). Approach 1 can be reformulated in terms of two spectra: one representing high-frequency events that is scaled to the UHS at 10 Hz, and a second representing low-frequency events that is scaled to the UHS at 1 Hz.

Using the amplitudes of 10 Hz and 1 Hz will simplify the analysis since, where magnitude values are required, they will be available from the rock PSHA results. The resulting soil UHS can be plotted and enveloped to obtain an overall UHS for soil. If more than two frequencies are necessary on rock to define specific events whose envelope matches the UHS, then these same frequencies can (and should) be used to calculate soil UHS. The use of two frequencies in this way is labeled "Approach 2A."

A variant of this approach recognizes that the magnitudes of earthquakes, for a given rock amplitude, may have a strong effect on non-linear soil behavior (through the duration of shaking and long period effects). The magnitude deaggregation at rock amplitude a' (at, say, 10 Hz) can be discretized into three magnitudes m_L , m_m , and m_H . Then the rock amplitude a' can be translated into soil distributions for each magnitude. These can be weighted (using weights derived from the deaggregation) to produce an overall distribution, the mean of which becomes a set of soil responses used to form the UHS. (The estimated UHS is the envelope of the mean soil responses calculated for 10 and 1 Hz.) This is labeled "Approach 2B." Because of nonlinear behavior in the soil, the mean soil amplitude considering M variability may be higher than if M variability is ignored.

Combination Approaches. It is possible to use combinations of the approaches described above, and in fact a combination of Approaches 3 and 2A is recommended below for calculating soil UHS. Specifically, it is recommended that Approach 3 be used to calculate UHS on soil, e.g. that z be determined for $P[A_S > z] = 1E-4$ and $1E-5$ in equations (6-5) and (6-6). Within equations (6-5) and (6-6), it is recommended that Approach 2A be used to calculate $P[A_S > z|m, a]$ or $P[AF > z/a|m, a]$.

6.2 Steps for estimating uniform hazard spectra for horizontal motions

The recommended approach for estimating soil UHS is a combination of Approaches 3 and 2A described in the previous section. We herein label this "Approach 2A/3."

The steps necessary to implement this combined approach are as follows:

1. Determine the soil distribution $P[A_S > z | m', a]$ or $P[AF > z/a | m', a]$ for several values of rock amplitude a and the corresponding dominant magnitude m' , using Approach 2A.
2. Integrate over rock amplitude a to calculate $P[A_S > z]$ using equation (6-5) or (6-6) for a range of soil amplitudes z (Approach 3).
3. Interpolate the results from step 2 at each frequency to obtain, the 10^{-4} and 10^{-5} UHS on soil.

We then use the slope of the soil hazard from 10^{-4} to 10^{-5} to calculate a soil URS from the 10^{-4} soil UHS.

An expanded description of these three steps for Approach 2A/3 follows. This is written in terms of the amplification factor AF, but a parallel procedure applies for computing soil response A_S directly.

Step 1. The soil response AF is calculated for three values of rock motion a : the amplitudes corresponding to the 10^{-3} , 10^{-4} and 10^{-5} hazard. This is achieved by making soil calculations with six sets of rock input motions: one with the high-frequency (10 Hz) magnitude shape scaled to the 10^{-3} UHS at 10 Hz, a second with the low-frequency (1 Hz) magnitude shape scaled to the 10^{-3} UHS at 1 Hz, and similarly for the 10^{-4} and 10^{-5} UHS. These calculations follow Approach 2A, include soil uncertainties, and yield the mean amplification AF for the scaled spectra at 10 and 1 Hz, from which the envelope is created. The calculations also yield a standard deviation of AF.

Step 2. Integrate over rock acceleration a using a simplification of equation (6-6) to calculate $P[A_S > z]$ for a range of soil amplitudes z :

$$P[A_S > z] = \int P[AF > \frac{z}{a} | a, m'(a)] f_A(a) da \quad (6-7a)$$

In this simplification the distribution of m given a has been replaced with a single value of m' (the mean value from deaggregation), representing a discrete distribution with a single value. This value of m' is different at the 10^{-3} , 10^{-4} , and 10^{-5} UHS levels. Step 1 gives us the mean and standard deviation of $[AF | a, m'(a)]$. Assuming a lognormal distribution we calculate $P[AF > z/a]$. (Because the standard deviation varies somewhat with amplitude and frequency in a non-monotonic way, it is convenient to use an average standard deviation for the calculation of $P[AF > z/a]$, which for the examples here is calculated to be 0.2.) For amplitudes below the 10^{-3} UHS or above the 10^{-5} UHS it is generally accurate to use the mean amplification at 10^{-3} and 10^{-5} , respectively (this can be confirmed with a sensitivity study).

An alternative solution to integrating over rock acceleration a in equation (6-7a) is to use the closed-form approximation:

$$z_{rp} = a_{rp} \overline{AF}_{rp} \exp\left(\frac{1}{2} k \sigma_8^2 / d_3^2\right) \quad (6-7b)$$

where z_{rp} is soil amplitude z associated with return period rp , \overline{AF}_{rp} is the mean amplification factor for the rock motion with return period rp , k and d_3 are derived from the slope of the rock hazard

curve and AF, and σ_δ is the log standard deviation of AF described above. Appendix A contains the derivation of equation (6-7b). This formulation, which is demonstrated below to be accurate, offers a convenient, intuitive way to obtain the soil UHS given a rock UHS and amplification factors. The first two terms on the right-hand-side of equation (6-7b) ($a_p \overline{AF}_p$) are Approach 2A, i.e. the rock UHS times the mean amplification factor. The last term ($\exp [1/2 k \sigma_\delta^2 / d_3^2]$) is a correction that accounts for uncertainty in soil amplification (σ_δ), the slope of the rock hazard curve (k), and the slope of AF (d_3). This term is typically 1.05 to 1.25.

Step 3. With the annual probability of exceedence for a range of soil amplitudes z , we interpolate to obtain the UHS on soil corresponding to 10^{-4} and 10^{-5} annual frequency (note that, at these levels, annual probability of exceedence = annual frequency of exceedence).

To derive the URS on soil, at each structural frequency we calculate A_R , which is the ratio of spectral amplitudes at 10^{-5} to those at 10^{-4} (see Section 7.3 of McGuire et al., 2001). We then calculate the scale factor SF:

$$SF = \max \{0.7, 0.35 A_R^{1.2}\} \quad (6-8)$$

which is equation (7-18) from McGuire et al., 2001 and equation (4-2) from this report. The 10^{-4} uniform reliability spectrum is calculated using the 10^{-4} UHS as:

$$URS = SF \times UHS \quad (6-9)$$

which is equation (4-1) from this report.

The specific form of SF in equation (6-8) depends on the assumptions of a seismic margin factor of 1.67 in the design level, and a factor of 20 to 40 between the UHS frequency and the component failure frequency. Other conservatisms or factors could be used, in which case the specific form of SF would change, but the calculation of the URS would be as represented here with a slightly different form for SF. See Section 9.1 for further discussion of the form of equation (6-8).

The advantage of procedure 2A/3 is that the UHS on soil can be calculated from the UHS on rock and from just a few soil amplification studies conducted at selected amplitude levels to establish the slope of AF. The procedure makes several approximations about the distribution of soil response but includes the major effect: soil amplification is a function of the rock input motion and the dominant earthquake magnitude.

6.3 Approaches for vertical motions

Assessment of site specific soil vertical motions to accompany corresponding horizontal motions is a perplexing issue, particularly if it is desirable to maintain hazard consistency with the horizontal motions. Rarely are separate hazard analyses performed for horizontal and vertical control or rock outcrop motions (currently no vertical relations are available for the CEUS) and there are no widely accepted site response methodologies currently available to accommodate vertical analyses (Silva, 1998).

Commonly, equivalent-linear site response analyses for vertical motions have used strain iterated shear moduli from a horizontal motion analysis to adjust the compression-wave velocities assuming either a strain independent Poisson's ratio or bulk modulus. Some fraction (generally 30% to 100%) of the strain iterated shear-wave damping is used to model the compression-wave damping and a linear analyses is performed for vertically propagating compression waves using the horizontal control motions scaled by some factor near 2/3.

Alternatively, fully nonlinear analyses can be made using two- or three-component control motions (Costantino, 1967; 1969; Li et al., 1992; EPRI, 1993). These nonlinear analyses require two- or three-dimensional soil models that describe plastic flow, yielding, and the accompanying volume changes as well as coupling between vertical and horizontal motions through Poisson's effect. These analyses are important to examine expected dependencies of computed motions on material properties and may have applications to the study of soil compaction, deformation, slope stability, and component coupling. However, the models are very sophisticated and require specification of many parameters, at least some of which are difficult to measure both in mean or central values as well as expected ranges (uncertainties).

The equivalent-linear approach implicitly assumes some coupling between horizontal and vertical motions. This is necessitated by the lack of well determined G/G_{max} and hysteretic damping curves for the constrained modulus. Ideally, the strain dependency of the constrained modulus should be determined independently of the shear modulus. Also, the conventional approach assumes vertically-propagating compression waves and not inclined P-SV waves. Additionally, the use of some fraction of the horizontal control motion is an approximation and does not reflect the generally greater high-frequency content of vertical component motions at rock sites due to lower kappa values (EPRI, 1993). More recently, use is made of V/H ratios for rock computed from empirical attenuation relations. This process accommodates observed trends in magnitude and distance dependencies of vertical motions (EPRI, 1993; Silva, 1998) and results in vertical control motions appropriate for the controlling earthquakes, generally based on UHS 1 Hz deaggregation, as this usually results in the largest earthquakes. For cases that result in very large distances (>100 km) for 1 Hz and very close distances for 10 Hz (< 10 km) or peak acceleration deaggregation, it would be more appropriate to use two design spectra (e.g. 1 Hz and 10 Hz) or to envelop the 1 Hz and 10 Hz (or PGA) V/H ratios to develop a conservative vertical rock outcrop spectrum. This approach should not be followed for cases where nonlinear (equivalent-linear) site response analyses are planned to estimate the vertical site specific soil motions. For these cases two (or more) spectra should be used.

The approach taken here makes use of generic soil V/H ratios to scale the site specific horizontal soil motions. This approach maintains as many site specific attributes as possible through the use of the horizontal soil motions (soil column) and generic soil V/H ratios (controlling magnitudes and distances) while avoiding the currently inherent ambiguity in vertical site response analyses. This is the case for WUS where vertical and horizontal component empirical attenuation relations for soil exist. For the CEUS, this approach relies on generic soil V/H ratios based on a validated site response methodology (EPRI, 1993; Silva, 1998). In this case, in an effort to preserve as many empirical attributes as possible and to remove any model deficiencies, we adopt an approach similar to that used in developing the recommended CEUS single- and double-corner spectral shapes (McGuire et al., 2001). In this approach WUS-to-CEUS scale factors are developed and used to scale an empirical

WUS deep soil V/H ratio. The scale factors are ratios of WUS and CEUS V/H ratios computed for generic deep soil, representative of deep soils beneath the WUS strong motion recording sites and assumed to occur both in the WUS and CEUS. To compute the V/H ratios, a generic deep soil column is placed on the generic WUS and CEUS crustal models in a manner analogous to developing the soil attenuation relations (Section 2). In this case, inclined P-SV waves are used to model the vertical motions. This approach was also used to supplement the CEUS analyses time history bins by scaling WUS records to CEUS conditions (McGuire et al., 2001; Section 3).

6.4 Horizontal motions for Mojave site

6.4.1 Results for Approaches 1, 2A, and 2B

Section 6.1 presented a number of approaches to estimating site-specific soil spectra that are consistent with a specified hazard level that accommodate uncertainties in soil properties. In this section, comparisons are made among several of these approaches, and site-specific soil UHS are computed for the Meloland soil profile located in the WUS at the Mojave site. The site-specific soil UHS (following Approach 4) reflect the desired hazard level with which to evaluate the various degrees of approximations using rock outcrop UHS and site response analyses. However, an issue exists in the soil UHS calculated with Approach 4 involving long return periods where the hazard may result from motions that significantly exceed the median ground shaking during earthquakes contributing to the hazard. Under these conditions for highly nonlinear profiles, the site-specific UHS may overestimate the hazard at high frequency, as the residual dispersion does not reflect the soils limited capacity to transmit high levels of motion (i.e. its non-linearity). This is an important issue and requires further elaboration.

Approach 4 was considered to represent “truth” in the context of the analyses of Section 6.1, as these spectra consist of amplitudes computed for the same probability of exceedence across structural frequency. However, at high strains soil profiles tend to saturate (material damping increases), transmitting proportionally less high-frequency motion as loading levels increase. This artifact is enhanced by the equivalent-linear approach and is one of the motivating factors for developing Approaches 2A and 2B. For soil columns near or into failure, when pore pressure has increased to very high levels, high frequency energy may again be transmitted through the column as hysteresis loops become S-shaped (material becomes dilatant) and material damping decreases with increasing strains. At this point, however, motions of significance to structures are generally lower and foundation stability is more of an issue than design ground motions. While this tendency to saturate is reflected in the convolution analyses used to develop both the site-specific soil motions and the soil attenuation relations, the residual dispersion computed in a conventional (homoskedastic) regression analysis is a combination over all event (causative) conditions (all magnitudes and distances). As a consequence, for long return periods, much of the contribution to the soil UHS results from motions that significantly exceed median estimates for the magnitudes and distances dominating the hazard. These contributions are reflected in the deaggregation ε values (McGuire, 1995). This process can conceivably result in soil motions that imply control motions sufficiently high enough to fail the soil column. This apparent paradox suggests that in the context of probabilistic seismic hazard analyses involving nonlinear site response, a magnitude- and distance-*independent* residual distribution (uncertainty about the median attenuation estimates) may be

inappropriate and can result in overly conservative soil motions. The “truth” or benchmark site-specific hazard analysis therefore should represent the distribution of residuals to be magnitude- and distance-*dependent*. There is also a possibility that, at high median response levels, the distribution should be negatively skewed, i.e. that a long positive tail would have very low probability. Detailed analysis of residual distributions from synthetic soil response calculations where Meloland soil properties were varied did not reveal such a skewness, however. Therefore the standard lognormal distribution of soil response was retained, but with a standard deviation dependent on magnitude and distance.

This treatment of soil response uncertainty should be viewed in the context of Meloland site characteristics. Although this profile is considered soft (Figure 2-6), its material strain dependencies are relatively weak (Figure 2-8) resulting in a system (initial stiffness and material strain dependencies) that is considered only moderately nonlinear (as implied by the recordings of the 1979 Imperial Valley earthquake across the El Centro array). Thus the use of a magnitude- and distance-dependent uncertainty in the attenuation relation (Section 3) is sufficient to capture the essential effects of soil saturation. For other profiles that exhibit more non-linear behavior, it would be appropriate to examine the distribution of residuals at high median response levels, to determine if skewness is apparent and should be modeled. For consistency in the current application, a heteroskedastic residual dispersion is used in developing the WUS rock UHS.

It should be noted that the use of a homoskedastic distribution for uncertainty in soil motion is consistent with current practice in the CEUS. WUS attenuation models typically include a magnitude dependency in their standard errors (Abrahamson and Shedlock, 1997) resulting in a large decrease as magnitude increases for $M \geq 6.5$. However, the high frequency motions (≥ 5 Hz) are affected most by nonlinear saturation because of the contribution of low-magnitude ($M < 6.5$) close-in earthquakes. The magnitude dependency currently incorporated in WUS attenuation relations does not represent soil response because it is site independent, and is applied at both rock and soil sites.

High soil responses may result from moderate or high input rock motions combined with randomly selected linear properties (a stiff column, high G/G_{\max} , or low damping curves). Therefore, a range of rock motions contribute to the frequency of exceeding a high soil spectrum. As a result, Approaches 1, 2A, and 2B (which are fundamentally deterministic in nature, being based on a fixed control motion and mean soil response) will underestimate the motions for Approach 4 (the site-specific UHS) at some low hazard level (high soil motion), unless higher fractile levels are used. For the Mojave site, this occurs at the annual probability of exceedence of 10^{-5} .

The development of Approach 3, described in Sections 6.1 and 6.2, avoids the deterministic aspects of Approaches 1, 2A and 2B, while approximating the integration over a range of input rock amplitudes.

Figure 6-1 shows a comparison of the WUS and CEUS rock outcrop UHS. The effects of both the hazard environment and attenuations relations (Section 2) are evident, with the WUS motions generally exceeding the CEUS motions by a factor of five or more for frequencies below about 10 Hz.

To correct the control motions to be appropriate for base-of-soil conditions (shear-wave velocity of 1 km/sec), the effects of the shallow (top 30m) soft rock profile (Figure 2-4) must be removed. Since the Meloland profile (Figure 2-6) was placed on top of the Wald and Heaton (1994) Southern California crustal model (Table 2-3), use of the WUS rock spectra as control motions contain the additional amplification of the materials above the 1 km/sec layer. To accomplish this, response spectral adjustment or correction factors have been developed (McGuire et al., 2001). These factors accommodate nonlinear response of the shallow material (Figure 2-5) and are based on the rock UHS peak acceleration value. The effects of these factors are shown in Figure 6-2, which compares the WUS rock UHS (Figure 6-1) and the corrected (to 1 km/sec material outcropping) UHS. The correction reduces the motions 10% to 20% over much of the frequency range with a maximum reduction near 2 Hz. The plots of control motions in this section include the corrections. Uncorrected motions are shown in Section 4.

Design spectra scaled to 1 and 10 Hz are shown in Figures 6-3 and 6-4 for the WUS and CEUS respectively. The difference in the hazard environments between the WUS and CEUS is evident in the large differences in the 1 Hz and 10 Hz magnitude values from deaggregation. The difference in magnitudes for the 1 Hz and 10 Hz design earthquakes is 1.2 units for the CEUS (Figure 6-4) and only 0.5 units for the WUS (Figure 6-3). The effects of magnitude distribution in the rock UHS on nonlinear soil response are much less an issue for WUS conditions than CEUS, at least for the example sites, which were chosen to maximize the differences at 1 and 10 Hz (Section 2).

In the site response analyses, two issues are important: the degree of fit of artificial motions to the control motion spectra and the effect of control motion variability on median soil spectra. The first issue involves developing appropriate Fourier amplitude spectra for use in the RVT equivalent-linear soil analyses that result in response spectra consistent with target response spectra. To illustrate the RVT spectral matching process (Silva and Lee, 1987), Figure 6-5 compares a target response spectrum to a spectrum resulting from spectral matching. The difference is less than a few percent over the entire frequency range.

The second issue involves the representation of control motion variability, and this is potentially significant because Approaches 1, 2A, and 2B assume fixed or constant control motion while varying site properties. This is different from the process used to develop site specific attenuation relations (Approach 4) where source, path, and site parameters are varied simultaneously. The implicit assumption involved in comparing results from these two different processes is that soil response is either independent or weakly dependent on control motion variability. To demonstrate the validity of this assumption, Figure 6-6 shows median and $\pm 1 \sigma$ spectral estimates for WUS conditions at $M = 7.5$ and $R = 1$ km varying only site properties while Figure 6-7 shows results for varying source, path, and site parameters simultaneously. Although the variability is significantly larger when source and path parameters variations are added ($\sigma_{\ln PGA}$ increases from 0.14 to 0.35, a factor of about 2), the median spectra are virtually identical as illustrated in Figure 6-8.

Meloland profile

The Meloland profile, located in the Imperial Valley of southern California and northern Mexico, is considered a soft profile (Figure 2-6) and has a column frequency of about 0.5 Hz. While it is

considered "bottomless" and extends kilometers in depth, it was truncated at a depth of 304m (1,000 ft) for these analyses. This site has a recently installed (Caltrans/CDMG) vertical strong motion array, and the nearby CDMG strong motion site recorded the M 6.5 1979 Imperial Valley earthquake at a rupture distance of 0.5 km (with an average horizontal component peak acceleration of about 0.3g). The modulus reduction and damping curves representing the Meloland profile are shown in Figure 2-8. They are based on modeling strong motions from the 1979 Imperial Valley earthquake recorded at Meloland and nearby sites (Silva et al., 1997) and reflect relatively weak strain dependencies. The profile is considered nonlinear to a depth of 150m (500 ft).

To begin the approach comparisons for the Mojave site, Figure 6-9 shows the soil UHS computed using Approaches 1, 2A, 2B, and 4. Approach 2A uses the envelope of the 1 Hz and 10 Hz mean spectra computed using 10 Hz and 1 Hz control motions to scale the rock UHS. The spectra may also be used independently to produce soil design spectra for cases where it may be desirable to perform two sets of design analyses. Approach 2B uses multiple (3) sets of control motions to compute both 1 Hz and 10 Hz weighted mean transfer functions. The envelope of the mean transfer functions times their respective control motion spectra becomes the Approach 2B spectrum (Table 6-1). Figure 6-9 shows very similar results for Approaches 2A and 2B, both of which show higher motions than Approach 1 for frequencies above about 1 Hz. This is a consequence of using a single broad UHS spectrum (Figure 6-3) as a control motion. The soil column is being softened more by the broad-banded rock motion of Approach 1 than by either of the scaled design spectra, each of which reflects a single earthquake. In general both Approach 2A and 2B approximate the motions of Approach 4 (soil UHS) from about 0.3 Hz to 100 Hz (PGA). In this case, little difference is seen in Approaches 2A and 2B and Approach 2A is recommended because of its simplicity. Approach 1 is not recommended.

To illustrate the levels of loading in the soil column, Figure 6-10 shows the median and $\pm 1\sigma$ effective strains for the Approach 1 analysis. The effective strains are large, with median values near 0.3 and $+ 1\sigma$ values near 0.6 in the intermediate portion of the profile.

The transfer functions (5% damped response spectra) used to scale the rock outcrop spectra are shown in Figures 6-11 to 6-13. Figure 6-11 shows the ratios computed for the 1 Hz scaled design earthquake and Figure 6-12 the corresponding ratios for the 10 Hz design earthquake. Figure 6-13 compares the two (1 Hz and 10 Hz) mean ratios, of which the envelope is used to scale the rock outcrop UHS (Approach 2B).

Magnitude dependencies in the transfer functions, Figures 6-11 and 6-12, are weak below 10 Hz for the 1 Hz scale design outcrop spectrum and strong below 10 Hz for the corresponding 10 Hz spectrum. Due to the similarity in the 1 Hz and 10 Hz scaled rock spectra (Figure 6-3), the corresponding weighted mean transfer functions are similar (Figure 6-13).

6.4.2 Results for Approach 2A/3

An example of the recommended procedure for calculating soil hazard was conducted at the Mojave site in California, using the Meloland soil profile, which was selected because it has the capability

of demonstrating the most non-linearity at high input amplitudes. The 10^{-3} , 10^{-4} , and 10^{-5} rock spectra are shown in Figure 6-14.

Deaggregation of the rock seismic hazard at 10^{-3} , 10^{-4} , and 10^{-5} leads to the M-R plots shown in Figures 6-15, 6-16, and 6-17 for 10 and 1 Hz. For each of the three amplitudes, soil motion was calculated by Approach 2A using the magnitudes and distances in Table 6-3.

The soil amplification factors calculated from Approach 2A are shown in Figure 6-18; Approach 2A is the recommended way to calculate soil amplitudes, as will be demonstrated below.

A soil seismic hazard analysis was conducted following Approach 3 (equation (6-7a)) at 25 frequencies using, for starting values of z , the rock amplitudes at 10^{-4} and 10^{-5} times the respective mean values of $AF(a, m')$. Once $P(A_s > z)$ was calculated for these values of z , the estimated 10^{-4} and 10^{-5} soil amplitudes were calculated by interpolation and extrapolation. These preliminary estimates of $A_s(10^{-4})$ and $A_s(10^{-5})$ then became the new values for z , and the process was repeated until stability was reached (always within five iterations). Approach 3 was also calculated with equation (6-7b), in which case no iteration is required.

The application of equation (6-7a) or (6-7b) requires an estimate of σ_s at each frequency, for the M and R value dominating the hazard for that calculation. These estimates come from the soil amplification studies conducted using as input the design spectra scaled to the UHS at 10 and 1 Hz. These indicated an average σ_s of 0.2.

Spectra estimated for 10^{-4} and 10^{-5} annual probabilities are shown in Figures 6-19 and 6-20, using several methods. Approach 4 is a direct calculation of seismic hazard on soil, using a site-specific soil attenuation equation with a standard deviation that varies with M and R. Approach 2A/3 applies equation (6-7a) using Approach 2A (which scales spectral shapes at 10 and 1 Hz) to estimate $P[AF > z/a]$. Table 6-3 indicates the M and R values for these spectral shapes. "Approximate Approach 2A/3" is identical to Approach 2A/3 except that it uses the approximate equation (6-7b).

Note that in this application, Approach 2A was applied using amplification factors from the 1 Hz spectrum at low frequencies ($f < 2$ Hz), and using the amplification factors from the 10 Hz spectrum at high frequencies ($f \geq 2$ Hz). This is slightly different from the Approach 2A application of the previous section, which uses the envelope of the amplification factor at any frequency (See Figure 6-13). Frequency 2 Hz was chosen as the cross-over frequency because the 1 Hz scaled spectrum dominates at lower frequencies and the 10 Hz scaled spectrum dominates at higher frequencies (see Figure 4-3).

Using Approach 4 as the spectra of merit, Figures 6-19 and 6-20 indicate that both Approaches 2A/3 are generally accurate. The integral Approach 2A/3 (equation (6-7a)) is slightly more accurate than the closed-form solution (equation (6-7b)) at 10^{-5} annual frequency (Figure 6-20). There is a slight underestimation of the Approach 4 spectral amplitudes from 7 to 30 Hz, amounting to less than 10%, for the 10^{-5} spectrum. This is acceptable, given that the soil conditions were chosen to accentuate nonlinear behavior and that the 10^{-5} amplitude is used only to calculate the slope in the soil hazard

curve, for purposes of deriving the URS. Approach 2A is slightly less accurate for both the 10^{-4} and the 10^{-5} spectrum.

If more accurate soil spectra are desired for a site, the best alternative is to develop site-specific soil attenuation equations for the site, and conduct a full seismic hazard analysis (Approach 4). If this is done, the soil attenuation equation must represent all epistemic and aleatory uncertainties in the soil amplitudes, and the resulting standard deviations should be compared to standard deviations from empirical soil equations.

6.5 Horizontal motions for Columbia site

6.5.1 Results for Approaches 1, 2A, and 2B

The Savannah River generic profile was adopted from measured shear-wave velocity profiles at the DOE Savannah River site. It is generally stiff but contains a broad soft zone at intermediate depths (around 25m) with a steep gradient thereafter (Figure 2-6b). The low-strain column resonance is near 0.8 Hz. G/G_{\max} and hysteretic damping curves based on modeling strong ground motions in the Los Angeles area recorded at cohesionless soil sites from the M 6.7 1994 Northridge earthquake are used for this site (Figure 2-8b).

For the approach comparison, Figure 6-21 shows results for 1, 2A, and 2B with Approach 4 reflecting the site specific soil UHS. As with the WUS site, Approach 1 underestimates the UHS at the higher frequencies while Approaches 2A and 2B are generally slightly above the UHS, except at very low frequency. Approaches 2A and 2B are nearly identical and both are conservative above 10 Hz while Approach 2B remains closer to the soil UHS at very low frequency (<0.4 Hz). Cyclic shear strain (effective) levels are illustrated in Figure 6-22, which shows much lower values than the corresponding WUS analyses. Maximum median strains developed in the soft zone have values near 0.02% compared to about 0.3% for the WUS Meloland profile (Figure 6-10). The loading levels are much lower and the profile is significantly stiffer.

The transfer functions (5% damped response spectra) are shown in Figures 6-23 to 6-25. Figures 6-23 and 6-24 show the amplification factors for the 1 Hz and 10 Hz scaled design spectra along with the weighted mean ratios. The effects of magnitude on the transfer functions are less than in the WUS (Figures 6-11 and 6-12) due to lower levels of control motions, a stiffer profile, and a smaller magnitude range (ML to MH), at least for the 1 Hz factors.

Figure 6-25 shows the weighted mean transfer functions. They show large differences at high frequency ($f > 30$ Hz). The 1 Hz transfer functions are larger than the 10 Hz transfer functions at high frequency due to lower loading levels (see Figure 6-4). The 10 Hz scaled rock outcrop design spectrum has significantly larger high frequency motions than the 1 Hz spectrum resulting in high cyclic shear strains in the soil column.

6.5.2 Results for Approach 2A/3

The procedure recommended in Section 6.2 was conducted at the Charleston site in the CEUS, using the generic Savannah profile. The 10^{-3} , 10^{-4} , and 10^{-5} spectra for rock conditions are shown in Figure 6-26 for the 1- and 2-corner ground motion models and for the mean. (Note that the mean is calculated by weighting the two ground motion models 0.5 each and calculating the hazard. The mean is not the average of the two uniform hazard spectra.)

Deaggregation of the rock seismic hazard at 10^{-3} , 10^{-4} , and 10^{-5} is different for each of the two ground motion equations. M-R deaggregation plots are shown in Figures 6-27, 6-28, and 6-29 for 10 and 1 Hz, for the 1-corner model (part a of each figure) and for the 2-corner model (part b). For each of the three amplitudes, soil motion was calculated by Approach 2A using the magnitudes and distances shown in Table 6-4.

A soil seismic hazard analysis was conducted following Approach 3 (equation (6-7a)) at 25 frequencies using an iterative procedure to calculate amplitudes associated with 10^{-4} and 10^{-5} annual frequencies. The iterative procedure was identical to that used for the Mojave site. For these calculations, σ_s was taken from the Approach 2A calculations of soil amplification (average of 0.2 over all frequencies). Equation (6-7b) was also applied, for which no iteration is required. Amplification factors used to apply Approach 3 are shown in Figure 6-30.

Spectra estimated for 10^{-4} and 10^{-5} annual frequencies are shown in Figures 6-31 and 6-32, using four methods. Approach 4 is the direct calculation of seismic hazard on soil, using the site-specific soil attenuation equation with a standard deviation that varies with M and R. Approach 2A/3 applies equation (6-7a), using Approach 2A to estimate $P[AF > z/a]$. In addition, "Approximate Approach 2A/3" uses equation (6-7b) to calculate $z_{.0001}$. Finally, "Approach 2A" is the direct scaling of the 10^{-4} rock UHS to the 10^{-4} soil UHS described in the previous subsection, using the envelope of the amplification factors at each frequency.

Using Approach 4 as the spectra of merit, Figures 6-31 and 6-32 indicate that "Approach 2A/3" and "Approximate Approach 2A/3" are very similar, and both give generally accurate estimates compared to Approach 4, particularly for 10^{-4} (Figure 6-21). These two Approaches underestimate the 10^{-5} UHS at high frequencies ($f > 15$ Hz), where the amplification factor is lowest (see Figure 6-30). Because the 10^{-5} UHS is used only to calculate the slope of the hazard curves in order to obtain the URS, this underestimation is acceptable. Approach 2A is accurate except for $f > 20$ Hz, where the 1 Hz amplification factor exceeds that for 10 Hz (see Figure 6-25). For the Columbia site, the hazard curve slope and amplification factors (Figure 6-30) are such that the "correction factor" (see the discussion of equation 6-7b) is on the order of 1.05, so Approach 2A is expected to be close to Approach 2A/3, except at high frequencies.

6.6 Vertical motions

6.6.1 Mojave site

To estimate vertical soil motions consistent with the horizontal soil motions, a WUS empirical generic soil V/H ratio was developed for $M = 6.6$ and $R = 18$ km, based on the rock UHS deaggregation at 1 Hz. The empirical V/H ratio (Figure 6-33) is an average of ratios from Abrahamson and Silva (1997) and Campbell (1997), which were selected because these two relations cover the widest frequency range. The vertical motions exceed the horizontal between 10 and 20 Hz due to the close distance (18 km) and large magnitude (EPRI, 1993; Silva, 1998). These ratios are used to develop vertical design spectra, as discussed in Section 7.1

6.6.2 Columbia site

As discussed in Section 6.3, the approach used to develop site specific vertical motions relies on modeling results to produce WUS-to-CEUS V/H scale factors for deep soil applied to a WUS empirical deep soil V/H ratio. This process results in a generic soil CEUS V/H ratio which is applied to the site specific horizontal design spectrum (smoothed version of Approach 2A/2B spectrum). To illustrate this process, Figure 6-34 shows the WUS-to-CEUS V/H scaling factors (dash-dotted line), the WUS deep soil empirical V/H ratio (dotted line), and the resulting CEUS deep soil V/H ratio (solid line). The empirical WUS deep soil V/H ratio was taken from Abrahamson and Silva (1997) as it is the only currently available ratio valid beyond 80 km (McGuire et al., 2001). The WUS-to-CEUS scale factors were taken from the factors used to scale the WUS analysis time histories to CEUS conditions (McGuire et al., 2001; Section 3). They are appropriate for the M and R of the 1 Hz CEUS rock UHS, 7.2 and 110 km respectively. These ratios are used to develop vertical design spectra as discussed in Section 7.2.

The exceedence of the vertical spectrum over the horizontal at high frequency ($f \geq 10$ Hz) is larger than expected for a distance of 110 km and should be closer to the horizontal, at least for rock sites (Atkinson, 1993). However, there is a large contribution to high-frequency hazard for $R = 10$ km (see Figure 3-29, particularly for the 1-corner model). This contribution at 10 km suggests an appropriate high frequency V/H ratio (Silva, 1997; McGuire et al., 2001) and indicates caution in selecting V/H ratios for cases where high and low frequency contributions to the UHS reflect both near and far distance contributions. Enveloping the 10 Hz and 1 Hz V/H ratios may be appropriate in these cases.

REFERENCES

- Abrahamson, N.A. and K.M. Shedlock (1997). "Overview," *Seis. Res. Let.*, 68(1), 9-23.
- Abrahamson, N.A. and W.J. Silva (1997). "Empirical response spectral attenuation relations for shallow crustal earthquakes," *Seis. Res. Let.*, 68(1), 94-127.
- Bazzurro, Paolo (1998). *Probabilistic Seis. Demand Analysis*, Ph.D. Thesis, Supervised by C.A. Cornell, Stanford Uni., Palo Alto, CA.

- Bazzurro, P., C.A. Cornell, and F. Pelli (1999). *Site- and Soil-specific PSHA for Nonlinear Soil Sites*, Proc., 4th Earthquake. Resist. Design Structures Conf. (ERES99), Catania, Italy, Jun. 15-17.
- Campbell, K.W. (1997). "Empirical near-source attenuation relationships for horizontal and vertical components of peak ground acceleration, peak ground velocity, and pseudo-absolute acceleration response spectra," *Bull. Seism. Soc. Am.*, 68(1), 154-179.
- Costantino, C.J. (1967). "Finite element approach to wave propagation problems," *J. Eng. Mech. Div.*, Am. Soc. Civil Engrs., 93.
- Costantino, C.J. (1969). "Two dimensional wave propagation through nonlinear media," *J. Comput. Physics*, 4.
- Electric Power Research Institute (1993). *Guidelines for Determining Dsgn. Basis Grnd. Motions*, Elec. Power Res. Inst., Palo Alto, CA, EPRI TR-102293, 1-5:
 vol. 1: "Methodology & guidelines for estimating earthquake ground motion in eastern NA."
 vol. 2: "Appendices for ground motion estimation."
 vol. 3: "Appendices for field investigations."
 vol. 4: "Appendices for laboratory investigations."
 vol. 5: "Quantification of seismic source effects."
- Li, X.S., Z.L. Wang, and C.K. Shen (1992). *SUMDES: A Nonlinear Proc. for Response Analysis of Horizontally-layered Sites Subjected to Multi-directional Earthquake Loading*, Dept. of Civil Eng., Uni. of Calif., Davis.
- McGuire, R.K., W.J. Silva, and C. Costantino (2001). *Tech. Basis for Rev. of Reg. Guidance on Dsgn. Grnd. Motions: Hazard and Risk-consistent Grnd. Motion Spectra Guidelines*, US Nuc. Reg. Comm., Rept NUREG/CR-6728, Oct.
- McGuire, R.K. (1995). "Probabilistic seismic hazard analysis and design earthquakes: closing the loop," *Bull. Seism. Soc. Am.*, 85, No. 5, 1275-1284, Oct.
- Silva, W.J. and K. Lee (1987). *WES RASCAL Code for Synthesizing Earthquake Grnd. Motions*, State-of-the-Art for Assessing Earthquake Hazards in the United States, Rept. 24, U.S. Army Engineers Waterways Exp. Station, Misc. Paper S-73-1.
- Silva, W.J., N. Abrahamson, G.R. Toro, and C. Costantino (1997). *Desc. and Validation of the Stochastic Grnd. Motion Mod.*, Rept. to Brookhaven Natl. Lab., Assoc. Uni., Inc., Upton, New York, Contract 770573.
- Silva, W.J. (1997). *Char. of Vert. Strong Grnd. Motions for Applications to Eng. Dsgn.*, Proc. FHWA/NCEER Workshop on the Natl. Rept. Of Seis. Grnd. Motion for New and Existing Highway Facilities, Tech. Rept. NCEER-97-0010.

USNRC (1997). *Ident. and Charact. of Seis. Sources and Determ. of Safe Shutdown Earthquake Grnd. Motion*, US Nuc. Reg. Comm., Reg. Guide 1.165, Mar.

Wald, D.J. and T.H. Heaton (1994). "A dislocation model of the 1994 Northridge, California, earthquake determined from strong ground motions," *U.S. Geol. Survey*, Open-File Rept. 94-278.

Table 6-1
Overview of Approaches for Developing Soil UHS

- Approach 1: Rock UHS used as control motions to drive soil column.
- Approach 2A: Use scaled 1 Hz and 10 Hz design earthquakes as control motions to develop 1 Hz and 10 Hz soil motions (R.G. 1.165 approach) or develop transfer function for 1 Hz and 10 Hz design earthquakes, using a single control motion (scaled shape) for each frequency; either envelope the transfer functions or switch from the 1 Hz transfer function to the 10 Hz transfer function at the frequency where the scaled spectra cross.
- Approach 2B: Develop weighted mean transfer functions for 1 Hz and 10 Hz design earthquakes accommodating magnitude distributions; use the 1 Hz transfer function at low frequencies and the 10 Hz transfer function at high frequencies, switching at the frequency where the scaled spectra cross.
- Approach 3: Perform PSHA with rock attenuation relation; deaggregate by M , and R and calculate soil response with appropriate control motions for each M , and R bin.
- Approach 4: UHS computed directly from PSHA using site-specific soil attenuation relations.

Table 6-2
Details of Approaches for Developing Soil UHS

<u>Description</u>	<u>Frequencies Used</u>	<u>Integration</u>	<u>Label</u>
PSHA using site-specific soil attenuation	multiple	over m and r	Approach 4
Calculate soil hazard from rock hazard and m and r deaggregation	several	over a , and over m and r given a	Approach 3
Scale rock UHS to soil UHS accounting for soil parameter uncertainty	two, e.g. 10 and 1 Hz	none	Approach 2A
Scale rock UHS to soil UHS accounting for soil parameter uncertainty and m deaggregation	two, e.g. 10 and 1 Hz	none	Approach 2B
Scale rock UHS to soil UHS using broadbanded input motion	none	none	Approach 1

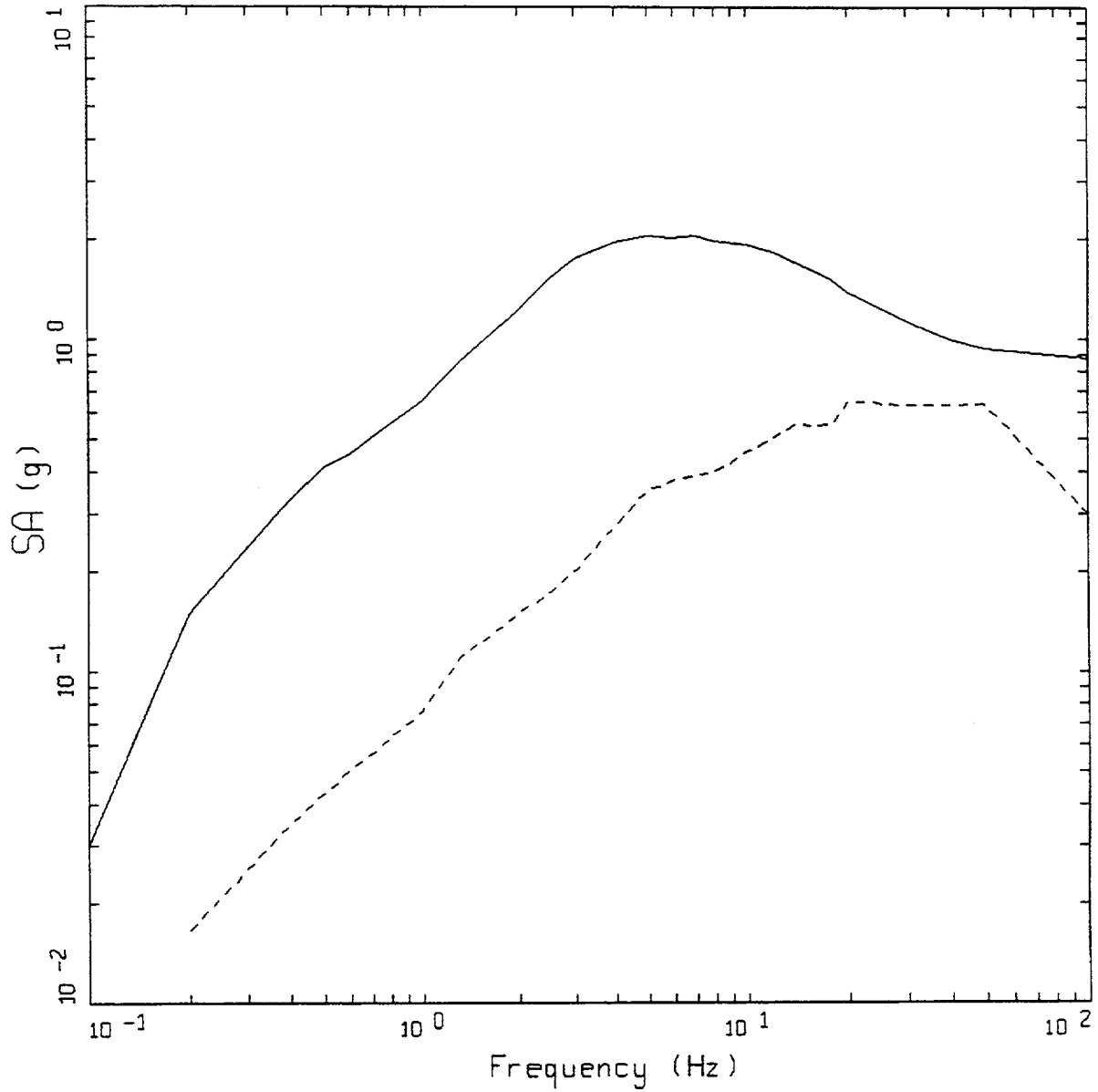
Table 6-3
Magnitudes and Distances Used for Soil Amplification Calculations
at Mojave Site

UHS	Approach	10 Hz			1 Hz		
		M	R	wt	M	R	wt
1E-3	1	M = 6.5, R = 22					
	2A	6.5	23	1.0	7.1	30	1.0
	2B	5.1	10	0.2	5.6	10	0.1
		6.5	22	0.6	7.0	28	0.6
	7.7	30	0.2	7.7	30	0.3	
1E-4	1	M = 6.1, R = 14					
	2A	6.1	14	1.0	6.6	18	1.0
	2B	5.1	10	0.2	5.4	10	0.2
		6.1	14	0.6	6.6	18	0.6
	7.8	30	0.2	7.8	30	0.2	
1E-5	1	M = 6.0, R = 12					
	2A	6.0	12	1.0	6.4	14	1.0
	2B	5.0	10	0.2	5.5	10	0.2
		6.0	12	0.6	6.4	14	0.6
	7.0	30	0.2	7.0	30	0.2	

Table 6-4
Magnitudes and Distances Used for Soil Amplification
Calculations at Columbia Site

UHS	Approach	Ground motion model	10 Hz			1 Hz			
			M	R	wt	M	R	wt	
1E-3	1	1-corner	M = 6.4, R = 85						
		2-corner	M = 6.8, R = 102						
		mean	M = 6.6, R = 94						
	2A	1-corner	5.9	62	1.0	6.9	109	1.0	
		2-corner	6.4	83	1.0	7.2	120	1.0	
		mean	6.2	73	1.0	7.1	115	1.0	
	2B (low)	1-corner	4.6	10	0.36	5.4	10	0.26	
		2-corner	5.4	10	0.50	6.0	10	0.12	
		mean	5.0	10	0.43	5.7	10	0.14	
	2B (mod)	1-corner	5.9	62	0.33	6.9	109	0.25	
		2-corner	6.4	83	0	7.2	120	0.59	
		mean	6.2	73	0.17	7.1	115	0.47	
	2B (high)	1-corner	7.4	130	0.31	7.7	7.7	0.49	
		2-corner	7.4	130	0.50	7.7	130	0.29	
		mean	7.4	130	0.40	7.7	130	0.39	
	1E-4	1	1-corner	M = 6.3, R = 64					
			2-corner	M = 6.9, R = 94					
			mean	M = 6.6, R = 79					
2A		1-corner	5.6	26	1.0	7.0	101	1.0	
		2-corner	6.4	66	1.0	7.4	121	1.0	
		mean	6.0	46	1.0	7.2	111	1.0	
2B (low)		1-corner	4.6	10	0.19	5.7	10	0.07	
		2-corner	4.7	10	0.24	6.2	10	0.07	
		mean	4.7	10	0.22	6.0	10	0.07	

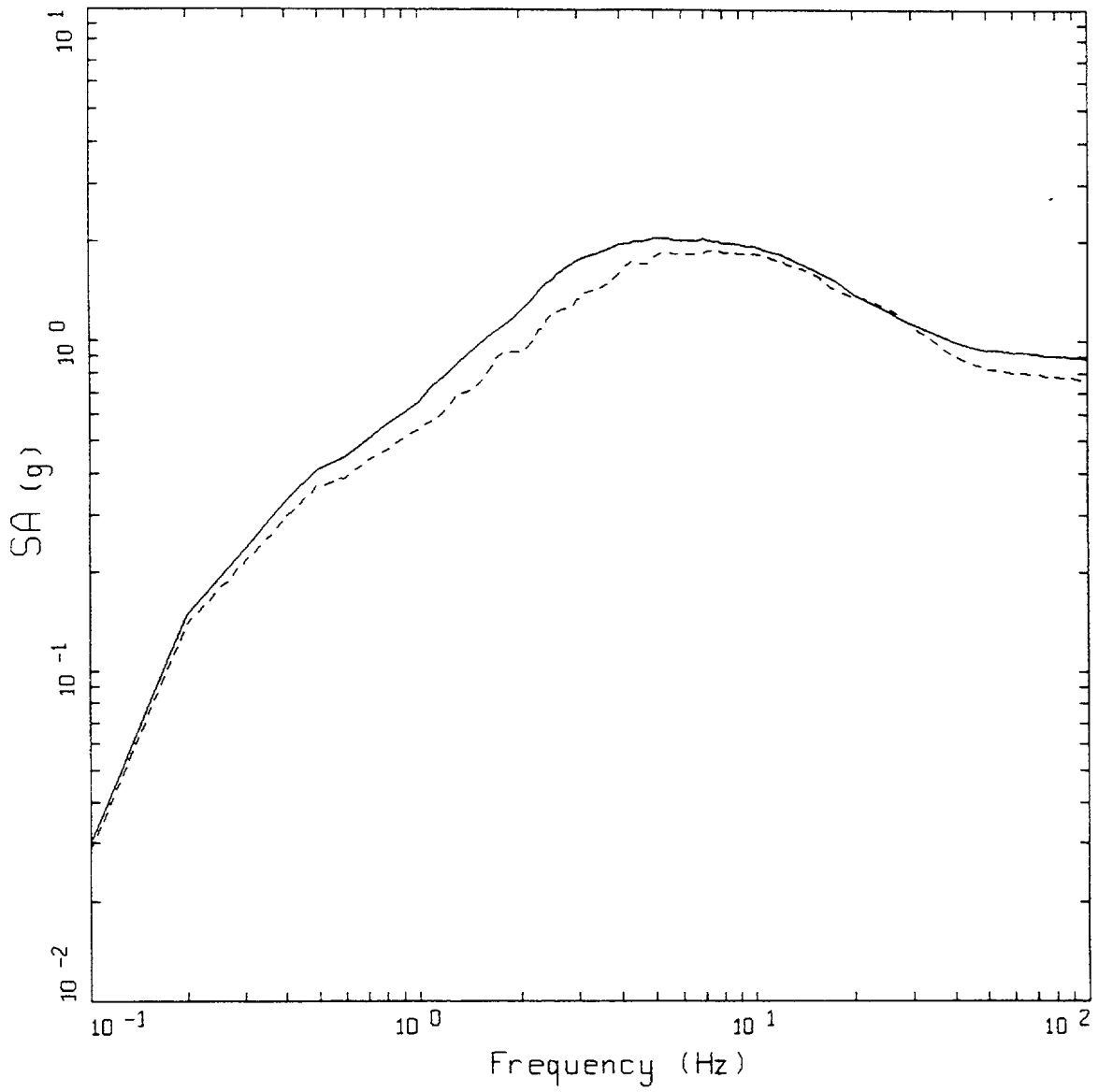
UHS	Approach	Ground motion model	10 Hz			1 Hz		
			M	R	wt	M	R	wt
1E-4 <i>(cont'd)</i>	2B (mod)	1-corner	5.6	26	0.72	7.0	101	0.80
		2-corner	6.4	66	0.45	7.4	121	0.65
		mean	6.0	46	0.58	7.2	110	0.72
	2B (high)	1-corner	7.7	130	0.09	7.7	130	0.13
		2-corner	7.7	130	0.31	7.7	130	0.28
		mean	7.7	130	0.20	7.7	130	0.21
1E-5	1	1-corner	M = 6.2, R = 40					
		2-corner	M = 6.7, R = 70					
		mean	M = 6.5, R = 55					
	2A	1-corner	5.5	10	1.0	6.8	69	1.0
		2-corner	6.0	30	1.0	7.4	110	1.0
		mean	5.8	20	1.0	7.1	90	1.0
	2B (low)	1-corner	4.6	10	0.02	6.1	10	0.40
		2-corner	4.7	10	0.21	6.4	10	0.16
		mean	4.7	10	0.11	6.3	10	0.28
	2B (mod)	1-corner	5.5	10	0.97	6.8	69	0.20
		2-corner	6.0	30	0.63	7.4	110	0.31
		mean	5.8	20	0.81	7.1	90	0.26
	2B (high)	1-corner	7.7	130	0.01	7.6	130	0.40
		2-corner	7.7	130	0.16	7.7	130	0.53
		mean	7.7	130	0.08	7.7	130	0.46



ROCK OUTCROP UHS SPECTRA

- LEGEND
- WUS ROCK UNIFORM HAZARD SPECTRA
 - - - CEUS ROCK UNIFORM HAZARD SPECTRA

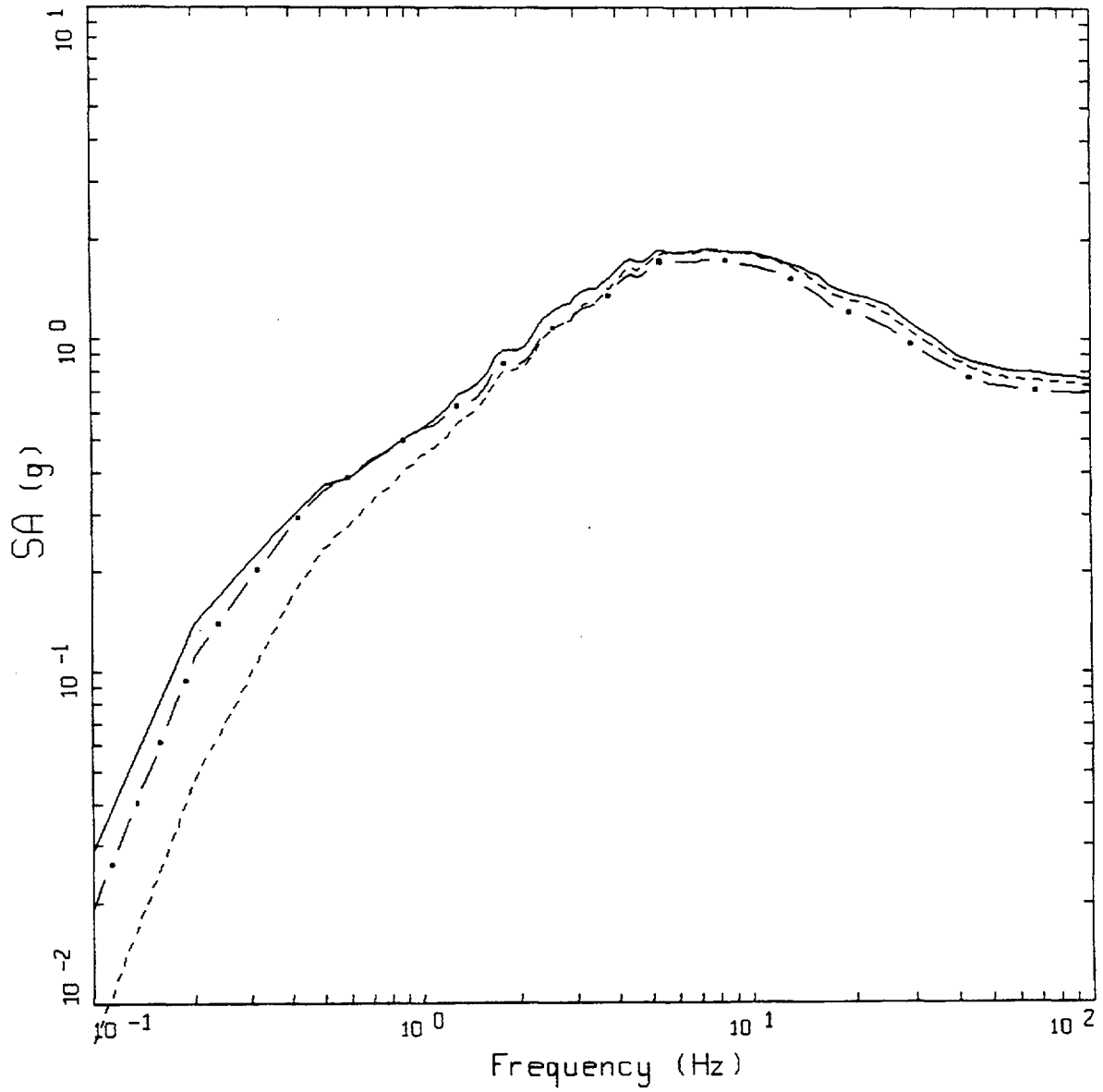
Figure 6-1. Comparison of 5% damped rock outcrop 10^{-4} UHS spectra for CEUS and WUS conditions.



ROCK OUTCROP UHS SPECTRA

- LEGEND
- WUS ROCK UNIFORM HAZARD SPECTRA
 - - - WUS BASEMENT ROCK UNIFORM HAZARD SPECTRA

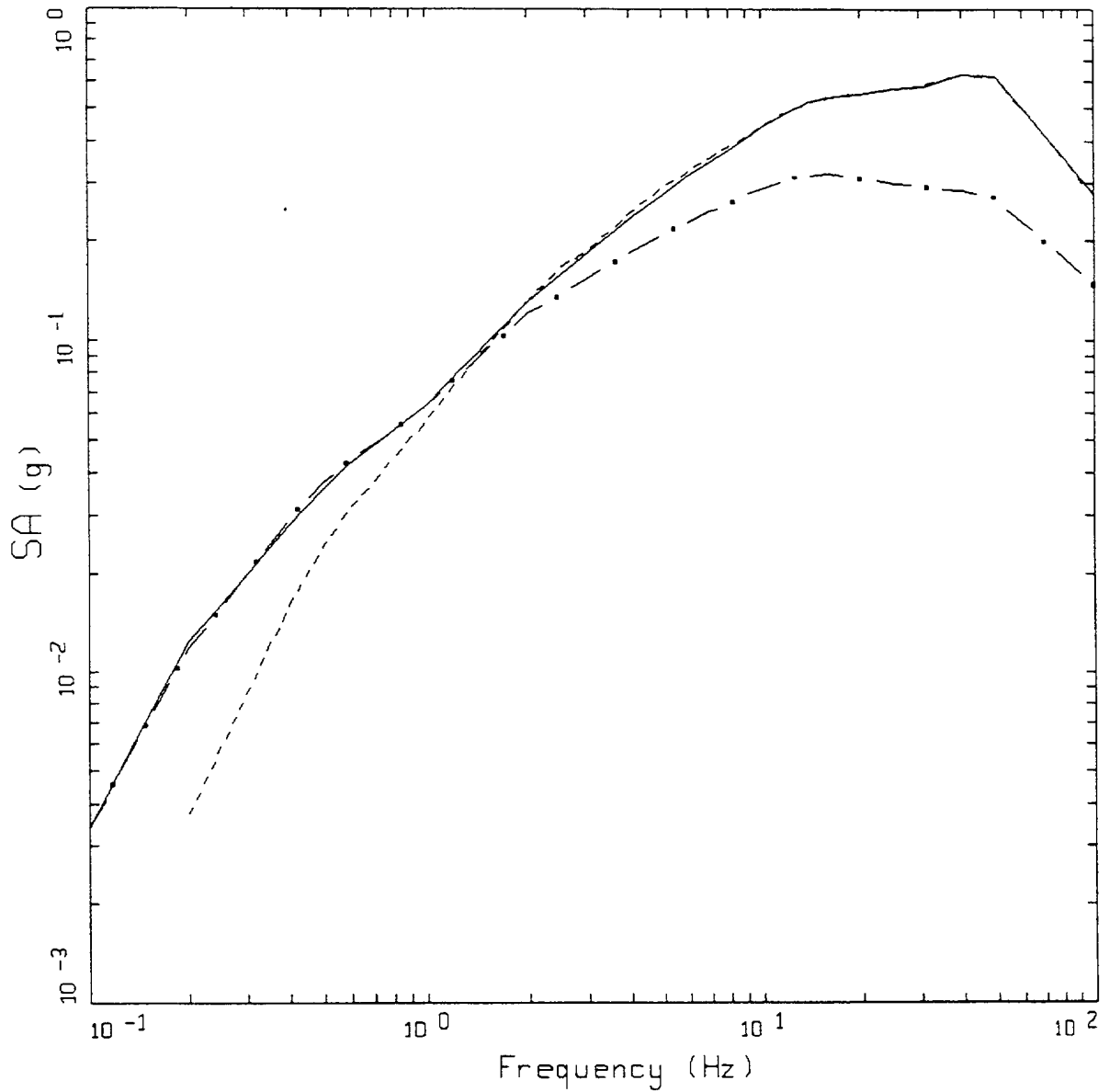
Figure 6-2. Comparison of WUS rock 10^{-4} UHS (solid line) with UHS corrected for base-of-soil conditions (dashed line).



WUS ROCK SPECTRA

- LEGEND
- BASEMENT ROCK UNIFORM HAZARD SPECTRUM
 - - - BASEMENT ROCK 10HZ DESIGN SPECTRUM
 - · - BASEMENT ROCK 1HZ DESIGN SPECTRUM

Figure 6-3. Mojave site, rock, 1 Hz, 10 Hz and UHS corrected to base of soil.



CEUS ROCK SPECTRA

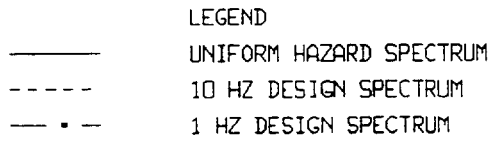
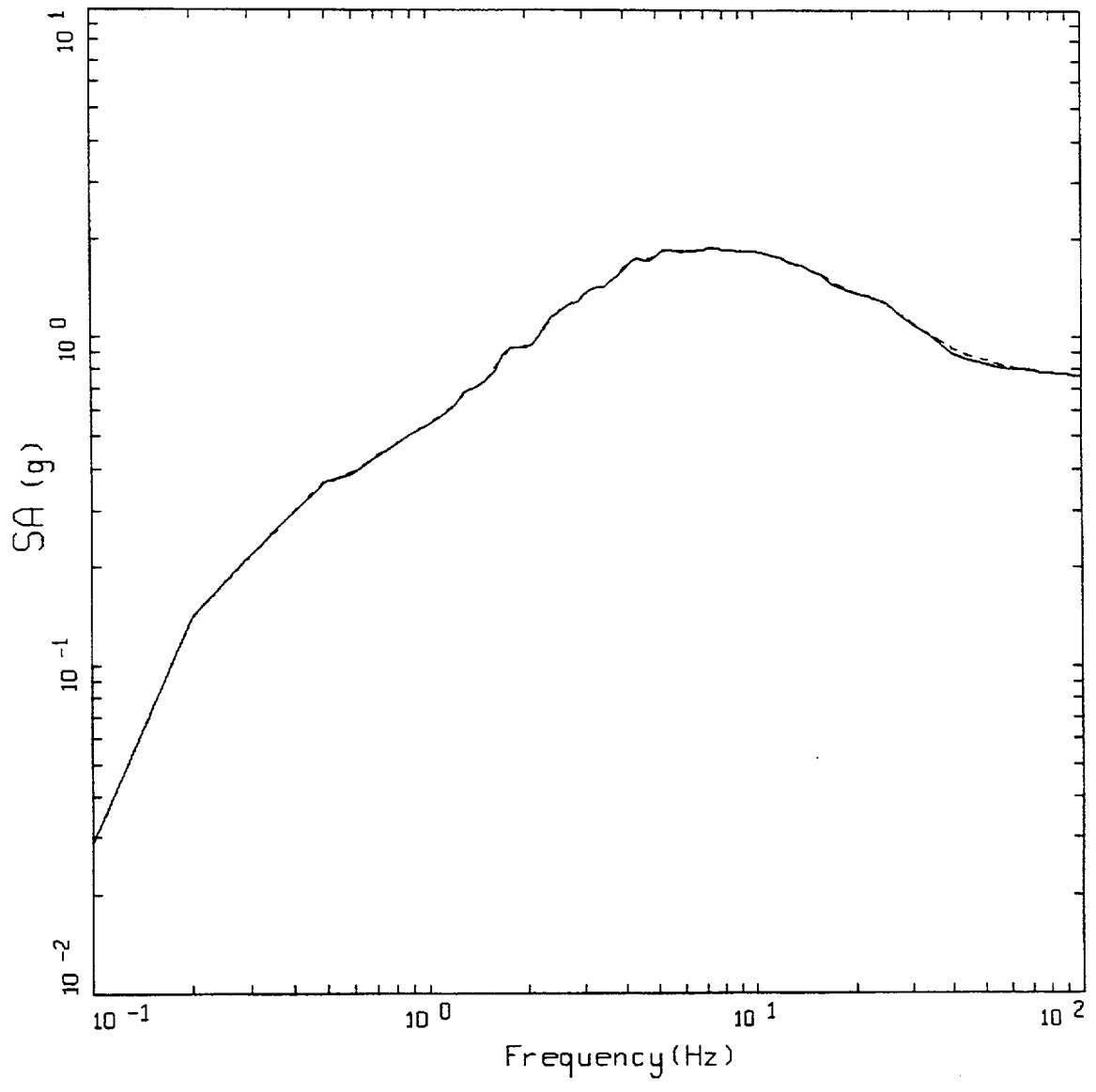


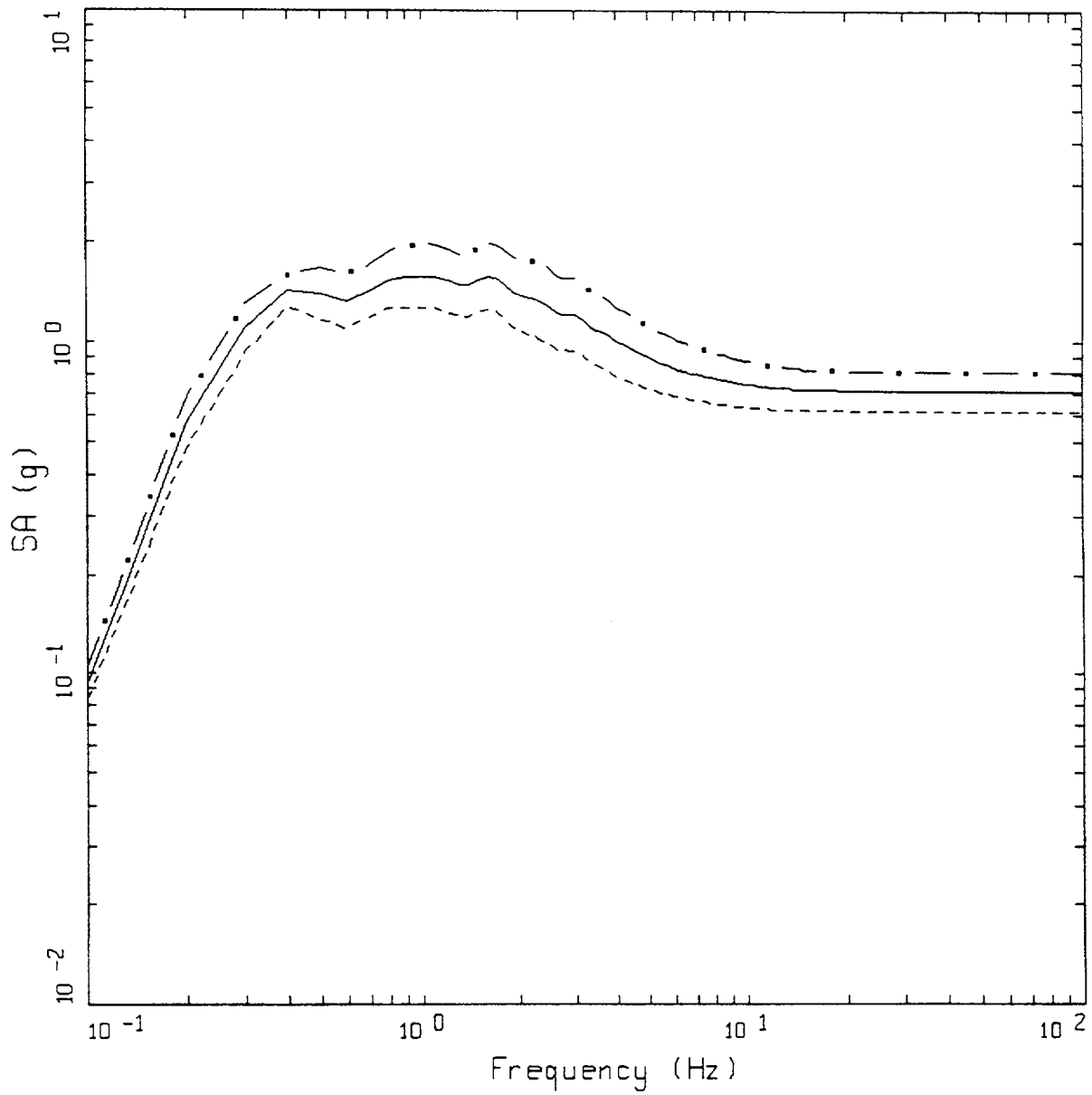
Figure 6-4. Columbia site, rock outcrop 1 Hz, 10 Hz and UHS.



WUS ROCK
MATCH TO CORRECTED UHS

LEGEND
 ——— 5 %, CORRECTED TARGET
 - - - - 5 %, SPECTRAL MATCH

Figure 6-5. Comparison of spectral match (dotted line) to corrected WUS rock UHS.

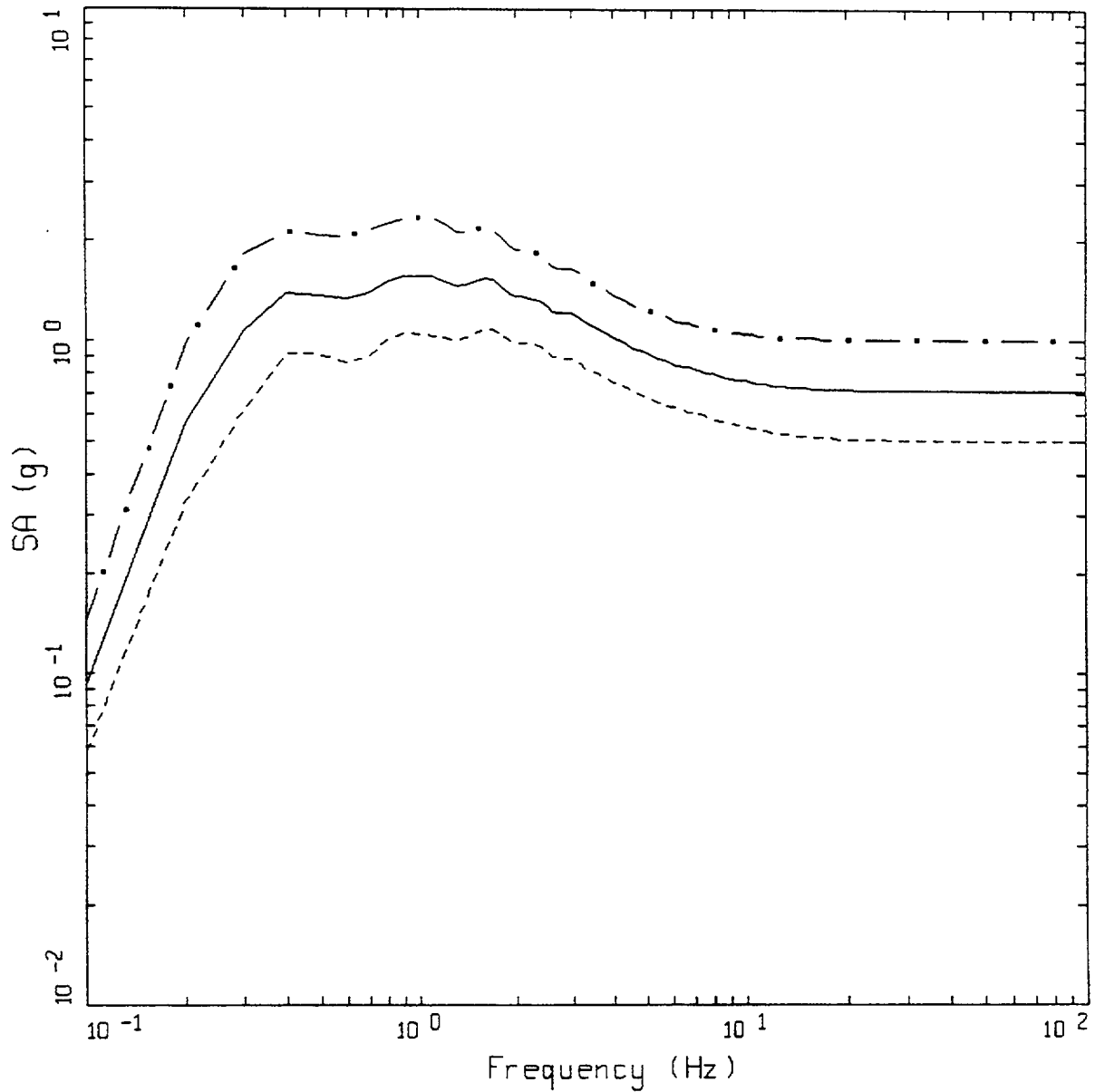


WUS, M = 7.5, D = 001 KM, H = 8 KM
 SD = 50 BARS, MELOLAND, SITE VARIABILITY

LEGEND

- . - 84TH PERCENTILE, PGA = 0.813 G
- 50TH PERCENTILE, PGA = 0.709 G
- - - 16TH PERCENTILE, PGA = 0.619 G

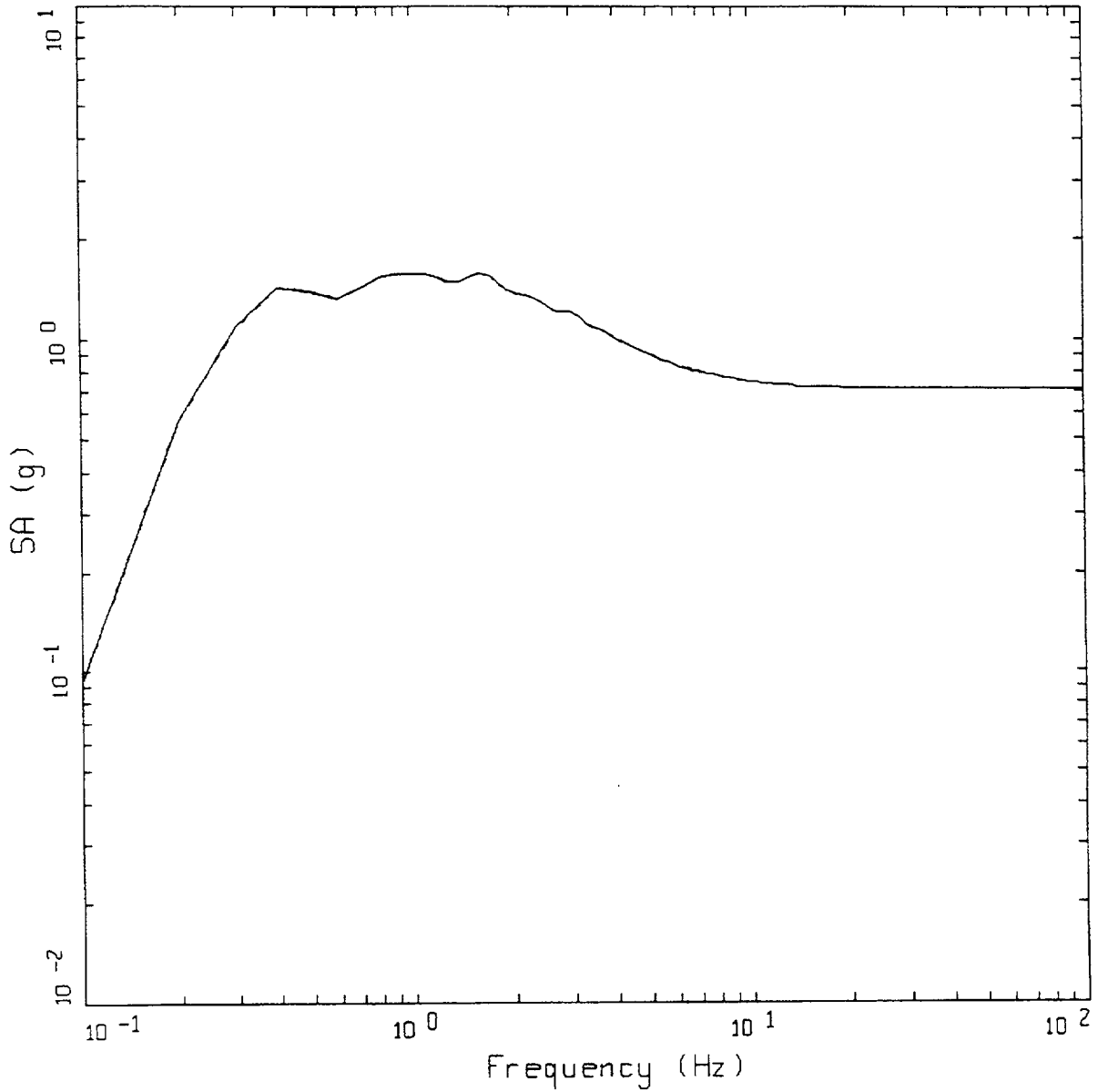
Figure 6-6. Median and $\pm \sigma$ spectra computed for $M = 7.5$ at a distance of 1 km using the Meloland profile with site variations only (profile, G/G_{max} , and hysteretic damping): WUS conditions.



WUS, $M = 7.5$, $D = 001$ KM, $H = 8$ KM
 SD = 50 BARS, MELOLAND, SOURCE+PATH+SITE VARIABILITY

LEGEND
 - . - 84TH PERCENTILE, PGA = 1.005 G
 ——— 50TH PERCENTILE, PGA = 0.709 G
 - - - - 16TH PERCENTILE, PGA = 0.501 G

Figure 6-7. Median and $\pm\sigma$ spectra computed for $M = 7.5$ at a distance of 1 km using the Meloland profile with source, path, and site variations: WUS conditions.

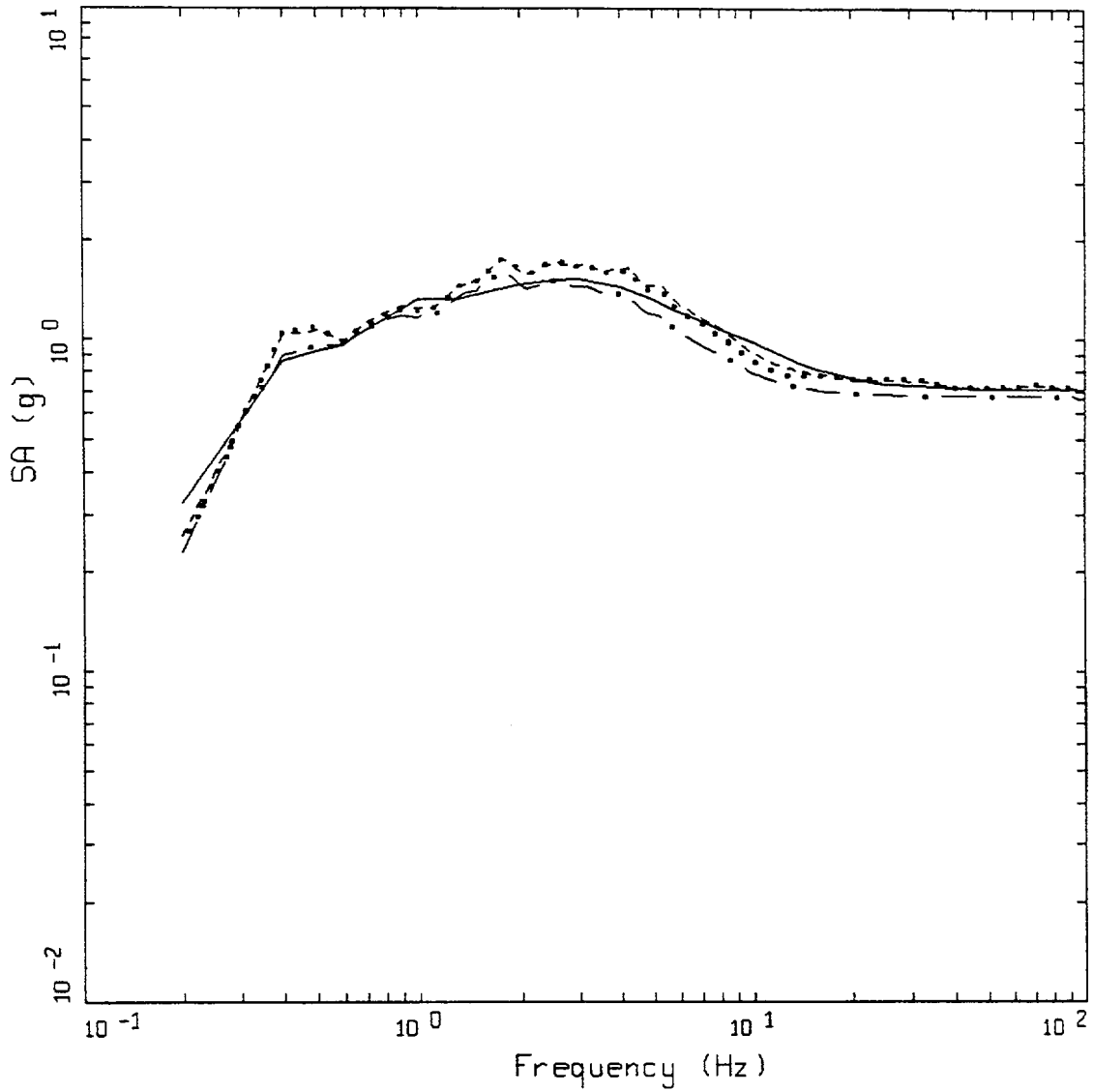


WUS, M = 7.5, D = 001 KM, H = 8 KM
 SD = 50 BARS, MELOLAND

LEGEND

- SITE; 50TH PERCENTILE, PGA = 0.709 G
- - - - SOURCE+PATH+SITE; 50TH PERCENTILE, PGA = 0.709 G

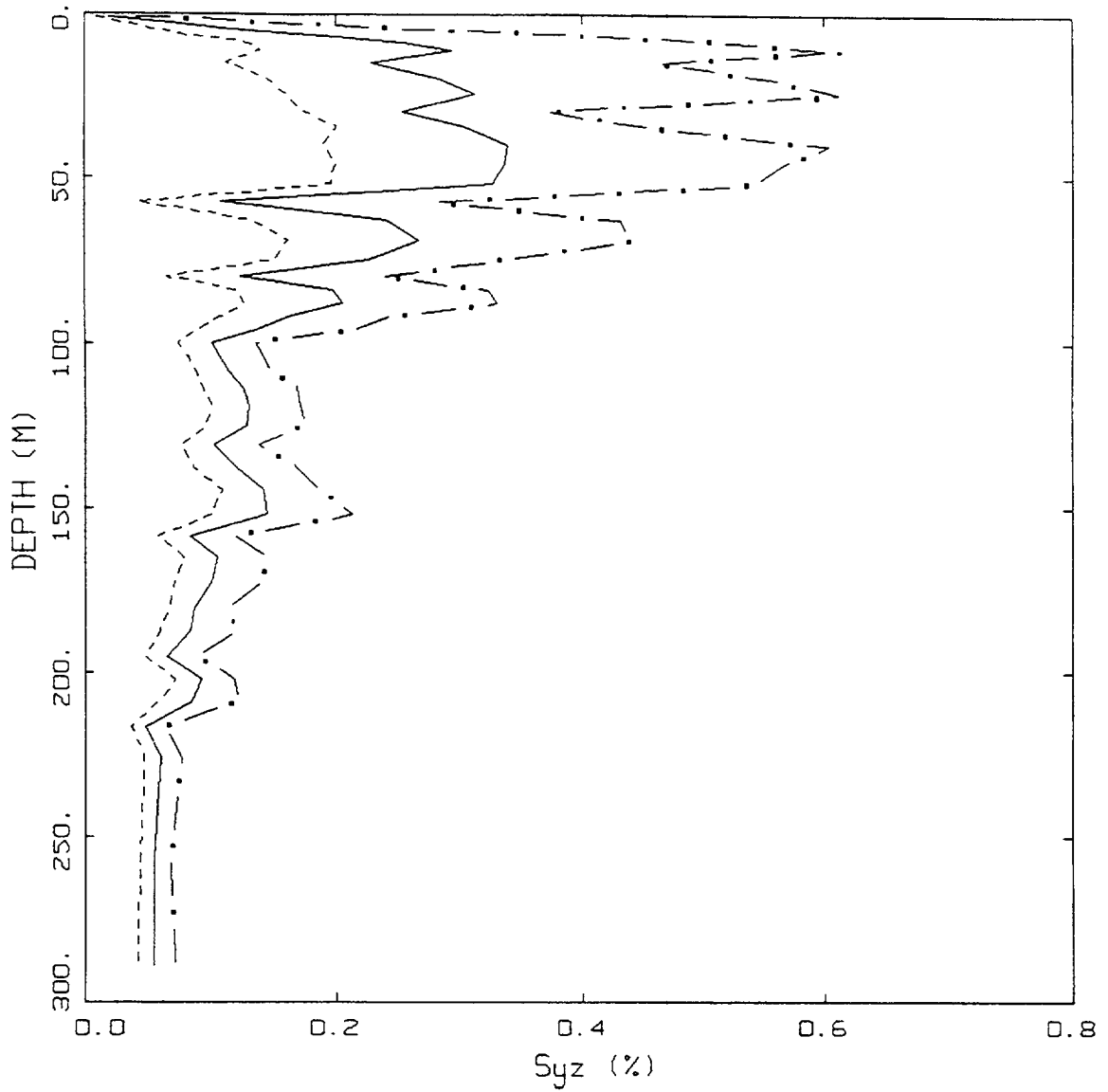
Figure 6-8. Comparison of median spectral estimates computed for $M=7.5$ at a distance of 1 km using the Meloland profile: varying site properties only (solid line) and varying source, path, and site properties (dashed line); WUS conditions.



WUS 10E-4 APPROACH COMPARISON, MELOLAND

- LEGEND
- APPROACH 4, 10⁻⁴ UHS SOIL UNIFORM HAZARD SPECTRUM
 - APPROACH 2A, 1 HZ AND 10 HZ DESIGN CONTROL MOTIONS
 - APPROACH 2B, 1 HZ AND 10 HZ DEAGGREGATION CONTROL MOTIONS
 - . - . APPROACH 1, 10⁻⁴ UHS ROCK CONTROL MOTION

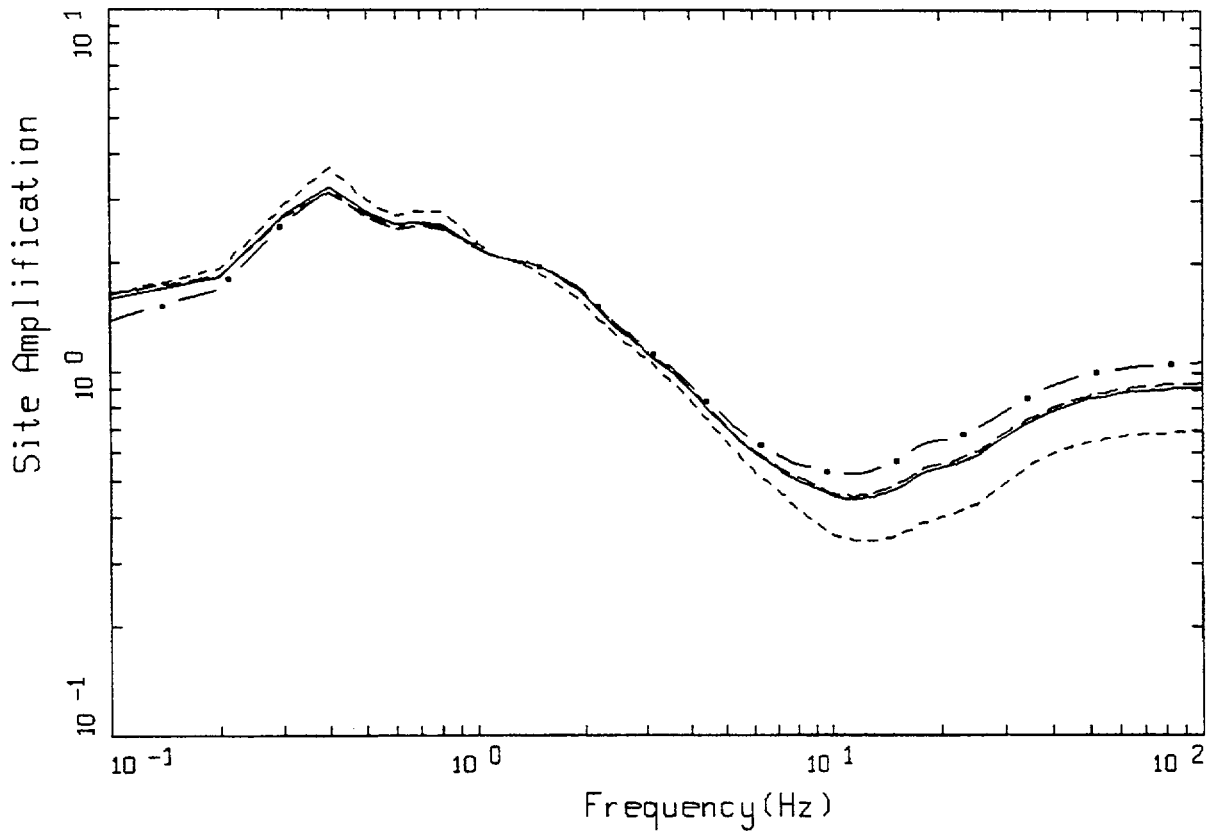
Figure 6-9. Comparison of soil spectra computed using Approaches 1, 2A, 2B, and 4 (Table 6-1) for Meloland profile, WUS conditions.



WUS, MELOLAND, APPROACH 1
EFFECTIVE STRAINS (SYZ)

LEGEND
 - · - 84TH PERCENTILE
 — 50TH PERCENTILE
 - - - 16TH PERCENTILE

Figure 6-10. Median and $\pm 1\sigma$ effective strains for Meloland profile using Approach 1, WUS conditions.

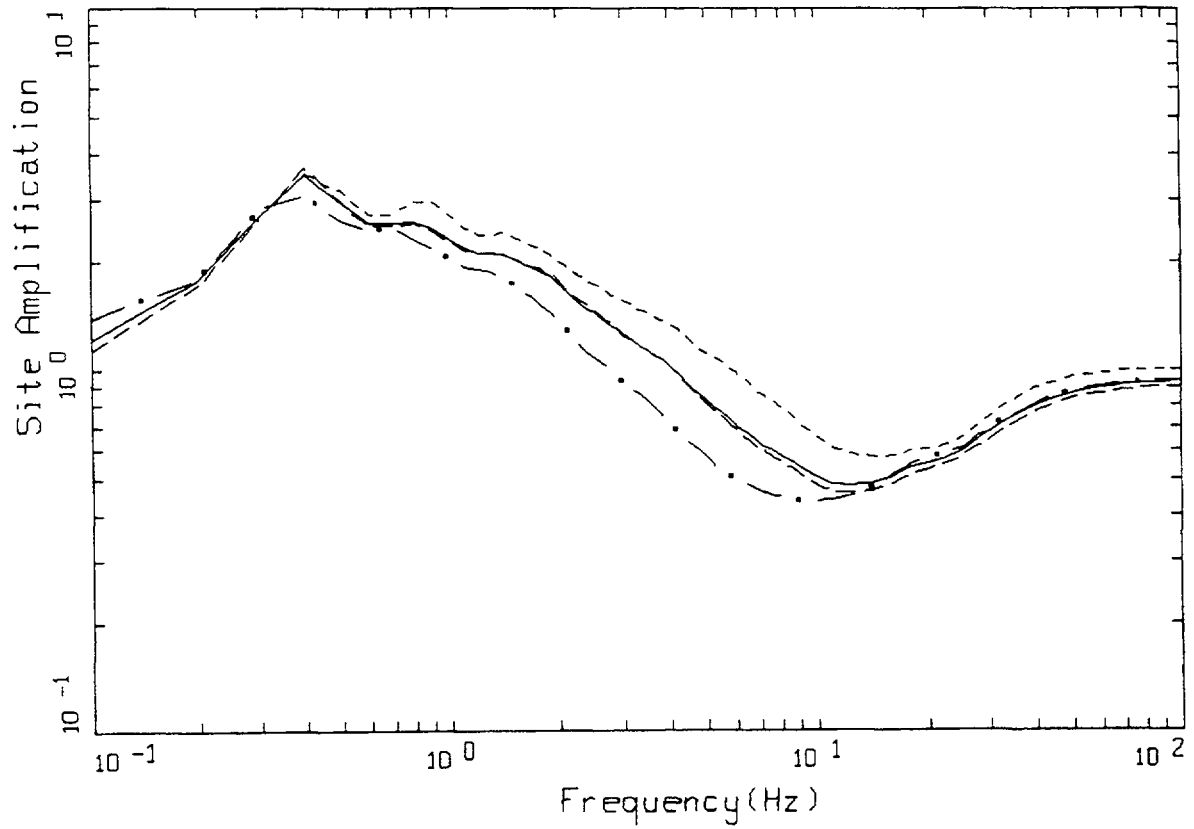


WUS 10E-4, MELOLAND
 1 HZ TRANSFER FUNCTION
 WEIGHTS: ML=0.20, MM=0.60, MH=0.20

LEGEND

- ML = 5.4, D = 10 KM, MEAN RATIO
- . - . MM = 6.6, D = 18 KM MEAN RATIO
- • — MH = 7.8, D = 30 KM MEAN RATIO
- WEIGHTED MEAN RATIO

Figure 6-11. Comparison of transfer functions computed for the scaled 1 Hz design earthquake for the Meloland profile, WUS conditions.

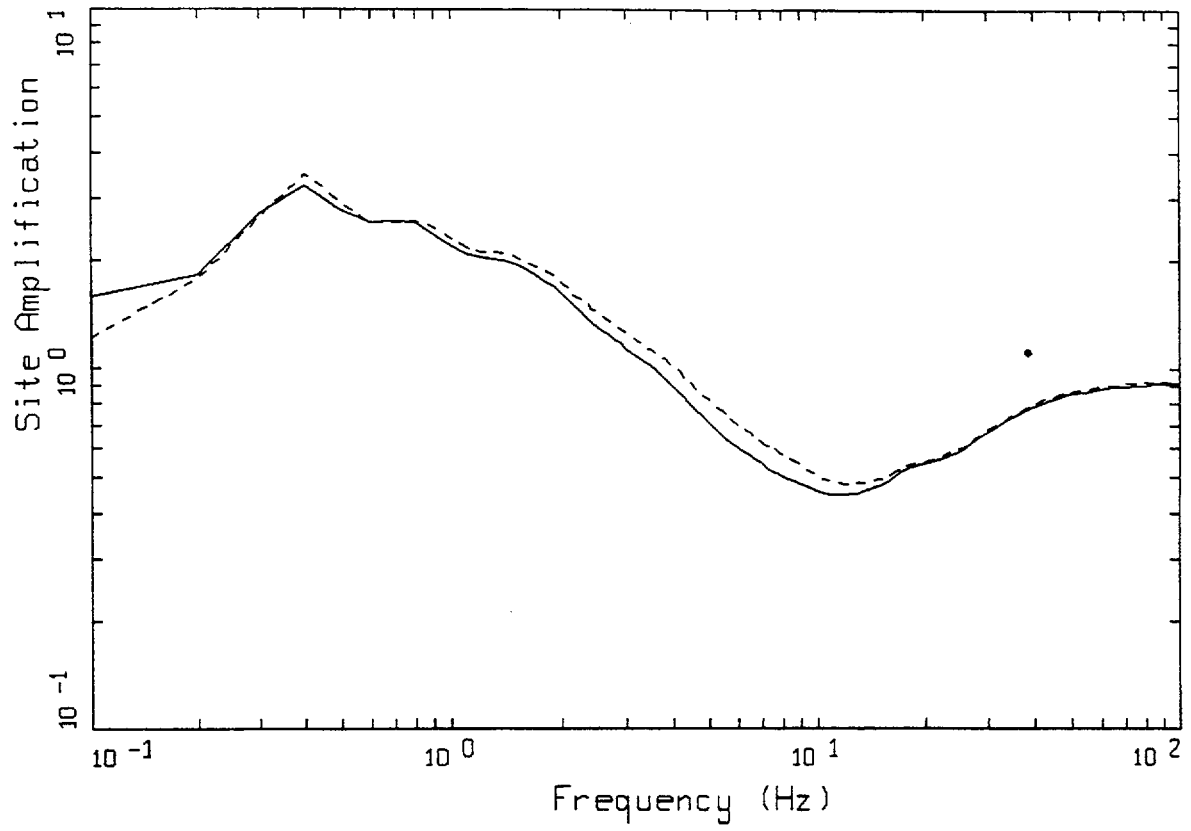


WUS 10E-4, MELOLAND
 10HZ TRANSFER FUNCTION
 WEIGHTS: ML=0.20, MM=0.60, MH=0.20

LEGEND

- ML = 5.1, D = 10 KM, MEAN RATIO
- · - · - MM = 6.1, D = 14 KM MEAN RATIO
- · — MH = 7.8, D = 30 KM MEAN RATIO
- WEIGHTED MEAN RATIO

Figure 6-12. Comparison of transfer functions computed for the scaled 10 Hz design earthquake for the Meloland profile, WUS conditions.



WUS, 10E-4, MELOLAND
 TRANSFER FUNCTIONS

LEGEND
 ——— 1 HZ WEIGHTED MEAN RATIO; WEIGHTS:ML=0.20,MM=0.60,MH=0.20
 - - - - 10 HZ WEIGHTED MEAN RATIO; WEIGHTS:ML=0.20,MM=0.60,MH=0.20

Figure 6-13. Comparison of weighted mean transfer functions computed for the 1 Hz and 10 Hz scaled spectra for the Meloland profile, WUS conditions.

Uniform hazard spectra, rock, Mojave site
Annual frequencies 1E-3, 1E-4, 1E-5

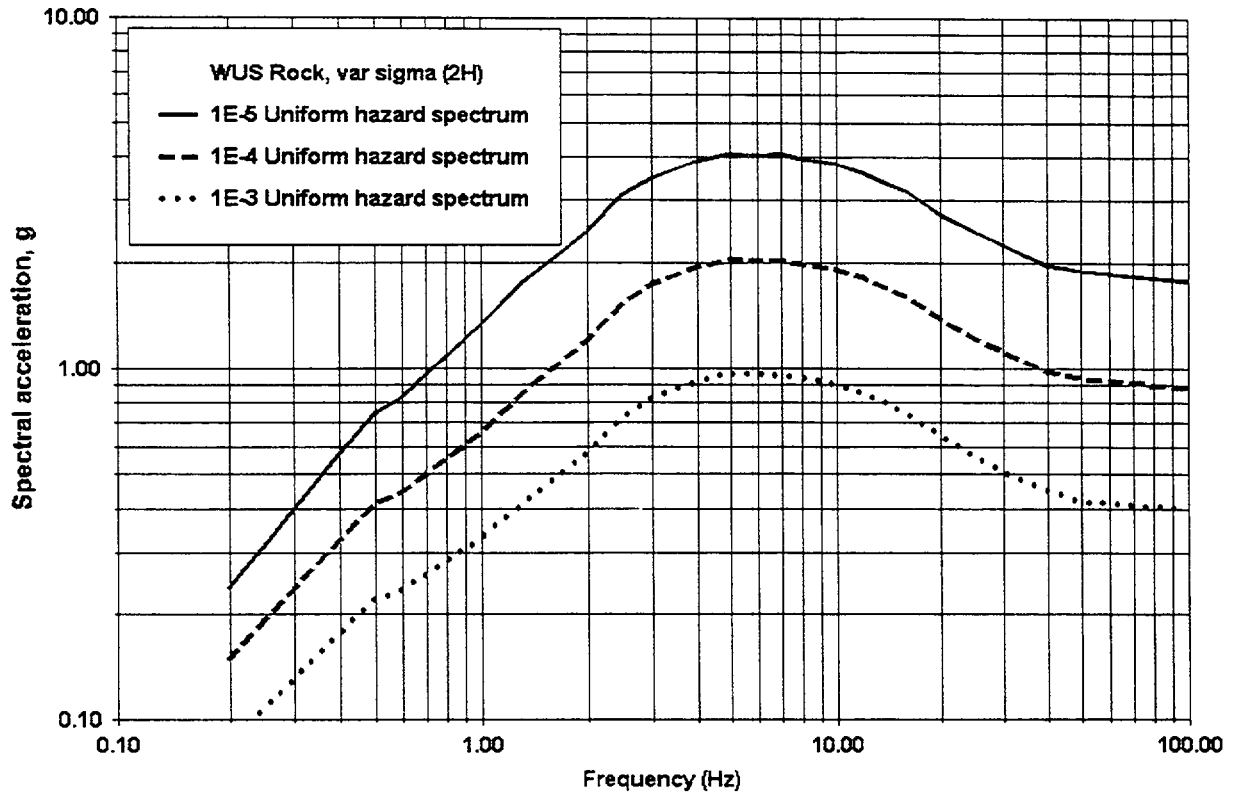
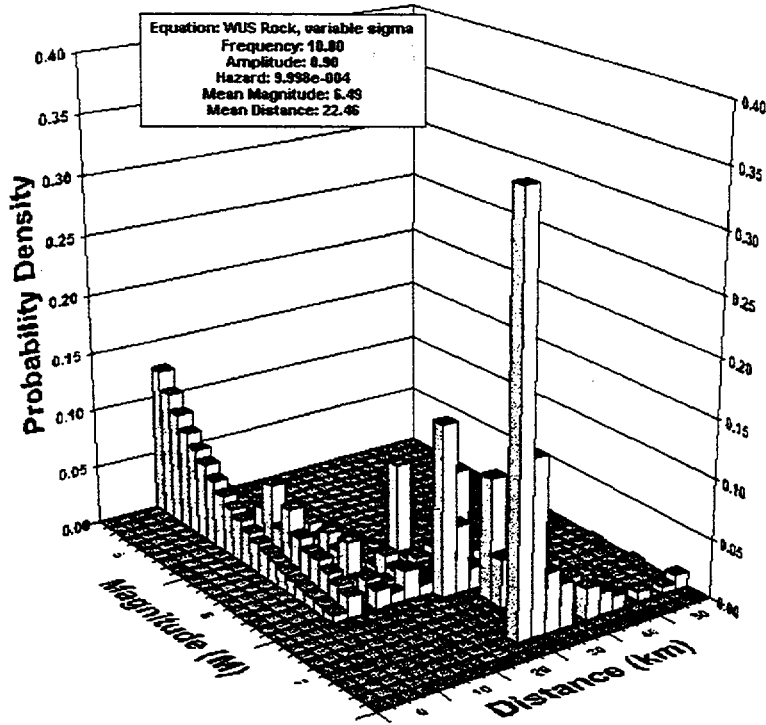


Figure 6-14. Mojave site rock spectra for 10^{-3} , 10^{-4} , and 10^{-5} annual frequencies.

Magnitude-Distance Deaggregation



Magnitude-Distance Deaggregation

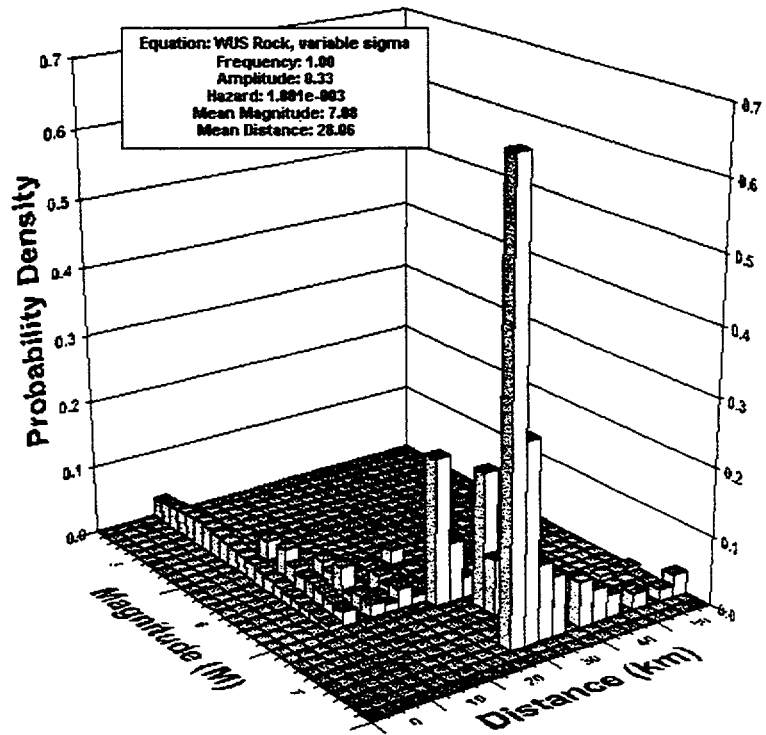
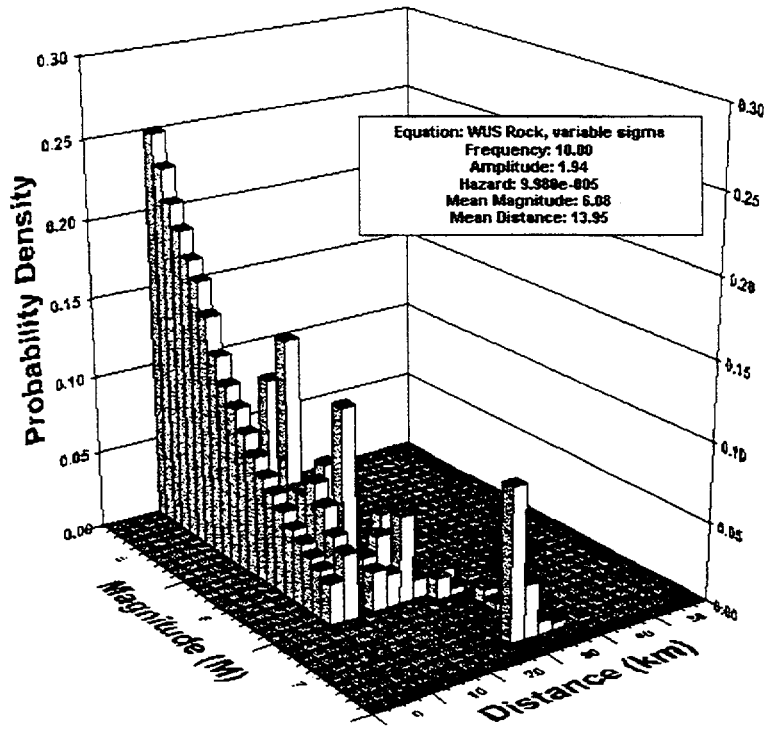


Figure 6-15. Mojave site, M-R deaggregation of rock seismic hazard for 10^{-3} . Top: 10 Hz Bottom: 1 Hz

Magnitude-Distance Deaggregation



Magnitude-Distance Deaggregation

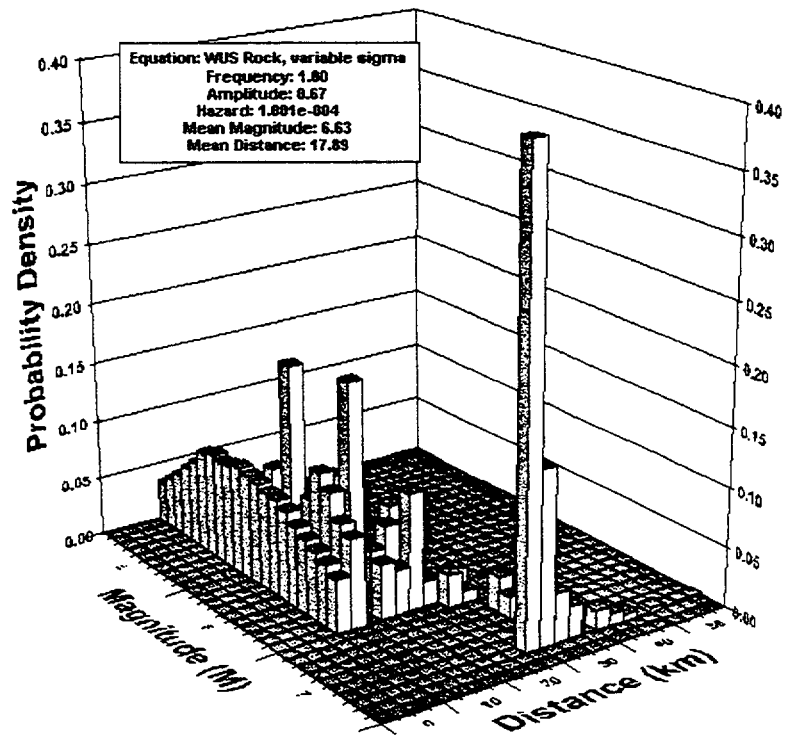
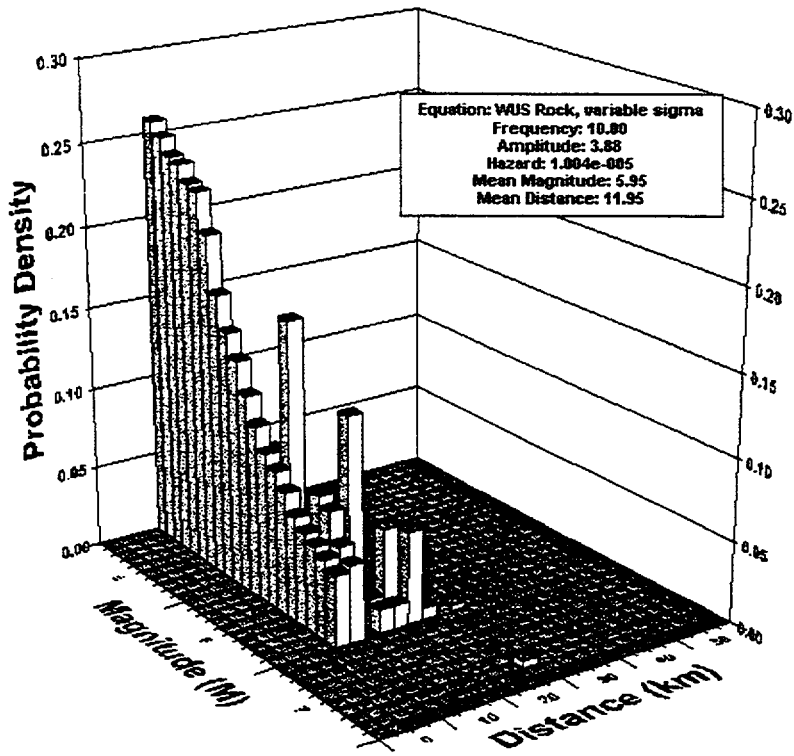


Figure 6-16. Mojave site,
 M-R deaggregation of rock
 seismic hazard for 10^{-4} . Top:
 10 Hz Bottom: 1 Hz

Magnitude-Distance Deaggregation



Magnitude-Distance Deaggregation

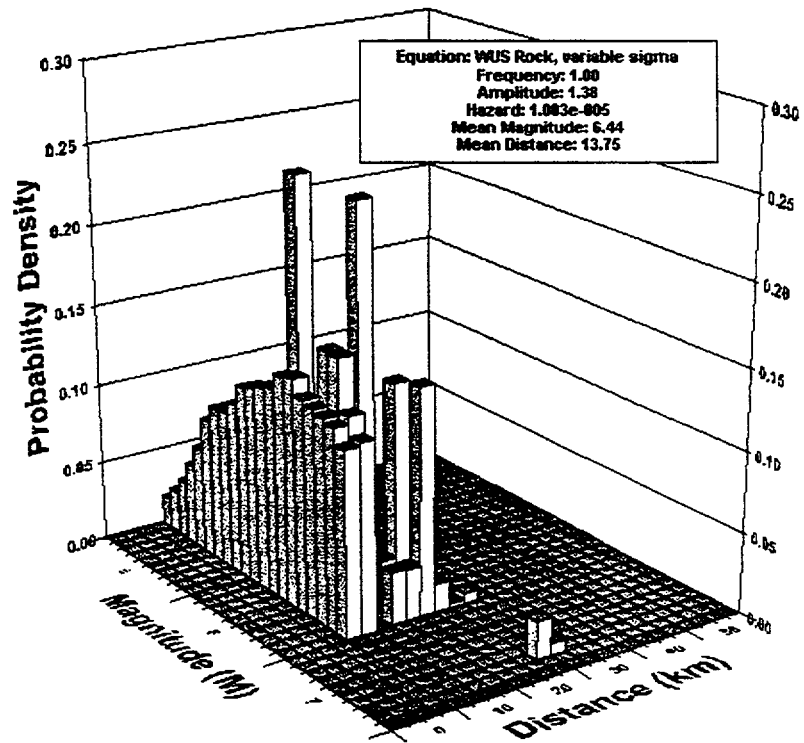


Figure 6-17. Mojave site, M-R deaggregation of rock seismic hazard for 10^{-5} . Top: 10 Hz Bottom: 1 Hz

WUS soil amplification factors

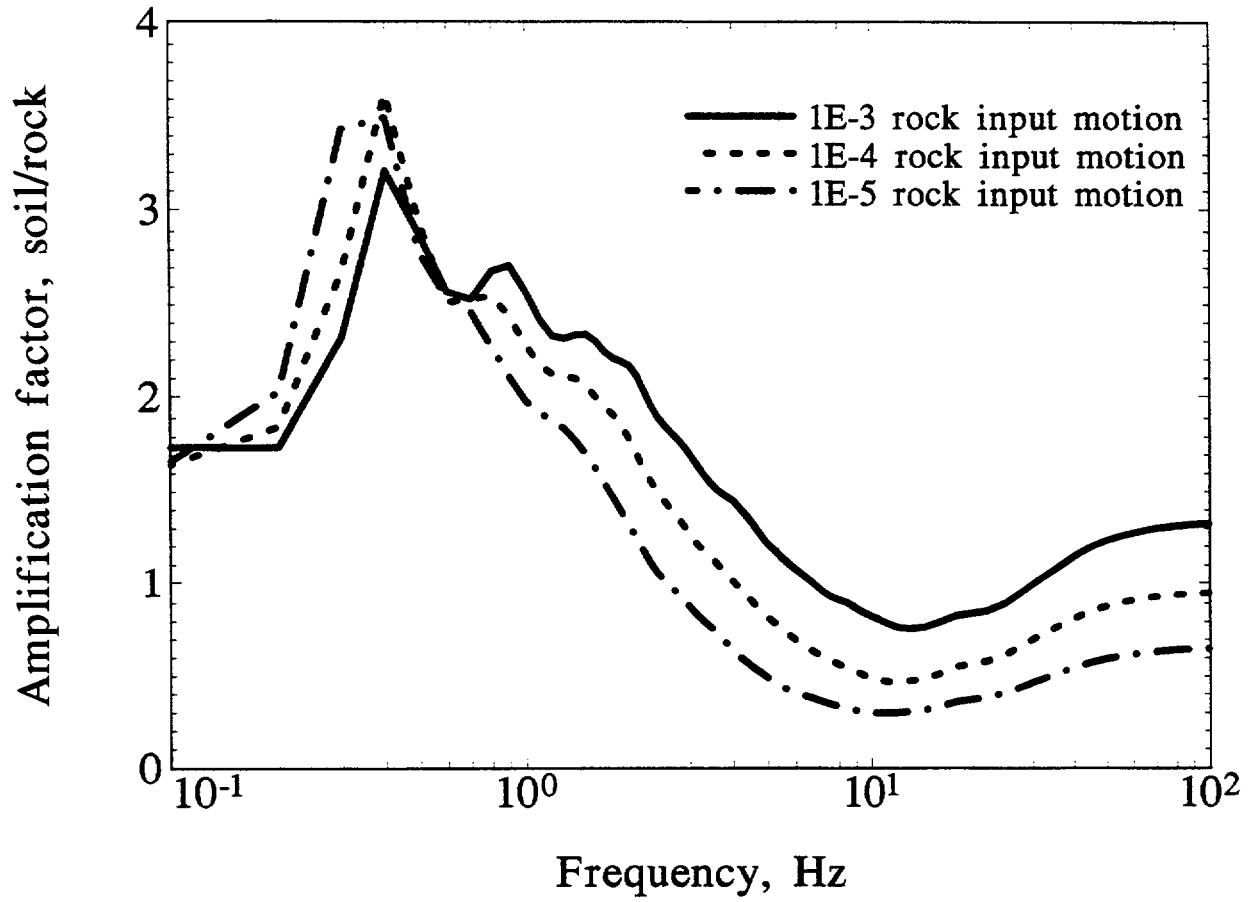


Figure 6-18. Mean amplification factor, soil/rock, from Approach 2A for 10⁻³, 10⁻⁴, and 10⁻⁵ rock input motions, Mojave site, Meloland profile.

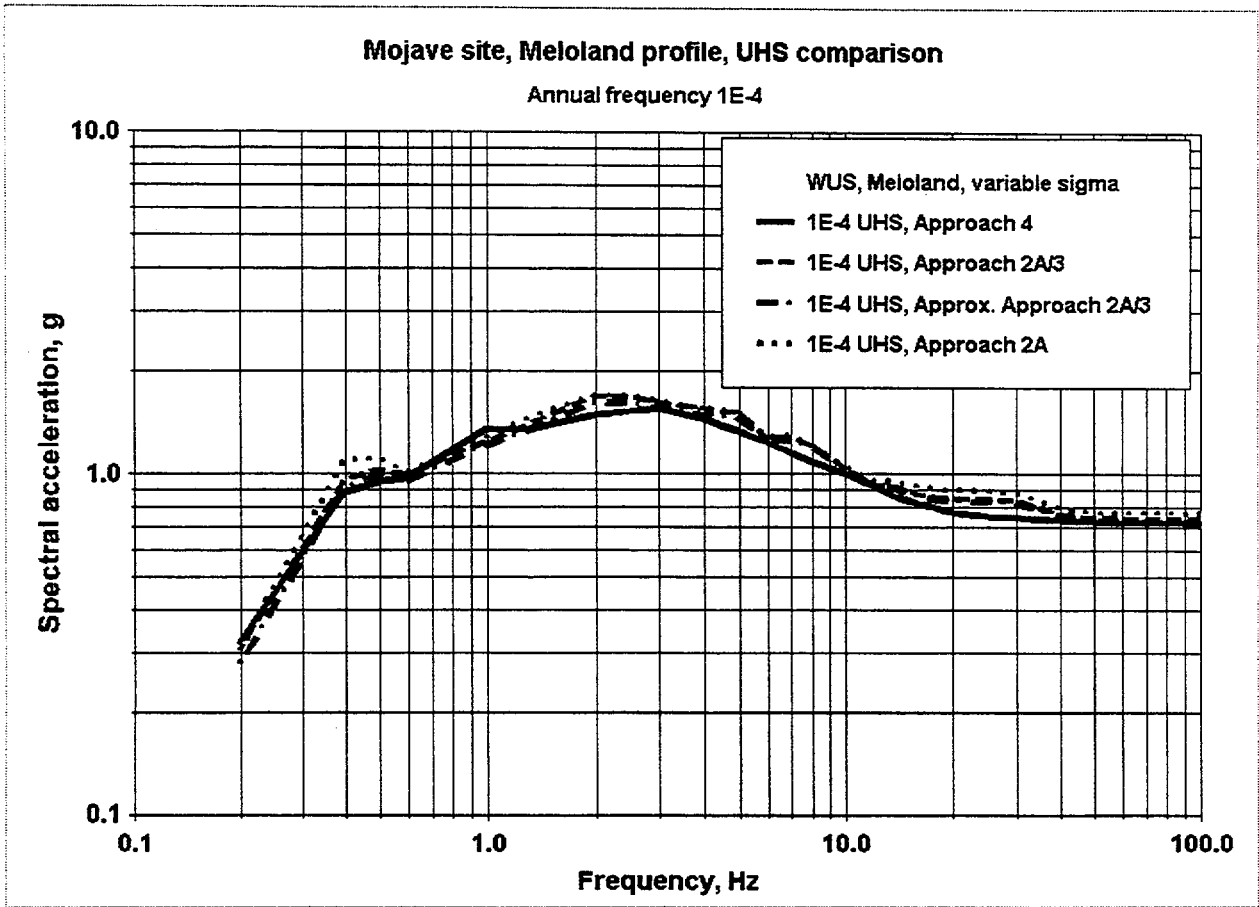


Figure 6-19. Mojave site 10^{-4} UHS for Meloland profile from Approach 4 (direct method) and Approaches 2A and 2A/3.

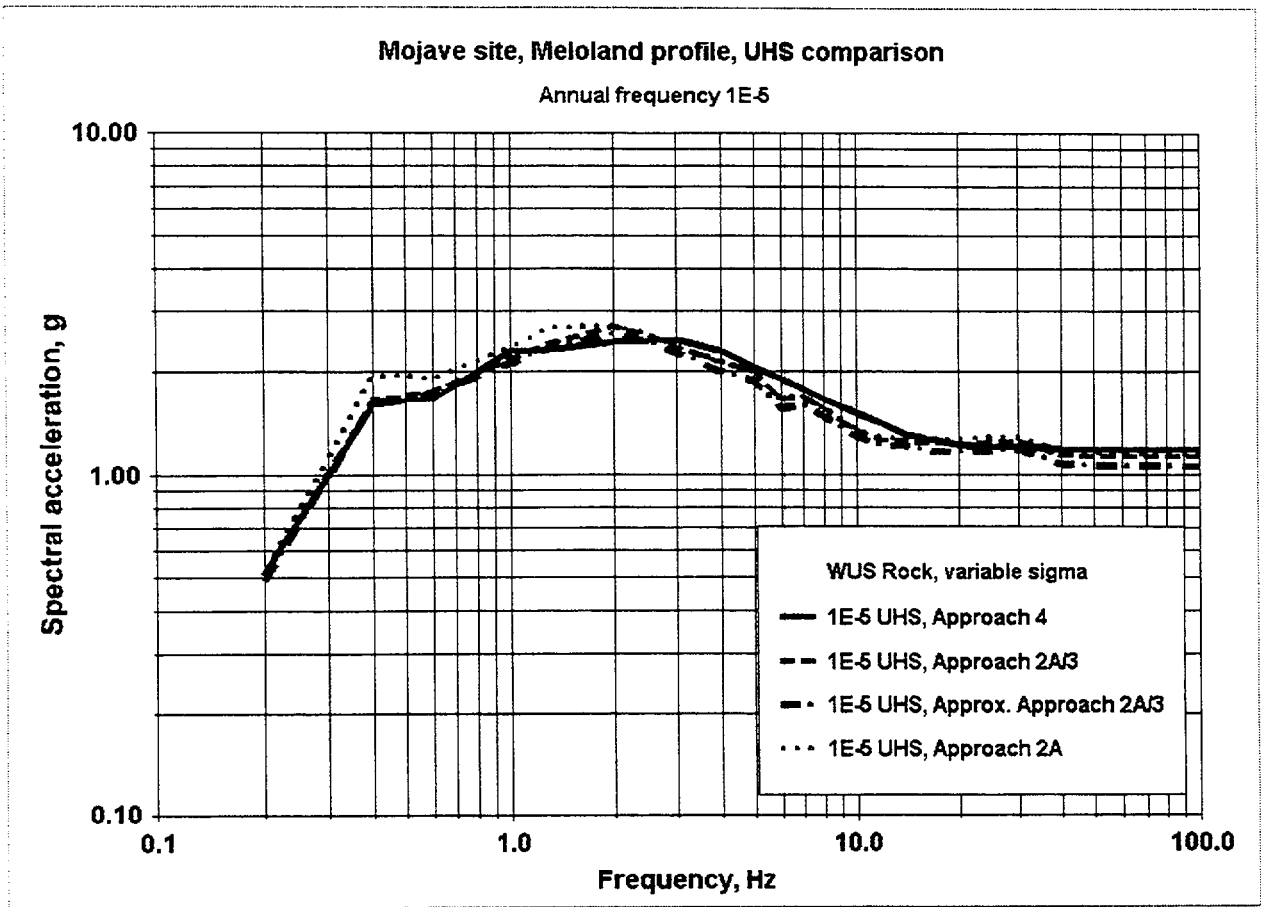
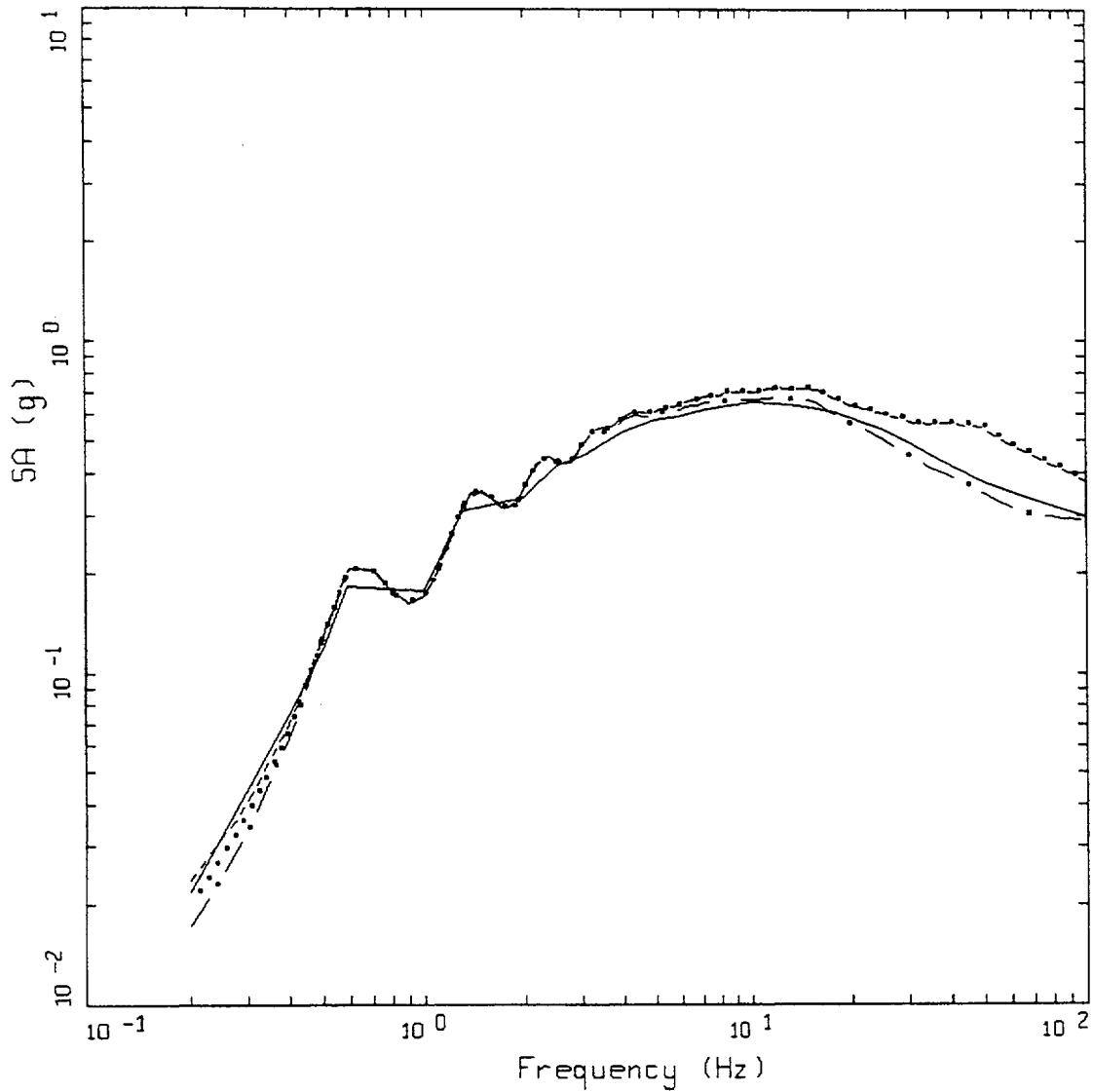


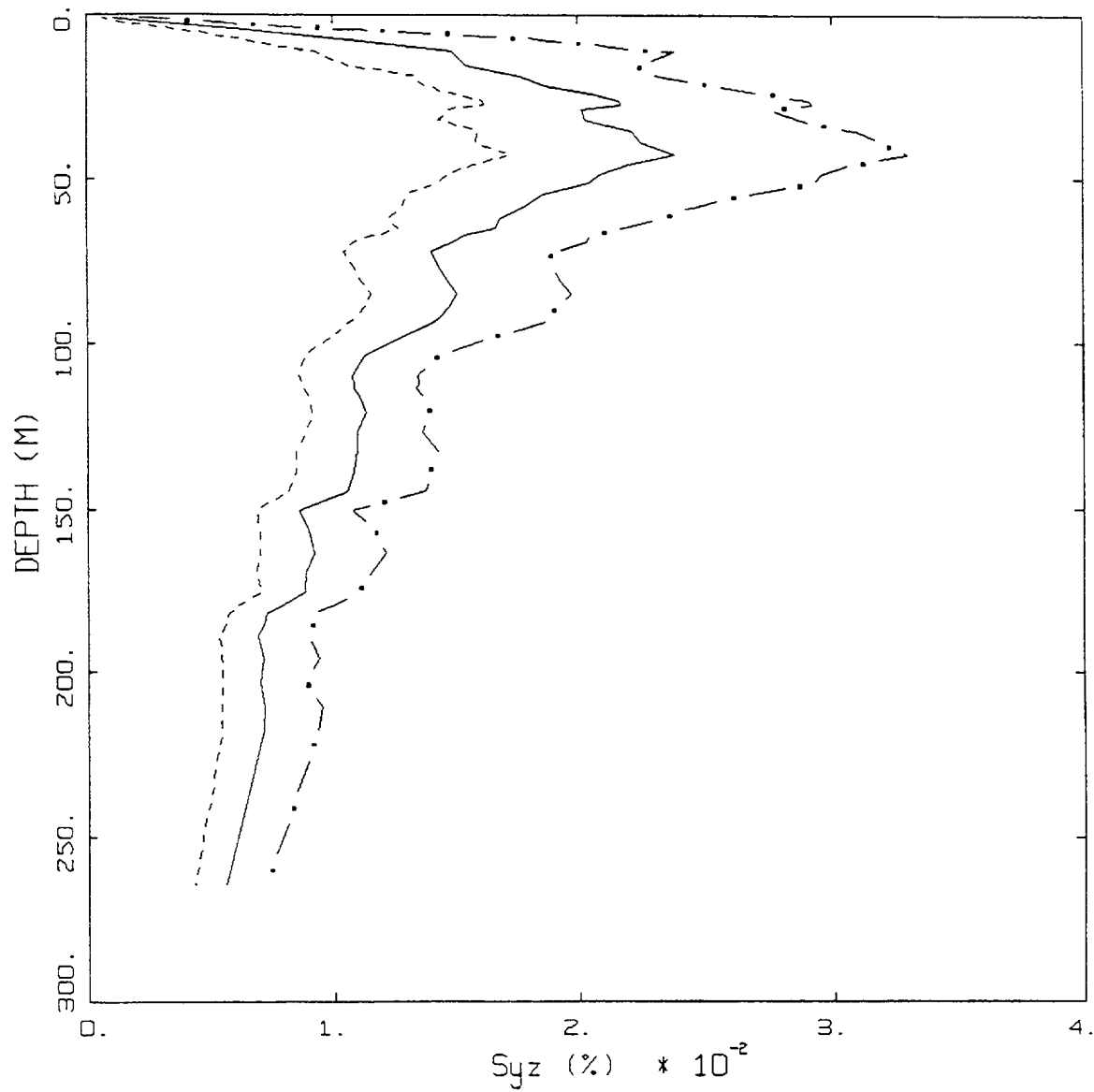
Figure 6-20. Mojave site 1E-5 UHS for Meloland profile from Approach 4 (direct method) and Approaches 2A and 2A/3.



CEUS 10E-4 APPROACH COMPARISON, SAVANNAH RIVER GENERIC

- LEGEND
- APPROACH 4, 10⁻⁴ UHS SOIL UNIFORM HAZARD SPECTRUM
 - APPROACH 2A, 1 HZ AND 10 HZ DESIGN CONTROL MOTIONS
 - APPROACH 2B, 1 HZ AND 10 HZ DEAGGREGATION CONTROL MOTIONS
 - · - · - APPROACH 1, 10⁻⁴ UHS ROCK CONTROL MOTION

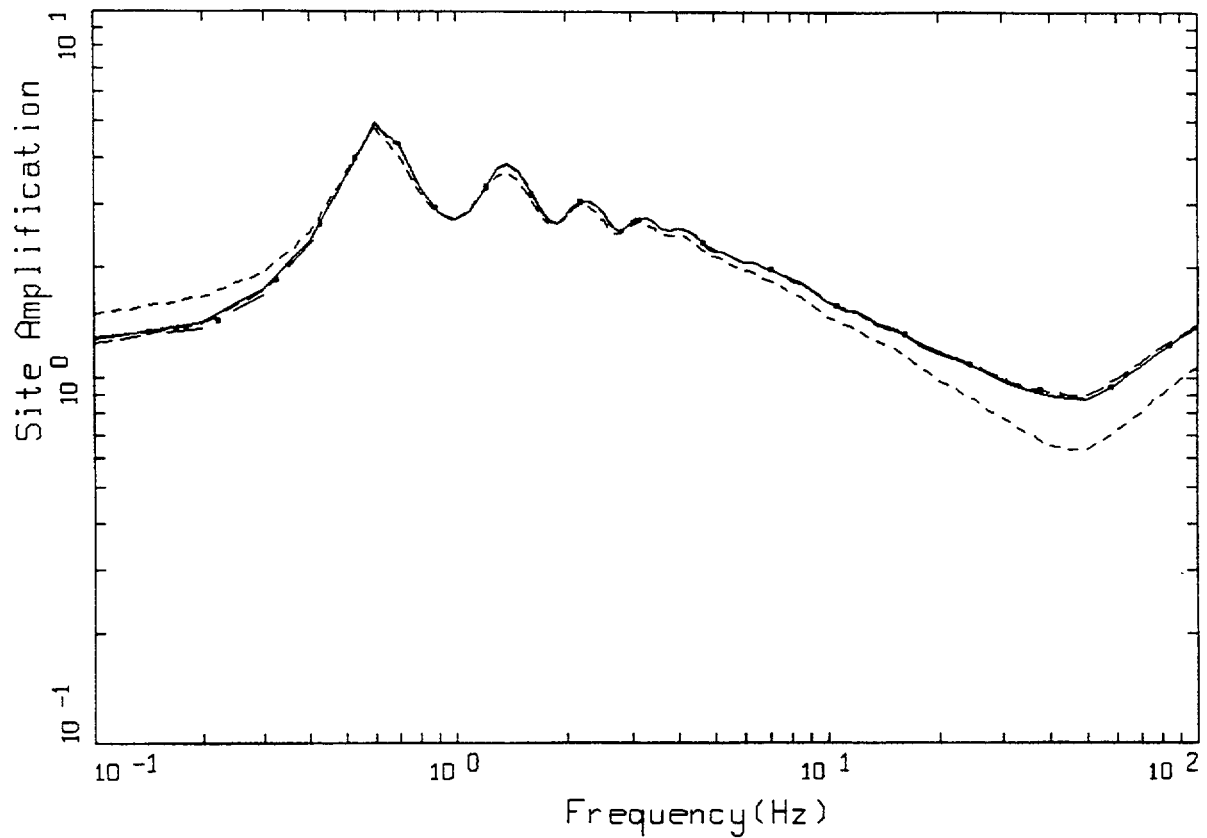
Figure 6-21. Comparison of soil spectra computed using Approaches 1, 2A, 2B, and 4 (Table 6-1) for Savannah profile, CEUS conditions.



CEUS, SAVANNAH RIVER GENERIC, APPROACH 1
EFFECTIVE STRAINS (SYZ)

LEGEND
 - . - 84TH PERCENTILE
 — 50TH PERCENTILE
 - - - 16TH PERCENTILE

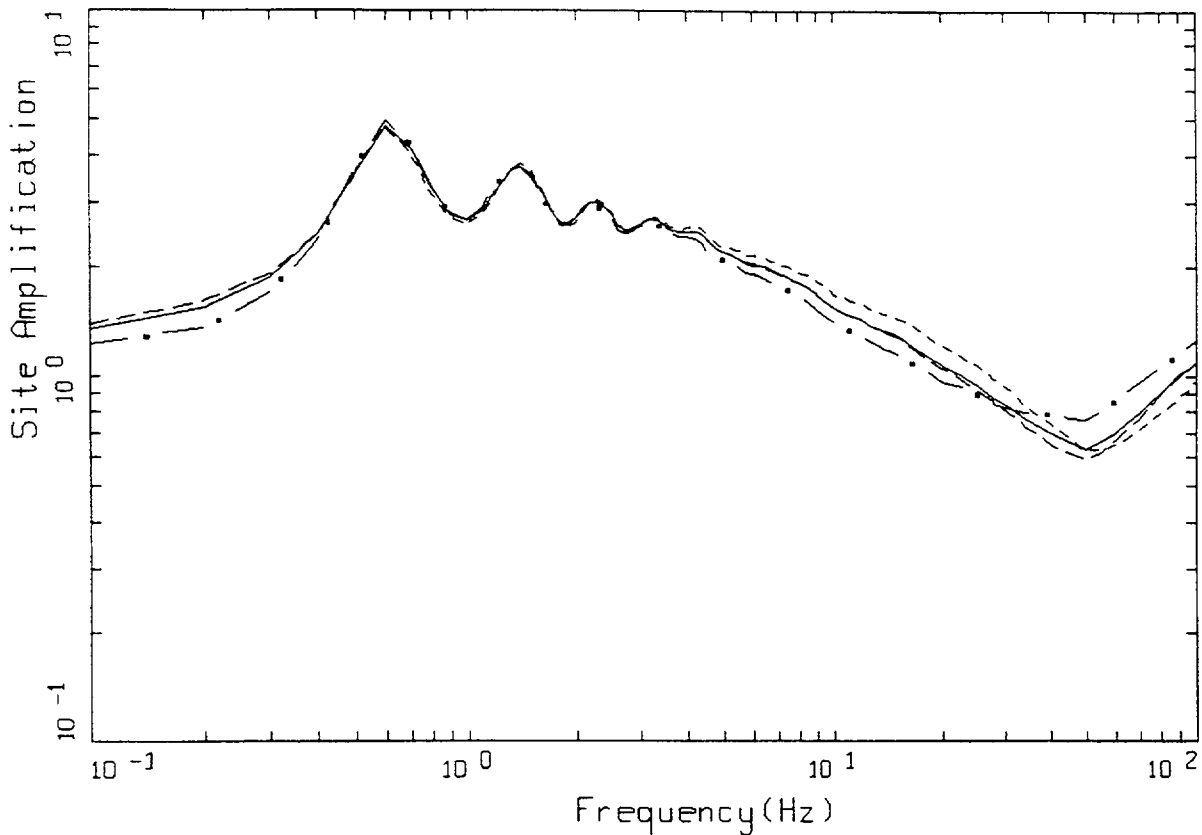
Figure 6-22. Median and $\pm 1\sigma$ effective strains for Savannah profile using Approach 1: CEUS conditions (note scale on strain axis).



CEUS 10E-4, SAVANNAH RIVER GENERIC
 1 HZ TRANSFER FUNCTION
 WEIGHTS: ML=0.07, MM=0.73, MH=0.20

LEGEND
 ----- ML = 6.0, D = 10 KM, MEAN RATIO
 - . - . - MM = 7.2, D = 110 KM MEAN RATIO
 — • — MH = 7.7, D = 130 KM MEAN RATIO
 ——— WEIGHTED MEAN RATIO

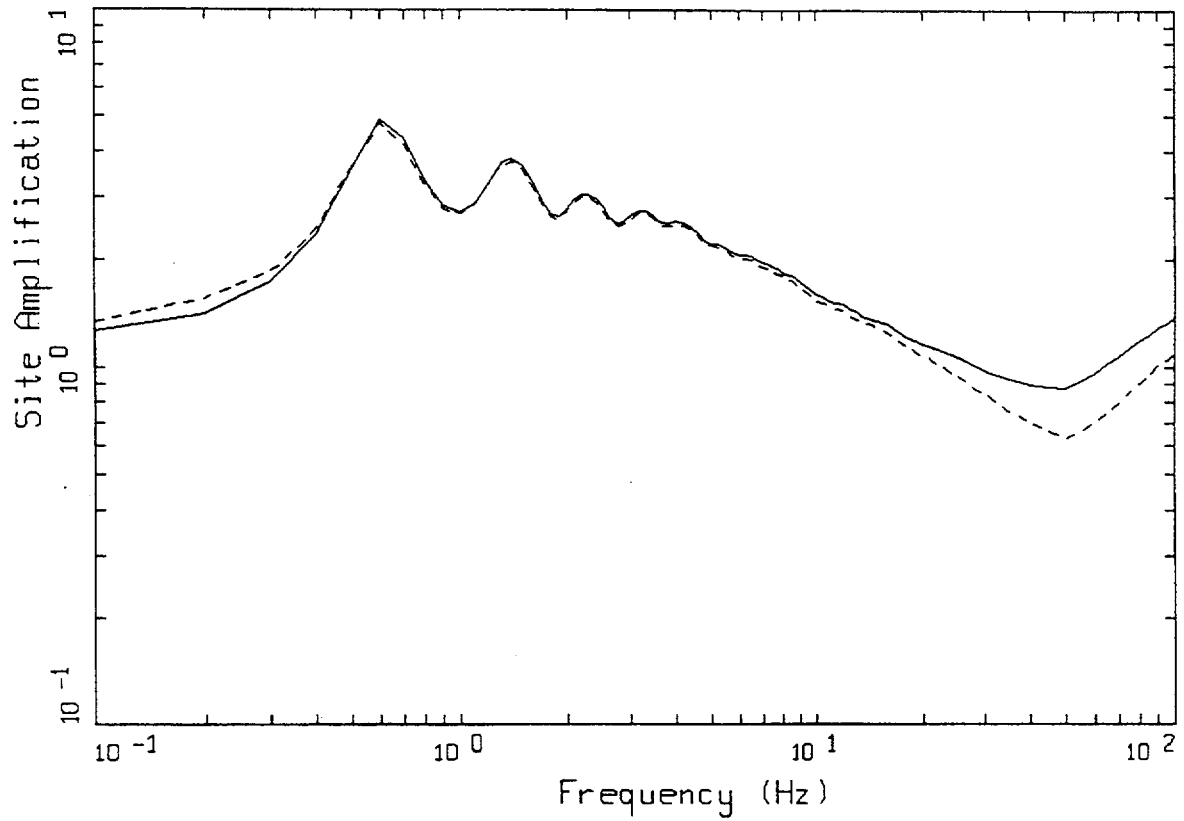
Figure 6-23. Comparison of transfer functions computed for the scaled 1 Hz motion for Savannah profile, CEUS conditions.



CEUS 10E-4, SAVANNAH RIVER GENERIC
 10HZ TRANSFER FUNCTION
 WEIGHTS: ML=0.22, MM=0.58, MH=0.20

LEGEND
 - - - - - ML = 4.7, D = 10 KM, MEAN RATIO
 - · - · - MM = 6.0, D = 46 KM MEAN RATIO
 — · — MH = 7.7, D = 130 KM MEAN RATIO
 ——— WEIGHTED MEAN RATIO

Figure 6-24. Comparison of transfer functions computed for the scaled 10 Hz motion for Savannah profile, CEUS conditions.



CEUS, 10E-4, SAVANNAH RIVER GENERIC
TRANSFER FUNCTIONS

LEGEND
 ——— 1 HZ WEIGHTED MEAN RATIO; WEIGHTS:ML=0.07,MM=0.73,MH=0.20
 - - - - 10 HZ WEIGHTED MEAN RATIO; WEIGHTS:ML=0.22,MM=0.58,MH=0.20

Figure 6-25. Comparison of weighted mean transfer functions computed for the scaled 1 Hz and 10 Hz motions for Savannah profile, CEUS conditions.

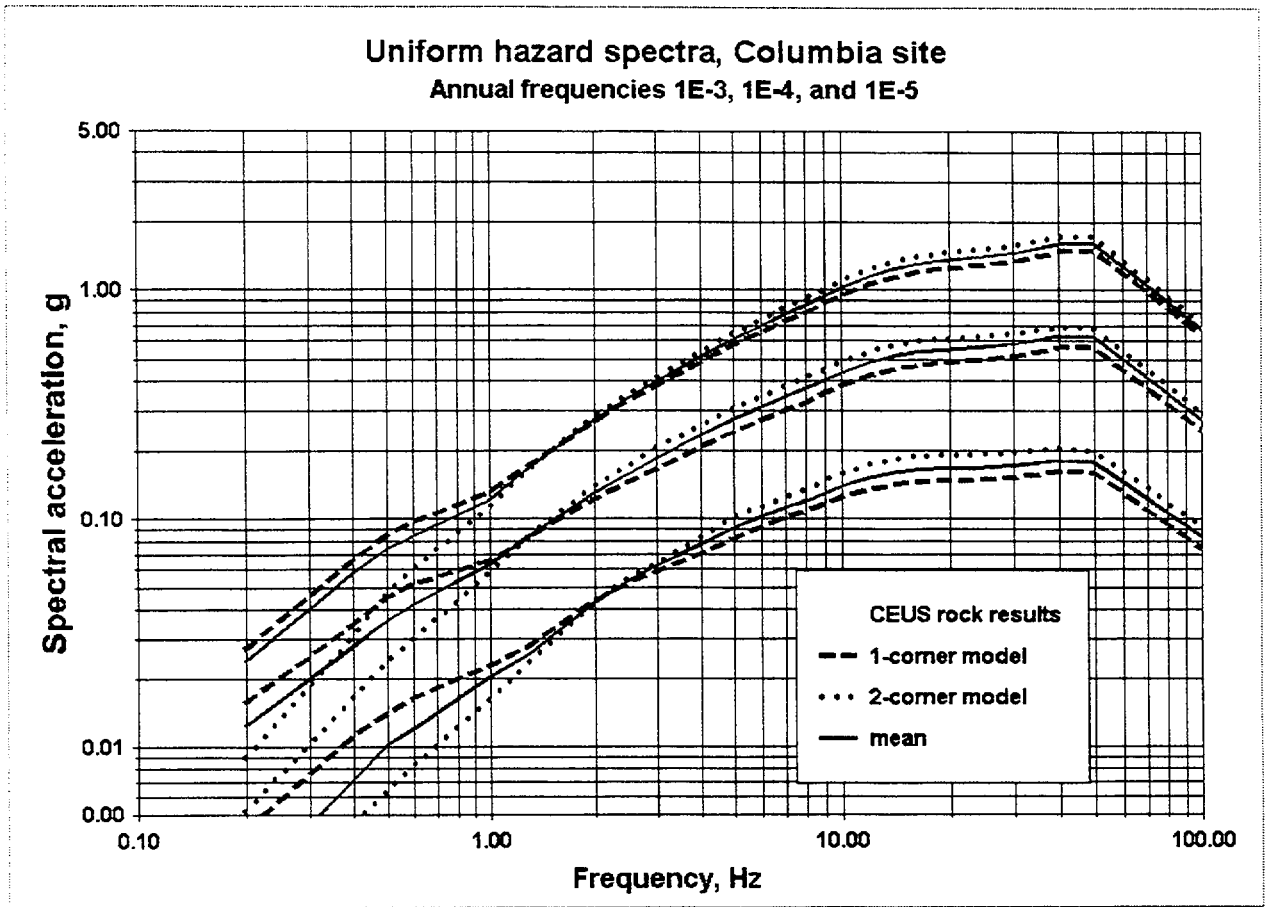
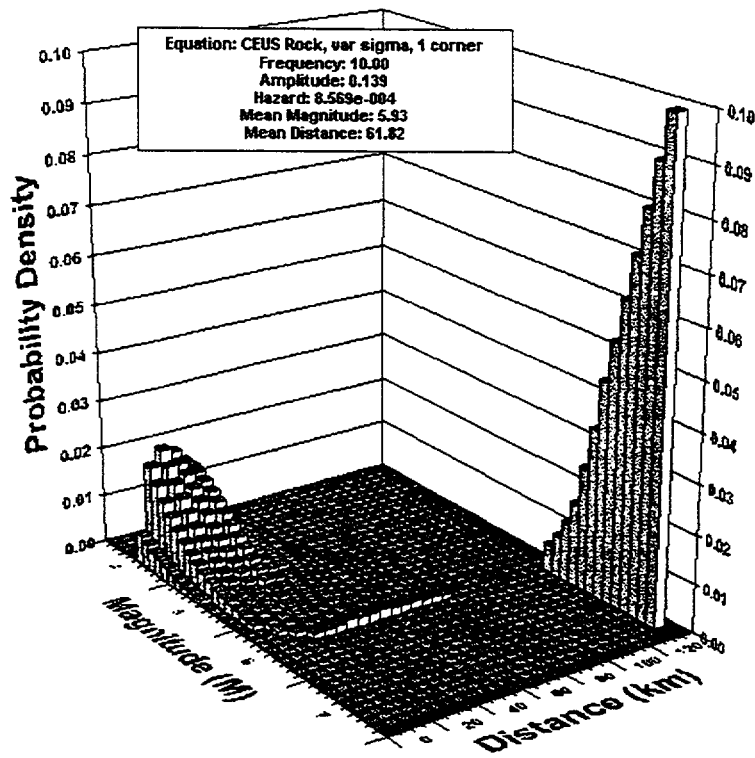


Figure 6-26. Columbia site UHS for 1- and 2-corner models and mean, for 10^{-3} (lower 3 curves), 10^{-4} (middle 3 curves), and 10^{-5} (top 3 curves).

Magnitude-Distance Deaggregation



Magnitude-Distance Deaggregation

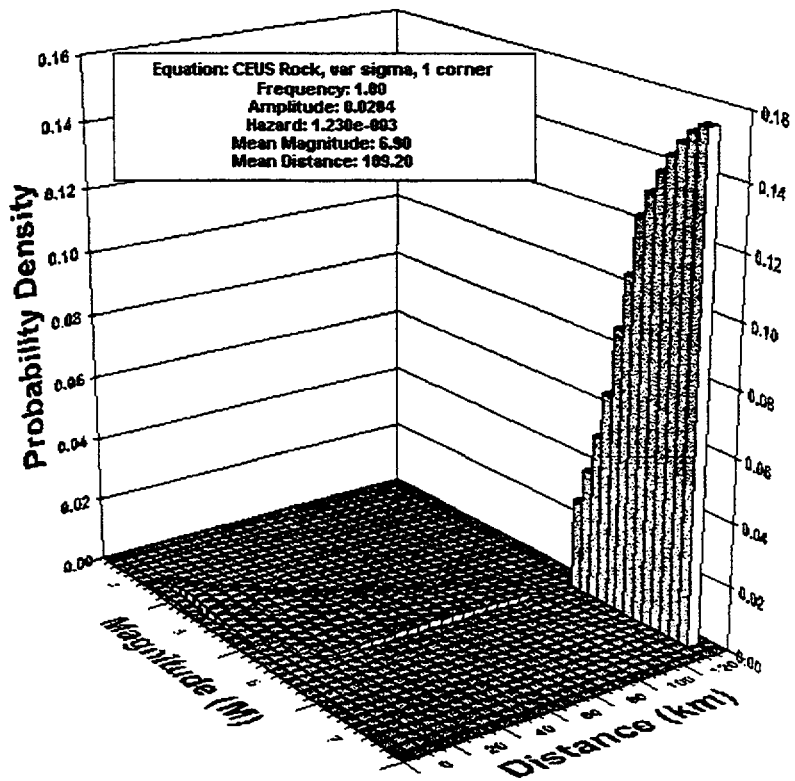
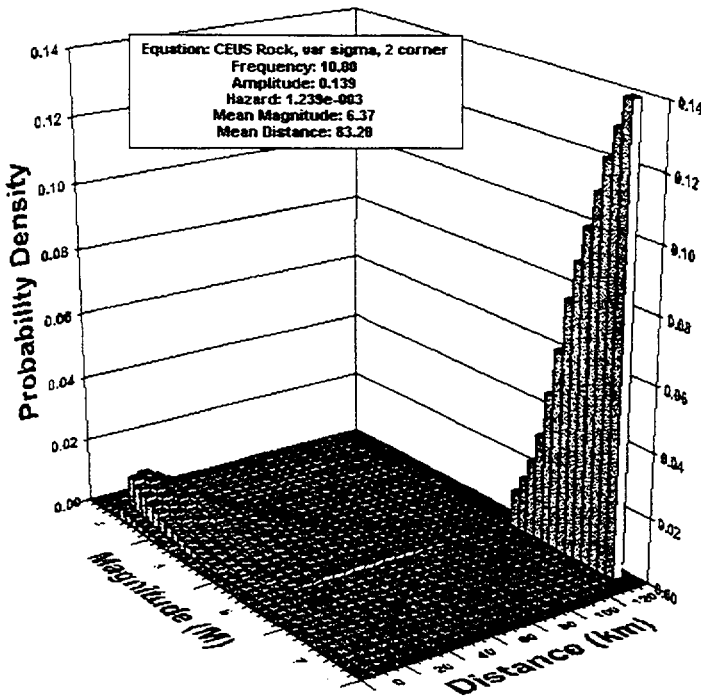


Figure 6-27a. Columbia site M-R deaggregation for 10^{-3} , 1-corner model, 10 Hz (top) and 1 Hz (bottom).

Magnitude-Distance Deaggregation



Magnitude-Distance Deaggregation

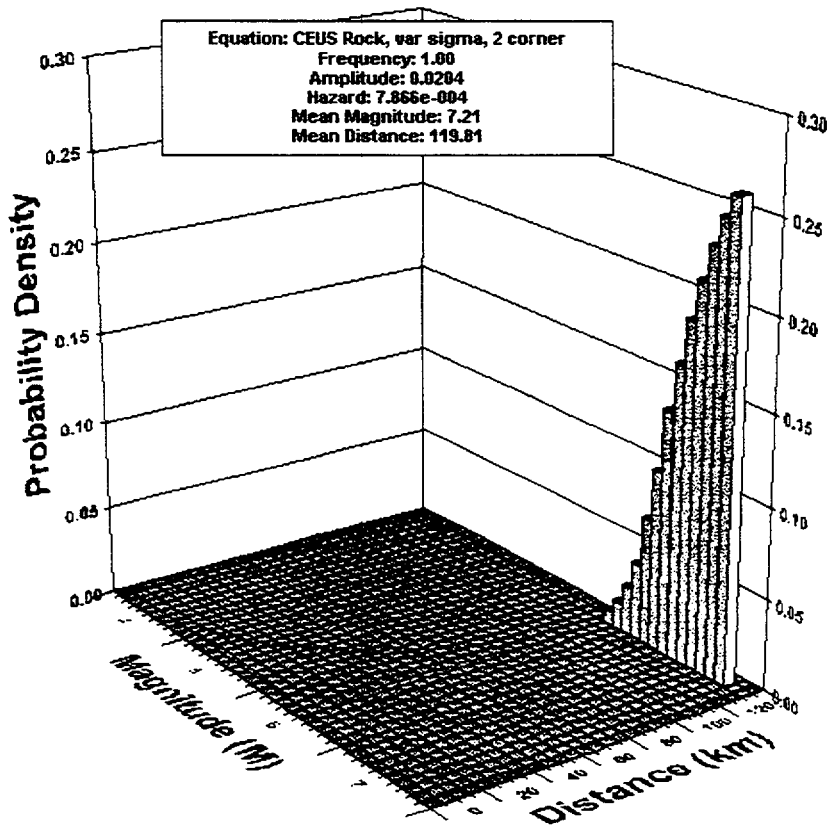
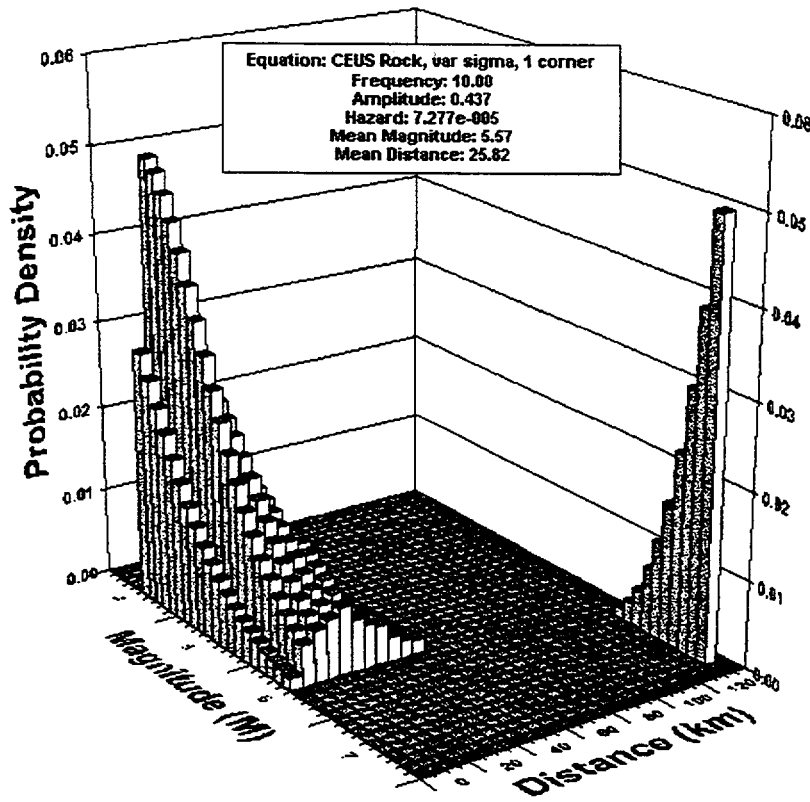


Figure 6-27b. Columbia site M-R deaggregation for 10^{-3} , 2-corner model, 10 Hz (top) and 1 Hz (bottom).

Magnitude-Distance Deaggregation



Magnitude-Distance Deaggregation

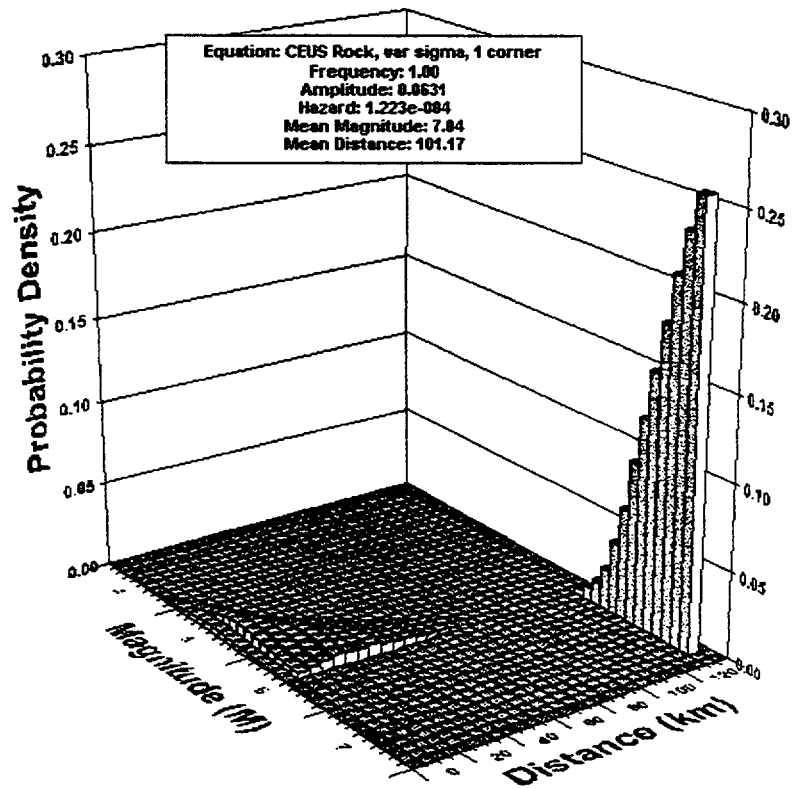
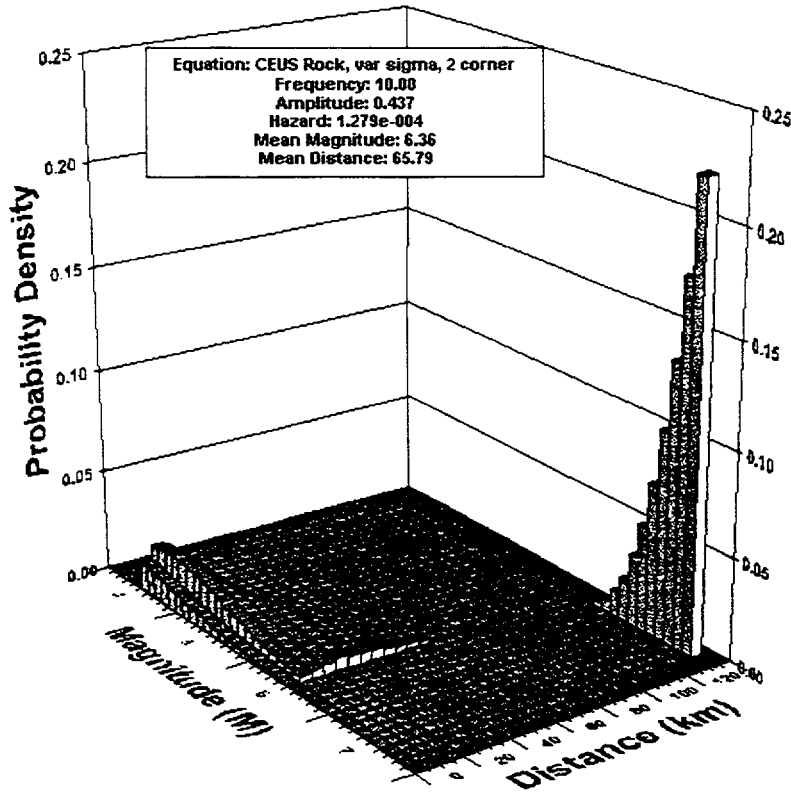


Figure 6-28a. Columbia site M-R deaggregation for 10^{-4} , 1-corner model, 10 Hz (top) and 1 Hz (bottom).

Magnitude-Distance Deaggregation



Magnitude-Distance Deaggregation

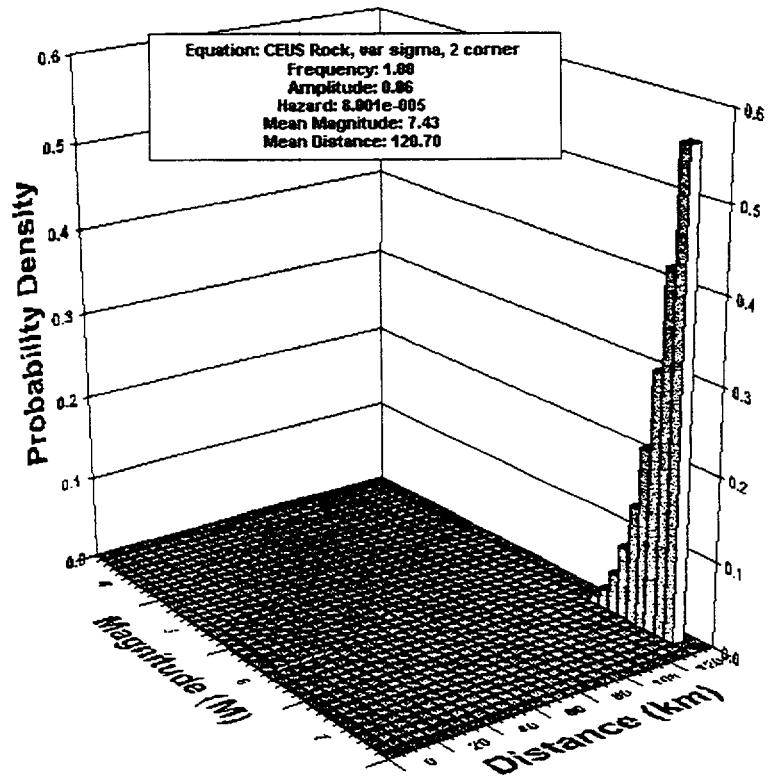
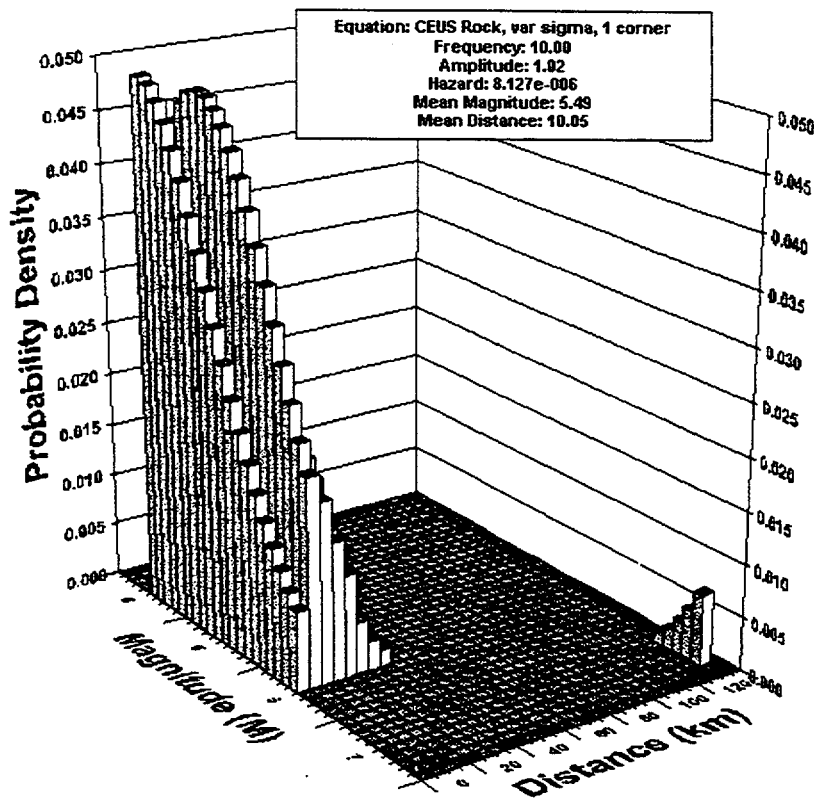


Figure 6-28b. Columbia site M-R deaggregation for 10^{-4} , 2-corner model, 10 Hz (top) and 1 Hz (bottom).

Magnitude-Distance Deaggregation



Magnitude-Distance Deaggregation

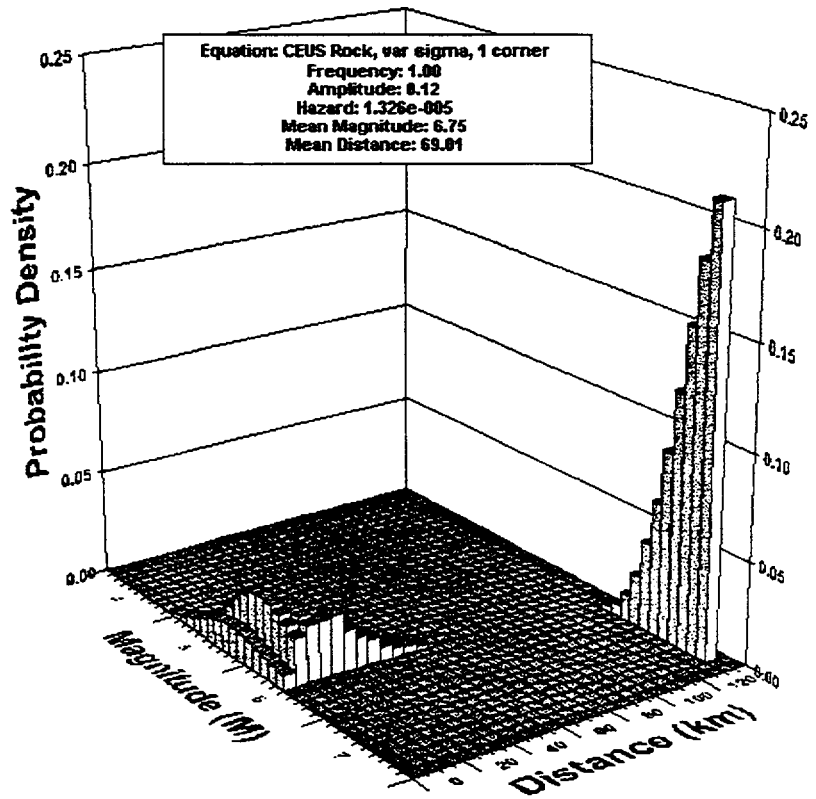
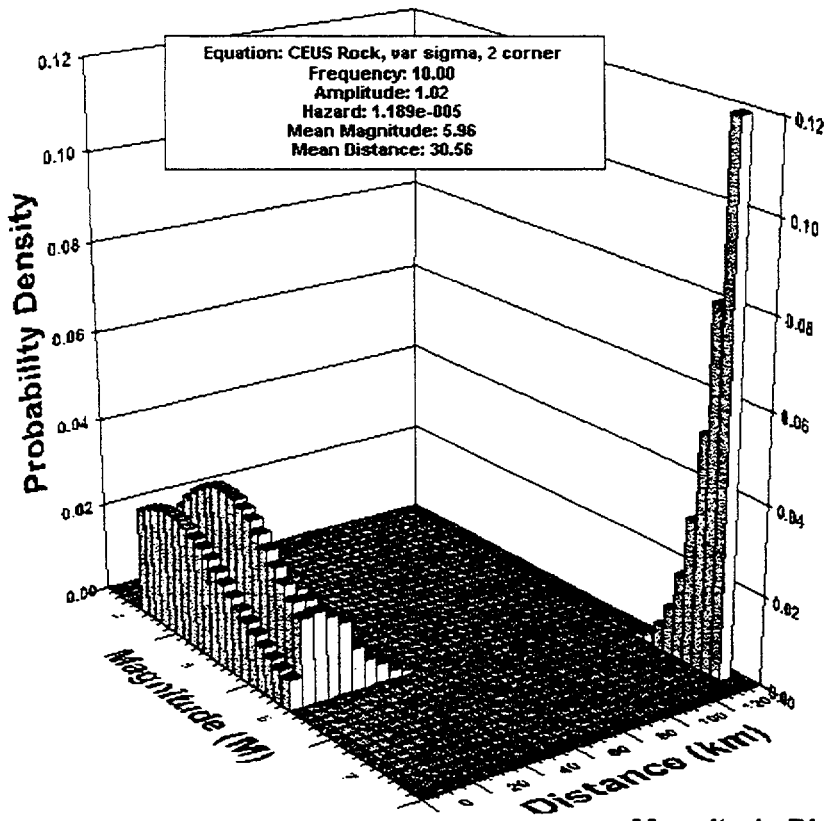


Figure 6-29a. Columbia site M-R deaggregation for 10^{-5} , 1-corner model, 10 Hz (top) and 1 Hz (bottom).

Magnitude-Distance Deaggregation



Magnitude-Distance Deaggregation

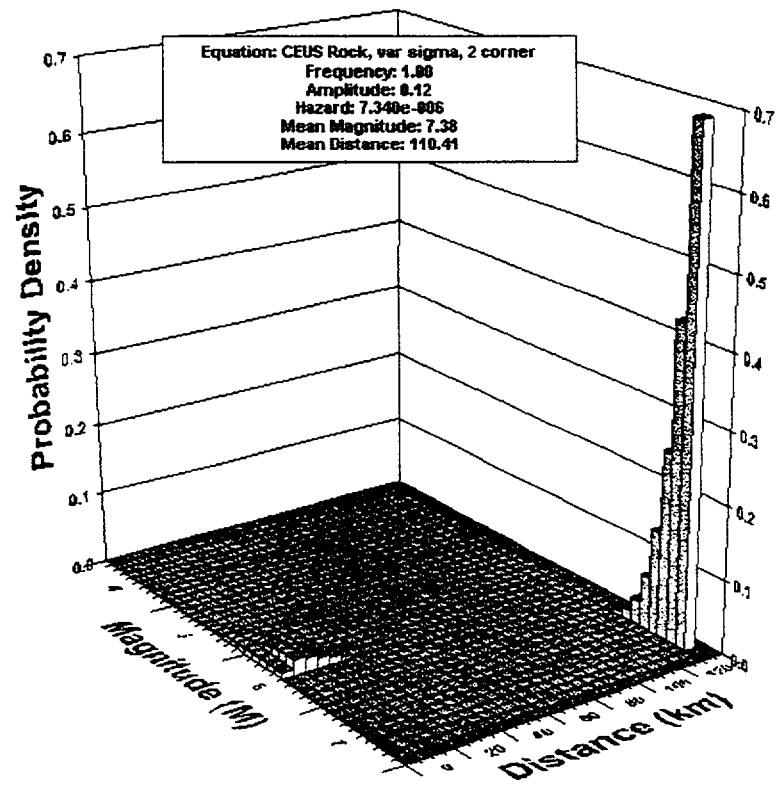


Figure 6-29b. Columbia site M-R deaggregation for 10^{-5} , 2-corner model, 10 Hz (top) and 1 Hz (bottom).

CEUS soil amplification factors

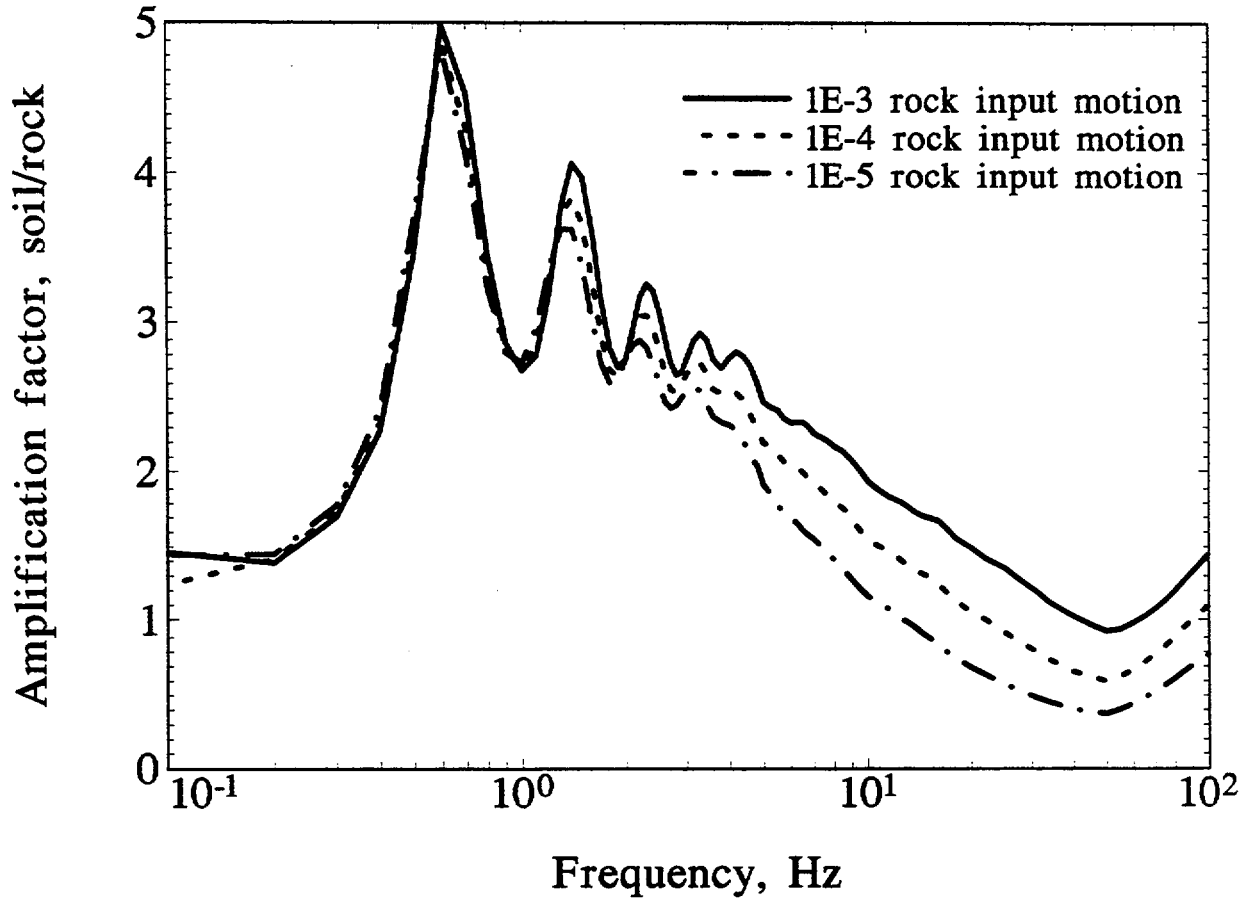


Figure 6-30. Mean amplification factor, soil/rock, from Approach 2A for 10⁻³, 10⁻⁴, and 10⁻⁵ rock input motions, Columbia site, Savannah profile.

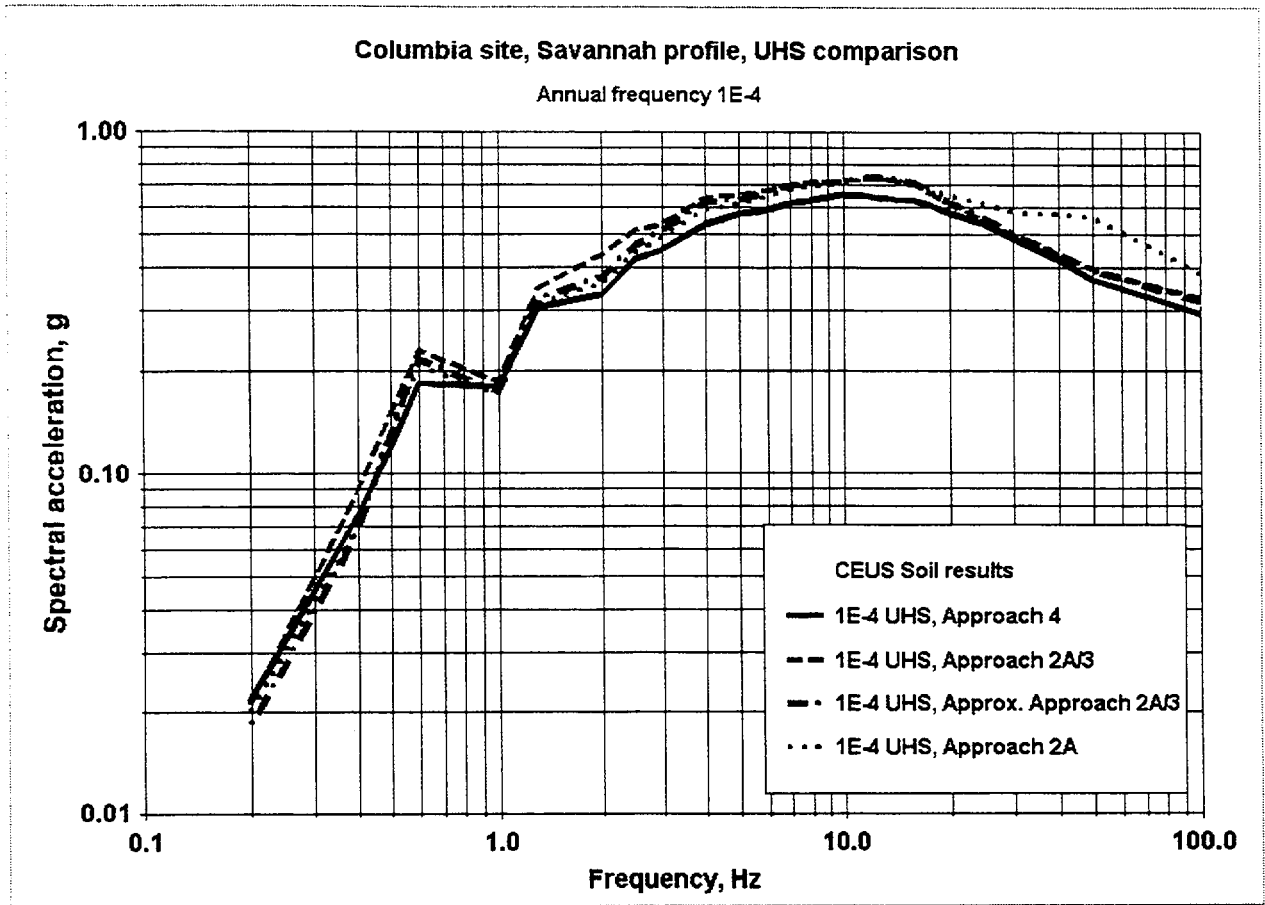


Figure 6-31. Columbia site 10^{-4} UHS for Savannah profile from Approach 4 (direct method) and Approaches 2A and 2A/3.

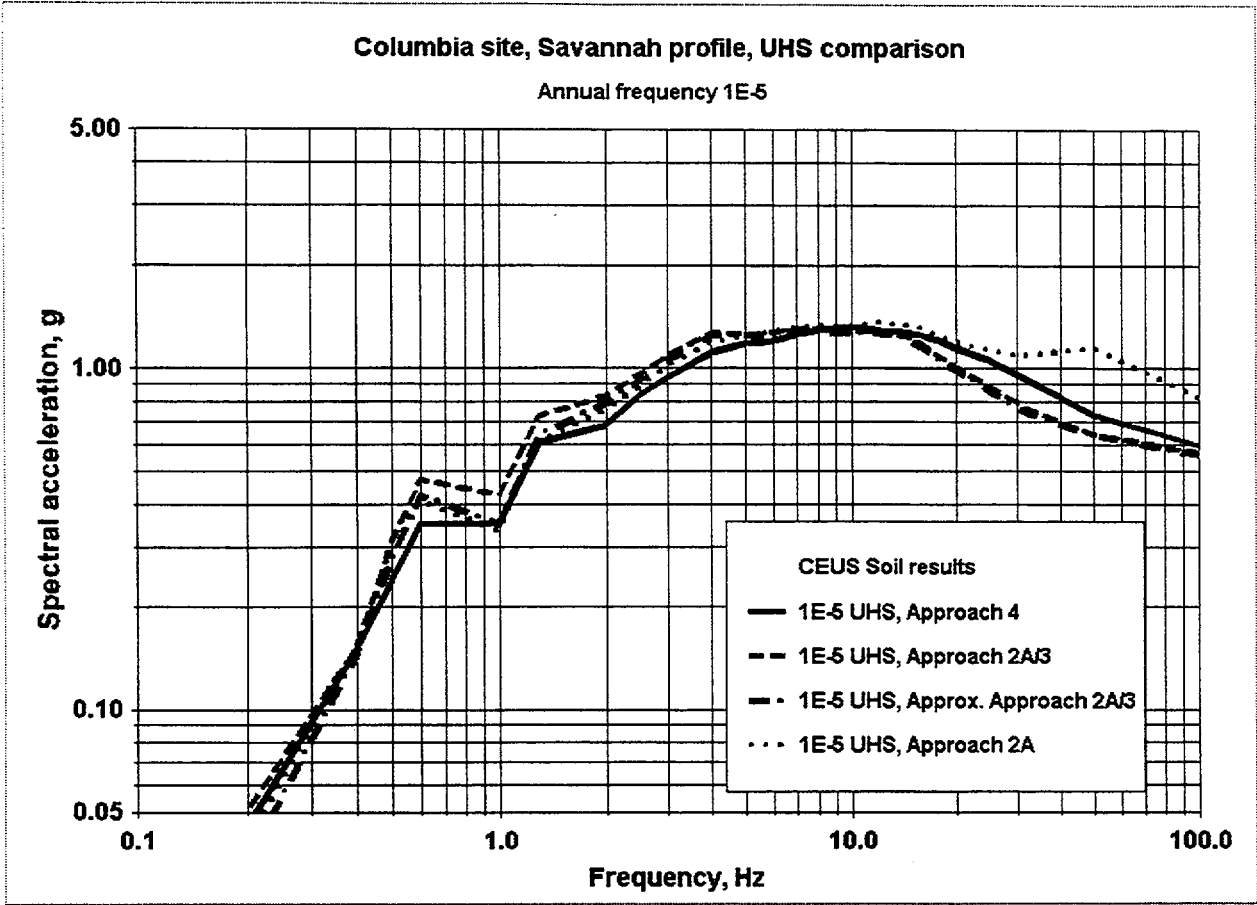
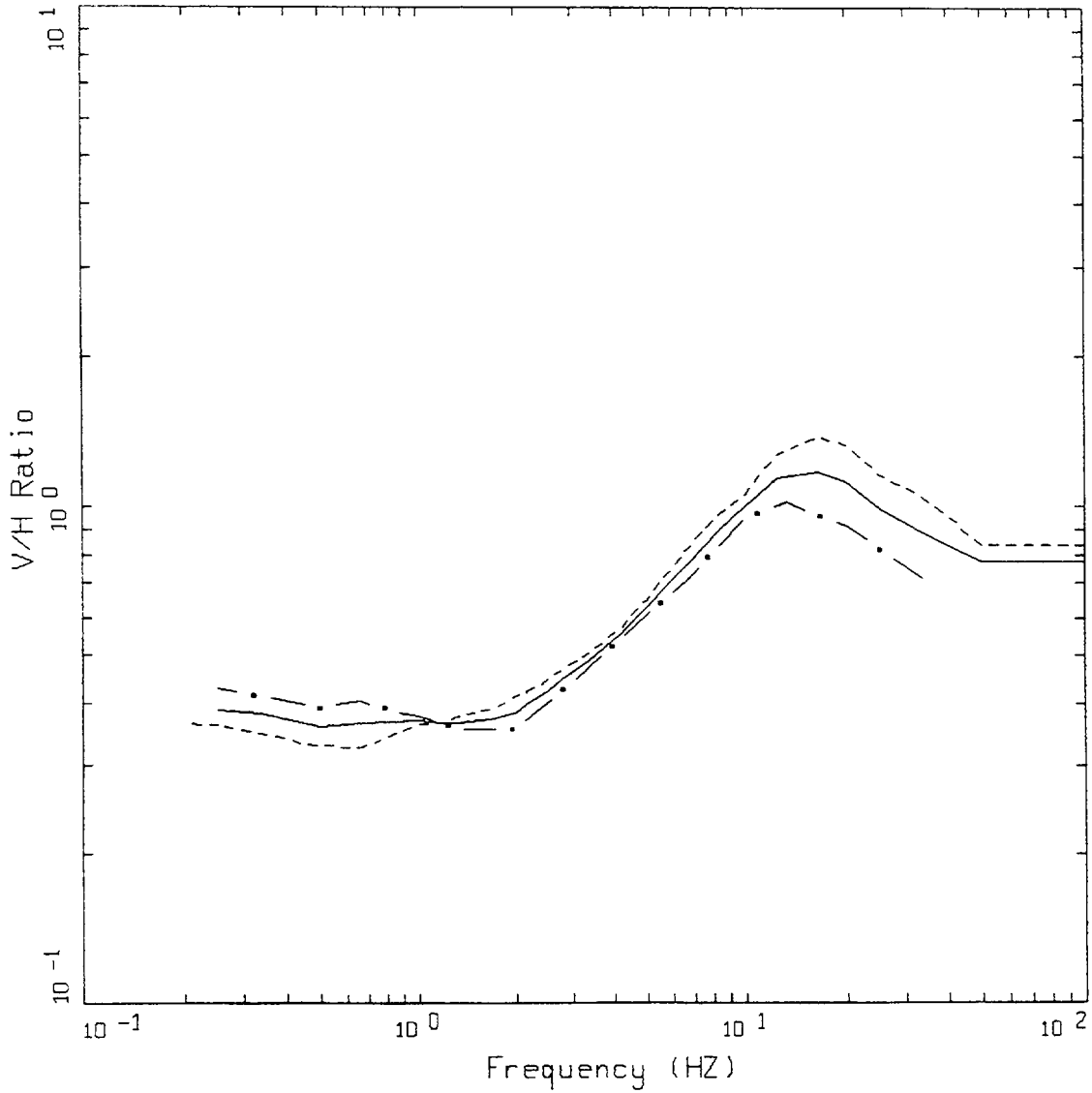


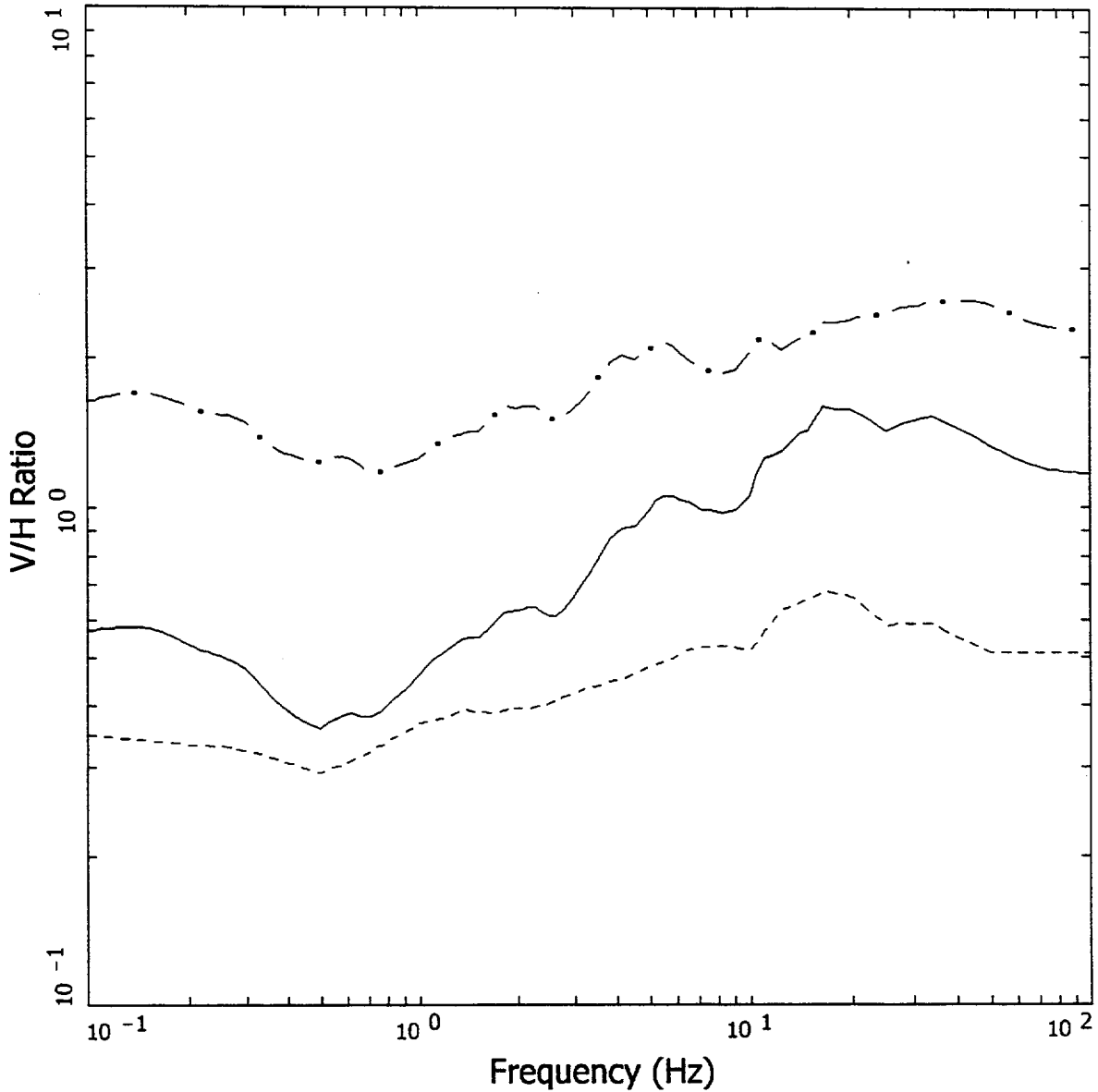
Figure 6-32. Columbia site 10^{-5} UHS for Savannah profile from Approach 4 (direct method) and Approaches 2A and 2A/3.



VERTICAL TO HORIZONTAL RATIO
 M = 6.6, D = 18 KM WUS SOIL

LEGEND
 ——— MEAN
 - - - - ABRAHAMSON AND SILVA (97)
 - . - . CAMPBELL (97)

Figure 6-33. Empirical WUS deep soil V/H ratios for 5% damped response spectra. Mean ratio is used to scale the horizontal soil design spectrum.



**VERTICAL TO HORIZONTAL RATIO
M = 7.2 , R = 110 KM CEUS SOIL**

- LEGEND
- CEUS SOIL V/H RATIO
 - - - ABRAHAMSON AND SILVA (97) WUS SOIL V/H RATIO
 - . - WUS TO CEUS SOIL V/H SCALE FACTOR

Figure 6-34. Elements used to develop CEUS deep soil V/H ratio. The solid line is used to scale the horizontal soil spectrum to produce the vertical soil spectrum.

7.0 UNIFORM RELIABILITY SPECTRUM ON SOIL

7.1 Mojave site

7.1.1 Derivation of uniform reliability spectrum (URS)

The URS for soil is derived in a manner similar to that used for rock conditions (Section 4), with several differences. The recommended steps are as follows:

1. Estimate the 10^{-4} and 10^{-5} UHS from Approximate Approach 2A/3 (equation (6-7b)) as described in Section 6.2.
2. Calculate factor A_R from the estimated 10^{-4} and 10^{-5} UHS, apply equations (4-1) and (4-2), and calculate the URS from the UHS estimated from Approximate Approach 2A/3.

These steps were applied to the Mojave site, and Table 7-1 documents the scale factor and URS. For this site, with its high seismic hazard, the soil response is well into the non-linear range at 10^{-4} annual frequency of exceedence levels, so the soil hazard curves are falling off very quickly (with a high negative slope). Hence the calculated scale factor is at its minimum value of 0.7 for all frequencies. Figure 7-1 shows the soil UHS and URS, the latter obtained by multiplying the UHS at each frequency by the scale factors in Table 7-1. For comparison purposes, Table 7-2 shows the URS calculated from Approach 4, and Figure 7-1 includes the URS from Approach 4. There is good agreement between the URS calculated by the two methods.

7.1.2 Scaled spectra on soil

Calculating scaled spectra for soil conditions requires calculating soil response for individual earthquakes and scaling those soil spectra to the soil URS. The dominant M and R values for the rock seismic hazard analysis are used to calculate the soil response, as there is no direct evaluation of the soil hazard and the contribution by M and R for soil conditions.

As documented in Section 3.1 and 4.1, deaggregation of the rock seismic hazard indicates that the following mean magnitudes and associated distances dominate for 10 and 1 Hz and for 10^{-4} annual frequency of exceedence:

$$\begin{aligned} 10 \text{ Hz:} & \quad M = 6.1, R = 14 \text{ km,} \\ 1 \text{ Hz:} & \quad M = 6.6, R = 18 \text{ km.} \end{aligned}$$

These M and R values are used to generate soil spectral shapes that are then scaled to the URS at 10 and 1 Hz, respectively.

For comparison purposes, Figure 7-2 shows the estimated UHS on soil (from Approach 2A) and two spectra obtained by multiplying the rock UHS at $1E-4$ annual frequency by soil amplification factors derived from 10 and 1 Hz design earthquakes. This illustrates that the simple scaling of rock UHS to estimate soil UHS is inaccurate.

Figure 7-3 shows the recommended scaling of soil spectra to the URS. The individual soil spectra estimated for the 10 and 1 Hz dominant earthquakes (with magnitudes and distances given above) are scaled to the 10 and 1 Hz URS amplitudes. This ensures that the site-specific soil characteristics are maintained in the final spectra. Figure 7-3 shows the 10^{-4} URS for the Meloland profile at the Mojave site, with the two scaled spectra representing the dominant earthquakes. In a design application the scaled spectra and the URS would be smoothed to remove calculated site resonances and frequency-to-frequency variations that result from attenuation coefficient variations. This has not been done here in order not to arbitrarily change the comparison between design spectra and scaled spectra. These individual spectra can be used to generate artificial time histories of motion, if desired, or a broad-band motion can be fit to the overall soil URS. These motions would be used as input to the analysis of structures and equipment founded on soil.

A vertical design spectrum is compared to the horizontal URS in Figure 7-4. The vertical spectrum is scaled from the horizontal spectrum as discussed in Section 6.

7.2 Columbia site

7.2.1 Derivation of URS

The URS for the Columbia site is derived in a manner similar to that for the Mojave site, using the two steps described in Section 7.1.1. Table 7-3 documents the scale factors and URS. The high frequency amplitudes show nonlinearity of soil response, with steep hazard curves. As a result the URS is below the UHS for high frequencies ($f \geq 10$ Hz) by the factor 0.7. At lower frequencies ($f < 10$ Hz) soil amplitudes are slightly more shallow, so the URS is below the UHS by factors that range from 0.71 to 0.87. For comparison purposes, Table 7-4 shows the URS calculated from Approach 4.

Figure 7-5 compares the $1E-4$ UHS and the URS calculated by approximate Approach 2A/3 and by Approach 4. The two URS spectra are very close, which confirms the use of Approximate Approach 2A/3 to derive the URS.

7.2.2 Scaled spectra on soil

At Columbia the scaled spectra are calculated similarly to these for the Mojave site, i.e. using mean magnitudes and associated distances from rock results. These were presented in Section 4 and are as follows (for 10^{-4} annual frequency of exceedence):

10 Hz	$M = 6.0, R = 46$ km,
1 Hz	$M = 7.2, R = 110$ km.

In Approximate Approach 2A/3 these magnitudes and distances were used to select rock records and compute soil response. The average soil spectra were computed for 10 Hz and 1 Hz, and are scaled to the URS at 10 Hz and 1 Hz, respectively.

For comparison purposes, Figure 7-6 shows the $1E-4$ UHS from Approach 2A compared to the spectra from deriving the soil with 10 Hz and 1 Hz motions scaled to the rock $1E-4$ UHS. This again indicates (as Figure 7-2 does) that simple scaling of the rock UHS to estimate the soil UHS is inaccurate.

The appropriate scaled spectra are shown in Figure 7-7, which indicates the 10 and 1 Hz spectra scaled to the 10^{-4} URS. This is the URS derived from Approximate Approach 2A/3 as shown in Figure 7-5. In a design application the scaled spectra and the URS would be smoothed to remove calculated site resonances and frequency-to-frequency variations that result from attenuation coefficient variations. This has not been done here in order not to arbitrarily change the comparison between design spectra and scaled spectra. The individual spectra can be used to generate artificial time histories, or a broad-banded motion can be fit to the URS. These motions would then be used for the design and analysis of structures and equipment founded on soil.

Figure 7-8 compares the 10^{-4} horizontal URS for the Columbia site to a vertical design spectrum obtained by scaling the horizontal spectrum. This scaling was discussed in Section 6.

Table 7-1
Scale factor for soil URS
Mojave site, Approximate Approach 2A/3

<u>Frequency, Hz</u>	<u>Approx. 10⁻⁴ UHS</u>	<u>Approx. 10⁻⁵ UHS</u>	<u>A_R</u>	<u>K_H</u>	<u>Scale Factor</u>	<u>10⁻⁴ URS</u>
100	7.40E-1	1.05	1.42	6.51	7.0E-1	5.18E-1
50	7.43E-1	1.05	1.42	6.58	7.0E-1	5.20E-1
40	7.63E-1	1.07	1.40	6.81	7.0E-1	5.34E-1
31	8.32E-1	1.17	1.41	6.73	7.0E-1	5.82E-1
25	8.41E-1	1.17	1.39	6.94	7.0E-1	5.89E-1
20	8.49E-1	1.16	1.36	7.43	7.0E-1	5.94E-1
18	8.56E-1	1.16	1.36	7.52	7.0E-1	5.99E-1
16	8.76E-1	1.18	1.34	7.80	7.0E-1	6.13E-1
14	9.15E-1	1.21	1.32	8.37	7.0E-1	6.41E-1
12	9.35E-1	1.21	1.29	8.97	7.0E-1	6.55E-1
10	1.05	1.29	1.23	11.07	7.0E-1	7.35E-1
8	1.26	1.48	1.18	13.82	7.0E-1	8.80E-1
7	1.34	1.59	1.19	13.02	7.0E-1	9.35E-1
6	1.33	1.56	1.17	14.74	7.0E-1	9.33E-1
5	1.57	1.88	1.19	12.96	7.0E-1	1.10
4	1.60	2.00	1.25	10.22	7.0E-1	1.12
3	1.65	2.27	1.37	7.24	7.0E-1	1.15
2.5	1.71	2.45	1.43	6.42	7.0E-1	1.20
2	1.71	2.57	1.50	5.67	7.0E-1	1.20
1.3	1.40	2.34	1.67	4.48	7.0E-1	9.78E-1
1	1.24	2.11	1.71	4.31	7.0E-1	8.66E-1
.6	9.84E-1	1.72	1.75	4.12	7.0E-1	6.89E-1
.5	1.01	1.66	1.64	4.67	7.0E-1	7.09E-1
.4	9.50E-1	1.62	1.70	4.32	7.0E-1	6.65E-1
.2	2.72E-1	4.83E-1	1.77	4.02	7.0E-1	1.91E-1

Table 7-2
Scale factor for soil URS
Mojave site, Approach 4

<u>Frequency, Hz</u>	<u>10⁻⁴ UHS</u>	<u>10⁻⁵ UHS</u>	<u>A_R</u>	<u>K_H</u>	<u>Scale Factor</u>	<u>10⁻⁴ URS</u>
100	7.18E-1	1.17	1.63	4.71	7.0E-1	5.03E-1
50	7.23E-1	1.18	1.63	4.71	7.0E-1	5.06E-1
40	7.29E-1	1.19	1.63	4.72	7.0E-1	5.10E-1
31	7.40E-1	1.21	1.63	4.73	7.0E-1	5.18E-1
25	7.47E-1	1.20	1.60	4.87	7.0E-1	5.23E-1
20	7.72E-1	1.22	1.58	5.04	7.0E-1	5.40E-1
18	7.97E-1	1.25	1.58	5.06	7.0E-1	5.58E-1
16	8.19E-1	1.27	1.55	5.24	7.0E-1	5.73E-1
14	8.55E-1	1.31	1.53	5.41	7.0E-1	5.98E-1
12	9.23E-1	1.41	1.53	5.43	7.0E-1	6.46E-1
10	9.98E-1	1.51	1.52	5.52	7.0E-1	6.98E-1
8	1.08	1.66	1.54	5.35	7.0E-1	7.58E-1
7	1.16	1.78	1.54	5.37	7.0E-1	8.10E-1
6	1.23	1.90	1.54	5.33	7.0E-1	8.64E-1
5	1.34	2.06	1.54	5.31	7.0E-1	9.35E-1
4	1.45	2.30	1.59	4.99	7.0E-1	1.01
3	1.55	2.49	1.61	4.85	7.0E-1	1.08
2.5	1.53	2.47	1.61	4.81	7.0E-1	1.07
2	1.49	2.43	1.63	4.69	7.0E-1	1.04
1.3	1.35	2.32	1.72	4.25	7.0E-1	9.44E-1
1	1.35	2.28	1.69	4.40	7.0E-1	9.47E-1
.6	9.74E-1	1.65	1.69	4.36	7.0E-1	6.81E-1
.5	9.49E-1	1.65	1.74	4.17	7.0E-1	6.64E-1
.4	8.80E-1	1.59	1.81	3.88	7.13E-1	6.27E-1
.2	3.23E-1	5.14E-1	1.59	4.96	7.0E-1	2.26E-1

Table 7-3
Scale factors for soil URS
Columbia site, Approximate Approach 2A/3

<u>Frequency, Hz</u>	<u>Approx. 10⁻⁴ UHS</u>	<u>Approx. 10⁻⁵ UHS</u>	<u>A_R</u>	<u>K_H</u>	<u>Scale Factor</u>	<u>10⁻⁴ URS</u>
100	3.18E-1	5.56E-1	1.75	4.12	7.00E-1	2.23E-1
50	3.95E-1	6.37E-1	1.61	4.84	7.00E-1	2.77E-1
40	4.41E-1	6.84E-1	1.55	5.24	7.00E-1	3.09E-1
31	4.95E-1	7.56E-1	1.53	5.43	7.00E-1	3.47E-1
25	5.60E-1	8.59E-1	1.53	5.37	7.00E-1	3.92E-1
20	6.20E-1	9.88E-1	1.59	4.95	7.00E-1	4.34E-1
18	6.59E-1	1.06	1.60	4.88	7.00E-1	4.62E-1
16	7.10E-1	1.15	1.62	4.77	7.00E-1	4.97E-1
14	7.27E-1	1.23	1.69	4.40	7.00E-1	5.09E-1
12	7.38E-1	1.26	1.71	4.27	7.00E-1	5.16E-1
10	7.16E-1	1.26	1.75	4.10	7.00E-1	5.01E-1
8	7.08E-1	1.28	1.81	3.89	7.13E-1	5.04E-1
7	6.95E-1	1.28	1.84	3.79	7.26E-1	5.05E-1
6	6.64E-1	1.24	1.87	3.66	7.44E-1	4.94E-1
5	6.33E-1	1.23	1.95	3.45	7.79E-1	4.93E-1
4	6.19E-1	1.24	2.00	3.33	8.02E-1	4.97E-1
3	5.12E-1	1.06	2.06	3.18	8.35E-1	4.27E-1
2.5	4.64E-1	9.20E-1	1.98	3.36	7.96E-1	3.69E-1
2	3.75E-1	7.87E-1	2.10	3.11	8.51E-1	3.19E-1
1.3	3.24E-1	6.37E-1	1.97	3.40	7.88E-1	2.55E-1
1	1.74E-1	3.48E-1	2.00	3.32	8.05E-1	1.40E-1
.6	2.17E-1	4.24E-1	1.96	3.43	7.83E-1	1.70E-1
.5	1.32E-1	2.77E-1	2.11	3.09	8.56E-1	1.13E-1
.4	6.73E-2	1.43E-1	2.13	3.04	8.68E-1	5.84E-2
.2	1.81E-2	3.56E-2	1.97	3.39	7.90E-1	1.43E-2

Table 7-4
Scale factors for soil URS
Columbia site, Approach 4

<u>Frequency, Hz</u>	<u>10⁻⁴ UHS</u>	<u>10⁻⁵ UHS</u>	<u>A_R</u>	<u>K_H</u>	<u>Scale Factor</u>	<u>10⁻⁴ URS</u>
100	2.94E-1	5.93E-1	2.02	3.28	8.12E-1	2.39E-1
50	3.70E-1	7.30E-1	1.97	3.39	7.91E-1	2.93E-1
40	4.22E-1	8.26E-1	1.96	3.43	7.84E-1	3.31E-1
31	4.83E-1	9.48E-1	1.96	3.42	7.86E-1	3.80E-1
25	5.39E-1	1.06	1.96	3.42	7.85E-1	4.23E-1
20	5.81E-1	1.15	1.97	3.38	7.92E-1	4.60E-1
18	6.06E-1	1.20	1.98	3.37	7.95E-1	4.82E-1
16	6.26E-1	1.24	1.98	3.37	7.95E-1	4.98E-1
14	6.36E-1	1.27	2.00	3.31	8.06E-1	5.13E-1
12	6.47E-1	1.29	2.00	3.33	8.03E-1	5.20E-1
10	6.54E-1	1.32	2.02	3.28	8.14E-1	5.32E-1
8	6.28E-1	1.28	2.04	3.23	8.24E-1	5.17E-1
7	6.17E-1	1.26	2.03	3.24	8.21E-1	5.07E-1
6	5.89E-1	1.20	2.03	3.25	8.19E-1	4.82E-1
5	5.75E-1	1.17	2.04	3.23	8.23E-1	4.73E-1
4	5.33E-1	1.10	2.07	3.16	8.39E-1	4.47E-1
3	4.52E-1	9.37E-1	2.07	3.16	8.40E-1	3.80E-1
2.5	4.22E-1	8.31E-1	1.97	3.40	7.88E-1	3.33E-1
2	3.34E-1	6.80E-1	2.03	3.24	8.20E-1	2.74E-1
1.3	3.06E-1	6.04E-1	1.97	3.39	7.90E-1	2.42E-1
1	1.79E-1	3.47E-1	1.94	3.47	7.76E-1	1.39E-2
.6	1.85E-1	3.51E-1	1.90	3.59	7.56E-1	1.40E-1
.5	1.19E-1	2.38E-1	2.00	3.32	8.04E-1	9.57E-2
.4	7.47E-2	1.49E-1	1.99	3.35	7.99E-1	5.97E-2
.2	2.18E-2	4.56E-2	2.09	3.12	8.49E-1	1.85E-2

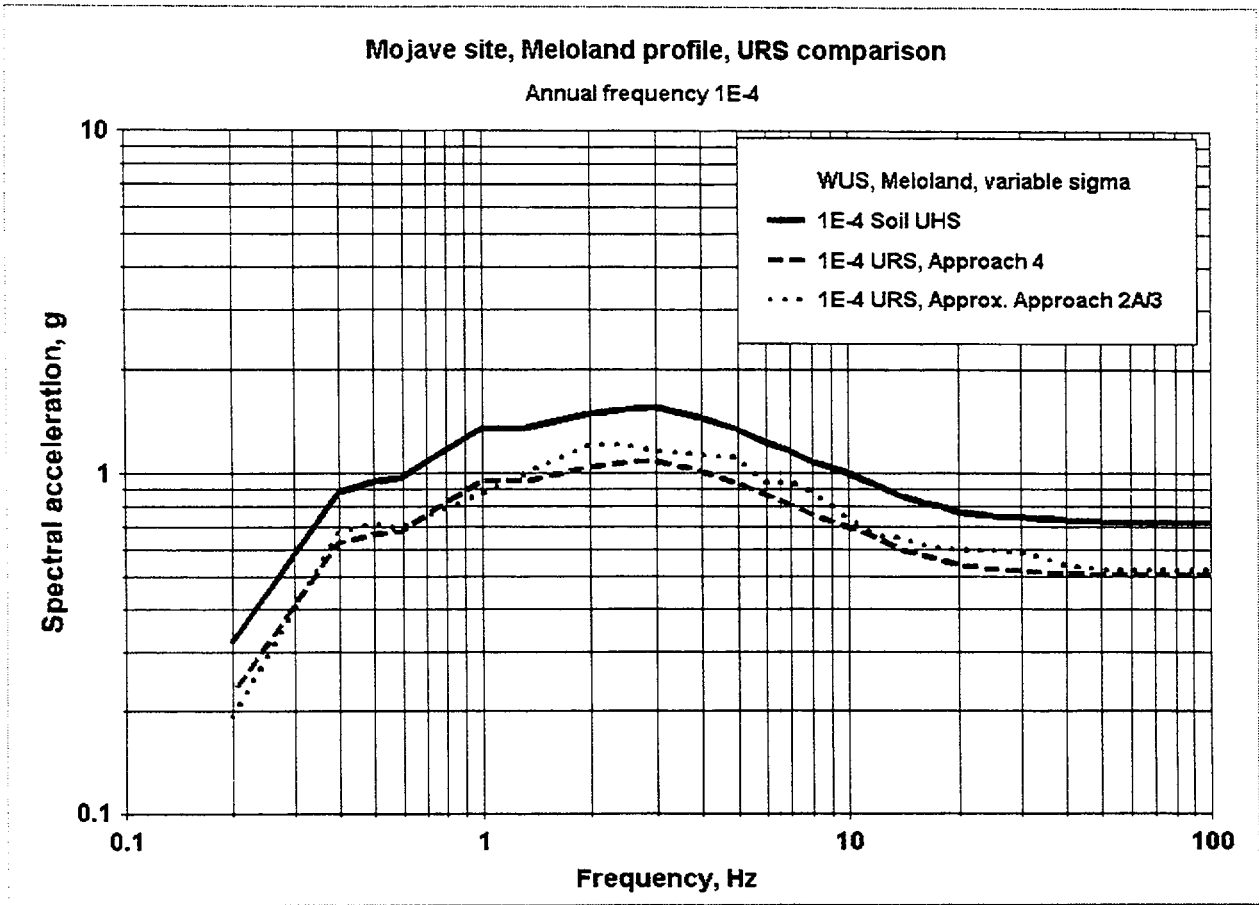
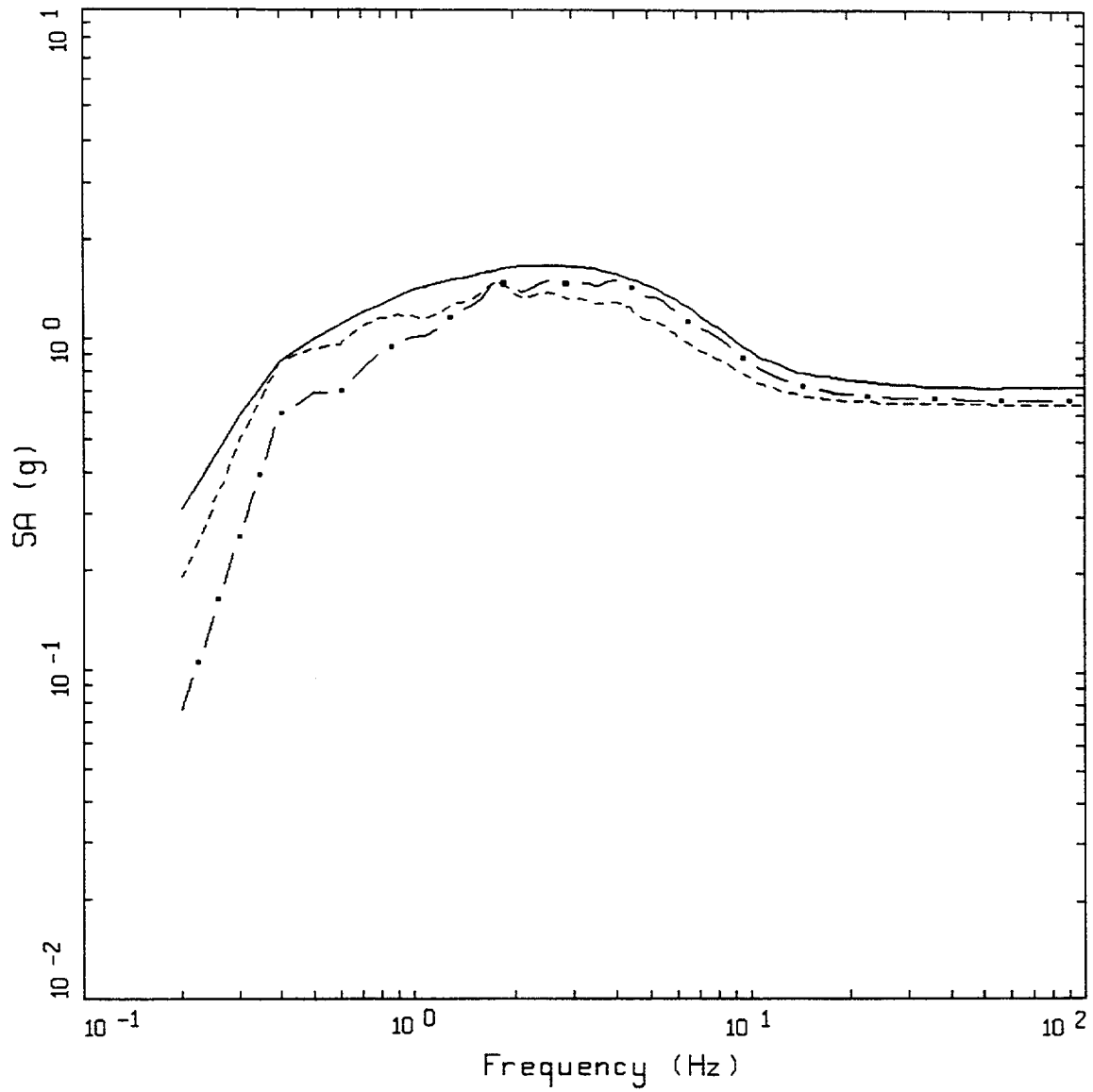


Figure 7-1. Mojave site, 10^{-4} soil URS from Approach 4 and Approximate Approach 2A/3, and 10^{-4} UHS from Approach 4.



WUS SOIL
MELOLAND

- LEGEND
- HAZARD CONSISTENT SOIL DESIGN SPECTRUM
 - - - MEAN 1 HZ SOIL DESIGN SPECTRUM
 - . - MEAN 10 HZ SOIL DESIGN SPECTRUM

Figure 7-2. Hazard consistent soil spectrum along with 1 Hz and 10 Hz soil spectra, horizontal motions, Mojave site.

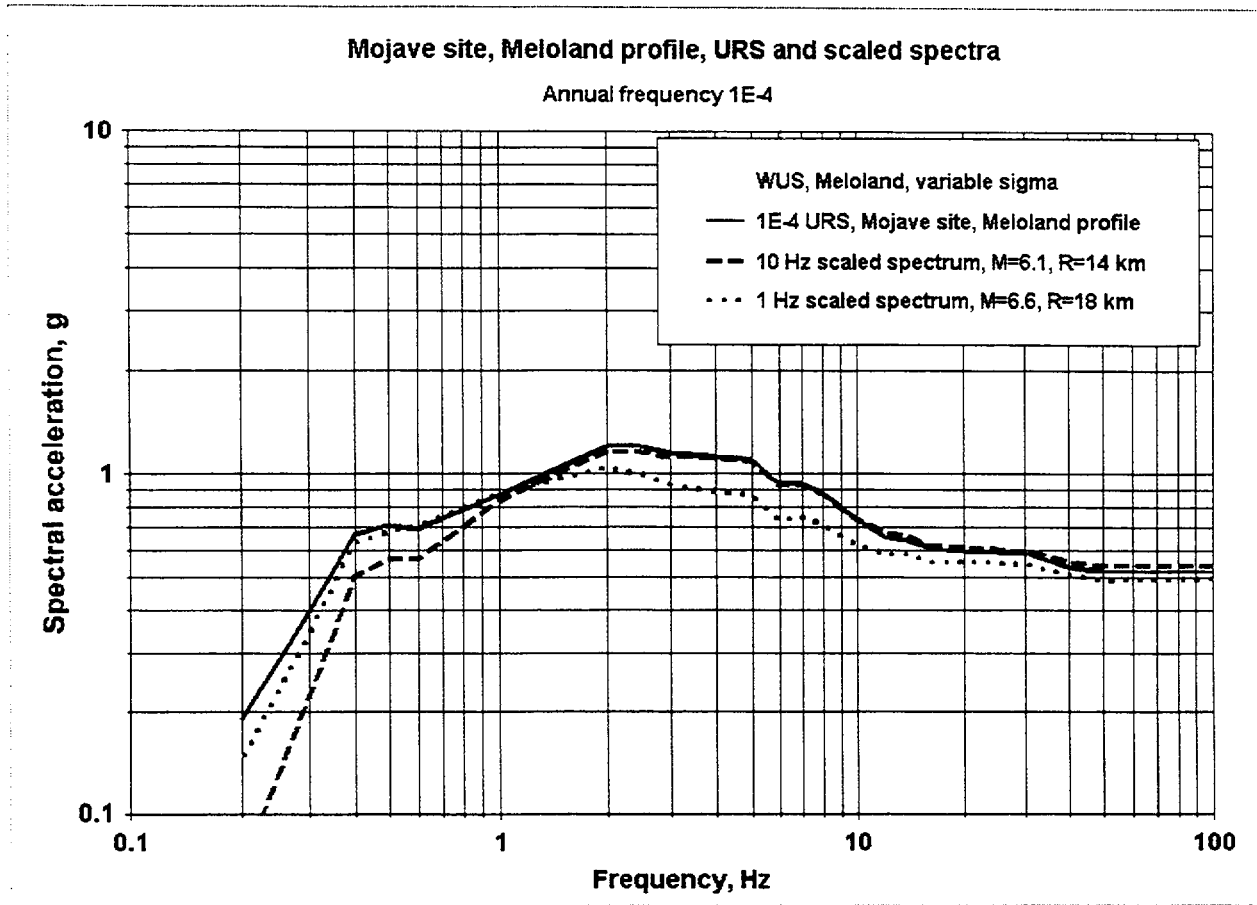


Figure 7-3. Mojave site 10^{-4} soil URS (Approximate Approach 2A/3) and 10 Hz and 1 Hz scaled spectra.

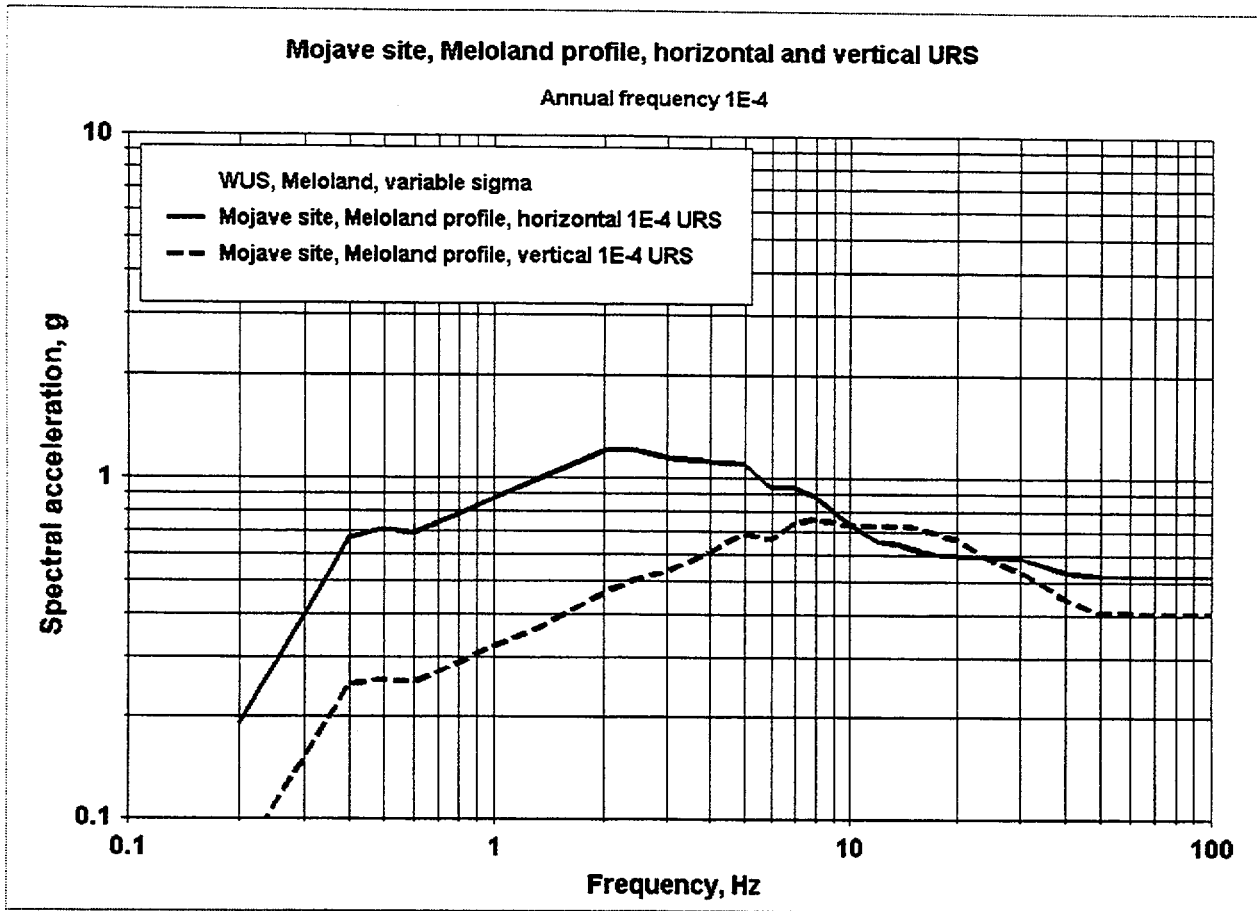


Figure 7-4. Horizontal and vertical URS for the Mojave site, Meloland profile.

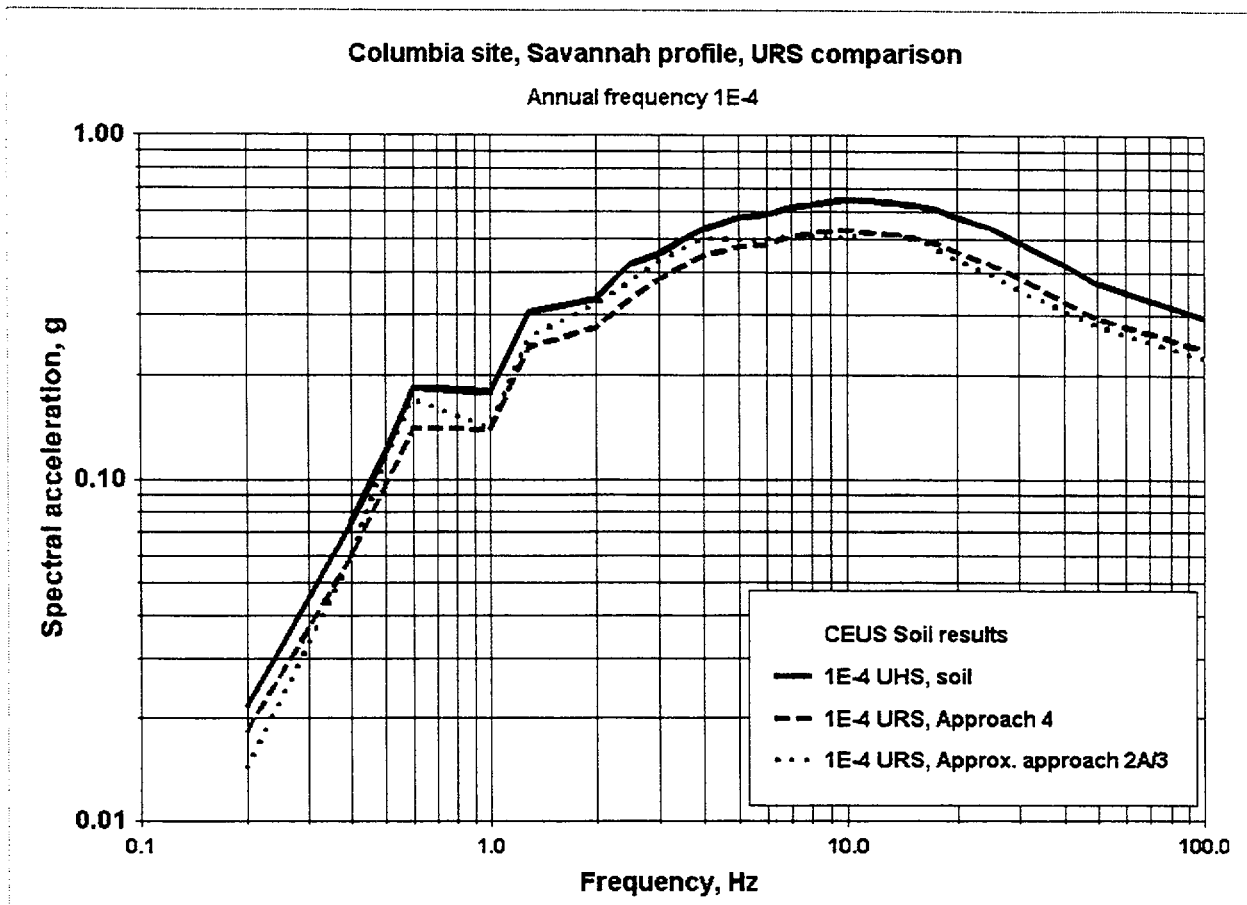
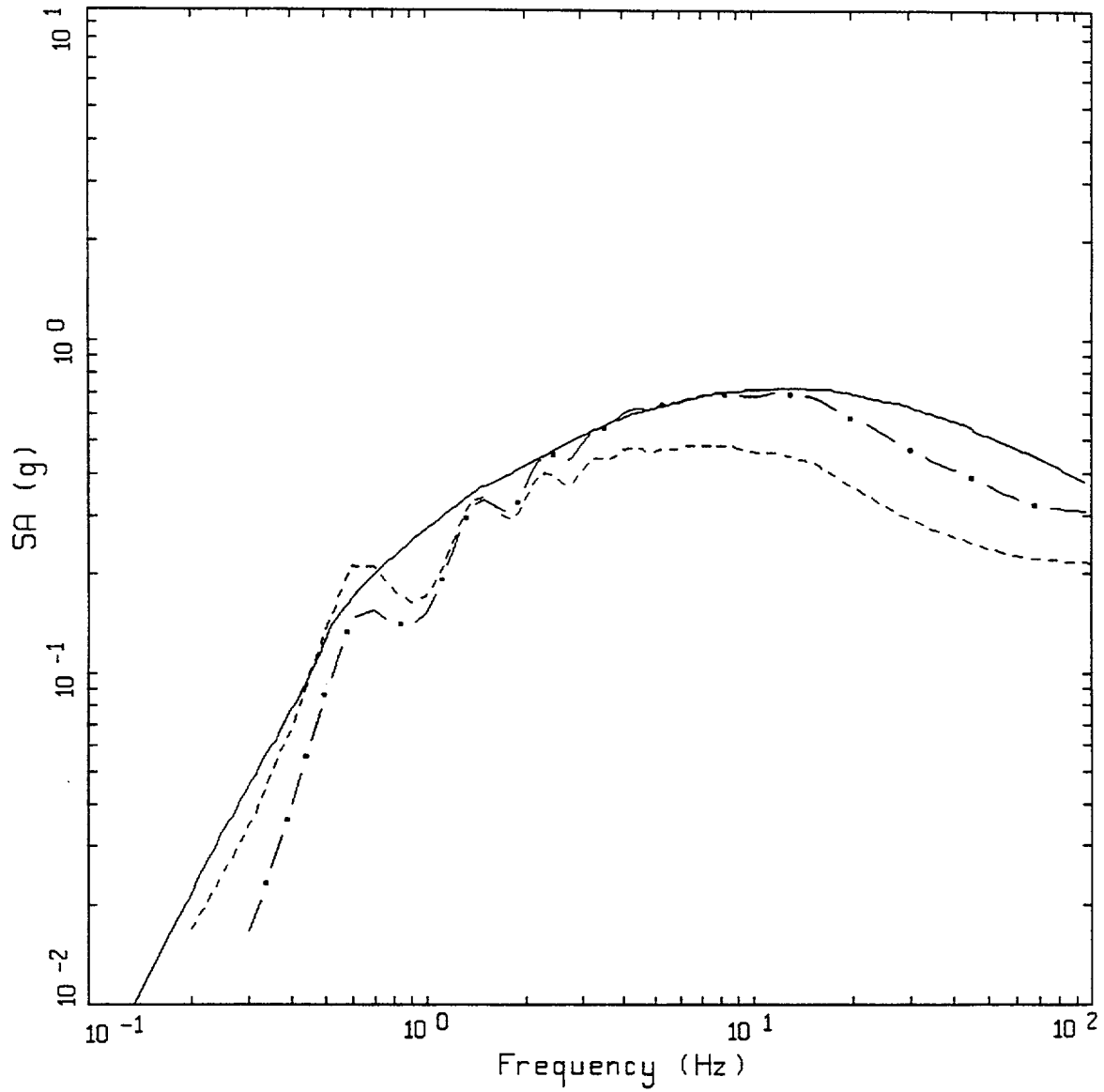


Figure 7-5. Columbia site, 10^{-4} soil URS from Approaches 4 and Approximate Approach 2A/3, and 10^{-4} UHS from Approach 4.



CEUS SOIL
SAVANNAH RIVER GENERIC

- LEGEND
- HAZARD CONSISTENT SOIL DESIGN SPECTRUM
 - - - MEAN 1 HZ SOIL DESIGN SPECTRUM
 - · - MEAN 10 HZ SOIL DESIGN SPECTRUM

Figure 7-6. Hazard consistent soil spectrum along with 1 Hz and 10 Hz soil spectra, horizontal motions, Columbia site.

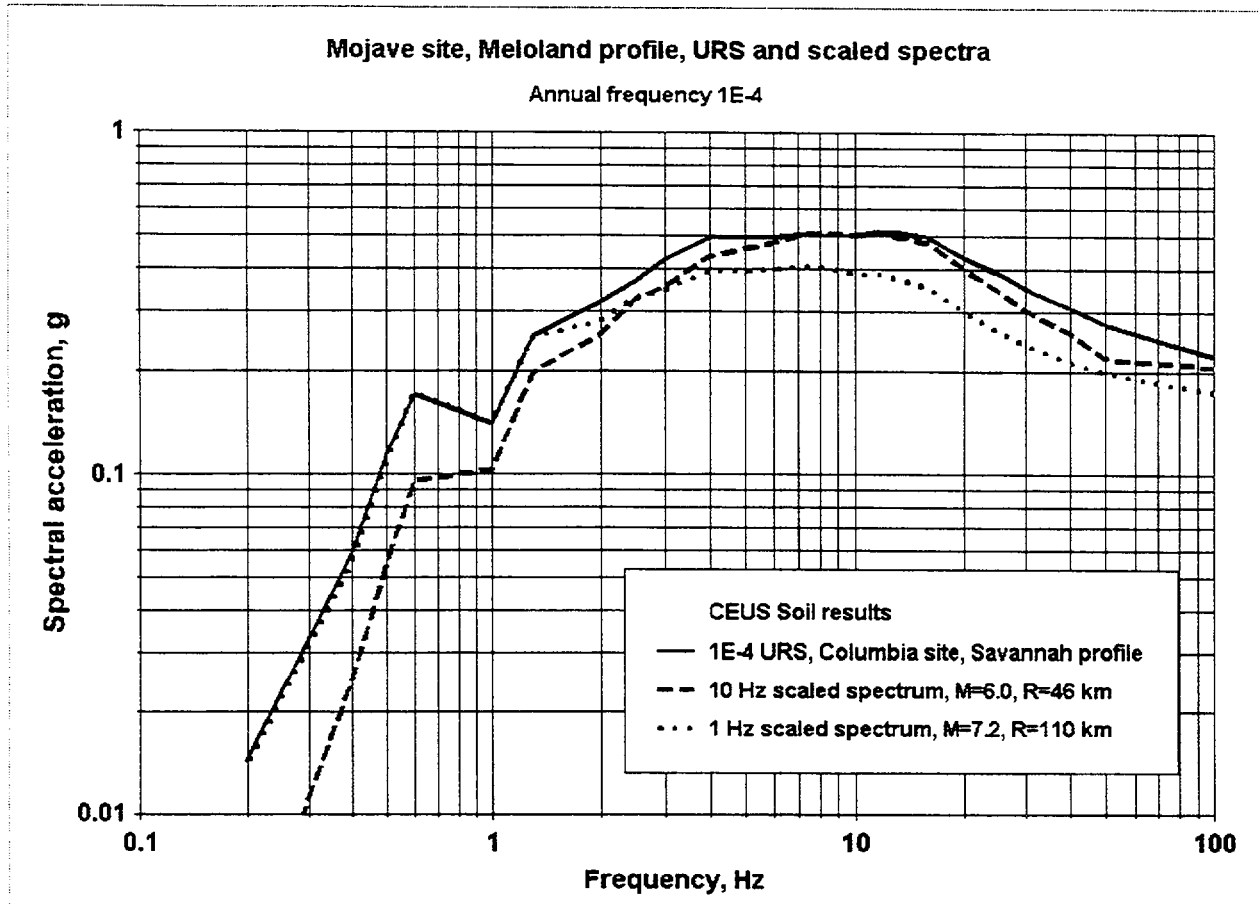


Figure 7-7. Columbia site 10^{-4} soil URS (Approximate Approach 2A/3) and 10 Hz and 1 Hz scaled spectra.

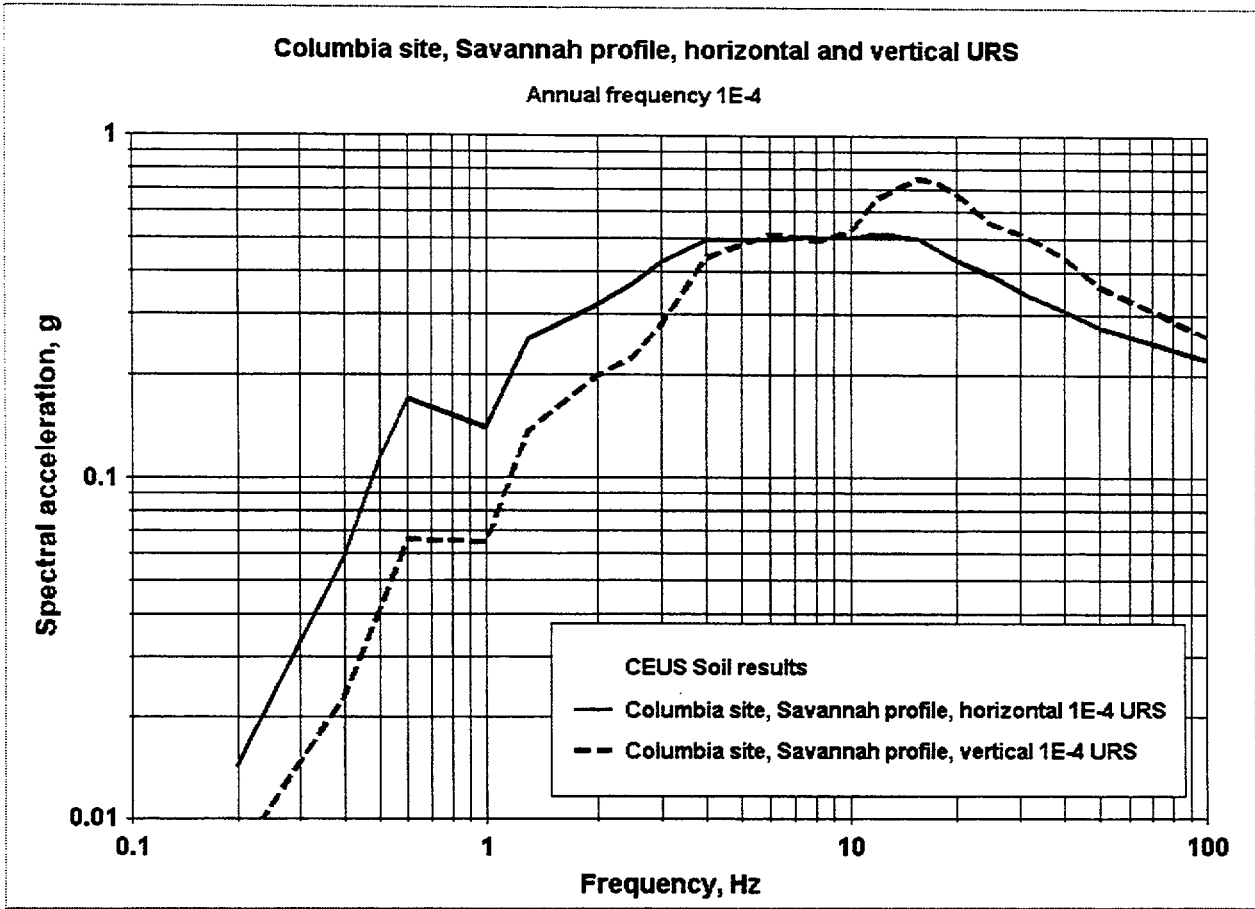


Figure 7-8. Horizontal and vertical URS for the Columbia site, Savannah profile.

8.0 GENERATING ARTIFICIAL MOTIONS FOR SOIL SITES

In this section we describe soil time histories that are generated for the Mojave and Columbia sites using a simple spectral matching procedure (Section 5.1). The guideline on number of spectral frequencies (100 per decade) recommended in McGuire et al., (2001) was followed. However, the corresponding matching criteria, which consist of a target exceedence maximum of 1.3 and minimum of 0.9 with not more than 20 points below the target (0.2 to 25.0 Hz and peak acceleration), was found to result in matched spectra that were biased high with respect to the target. To achieve spectral matches more representative of desired risk levels implied by the uniform reliability spectra (Section 7), an alternative criterion was developed. A band is defined between 95% and 110% of the target spectrum, and virtually all points must fall within the band (up to 5 or 10 points may fall outside the band, but not at adjacent frequencies). This criterion results in a mean-based fit (Chi-square near 1.0) with about 60 to 80 points being below the target (but only slightly), and more than 200 points above the target. The fit is easily obtainable, represents the desired spectral level, and does not permit significant notches or holes to develop in the Fourier amplitude spectrum, as the plots of power spectral density show.

For the WUS Mojave and CEUS Columbia sites, the deaggregation magnitudes (rock outcrop UHS) and distances are listed in Tables 8-1 and 8-2 along with the duration guideline (Table 5-2). The time histories selected from the WUS soil time histories bins for inputs to the spectral matching are listed in Table 8-1 along with their associated durations, both prior, as well as subsequent, to the matching process. For the CEUS Columbia site, WUS records scaled to CEUS conditions (see Section 3 of McGuire et al., 2001) were selected with corresponding parameters listed in Table 8-2. The resulting target spectra, spectral matches, power spectral densities, and time histories are shown in Figure 8-1 through 8-12 for the horizontal (H1 and H2) and vertical (V) components of the WUS motions and in Figures 8-13 through 8-24 for the CEUS motions. The horizontal component target spectra are the URS while the vertical target spectra were developed by applying generic deep soil V/H ratios to the hazard consistent soil spectra (Section 7).

The accompanying smoothed power spectral density (PSD) plots ($\pm 20\%$) were computed using the 5 to 75% Arias intensity durations (Tables 8-1 and 8-2) and show no rapid oscillations or deep minima. The resulting time histories appear realistic in acceleration, velocity, and displacement.

Peak particle ratios (PGV/PGA and $PGA \cdot PGD/PGV^2$) computed from the matched time histories are listed in Tables 8-1 (WUS) and 8-2 (CEUS) along with statistical shape bin median values (Table 5-2). For the WUS soil motions, the time histories show large PGV/PGA ratios compared to bin medians (~ 180 cm/sec/g compared to 79 cm/sec/g). These large values are consistent with recorded motions from the $M 6.5$ 1979 Imperial Valley earthquake at sites located near the fault rupture ($PGA \geq 0.3g$). The average horizontal PGV/PGA value for the Meloland site is about 260 cm/sec/g, which is elevated due to the effects of rupture directivity being located near (≤ 5 km) the fault trace and with rupture toward the site. With the 1 Hz controlling earthquake at 18 km, extreme directivity enhancements at low frequency (≤ 1 Hz) would not be expected but site location relative to the mapped faults should be investigated for cases with M greater than about 6.5 and deaggregation distances within about 20 km. These conditions are considered to apply to spectral levels for

frequencies as low as 0.5 Hz as lower frequency considerations are only to assure reasonable PGV/PGA and $PGA \cdot PGD / PGV^2$ values for the matched time histories.

The $PGA \cdot PGD / PGV^2$ ratios are 2.6 (Table 8-1), close to the bin medians of 3.1. The cross correlations (Table 8-2) are low (less than 0.1) among all three components.

For the CEUS, the 1 Hz deaggregation magnitude and distance are 7.2 and 130 km respectively (Table 8-2). The bin median PGV/PGA and $PGA \cdot PGD / PGV^2$ ratios are about 225 cm/sec/g and 3 respectively. The spectral match values are near 50 cm/sec/g for PGV/PGA ratios and around 7 for the $PGA \cdot PGD / PGV^2$ ratios. These are driven by the low PGV values (Figures 8-16 and 8-20), which are caused by the influence of the double corner source model in the hazard analyses. The difference in the low frequency (≤ 1 Hz) rock motion between the single- and double-corner source models is very large (Figures 2-17a and 2-17b).

As with the WUS site, the cross correlations (Table 8-2) are low for the CEUS, with a maximum of 0.04.

REFERENCES

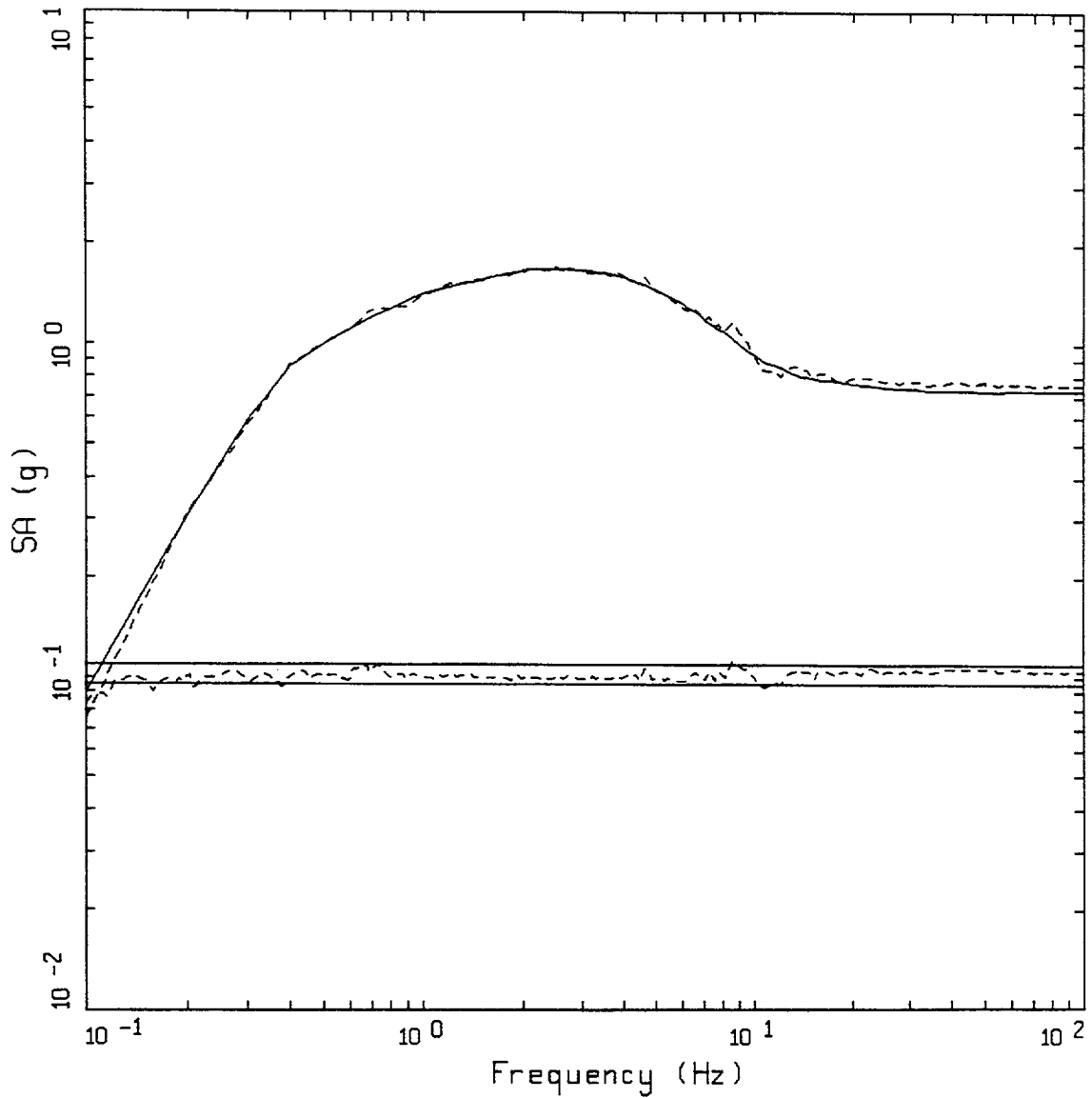
McGuire, R.K., W.J. Silva, C.J. Costantino (October 2001). "Technical Basis for Revision of Regulatory Guidance on Design Ground Motions: Hazard- and Risk-Consistent Ground Motion Spectra Guidelines." U.S. Nuclear Reg. Comm., Rept NUREG/CR-6728, October.

Table 8-1
WUS Soil Motion Durations

Rock UHS (10 ⁻⁴)	Magnitude	Distance (km)	Durations (5 to 75%) (sec)		
			Input	Match	Target
1 Hz	6.7	18	000(H1) 6.20	13.99	3.6 - 8.2
			090(H2) 8.01	14.82	3.6 - 8.2
			up 7.54	12.48	3.6 - 8.2
RECORDS SELECTED					
Target M	Earthquake	M	Site	Distance (km)	Site Condition
6.7	Loma Prieta	6.9	USGS, WAHO	18.1	Soil
PEAK PARTICLE RATIOS					
Component	PGV/PGA (cm/sec/g)	Bin Median PGV/PGA (cm/sec/g)	PGA•PGD/ PGV ²	Bin Median PGA•PGD/PGV ²	
H1	175.0	78.8	2.6	3.1	
H2	183.0	78.8	2.6	3.1	
V	113.0	----	4.0	----	
ABSOLUTE CROSS CORRELATIONS					
Component	Cross Correlation				
H1 H2	0.01				
H1 V	0.04				
H2 V	0.02				

Table 8-2
CEUS Soil Motion Durations

Rock UHS (10 ⁻⁴)	Magnitude	Distance (km)	Durations (5 to 75%) (sec)		
			Input	Match	Target
1 Hz	7.2	130	310(H1) 22.23	26.00	16.2 - 36.5
			220(H2) 24.33	28.48	16.2 - 36.5
			up 23.75	23.76	16.2 - 36.5
RECORDS SELECTED					
Target M	Earthquake	M	Site	Distance (km)	Site Condition
7.2	Landers	7.2	CDMG 90094 Jaboneria	153.9	Soil
PEAK PARTICLE RATIOS					
Component	PGV/PGA (cm/sec/g)	Bin Median PGV/PGA (cm/sec/g)	PGA•PGD/ PGV ²	Bin Median PGA•PGD/PGV ²	
H1	47.0	224.8	7.5	3.0	
H2	47.0	224.8	6.8	3.0	
V	22.7	----	13.9	----	
ABSOLUTE CROSS CORRELATIONS					
Component	Cross Correlation				
H1 H2	0.01				
H1 V	0.04				
H2 V	0.03				



WUS, MELOLAND
HORIZONTAL 1

- LEGEND**
- 5 %, SOIL TARGET; PGA = 0.730 G
 - 5 %, SPECTRAL MATCH; PGA = 0.761 g
 - 5 %, UPPER BOUND 1.10 (SCALED BY 0.1)
 - 5 %, RATIO: SPECTRAL MATCH TO SOIL TARGET (SCALED BY 0.1)
 - 5 %, LOWER BOUND 0.95 (SCALED BY 0.1)

Figure 8-1. Target spectrum, spectral match and spectral ratio, component H1, Mojave site, soil.

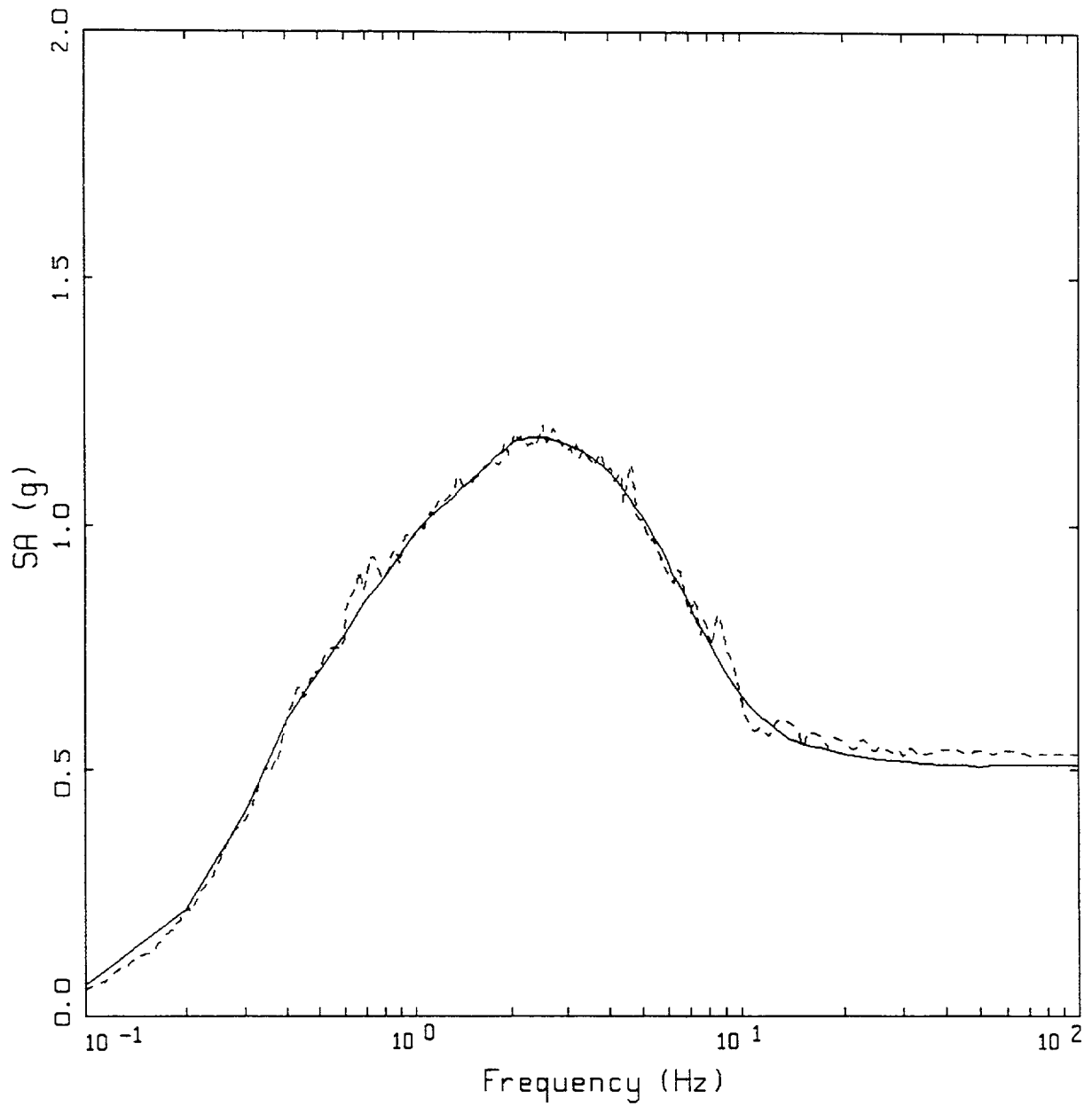
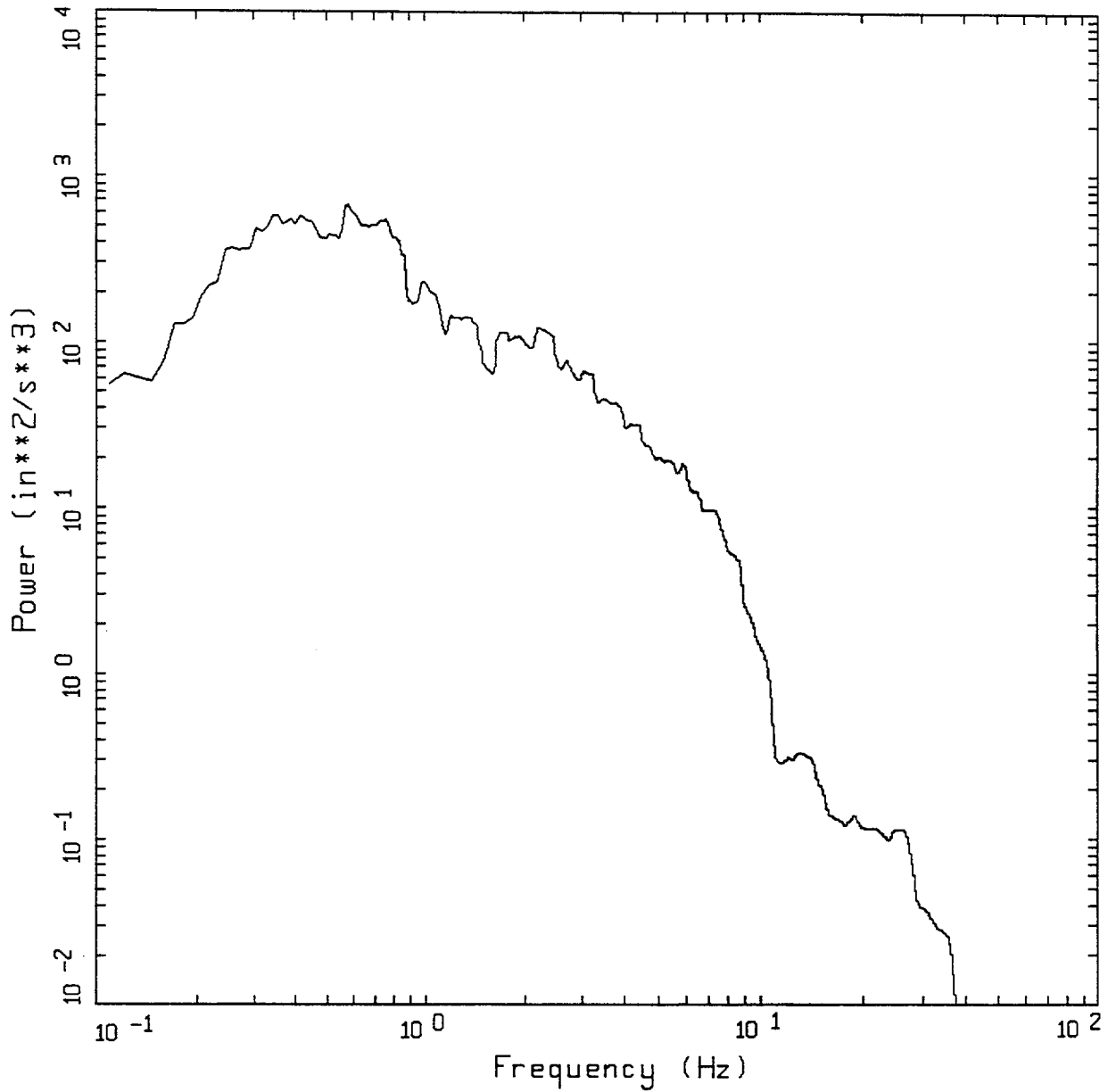


Figure 8-2. Target spectrum and spectral match on linear scale, component H1, Mojave site, soil.

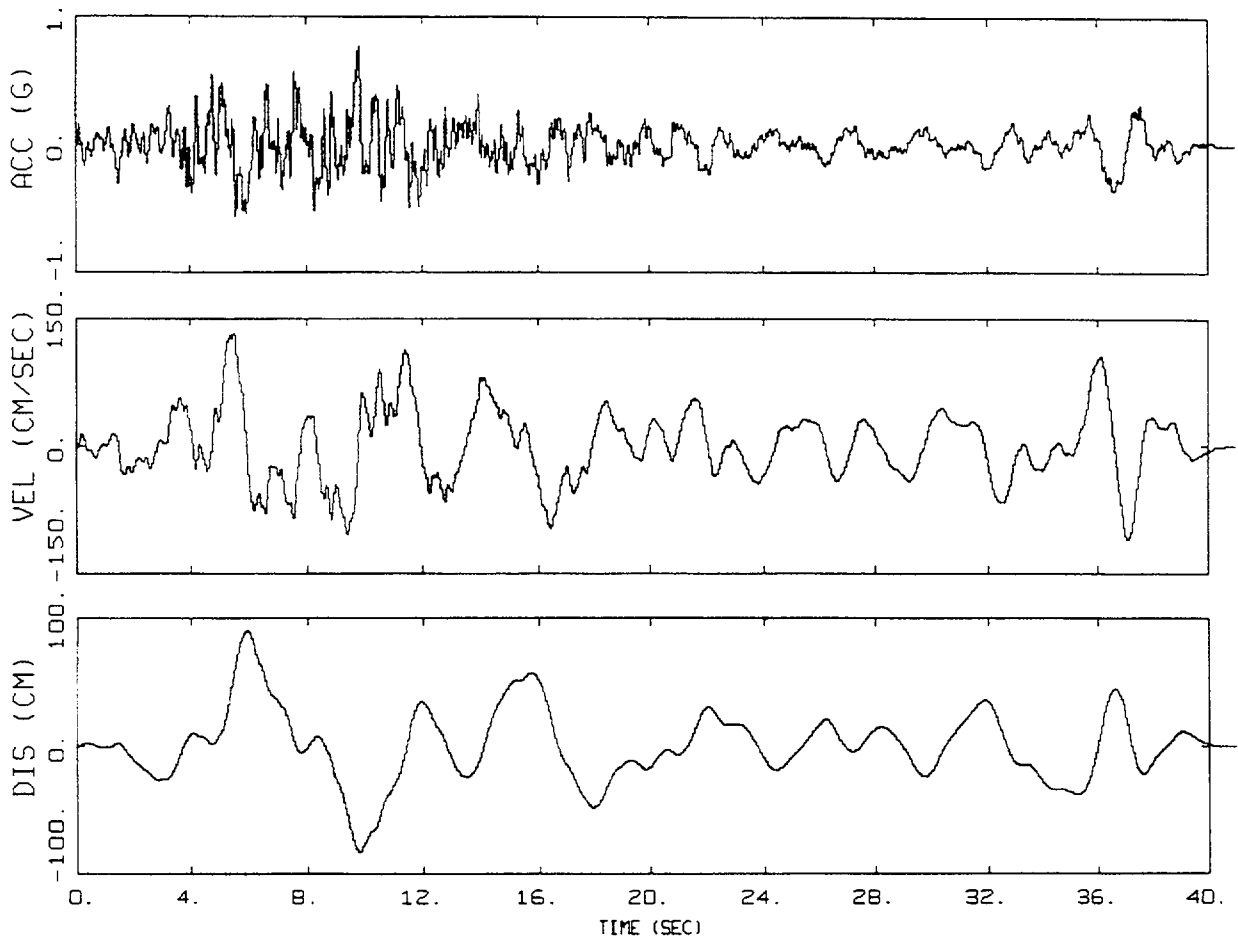


WUS, MELOLAND, H1
 POWER SPECTRAL DENSITY (PSD)

LEGEND

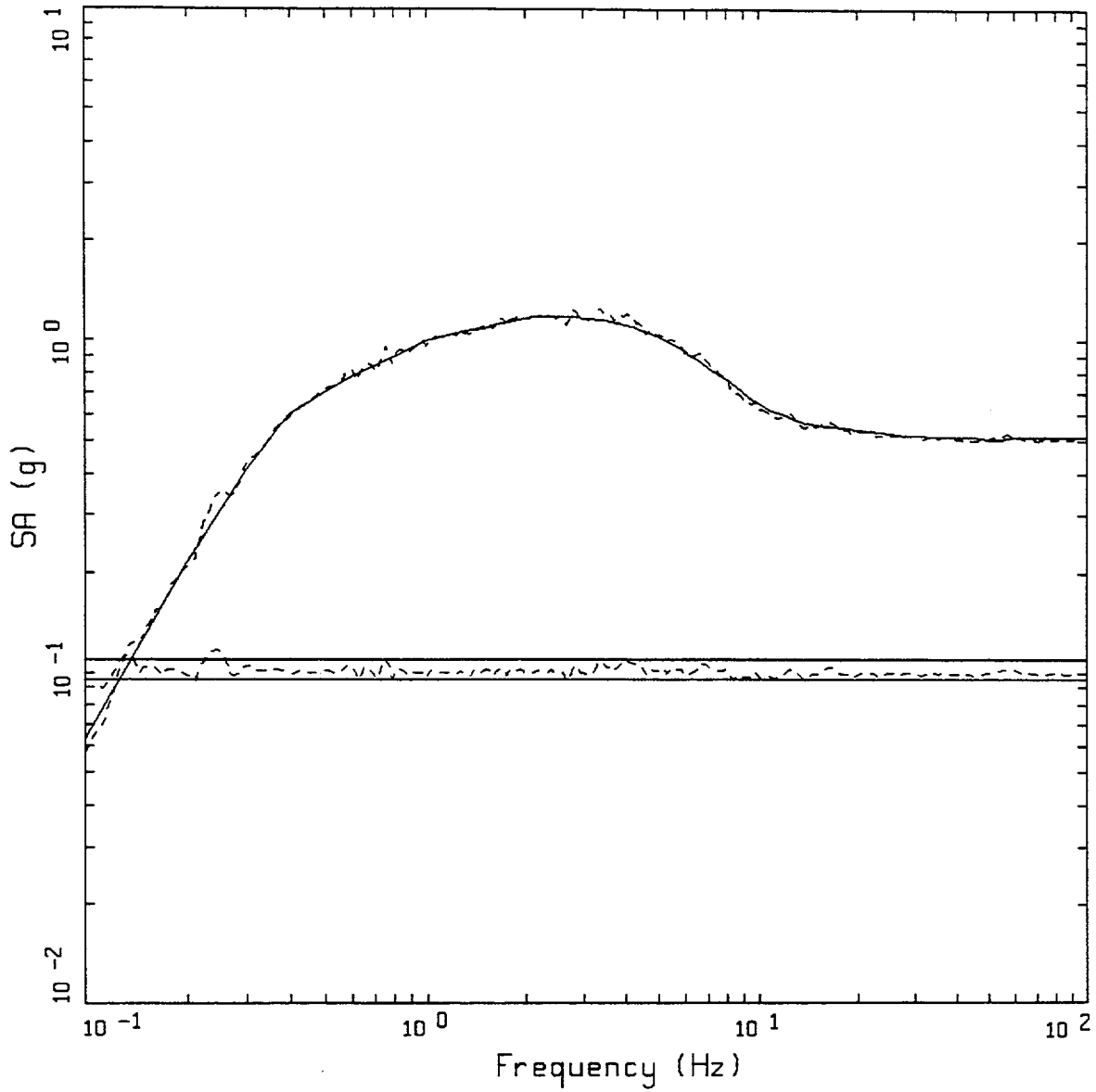
— HORIZONTAL 1, 5%-75% ARIAS DURATION = 13.99 SEC

Figure 8-3. Power spectral density for component H1, Mojave site, soil.



WUS, MELOLAND, H1

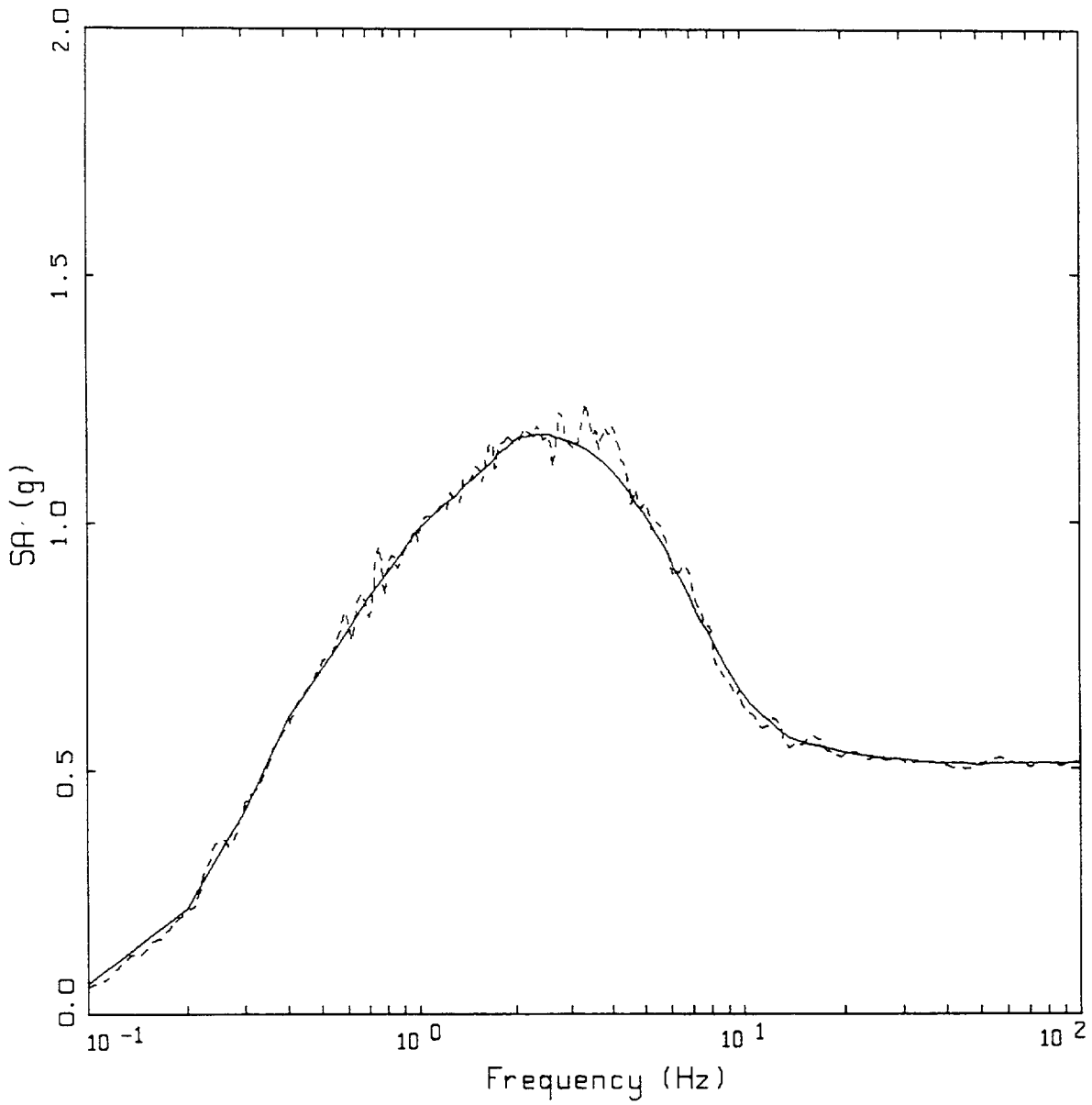
Figure 8-4. Time histories for component H1, Mojave site, soil.



WUS, MELOLAND
HORIZONTAL 2

- LEGEND
- 5 %, SOIL TARGET; PGA = 0.511 G
 - - - - 5 %, SPECTRAL MATCH; PGA = 0.512 g
 - 5 %, UPPER BOUND 1.10 (SCALED BY 0.1)
 - - - - 5 %, RATIO: SPECTRAL MATCH TO SOIL TARGET (SCALED BY 0.1)
 - 5 %, LOWER BOUND 0.95 (SCALED BY 0.1)

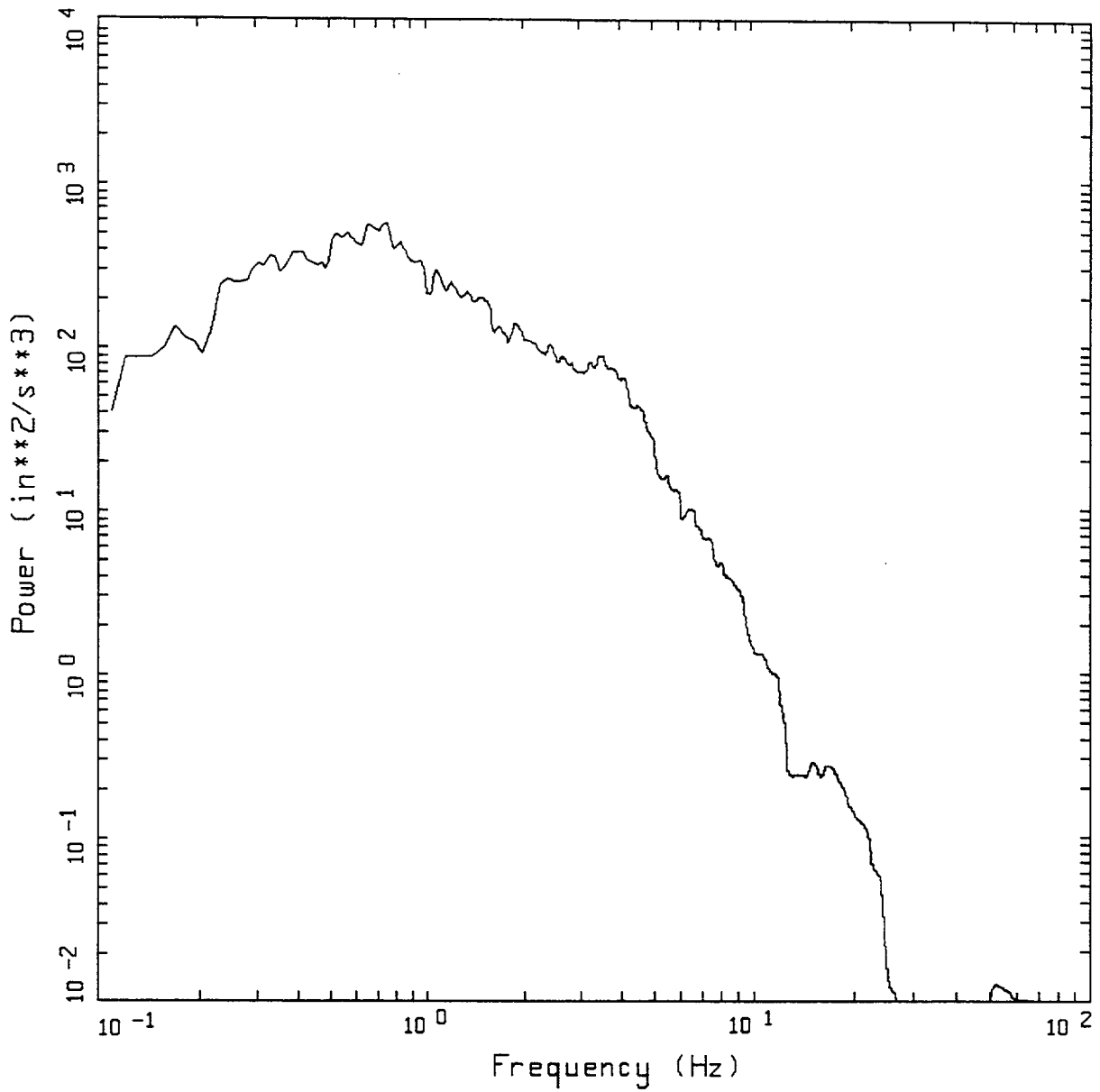
Figure 8-5. Target spectrum, spectral match and spectral ratio, component H2, Mojave site, soil.



WUS, MELOLAND
HORIZONTAL 2

- LEGEND
- 5 %, SOIL TARGET; PGA = 0.511 G
 - 5 %, SPECTRAL MATCH; PGA = 0.512 g

Figure 8-6. Target spectrum and spectral match on linear scale, component H2, Mojave site, soil.



WUS, MELOLAND, H2
 POWER SPECTRAL DENSITY (PSD)

LEGEND

— HORIZONTAL 2, 5%-75% ARIAS DURATION=14.82 SEC

Figure 8-7. Power spectral density for component H2, Mojave site, soil.

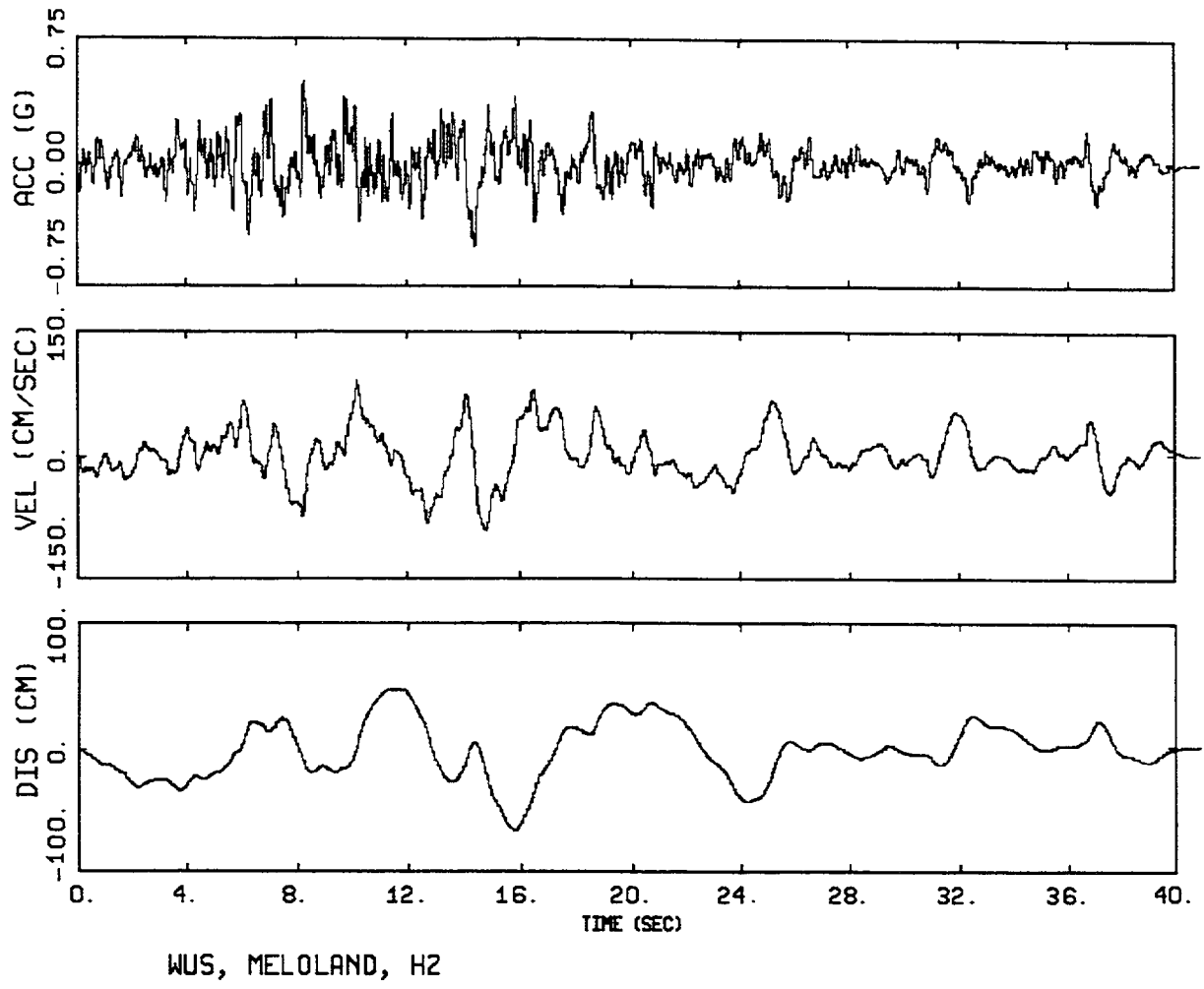
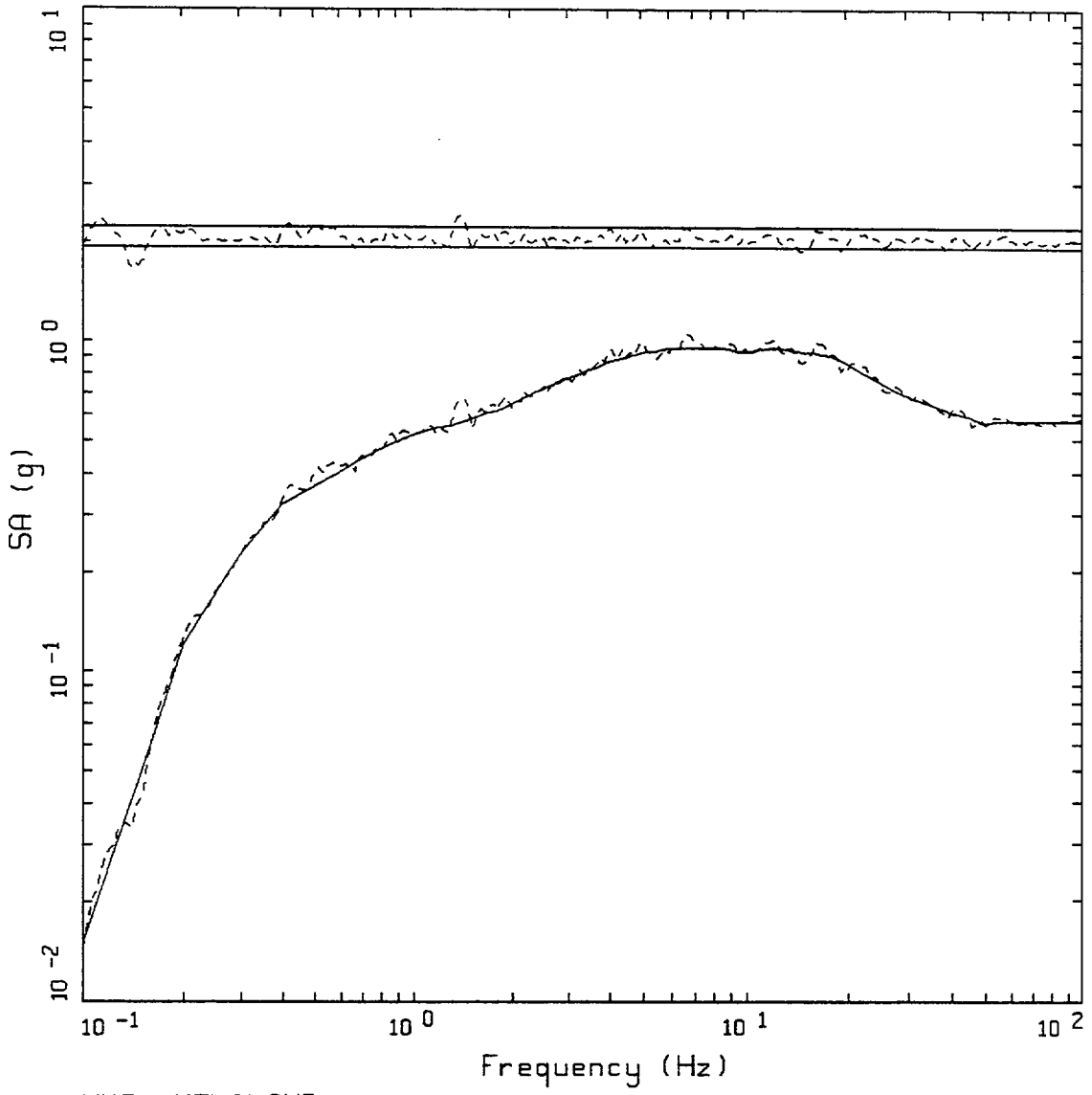


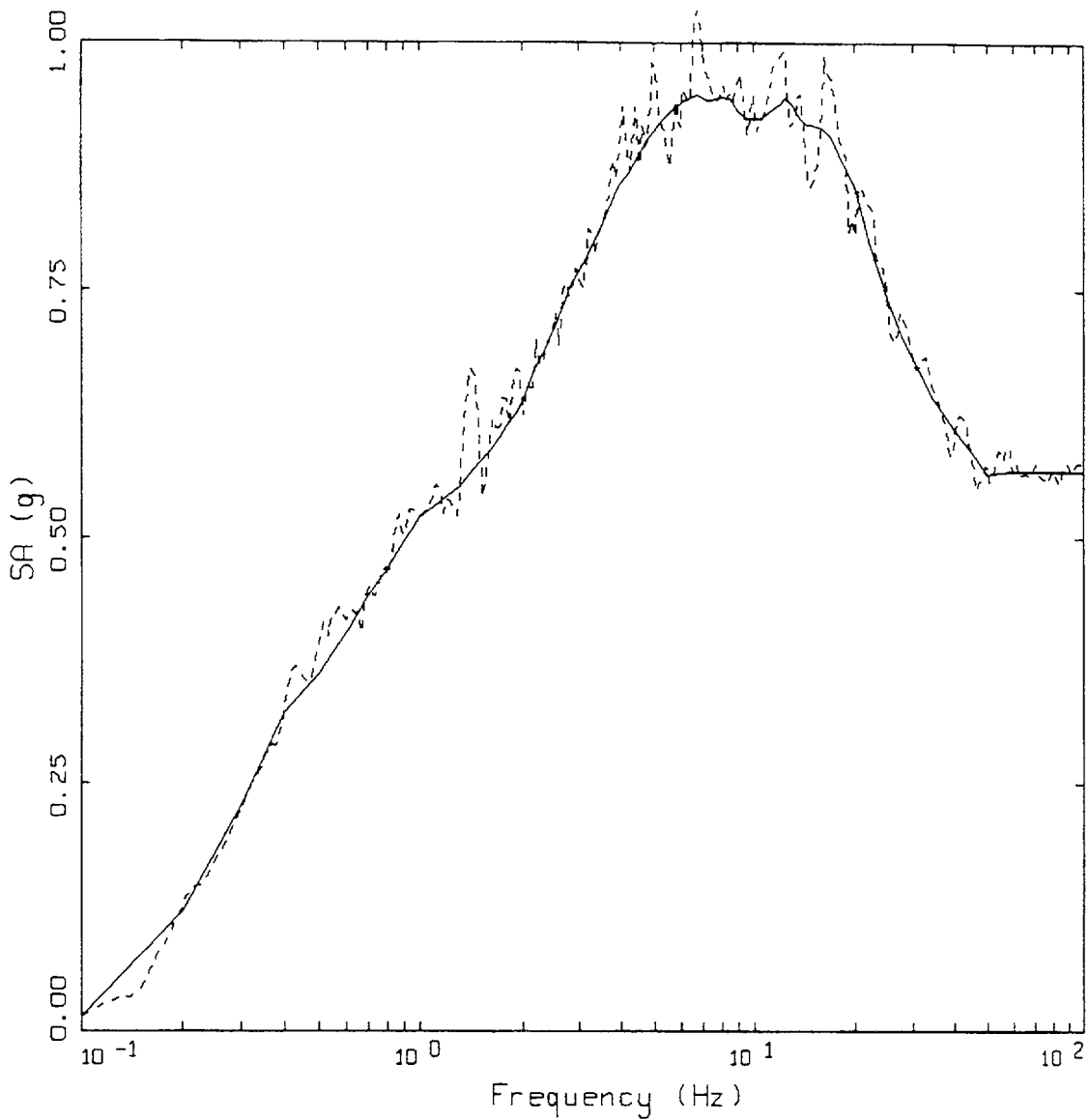
Figure 8-8. Time histories for component H2, Mojave site, soil.



WUS, MELOLAND
VERTICAL

- LEGEND
- 5 %, SOIL TARGET; PGA = 0.568 G
 - - - - - 5 %, SPECTRAL MATCH; PGA = 0.598 g
 - 5 %, UPPER BOUND 1.10 (SCALED BY 2.0)
 - - - - - 5 %, RATIO: SPECTRAL MATCH TO SOIL TARGET (SCALED BY 2.0)
 - 5 %, LOWER BOUND 0.95 (SCALED BY 2.0)

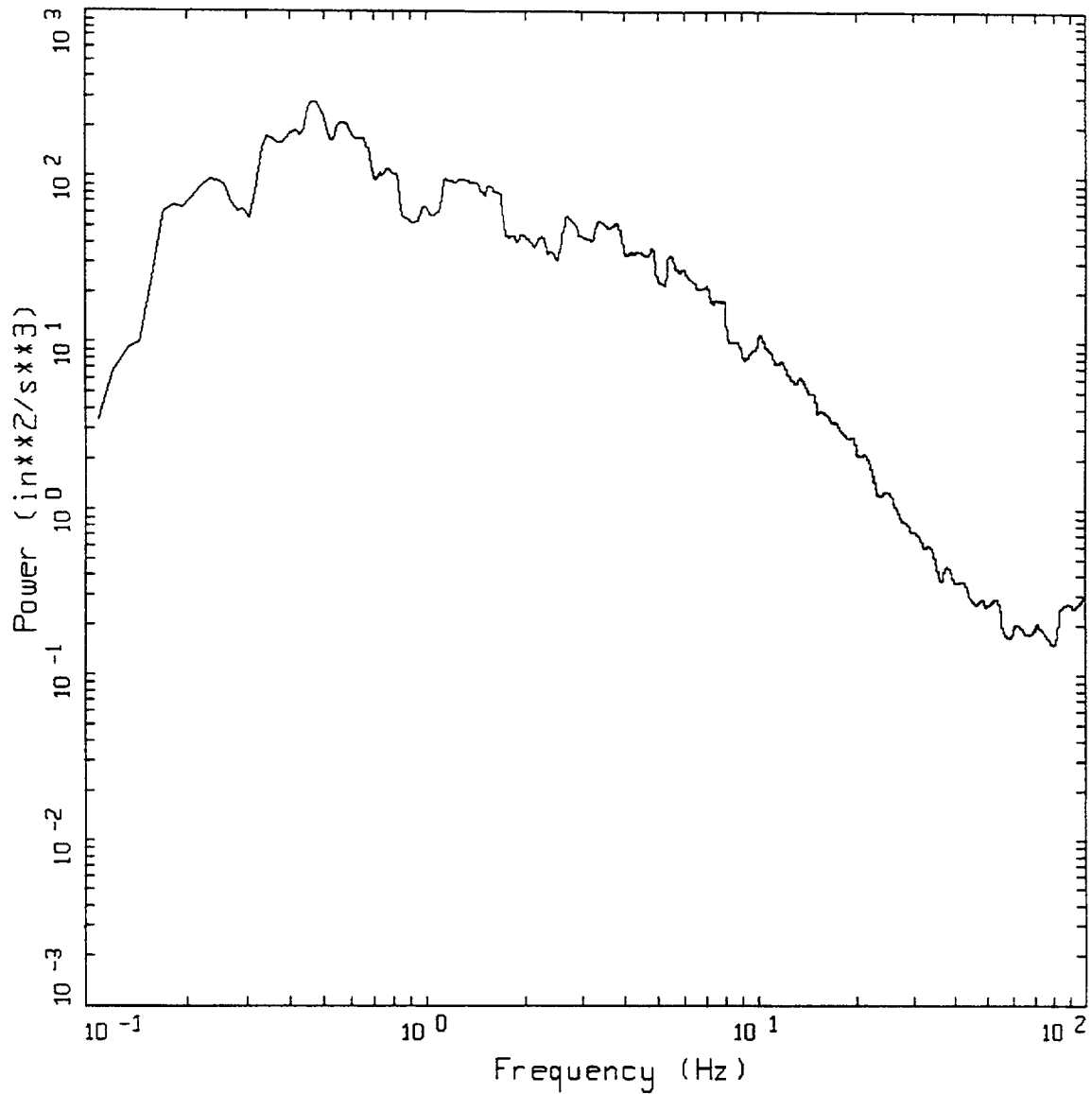
Figure 8-9. Target spectrum, spectral match and spectral ratio, component V, Mojave site, soil.



WUS, MELOLAND
VERTICAL

LEGEND
 ——— 5 %, SOIL TARGET; PGA = 0.568 G
 - - - - 5 %, SPECTRAL MATCH; PGA = 0.598 g

Figure 8-10. Target spectrum and spectral match on linear scale, component V, Mojave site, soil.



WUS, MELOLAND, VERTICAL
POWER SPECTRAL DENSITY (PSD)

LEGEND

— VERTICAL, 5% - 75% ARIAS DURATION=12.48 SEC

Figure 8-11. Power spectral density for component V, Mojave site, soil.

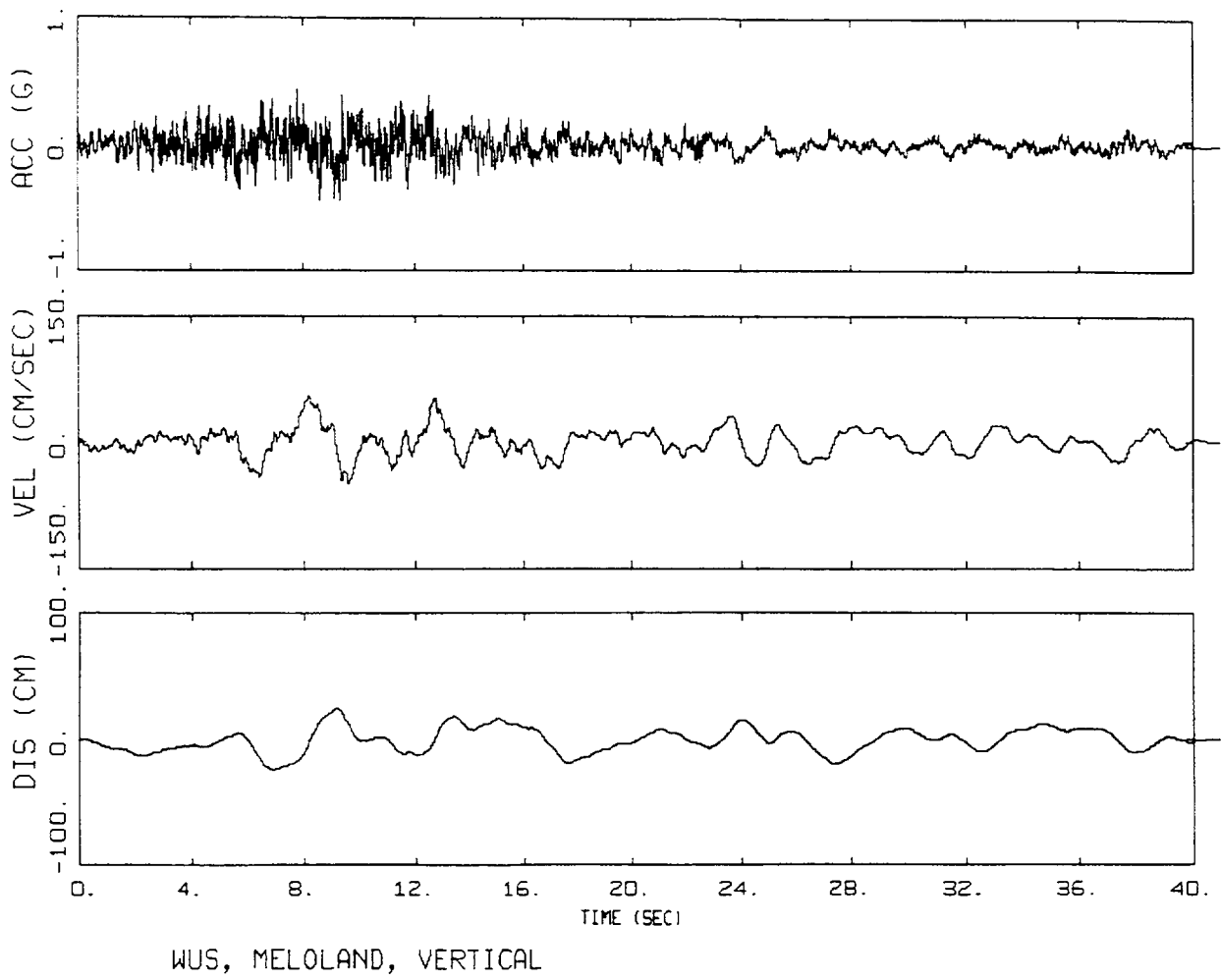
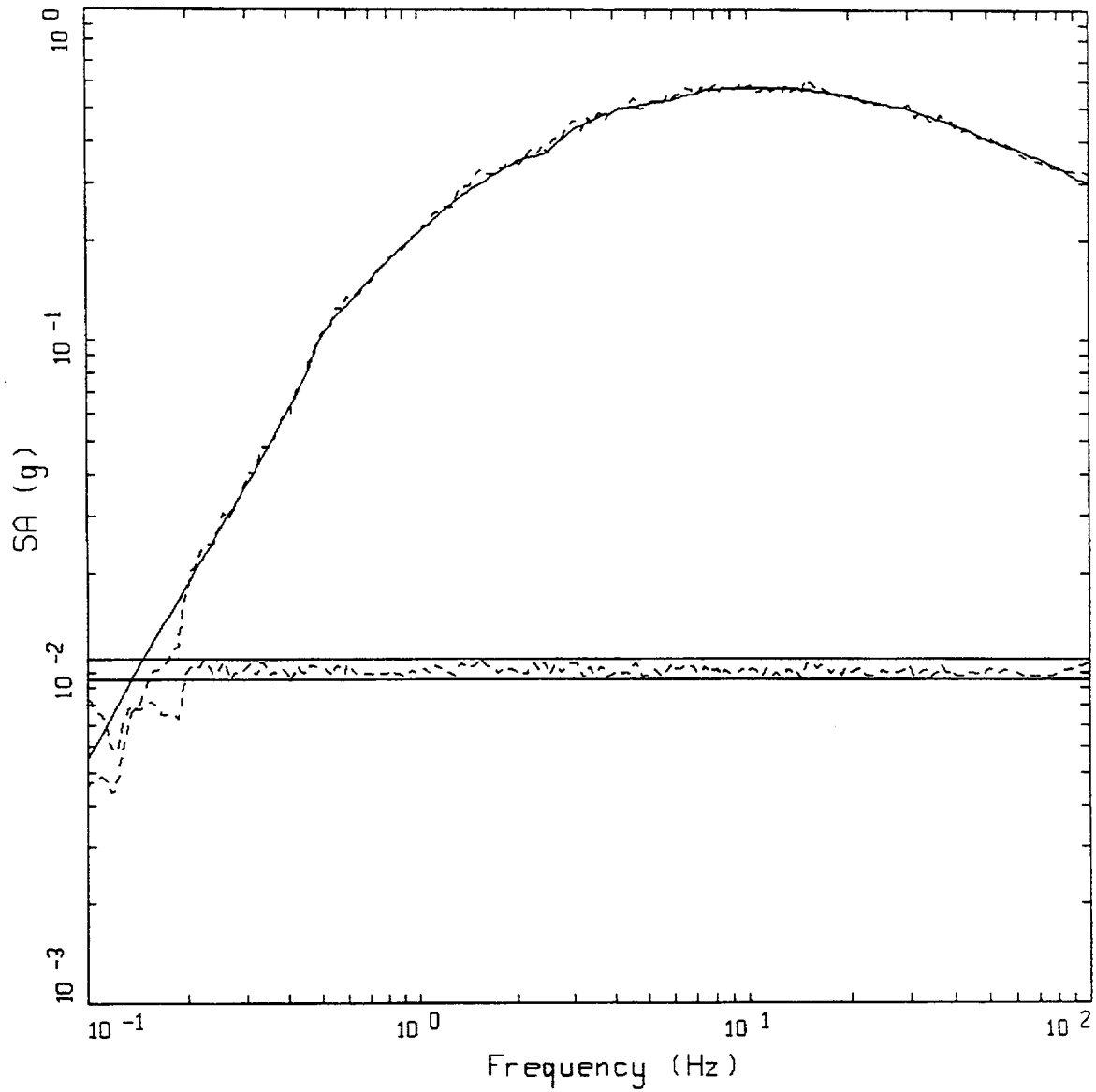


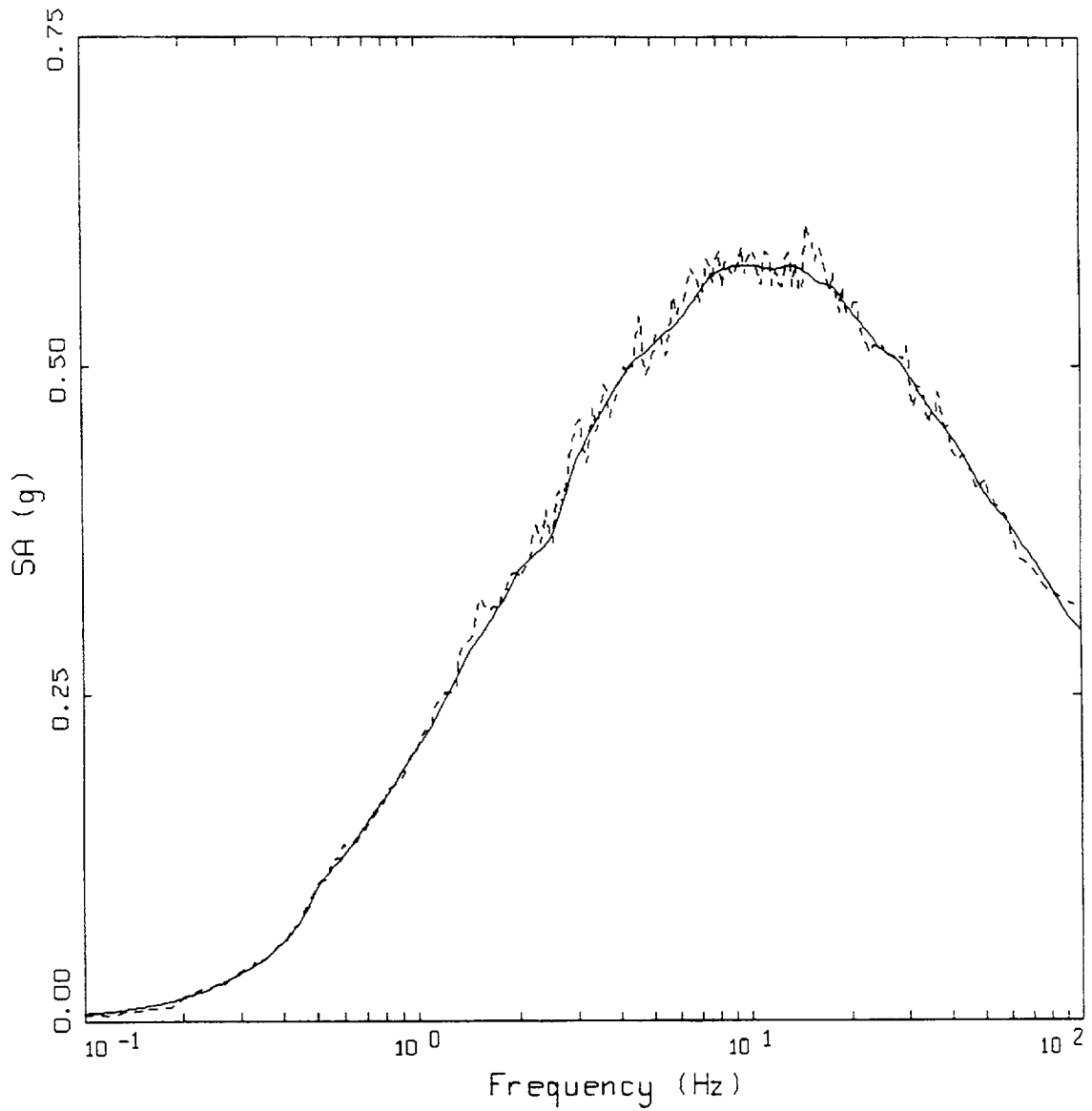
Figure 8-12. Time histories for component V, Mojave site, soil.



CEUS, SAVANNAH RIVER
HORIZONTAL 1

- LEGEND
- 5 %, SOIL TARGET; PGA = 0.300 G
 - 5 %, SPECTRAL MATCH; PGA = 0.315 g
 - 5 %, UPPER BOUND 1.10 (SCALED BY 0.01)
 - 5 %, RATIO: SPECTRAL MATCH TO SOIL TARGET (SCALED BY 0.01)
 - 5 %, LOWER BOUND 0.95 (SCALED BY 0.01)

Figure 8-13. Target spectrum, spectral match and spectral ratio, component H1, Columbia site, soil.

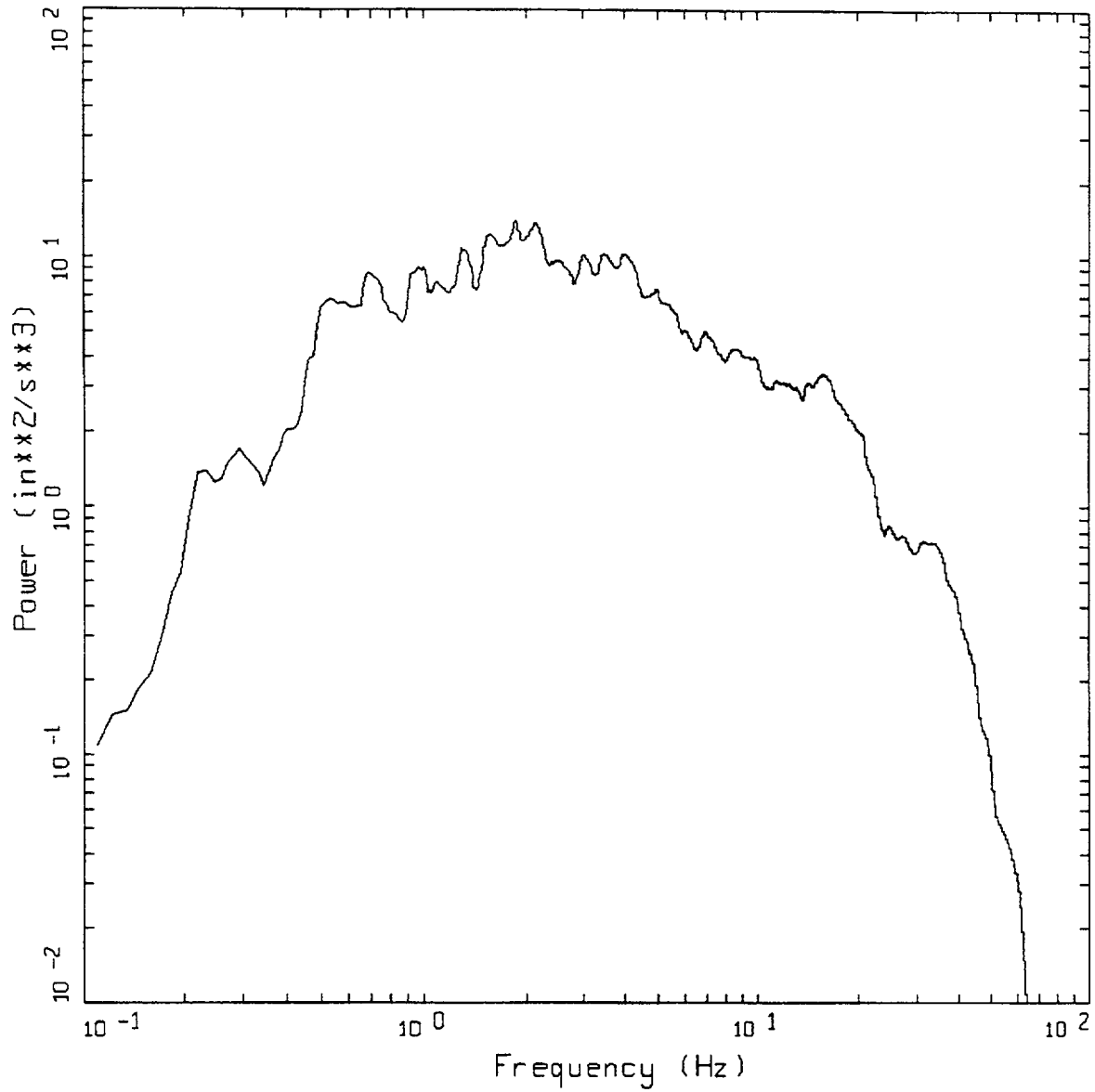


CEUS, SAVANNAH RIVER GENERIC
HORIZONTAL 1

LEGEND

- 5 %, SOIL TARGET; PGA = 0.300 g
- 5 %, SPECTRAL MATCH; PGA = 0.315 g

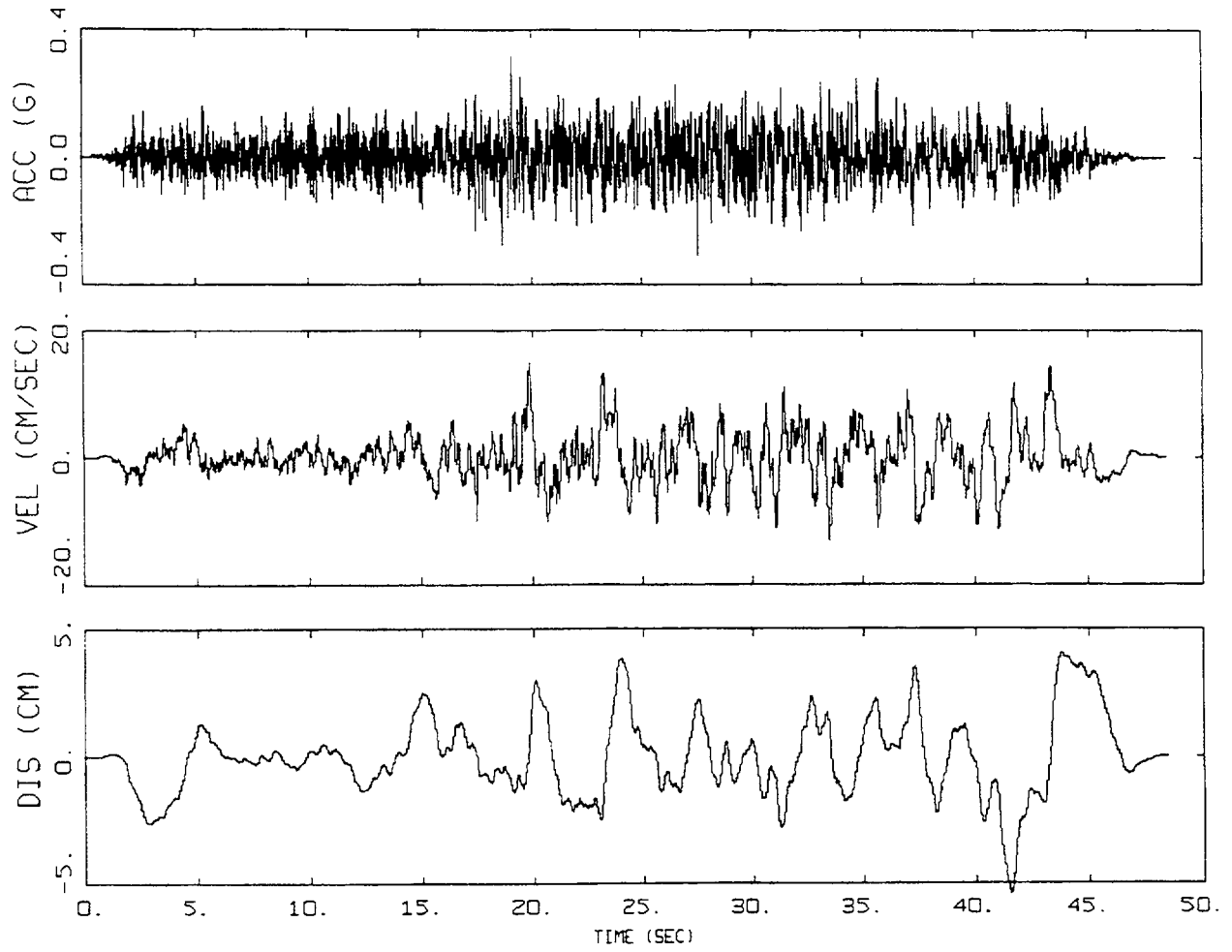
Figure 8-14. Target spectrum and spectral match on linear scale, component H1, Columbia site, soil.



CEUS, SAVANNAH RIVER, H1
POWER SPECTRAL DENSITY (PSD)

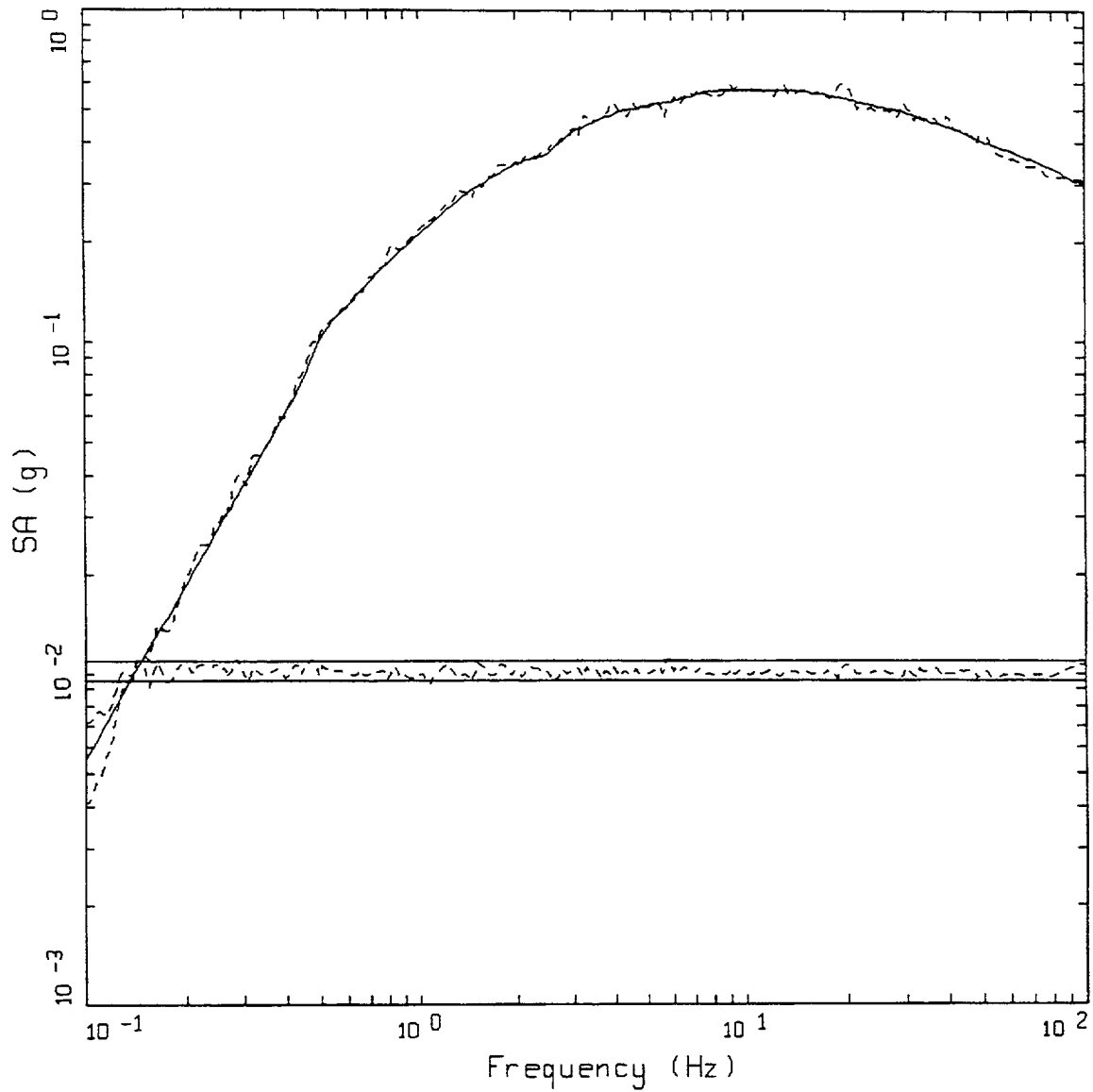
LEGEND
 ——— HORIZONTAL 1, 5% - 75% ARIAS DURATION=26.00 SEC

Figure 8-15. Power spectral density for component H1, Columbia site, soil.



CEUS, SAVANNAH RIVER, H1

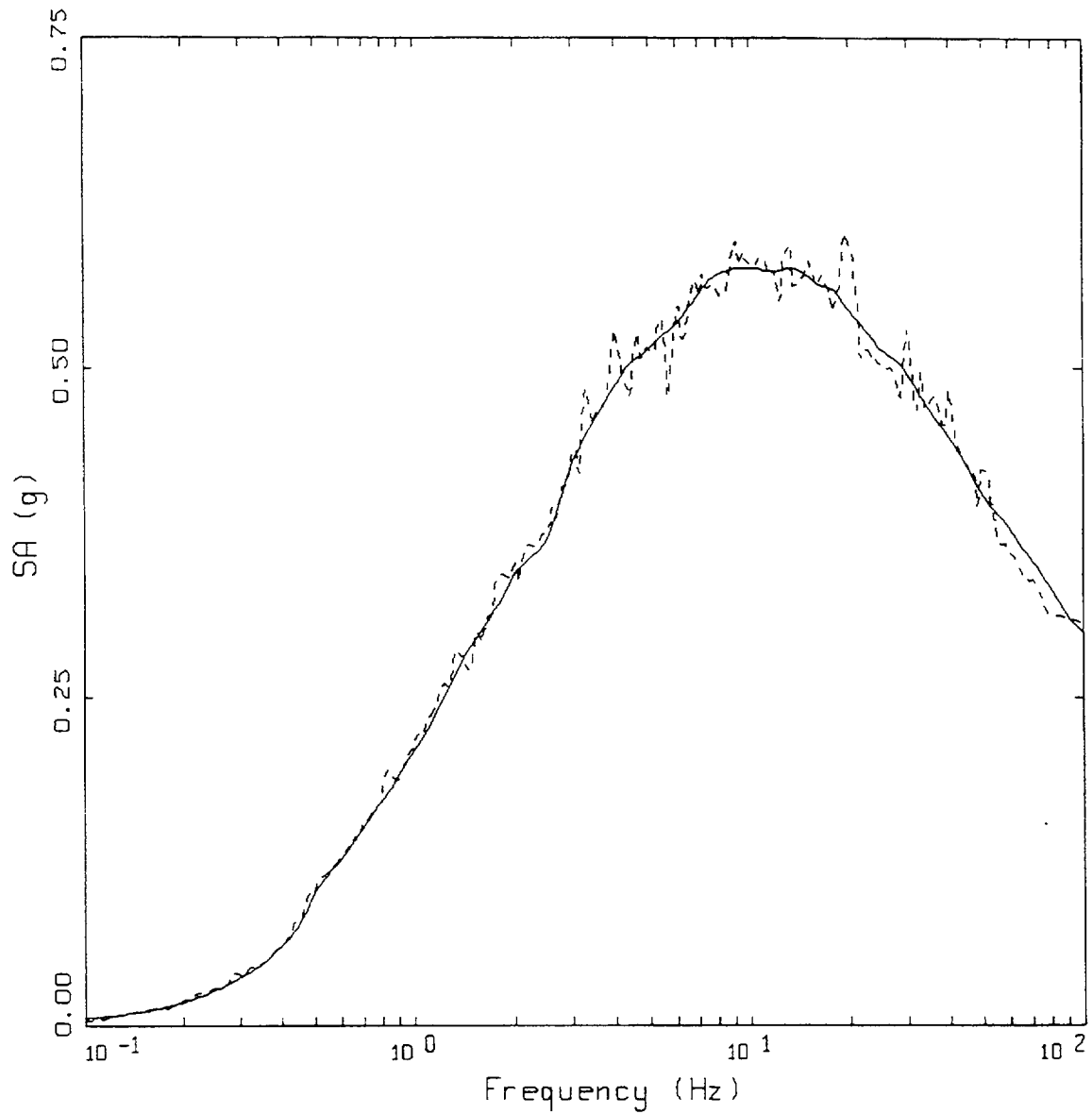
Figure 8-16. Time histories for component H1, Columbia site, soil.



CEUS, SAVANNAH RIVER
HORIZONTAL 2

- LEGEND
- 5 %, SOIL TARGET; PGA = 0.300 G
 - 5 %, SPECTRAL MATCH; PGA = 0.307 g
 - 5 %, UPPER BOUND 1.10 (SCALED BY 0.01)
 - 5 %, RATIO: SPECTRAL MATCH TO SOIL TARGET (SCALED BY 0.01)
 - 5 %, LOWER BOUND 0.95 (SCALED BY 0.01)

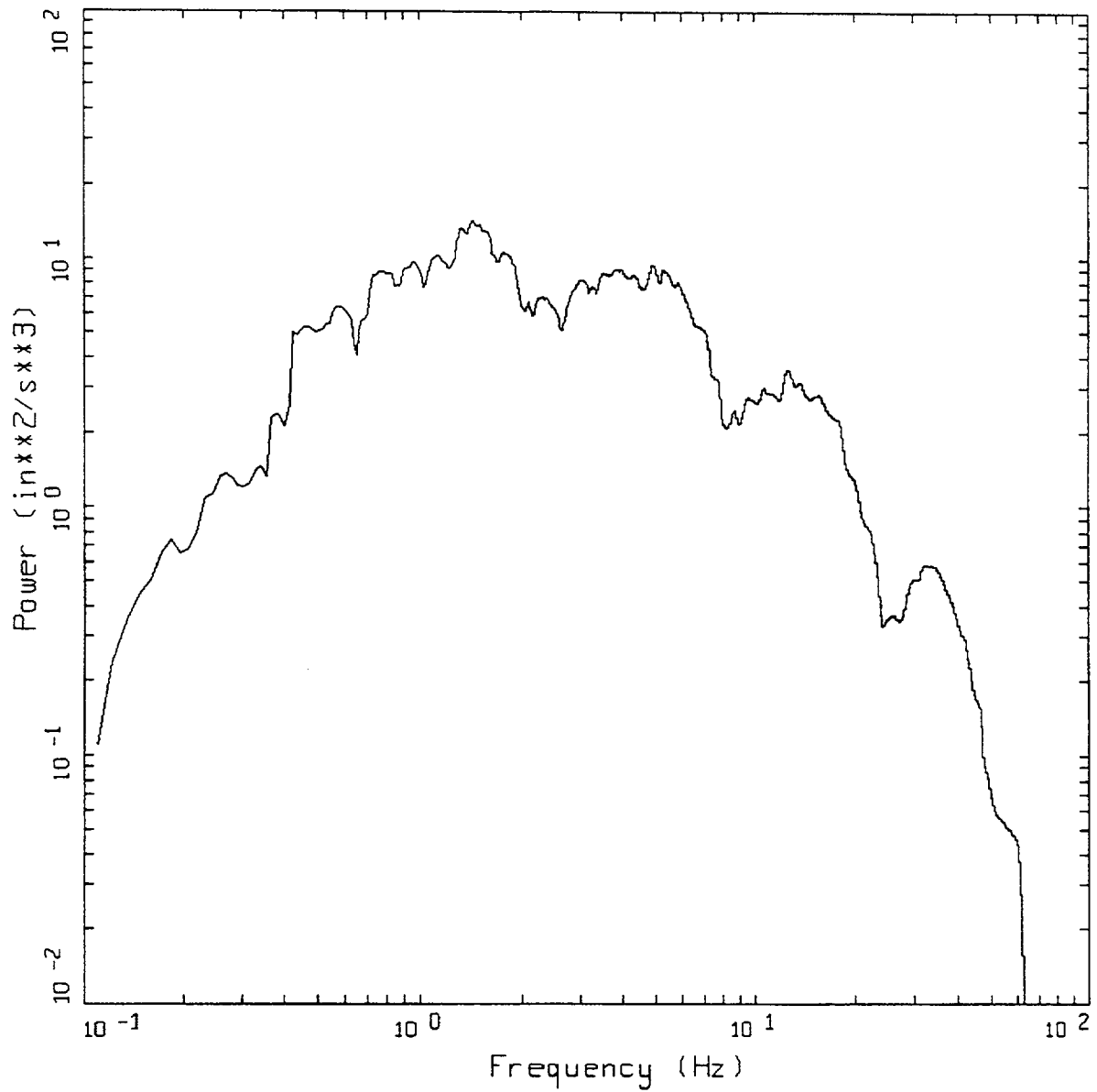
Figure 8-17. Target spectrum, spectral match and spectral ratio, component H2, Columbia site, soil.



CEUS, SAVANNAH RIVER
HORIZONTAL 2

LEGEND
 ——— 5 %, SOIL TARGET; PGA = 0.300 g
 - - - - 5 %, SPECTRAL MATCH; PGA = 0.307 g

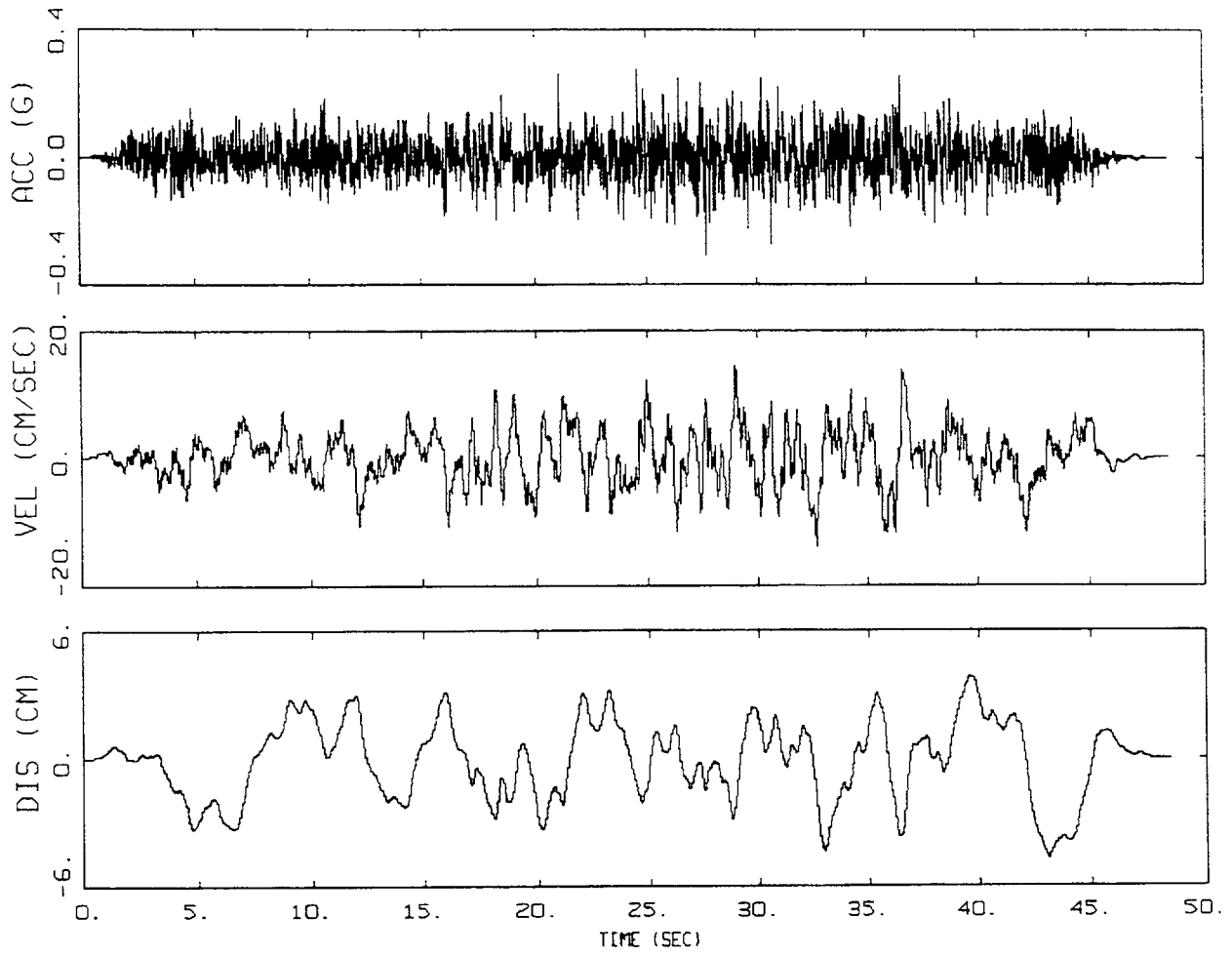
Figure 8-18. Target spectrum and spectral match on linear scale, component H2, Columbia site, soil.



CEUS, SAVANNAH RIVER, H2
 POWER SPECTRAL DENSITY (PSD)

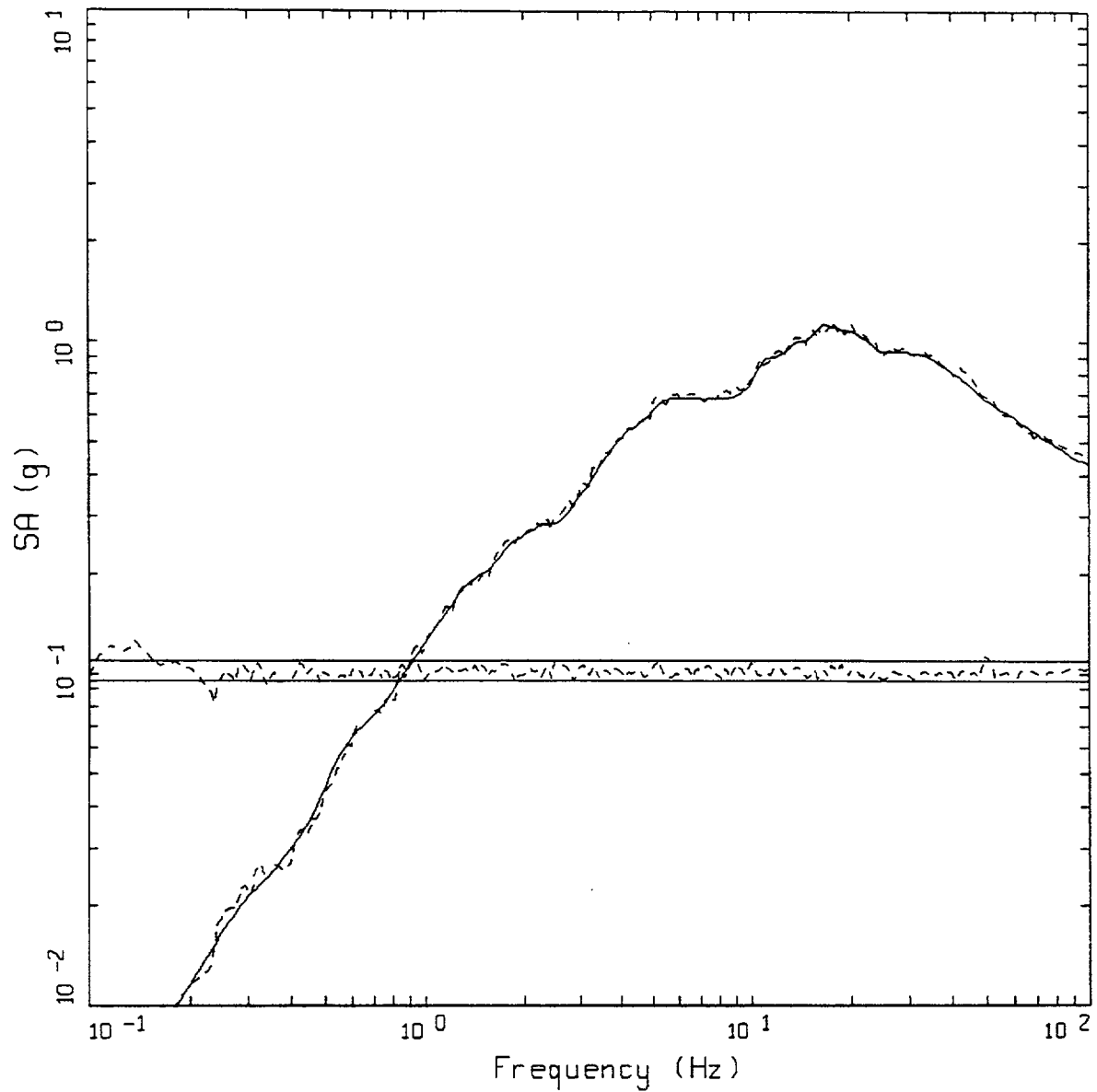
— LEGEND
 HORIZONTAL 2, 5% - 75% ARIAS DURATION=28.48 SEC

Figure 8-19. Power spectral density for component H2, Columbia site, soil.



CEUS, SAVANNAH RIVER, H2

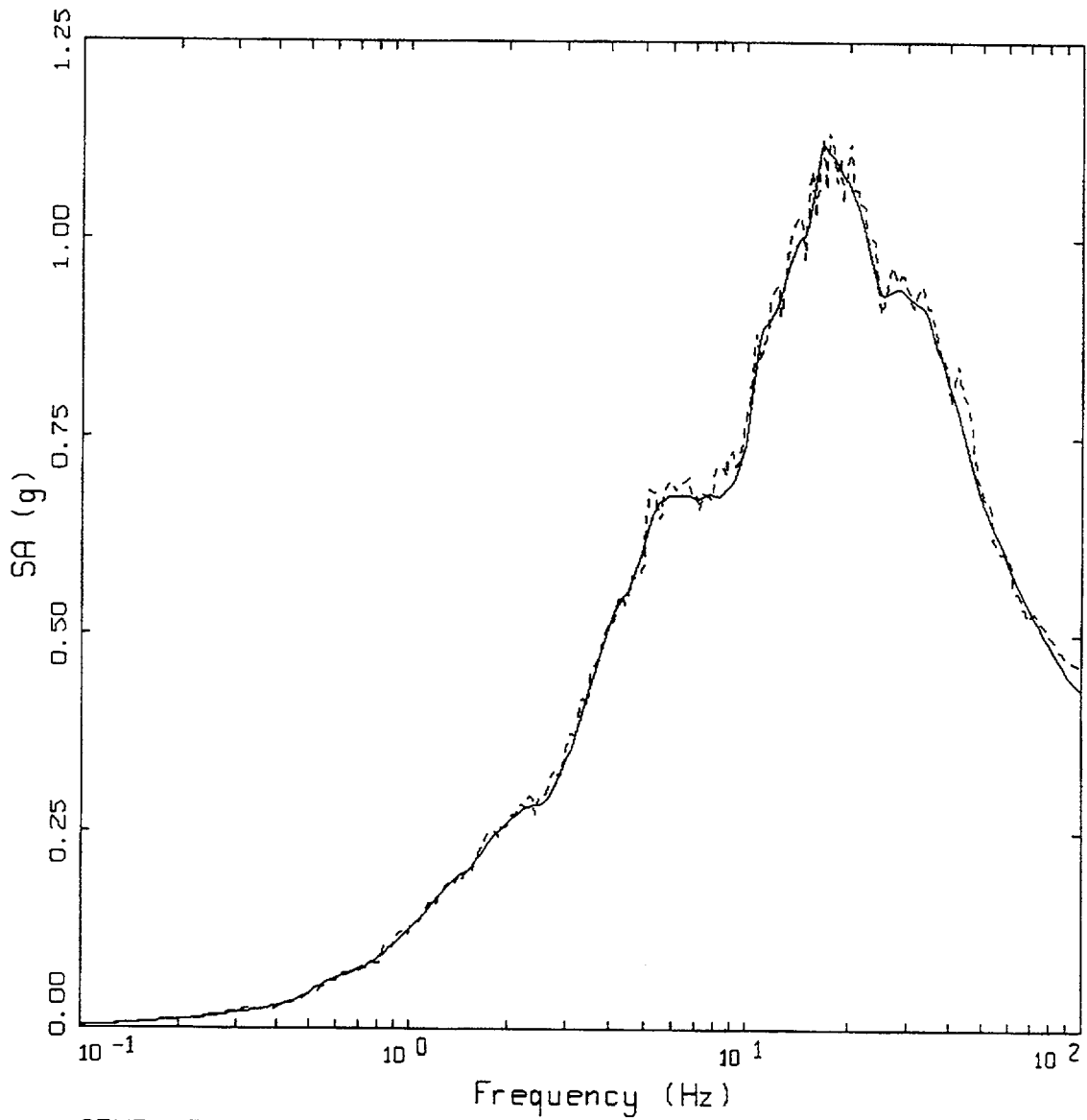
Figure 8-20. Time histories for component H2, Columbia site, soil.



CEUS, SAVANNAH RIVER
VERTICAL

- LEGEND
- 5 %, SOIL TARGET; PGA = 0.431 G
 - 5 %, SPECTRAL MATCH; PGA = 0.451 g
 - 5 %, UPPER BOUND 1.10 (SCALED BY 0.10)
 - 5 %, RATIO: SPECTRAL MATCH TO SOIL TARGET (SCALED BY 0.10)
 - 5 %, LOWER BOUND 0.95 (SCALED BY 0.10)

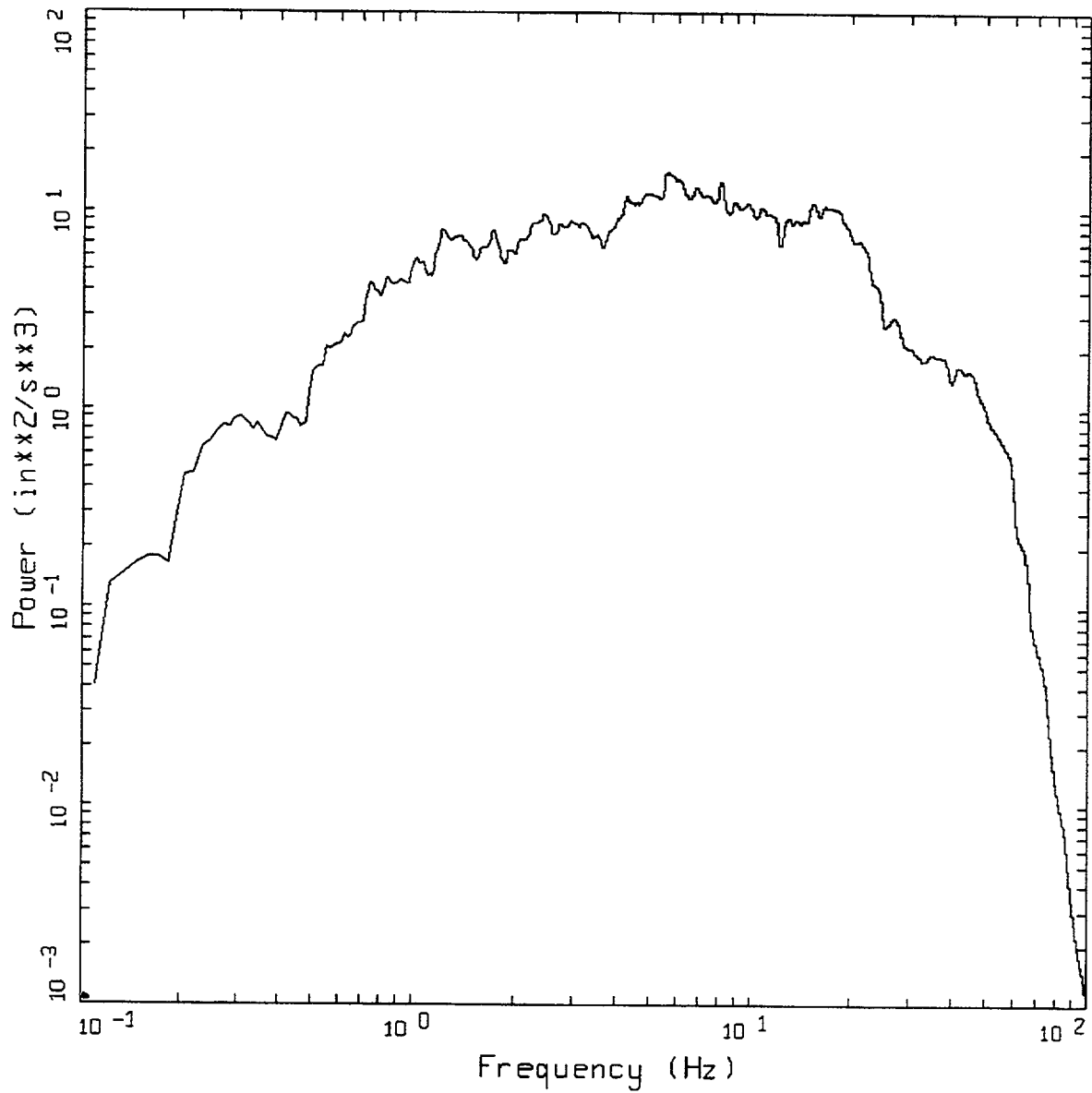
Figure 8-21. Target spectrum, spectral match and spectral ratio, component V, Columbia site, soil.



CEUS, SAVANNAH RIVER
VERTICAL

- LEGEND
- 5 %, SOIL TARGET; PGA = 0.431 g
 - 5 %, SPECTRAL MATCH; PGA = 0.451 g

Figure 8-22. Target spectrum and spectral match on linear scale, component V, Columbia site, soil.



CEUS, SAVANNAH RIVER, VERTICAL
POWER SPECTRAL DENSITY (PSD)

LEGEND

— VERTICAL, 5% - 75% ARIAS DURATION=23.76 SEC

Figure 8-23. Power spectral density for component V, Columbia site, soil.

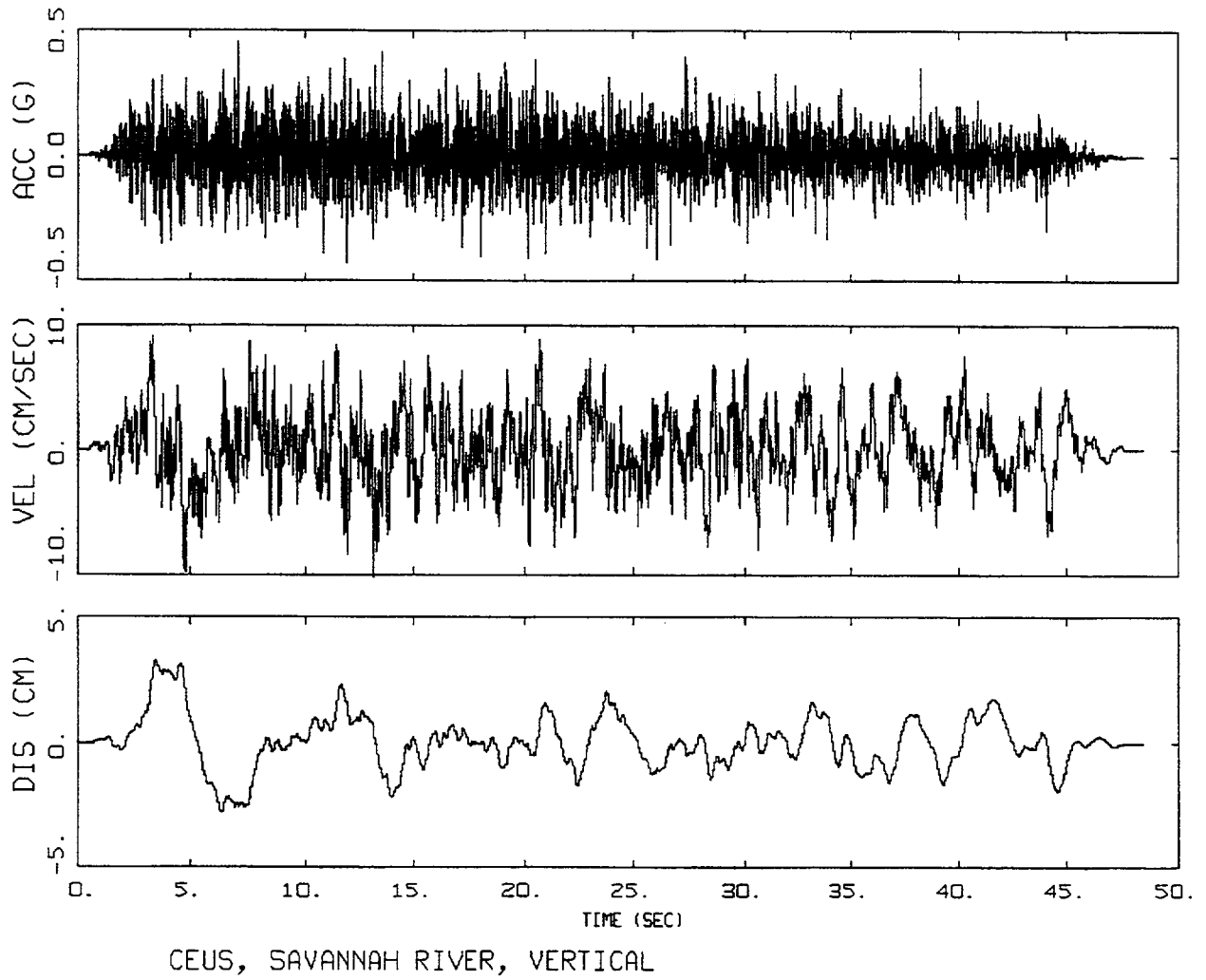


Figure 8-24. Time histories for component V, Columbia site, soil.

9.0 SUMMARY OF RECOMMENDATIONS

This section summarizes recommendations on developing seismic ground motion spectra appropriate for use in designing or evaluating nuclear facilities at any location in the US. This summarizes the work reported herein and in McGuire et al., (2001). The procedure for deriving ground motion spectra for rock sites is summarized in Figure 1-1, and for soil sites is summarized in Figure 1-2.

9.1 Rock sites

Probabilistic seismic hazard analysis

Developing seismic ground motions starts with a probabilistic seismic hazard analysis (PSHA) conducted with up-to-date interpretations of earthquake sources, earthquake recurrence, and strong ground motion estimation, using methods described in the SSHAC report (1997). Epistemic uncertainties must be characterized in a complete and defensible fashion. In particular for the CEUS, our understanding of single- and double-corner ground-motion models is evolving, and future PSHAs must fully document the appropriateness of using either or both of these models. A complete PSHA includes hazard for structural frequencies from 100 Hz to 0.2 Hz, and calculates results for annual frequencies of exceedence from 10^{-2} to 10^{-5} . The PSHA must be conducted at a minimum of 25 frequencies, approximately equally spaced on a logarithmic frequency axis between 100 and 0.2 Hz.

The PSHA must deaggregate the mean seismic hazard by M and R to determine the relative contributions to hazard, at 10 Hz and at 1 Hz. Assuming that 10^{-4} is the target hazard level for design, this deaggregation must be done at 10^{-4} . If multiple attenuation equations have been used to characterize epistemic uncertainties, the deaggregation must be done with each attenuation equation weighted by the subjective probabilities that are justified and used in the PSHA.

The current (year 2001) procedure is to conduct the PSHA for horizontal ground motion and to develop vertical motions by scaling the the horizontal motions. This ensures that we derive vertical motions consistent with the horizontals. If defensible attenuation equations are developed for vertical motions, they may be used in a PSHA, but the vertical and horizontal design motions should be evaluated to determine that they are consistent.

Uniform hazard spectra (UHS) and uniform reliability spectrum (URS)

From the PSHA, we should derive the 10^{-4} and 10^{-5} mean uniform hazard spectra (UHS). From these spectra we determine the ratio $A_R(f)$ of the spectral amplitudes at each frequency f . That is,

$$A_R(f) = SA(f, 10^{-5})/SA(f, 10^{-4}) \quad (9-1)$$

where SA is spectral acceleration. An additional parameter used to characterize the slope is K_H , which is the negative slope of the hazard curve in log space. The two are related by

$$A_R = 10^{\frac{1}{K_H}} \quad \text{or} \quad K_H = \frac{1}{\log_{10} A_R}$$

We calculate the *uniform reliability spectrum* URS by multiplying the UHS at each frequency by a scale factor SF:

$$\text{URS} = \text{UHS} \times \text{SF} \quad (9-2)$$

The scale factor SF depends directly on two important policy/decision parameters:

- 1) the desired probability ratio R_p defined as the ratio of the hazard exceedence frequency H_D for which the UHS is chosen, to the permissible annual frequency P_f of unacceptable seismic performance of a structure, system, or component, i.e.:

$$R_p = \frac{H_D}{P_f}$$

- 2) the desired minimum seismic margin factor F_{SM} expected to be achieved for structures, systems, and components designed to the Standard Review Plan, and specified Codes and Standards (ACI, AISC, ASME, etc.). F_{SM} is defined by:

$$F_{SM} = \frac{\text{HCLPF Capacity}}{\text{URS}}$$

in which the HCLPF Capacity corresponds to the ground motion level for which there is approximately a mean one-percent conditional probability of unacceptable seismic performance.

In order to achieve a reliability-based design, the NRC must set target values for these two parameters R_p and F_{SM} . Current codes and standards coupled with the Standard Review Plan achieve variable minimum seismic margin factors F_{SM} ranging from about 1.0 to 2.0 with the lower half of this range being typically applicable for brittle failure modes and the upper half of this range being typically applicable for ductile failure modes.

For purposes of this study, the following example values were selected:

Desired $R_p \approx 20$ to 40
 Minimum $F_{SM} \approx 1.67$

for which the following scale factor SF is appropriate:

$$SF = \max \{0.7, 0.35 A_R^{1.2}\} \quad (9-3)$$

The above R_p and F_{SM} values were chosen only for example purposes. For other desired R_p and F_{SM} values the following table applies:

SF for different F_{SM} and R_p values		
F_{SM}	Desired R_p range	
	10 to 20	20 to 40
1.0	$\max \{1.0, .60 A_R^{0.9}\}$	$\max \{1.2, .60 A_R^{1.2}\}$
1.33	$\max \{0.8, .45 A_R^{0.9}\}$	$\max \{0.9, .45 A_R^{1.2}\}$
1.5	$\max \{0.7, .40 A_R^{0.9}\}$	$\max \{0.8, .40 A_R^{1.2}\}$
1.67	$\max \{0.6, .35 A_R^{0.9}\}$	$\max \{0.7, .35 A_R^{1.2}\}$
2.0	$\max \{0.5, .30 A_R^{0.9}\}$	$\max \{0.6, .30 A_R^{1.2}\}$

Depending upon the desired R_p range and minimum F_{SM} selected, the scale factor SF can be either generally less than or generally greater than unity. In all cases SF increases with increasing A_R for $A_R \geq 1.8$.

Scaled spectra

Scaled spectra are used in two ways: as a consistency check on the UHS, and to derive multiple earthquake design spectra (if desired) from the URS. For the consistency check, we use the appropriate mean M and R values from deaggregation of the 10^{-4} amplitudes at 10 and 1 Hz to calculate spectral shapes from each attenuation equation used in the PSHA and from the spectral shapes developed in this project. That is, we use the M - R deaggregation values for 10 Hz to calculate the 10 Hz spectral shape, and similarly for 1 Hz. From the attenuation equations we calculate representative spectral shapes using the attenuation equation weights from the PSHA. A representative spectral shape is calculated as the antilog of the average weighted logarithmic spectral values from each attenuation equation. These representative spectral shapes are scaled so that they equal the 10^{-4} UHS at 10 and 1 Hz.

We also derive spectral shapes from the shapes recommended in McGuire et al., (2001) for the mean M and R values from deaggregation at 10 and 1 Hz, for the 10^{-4} hazard. This procedure consists of applying either equation (4-8) (for the WUS) or equation (4-9) (for the CEUS) of McGuire et al., (2001), using the coefficients of Table 4-3 of that reference. To calculate the coefficients, we use the appropriate deaggregation M - R values. These spectral shapes are scaled to equal the 10^{-4} UHS at 10 and 1 Hz. Again, if both the 1- and 2-corner source models are used for the CEUS (see Table 4-3 of McGuire et al., 2001), we calculate the antilog of the average weighted logarithmic spectral values from each equation.

We compare these sets of spectral shapes (one set from the attenuation equations, a second set from McGuire et al., 2001) to the 10^{-4} UHS. Any substantial differences in shapes (greater than about 20%) must be understood and explained. For example, the CEUS spectral shapes were developed

for hard rock conditions, and applications to a site in Texas founded on softer rock would indicate high frequency amplitudes that are too high. Presumably the region-specific attenuation equations used in a PSHA for the Texas site would reflect the correct rock characteristics and would explain why the spectral shapes derived from equation (4-9) of McGuire et al., (2001) do not apply to this site.

The second use of scaled shapes is to develop design spectra for individual earthquakes. One option available to the designer is to use the broad-banded 10^{-4} URS for design, in which case spectra need not be scaled to the URS. However, the designer may wish to avoid having to design to this broad-banded spectrum. If so, the representative spectral shapes from the attenuation equations described above are scaled to the 10^{-4} URS values at 10 and 1 Hz. Only the representative spectral shapes from the attenuation equations used in the PSHA are used for this application, as they will be the most current, up-to-date, and justified spectra. The two scaled spectra must not fall below the URS by more than 10% at any frequency. If the 10 Hz scaled spectrum falls below the URS by more than 10% at a frequency higher than 10 Hz, the 10 Hz scaled spectrum may be increased until the 10% criterion is met. Alternatively, an additional scaled spectrum may be added at the frequency with the largest discrepancy, deaggregating the hazard and calculating the spectral shape from the *M* and *R* values from hazard deaggregation at this frequency. A similar rule applies for a discrepancy larger than 10% at a frequency below 1 Hz. For frequencies between 10 and 1 Hz, if the envelope of the two scaled spectra falls more than 10% below the URS, both spectra must be increased by the same factor so that the 10% criterion is met. Alternatively, an additional spectrum may be scaled at the frequency with the largest discrepancy, using *M* and *R* values from deaggregation of the hazard at this frequency to calculate the spectral shape. For application of the 10% criterion, the PSHA must be conducted at a minimum of 25 frequencies, approximately equally spaced on a logarithmic frequency axis between 100 and 0.2 Hz.

Vertical motions

Vertical motion design spectra are scaled from the horizontal motion design spectra using V/H ratios documented in McGuire et al., (2001). The appropriate ratios are listed in Tables 4-4 (for the WUS) and 4-5 (for the CEUS) of that reference. These ratios are based on the horizontal peak acceleration, which should be taken to be the 10^{-4} URS spectral acceleration at 100 Hz.

An alternative is to conduct a PSHA for vertical motions separately from horizontal motions. If this is done, the same procedures are followed as for horizontal motions. Once the vertical design spectra are obtained, they must be compared to the horizontal design spectra to ensure that consistent motions have been derived.

Damping other than 5%

The procedures above derive design spectra for 5% damping. To obtain spectra for other dampings, three procedures are described in Section 4.9 of McGuire et al., (2001). Any of these three procedures may be used. In these procedures the spectra for other dampings are calculated as multiplicative ratios to the 5% damped spectrum.

Analysis time histories

For analysis, either a single set (3 components) of statistically independent (as defined in McGuire et al., 2001, Section 5.5.3) time histories, or multiple sets may be generated. The time histories must meet the spectral matching criteria described in McGuire et al., (2001), Section 5.6, either individually (for a single set) or in the mean (for multiple sets). These matching criteria are as follows. For a broad-banded spectrum, the 5% damped response spectrum must not be less than 10% below, nor 30% above, the URS, i.e.:

$$0.9*URS < RS < 1.3*URS \quad \text{for } 0.2 \text{ Hz} < f < 25 \text{ Hz}$$

where RS is the 5% damped response spectrum of the artificial record. For spectra represented by two (or more) scaled spectra, an intersection frequency f_c is defined where the two scaled spectra intersect. The criterion for the artificial motion representing the 1 Hz scaled spectrum is:

$$\begin{aligned} 0.9*URS < RS < 1.3*URS & \quad \text{for } 0.2 \text{ Hz} < f < f_c \\ 0.9*DES1 < RS < 1.3*DES1 & \quad \text{for } f_c < f < 25 \text{ Hz} \end{aligned}$$

where DES1 is the spectrum scaled to the URS at 1 Hz. That is, the response spectrum must fall between 90% and 130% of the URS at low frequencies, and between 90% and 130% of the scaled 1 Hz spectrum at high frequencies. Analogous rules apply for the 10 Hz scaled spectrum, DES10:

$$\begin{aligned} 0.9*DES10 < RS < 1.3*DES10 & \quad \text{for } 0.2 \text{ Hz} < f < f_c \\ 0.9*URS < RS < 1.3*URS & \quad \text{for } f_c < f < 25 \text{ Hz} \end{aligned}$$

If three (or more) scaled spectra are used to represent the URS, analogous rules apply for artificial records used to represent each scaled spectrum. That is, in the frequency range represented by a particular scaled spectrum, RS must match the URS, within 90% to 130%. Outside that range, RS must match the scaled spectrum, within 90% to 130%. The check for response spectrum matching is made for 5% of critical damping only.

Spectral matching procedures that require an input motion (basis time history) are preferred since these approaches preserve a realistic phase spectrum and thereby preserve the character of resulting acceleration, velocity, and displacement time histories. Suites of time histories aggregated by **M**, **R**, and site condition bin are available for use as basis motions (McGuire et al., 2001). Alternative motions may be used if justified. Final spectrally matched motions must have appropriate time domain characteristics. Specifically, PGV/PGA and $PGA*PGD/PGV^2$ ratios should be within $\pm 1\sigma$ of bin medians, and durations should be within the bin target ranges (± 1.5 of bin medians). Motions with ratios that fall outside these ranges will be acceptable as long as the difference is documented and justified. For a single 3-component set of motions, each time history should meet these criteria and for multiple sets, median values should be within the specified ranges and the uncertainties should not exceed those of the bin motions.

9.2 Soil sites

Soil sites are those for which a site-specific response analysis is required. The dynamic nonlinear properties (shear wave velocity, modulus reduction and material damping) of the near-surface layers of such soil sites differ significantly from those of rock sites, for which the attenuation equations were derived for use in the PSHA. One alternative is to conduct the PSHA for site-specific conditions (designated "Approach 4" in Section 6.1). In this case, an appropriate profile must be used along with nonlinear properties in developing the site-specific attenuation relations. Also, site-specific variabilities in profile depth, velocities, and layer thicknesses, and dynamic nonlinear material properties, must be included in developing the attenuation relations. Uncertainties in source and path properties should also be modeled, either as aleatory or epistemic uncertainty in the attenuation or in the PSHA. If this method is used, the procedure follows that described in Section 9.1 for rock sites.

For several reasons it may not be desirable to conduct the PSHA for soil conditions. Site-specific soil data may be available only in preliminary form, or different structures at a nuclear facility may rest on different soil properties and/or depths. In these cases it will be appropriate to conduct the PSHA for rock conditions, and then modify the rock results to develop design spectra for the different soil conditions that exist. This means that multiple soil design spectra can be calculated for different structures at a facility, all consistent with a single rock PSHA. Also, soil spectra can be updated at a later time based on additional site-specific data that may be collected.

Defining motions and time histories for rock outcrop as input to soil

For soil design motions developed from rock PSHA, the procedure is outlined in Figure 1-2. The first five steps are similar to those for rock sites, except that the target spectra are scaled to the UHS rather than the URS, because the first goal is to estimate accurate UHS on the soil surface, from which URS can be derived. Control motions corresponding to the target spectra are defined for rock outcrop at the base of the soil column, rather than for rock outcrop at the ground surface. For the CEUS these definitions are identical; for the WUS they differ in that the near-surface highly fractured rock zone is removed to a depth corresponding to the shear-wave velocity at the base of the soil (or to a depth of 150 m [500 ft] in the case of deep profiles). This definition of outcrop rock motion results in rock conditions more reflective of the actual conditions at the base of the soil column. The first five steps are:

- 1) conduct a PSHA for rock conditions.
- 2) deaggregate the mean hazard for 10^{-4} at 10 and 1 Hz.
- 3) define target spectra at 10 and 1 Hz based on spectra (from rock attenuation equations and from the spectral shapes in Section 4 of McGuire et al., 2001) calculated for M and R scaled to the 10^{-4} UHS. These sets of spectra are used for a consistency check on the shape of the rock UHS. Once the UHS has been checked and justified, the scaled spectra from the rock attenuation equations are used as target spectra. If the envelope of these spectra falls more than 10% below the 10^{-4} UHS at any frequency between 0.2 and 100 Hz, the spectra must be increased or an additional spectrum must be added, following the rules described in Section 9.1 for rock sites.

- 4) pick rock time histories from appropriate M and R bins.
- 5) adjust rock time histories to match the target spectra.

For steps 4 and 5, bin time histories from rock records would of course be used for the appropriate region (WUS or CEUS). The subsequent steps to developing soil design motions are as follows.

Site response analysis

We use the spectrally matched rock (i.e. base of soil) time histories as control motions for site response analyses, for horizontal motions (and for vertical motions, if desired). For frequency domain analysis we start with the rock outcrop scaled spectra to define the control motion. Uncertainties in soil depth, velocities, layer thicknesses, and dynamic nonlinear material properties must be modeled. Site response analyses should be performed with the 1 Hz and 10 Hz design spectra to develop mean transfer functions for 10^{-3} , 10^{-4} , and 10^{-5} input motions, and to develop logarithmic standard deviations of soil response at each frequency. This method is labeled "Approach 2A" in Section 6.1. Note that it is *required* to use the two rock outcrop scaled spectra (at 1 and 10 Hz) to calculate soil response, unless one spectrum lies within 10% of the UHS for frequencies between 0.2 to 25 Hz. This requirement is made in order not to drive the soil column with an unrealistically broad-banded motion that will not occur at the site.

Implicit in this process for determining ground spectra (UHS and URS) at soil sites is the requirement to have appropriate nonlinear soil models for use in the site convolution evaluations. These soil models consist of both degradation of shear modulus and increase in hysteretic damping ratio with induced shear strains and have a controlling effect on soil motions at moderate to high loading levels.

It is therefore critical to ensure that where soil models are deduced from laboratory studies, the sampling and testing programs are critically peer reviewed to ensure that the generated soil dynamic nonlinear properties are appropriate to properly characterize site response.

Uniform hazard spectra (UHS)

The UHS on soil is calculated using the method labeled "Approximate Approach 2A/3" in Section 6.2. In this method, the 10^{-4} and 10^{-5} UHS on soil are estimated from equation (6-7b):

$$z_{rp} = a_{rp} \overline{AF}_{rp} \exp\left(\frac{1}{2} k \sigma_8^2 / d_3^2\right) \quad (9-4)$$

where z_{rp} is soil amplitude z associated with return period rp , \overline{AF}_{rp} is the mean amplification factor for the rock motion with return period rp , k and d_3 are derived from the slope of the rock hazard curve and AF, and σ_8 is the log standard deviation of AF. Equation (9-4) is called Approximate Approach 2A/3 in Section 6.

Uniform reliability spectrum (URS)

With estimated 10^{-4} and 10^{-5} UHS on soil, we calculate the ratio A_R at each frequency (see equation (9-1)). We modify the 10^{-4} UHS by the scale factor SF to determine the URS on soil (see equations (9-2) and (9-3)). Note as discussed in connection with equation (9-3) that SF depends on the selection of a desired probability ratio R_p and a minimum seismic margin factor F_{SM} .

Vertical motions

An acceptable procedure for defining vertical motions is as follows. The final soil surface horizontal design spectra is scaled by a suitable generic or site-specific soil V/H ratio, suitable in the sense of an appropriate M , R , and soil condition. For WUS conditions, the use of one or several empirical soil V/H ratios is preferred (see, for example, Figure 6-33). For the CEUS, if appropriate empirical V/H ratios are unavailable, either of the following approaches may be used.

First, the generic soil category CEUS V/H ratios documented in EPRI (1993) may be used. These ratios were developed using a well-validated model, and they have undergone technical review. This method is preferred if the site conditions match those used in EPRI (1993).

Second, the approach used here (Figure 6-34) may be used. This procedure scales a WUS deep soil empirical V/H ratio to CEUS conditions. The scaling must be done by a well-validated model that reproduces the M , R , and site condition dependencies of empirical WUS V/H ratios and also that models V/H ratios at rock sites in the CEUS (McGuire et al., 2001, Sections 6.3 and 6.4). For the CEUS, to assess the reasonableness of results, vertical motions computed using multiple methods are encouraged, particularly if either the 1 Hz or 10 Hz controlling earthquakes are within about 20 to 30 km of the site.

As an alternative to scaling horizontal design motions, site response analyses may be performed for vertical motions, in which case the development of vertical design spectra parallels that for horizontal design spectra.

Damping other than 5%

For soil sites, the procedure for calculating spectra for damping other than 5% is the same as for rock sites.

Analysis time histories

For soil sites, the selection and adjustment of analysis time histories is the same as for rock sites.

REFERENCES

EPRI (1993). *Guidelines for determining design basis ground motions*, Elec. Power Res. Inst., Palo Alto, CA, Rept. TR-102293, 3 vols, Nov.

McGuire, R.K., W.J. Silva, and C.J. Costantino (2001). "Technical Basis for Revision of Regulatory Guidance on Design Ground Motions: Hazard- and Risk-consistent Ground Motion Spectra Guidelines," U.S. Nuclear Reg. Comm., Rept. NUREG/CR-6728, October.

SSHAC (1997). *Recommendations for probabilistic seismic hazard analysis: guidance on uncertainty and use of experts*, Senior Seismic Hazard Analysis Committee (SSHAC), US Nuclear Reg. Comm. Rept. NUREG/CR-6372, 256p, April.

APPENDIX A APPROXIMATE METHOD TO CALCULATE SOIL HAZARD

This approximation to the probability of exceeding a soil amplitude z was derived by G. Toro; it leads to a simple, closed-form expression for the hazard at a soil site. The derivation is made for the case of correlation between deviations of rock amplitude a and the amplification factor AF from their mean values, although the final recommended form simplifies when zero correlation is assumed. Throughout this discussion, the deviations of rock amplitude and soil amplification are assumed to be logarithmic deviations from the mean logarithmic values.

The rock hazard is written as:

$$P[A > a] = \int \int \int P[A > a | m, r, \varepsilon] f_M(m) f_R(r) f_\varepsilon(\varepsilon) dm dr d\varepsilon \quad (\text{A-1})$$

where ε is the logarithmic deviation of rock amplitude and where $P[\cdot]$ within the integrand is either 0 or 1 depending on the values of a , m , r , and ε . If the uncertainty in ground motion is zero, i.e. $\sigma_\varepsilon = 0$, Equation A-1 simplifies to what we can call the "central hazard curve \bar{H} ," as follows:

$$\begin{aligned} \bar{H}(a) &= P[A > a \text{ when } \sigma_\varepsilon = 0] \\ &= \int \int P[A > a | m, r, \sigma_\varepsilon = 0] f_M(m) f_R(r) dm dr \end{aligned} \quad (\text{A-2})$$

If $\sigma_\varepsilon \neq 0$ but is constant over all values of m and r , the following holds:

$$\int \int P[A > a | m, r, \varepsilon] f_M(m) f_R(r) dm dr = \bar{H}(a e^{-\varepsilon}) \quad (\text{A-3})$$

That is, the probability of exceeding a can be calculated from the central hazard curve at amplitude $a e^{-\varepsilon}$. If we assume further that the mean rock hazard curve is linear in log-log space:

$$\bar{H}(a) = c(a)^{-k} \quad (\text{A-4})$$

then we can substitute (A-3) and (A-4) into (A-1) so that the rock hazard can be written:

$$P[A > a] = c a^{-k} \int e^{\varepsilon k} f_\varepsilon(\varepsilon) d\varepsilon \quad (\text{A-5})$$

$$\begin{aligned}
&= ca^{-k} e^{k^2 \sigma_\varepsilon^2 / 2} \\
&= c' a^{-k}
\end{aligned}
\tag{A-6}$$

where $c' = c \exp(k^2 \sigma_\varepsilon^2 / 2)$ and σ_ε is the standard deviation of the logarithmic deviation ε . Equation A-6 implies that hazard curves for $\sigma_\varepsilon = 0$ and $\sigma_\varepsilon \neq 0$ have the same slope, provided σ_ε is constant with a .

We write the soil amplification factor AF as:

$$AF = d_1 a^{-d_2} e^\delta \tag{A-7}$$

where δ is the logarithmic deviation of AF, which might be correlated with ε . The soil amplitude is then:

$$\begin{aligned}
z &= a \cdot AF \\
&= a d_1 a^{-d_2} e^\delta \\
&= d_1 [\bar{a} e^\varepsilon]^{1-d_2} e^\delta
\end{aligned}
\tag{A-8}$$

where \bar{a} is the mean rock amplitude. Solving for \bar{a} gives:

$$\bar{a} = [z e^{-\delta} / d_1]^{1/d_3} e^{-\varepsilon} \tag{A-9}$$

where $d_3 = 1 - d_2$.

We can write the probability of exceeding soil amplitude z as

$$P[A_S > z] = \iint P[\bar{a} > (z e^{-\delta} / d_1)^{1/d_3} e^{-\varepsilon}] f_\varepsilon(\varepsilon) f_\delta(\delta) d\varepsilon d\delta \tag{A-10}$$

The probability in the integrand can be written using equation A.4 as:

$$\begin{aligned}
P[\cdot] &= c [(z e^{-\delta} / d_1)^{1/d_3} e^{-\varepsilon}]^{-k} \\
&= c (z / d_1)^{-k/d_3} e^{k(\delta/d_3 + \varepsilon)}
\end{aligned}
\tag{A-11}$$

This probability depends only on the parameter $y = \delta/d_3 + \varepsilon$, which is normally distributed with mean = 0 and standard deviation:

$$\sigma_y = (\sigma_\varepsilon^2 + \sigma_\delta^2/d_3^2 + 2\rho\sigma_\varepsilon\sigma_\delta/d_3)^{1/2} \quad (\text{A-12})$$

where ρ is the correlation coefficient between ε and δ . In terms of y , equation A-10 can be written:

$$P[A_S > z] = \int e^{ky} c(z/d_1)^{-k/d_3} f_Y(y) dy \quad (\text{A-13})$$

which simplifies to:

$$P[A_S > z] = c(z/d_1)^{-k/d_3} \exp \frac{1}{2} k^2 [\sigma_\varepsilon^2 + \sigma_\delta^2/d_3^2 + 2\rho\sigma_\varepsilon\sigma_\delta/d_3] \quad (\text{A-14})$$

This can be further simplified to:

$$P[A_S > z] = c' [(z/d_1)^{1/d_3}]^{-k} \exp \left\{ \frac{1}{2} k^2 [\sigma_\delta^2/d_3^2 + 2\rho\sigma_\varepsilon\sigma_\delta/d_3] \right\} \quad (\text{A-15})$$

The first two terms on the right side of the equation A-15, $c'[\cdot]^{-k}$, give the rock hazard associated with a rock amplitude of $\frac{z}{\overline{AF}}$ (see equations A-6 and A-9). The third term, $\exp\{\cdot\}$, is a correction for uncertainties in \overline{AF} and for correlation. If the correlation is zero, the soil hazard simplifies to:

$$P[A_S > z] = P[A > \frac{z}{\overline{AF}}] \exp \left\{ \frac{1}{2} k^2 \sigma_\delta^2 / d_3^2 \right\} \quad (\text{A-16})$$

where \overline{AF} is the mean amplification factor.

Further, if the soil uncertainty is constant with amplitude, the soil hazard curve will have slope k/d_3 , and the soil amplitude associated with a given return period (e.g. 10,000 years) can be computed as:

$$z_{10,000} = a_{10,000} \overline{AF}(a_{10,000}) \exp \left(\frac{1}{2} k \sigma_\delta^2 / d_3^2 \right) \quad (\text{A-17})$$

Equation (A-17) provides a simple interpretation of the effects of soil amplification and its uncertainty. The first two terms on the right side of equation (A-17), $a_{10,000} \overline{AF}(a_{10,000})$, give the soil amplitude at 10,000 years for a rock amplitude $a_{10,000}$ and a deterministic (i.e. perfectly known) soil amplification. The last term, $\exp(\cdot)$, is a correction factor that accounts for the slope k of the rock

hazard curve, the uncertainty in soil amplification σ_s , and the change in soil motion with rock motion d_3 . This correction factor is typically in the range 1.05 to 1.25.

APPENDIX B COMPARISON OF HORIZONTAL SOIL RESPONSE USING EQUIVALENT LINEAR AND NONLINEAR METHODS

B.1 Methods of analysis

This section of the report presents results obtained from site response calculations performed using both equivalent linear and fully nonlinear methods of analysis of site response. Calculations were performed for a number of different rock outcrop motions that have been described previously in this report. In all cases, site response evaluations were performed under the simplifying assumption of vertically propagating shear waves moving through a horizontally layered soil column. The analysis therefore is one dimensional, significantly simplifying the response evaluations. This assumption is widely used to estimate surface ground motions and horizontal shear strains developed throughout the soil column. A further benefit from this approach results from the fact that it reduces the complexity of the constitutive models required to define stress-strain properties of the site soils. At any one location in the soil column, one must only be concerned with the shear stress-strain relationship, and the effects of other components of the wave field can be neglected. In addition, the shear properties of the materials can be relatively easily related to test data obtained from relatively simple laboratory tests conducted on soil samples. Of course, the appropriateness of this simplification must be properly evaluated before acceptance of its predictions of site response.

Two separate equivalent linear methods of analysis were used, namely the random vibration model of the RASCAL computer code (Silva and Lee, 1987), in which time histories are defined in terms of power spectral density and conversions between time domain and frequency domain are made in terms of RVT assumptions, and the deterministic method of the CARES computer code (Miller and Costantino, 2000) in which the transfer between time domain and frequency domain is made exactly using Fourier transform calculations. The material constitutive models are assumed to be viscoelastic, and any nonlinearities in site response calculations are treated in an approximate fashion by changing the effective moduli of any soil layer after each calculation based on results from the previous response calculation. The approach is based on the well known procedures presented by Idriss and Seed (1968) and described in many subsequent publications (e.g., Seed and Idriss, 1982; Schnabel, Seed and Lysmer, 1972).

The fully nonlinear analyses were made using the TESS computer code (Pyke, 1984), which performs a deterministic response calculation in the time domain but treats the soil shear stress-strain relation as fully nonlinear throughout the calculation. The shear stress-strain relationship used in TESS is based on the Hardin-Drnevich hyperbolic relationship (Hardin & Drnevich, 1972) modified by the Cundall-Pyke hypothesis (Cundall, 1975; Pyke, 1979) to control cyclic behavior. The soil model simulates in a relatively simple manner the well known shear behavior of degradation of shear modulus and shear strength with cyclic strain levels and change of shape of the shear stress-strain curve with the magnitude of applied cyclic strain. The code also allows evaluation of the impact of saturation on shear behavior, but these features were not used in these calculations.

B.2 Site model

The base case profile of the site soil column analyzed in these calculations is the Imperial Valley soil column described previously. The initial low strain shear wave velocity profile of this site is shown in Figure B-1 in which the site soils extend to a depth of 1000' to bedrock. The bedrock is assumed to have a shear wave velocity of about 3,300 fps. For these site response calculations, the material below this depth is assumed to be a uniform elastic half-space. The low strain shear wave velocity of the site soils vary from 400 fps at the surface to about 2,300 fps immediately above the bedrock contact. For all response calculations using either CARES, RASCAL or TESS programs, an "individual" site response was determined as the mean response resulting from 30 different approximations to the soil column. In each of the 30 cases, properties of the individual soil layers were selected randomly based upon typical values of median and one-sigma percentiles to capture the expected uncertainties of these properties based on typical field results. The variations included variability in low strain shear modulus and damping of each soil layer, thickness of individual soil layers, and total thickness of the soil column. The approach used for selecting specific values of the individual properties is based on the generic results presented by Toro (1997). Variability in shear moduli and damping was assumed to be lognormal while the variability in layer thickness was assumed to be normal.

The variation in total thickness of the soil column for the 30 cases considered in each evaluation extended from 950' to 1050'. For each soil column, surface motions were generated by each analysis (CARES, RASCAL or TESS) and the mean of the surface (5% damped) response spectrum was calculated. The site amplification function was then determined as the ratio (frequency by frequency) of the mean surface spectrum divided by the (5% damped) spectrum of the outcrop motion used as input to the set of calculations. Comparisons of the mean spectrum and site amplification functions from the three approaches were then made.

For the equivalent linear models (CARES and RASCAL) of site response, the viscoelastic soil properties are defined in terms of their low strain shear moduli (or shear velocity) as indicated in Figure B-1 together with the strain degradation properties shown in Figure B-2. As described previously, these degradation properties were determined by inversion methods from recorded site earthquake data. The deeper soils below a depth of 295' were slightly less nonlinear, having both less degradation and damping with peak cyclic shear strain. Soils below 626' were assumed to behave linearly with no degradation considered with shear strain. Calculated shear strains in these lower layers were generally found to be about 0.05% or less.

For the fully nonlinear calculation using TESS, it was first necessary to generate nonlinear soil properties which hopefully closely reproduce the degradation properties developed for the equivalent linear models. This would then allow for a direct comparison of the effects of nonlinear and equivalent linear calculational approaches in the prediction of site response. A sample of the cyclic behavior model assumed in the TESS calculation is shown in Figure B-3 for three different levels of applied cyclic strain. As strain levels increase, the average slope of the shear loops decreases, which simulates the decrease in shear modulus used in the equivalent linear calculation. The increased hysteretic behavior of the loops simulates the increase in cyclic damping ratio with strain

used in the equivalent linear model. The resulting TESS degradation properties depend upon the selection of a number of parameters for each soil layer.

After a number of trial calculations, a set of TESS soil parameters were selected that were used to generate equivalent degradation properties. Figures B-4 and B-5 show comparisons of degradation models developed from the TESS site response calculations with the equivalent linear degradation models used in CARES and RASCAL for the two upper soil models of the soil column. For the deeper linear soils below 626', an additional TESS model was developed that matched the linear low strain shear damping of 0.5% used in the linear calculations. As may be noted from these comparisons, the degradation of shear modulus for the linear and nonlinear analyses are reasonably close for shear strain levels below about 1%. However, it was found that with these selected parameters, the resulting hysteretic soil damping moduli in the TESS model were about double the values used in the equivalent damping model for effective soil strains above about 0.1%. In the TESS nonlinear soil model, it was difficult to match results of both shear modulus and hysteretic damping. Since the degradation in shear modulus was considered to be most significant to site response, the parameters that best fit these properties were selected for use.

B.3 Initial computations

In the initial set of calculations performed for this evaluation, the rock outcrop motion used as input to the soil columns was defined in terms of a 5% damped Uniform Hazard Spectrum (UHS) with a PGA of almost 1g. A time history was generated that closely enveloped this spectrum and had a total duration of 20 seconds with a strong motion duration (time from 5% to 75% Arias intensity) of about 6 seconds. This input motion was then used as an outcrop input to the 30 soil columns in each set of calculations, and mean surface spectra were generated. The results obtain from the 30 CARES equivalent linear runs are shown in Figure B-6 and these are considered as typical results from this exercise. The mean surface spectrum computed from either the average of the individual spectra or the average of the logs of the individual spectra is essentially the same across the frequency range considered. Figure B-7 presents a comparison of the mean spectra generated from the two equivalent linear calculations and indicates very similar results. The smoothness of the calculated RASCAL spectrum as compared with the deterministic CARES spectrum results from the assumed smoothness in the RVT conversion of time histories to the frequency domain as opposed to the deterministic calculation in CARES. Figure B-8 presents results comparing the CARES equivalent linear response with the nonlinear TESS calculations while Figure B-9 is a similar comparison of the CARES, RASCAL with the TESS calculations. These figures generally indicate that the equivalent linear assumptions tend to amplify surface responses as compared to the nonlinear calculation, particularly at the higher frequencies above 10 Hz. This behavior at the higher frequencies probably results from the significantly higher equivalent damping embedded within the TESS soil models.

B.4 Revised input motions for WUS sites

Following this initial set of calculations, revised calculations were made using new rock outcrop site motions associated with new UHS definitions and with new spectra for characteristic events associated with this new UHS. These characteristic spectra were then scaled back to the UHS at frequencies of 1 Hz and 10 Hz as is currently recommended for development of design response

spectra. Figure B-10 presents these various outcrop spectra considered in these revised site response calculations. It should be noted that the low magnitude characteristic event, when scaled back to the UHS at 1 Hz, leads to the relatively high rock outcrop motion for frequencies greater than 1 Hz, with a PGA significantly higher than 1g.

The first set of calculations performed with CARES, RASCAL and TESS was for the case of an input rock outcrop motion defined by the new UHS spectrum. Again, an artificial time history was generated that closely envelops this target spectrum and that has duration estimates similar to the mean magnitude event (M6.7) associated with the UHS. Figure B-11 presents the mean surface spectra results generated from the CARES and RASCAL equivalent linear methods of analysis. These results are similar to those previously described, with the deterministic CARES and RVT RASCAL approaches yielding similar estimates of surface spectra over the entire frequency range of interest. Again, the CARES spectra are "hashier" than the RASCAL results due to the greater variability in the time/frequency domain transfer in the deterministic approach as opposed to the RVT model. Figures B-12 and B-13 present similar comparisons of the equivalent linear and nonlinear TESS results for the same outcrop input motion. Again, the comparison indicates that the equivalent linear models overpredict the surface motions as compared to the nonlinear model, particularly at frequencies above 10 Hz. Figure B-14 presents comparisons of the spectral ratios (defined as the mean surface spectral acceleration divided by the corresponding outcrop spectral acceleration, all calculated for 5% equipment damping) for the three methods of analyses. The spectral ratios from the nonlinear calculation are lower than the equivalent linear results, particularly at frequencies above 10 Hz.

Figures B-15 through B-18 present similar results obtained for the case of the rock outcrop spectrum defined from the time history which closely envelops the high magnitude event (M7.8) scaled to the UHS spectrum at 1 Hz. As can be noted in Figure B-10, this spectrum is similar in shape and magnitude to the UHS spectrum. The results from the site response calculations lead to similar conclusions as mentioned for the results using the UHS rock outcrop. Figures B-19 through B-21 present results of spectral ratios determined for the median magnitude (6.7) and low magnitude (5.1) outcrop motion scaled back to the UHS at 1 Hz as well as the high magnitude (7.8) event scaled back to the UHS at 10 Hz. Again, the results for the low magnitude event scaled back to the UHS at 1 Hz leads to the highest outcrop input motions at frequencies above 1 Hz, although its spectral accelerations at frequencies below 1 Hz are lower than the UHS. Since these soil columns have their fundamental frequency significantly lower than 1 Hz (mean value about 0.4 Hz), the expected responses relative to the UHS cannot be predicted directly.

The spectral ratios in Figures B-22 through B-24 have similar characteristics to those previously described for the UHS case although some differences in magnitude of these ratios can be noted depending upon the input outcrop motions used. Figure B-22 presents a comparison of the spectral ratios obtained from the CARES equivalent linear computations, Figure B.23 presents a comparison from the RASCAL computations while Figure B.24 presents results from the nonlinear TESS computations. These plots show that the characteristic behavior from the three approaches is relatively similar, with the low magnitude event scaled back to the UHS at 1 Hz always resulting in lower amplifications at the higher frequency range. As was indicated previously, this rock outcrop motion has significantly higher input accelerations than the other characteristic events.

B.5 Conclusions

The results from these many site response calculations performed for this deep soil column, which extends to a depth of over 1,000' to bedrock, can be summarized with two primary conclusions. First, the equivalent linear methods of analysis based upon either deterministic (CARES, SHAKE, etc.) or RVT approaches lead to very similar estimates of site response over the entire frequency range of interest. Second, the fully nonlinear calculation from the TESS soil model leads to generally lower estimates of site response over the entire frequency range of interest, but particularly at frequencies above 10 Hz. Spectral ratios at frequencies above 10 Hz are about 30% lower in the fully nonlinear calculation as compared to the equivalent linear models. This is primarily the result of the higher effective soil damping used in the stress-strain model contained in TESS.

REFERENCES

- Cundall, P.O. (1975). "Quake - A Computer Program to Model Shear Wave Propagation in a Hysteretic, Layered Site," Technical Note, Dames & Moore, ATG London.
- Hardin, B.O. and V.P. Drnevich (1972). "Shear Modulus and Damping in Soils: Design Equations and Curves", Proc. ASCE, vol 98, no. SM7, July.
- Idriss, I.M. and H.B. Seed (1968). "Seismic Response of Horizontal Soil Layers," Journal, Soil Mechanics and Foundation Engineering, vol. 94, no. SM4, pp. 1003-1031.
- Miller, C.A. and C.J. Costantino (2000), "CARES, (Computer Analysis for Rapid Evaluation of Structures)," Version 1.3, Costantino, Miller and Associates for Office of Nuclear Regulatory Research, U.S. Nuclear Regulatory Commission.
- Pyke, R. (1984). "TESS1, A Computer Program for Nonlinear Ground Response Analysis", TAGA Engineering Software Services, Berkeley CA.
- Pyke, R.M. (1979). "Nonlinear Soil Model for Irregular Cyclic Loadings," Journal, Geotechnical Engineering, ASCE, vol 105, pp. 715-726.
- Schnabel, P.B., H.B. Seed, and J. Lysmer, (1972). "Modification of Seismograph Records for Effects of Local Soil Conditions", Report No. EERC 71-8, UC Berkeley, Dec.
- Seed, H.B. and Idriss, I.M. (1982). "Ground motions and soil liquefaction during earthquakes", Monograph Series, EERI, Berkeley.
- Silva, W.J. and K. Lee, (1987). "*WES RASCAL code for synthesizing earthquake ground motions.*" State-of-the-Art for Assessing Earthquake Hazards in the United States, Report 24, U.S. Army Engineers Waterways Experiment Station, Miscellaneous Paper S-73-1.

Silva, W.J., N. Abrahamson, G. Toro, C. Costantino (1997). "Description and validation of the stochastic ground motion model." Report to Brookhaven National Laboratory, Associated Universities, Inc. Upton, New York, Contract 770573.

Toro, G.R. (1997). "Probabilistic Models of Site Velocity Profiles for Generic and Site-Specific Ground Motion Amplification Studies." Published as an appendix in Silva et al (1997).

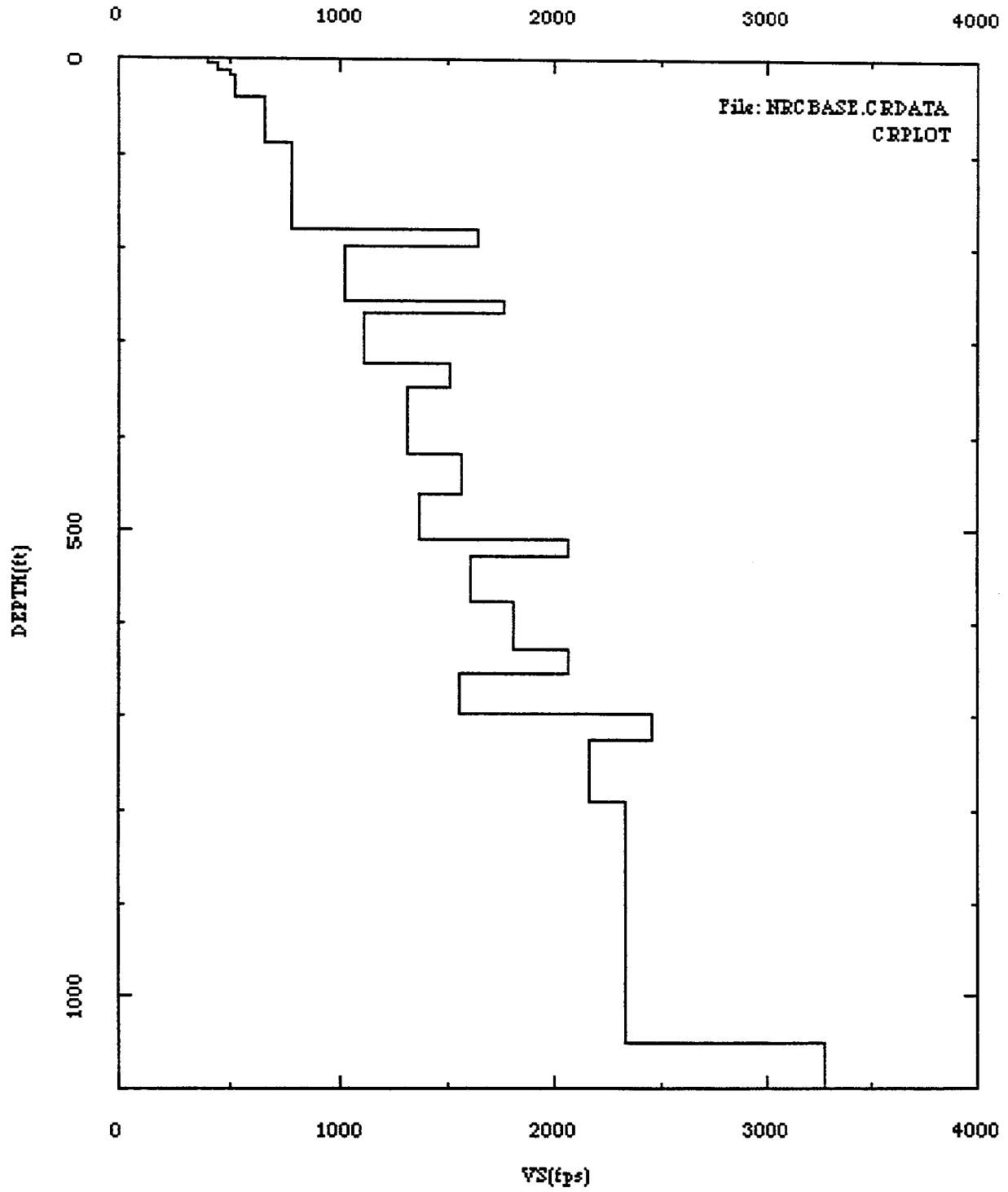


Figure B-1. Initial shear modulus for Imperial Valley soil column.

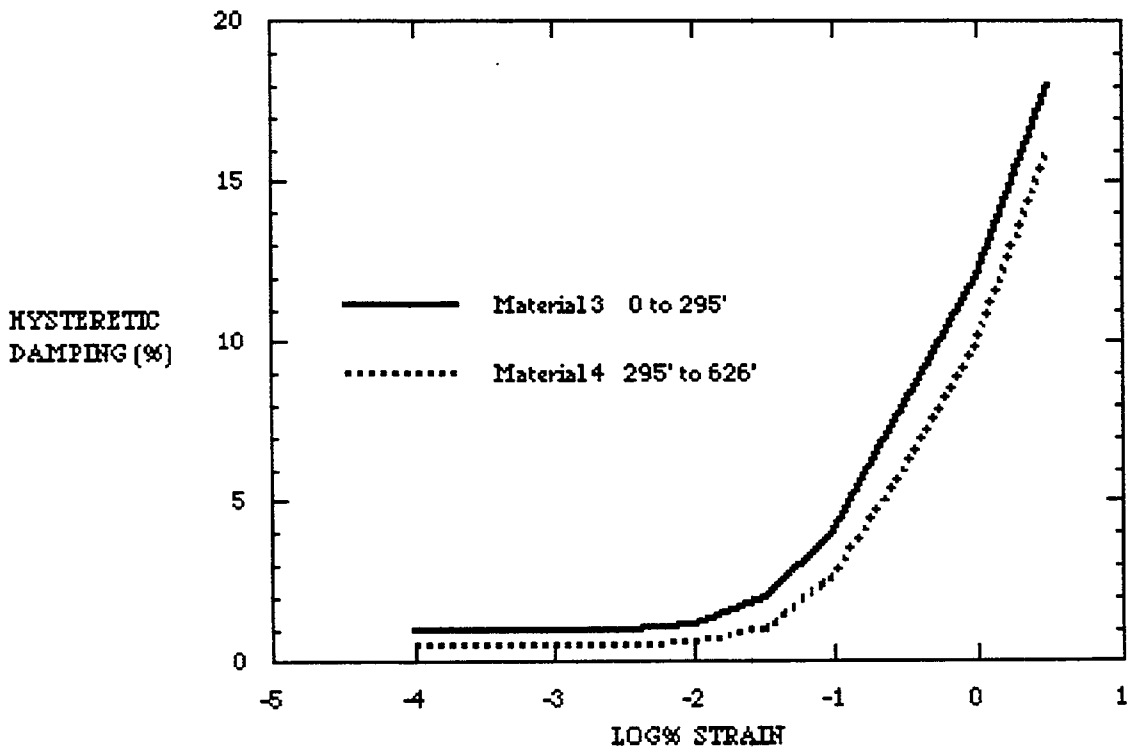
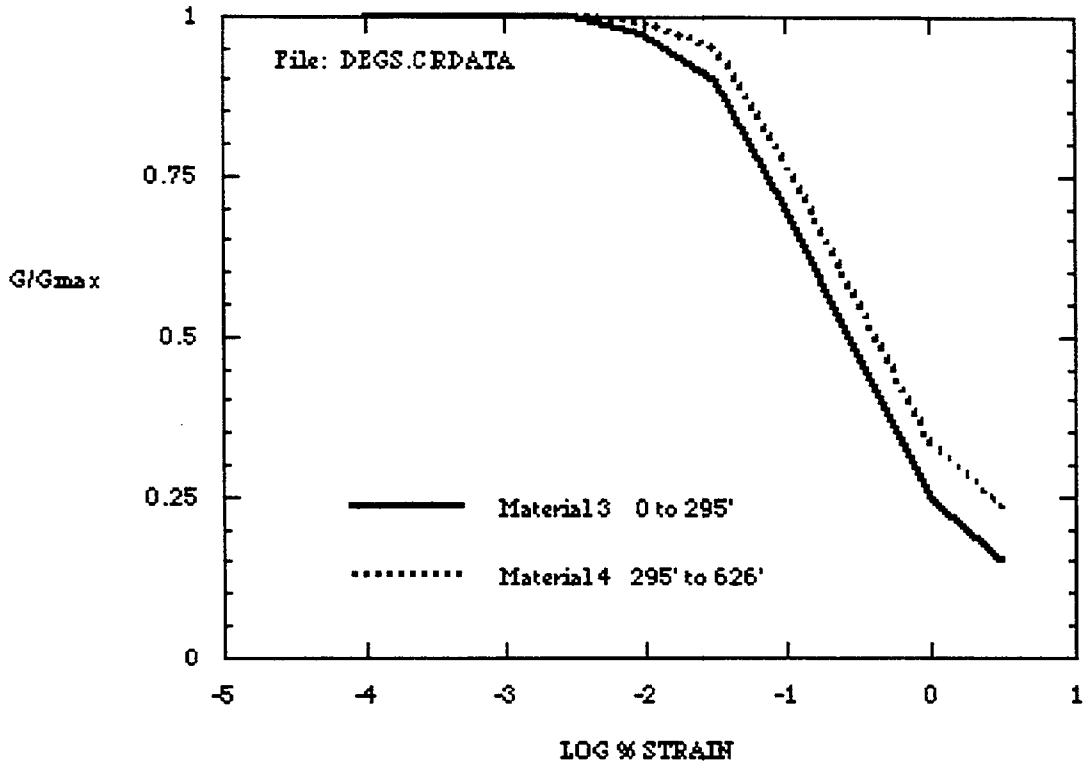


Figure B-2. Imperial Valley degradation model.

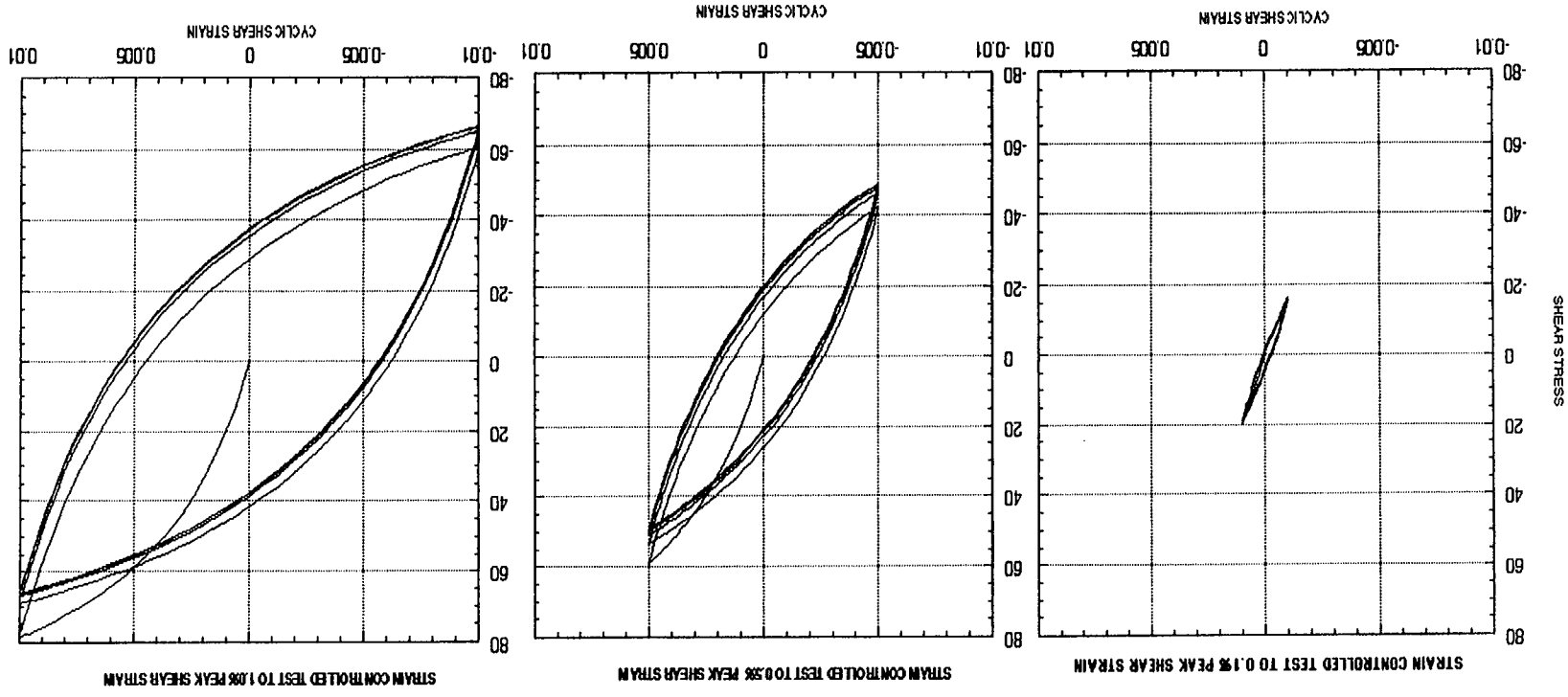


Figure B-3. Cyclic behavior for 5 cycles of loading for strain-controlled cyclic shear test; reference strain = 0.5%.

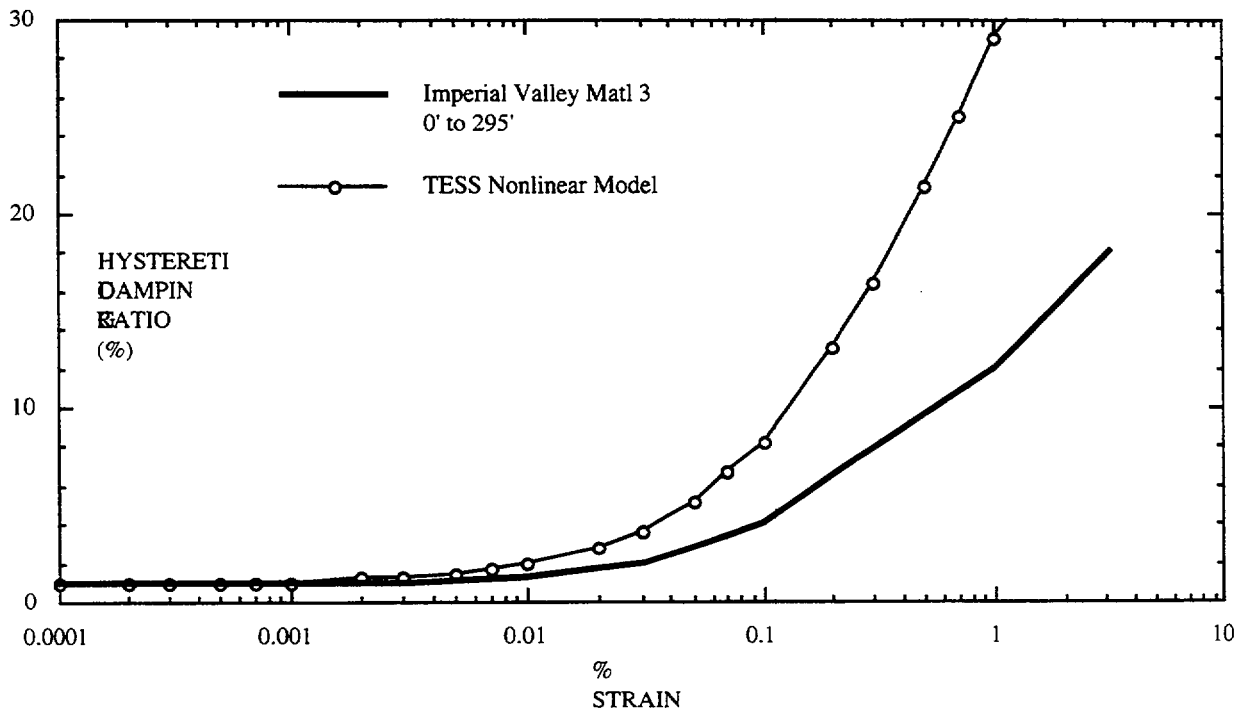
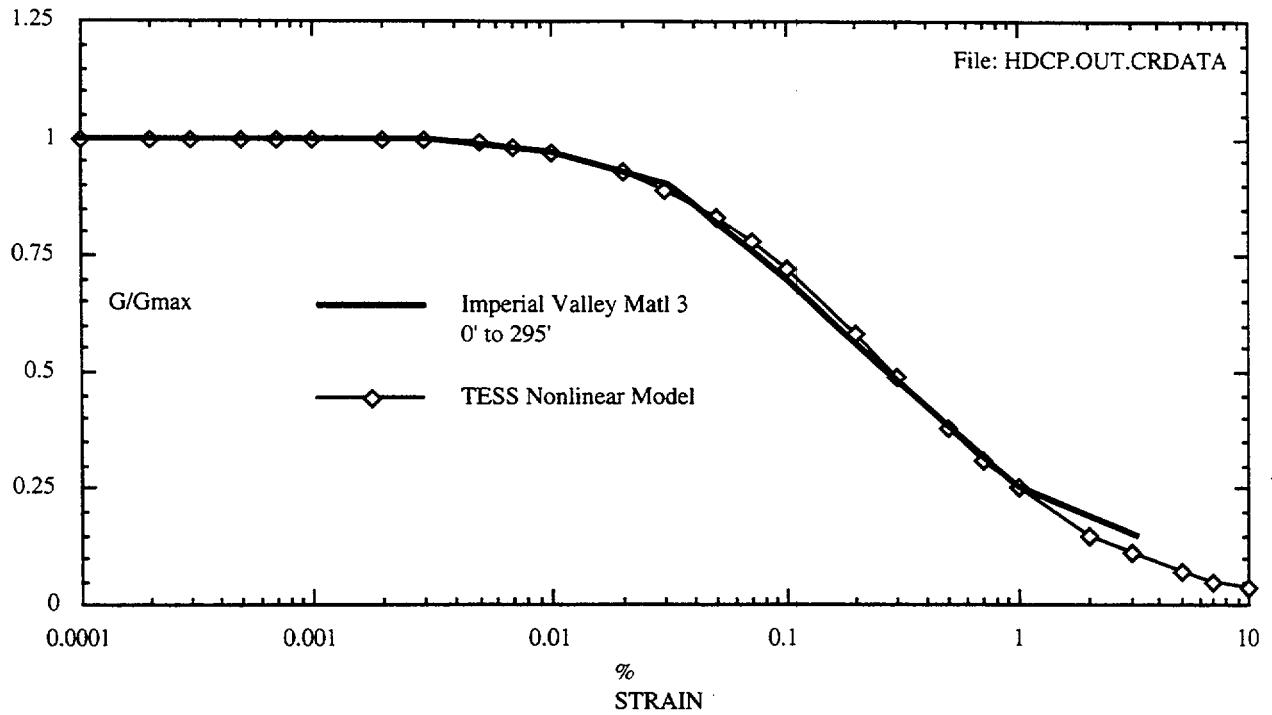


Figure B-4. Comparison of nonlinear degradation model with equivalent linear assumption for Imperial Valley near-surface soils from 0' to 295'.

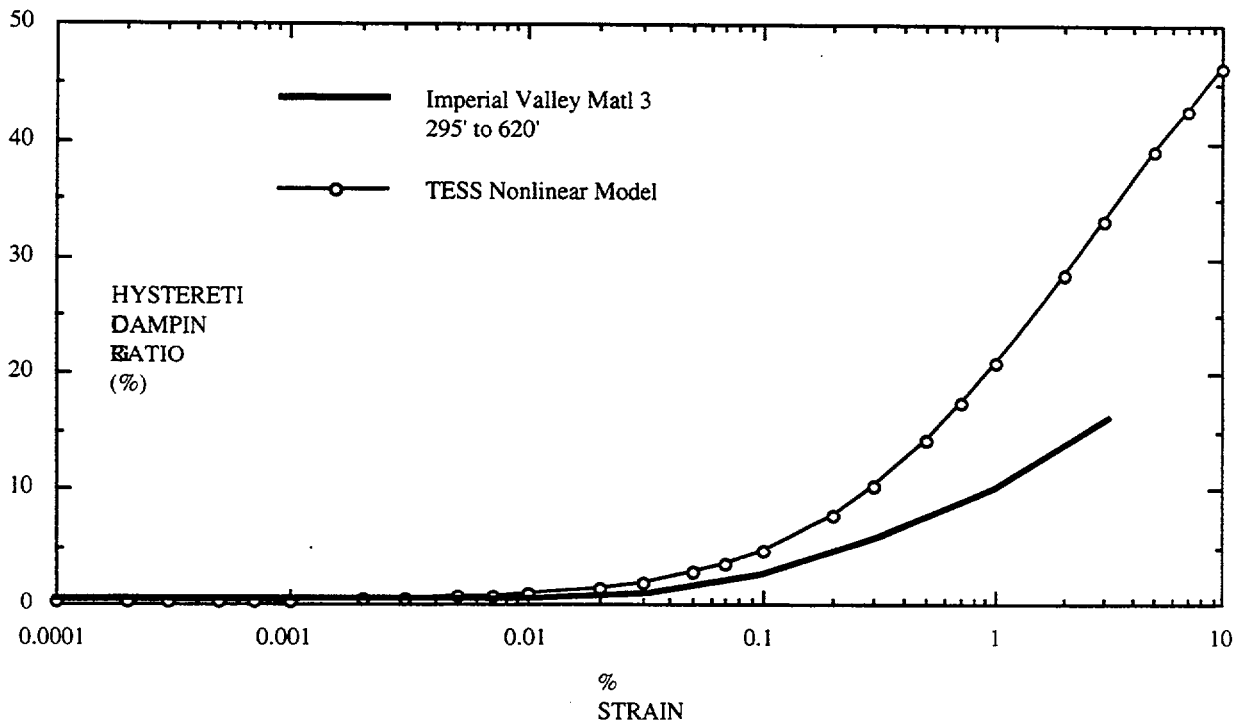
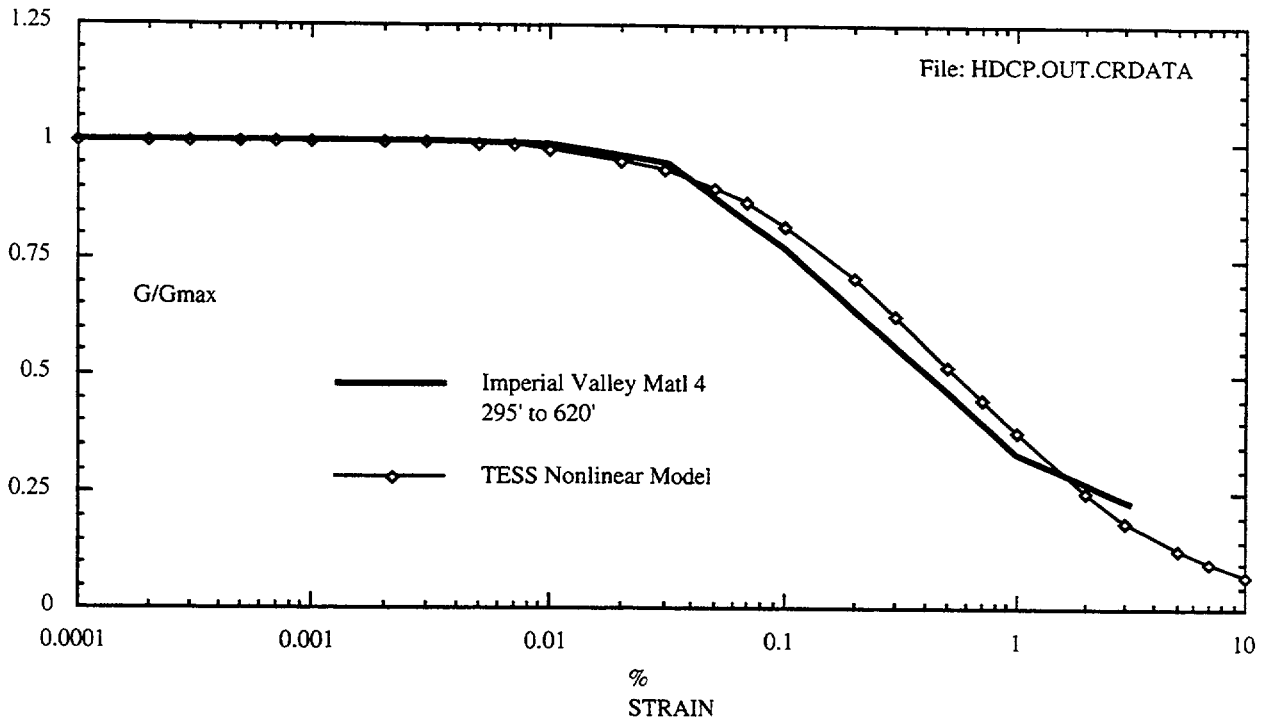


Figure B-5. Comparison of nonlinear degradation model with equivalent linear assumption for Imperial Valley deep soils from 295' to 626'.

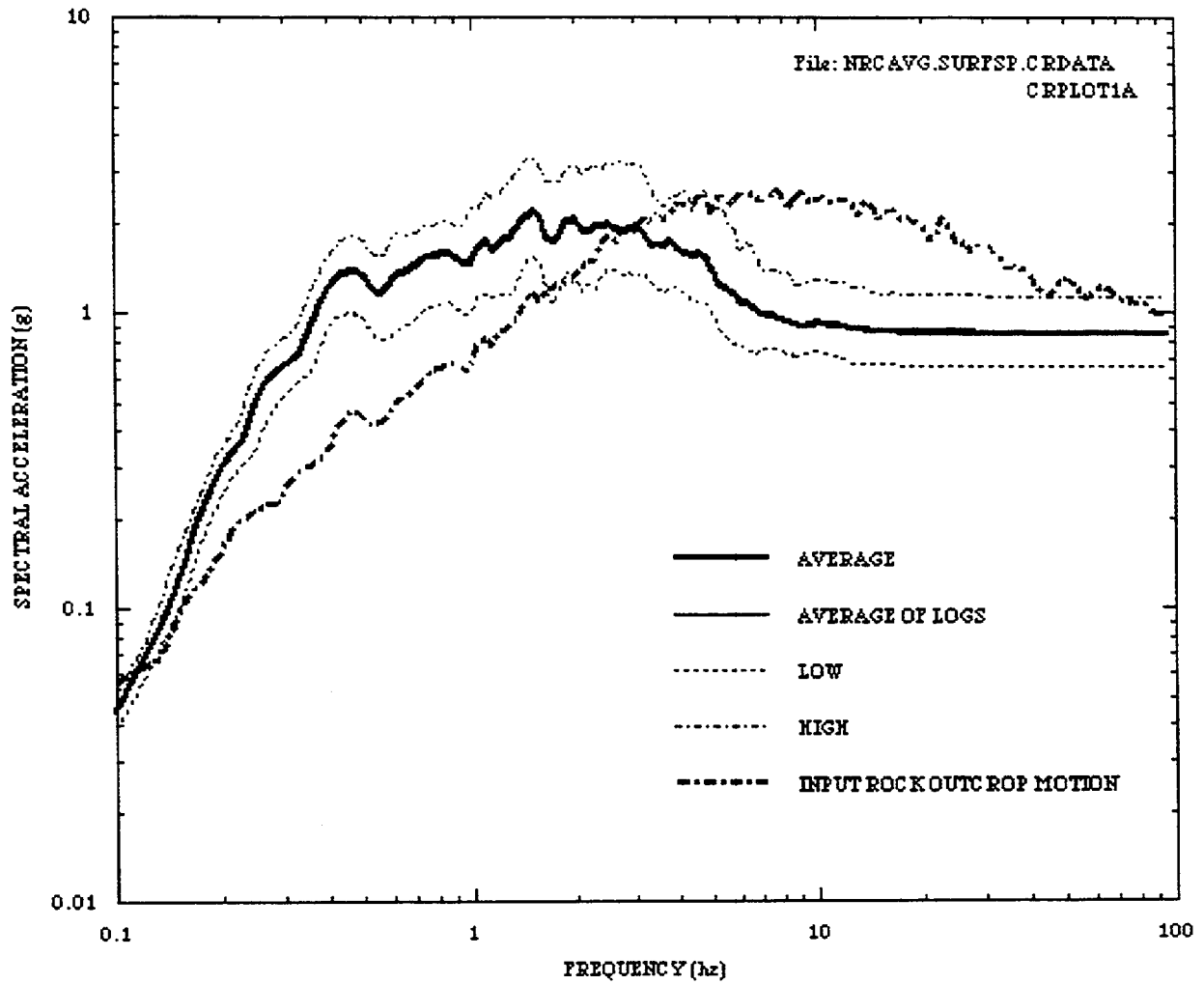


Figure B-6. Mean 5% damped surface spectra for Imperial Valley site column from 30 runs using UHS rock outcrop (CARES equivalent linear time domain solution).

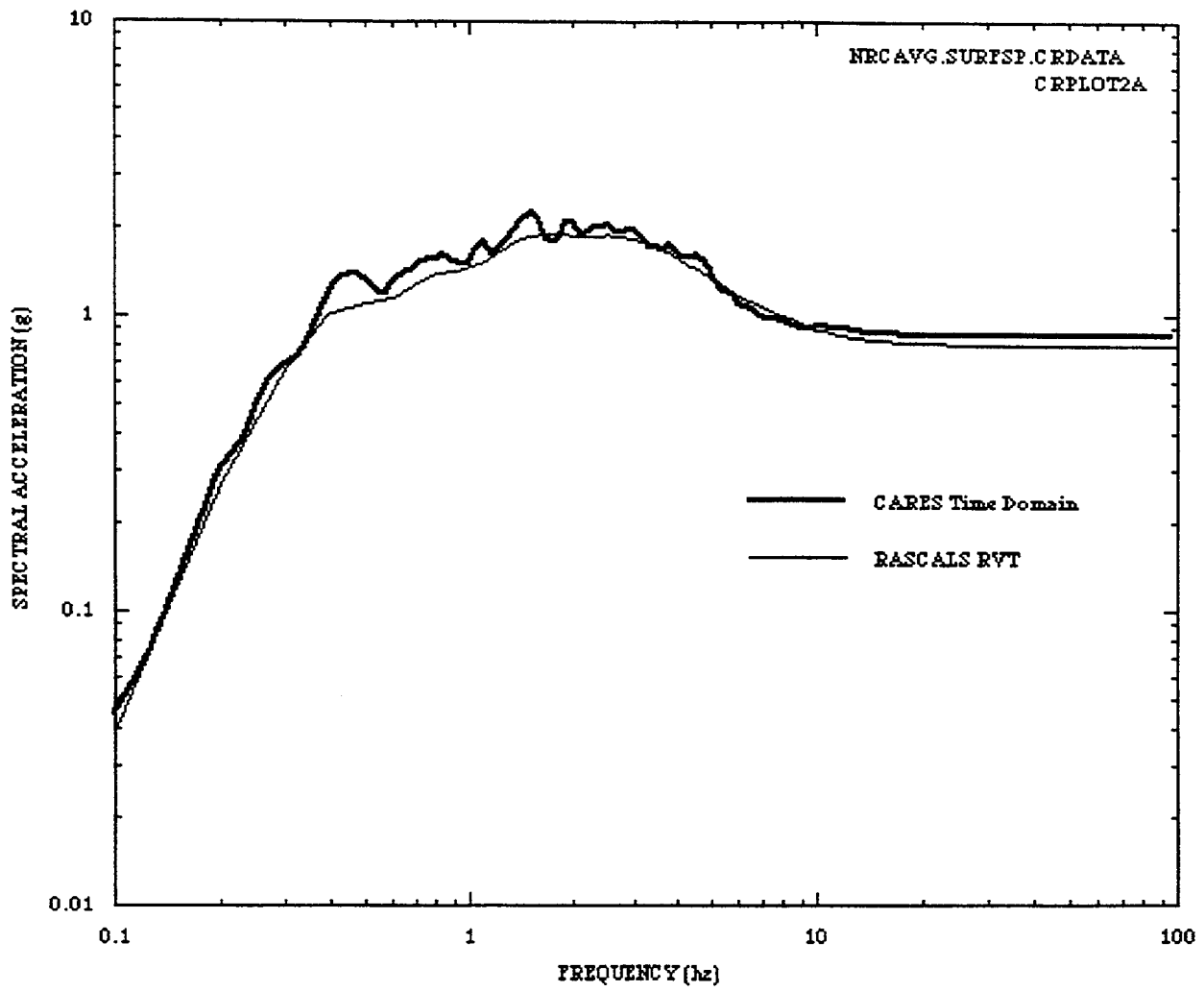


Figure B-7. Comparison of equivalent linear models: mean 5% damped surface spectra Imperial Valley site column from 30 runs using UHS rock outcrop.

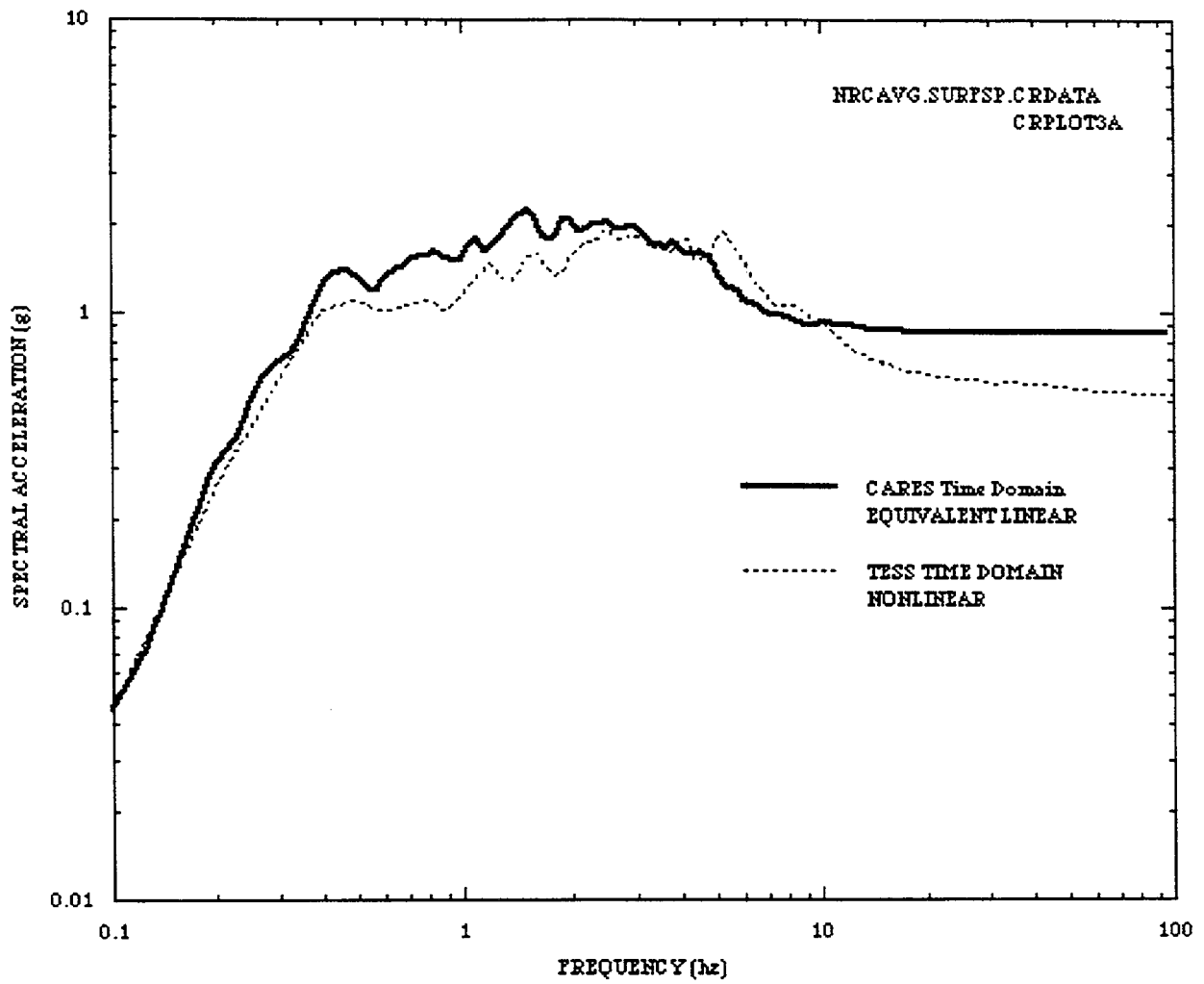


Figure B-8. Comparison of CARES equivalent linear with TESS nonlinear mean 5% damped surface spectra Imperial Valley site column from 30 runs UHS rock outcrop.

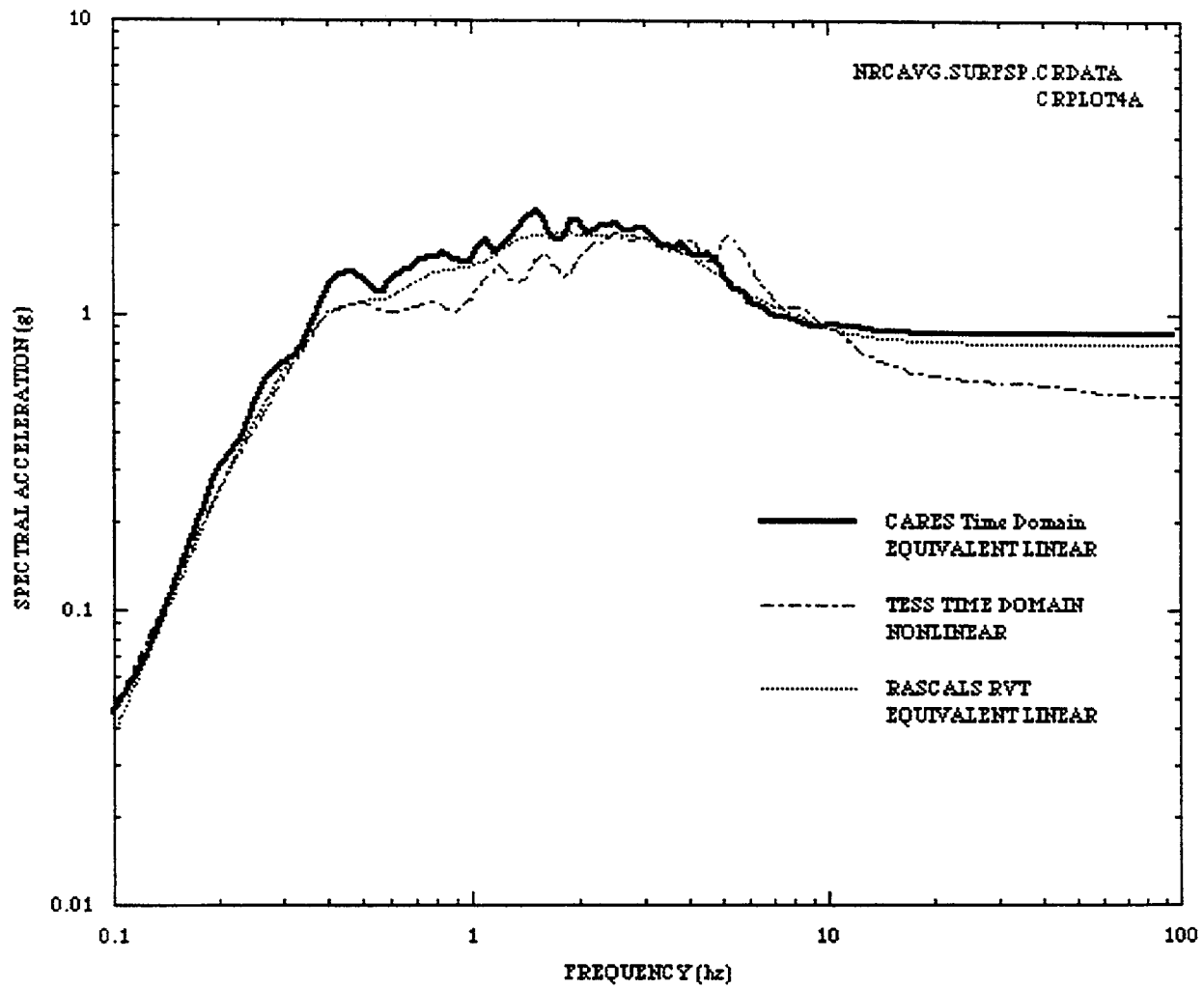


Figure B-9. Comparison of RASCAL equivalent linear with TESS nonlinear mean 5% damped surface spectra Imperial Valley site column from 30 runs UHS rock outcrop.

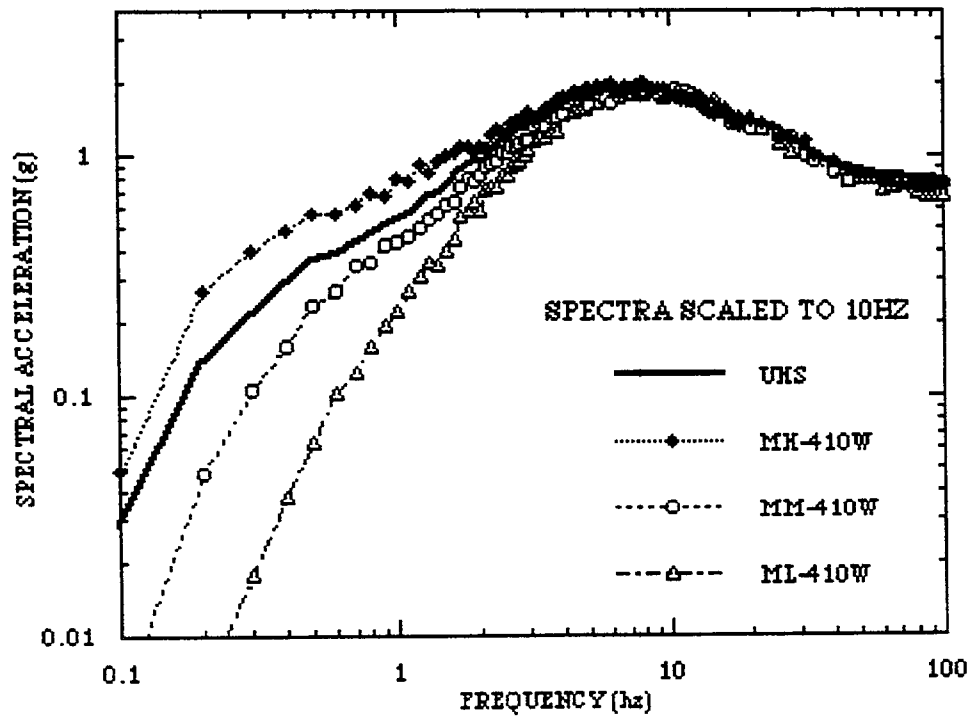
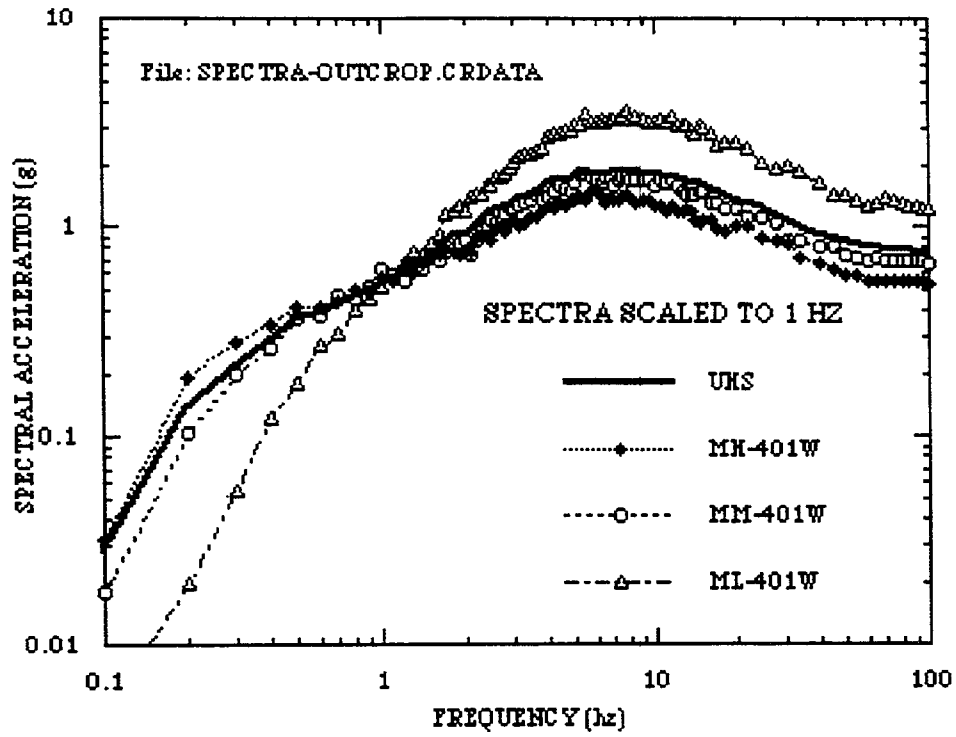


Figure B-10. 5% damped outcrop spectra definitions.

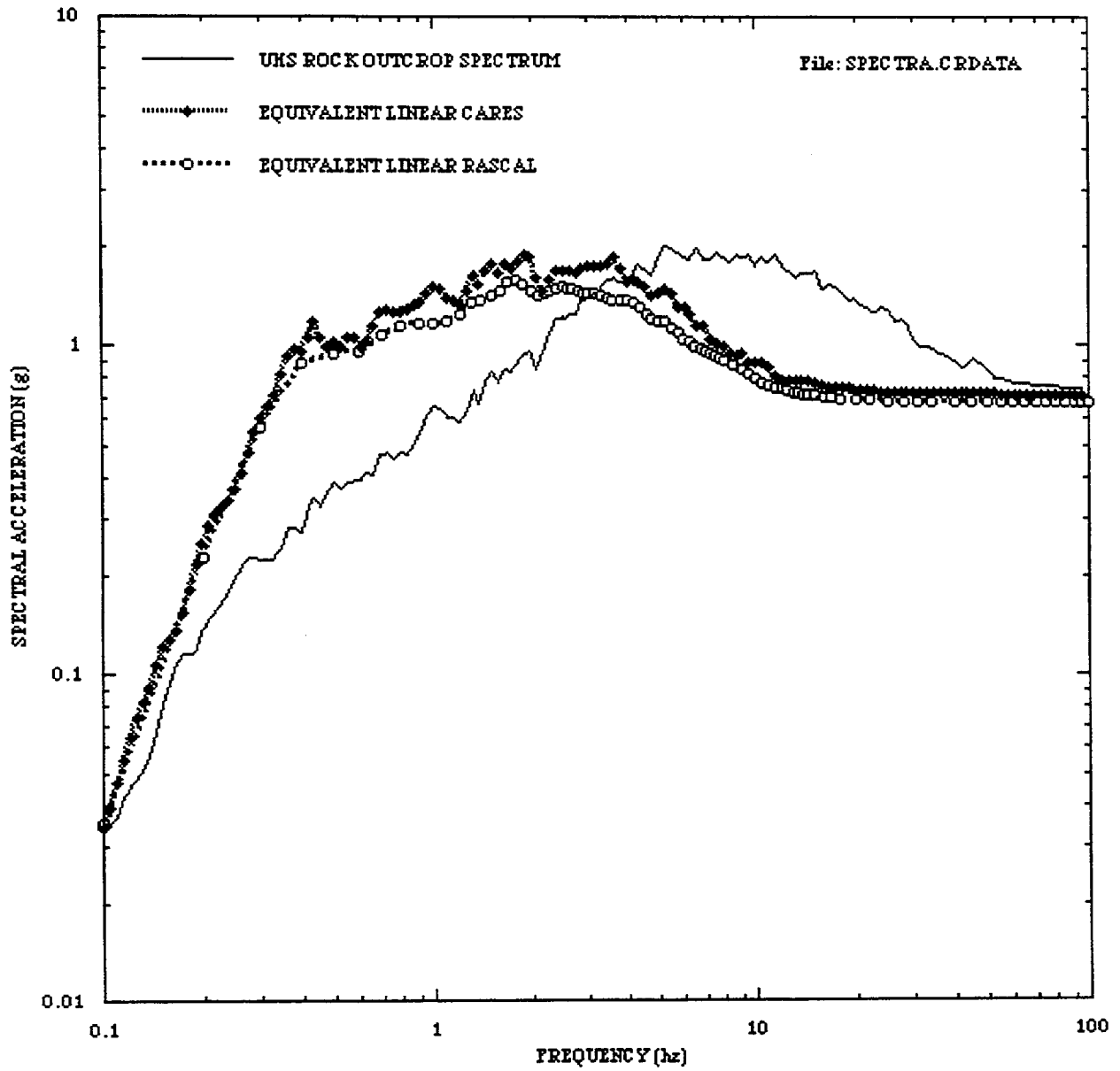


Figure B-11. Comparison of mean surface spectra for Imperial Valley soil columns from equivalent linear CARES and RASCAL calculations (UHS rock outcrop).

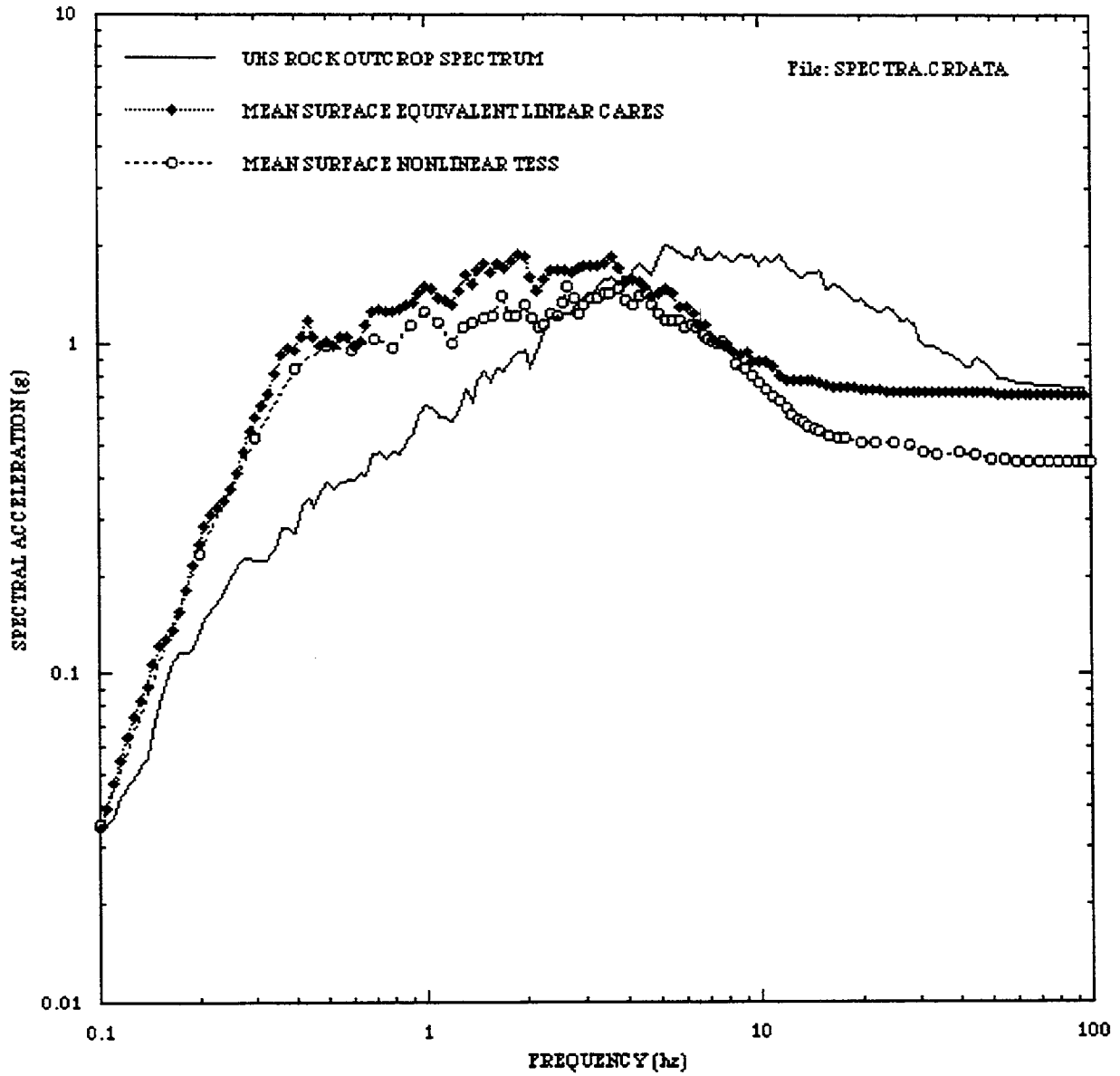


Figure B-12. Mean surface spectra for Imperial Valley soil columns from equivalent linear CARES and nonlinear TESS calculations (UHS rock outcrop motion).

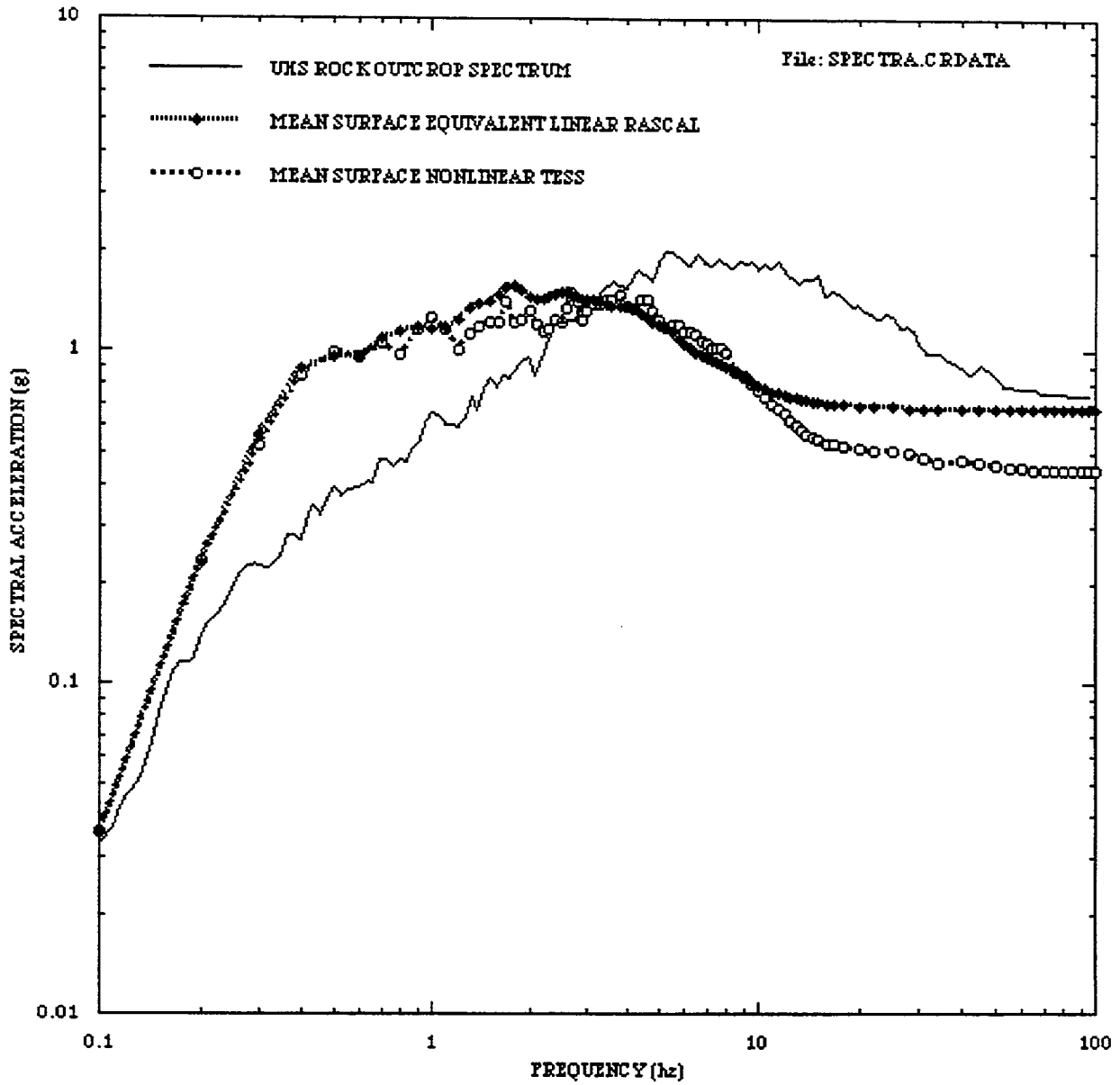


Figure B-13. Comparison of mean surface spectra for Imperial Valley soil columns from equivalent linear RASCAL and nonlinear TESS calculation (UHS rock outcrop).

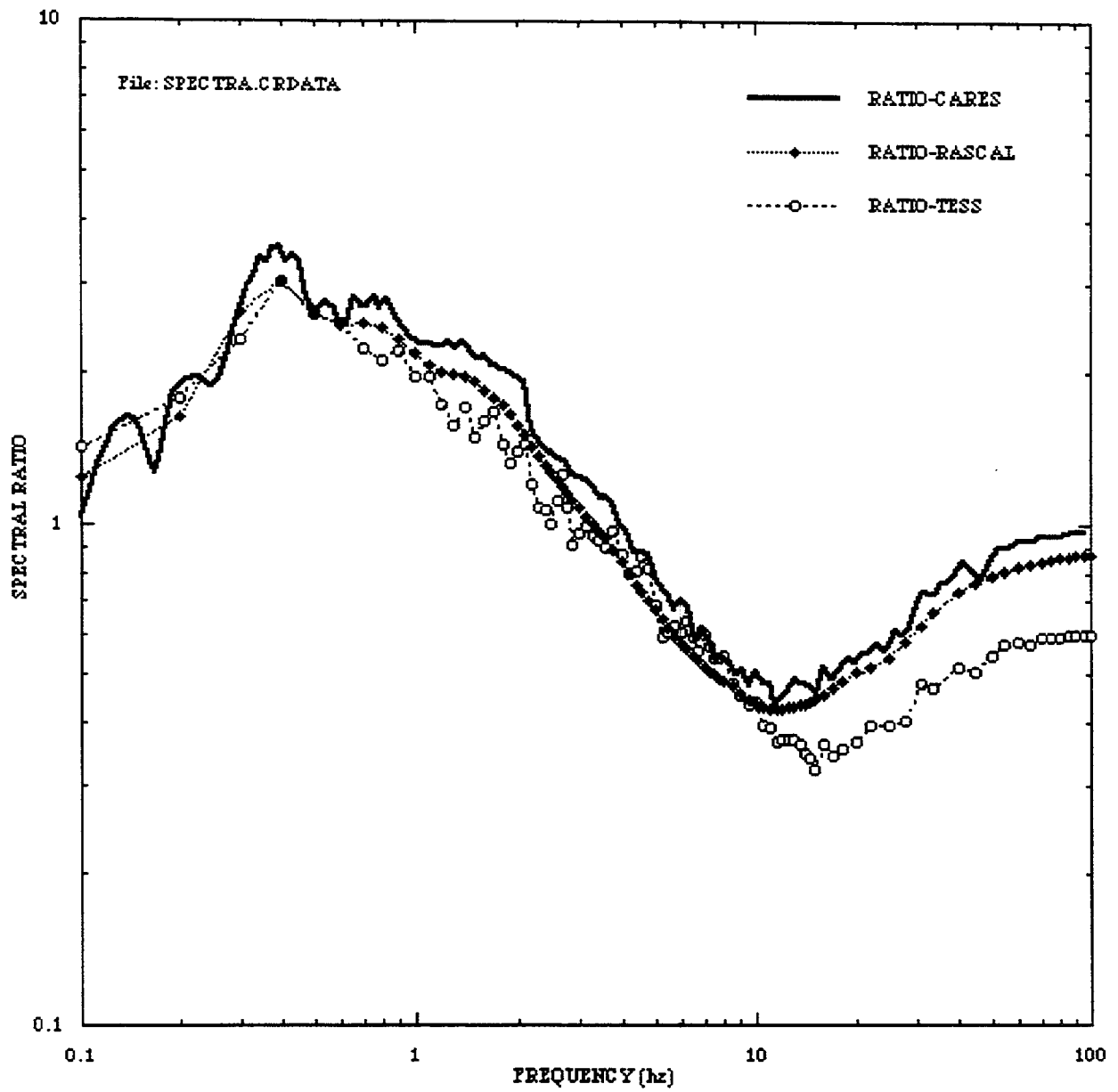


Figure B-14. Mean spectral ratios for Imperial Valley soil columns from CARES, RASCAL and TESS computations for UHS bedrock outcrop input motions.

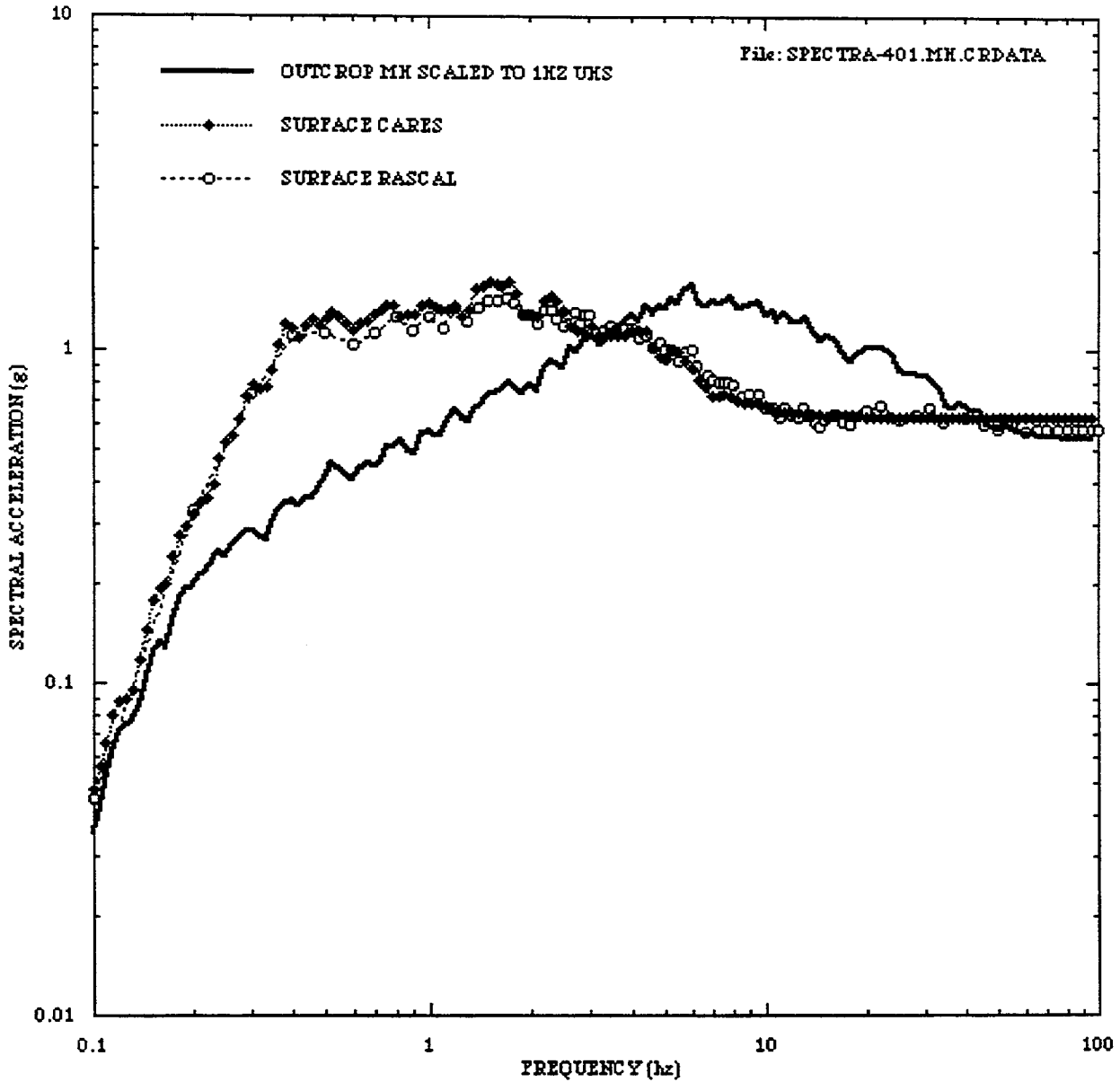


Figure B-15. 5% damped surface spectra for Imperial Valley soil columns from equivalent linear CARES and RASCAL runs for high magnitude event scaled to 1 Hz UHS spectrum.

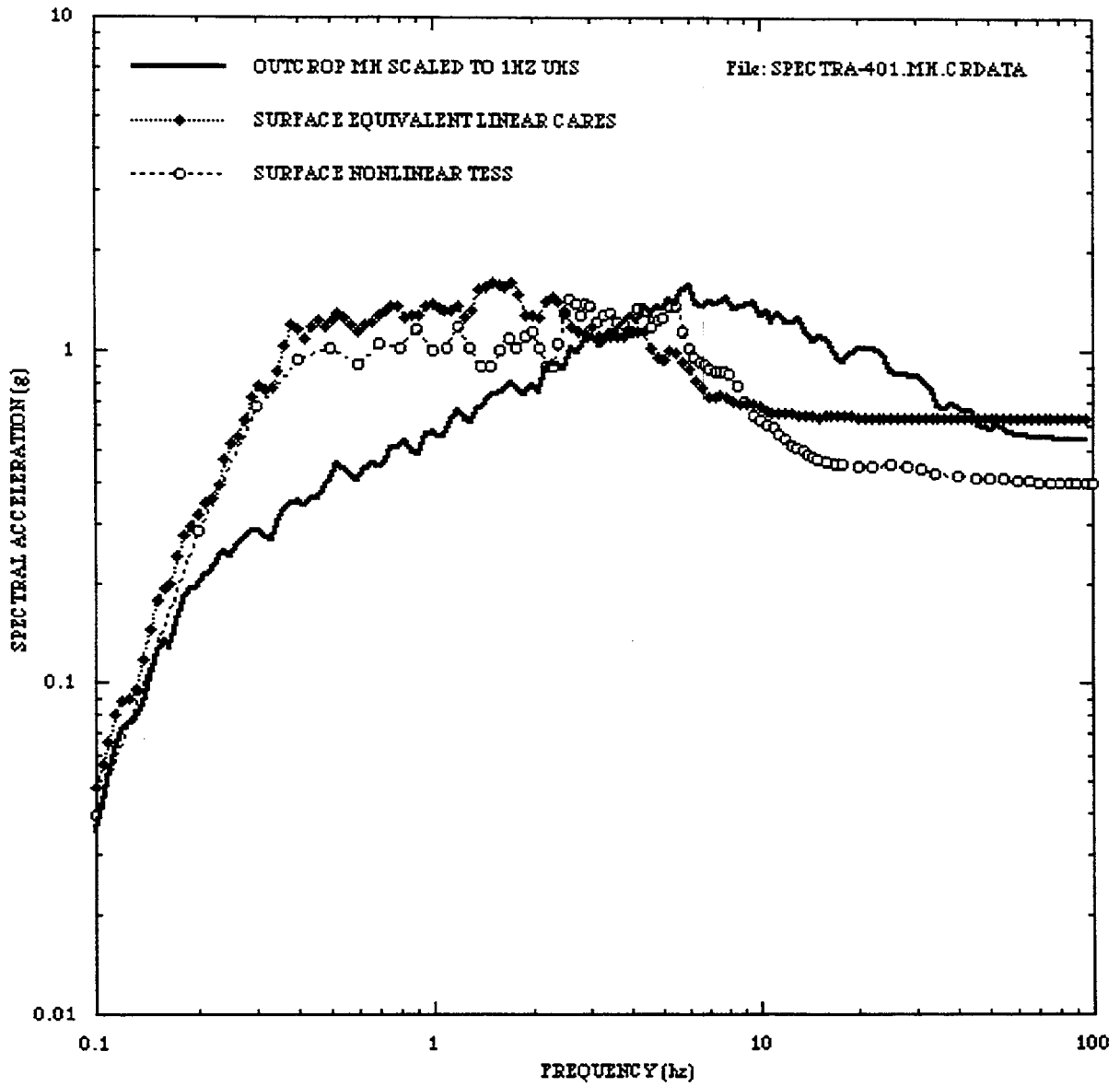


Figure B-16. 5% damped surface spectra for Imperial Valley soil columns from equivalent linear CARES and nonlinear TESS runs for high magnitude event scaled to 1 Hz UHS spectrum.

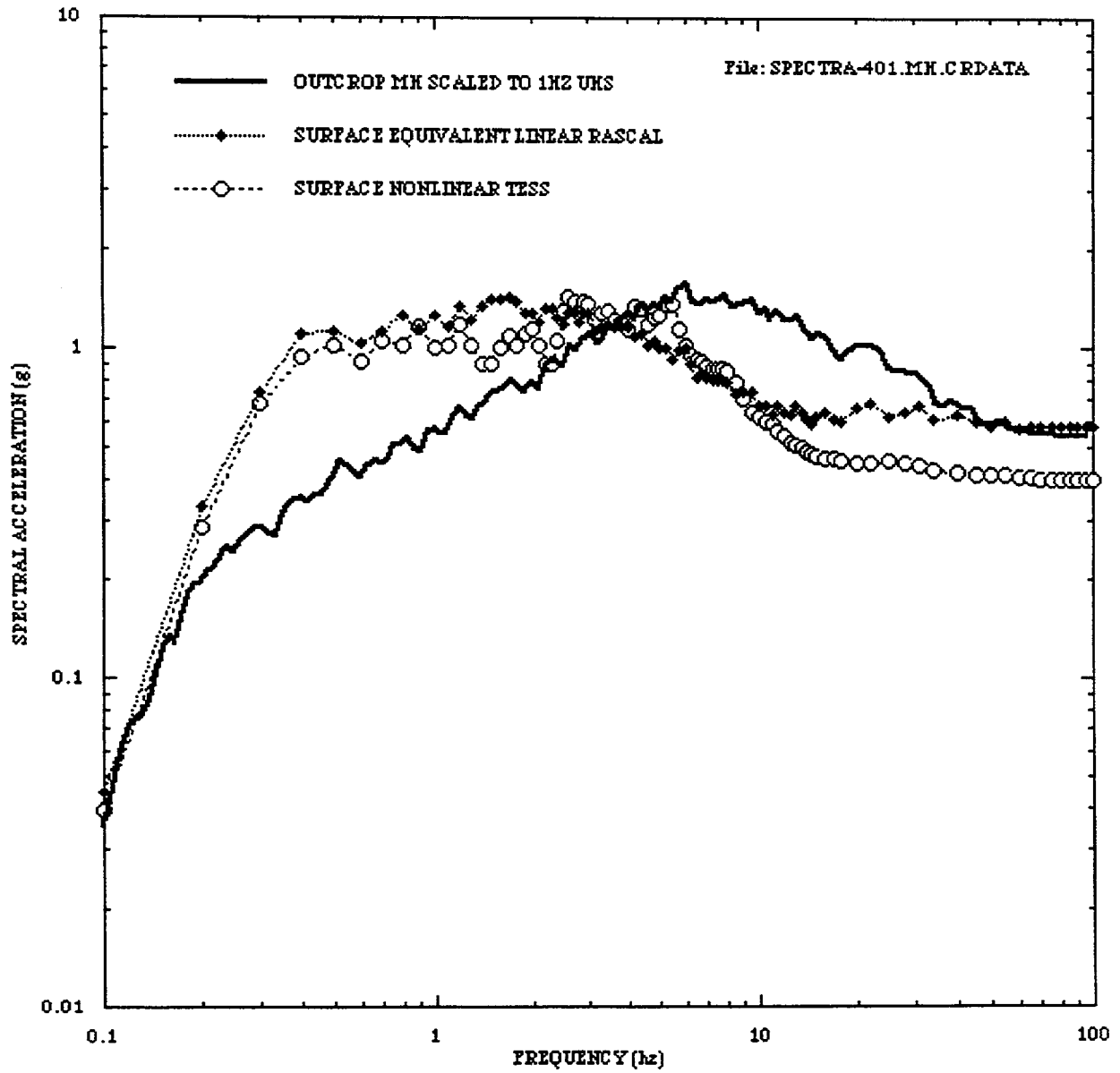


Figure B-17. 5% damped surface spectra for Imperial Valley soil columns from equivalent linear RASCAL and nonlinear TESS runs for high magnitude event scaled to 1 Hz UHS spectrum.

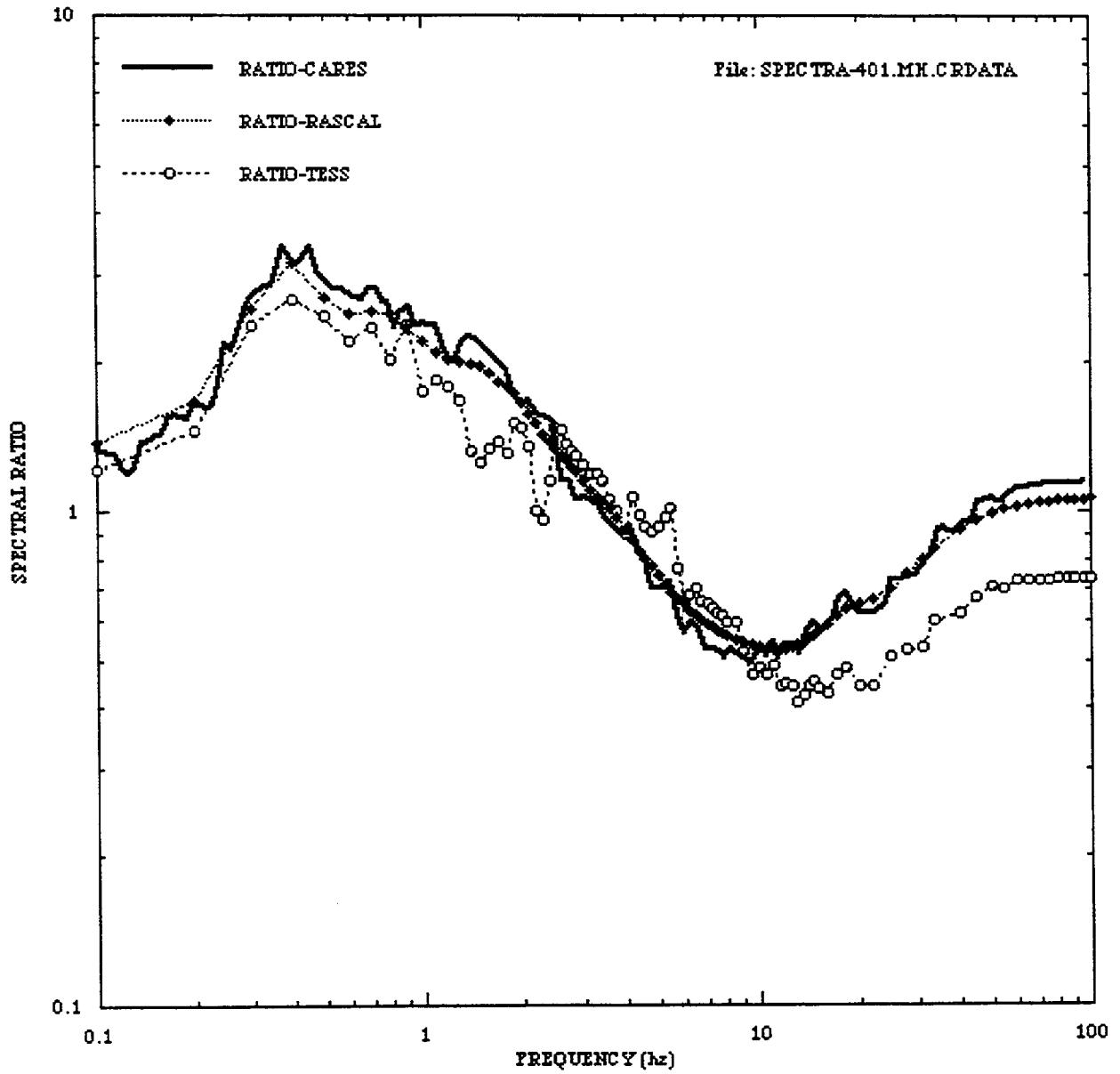


Figure B-18. Mean 5% damped spectral ratios for Imperial Valley soil columns from high magnitude event scaled to 1 Hz UHS spectrum.

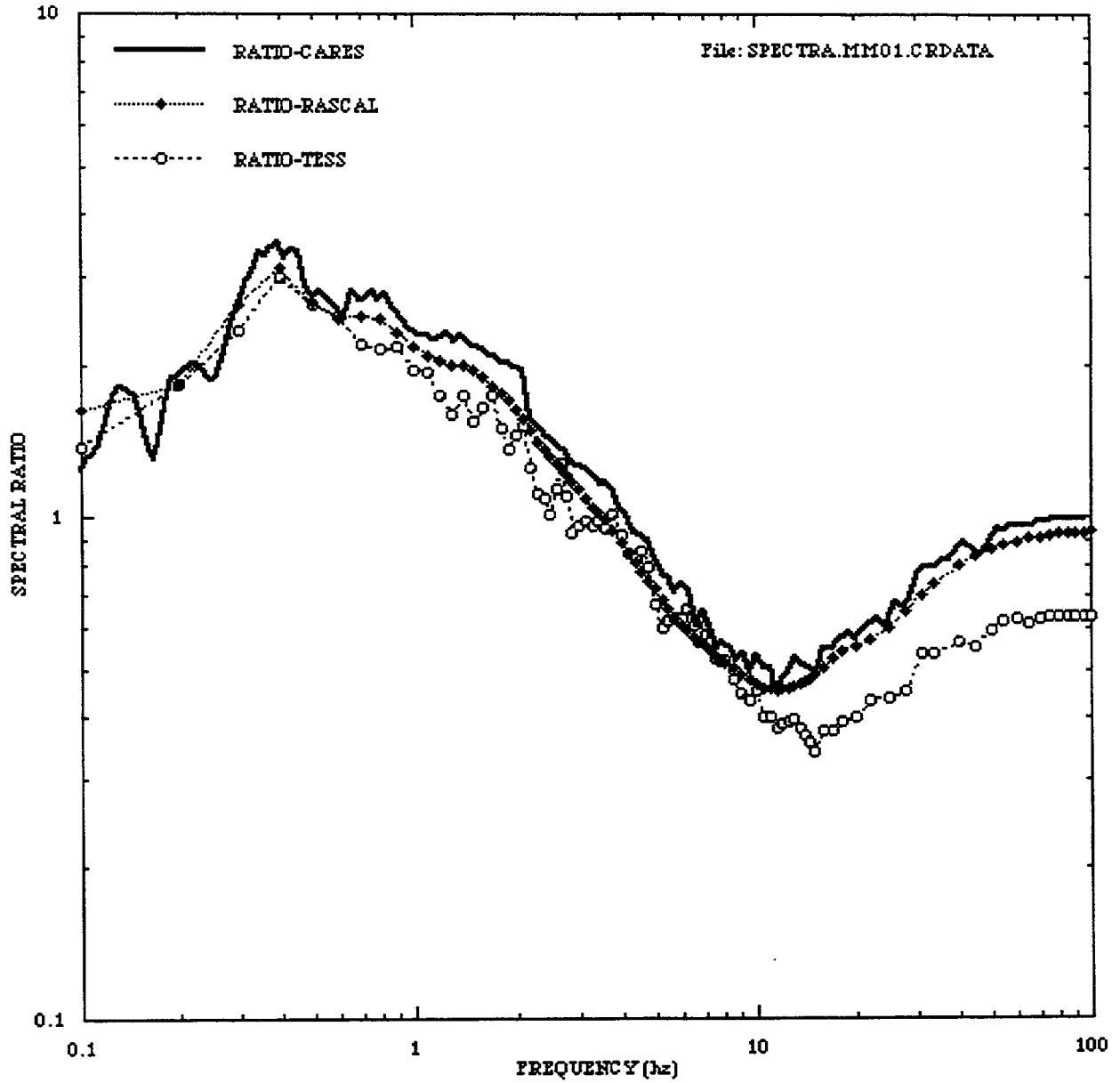


Figure B-19. Mean 5% damped spectral ratios for Imperial Valley soil columns for median magnitude event scaled to 1 Hz UHS spectrum.

BIBLIOGRAPHIC DATA SHEET

(See instructions on the reverse)

2. TITLE AND SUBTITLE
Technical Basis for Regulatory Guidance on Design
Ground Motions: Development of Hazard- and Risk-consistent Seismic
Spectra for Two Sites

NUREG/CR-6769

3. DATE REPORT PUBLISHED

MONTH YEAR
April 2002

4. FIN OR GRANT NUMBER

W6248

5. AUTHOR(S)
R.K. McGuire, Risk Engineering, Inc.; W.J. Silva, Pacific
Engineering and Analysis; C.J. Costantino, Consultant

6. TYPE OF REPORT

Technical

7. PERIOD COVERED (Inclusive Dates)

04/1996 - 03/2001

8. PERFORMING ORGANIZATION - NAME AND ADDRESS (If NRC, provide Division, Office or Region, U.S. Nuclear Regulatory Commission, and mailing address; if contractor, provide name and mailing address.)

Risk Engineering, Inc.
4155 Darley Avenue, Suite A
Boulder, Colorado 80305

9. SPONSORING ORGANIZATION - NAME AND ADDRESS (If NRC, type "Same as above"; if contractor, provide NRC Division, Office or Region, U.S. Nuclear Regulatory Commission, and mailing address.)

Division of Engineering Technology
Office of Nuclear Regulatory Research
U.S. Nuclear Regulatory Commission
Washington, DC 20555-0001

10. SUPPLEMENTARY NOTES

R. M. Kenneally, NRC Project Manager

11. ABSTRACT (200 words or less) We illustrate recommendations for design spectra at two example sites, one in the Mojave desert, California, and the second at Columbia, South Carolina. For rock conditions, the uniform hazard spectrum (UHS) is determined at each site with a probabilistic seismic hazard analysis (PSHA). We calculate a scale factor to derive a rock uniform reliability spectrum (URS) based on the slopes of the hazard curves across the frequency range of interest at each site. The database of strong motion records provides a source of rock motions with the correct magnitudes and distances. For soil sites, we illustrate the development of design spectra using a profile of the Savannah River site in South Carolina assumed to lie at the Columbia site. We scale soil spectra to the 10 Hz and 1 Hz UHS and URS, using soil-specific amplification studies, because generic shapes for soil sites are not appropriate. Artificial motions for soil sites are created in a manner similar to that for rock sites. These recommendations for design spectra illustrate that reliability-consistent spectra can be calculated for both rock and soil sites.

12. KEY WORDS/DESCRIPTORS (List words or phrases that will assist researchers in locating the report.)

seismic hazard, spectral shapes, risk-consistent spectra, soil spectra,
soil response, uniform hazard spectra, uniform reliability spectra,
artificial motions

13. AVAILABILITY STATEMENT

unlimited

14. SECURITY CLASSIFICATION

(This Page)

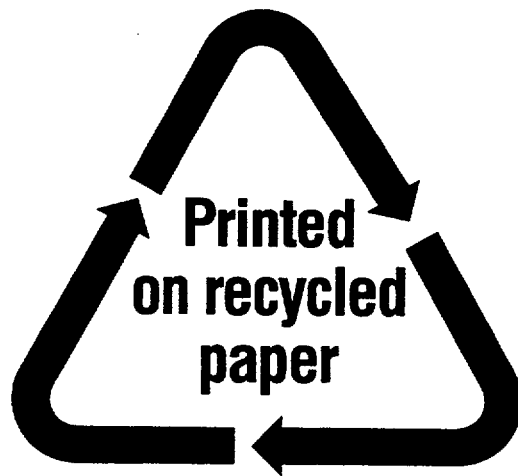
unclassified

(This Report)

unclassified

15. NUMBER OF PAGES

16. PRICE



Federal Recycling Program

**UNITED STATES
NUCLEAR REGULATORY COMMISSION
WASHINGTON, DC 20555-0001**

**OFFICIAL BUSINESS
PENALTY FOR PRIVATE USE, \$300**